Petrogenesis of Palaeocene granites,

Island of Skye,

N. W. Scotland.

BY
ALI SALEH ALI ABOAZOUM.

Department of Geology and Applied Geology,
University of Glasgow,
Glasgow,
June 1995.

Thesis submitted for the degree of Doctor of Philosophy.

ACKNOWLEDGEMENTS

I would like to express my thanks to my father and mother, without whose advice, encouragement, patience and understanding, together with their prayer for me, I would not have started this research, rather than complete it. My thanks also to libyan people for their financial support .

I am indebted to my supervisor, Dr Brian R. Bell, for his guidance, encouragement, constant support, fruitful discussion, valuable advice and his patience during the period of this research.

Drs Graeme Rogers and Tony Fallick are also thanked for their enormous help, encouragement and valuable discussion. I am also grateful to Dr Tim Dempster for his comments in the early stages of this research, Dr George Bowes for his computer assistance, and Drs Gawen Jenkin and Joe Crummy for their help and discussions regarding the fluid inclusions.

I wish to thank my colleague Gary Kitchner for his generous assistance in the field during the collection of samples. Discussions with Abdulhamid Alhurmezi, Abdulrahman Bumezbeur and Ahmed Alkotbah are highly appreciated.

Pete Ainsworth, Jim Gallagher, William Higgison (Bill), Dugald Turner, Robert MacDonald, John Gilleece, Jim Kavanagh, Douglas Maclean, Murdo Macleod, and Roddy Morrison from the Geology Department, together with Anne Kelly, Allison MacDonald, Joss, Martin McCartney and Juile Gerc from SURRC, East Kilbride, are all thanked for their contributions to this research, which are highly appreciated.

Finally, thanks to my wife, for her support, patience and understanding, without which this research would not have been completed. My best wishes, deep thanks and love to all my sons, Abdulmonim, Saleh, Abdulsalam and Ahmed.

DECLARATION

I declare here that the material presented in this thesis is the result of independent research carried out between September 1991 and May 1995 in the Department of Geology and Applied Geology, University of Glasgow, under the supervision of Dr Brian R. Bell. Any published or unpublished materials used herein have been given full acknowledgement in the text.

Ali S. A. Abouazoum

[redacted]

June 1995

TABLE OF CONTENTS

CHAPTER III

Petrography

CHAPTER IV

Mineral chemistry

CHAPTER VII

Stable isotope geochemistry

CHAPTER VIII

Radiogenic isotope geochemistry

LIST OF FIGURES

Chapter VII

LIST OF TABLES

ABSTRACT

This thesis documents an investigation of selected intrusions of the Palaeocene granites on the Isle of Skye, and includes: petrography, mineral chemistry (include REE concentrations), fluid inclusions, whole rock major-, trace- and rare-earth-elements, together with stable oxygen and hydrogen and Sr-Nd isotope geochemistry on whole rocks and mineral separates.

The data presented indicate that the granites are geochemically related and have been severely affected by 'associated ' hydrothermal fluid(s), especially the Loch Ainort Granite. The hydrothermal fluids most likely represent the limited mixing between magmatic and meteoric waters in Beinn an Dubhaich Granite. In contrast, the other granites are likely to have been affected by meteoric water alone, with water-rock interaction having occurred below 500°C.

The coarsening of granophyric texture outwards from alkali feldspar phenocrysts, the low concentration of Fe^{3+} in pyroxenes, together with the slight variations in Fe^{2+}: Mg ratio of biotites, suggest a slow cooling history for the granites. The (two feldspar) Beinn an Dubhaich and Glamaig granites have small negative Eu anomalies compared with the (single feldspar) Loch Ainort and Marsco granites, suggesting the important role of plagioclase fractionation during granite evolution. The most important reservoirs for the REE in the Skye granites are amphibole, pyroxene and apatite.

The inflection present in the plot of MnO against SiO_2, the non-linear and divergent relationships between K_2O, Rb, Sr and ?Nb against SiO_2, and the presence of an anomalous group of granites which are characterised by *low* Zr , Y and Nb, but with *high* SiO_2 contents, mitigates against simple mixing as the dominant process responsible for the compositional diversity of the granites.

The ^{18}O-depleted signature of quartz from the Loch Ainort and Marsco granites, together with the equilibrium value of $\Delta_{Q\text{-}Af}$ from the Marsco Granite, suggest that these granites contain a crustal component

which was derived by partial melting of an ^{18}O-depleted protolith. In contrast, the Beinn an Dubhaich and Glamaig granites appear to have crystallised with normal $^{18}O/^{16}O$ signatures and were subsequently depleted in ^{18}O by subsolidus reaction with meteoric waters. The low δD values for amphiboles from the Loch Ainort and Glamaig granites are attributed to a high w/r ratio during hydrothermal alteration and the involvement of a low-D protolith in the Loch Ainort Granite, whereas in the Glamaig Granite, interaction with meteoric water and chloritisation are the most reasonable explanations for the δD values of the amphiboles.

Zircons from the Glamaig and Marsco granites contain refractory cores and have unusually low Sm/Nd ratios, unlike the zircons from the Beinn an Dubhaich and Loch Ainort granites, which have normal Sm/Nd ratios, indicating that the inherited zircons had very low Sm/Nd ratios. These refractory zircons, together with high crystallisation temperatures recorded for these granites by feldspar thermometry (800-950°C) and zircon solubility data (812-986°C) (Loch Ainort and Marsco in particular), indicate the dual importance of mantle-derived materials and crustal components in the origin of the granites.

The radiogenic isotope data reveal that the crystallisation of the analysed samples appears to have occurred within a very short period of time (5Ma) at approximately 55-60Ma, and each intrusion has a distinct and different initial $^{87}Sr/^{86}Sr$ and εNd isotopic composition. Such variations are attributed to magma-crust interaction, with different proportions of crustal components (around 70% for Beinn an Dubhaich, 10% for Loch Ainort, 40% for Marsco and 50% for Glamaig). In contrast, the variations in initial $^{87}Sr/^{86}Sr$ ratios between minerals from the Marsco and Loch Ainort granites are attributed to hydrothermal alteration processes.

The wide range of T_{DM}^{Nd} model ages for the Skye granites is interpreted as representing variable mixtures of old crust and Palaeocene mantle-derived materials, rather than a major crust-formation event. The intermediate isotopic composition of the granites between Hebridean mantle and crustal compositions, together with the heterogeneous isotopic compositions of basement Lewisian amphibolites and granulites, indicate that they are the products of the differentiation of different pulses of basaltic magma, and that each magma was contaminated with crustal lithologies which had distinct and different Sr and Nd isotope signatures.

CHAPTER I

An outline of this study and an introduction to granites and granitic rocks: Some definitions and general concepts

1.1 Introduction and outline of this study

This study is concerned with the geochemistry and petrogenesis of granitic rocks, specifically the Palaeocene granites of the Skye Intrusive Centre, NW Scotland. The aim of the study is to investigate the mineralogy and geochemistry of Skye granites in order to determine the origin of the magmas and the processes by which the intrusions achieved their present-day mineralogies and geochemical characteristics.

Skye granites have been the subject of many investigations which have focused on two quite different aspects of their mineralogy and geochemistry. First, a number of studies have been concerned with the origin(s) of the magmas, specifically if they represent partial melts of crustal rocks, or, alternatively, if they represent evolved liquids derived by extreme fractional crystallisation of a more primitive (basaltic) parental magma. The possibility

that they contain components from both generation mechanisms has, of course, also be considered. Second, a number of studies have been concerned with the modification of Skye granites by subsolidus reaction with circulating meteoric waters subsequent to their emplacement. Consequently, Skye granites have been examined in order to solve problems of granite magma genesis, whilst at the same time it has been demonstrated that they have undergone substantial modifications with respect to stable isotopes (oxygen and hydrogen), together, possibly, with other chemical components.

This dichotomy of interests has lead to the present investigation. In its simplest form, this investigation sets out to characterise Skye granites in terms of their mineralogy and geochemistry, and to determine the relative magmatic and hydrothermal signatures of the component minerals and how these data compare to previous, predominantly whole-rock, geochemical studies. As such, this study reports details on the following aspects of Skye granites: (i) mineralogy; (ii) mineral textures; (iii) mineral chemistry data (including the rare-earth-elements); (iv) fluid inclusion data; (v) whole-rock compositions (major-, trace- and rare-earth-elements); (vi) O and H isotope geochemistry of individual minerals and whole-rocks; and, (vii) Rb-Sr and Sm-Nd isotope geochemistry of individual minerals and whole-rocks. All of these data are synthesised into a coherent model which sets out to interpret and explain the geochemistry of Skye granites and to unravel the processes involved in their origin and evolution.

Detailed accounts of the petrology and geochemistry of granites and granitic rocks are available in a number of excellent recent textbooks, noteworthy amongst which are: Didier and Barbarin (1991); Clarke (1992), and Pitcher (1993). As such, only concepts and data relevent to the present study are included in this text.

1.2 A definition of granite and the mineralogy of granites

The name **granite** is very old and, ultimately, of unknown origin. Possibly, it may have been derived from ancient Welsh, as *gwenith faen*, a wheatstone for the grinding of flour. Another possibility is that it is derived from the Italian word *granito* (Latin: *granum*), meaning grained. However, there is considerable doubt over either derivation (see: Johannsen, 1931, vol. 1, p. 254; Pitcher, 1993, p.1).

In general terms, granite may be defined as a holocrystalline igneous rock, composed essentially of quartz, alkali feldspar and plagioclase, with or without, ferromagnesian silicate minerals and oxides.

Typically, quartz should constitute at least 10 vol.% of the rock. According to Nockolds et al. (1978) a value of 10 vol.% is required, whereas Hatch et al. (1972) suggest a value of at least 20 vol.%. More recently, on behalf of the International Union of Geological Sciences (IUGS) Subcommission on the Systematics of Igneous rocks, Le Bas and Streckeisen (1991) recommend that quartz should constitute 20-60 vol.% of the total [quartz + alkali feldspar + plagioclase] *and where [quartz + alkali feldspar + plagioclase] constitutes at least 10 vol. % of the rock.* Figure 1.1 sets out the classification according to Le Bas and Streckeisen (1991). Rocks richer in quartz (and therefore poorer in feldspar) fall within either the field of quartz-rich granitoids (60-90 vol.% quartz) or, at ≥ 90 vol. %, into the field of quartzolites (silexites). Less specifically, Johannsen (1931) quotes that the combined quartz + feldspars in a granite should be ≥ 50 vol.% of the total rock.

The total vol.% of feldspar (both alkali feldspar and plagioclase) in granites has been less clearly defined. By inference from Fig. 1.1, Le Bas and Streckeisen (1991) suggest that the total vol.% of feldspar should be *at least*

40 vol.% and that alkali feldspar should dominate over plagioclase. In reality, most accepted definitions of the total vol.% of feldspar are much higher, although not defined (for example, Johannsen, 1931; Hatch et al., 1972; Nockolds et al., 1978).

Depending upon the relative proportion of alkali feldspar to plagioclase, Le Bas and Streckeisen (1991) and Nockolds et al. (1978) suggest the following names (Fig. 1.2): alkali granite (≥ 90 vol. % alkali feldspar); granite (alkali feldspar = at least 40 vol.%); granodiorite (alkali feldspar = 10-40 vol.%); and, tonalite (alkali feldspar ≤ 10 vol.%). Fine-grained equivalents to these lithologies are: alkali rhyolite, rhyolite, rhyodacite, and dacite, respectively (Nockolds et al. , 1978).

Based upon the type(s) of alkali feldspar present, two types of granites may be defined. These are: (i) hypersolvus granites, which contain a single alkali feldspar, typically a microperthite; and, (ii) subsolvus granites, which contain two alkali feldspars, typically microperthite and independent albite (Tuttle and Bowen, 1958).

Plagioclase typically is subhedral, either unzoned or zoned, and typically lies within the compositional range oligoclase - andesine ($Ab_{90}An_{10}$ - $Ab_{50}An_{50}$).

Ferromagnesian silicates, oxides and phosphates are considered, by definition, to be accessory in granites and constitute wide and varied groups. Important amongst the ferromagnesian silicates are: amphiboles (calcic, Fe-Mg-rich, or alkali-rich), Mg-Fe micas (eastonite - siderophyllite), Al micas (muscovite), pyroxenes (aegirine, hedenbergite), olivines (fayalite), garnets, cordierites, epidote group minerals (including allanite), and zircon. Oxides include members of the spinel group and sphene (or titanite). Phosphates include apatite, monazite and xenotime.

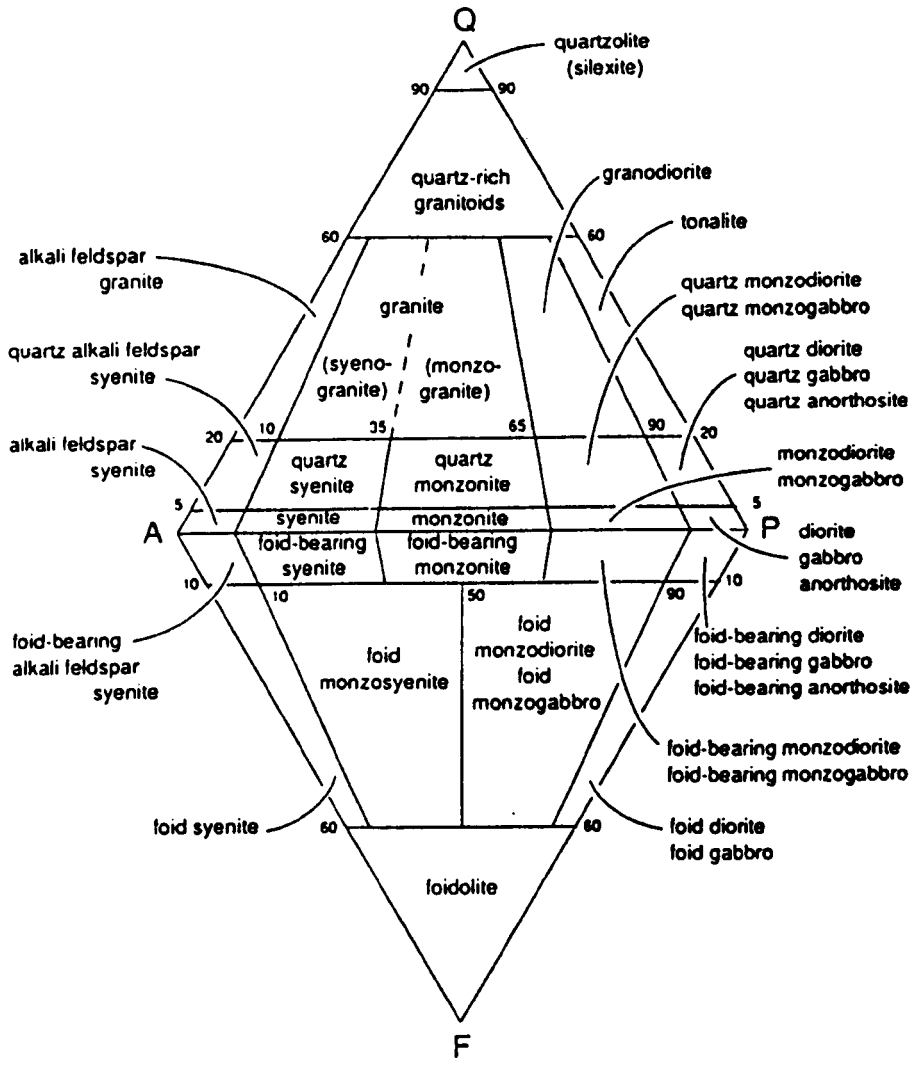

Fig. 1.1 Classification and nomenclature of the plutonic igneous rocks according to their felsic modal contents when mafic mineral content is less than 90%. Q, quartz; A, alkali feldspar; P, plagioclase; F, feldspathoid(foid). (after Le Bas and Steckeisen, 1991).

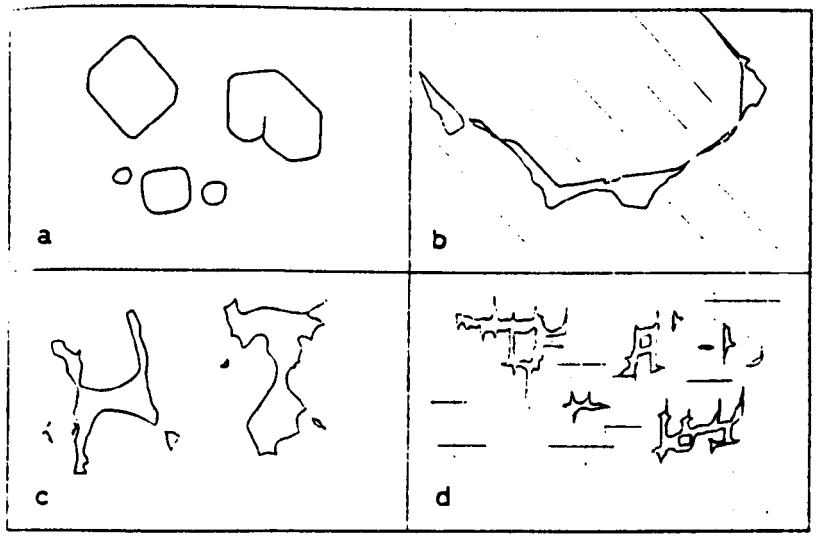

Fig. 1.2 Variations of quartz shapes in granites. **(a)** Euhedral hexagonal crystals; **(b)** Anhedral quartz surrounding a core of alkali feldspar; **(c)** Concave quartz simultaneously crystallized with alkali feldspar; **(d)** Net-like quartz forming veinlets or garlands in alkali feldspar subparallel to the cleavage planes. (after Mehnert, 1968).

1.3 Textural characteristics of granitic rocks

The textural characteristics of granites are extremely variable. However, their interpretation is critical to an understanding of the crystallisation history and any post-crystallisation modifications which may have occurred. Clarke (1992, Chapter 3) provides a useful summary of the many recognised textures in granites, together with explanations as to their possible origin(s). Relevant to Skye granites are the following textural characteristics:

(i) equigranular: all grains are essentially same size;

(ii) inequigranular: a range of grain sizes, for example, porphyritic;

(iii) euhedral, subhedral and anhedral: grains have all faces developed, some faces developed, no faces developed;

(iv) crystal zoning: compositional variation from core to rim, may be continuous or stepped;

(v) poikilitic texture: one mineral encloses or partially encloses another;

(vi) granular texture: most grains are equant in shape, typically subhedral;

(vii) granophyric texture: quartz and alkali feldspar in a radiating intergrowth: possibly a disequilibrium eutectoid growth, or fluid-related;

(viii) perthite and antiperthite: exsolution or unmixing of two feldspars;

(ix) coronas and epitaxial overgrowths: reaction between a nucleus mineral and a melt, for example, due to a peritectic reaction.

Other textural characteristics include: the development of aphanitic chills at the margins of intrusions due to rapid crystallisation rates; the alignment of crystals, either due to recrystallisation in a differential stress field or flow

alignment during intrusion; the presence of xenocrysts, certain of which may show reaction (resorption) or overgrowth characteristics; xenoliths (again possibly showing evidence of mineral resorption or overgrowth, and possibly either recrystallised or in a state of disaggregation due to mechanical breakdown or partial melting).

Typically, early-crystallised minerals tend towards euhedral forms, whereas later minerals are anhedral due to their impingement on other minerals during growth. During mineral growth, melt inclusions may be trapped by minerals, as can early precipitated minerals. During hydrothermal alteration (mineral-fluid reaction) samples of the fluid may be trapped (any possible combination from solids, (crystals), liquid, and vapour).

Mineral intergrowths can be produced during eutectoid crystallisation of a melt, for example, granophyric intergrowth involving quartz and alkali feldspar), or involving a mineral and a melt, for example, epidote coronas on amphiboles, or involving the solid-state, for example, perthites.

1.4 Classifications of granites and granitic rocks: mainly chemical

Chemical classifications of granitic rocks are numerous. Linking mineralogy to whole-rock composition can be achieved by use of schemes such as the normative mineralogy procedure set out by Cross, Iddings, Pirsson and Washington (hence, CIPW norm). Granites, by definition, contain normative quartz *(Q)*, orthoclase *(Or)*, albite *(Ab)* and, usually, some anorthite *(An)*. Granites rich in aluminium will contain normative corundum *(C)*, whereas those rich in the alkalies contain normative acmite *(Ac)*; such compositional characteristics typically show as modal muscovite or alkali-rich amphiboles and pyroxenes such as arfvedsonite and aegirine, respectively.

The relationship between the amounts (in moles) of the CaO (=C), Na_2O (=N) and K_2O (=K), and, Al_2O_3 (=A) can also be applied to the classification of granites, as follows (Shand, 1947):

If A/(C+N+K) = 1, then if only quartz and feldspar are present, we have a so-called haplogranite; the presence of other minerals which contain any of these constituents will modify the ratio either to values <1 (for example, amphibole) or values >1 (for example, almandine garnet). Certain terms have been applied depending upon the relative values of A, C, N and K: if A/(C+N+K) > 1 the granite is peraluminous; if A/(C+N+K) <1 the granite is metaluminous; and, if A < (N+K) the granite is peralkaline. Peraluminous granites are typified by modal muscovite, biotite, garnet, cordierite or andalusite, whereas metaluminous granites may contain pyroxene, hornblende or biotite, and peralkaline granites contain alkali-rich minerals such as aegirine, arfvedsonite and riebeckite.

Chayes (1985) and Clarke (1992) produced average major-element compositions of peraluminous, metaluminous and peralkaline granites. These data are reproduced here in Table 1.1.

	Peraluminous	Metaluminous	Peralkaline
SiO_2	71.45	67.43	74.01
TiO_2	0.32	0.55	0.23
Al_2O_3	14.76	14.67	11.59
FeOT	2.49	4.13	3.08
MnO	0.13	0.12	0.10
MgO	0.78	1.64	0.55
CaO	2.01	3.53	0.48
Na_2O	3.72	3.72	4.33
K_2O	3.52	3.20	5.09
P_2O_5	0.14	0.17	0.06
Total	99.32	99.16	99.52
A/CNK	1.10	0.93	0.86
NK/A	0.67	0.65	1.09

Table 1.1 Average major-element compositions for peraluminous, metaluminous and peralkaline granites (after Clarke, 1992; however, the reported NK are less than Al in peralkaline granite ?).

More complex classifications have attempted to utilise combined major- and trace-element data, together, in certain cases, with radiogenic and stable isotope signatures. Some of the classifications and discriminations which have been identified are aimed at linking granite composition and tectonic setting, whereas others attempt to link composition and genesis of the magma. One of the more popular and apparently successful schemes has been developed by Chappell and White and their co-workers. Clarke (1992) summarises the four identified granite types as follows:

(i) **I-type:** with A/(C+N+K) < 1.1; $^{87}Sr/^{86}Sr_i < 0.705$; $\partial^{18}O < 9$ °/oo ; implying source materials of basic or intermediate igneous composition or infracrustal derivation (Chappell and White, 1974; Chappell and Stephens, 1988);

(ii) **S-type:** with A/(C+N+K) > 1.1; $^{87}Sr/^{86}Sr_i > 0.707$; $\partial^{18}O > 9$ °/oo ; implying source rocks of sedimentary or supracrustal protoliths (Chappell and White, 1974; White and Chappell, 1988);

(iii) **M-type:** with A/(C+N+K) < 1; $^{87}Sr/^{86}Sr_i < 0.705$; $\partial^{18}O < 9$ °/oo ; implying mantle sources, either indirectly through partial melting of subducted oceanic crust, or directly by extended fractional crystallisation of basaltic magma (White, 1979; Pitcher, 1982);

(iv) **A-type:** with A/(C+N+K) > 1; $^{87}Sr/^{86}Sr_i$ and $\partial^{18}O$ comparable to I-, S- and M-types; low CaO; high Fe/Mg; high Ta, Nb, Zr, REEs and F; and are anorogenic (Loiselle and Wones, 1979; Collins et al., 1982; Clemens et al., 1986; Creaser et al., 1991).

It is clear that the classification of granites into I- and S-types has a genetic connotation: that the source materials for the magmas were either igneous or sedimentary, respectively. This still holds for the M-type, but is not applicable to the so-called A-type, which is based upon tectonic setting, not

source material.

Another complication with schemes of this type is that it has been shown that I-type granitic magmas may evolve (that is, change composition by some process, or combination of processes) and produce S-type (peraluminous) magmas (for example, Halliday et al., 1981; Zen, 1986; Liggett, 1990; Miller et al., 1990). Factors such as variable degrees of melting of the source material and the melting of heterogeneous source materials, together with processes such as magma-crust interaction (assimilation), magma-mixing and hydrothermal alteration may all cause magmas to evolve across the simple I- and S-type boundaries. As such, all classification schemes are limited with respect to identifying the predominant source materials and hence the mechanism of magma generation.

Certain classification schemes have been devised based upon the concentrations and ratios of a number of identified immobile trace-elements, for example, Ta, Hf, Nb, Ti, Zr and Y (for example, Floyd and Wichester, 1975; Brown et al., 1984; and, Pearce et al., 1984). Such schemes have, typically, been used to distinguish between granites in different tectonic settings, such as syn-tectonic and post-tectonic collision granites, volcanic arc granites, and within-plate granites.

Finally, a useful summary of proposed schemes of granite classification is presented by Pitcher (1993) (Table 1.2), encompassing certain of the schemes outlined above (for example that of Shand 1947; and the Chappell and White I-S-M-A scheme). Use will be made of parts of certain of these schemes, where appropriate. However, the main objective of this investigation is concerned with the genesis of the magma(s) and their subsequent evolution, and not merely with their classification or tectonic setting.

Table 1. 2 Comparison of the main petrogenetic classifications of granitic rocks (after Pitcher, 1993), where: **MA** or **AM**, magmatic association; **A**, alumino; **K**, potassic; **G**, granodiorite; **L**, leucogranite; **SA**, subalkaline; **CA**, calcalkaline; **TH**, tholeiitic; **A-PA**, alkaline-peralkaline, according to La Roche abbreviations. Other abbreviations are: **IA**, Island arc; **CA**, continental arc; **CC**, continental collision; **PO**, post-orogenic; **RR**, rift related; **CE**, continental epeirogenic; **CEU**, continental epeirogenic uplift; **OP**, oceanic plagiogranite; S-and I-type indicate derivation from sedimentary and igneous sources, respectively. Within Barbarin's suggested synthetic classification the acronyms signify: C_{ST}, crustal shearing and thrusting; C_{CA}, C_{CI}, crustal collision autochthonous or intrusion; H_{LO}, hybrid late orogenic, H_{CA}, hybrid continental arc; T_{IA}, and T_{OR}, tholeiitic island arc and tholeiitic ocean ridge; **A**, alkaline. (after Pitcher, 1993).

Classification Basis		Origin						
		Crustal		Mixed			Mantle	
First chemical	Shand (1943)	Peraluminous		Metaluminous				Peralkalines
Nomenclatures	Lacroix (1898)	Roches Calco-alc. hyperalumineuses		Roches calco-alcalines				Roches alcalines
Petrography	Capdevila and Floor (1970) Capdevila et al. (1973)	Granite s mesocrustaux		Granite Mixtes	Granites basicrustaux			
	Orsini (1979)			AM sub-alc. alumineux	AM sub-alc. AM. hypoalum	Calco-alc.		
	Yang Chaoqun (1982)		MM-type	CR-type	M S-type		MD-type	
	Tischendorf and Palchen (1985)	Si	Ss	Si	IKK	IOK	IMT	IMA
Enclaves	Didier and Lameyre (1969) Didier et al. (1982)	C-type (crustal) (Leucogranites)		M-type (Mixed or Mantle) (Monzogranites & granodiorites)				
Mineralogy (QAP system)	Lameyre (1980) Lameyre and Bowden (1982)	(Leucogranites) (crustal fusion)		Calc-alkaline series (High K, Medium K or Low K)			Tholeiitic (series) Series	(Per)alkaline
Mafic minerals	Rossi and Chevremont (1987)	AM aluminopotassique (s.s. Ou composites)		AM monzonitique		AM calco. alcaline	AM tholeitique	AM (PSer) alcaline
Biotite composition	Nachit et al. (1985)	Lignees alumino-potassi		Lignees calcoalclines et subalcalines				Lignees alcalines et hyperalcalines
Zircon morphology	Pupin (1980, 1985)	Type 1	Type 2	Type 3	Type 4 & 5		Type 7	Type 6
Opaque oxides	Ishihara (1977) Czamanske et al. (1981)	Ilmenite series			Magnetire series			
Geochemistry (major elements)	Chappell and White (1974, 1984) Collins et al. (1982) Whalen et al. (1987)		S-type	I-type			M-type	A-type
	De La Roche (1986) De La Roche et al. (1980)	Ak-L MA	Ak-G MA	SA MA	CA MA		TH MA	A-PAMA
	Debon and Le fort (1988)	Aluminous MA			Alumino-cafemic and cafemic MA (Subalkaline, calc-alkaline, tholeiitic and (per)alkaline)			
	Manier and Piccoli (1989)	CCG		POG	CAG		IAG / OP	PRG / CEUG
Geochemistry (trace elements)	Tauson and Kozlov (1973)	Plumasitic leucogranites	Ultra-MM granites	Palingenic granites (normal & subalkalines)			Plagio-granites	Agpaitic leucogranites
	Pearce et al. (1984)	C O L G- Collision Granites (Syntectonic) (post-tectonic)		VAG Volcanic arc granites			ORG	WPG within plate granites
Associated mineralizations	Xu Kegin et al. (1984)	Transformation type (continental crust)		Synttexis type (transitional crust)			Mantle -derived type	
Tectonic environment	Pitcher (1983, 1987)	Hercyno type		Caledonian type		Andinotype	W. Pacific type	Nigeria type
Suggested classification by Barbarin (1990)		C_{ST}	C_{CA}	C_{CI}	H_{LO}	H_{CA}	$_{IA}T_{OR}$	A

1.5 Subsolidus modifications of granites

In the following discussion, reference is made, where appropriate, to previous studies of alteration processes which affected Skye granites.

1.5.1 Recrystallisation of granites

The mineralogy and structural features of granites and their fabric are not the result of a single petrogenetic process, but are the product of a sequence of processes, as admitted by many authors (for example, Mehnert, 1968). Among these processes is recrystallisation.

The term recrystallisation from a petrological point of view is the changing of crystal fabric or crystal size without an accompanying change in mineral chemistry (Bates and Jackson, 1980). During recrystallisation some crystals grow in size by consuming neighbouring crystals, whereas others simply replace their polymorphs, for example inversion of quartz.

The factors favouring recrystallisation are chiefly water and heat (Huang, 1962; Cox et al., 1979; Ferry, 1985). This association suggests that an especially favourable agent would be hydrothermal fluids. In addition, chemical agents play an important role, whereas stresses influence the resulting fabrics (Huang, 1962).

Evidence for recrystallisation in granitic rocks comes from studies of quartz and feldspar, for example, Tuttle (1952) and Mehnert (1968), and may be summarised as follows:

Quartz in granites is formed over a long period of crystallisation and hence a sequence of different generations can be produced:

(i) Euhedral quartz (Fig.1.2a), which is identical to that of the phenocrysts in

porphyries (volcanic rocks). Their hexagonal symmetry is taken as an indication of their formation above the inversion temperature of high-low quartz, i.e. above 573°C and confirms their crystallisation before K- feldspar megacrysts, as this type of quartz typically occurs as inclusions inside alkali feldspar megcrysts (Mehnert, 1968)

(ii) Anhedral quartz, which is the main variety of quartz in granites, and occurs in the interstices between earlier-crystallised minerals including primary alkali feldspar (Fig. 1.2b). Such quartz may form simultaneously with post-magmatic alkali feldspar rims of megacrysts, and occur as anhedral crystals (Mehnert, 1968).

(iii) Concave quartz, described by Mehnert (1968) as inclusions of quartz in K-feldspar with concave borders, or more rarely parallel to it (Fig. 1.2c). He attributes their origin to a graphic intergrowth between quartz and K-feldspar accompanied by corrosion of quartz edges.

(iv) Net-like quartz, which is uncommon in normal granites, but when it does occur, generally forms thin veinlets or garlands in alkali feldspar, or more rarely in plagioclase (Fig. 1.2d).

Rapidly quenched quartz crystals (e.g. quartz in rhyolites) contain glass inclusions, whereas slowly cooled quartz (e.g. quartz in granites) does not contain such inclusions (Tuttle, 1952). The quartz from granites goes through the high-low inversion at slightly higher temperatures than the quartz phenocrysts of rhyolites (Tuttle and Keith, 1954). This difference is illustrated in Fig. 1.3, (after Keith and Tuttle, 1950), which is a plot of the temperatures of beginning of transformation on heating and cooling through the inversion.

Therefore, the evidence from polymorph inversion, the presence of inclusions and petrofabric differences between rhyolite and granite, strongly

suggest that some quartz in granites is the product of recrystallisation.

Alkali feldspar in granite can crystallise at two different stages, magmatic and post-magmatic. The crystallisation of post-magmatic alkali feldspar is related to the primary magmatic formation of alkali feldspar (Mehnert, 1968).

The inner parts of alkali feldspar megacrysts are typically euhedral and have a slightly higher Na content, when compared with their outer rims and smaller crystals in the groundmass of the granite. This difference in Na content can be attributed to the degree of perthite formation in the alkali feldspar megacrysts, which may be another indication of recrystallisation processes in granites (Mehnert, 1968).

Plagioclase, in intrusive felsic rocks, is rarely zoned, whereas in their extrusive equivalents, is almost always zoned. The high temperature form of albite is found only in extrusive rocks and meteorites, whereas the low form is found in plutonic rocks (Tuttle and Bowen, 1950).

Low-temperature albite often exhibits some forms of albitization, consisting of the partial or complete replacement of pre-existing plagioclase or alkali feldspar by albite, or as fringes or lobes around earlier plagioclase and alkali feldspar crystals (Mehnert, 1968). Euhedral alkali feldspar and/or plagioclase phenocrysts can microscopically be composed of an aggregate of small albite crystals replacing them completely, whereas this feature is absent in high albite (Mehnert, 1968). The difference between low temperature and high temperature plagioclase, in terms of chemical zonation and optical properties, indicates that the recrystallisation can take place in plutonic rocks (Tuttle, 1952).

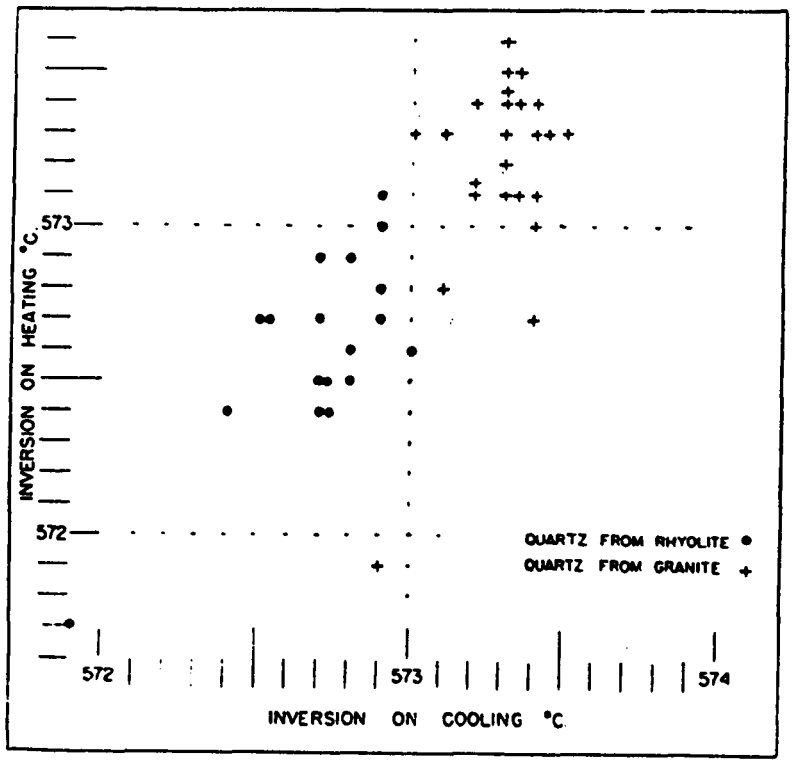

Fig. 1.3 Plot showing the relation between the beginning of the high-low inversion on heating and cooling in quartz from granites and rhyolites. (after Keith and Tuttle, 1950).

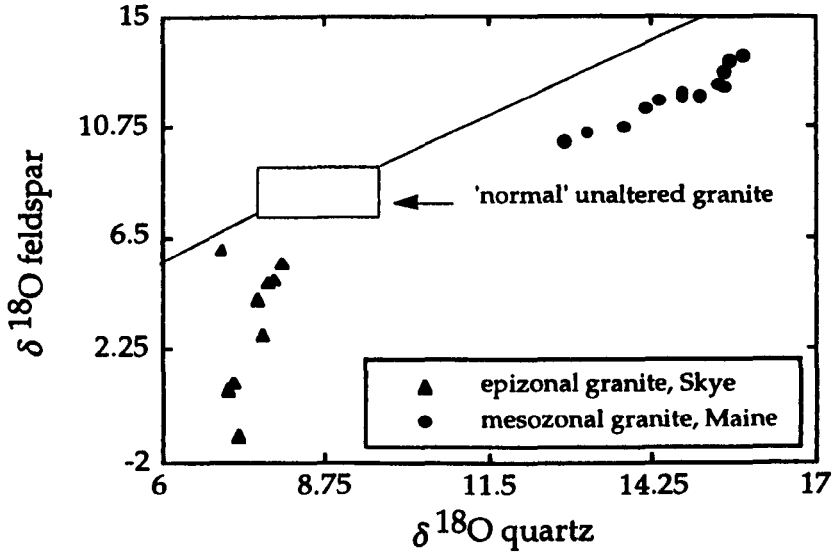

Fig. 1.4 Oxygen isotope compositions of quartz and feldspar from hydrothermally-altered (epizonal and mesozonal) granites (after Ferry, 1985). Box represents the inferred composition of feldspar and quartz from unaltered 'normal' granite; line represents approximate equilibrium ^{18}O-^{16}O fractionation between magmatic quartz and alkali feldspar.

1.5.2 Exsolution of alkali feldspars

Homogeneous alkali feldspar in granites unmixed during cooling under high water pressure (PH_2O = 5000 bars) to Na-and K-rich components, to form perthite (Smith, 1974).

Practically all of the alkali feldspar of any particular composition starts to exsolve as temperature decreases to the minimum temperature of its stability at that composition, i.e. when the surface of the solvus is reached. The position of the solvus, unlike the solidus and liquidus curves, does not change with changes in pressure of water, because water does not participate in the equilibria involved at the solvus, whereas it does participate in the solidus-liquidus equilibria by entering into the composition of the liquid phase (Tuttle and Bowen, 1958).

Many granites contain two different types of feldspar, one K-rich and the other Na-rich, which crystallise independently. These are the so-called subsolvus granites, and contain magmatic sodium feldspar as discrete grains of albite or albite-oligoclase beside magmatic potassium feldspar (Tuttle & Bowen, 1958). In hypersolvus (one feldspar) granites the sodium feldspar is held in solid-solution with potassium feldspar (Philpotts, 1990).

Hypersolvus granite crystallisation takes place above the solvus, due to the generally anhydrous nature of the melt. In contrast, subsolvus granite crystallisation occurs in a water-saturated system; thus, the crystallisation occurs when the alkali feldspar minimum intersects the solvus (Fig. 1.5a) (Morse, 1983; Philpotts, 1990).

Philpotts (1990) pointed out that the addition of water to an alkali feldspar melt at 500 bars will decrease the liquidus temperatures and the melt will become saturated in water when it reaches 10 wt.% (Fig. 1.5b). At this pressure any additional water will form a vapour phase, but if pressure

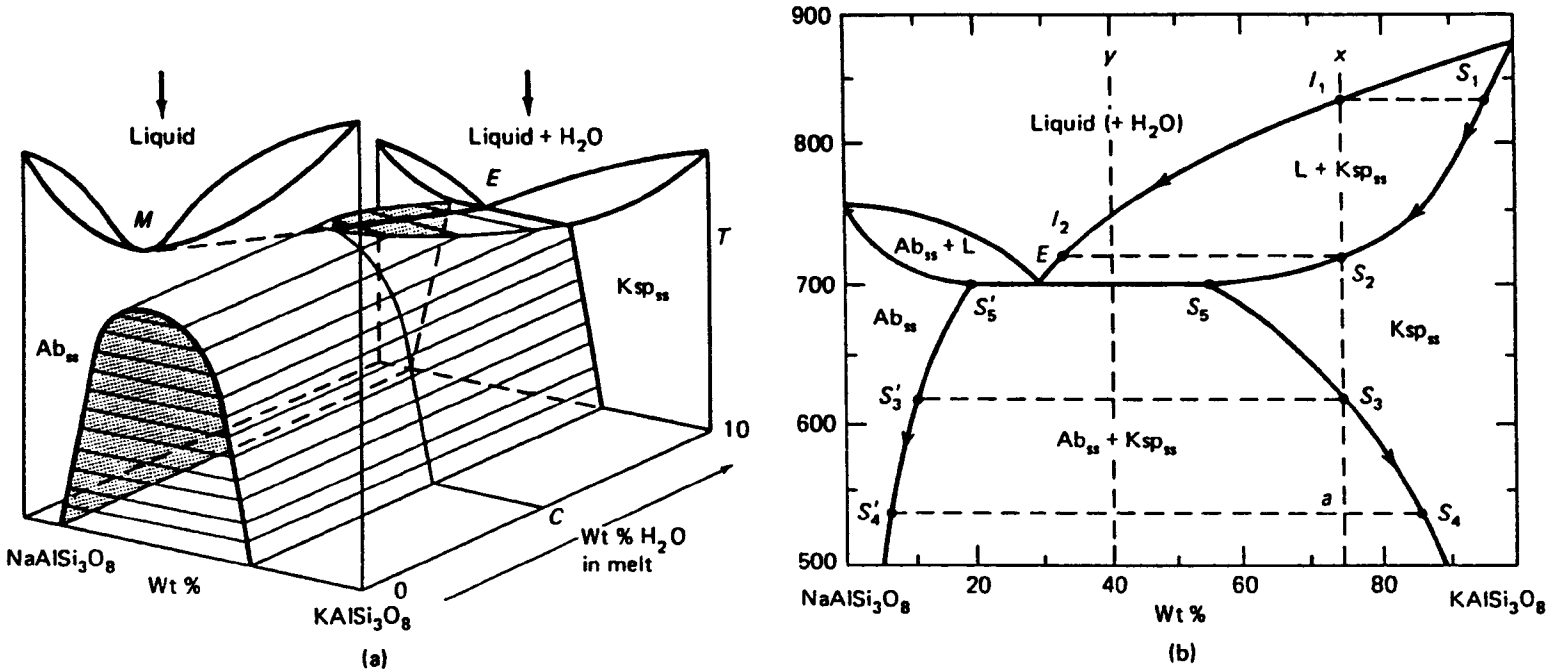

Fig. 1.5 (a) Schematic diagram illustrating the effect of the addition of H_2O in the system $NaAlSi_3O_8$-$KAlSi_3O_8$ at 500 bars. Where, (M) is the minimum in the anhydrous system and changes to an eutectic (E) beyond a critical concentration (C) of water in the melt. **(b)** H_2O-saturated phase diagram for alkali feldspars at 500bars (after Philpotts, 1990).

increases, this additional water will dissolve in the melt and (eventually) lower the liquidus temperature.

The presence of two distinct feldspars in granites can be the result of either magmatic crystallisation, or be post-magmatic, forming below 660°C, i.e., corresponding to the exsolution area (when both albite and alkali feldspar start crystallising simultaneously) (Mehnert, 1968). This temperature (660°C), as identified by Tuttle and Bowen (1958), is a maximum temperature for the solvus, at compositions close to 55% sodium feldspar at 1 Kbar, and is the minimum temperature for the stable existence of a feldspar of that composition.

Yoder et al. (1957) identified a region of complete miscibility of Na-rich and K-rich components at high water pressures (5000 bars), whereas the solvus and solidus curves intersect in the binary system Or-Ab at 695 °C and results in the crystallisation of two feldspars.

In high temperature rocks, a single feldspar with high contents of both alkalis is normally found, whereas in rocks believed to have formed at lower temperatures a sodium-rich feldspar and a potassium-rich feldspar coexist. This indicates that the alkali feldspars form a complete solid-solution series at high temperatures, but have only limited miscibility in the crystal state at low temperatures (Tuttle and Bowen, 1958).

The change in composition of homogeneous alkali feldspars during exsolution, towards the pure end-member components, occurs as temperature decreases. The purer the feldspar composition, the lower the temperature of crystallisation has to be if equilibrium was established. Thus, the crystallisation or recrystallisation of two feldspars in granites can result in compositions of, for example, Or_{65-75} Ab_{35-25}, or even Or_{10-15} Ab_{90-85}.

1.5.3 Alteration of primary minerals to secondary minerals

Relatively few granitic rocks remain entirely unaltered after their crystallisation. Alteration implies any changes that occur to primary magmatic minerals (quartz, feldspar, Fe-Ti oxides and ferromagnesian minerals), caused by changes in the temperature and chemical composition of the environment, possibly as a result of interaction with a fluid or with their respective host rocks. Weathering is excluded from this definition.

Types of alteration associated with granitic rocks are summarised by Clarke (1992). The temperature of alteration decreases from type (1), which occurs at high temperatures, towards type (9), which occurs at near-surface temperatures:

(1) Potassic alteration. Secondary potash-rich minerals appear: at high temperatures plagioclase is replaced by secondary alkali feldspar, and, hornblende is replaced by biotite.

(2) Sodic albitization. Secondary albite appears: plagioclase is replaced by albite and K-feldspar is replaced by albite.

(3) Episyenitisation desilicification. The silica content of the rock decreases with or without the formation of secondary feldspar.

(4) Phyllic sericitisation or greisenisation. White mica appears: feldspar is replaced by white mica or topaz, and biotite is replaced by muscovite + rutile + quartz.

(5) Argillic. Clay minerals appear: plagioclase is replaced by kaolin + sericite and ferromagnesian minerals are replaced by montmorillonite + sericite.

(6) Advanced argillic desilicification. Formation of non-silicates: removal of silica from the rock and formation of pyrophyllite, diaspore and corundum

(T > 50°C).

(7) Silicification. Silica content of the rock increases: secondary quartz is introduced.

(8) Propylitic chloritisation. Formation of chlorite: ferromagnesian minerals change to chlorite + epidote.

(9) Supergene oxidation and dissolution of sulphides: Formation of gossans at surface conditions and temperatures.

The degree of alteration depends on the type and origin of the fluid that reacts with the granite. Epizonal (high level) granites which are emplaced into permeable upper crustal country-rocks are the most likely to be altered by reaction with large amounts of meteoric water in short-lived hydrothermal systems (Taylor, 1974). In contrast, fluids responsible for the alteration of mesozonal (mid crustal) granites may be metamorphic in origin (for example, Ferry, 1985).

In altered epizonal granites, the two types of feldspars show a large departure from chemical equilibrium with each other, and quartz and feldspar also show departure from oxygen isotope (exchange) equilibrium because shallow hydrothermal events are short-lived and consequently isotopic and chemical exchange reactions among minerals do not proceed to equilibrium (Ferry, 1985). In contrast, mesozonal granites show a close approach to chemical and isotopic equilibrium, because of long-lived interaction with fluids (Ferry, 1985).

During hydrothermal activity associated with epizonal granites, the chemical and isotopic compositions of some minerals are completely changed, whereas others are partially changed or not changed at all. In contrast, in long-lived systems, the fluid may change most or all of the

minerals (Ferry, 1985).

By using oxygen isotope compositions of quartz and feldspar from epizonal and mesozonal granites, Ferry (1985) identified how the kind of fluids can increase or decrease the isotopic compositions of the rock according to their own composition (Fig. 1.4). It is clear that the meteoric water which reacts with epizonal granites causes reductions in O-isotopic composition of both quartz and alkali feldspar, particularly the latter; whereas the metamorphic fluid which reacts with mesozonal granites causes increases in O-isotope compositions of both quartz and alkali feldspar.

Two different kinds of alteration were recognised by Ferry (1985) for Skye granites. These are:

(i) Turbidity: a process by which clear feldspar changes from having a smooth featureless surface to a surface covered with a myriad of tiny pits, with exposed fluid inclusions. Turbid feldspar has a composition that records physical conditions of hydrothermal alteration at temperatures of 350-450°C, and therefore the turbidity is a subsolidus phenomenon (Ferry, 1985).

As the turbidity is considered to be the result of reaction with water, Folk (1955) pointed out that this phenomenon is common in igneous rocks that crystallise from a hydrous magma. By using scanning and transmission electron microscopy, Guthrie and Veblen (1991) recognised two different types of turbidity in alkali feldspars from a sample from the Loch Ainort Granite of Skye: one concentrated at the rims of crystals and referred to as blackish turbid regions and characterised by the presence of relatively large fluid inclusions, the other occurring between the former region and clear cores, and referred to as reddish-brown regions and characterised by smaller fluid inclusions. In a sample from the Beinn an Dubhaich Granite, which

has near normal values of $^{18}O/^{16}O$, only feldspar with the reddish-brown regions were identified.

Therefore, two generations of turbidity were recognised by Guthrie and Veblen (1991), indicating that different kinds of fluids may be responsible for the formation of each of the types of turbidity regions: one reacting with both granites, whereas the other reacting with only the Beinn an Dubhaich Granite. Such a two-stage mechanism is supported by the difference in bulk-rock oxygen isotope compositions of the two granites, and consequently suggests that the fluid which caused the reddish-brown turbidity in feldspars is possibly different from the fluid responsible for the isotopic alteration (Guthrie and Veblen, 1991).

(ii) The formation of secondary mafic minerals, including: chloritisation of biotite with exsolution of Fe-Ti oxide; uralitisation of primary pyroxene to a fibrous mass of amphibole which usually begins along the cleavages; calcic plagioclase which may be altered to a mixture of zoisite (or epidote), calcite, and secondary white mica. Along side the alteration of primary mafic minerals to secondary mafic minerals, alkali feldspar can also altered to white mica (sericite). In general, plagioclase is more resistant to alteration processes than alkali feldspar. Quartz and primary white mica are unaffected by hydrothermal fluids, whereas amphibole usually remains unchanged or is partially altered to chlorite (Nockolds et al., 1978).

Ferry (1985) used a Turbidity Index and an Alteration Index to investigate whether the formation of turbid feldspar and other secondary mafic minerals in Skye granites was isochemical or not. [where: Turbidity Index (TX) = the volume of turbid feldspar in a sample divided by the total volume of feldspar; Alteration Index (AX) = total volume of secondary mafic minerals (chlorite and/or montmorillonite) divided by the total volume of mafic minerals (amphibole, biotite, pyroxene, olivine and

secondary mafic minerals)]. He concluded that the formation of turbid feldspar during hydrothermal alteration appears to have been isochemical, or nearly so, since there is no significant change in the K or Na contents with progressive formation of turbid feldspar. In contrast, during mineralogical alteration and the formation of secondary mafic minerals there is an increase in water content, a significant decrease in Ca and Fe, and a slight decrease in Na, with increase in Alteration Index, whereas there is no significant change in Al, Si, and Mg contents with progressive alteration.

Granitic rocks consist of anhydrous (olivine, pyroxene, plagioclase, alkali feldspar and quartz) and hydrous (mica and amphibole) minerals. The stability of these minerals is a function of temperature, water pressure, and oxygen fugacity (McBirney, 1984). However, anhydrous minerals melt at lower temperatures with increasing water pressure, whereas hydrous minerals melt at higher temperatures with decreasing water pressure.

Fig. 1.6 illustrates the stability relations of minerals in a granodiorite magma as a function of temperature and water pressure (from McBirney, 1984, Fig. 10-13). During crystallisation at high water pressures, the paragenetic sequence is: amphibole, then mica, then plagioclase, then alkali feldspar, then quartz; whereas at low water pressures the sequence is: clinopyroxene (altering to amphibole: uralite), then plagioclase and alkali feldspar (altering to mica: sericite), then quartz.

For Skye granites, coexisting clear plagioclase and alkali feldspar, and coexisting magnetite and ilmenite, record temperatures within 100°C of granitic magma crystallisation temperatures and, with the rest of the primary minerals, record almost the same oxygen fugacity within 100°C of the crystallisation temperatures of granites (Ferry, 1985). Thus, these minerals have chemical compositions which they acquired during their crystallisation from the magma, or at temperatures only slightly below their

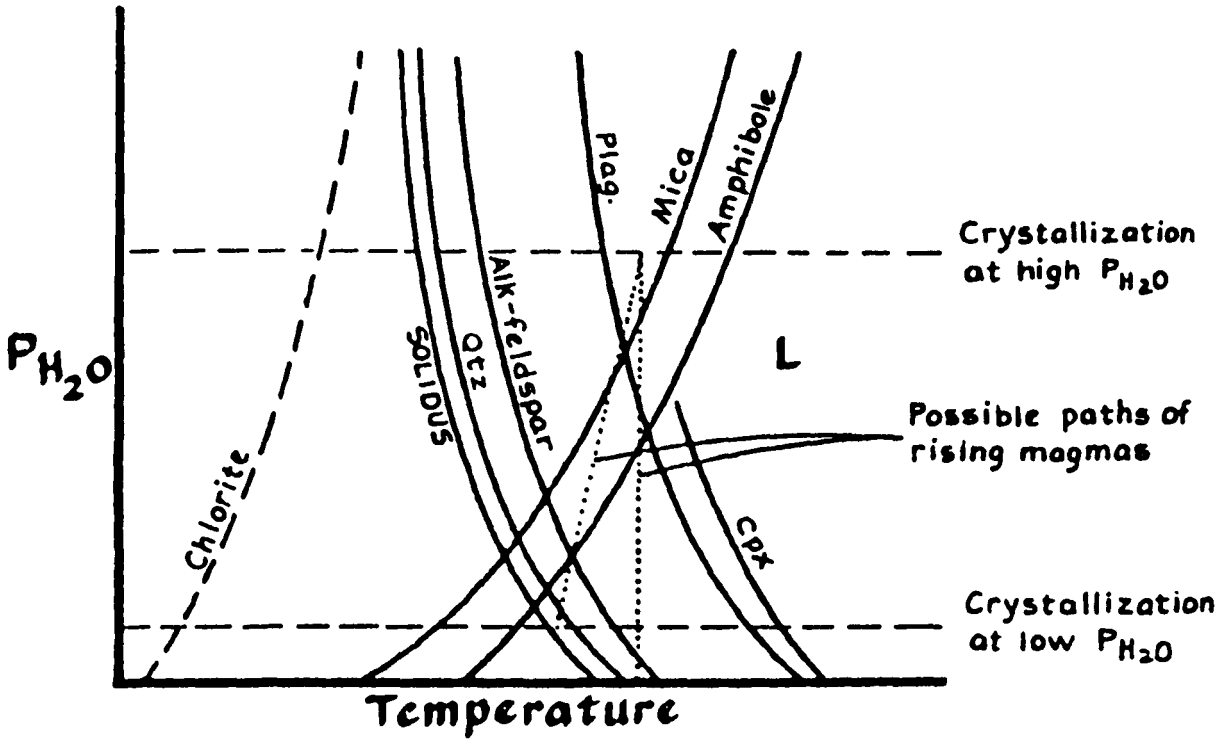

Fig. 1.6 Stability relations of minerals in a granodiorite magma as function of temperature and water pressure (after McBirney, 1984, Fig. 10-13). See text for further details.

crystallisation temperatures (Ferry, 1985). In contrast, it has been shown that coexisting turbid feldspar and secondary mafic minerals record temperatures of 350-450°C, indicating that the granites contain a subset of minerals whose chemical compositions were acquired during hydrothermal alteration processes (i.e. at temperatures of less than 450°C) (Ferry, 1985). Secondary mineral grains are often smaller in size than the primary crystals which they partially or wholly replace. However, there may be no detectable differences between the compositions of unaltered and partially altered minerals in the same specimen (Ferry, 1985).

CHAPTER II

Granites of the Skye Intrusive Centre: An outline of their field relationships and a summary of previous studies

2.1 Introduction

This Chapter is concerned mainly with the location and field relationships of the Skye Intrusive Centre in general, and a more detailed account of the granite centres. A summary of previous studies is presented, including possible origins of the magma(s).

2.2 Location, age and field relationships

The British Tertiary Volcanic Province (BTVP) is one of several regions around the North Atlantic where extrusive and intrusive magmatism occurred during the Palaeocene caused possibly by the uprise of a narrow, hot, mantle plume, centred near East Greenland, which spread laterally beneath the overlying plate to form a mushroom-shaped dome (Emeleus, 1989) (Fig. 2.1).

The intrusive complex on the Isle of Skye is part of the BTVP and has been the subject of much research over the past 150 years.

Initial investigations by Macculloch (1819), Von Oeynhausen and Von Dechen (1829) and Forbes (1845), established the igneous origin of the rocks in central Skye.

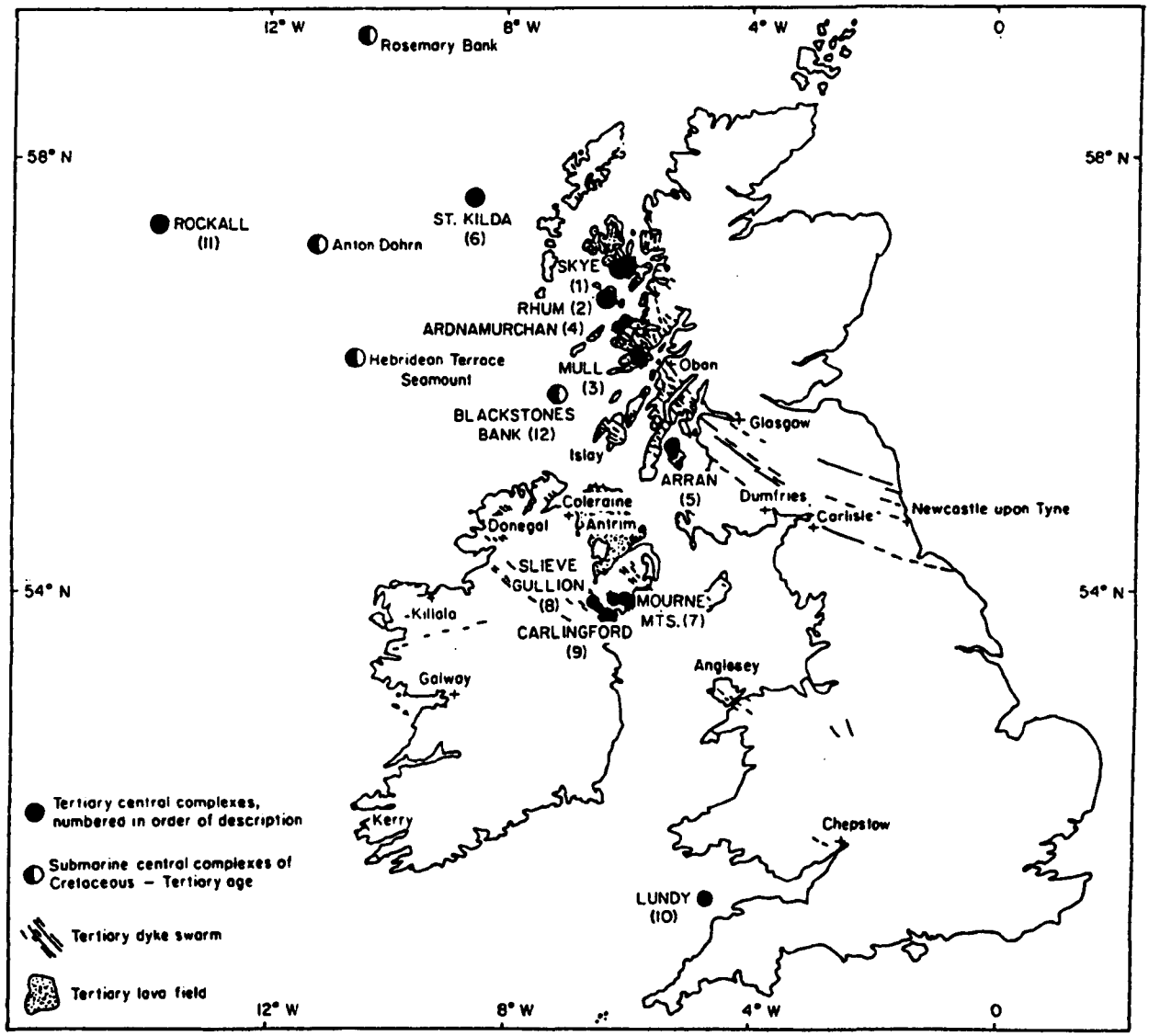

Fig. 2.1 Map illustrating the distribution of British Tertiary central complexes and submarine central complexes, along with Tertiary dyke swarms and lava fields (after Emeleus, 1982).

Subsequently, studies were carried out by Judd (1874), Geikie (1897) and Harker (1904) on the field relationships of the igneous complex and surrounding lava field of central Skye. Harker (1904) proposed that the granite intrusions were either boss-like or laccolithic in form.

Fig. 2. 2 illustrates the geology of the Isle of Skye. The island is composed of three distinctive geological parts, as follows:

(i) The south-east part, which is composed of Lewisian gneiss, Torridonian sandstone, Moine Schists and Cambro-Ordovician sedimentary rocks. Their field relationships are controlled by the Lower Palaeozoic Moine Thrust Belt.

(ii) The north of the island, including Trotternish, Waternish and Duirinish, separated from each other by large sea-lochs such as Loch Dunvegan and Loch Snizort (Fig. 2.2), consists of Palaeocene plateau lavas, with underlying Jurassic sedimentary rocks intruded by a Palaeocene sill complex along the east coast. All lithologies dip gently toward the west. The plateau lavas are dominated by basalts and hawaiites.

(iii) The central part of the island is composed mainly of Palaeocene intrusive rocks, which are younger than the plateau lavas of north Skye. This area contains the Cuillin Hills which are composed mainly of basic and ultrabasic rocks, typified by gabbros, and the younger Redhills, composed of granitic rocks and exhibiting a more rounded topography, lying to the north and east of the Cuillin Hills.

The distribution of the Cuillin Igneous Complex and the three younger Redhills granite centres is shown in Fig. 2. 3.

The earliest centre consists of various ultrabasic and basic ring intrusions of the Cuillin Igneous Complex. The Cuillin Igneous Complex is post-dated by the

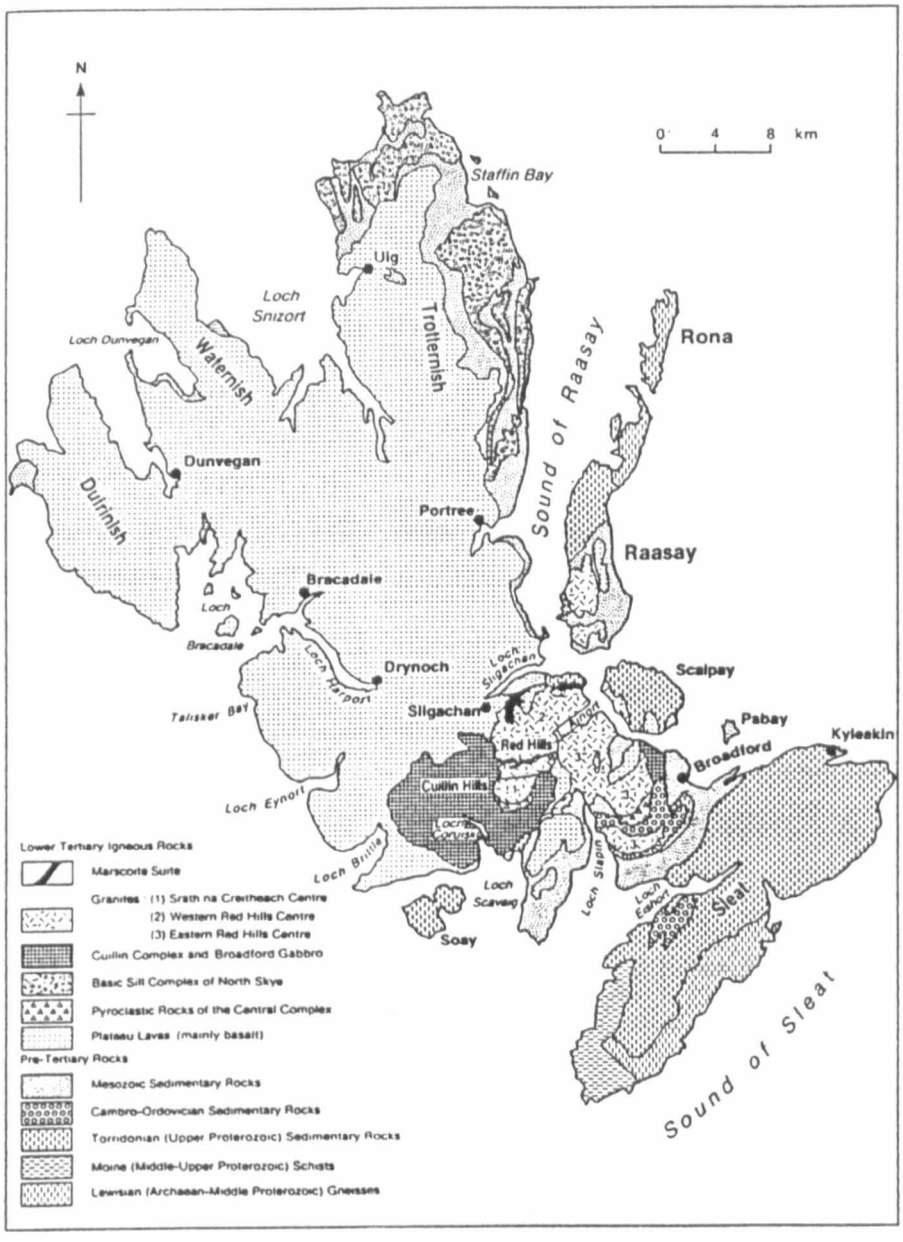

Fig. 2.2 Geological map of the Isle of Skye (after Bell and Harris, 1986).

granites of the small Srath na Creitheach Centre, and by the later Western Redhills Centre. The Eastern Redhills Centre is the youngest granitic centre.

The Cuillin Igneous Complex contains a few silicic intrusions, the most important of which is the Coire Uaigneich Granite, which was emplaced before all of the main Skye granites (Emeleus, 1982).

The sequence of granite intrusions in the four centres on Skye has been summarised from Bell (1976). From oldest to youngest these are as follows:

A-CUILLIN COMPLEX:
Coire Uaigneich (and other minor granites).
B-SRATH NA CREITHEACH CENTRE:
1-Ruadh Stac ; 2-Meall Dearg;
3-Blaven .
C-WESTERN RED HILLS CENTRE:
1-Glamaig; 2-Maol na Gainmhich;
3-Eas Mor; 4-Beinn Dearg Mhor;
5-Loch Ainort; 6-Glen Sligachan;
7-Southern Porphyritic (Felsite); 8-Southern Porphyritic;
9-(Marscoite Suite;) 10-Meall Buidhe granite;
11-Marsco .
D-EASTERN RED HILLS CENTRE:
1-Glas Bheinn Mhor; 2-Beinn na Cro;
3-Allt Fearna; 4-Beinn An Dubhaich;
5-Beinn na Caillich; 6-Creag Strollamus.

As the scope of this study is restricted to the granite centres on Skye, the following aspects of the geology are important:

First, the Srath na Creitheach Centre is the oldest of all the granite centres, and contains the smallest number of distinct intrusions. The three intrusions are (from oldest to youngest) Ruadh Stac, Meall Dearg, and Blaven. This centre is located at the southern end of Glen Sligachan, and extends below the gabbros

of the Cuillin Igneous Complex on the north-west side of Blaven. Emeleus (1982) believes that the Meall Dearg intrusion is the youngest, located along the northern edge of the centre.

The absence of cone-sheets in these intrusions is an indication of their formation after the Cuillin Igneous Complex, whereas the truncation of the Meall Dearg Granite by the Marsco Granite (of the Western Redhills), indicates that they pre-date the Western Redhills granites (Bell, 1976).

Second, the younger Western Redhills Centre was emplaced. Many studies have been carried out on these rocks by, for example, Wager & Vincent (1962), Wager, et al. (1965), Bell (1966, 1976) and Thompson (1969, 1980, 1982).

The Western Redhills Centre lies further to the north (Fig. 2.3), and is composed of twelve distinct granitic intrusions, mostly ring-shaped. The order of intrusion has been listed above. The Marscoite Suite has the form of a discontinuous composite ring-dyke, comprising an acidic member (the Southern Porphyritic Felsite), a basic member (ferrodiorite) and a mixed magma member (marscoite) (Wager et al., 1965).

Third, the Eastern Redhills, the last granite centre in the Skye Intrusive Centre, which is located to the west of Broadford in three fairly isolated groups of intrusions (Fig. 2.3). Their younger age is demonstrated as the Glas Bheinn Mhor Granite cuts across members of the Western Redhills Centre between Loch Ainort and Belig (Fig. 2.3), (Emeleus, 1982). Several authors have presented data on the mineralogy and structure of the Beinn an Dubhaich Granite (King, 1960; Tuttle and Keith, 1954; Tuttle and Bowen, 1958; Nicholson, 1970), but no great attention has been paid towards the nature of the centre as a whole and the age relationships of their components. The Beinn an Dubhaich Granite is believed to be one of the youngest intrusions and was emplaced

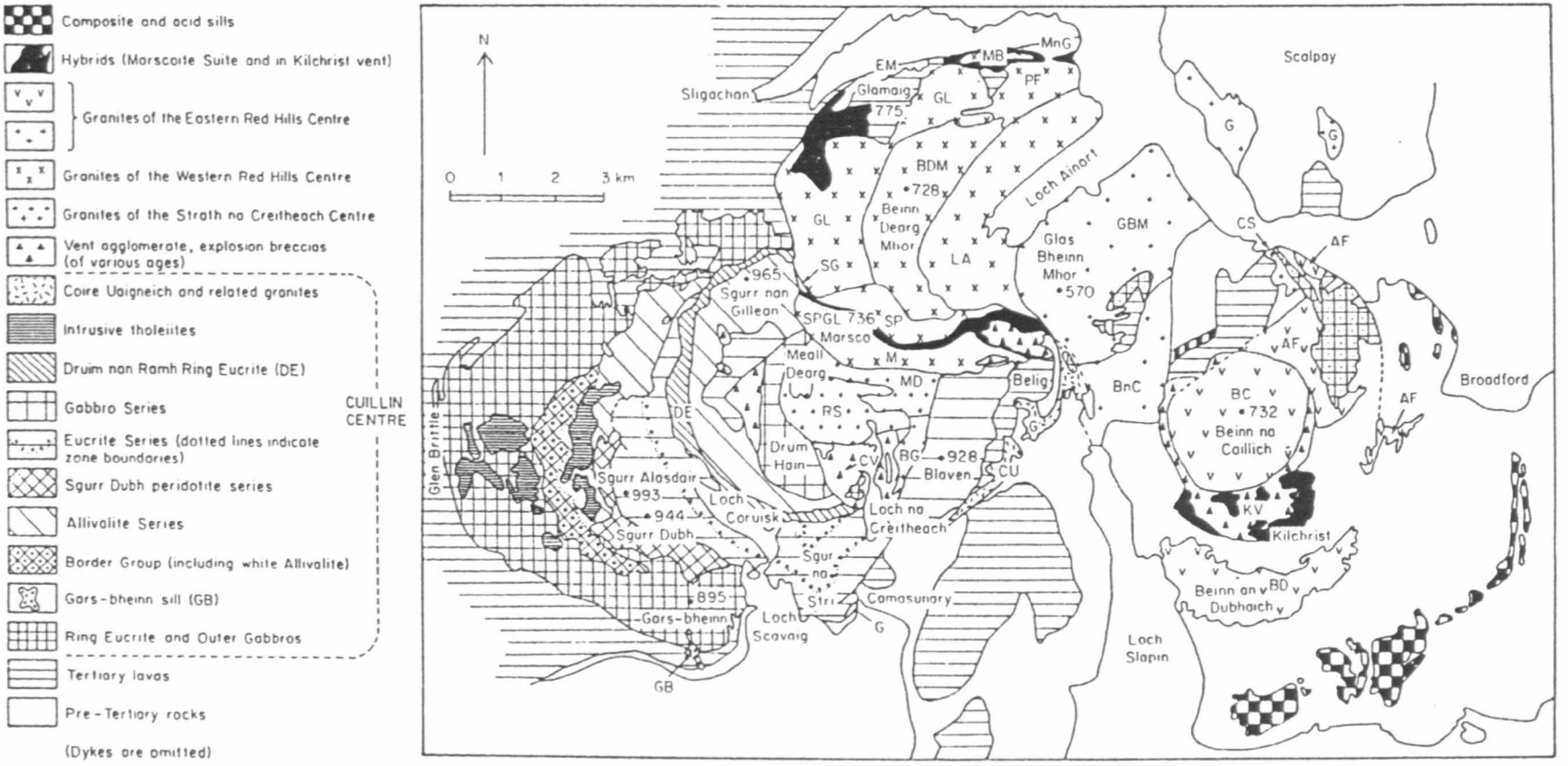

Fig. 2.3 Geological sketch map of the Skye Intrusive Centre. (after Bell, 1976; Emeleus, 1982).

wholly within Cambro-Ordovician limestones (Emeleus, 1982). Harker (1904) considers this granite as being boss-like, but later King (1960) argued strongly that it is a sheet overlying the limestones. The Beinn na Caillich Granite to the north, appears to be the youngest granite of the Centre and is emplaced into various pyroclastic deposits (Emeleus, 1982).

The following paragraphs outline more details on the age and field relationships of the Glamaig, Loch Ainort, Marsco and Beinn an Dubhaich granites, since more attention is paid to these intrusions in later chapters in terms of their mineralogy, mineral chemistry and isotopic characteristics as they cover the compositional spectrum of Skye granites. The following review is summarised from Harker (1904), Richey et al. (1946, 1947), Bell (1966, 1976), Thompson (1969, 1980) and Bell and Harris (1986):

(i) The Glamaig Granite was first defined by Richey et al. (1946) and described in detail by Wager et al. (1965). The presence of mafic inclusions (up to 5 vol.% of the rock) have been interpreted by Thompson (1980) as due to the injection of basic magma into the base of a magma chamber dominated by acid magma. The contact of the Glamaig Granite with the Cuillin Igneous Complex is in part tectonic, with sub-vertical crush planes, and is similar to its other main contact with the younger Beinn Dearg Mhor Granite.

(ii) The Loch Ainort Granite crops out on to the east of the Beinn Dearg Mhor Granite around the head of Loch Ainort, between Maol Ban in the north, and Coire Choinnich in the south, and in plan is approximately L-shaped. The boundary of this intrusion with all adjacent rocks is complicated by crushing, apart from the eastern margin which is truncated by the first intrusion of Eastern Redhills Centre (Glas Bheinn Mhor). Its similarity in many respects to the Beinn Dearg Mhor Granite, and the discovery of a zone of strong crushing

along the shallow valley between Druim nan Cleochd and Leathad Chrithin, lead Bell (1966) to conclude that the two intrusions are spatially, temporally and compositionally closely related.

(iii) The Marsco Granite forms the lower southern and western parts of Marsco in Glen Sligachan and extends eastwards as far as Belig. This intrusion is in contact along its northern margin with the older Marscoite Suite: these time relationships are suggested by rare veins of Marsco Granite which penetrate the ferrodiorite of the Marscoite Suite, and by occasional disruption of the ferrodiorite by the Marsco Granite along their contact (Bell and Harris, 1986).

(iv) The Beinn an Dubhaich Granite is the most studied granite in the Eastern Redhills, and occupies an area of about 3 km^2. This granite is wholly intruded into a broad anticline of Cambro-Ordovician limestones and contains numerous enclosures of these country-rocks (Bell and Harris, 1986). The limestones have been metamorphosed up to olivine grade (Hoersch, 1981). The intrusion is considered to be a steep-sided mass by several authors (for example, Harker, 1904; Stewart, 1965; Bell, 1982) but as a sheet-like structure by others (for example, King 1960; Whitten, 1961).

2 .3 Previous studies

2 .3 .1 Harker (1904)

Skye was the first of the Scottish Tertiary igneous centres to be investigated by the Geological Survey (Bell 1966). The survey was undertaken by Alfred Harker during field seasons from 1895-1901. His conclusions were published in 1904.

From Harker's study, the following summary can be made:

The granitic rocks of Skye occur over an area almost equal to, or exceeding, that occupied by the gabbro of the Cullin Hills, and have the general form of a large irregular laccolith, dipping towards the south. The granite intrusions which form the Eastern Redhills are considered as representing a distinct intrusive centre and having boss-like forms (e.g. the Beinn an Dubhaich Granite).

In some places, at the margins of the granites, the rocks become fine-grained and felsitic, sometimes with visible spherulites, although sometimes a relatively coarse granophyre occurs up to the actual margin. These differences Harker attributed to the varying habits of the intrusions: (i) the sheet-like or laccolithic habit giving the fine-grained lithologies; or (ii) the boss-like habit where fine-grained margins are absent.

Where the sheet-like habit (i) breaks down or becomes very irregular, as for example in the Camasunary district, there is little or no chill facies, but if the magma was intruded strictly in the sheet-like form following bedding or other planar surfaces, there is typically a marginal chill facies.

The boss-like form(s) (ii), as in the Beinn an Dubhaich and other Eastern Redhills granites, has in general little or no development of marginal chill facies.

In terms of whole-rock compositions the (British Tertiary) granites fall into two groups:

(i) A group with silica contents between 75-77wt.%, and with biotite as the only ferromagnesian mineral. This group is represented in Skye only by the Beinn an Dubhaich Granite.

(ii) A group with silica contents of 70-72wt.%, and containing hornblende and augite. This group includes most Skye granites.

Two feldspars are typically present, a plagioclase and orthoclase. Turbidity occurs in many of the feldspars and is widely distributed. Quartz occurs either in rather rounded irregular grains or enclosed in orthoclase , and sometimes in an intimate intergrowth with alkali feldspar. Augite occurs mainly in roughly euhedral crystals, and in some intrusions is present in two rather different habits, which may indicate two distinct generations. Hornblende is similar to augite, and occasionally shows two distinct habits, and is always untwinned. Biotite in Skye granites occurs in flakes of deep brown colour, and decomposes to chlorite and epidote. The Fe-Ti oxide seems to be always magnetite, and occurs only in a quite subordinate quantity, associated with augites.

Accessory minerals are sphene, which is mainly associated with hornblende, and is concentrated in the granitoid rather than the granophyric varieties. Apatite occurs as needles usually enclosed by other minerals, among them quartz. Zircon is present as well-shaped crystals, but less widely distributed, and allanite is occasionally present as brown untwinned single crystals with strong pleochroism.

Quartz has tended to crystallise before the alkali feldspar, but often the two minerals have formed almost simultaneously, to produce granophyric textures. Spherulitic texture is not found in the Skye granites, except within marginal facies.

Two different hypotheses were examined by Harker concerning the origin of Skye granites:

(i) A single early event which produced acid magma from the differentiation of a basic magma;

(ii) The repeated production of acid magma from the differentiation of basic magmas throughout the igneous episode.

Harker (1904) concludes that the former mechanism is more likely, based upon the repeated and varied associations of acid rocks throughout the lava field and intrusive complexes on Skye.

2 .3 .2 Pre-1970

After Harker (1904), a few researchers concentrated their attention towards the relationships between the granites and the Marscoite Suite, whilst some of them paid more attention to the origin of the granite magmas by using chemical data available at that time.

Richey et al. (1946) found marscoite at certain localities to be chilled against granite and concluded that the marscoite was latter than the granite. This conclusion contrasted with Harker's conclusion, who had found the inclusion of relics of marscoite within the granites at these localities, and presumed the marscoite to be earlier than the granite.

Later, McIntyre and Reynolds (1947) concluded that the marscoite is seen to be chilled against the granite and occurred as inclusions within it. However, Bailey (1947) assumed there are two generations of granite or two marscoite generations to solve this controversy. This idea were supported by Richey et al.(1947), who confirmed there were two granites of different ages involved.

The origin of the Coire Uaigneich Granite was considered by Wager et al. (1953) to be the result of the fusion of (Proterozoic) Torridonian sandstone adjacent to the basic rocks of the Cullin Igneous Complex. They supported this conclusion

by describing some relics of arkose in the main part of the intrusion , but not in the marginal chilled material.

The composition of the Coire Uaignech Granite, away from the usual eutectic-like composition of many granites, indicated to Wager et al. (1953) that its origin was by refusion of an original, quartz-rich material which did not suffer subsequent fractional crystallisation.

Experimental studies concerned with the nature of Skye granites and their recrystallisation were carried out by Tuttle and Keith (1954) and Tuttle and Bowen (1958) (see Chapter I).

King (1960) and Whitten (1961) concentrated their studies on the field relations and form of the Beinn an Dubhaich Granite, and concluded that this granite has a sheet habit, rather than the boss-like model as proposed by Harker (1904). King, in particular, observed the inclusion of marble within the granite, along with some granite tongues and dyke-like masses in the limestone.

Examining the Ab-Or-Q-H_2O system at moderate to low pressures of water vapour, Brown (1963) explained the origin of a variety of granitic rocks in Skye, all having formed at about the same time and in a similar environment, by partial melting of rocks containing a large amount of total normative alkali feldspar and quartz, with feldspar in excess of quartz, and feldspar being relatively rich in potassium.

A detailed study of the Marscoite Suite of rocks, and other granitic rocks related to it, by Wager et al. (1965), lead them to reject the conclusion by Harker (1904), in which he suggested that the time of marscoite emplacement was between the early stage of basic intrusions and the later stage of acidic intrusions. Wager et al. (1965) agreed with McIntyre and Reynolds (1946) and

Richey et al.(1947), by distinguishing two separate acid intrusions. Marscoite is chilled against one, which it post-dates , and occurs as inclusions in the other, which it pre-dates.

	A	B	C	D	E
SiO_2	76.41	54.18	61.96	60.07	60.85
Al_2O_3	11.71	13.74	13.03	14.22	13.13
Fe_2O_3	1.68	1.88	1.81	3.71	1.82
FeO	0.77	10.79	7.28	6.65	7.78
MgO	0.17	2.42	1.63	1.39	1.74
CaO	0.42	6.34	4.27	4.35	4.57
Na_2O	3.62	3.46	3.52	4.02	3.51
K_2O	4.92	1.85	2.93	2.75	2.78
MnO	0.002	0.3	0.2	0.26	0.211
TiO_2	0.14	1.97	1.33	1.53	1.42
P_2O_5	0.04	1.30	0.86	0.60	0.92
H_2O+	0.50	1.40	1.09	0.67	1.13

Table 2.1 Analysed and calculated chemical compositions of marscoite (after Wager et al., 1965), where: **A**, Southern Porphyritic Felsite (SPF); **B**, Ferrodiorite; **C**, Composition of mixture of 35% SPF and 65% ferrodiorite; **D**, Analysed marscoite; and **E**, Composition of mixture of 30% SPF and 70% ferrodiorite.

The origin of marscoite was identified to be a mixture of ferrodiorite and Southern Porphyritic Felsite, by using the composition of ferrodiorite, Southern Porphyritic Felsite and marscoite as indicated in Table 2. 1. A graphical representation of the data given in Table 2. 1 is presented in Fig. 2. 4.

Wager et al. (1965) also noted that the acidic rocks of the the Western Redhills Centre vary in texture from granitic to granophyric to felsitic. Other distinguishing features include miarolitic cavities, the absence of pegmatites and rare aplites. These textural characteristics are typical of crystallisation at a high crustal level, under a low hydrostatic pressure.

By using strontium isotopic abundance data Moorbath and Bell (1965) investigated the origin of Skye granites. The following summary is made from their study:

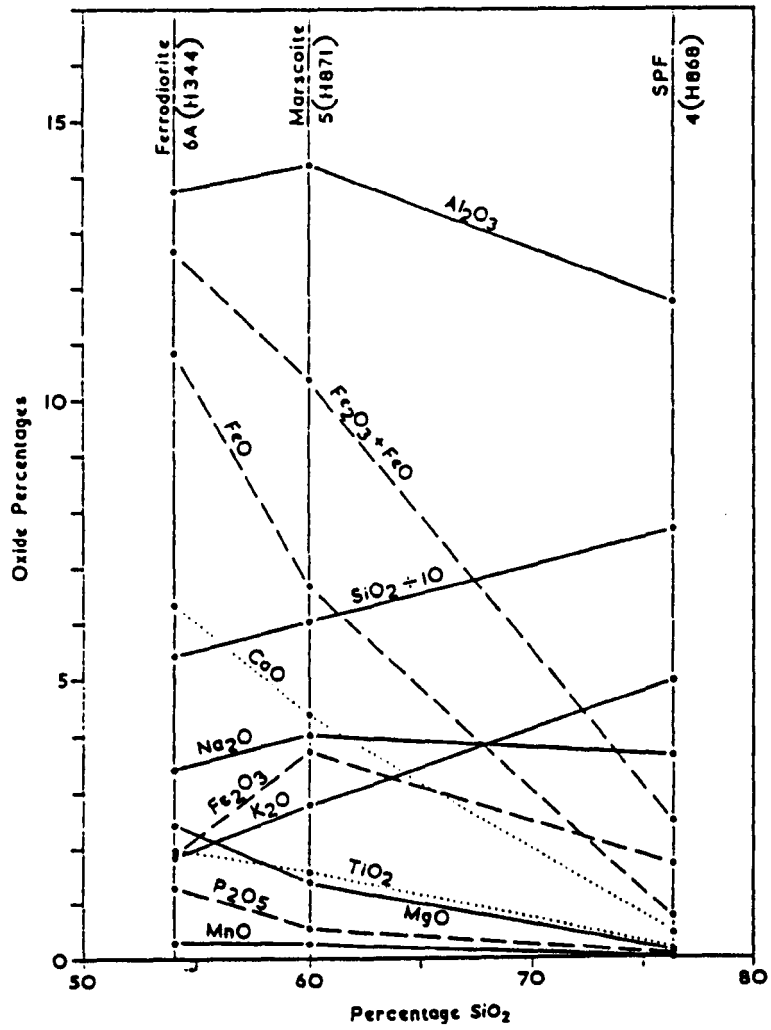

Fig. 2.4 Variation diagram, with wt.% silica against wt.% of all other oxides, for marscoite and the Southern Porphyritic Felsite. Data from Table 2.1 (both data and diagram after Wager et al., 1965).

Twelve basalts, dolerites, gabbros and peridotites, give an average ($^{87}Sr/^{86}Sr$) initial value of 0.7058 ± 0.0010. Three granites from the Western Redhills Centre give an average ($^{87}Sr/^{86}Sr$)initial value of 0.7115 ± 0.0011. One granite from the Eastern Redhills Centre gives a ($^{87}Sr/^{86}Sr$)initial value of 0.7137 ± 0.0010. Ferrodiorite and the hybrid rock marscoite give an average ($^{87}Sr/^{86}Sr$)initial value of 0.7126 ± 0.0008, whereas the Southern Porphyritic Felsite from the Marscoite Suite yielded a ($^{87}Sr/^{86}Sr$)initial value of 0.7213 ±0.0020.

From these isotopic data, Moorbath and Bell (1965), concluded that both the granites and the rocks of the Marscoite Suite all have significantly higher ($^{87}Sr/^{86}Sr$)initial ratios than those of the basalt and related rocks, and were derived from a source with a higher Rb/Sr ratio than that of the basalt.

These isotopic data support the hypothesis that the granites and members of the Marscoite Suite originated by partial melting of the underlying (Archaean) Lewisian Gneiss basement complex, and contradicts the hypothesis of crystal fractionation of basaltic magma for the origin of the granites and the Marscoite Suite.

Moorbath and Bell (1965) assumed that the heat required for partial melting of the basement rocks to produce the granite magma was provided by basic plutonic intrusions in the crust during the Palaeocene igneous episode.

Bell (1966) described the Skye granites as high-level granophyric intrusions, with different types of feldspar phenocrysts which have different optical and chemical characteristics, and which he used as an indication of high temperature modifications.

Since the Skye granites plot in the K-feldspar field in the system Ab-Or-SiO_2-H_2O, (Brown, 1963), and fractional crystallisation or melting of basalts

produces liquid either in the Ab-Q region or in the Ab field, then the formation of the Skye granites by partial melting of underlying basement gneiss appears reasonable, and the heat necessary for this process could have been provided by the abundant basic magmas involved in the igneous complex (Bell, 1966).

Studies concerning the origin of Skye granitic magmas were presented and discussed by Kleeman (1965), Dunham and Thompson (1967) and Kleeman (1967). Kleeman (1965) argued strongly for the formation of granitic magmas by fractional crystallisation of basic magmas or by melting of pre-existing igneous material.

The composition of an alkali feldspar does not indicate precisely the composition of its host (i.e it is quite possible for any rock with a potassium-rich feldspar to lie in the low temperature field at P_{H2O} between 500-1000 bars (Kleeman, 1967). Kleeman (1967) concluded that it is possible that granitic rocks could form from the differentiation of contaminated basic magma which had a water pressure of about 1000 bars during cooling. Such granitic magmas would be enriched in Fe relative to Mg, and the presence of fayalite and ferrohedenbergite argue strongly for a basic parent (Kleeman, 1967).

Dunham and Thompson (1967), followed Wager et al. (1953) and Brown (1963), and concluded that the generation of the Coire Uaigneich Granite was by the fusion of Torridonian arkose at a shallow depth.

Since some Skye granites plot in the primary phase field of alkali feldspar in the Or-Ab-An-SiO_2 system, lead Dunham and Thompson (1967) to concluded that these granites cannot have been derived from the differentiation of a basic magma. Such conclusion is consistent with the studies of Brown (1963) , Moorbath and Bell (1965), and Bell (1966).

From a study of lead isotopic data, Moorbath and Welke (1969) confirmed a general parallelism between their Pb isotope results and the Sr isotope results of Moorbath and Bell (1965), based on the same samples (i.e. low radiogenic Pb and high radiogenic Sr), indicating the important role played by the underlying Lewisian Gneiss basement complex, which has low U/Pb and high Rb/Sr ratios, relative to upper mantle source regions.

As the partial melting of Lewisian Gneiss was the currently favoured hypothesis concerning the origin of Skye granites, Moorbath and Welke (1969) went along with this hypothesis, but they did not exclude the generation of the Skye granites by a combination of crystal-liquid fractionation of basic magma and the partial melting of crustal rocks.

The intrusive igneous rocks of the Marsco area of the Western Redhills Complex were studied by Thompson (1969). His study considered seven different granites in terms of textures, mineralogy and time of emplacement. By using time of emplacement, and compositional trends for four of the main Western Redhills granites, Thompson (1969) rejected the role of crystal-liquid fractionation of basic magmas to produce the granite magmas.

Similar to Brown (1963), Thompson (1969) argued by analogy with the synthetic system Ab-Or-Q-H_2O (Tuttle and Bowen, 1958) that the Skye granites were generated by partial melting of crustal rocks . Based on the composition of the rocks examined and where they plotted in the Ab-Or-Q-H_2O system, Thompson (1969) concluded that the origin of the granite magmas was by partial melting of acid Lewisian Gneiss and Torridonian arkose by variable amounts.

2.3.3 Post-1970

A significant number of geochemical studies of Skye granites have been published since 1970.

As the early work by Moorbath and Bell (1965) showed that the granitic rocks of Skye have higher Sr initial ratios than the exposed basic rocks, they adopted a partial melting hypothesis of crustal rocks for the origin of Skye granites. Subsequently, Taylor and Forester (1971) showed from a study of oxygen isotope signatures of minerals and rocks from the Skye Intrusive Centre that there has been. significant mineral-fluid reactions involving meteoric-hydrothermal convection systems. They concluded that the Skye granites might have had low Sr initial ratios at the time of emplacement, similar to those of the associated basic rocks, and that the hydrothermal solution(s) which had Sr initial ratios of about 0.721, or higher, might have been responsible for the higher Sr initial ratios of the granites, thus, the partial melting of crustal rocks hypothesis favoured by Moorbath and Bell (1965) on the basis of their strontium isotope study was questioned by Taylor and Forester (1971).

The subsequent more detailed oxygen isotope investigation by Forester and Taylor (1977) concluded that the granite quartz from Skye is depleted in ^{18}O relative to granite quartz from other igneous provinces. As there is no correlation between grain- size and the oxygen isotope signature of Skye granite quartz, and quartz is the most resistant rock-forming mineral to oxygen isotope exchange, they suggested that the significant ^{18}O depletion might be a primary igneous feature. Thus, Forester and Taylor (1977) suggested that some Skye granites formed by partial melting of hydrothermally-altered country-rocks at depth.

Due to the immobility of the rare-earth-elements (REE) during hydrothermal activity, Thorpe et al. (1977) used whole-rock REE data to investigate the origin of Skye granites. The crustal country-rocks in Skye have $(Ce/Yb)_N$= 8-18, whereas the granites have $(Ce/Yb)_N$= 3-8, and the absolute abundances of the REE in the crustal country-rocks are much lower than that in the granites (Thorpe et al., 1977). These features exclude the possibility of generating granitic melts from crustal material by partial melting processes, and suggest the formation of the granites by fractional crystallisation of different basic magmas (Thorpe et al., 1977).

A subsequent model presented by Thorpe (1978), which depends on changes in Sm_N and $(Ce/Yb)_N$ during the fractionation of different minerals, suggests that the fractional crystallisation of basic magmas is a plausible mechanism by which the granites formed.

From a consideration of the homogeneity of British Tertiary granitic intrusions, their general lack of any xenoliths, the immobility of zirconium during hydrothermal alteration, zirconium concentrations, and the differences in REE abundance between the granites and Lewisian and Torridonian country-rocks, Meighan (1979) argued strongly in favour of differentiation of basic magmas of variable compositions as a possible origin for significant amounts of granitic magmas, including the xenolith-bearing Coire Uaigneich Granite (see below).

Dickin and Exley (1981) proposed an alternative theory that the Coire Uaigneich Granite was formed by the mixing of two magmas. They identified the following geochemical characteristics:

(i) the heterogeneity of Sr initial ratios between early and later minerals; (ii) the Pb isotope composition of the intrusion, which falls within the range of Torridonian sandstone (i.e. between the composition of Torridonian sandstone

xenoliths in the intrusion and the composition of Torridonian sandstone in outcrop) and not far from a Lower Tertiary mantle composition; (iii) the presence of detrital zircons within the intrusion which are characterised by high Th,Y, and heavy REE contents compared to primary igneous zircons; (iv) the high concentration of zirconium in Torridonian sandstones compared to that in the Coire Uaigneich Granite. From these data, they concluded that the formation of the intrusion was by mixing of different magmas, one formed by partial melting of Torridonian sandstone and the other formed by the differentiation of a basaltic magma.

Dickin (1981), in his isotope study of Tertiary igneous rocks from Skye, restated his previous theory with Exley (Dickin and Exley, 1981) that the granites were formed by contamination of acid differentiates of mantle-derived parentage with partial melts of crustal rocks. The Pb isotope compositions of the Skye granites, between mantle and crustal rock compositions, the presence of granitic intrusions above older basic rocks, and the intermediate Sr initial ratios of the granites between Sr initial ratios for the Hebridean mantle and upper crustal rocks, suggests the formation of Skye granites by crustal contamination of mantle-derived components differentiated at a relatively high crustal level (Dickin, 1981).

The upper crustal contribution to the granitic melts is estimated from 5 up to 33 percent of the mass of each intrusion; this crustal fraction increases within the younger intrusions. This phenomenon suggests that the differentiating basic magma(s) which gave rise to the younger intrusions had longer times in the upper crust before their crystallisation, allowing more contamination by crustal melts. On the basis of a single source magma, this seems to be unlikely, because a batch of basaltic magma cannot be maintained in the upper crust for a long period of time (up to 7 Ma based on the age data of Dickin (1981)) without

complete crystallisation. These arguments, along with the magnetic evidence of Brown and Mussett (1976) which suggests that the Skye granites are underlain by basic plutons, led Dickin (1981) to conclude that differentiation from different basic magmas is a more likely explanation for Skye granite formation.

According to Thompson (1982), the uprise of large quantites of acid differentiates from basaltic parents into upper crustal Lewisian Gneiss, would cause partial melting of these country- rocks, and the formation of substantial amounts of acid 'partial melt' magmas. In general, the mantle-derived basic magmas upwelling beneath the BTVP were affected by fractional crystallisation and crustal contamination to varying extents as they rose through the continental crust (Thompson, 1982).

In summary, the formation of Skye granites, by contributions from both basaltic differentiates and crustal melts, was first proposed by Moorbath and Welke (1969). This model has been emphasised by, for example, Dickin (1981), Dickin and Exley (1981), and Thompson (1982). More recently, Dickin et al. (1984) favoured this model based on a study of Nd and Sr isotope compositions and suggested that the mantle material which was parental to the granites was contaminated first with lower crustal rocks, and then with upper crustal materials. The contribution of lower crustal rocks is significant in the early granite intrusions, whereas the contamination with upper crustal rocks increases with time (Dickin et al., 1984).

This evidence lead Dickin et al. (1984, 1987) to suggest the involvement of long-lived magma chamber(s) in the petrogenesis of the Skye granites. This observation is consistent with the conclusions of Dickin (1981), who suggested that the contribution of the upper crust in the granitic melts increased with time.

In conclusion, from this short review of previous studies, it is safe to conclude that most studies ensure that both mantle-derived materials and crustal components are invoked for the formation of Skye granites.

CHAPTER III

Petrography

3.1 Introduction

This chapter is concerned with the mineralogy and microscope petrography of Skye granites. Typically, the Skye granites are holocrystalline, medium-to coarse-grained, commonly with megacrysts (up to 20mm long) of euhedral alkali feldspar. The alkali feldspar megacrysts occur as both orthoclase and perthite, constituting 40-60 vol.% of each granite in a concertal texture.

Quartz and alkali feldspar commonly occur together in a micrographic or granophyric intergrowth, indicating the simultaneous crystallisation of these two minerals from a melt at the eutectic composition (Carstens, 1983). Two generations of plagioclase are observed, a slightly zoned euhedral variety and an anhedral type.

The main ferromagnesian minerals are amphibole and biotite, although pyroxene is present in a few intrusions, and olivine as a trace in some intrusions. Accessory minerals are Fe-Ti oxide, zircon, and apatite.

Due to the severe interaction between heated meteoric water and Skye granites (Ferry, 1985), as indicated from microscopic studies (i.e. the turbidity of

feldspar and presence of secondary minerals after primary minerals)(see for example, Ferry 1979), and the distribution of secondary fluid inclusions in quartz (see Chapter 5), the modal compositions of the samples have been obtained on the basis of the discrimination between primary and secondary phases.

The Turbidity Index (TX) and Alteration Index (AX) were defined by Ferry (1985) as the volume of turbid feldspar divided by the total volume of feldspar, and the total volume of secondary mafic minerals (chlorite/or clay minerals) divided by the total volume of mafic minerals (amphibole + biotite + pyroxene + olivine + secondary mafic minerals), respectively.

The most common order of crystallisation for the Skye granites examined in this study is: apatite, zircon, olivine, pyroxene, amphibole, plagioclase, biotite, alkali feldspar and quartz, although quartz and alkali feldspar have commonly crystallised at the same time producing a granophyric intergrowth. In one case biotite appears to have crystallised before amphibole (the Beinn an Dubhaich Granite).

More detailed microscopic studies have been carried out on certain selected intrusions (Beinn an Dubhaich, Loch Ainort, Marsco and Glamaig), which have been the subject of mineral chemistry (see Chapter IV) and isotope studies (see Chapters VII and VIII).

Assemblages of primary and secondary minerals and their modes are presented in Table 3.1. These data have been obtained by studying the amounts of the main minerals in each specimen by means of modal analyses (average 2,000 points).

The modal analysis data (Table 3.1) are plotted on the QAP classification triangle of Le Maitre et al. (1989) and Le Bas and Streckeisen (1991) (Fig. 3.1). The following points may be summarized:

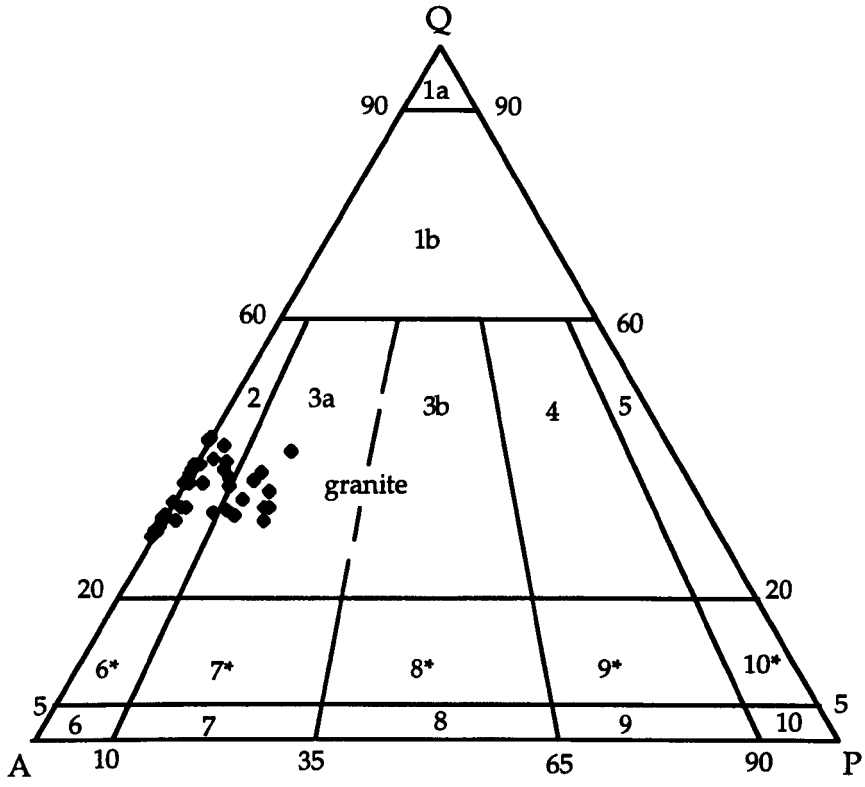

Fig.3.1 The IUGS Q-A-P ternary plot for classification and nomenclature of plutonic igneous rocks on the basis of their modal mineralogies (Le Maitre et al., 1989; Le Bas and Streckeisen, 1991). Q-quartz, A-alkali feldspar and P-plagioclase.

1a quartzolite, **1b** quartz-rich granitoids, **2** alkali feldspar granite, **3a** syenogranite, **3b** monzogranite, **4** granodiorite, **5** tonalite, **6*** quartz alkali feldspar syenite, **7*** quartz syenite, **8*** quartz monzonite, **9*** quartz monzodiorite and quartz monzogabbro, **10*** quartz diorite, quartz gabbro and quartz anorthosite, **6** alkali feldspar syenite, **7** syenite, **8** monzonite, **9** monzodiorite and monzogabbro, and **10** diorite, gabbro and anorthosite.

(i) all Skye granites are clustered in the alkali feldspar granite and syenogranite fields, reflecting the domination of alkali feldspar over plagioclase.

(ii) along with the variation in the amount of mafic minerals, there are significant variations involving the abundance of quartz, alkali feldspar and plagioclase.

(iii) most granites cannot be distinguished from each other by modal analysis, as there is considerable overlap between several analyses in the range of modal values of each mineral.

3.2 Granite Petrography

3.2.1 The Beinn an Dubhaich Granite

Six samples were examined from this intrusion, and may be summarized as follows: It is a two feldspar granite, containing about 40-50 vol.% alkali feldspar, 8-11 vol.% plagioclase, 1-9 vol.% amphibole, 28-35 vol.% quartz, and 0.2-2 vol.% biotite, together with accessory zircon and apatite and alteration products such as chlorite, epidote and muscovite after biotite and/or amphibole, plagioclase and alkali feldspar and/or plagioclase, respectively.

It is a coarse-grained, inequigranular granite, with larger crystals of both alkali feldspar and plagioclase (up to 15mm), whereas the average grain-size of the smaller crystals is 5mm. Quartz and alkali feldspar commonly occur in a micrographic intergrowth. The ferromagnesian minerals commonly occur in clots, typically enclosing early-precipitated crystals of apatite, zircon and Fe-Ti oxides.

These ferromagnesian minerals are partially or completely replaced by chlorite, whereas secondary muscovite is restricted to alkali feldspar and plagioclase

crystals, and epidote is restricted to plagioclase crystals. The main minerals are presented in **Fig. 3. 2 (i).**

Primary minerals

1-Quartz: Sub-angular to rounded, 1-5mm (occasionally up to 10 mm) across in consertal texture, characteristically concentrated in linear aggregates, suggestive of some form of recrystallisation (**Fig. 3. 2 (ii)**). Fluid inclusions trails are common, as are isolated inclusions (**Fig. 3. 2 (iii)**), both in linear and random distributions.

2-Clear alkali feldspar: Alkali feldspar occurs in the form of subhedral to euhedral prismatic crystals, on average 5-8mm across, but also up to 12mm. Clear alkali feldspar is colourless, and exhibits no chemical zoning. There are no individual complete crystals of clear alkali feldspar, although clear material is present in the cores of crystals which are partially altered to turbid alkali feldspar along their rims (Ferry, 1985) (see Secondary Minerals, below). These rims of altered alkali feldspar typically constitute 80-90 vol.% of any one crystal.

3-Clear plagioclase: Plagioclase occurs mainly in the form of euhedral to subhedral prismatic crystals, on average 3-6mm (but up to 10mm) across. Most show albite twin lamellae, and occasionally are enclosed in alkali feldspar megacrysts (**Fig. 3. 2 (iv)**). Like alkali feldspar, plagioclase becomes turbid with progressive alteration, but also is partially altered to secondary minerals such as epidote and muscovite (Ferry, 1985). Cores are commonly cracked and show signs of alteration to sericite. Typically plagioclases are mantled with clear/turbid alkali feldspar (cf. Bryon et al., 1994), and are more commonly clear in contrast to the typically turbid appearance of alkali feldspar.

4-Amphibole: Amphibole is green to pale green, and it is the main ferromagnesian mineral in this granite. Typically, it is up to 6mm across, and

Fig. 3. 2 (i) The main rock-forming minerals. Where: **A**, amphibole; **B**, biotite; **C**, alkali feldspar; **D**, plagioclase; **E**, quartz; **F**, zircon; and, **G**, Fe-Ti oxide. **Beinn an Dubhaich Granite**. Crossed-polars. Field of view: 1.25mm x 0.84mm.

Fig. 3. 2 (ii) Two sets of aggregates of quartz crystals as inclusions within an alkali feldspar crystal. Where: **A**, alkali feldspar; and, **B**, quartz. **Beinn an Dubhaich Granite**. Crossed-polars. Field of view: 1mm x 0.70mm.

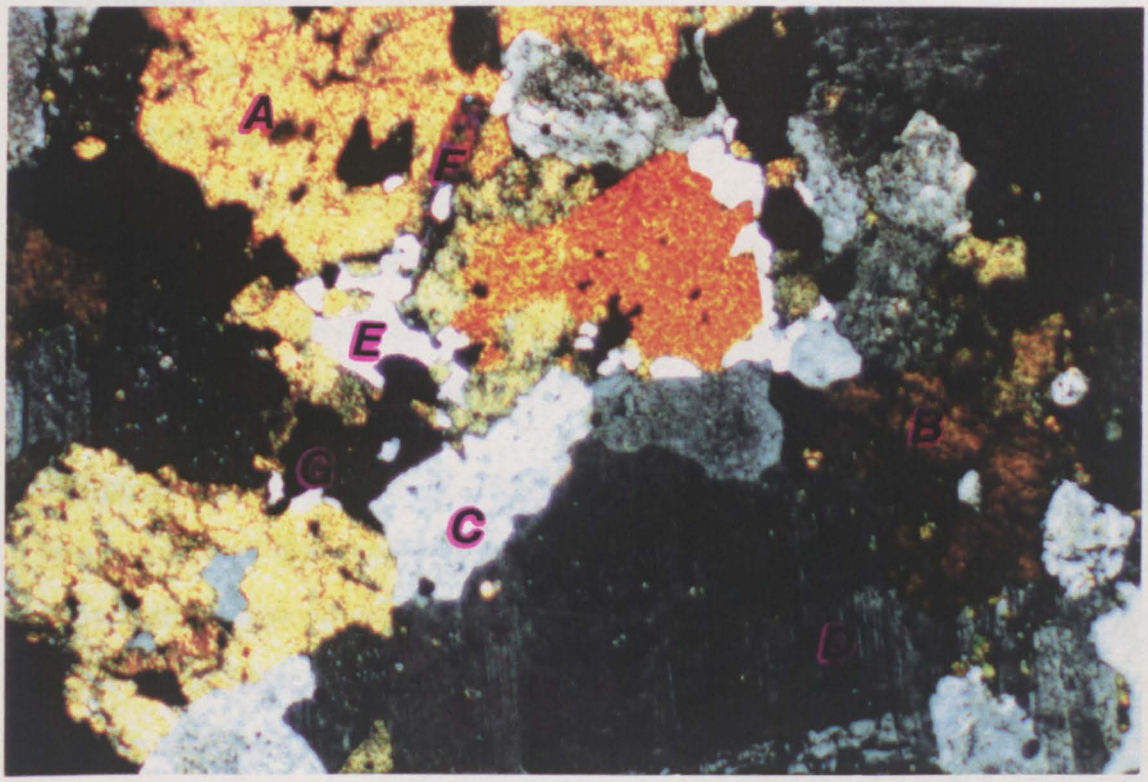
A
E
E
C
C
B
D


A
B

commonly occurs as subhedral grains in close association with crystals of biotite, Fe-Ti oxide and zircon in the form of mineral aggregates. Individual crystals of near-euhedral form are also present. There are numerous inclusions within the amphiboles, most commonly of zircon and apatite. Biotite is a common secondary mineral replacing amphibole (**Fig. 3. 2 (v)**), although the mantling of well-developed crystals of apparently primary biotite suggests that amphibole crystallisation was at least in part after biotite crystallisation.

5-Biotite: Biotite occurs in the form of subhedral-euhedral crystals, along with some anhedral flakes (i.e. as alteration products), (**Fig. 3. 2 (v)**). It occurs as brownish yellow crystals, typically associated with crystals of amphibole in mafic clots. Their average size is 0.8-2mm (but up to 3mm across). Biotite is usually fresh, with chloritisation affecting only a few flakes along cleavages (**Fig. 3. 2 (vi)**).

6-Fe-Ti oxides: This is one of the most common and ubiquitous accessory phases in the Skye granites, and occurs predominantly as subhedral to anhedral inclusions, up to 1mm across within clots of mafic minerals such as amphibole and biotite (**Fig. 3. 2 (vi)**).

7-Zircon: Whitish to colourless, similar to Fe-Ti oxide, zircon occurs within early- precipitated crystals of amphibole, and sometimes in plagioclase, in anhedral and euhedral forms. Identified magmatic zircons are up to 0.4mm across. Rarer crystals of anhedral, possibly secondary (inherited), zircons are identified by their corroded, anhedral shapes, within amphibole crystals (**Fig. 3. 2 (vii)**), suggestive of some sort of inheritance from the partial melting of crustal rocks. The relative proportion of the two identified zircon types is 2:3 (euhedral: anhedral).

8-Apatite: Apatite occurs in the form of needles up to 0.2mm long, typically within amphibole crystals, biotite crystals, plagioclase crystals (**Fig. 3. 2 (iv &**

Fig. 3. 2 (iii) Fluid inclusion distribution within a quartz crystal. Both random and linear trends are present. **Beinn an Dubhaich Granite.** Crossed-polars. Field of view: 1.25mm x 0.84mm.

Fig. 3. 2 (iv) Plagioclase crystals included within an alkali feldspar crystal. The plagioclase crystals show albite lamellae and one contains an apatite needle (A). **Beinn an Dubhaich Granite.** Crossed-polars. Field of view: 1.25mm x 0.84mm.

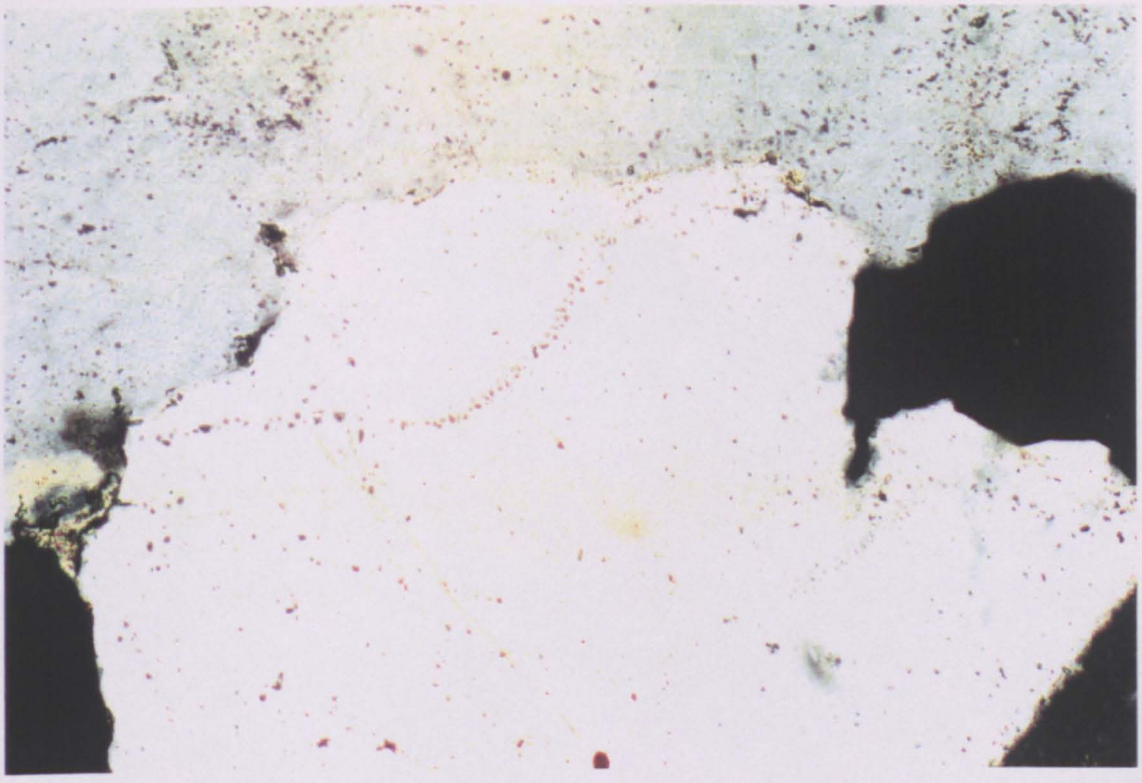

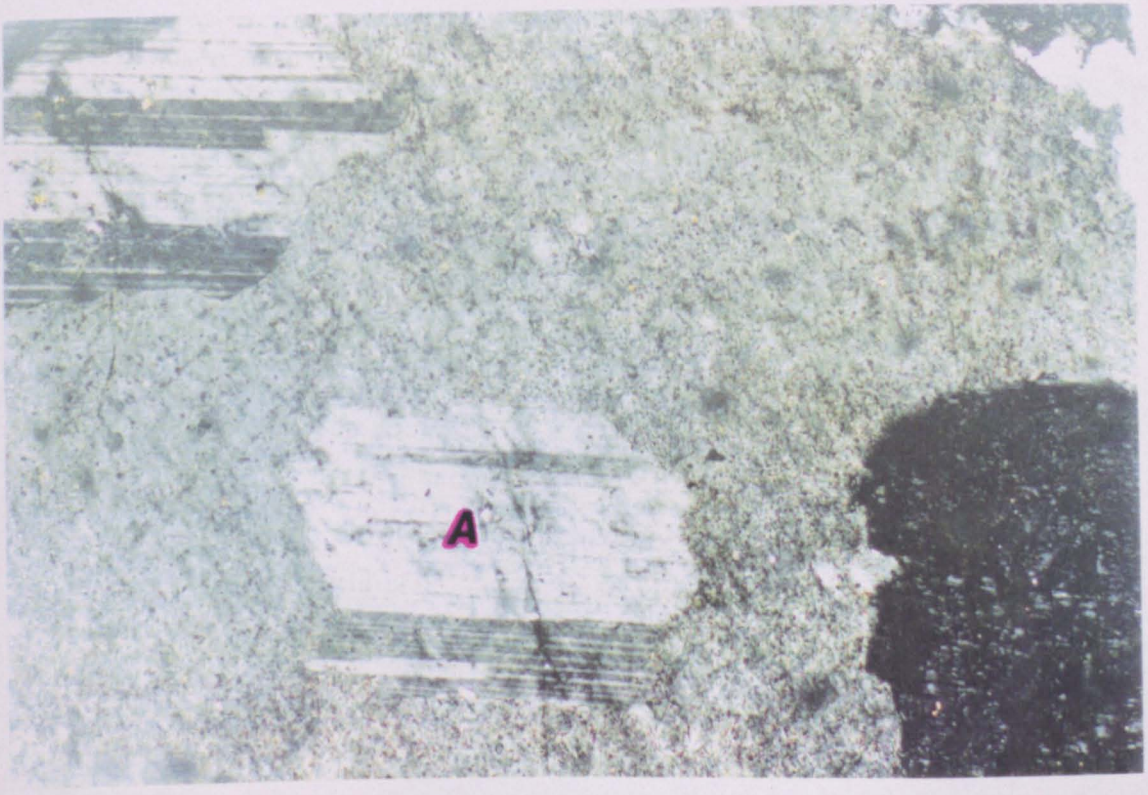
A

Fig. 3. 2 (v) A large amphibole crystal, partially replaced by secondary biotite and chlorite, and containing what appears to be primary biotite. Clear and turbid areas within the alkali feldspar crystals are also evident. Where: **A**, amphibole; **B**, alteration product of amphibole (biotite and/or chlorite); **C**, primary biotite; **D**, clear region in alkali feldspar; **E**, turbid region in alkali feldspar; **F**, plagioclase; **G**, quartz; and, **H**, Fe-Ti oxide. **Beinn an Dubhaich Granite**. Crossed-polars. Field of view: 3mm x 2mm.

Fig. 3. 2 (vi) Typical euhedral biotite grains which show some form of alteration to secondary chlorite, and contain Fe-Ti oxide and apatite as inclusions. Surrounded by other rock-forming minerals. Where: **A**, amphibole; **B**, alkali feldspar; and, **C**, quartz. **Beinn an Dubhaich Granite.** Crossed-polars. Field of view: 1.25mm x 0.84mm.

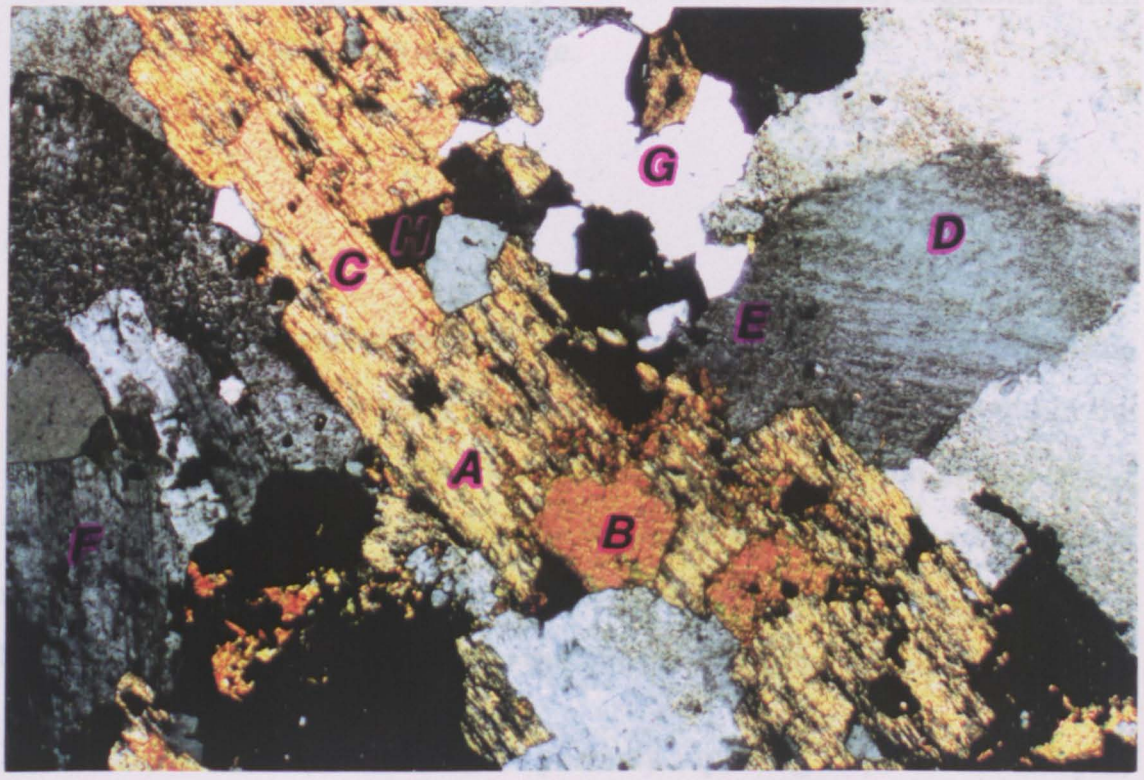
G
H
C
D
E
A
B
F

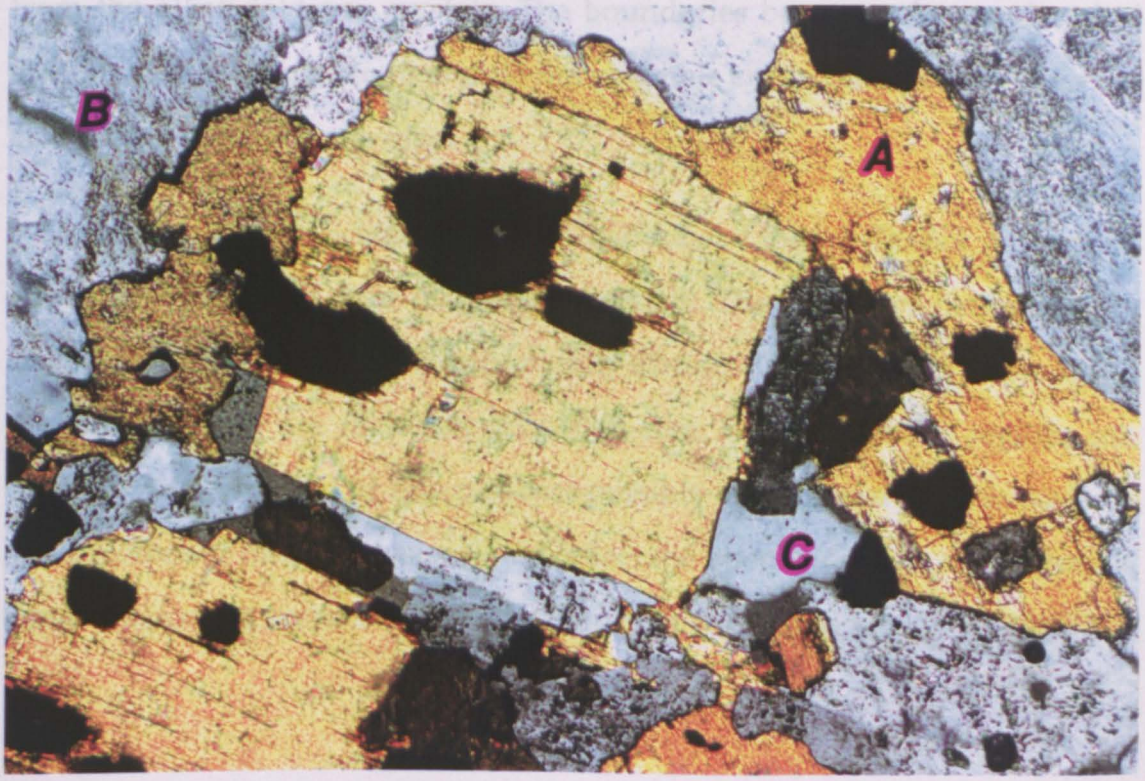
B
A
C

vi)) and, less commonly within crystals of alkali feldspar, suggesting their crystallisation at a relatively early stage.

Secondary minerals

A value of TX was computed from the data in Table 3. 1, and is within the range 0.67 to 0.78. This implies 67-78vol.% of the feldspar is turbid within the Beinn an Dubhaich Granite. In contrast, the AX values are within the range 0.11 to 0.52, which means 11-52 vol. % of the ferromagnesian minerals are altered to secondary minerals. Thus, the formation of turbid feldspar appears to have been, at least in part, independent of the formation of other secondary minerals.

1-Turbid alkali feldspar: Wholly or partially replacing clear alkali feldspar, occurs as both larger and small crystals and can be easily distinguished from coexisting plagioclase which is clearer (i.e. less altered). This turbid alkali feldspar comprises microperthites with strings of unmixed sodic feldspar (**Fig. 3. 2 (v)**). The strings of unmixed sodic feldspar are a product of late exsolution from the alkali feldspar crystals. The boundaries between clear and turbid alkali feldspar are not sharp and do not resemble crystal faces; turbid rims cut across clear cores in some cases.

2-Turbid plagioclase: Forms only a small volume of the whole rock and occurs along the margins of clear plagioclase crystals. The boundary between clear and turbid plagioclase is microstructurally distinct (Guthrie and Veblen, 1991): the clear regions are relatively inclusion-free, whereas turbid regions are covered with a myriad of tiny pits that possibly are exposed fluid inclusions. The presence of these inclusions may reflect the interaction with a fluid phase. Some plagioclase crystals are highly altered to secondary muscovite (**Fig. 3. 2 (viii)**).

Fig. 3. 2 (vii) Amphibole crystals containing anhedral zircon grains as inclusions, in close association with Fe-Ti oxide and secondary epidote. Fluid inclusions are evident in the quartz crystals. Where: **A**, amphibole; **B**, zircon; **C**, Fe-Ti oxide; **D**, quartz; **E**, epidote; and, **F**, chlorite. **Beinn an Dubhaich Granite**. Crossed-polars. Field of view: 1.25mm x 0.84mm.

Fig. 3. 2 (viii) White mica (sericite) concentrated in the core of a plagioclase crystal. **Beinn an Dubhaich Granite**. Crossed-polars. Field of view: 1mm x 0.70mm.

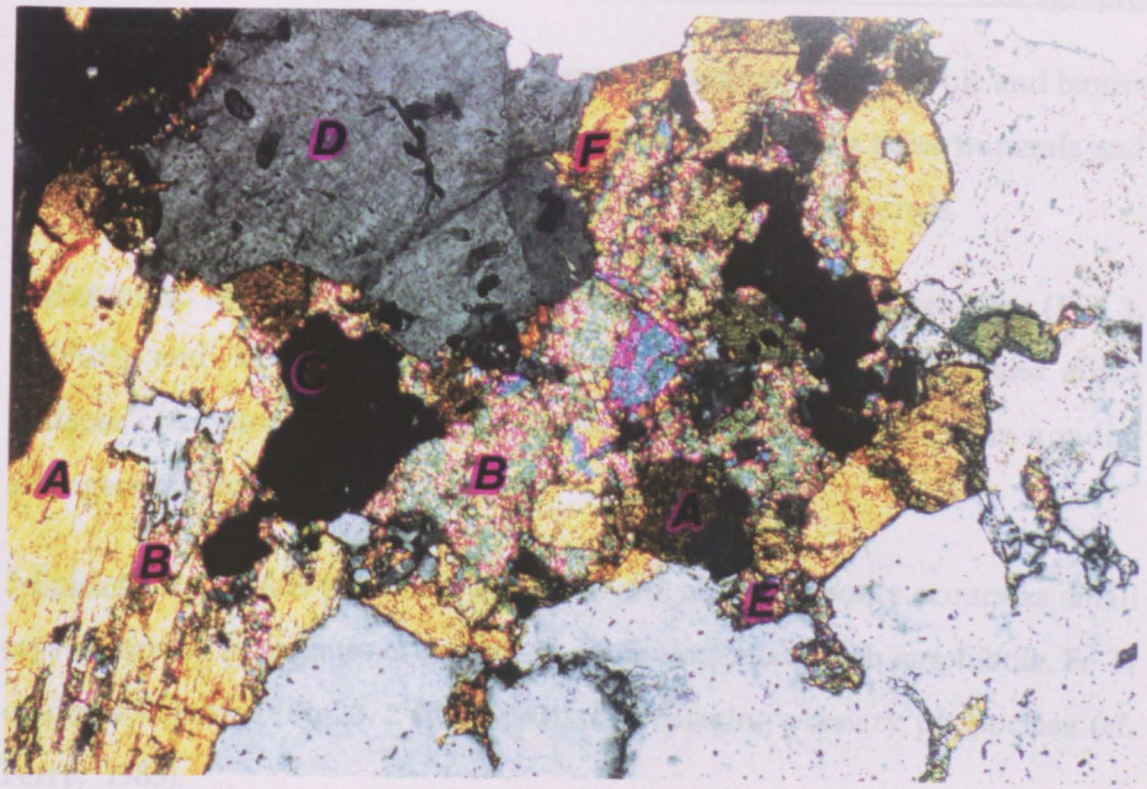
D
F
C
A
B
B
A
E

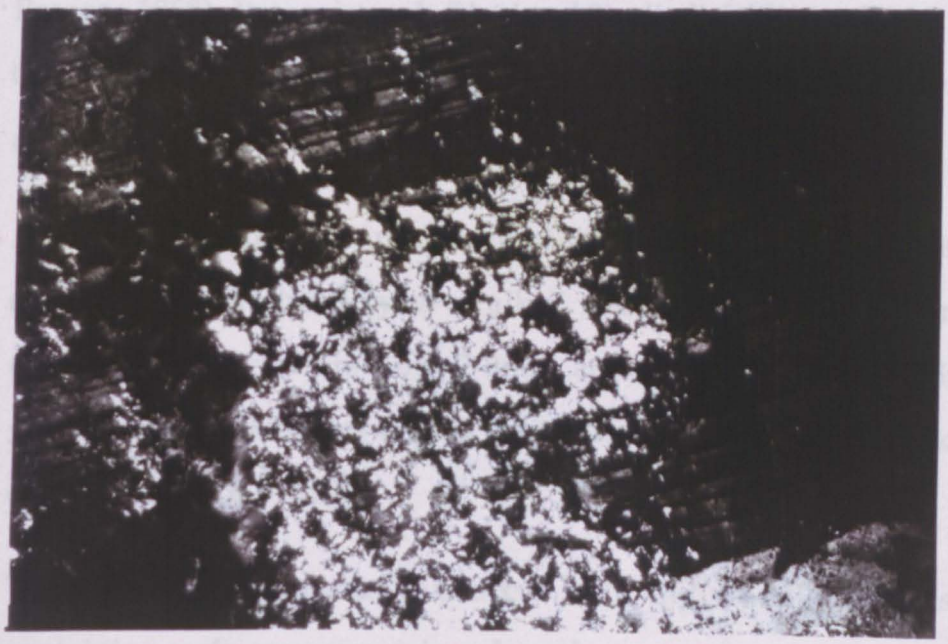

3-Chlorite: Chlorite is concentrated along the margins of amphibole and biotite crystals (**Fig. 3. 2 (vi)**), and sometimes completely replaces these minerals and takes their shape. It is typically yellowish, and up to 0.4mm across.

4-Muscovite: Muscovite is present as a sericitic alteration of plagioclase (**Fig. 3. 2 (viii)**), and as larger individual flakes, set in both plagioclase and alkali feldspar often along the elongation (cleavage) direction, as well as in a radial arrangement, up to 0.4mm across.

5-Epidote: Epidote is yellowish to pale green, and commonly occurs as small crystals and as aggregates of crystals in mafic clots along with amphibole, Fe-Ti oxides and zircon (**Fig. 3. 2 (vii)**), partially replacing primary plagioclase (cf. Ferry, 1985).

3.2.2 The Loch Ainort Granite

A hypersolvus granite with a single feldspar, except a few plagioclase lamellae as a component of perthites representing less than (0.25 vol.%) (Tuttle & Bowen, 1958). It consists of 54-64 vol.% alkali feldspar, 27-32 vol.% quartz, 0.25-3.75 vol.% pyroxene, 0-7 vol.% amphibole, and 0-3 vol.% biotite. Zircon, along with rare apatite, are present as accessory minerals.

An inequigranular (i.e. porphyritic) granite, most crystals are anhedral to subhedral, with phenocrysts of alkali feldspar up to 20mm across, whereas quartz phenocrysts are only 7-8mm across. The average grain-size of the groundmass is 0.5-2mm (**Fig. 3. 3 (i)**). Granophyric and graphic textures are common (**Fig. 3. 3 (ii)**).

The ferromagnesian minerals occur both individually and as aggregates, containing early accessory minerals such as apatite and zircon. Modal data are presented in Table 3.1.

Fig. 3. 3 (i) Alkali feldspar phenocryst (**A**) set in a fine-grained matrix of quartz, alkali feldspar, amphibole, pyroxene and Fe-Ti oxide. Where: **B**, alkali feldspar; **C**, quartz; **D**, amphibole; **E**, pyroxene; **F**, Fe-Ti oxide; **G**, secondary white mica; and, **H**, chlorite partially replacing pyroxene. **Loch Ainort Granite**. Crossed-polars. Field of view: 3mm x 2mm.

Fig. 3. 3 (ii) Typical granophyric intergrowth around alkali feldspar phenocrysts. This intergrowth is coarser away from the phenocrysts (see text for further discussion). Where: **A**, alkali feldspar phenocryst; **B** & **C**, alkali feldspar and quartz patches, respectively; **D**, quartz; and, **F**, amphibole. **Loch Ainort Granite**. Crossed-polars. Field of view: 3mm x 2mm.

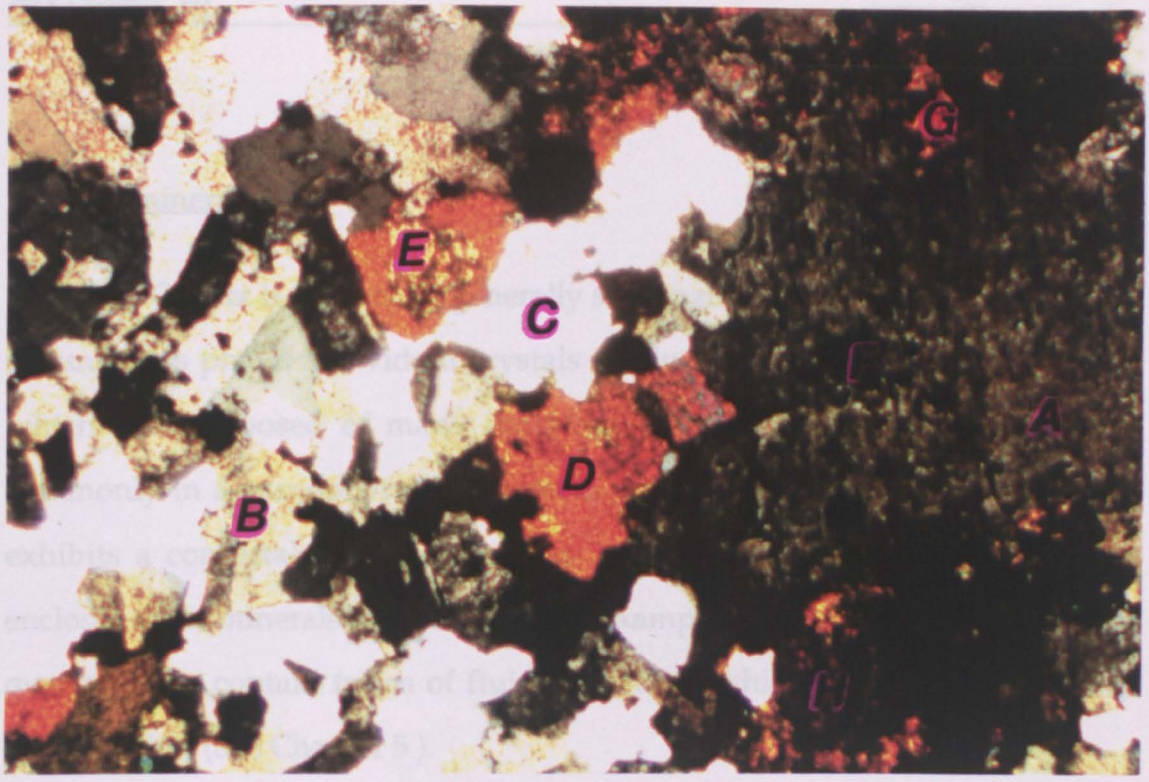
G
E
C
F
A
D
B
C

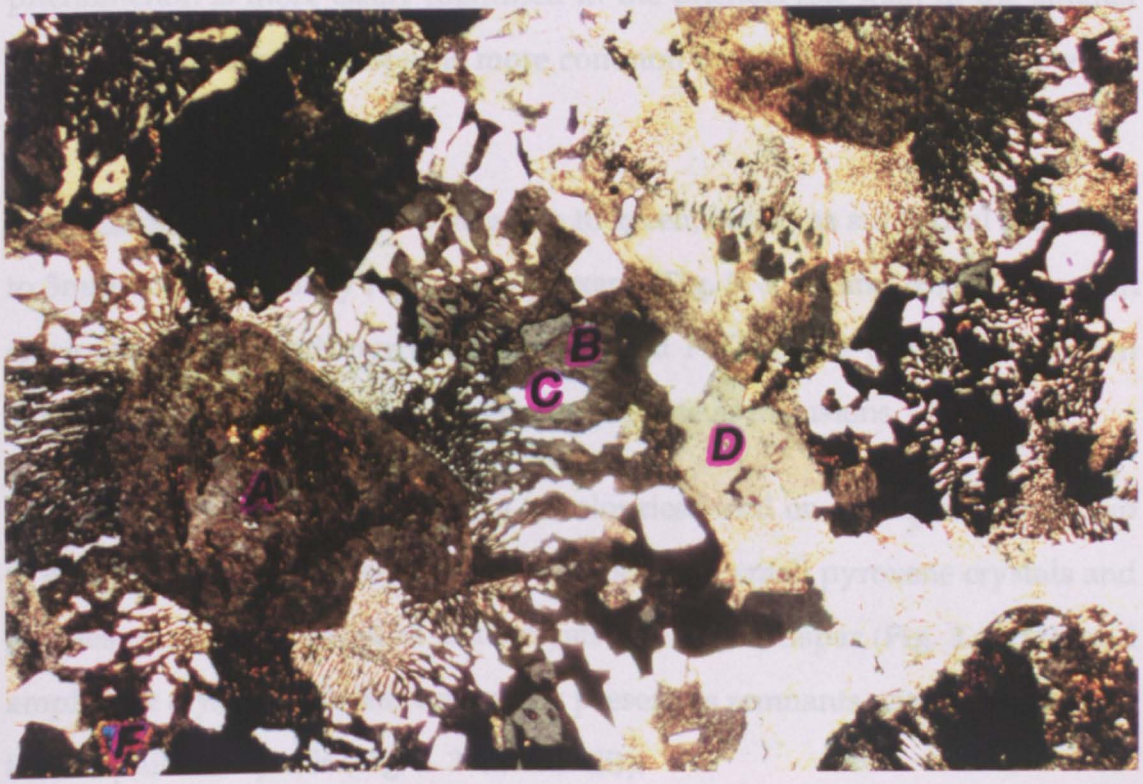
B
C
D
A
F

Primary minerals

1-Quartz: Quartz is colourless, generally sub-angular to rounded, and always a groundmass phase; individual crystals rarely exceed 7mm. Clots also occur which are composed of many individual grains of quartz. The quartz is commonly in a granophyric intergrowth with alkali feldspar. As quartz also exhibits a consertal texture involving early-formed crystals, it commonly encloses these minerals as inclusions, for example, apatite (**Fig. 3. 3 (iii)**). Most quartz grains contain trains of fluid inclusions, which are mainly secondary (**Fig. 3. 3 (iv)**) (See Chapter 5).

2-Clear alkali feldspar: Alkali feldspar forms anhedral to subhedral, strongly perthitic phenocrysts, with rare cross-hatched twinning. Clear alkali feldspar comprises only a small vol% of the total alkali feldspar present. It occurs both as phenocrysts, and as small crystals in the groundmass, and the turbidity phenomenon is more easily identified in the phenocrysts than in the smaller crystals. Clear alkali feldspar is more common in crystal cores and shows no chemical zonation.

3-Amphibole: Amphibole is pale green to green, occurs as subhedral grains up to 3mm across, partially replacing pyroxene (**Fig. 3. 3 (i) and (ii)**). It occurs in close association with pyroxene, zircon, and Fe-Ti oxide in ferromagnesian aggregates, and contains some zircon and apatite as inclusions.

4-Pyroxene: Pyroxene is pale green to colourless, and on average 0.5-2mm (up to 4mm) across. It is present in clots composed of small pyroxene crystals and needles of apatite, as well as chadacrysts in alkali feldspar (**Fig. 3. 3 (iv)**) and amphibole crystals. It is less commonly present as remnants within the cores of the amphibole crystals (**Fig. 3. 3 (i) and (ii)**).

Fig. 3. 3 (iii) Pyroxene surrounded by later amphibole crystals; and, quartz containing apatite needles as inclusions. Where: **A**, pyroxene; **B**, amphibole; **C**, quartz; and, **D**, alkali feldspar. **Loch Ainort Granite.** Crossed-polars. Field of view: 1mm x 0.70mm.

Fig. 3. 3 (iv) Pyroxene crystal included within an alkali feldspar crystal. Hydrothermal alteration is evident from the turbidity of the feldspar, fluid inclusions in the quartz, and the presence of chlorite after pyroxene. Where: **A**, pyroxene; **B**, alkali feldspar; **C**, quartz; and, **D**, chlorite. **Loch Ainort Granite.** Crossed-polars. Field of view: 1.25mm x 0.84mm.

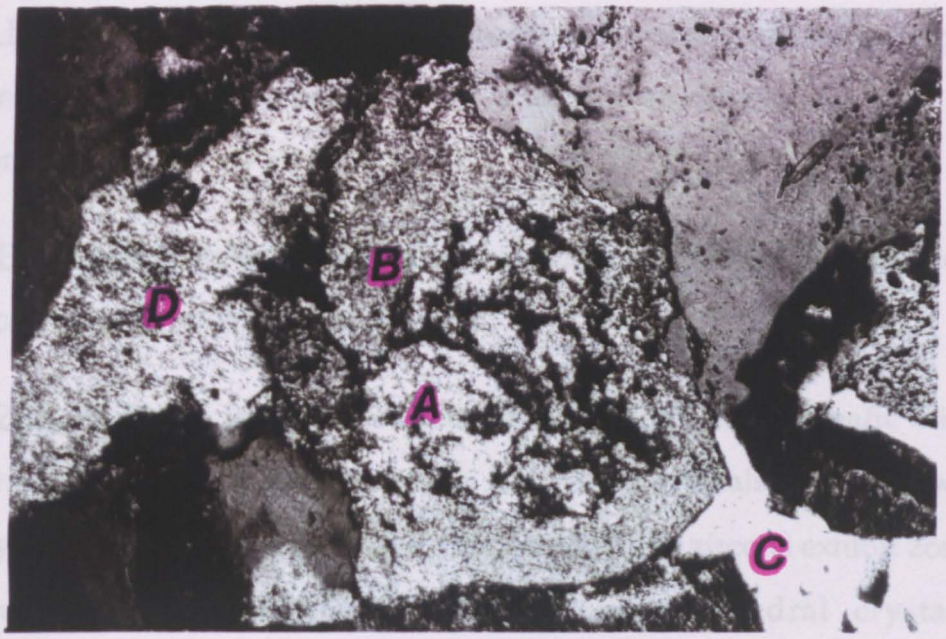
D
B
A
C

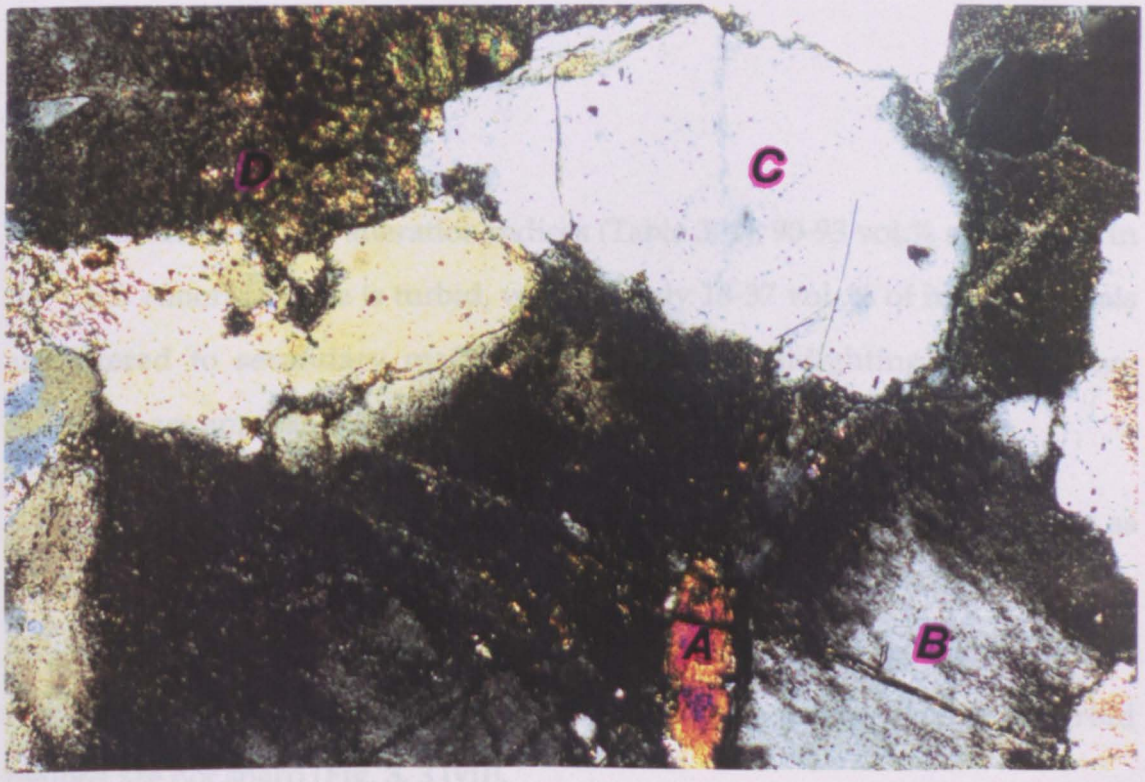
D
C
A
B

5- Biotite: Biotite is brown to light brown and is present as irregular plates up to 2mm across, always showing some alteration to chlorite, which is sometimes complete.

6-Fe-Ti oxides: Fe-Ti oxides are always present within clots of mafic minerals, along with pyroxene and amphibole.

7-Zircon: Zircon is colourless, and occurs within clots of mafic minerals (i.e. pyroxene and amphibole), and as individual crystals. They show euhedral crystal shapes with sharp edges. Commonly these zircons exhibit zonal growth lines; possible inherited zircons occur as anhedral crystals within ferromagnesian clots, along with pyroxene, amphibole and Fe-Ti oxides.

8-Apatite: Apatite occurs as needles in trace amounts up to 0.1mm across, mostly within clots of ferromagnesian minerals, although occasionally within alkali feldspar crystals (**Fig. 3. 3 (v)**). The apatites are homogeneous and without any sort of chemical zonation.

Secondary minerals

From the turbidity and alteration indices (Table 3. 1), 90-93 vol.% of feldspar in the Loch Ainort Granite is turbid, whereas only 18-37 vol. % of mafic minerals are altered to secondary mafic minerals, thus highlighting that the two processes are apparantly independent.

1-Turbid alkali feldspar: Wholly or partially replacing clear alkali feldspar as microperthite, with strings of exsolved sodic plagioclase. This exsolved feldspar indicates that the development of turbidity occurred below the alkali feldspar solvus (i.e. at low temperature). The boundaries between clear and turbid regions are not sharp (**Fig. 3. 3 (vi)**).

Fig. 3. 3 (v) Crystal of alkali feldspar containing an apatite needle. Where: **A,** alkali feldspar; **B**, quartz; and, **C**, apatite. **Loch Ainort Granite.** Crossed-polars. Field of view: 1mm x 0.70mm.

Fig. 3. 3 (vi) The distribution of turbidity along the grain boundaries of alkali feldspar, in contact with quartz crystals, suggesting the circulation of water along the crystal edges (see text). Where: **A**, a clear alkali feldspar region; **B**, a turbid alkali feldspar region; and, **C**, quartz. **Loch Ainort Granite.** Crossed-polars. Field of view: 1.25mm x 0.84mm.

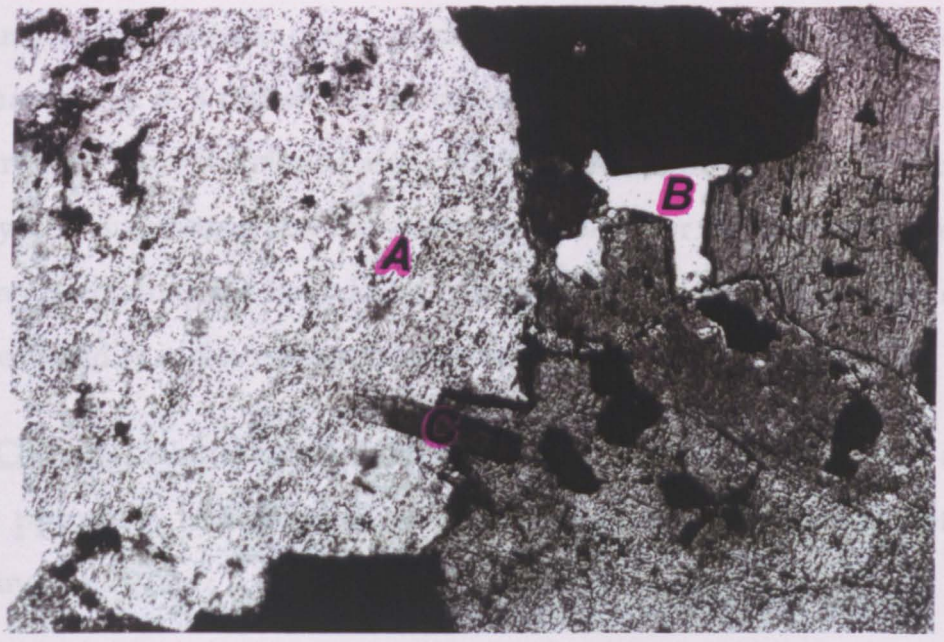
A
B
C

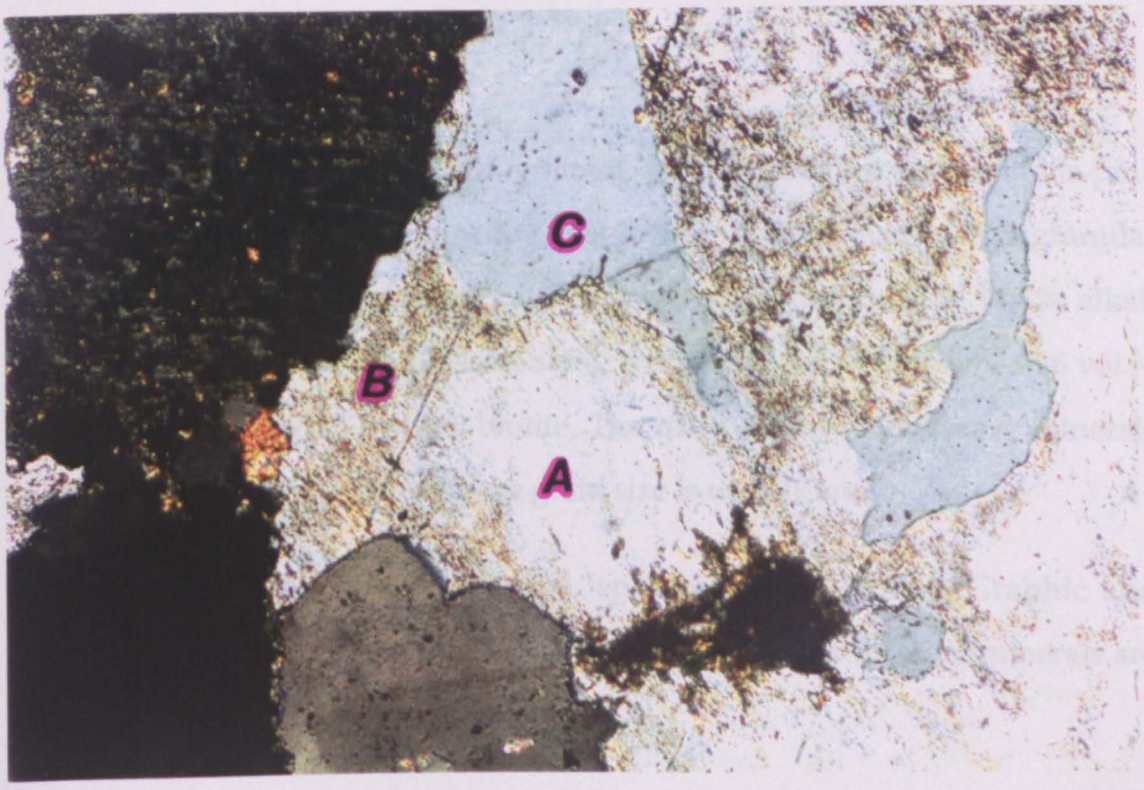
C
B
A

Turbid alkali feldspar occurs predominantly in granophyric intergrowthss with quartz. **Fig. 3. 3 (vi)** shows an inclusion of quartz in alkali feldspar, and the turbidity more developed along the boundaries of quartz and alkali feldspar crystals, suggesting that the water responsible for the alteration preferentially circulated along the boundaries of the crystals, explaining to some extent why the turbidity is concentrated along the edges of feldspar crystals.

2-Chlorite: Chlorite appears either as a direct replacement of biotite, amphibole, or pyroxene, in individual crystals , or along grain margins of all mafic minerals .

3-Epidote: Epidote is pale greenish yellow and occurs as small aggregates in trace amounts restricted to samples which contain plagioclase.

4-Muscovite: Muscovite occurs as very fine aggregates replacing or partially replacing the interior of alkali feldspar crystals.

3.2.3 The Glamaig Granite

The Glamaig Granite is medium-grained, grey-weathering and contains pink alkali feldspar surrounding white plagioclase predominantly equigranular (Thompson, 1969). It consists of 27-33 vol.% of quartz, 50-59 vol.% alkali feldspar and 0-8 vol.% plagioclase, along with 0-0.65 vol.% pyroxene, 0-6 vol.% amphibole, and 0.75-5.3 vol.% biotite. The main observed accessory minerals are zircon and apatite. The average grain size is up to 15mm.

Secondary minerals include chlorite, epidote and muscovite. Graphic and granophyric textures are common. Most of the main rock-forming minerals are illustrated in **Fig. 3. 4 (i)**.

Also present are rounded to subangular mafic inclusions, which range from 4-

Fig. 3. 4 (i) The main rock-forming minerals. Where: **A**, alkali feldspar; **B**, amphibole; **C**, quartz; **D**, biotite; **E**, zircon; and, **F**, Fe-Ti oxide. Secondary chlorite (**G**) is evident, partially replacing amphibole and biotite, and apatite occurs as inclusions within other minerals such as alkali feldspar and quartz. **Glamaig Granite**. Crossed-polars. Field of view: 1.25mm x 0.84mm.

Fig. 3. 4 (ii) Granophyric texture, resulting from the simultaneous crystallisation of quartz and alkali feldspar. Where: **A**, alkali feldspar; **B**, quartz; and, **C**, secondary white mica (sericite). **Glamaig Granite**. Crossed-polars. Field of view: 1.25mm x 0.84mm.

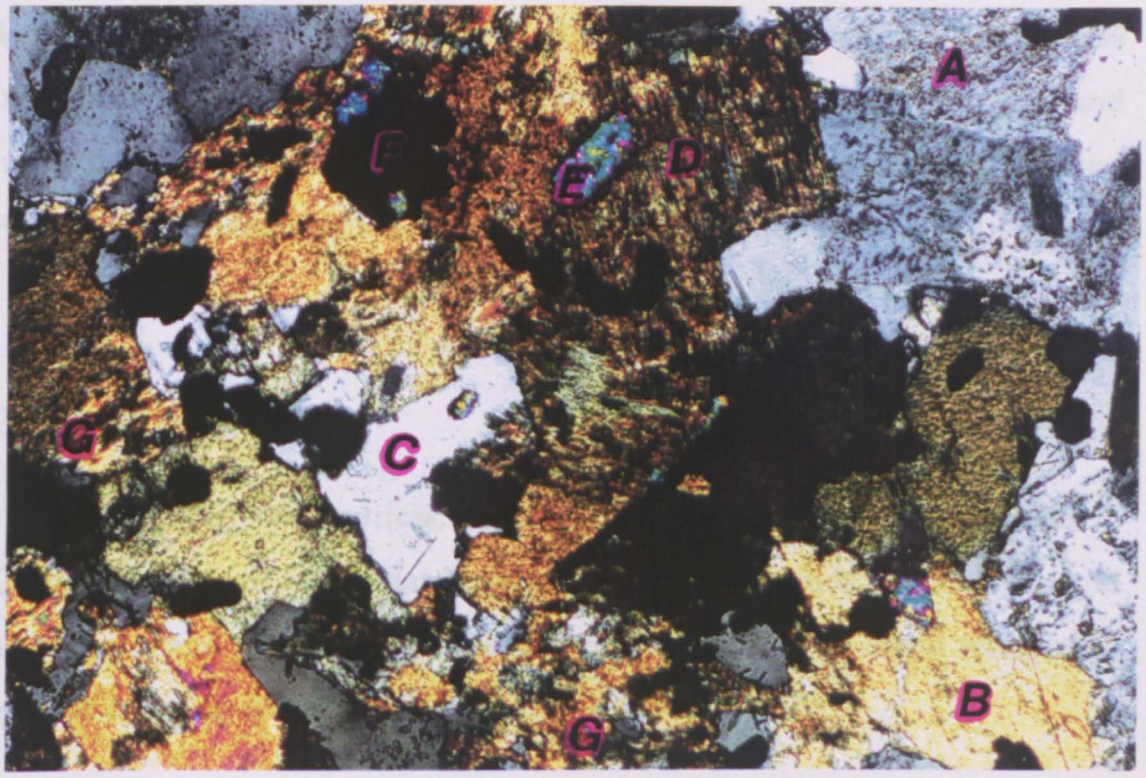
A
F
E
D
G
C
B
G

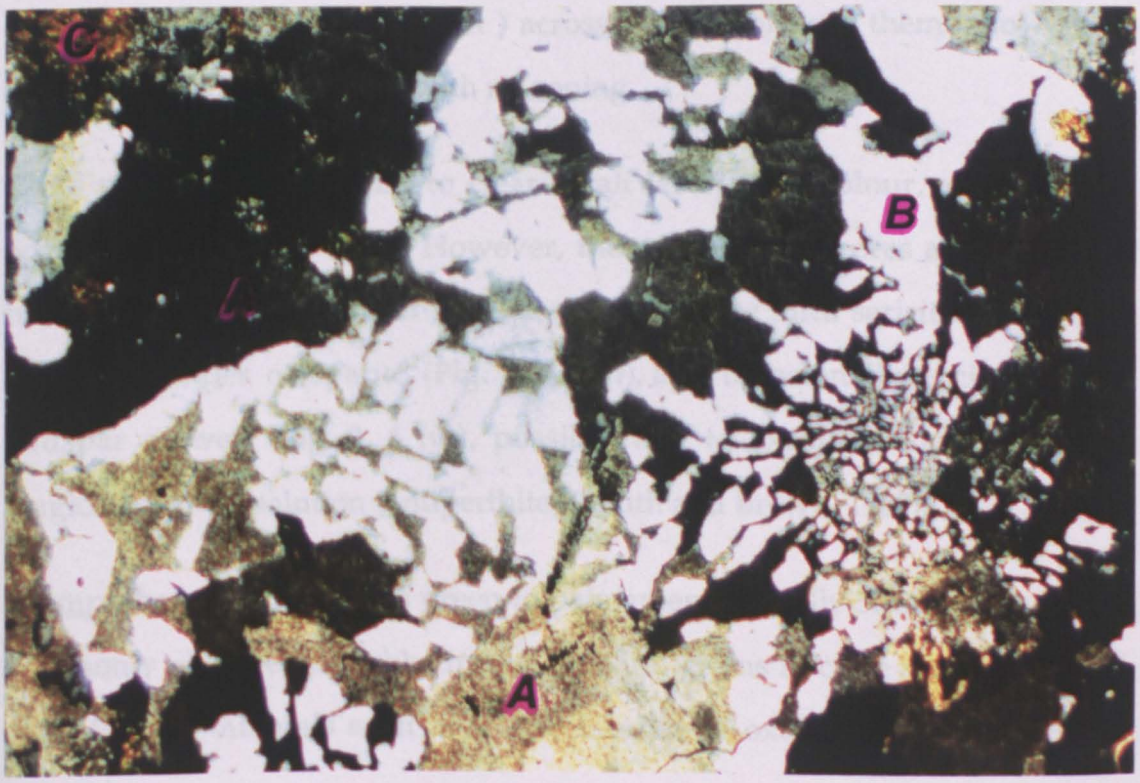
C
B
A

45mm in diameter, and form up to 5 vol.% of the rock (Thompson, 1980). These inclusions occur in almost every hand-specimen (Wager et al., 1965), and normally consist of alkali feldspar, zoned plagioclase, amphibole, biotite and Fe-Ti oxides (Thompson, 1980). Modal data are presented in Table 3. 1.

Primary minerals

1-Quartz: Whitish or colourless, anhedral grains, on average 2.5-3.5 mm across. Quartz appears to be the latest mineral, as it surrounds both biotite and amphibole, and possibly crystallised simultaneously with alkali feldspar in graphic and granophyric (hourglass) textures (**Fig. 3. 4 (ii)**).

2-Clear alkali feldspar: Alkali feldspar occurs in the form of anhedral to subhedral prismatic crystals, on average 8-10mm (up to 15mm) across. Clear alkali feldspar is colourless to white, and is restricted to the core of some alkali feldspar crystals which have been partially affected by turbidity (**Fig. 3. 4 (iii)**).

3-Clear plagioclase: Plagioclase forms subhedral to euhedral prismatic crystals on average 3-5mm (up to 10mm) across. The majority of them show albite twin lamellae (**Fig. 3. 4 (iv)**), with no zoning.

Clear plagioclase is similar to clear alkali feldspar in colour, and similarly occurs within crystal cores. However, these plagioclase cores are commonly fractured and show signs of alteration to the white mica sericite. Plagioclase encloses needles of apatite (**Fig. 3. 4 (iv)**), and occasionally encloses alkali feldspar as well (**Fig. 3. 4 (v)**), possibly due to exsolution of an original plagioclase solid-solution (antiperthite) (Smith and Brown, 1988).

4-Amphibole: Amphibole is green to pale green, typically 5mm across, and is commonly observed as subhedral to euhedral grains in close association with early-formed minerals such as plagioclase, Fe-Ti oxide and biotite in mafic

Fig. 3. 4 (iii) Alkali feldspar crystal illustrating the distribution of turbidity along the edge of the grain, whereas its core contains some fluid inclusions, and apatites are present as inclusions in quartz. Where: **A**, alkali feldspar; **B**, quartz; and, **C**, biotite completely replaced by secondary chlorite. **Glamaig Granite**. Crossed-polars. Field of view: 1.25mm x 0.84mm.

Fig. 3. 4 (iv) Plagioclase crystal partially affected by the turbidity process along its margin. Primary minerals are alkali feldspar, quartz, amphibole and biotite, along with apatite needles as inclusions in the plagioclase. Chlorite has partially replaced some of the amphibole crystals. Where: **A**, plagioclase; **B**, alkali feldspar; **C**, quartz; **D**, amphibole; **E**, biotite; **F**, Fe-Ti oxide; and, **G**, Chlorite. **Glamaig Granite**. Crossed-polars. Field of view: 1.25mm x 0.84mm.

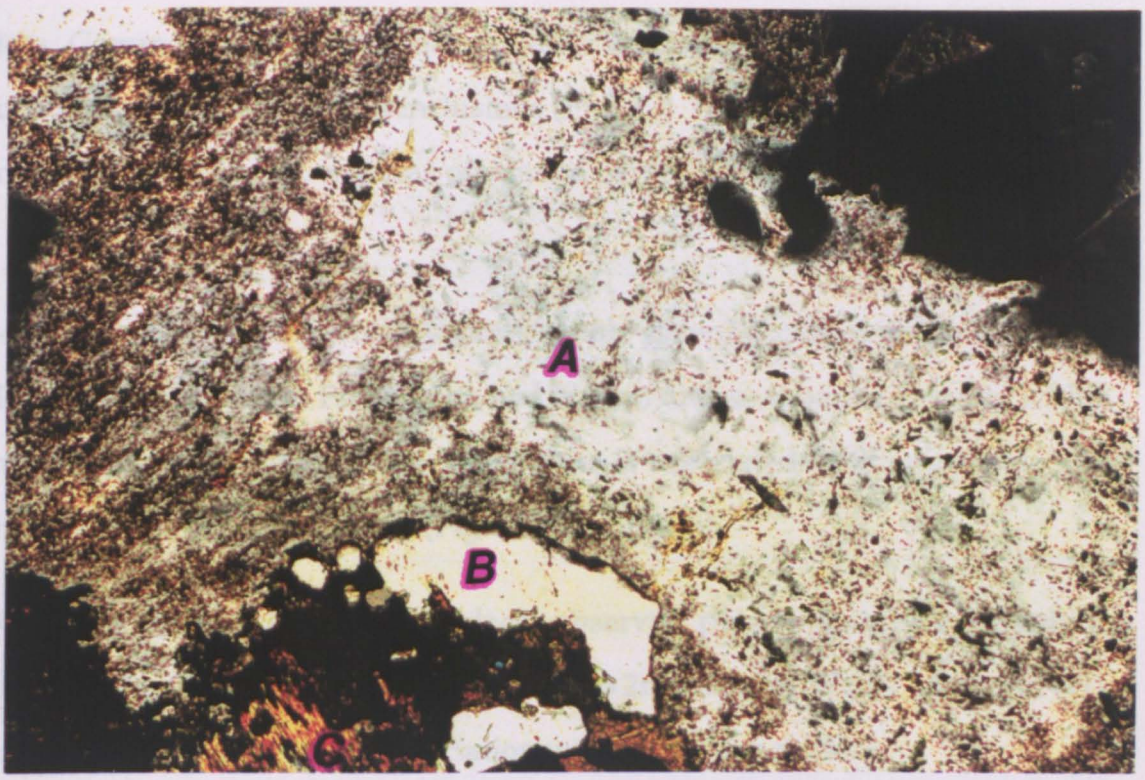
A
B
C

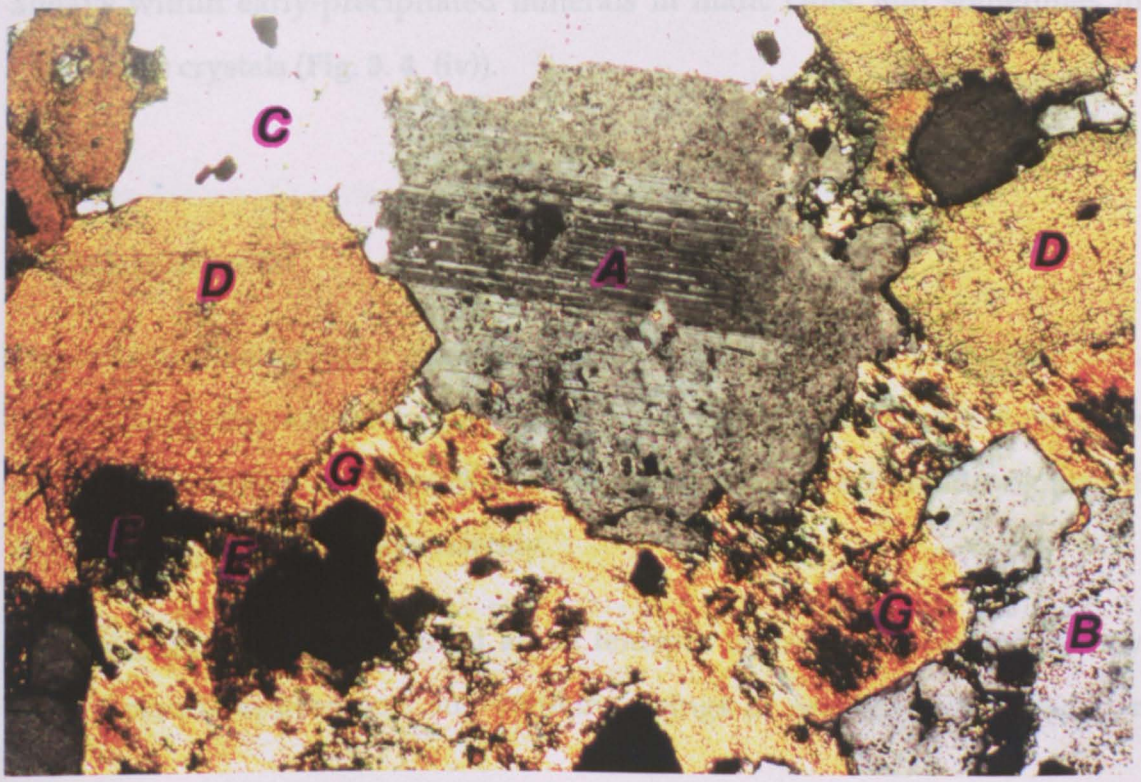
C
D
A
D
G
F
E
G
B

clots. Commonly the amphibole contains some early-precipitated minerals such as zircon and apatite as inclusions (**Fig. 3. 4 (i)**). Some of these amphibole crystals are quite fresh, whereas others are partially replaced by chlorite (**Fig. 3. 4 (iv)**).

5- Biotite: Biotite is brownish yellow to pale green, occurs within mafic clots along with amphibole, Fe-Ti oxide and zircon, and as separate crystals within the granite, up to 4mm across. The biotite is associated with amphibole and chlorite in the mafic inclusions (**Fig. 3. 4 (i) and (iv)**).

6-Fe-Ti oxides: Dark, brownish black, observed predominantly in the mafic clots along with amphibole and biotite, up to 2mm across (**Fig. 3. 4 (iv) and (v)**). Some crystals occur in close association with secondary chlorite.

7-Zircon: Zircon occurs as colourless euhedral grains, always as inclusions within later-precipitated minerals such as amphibole, biotite, and alkali feldspar (**Fig. 3. 4 (i)**). Anhedral crystals are very rare.

8-Apatite: Apatite occurs as colourless needles, up to 0.4mm in length, and always within early-precipitated minerals in mafic clots, and sometimes in plagioclase crystals (**Fig. 3. 4 (iv)**).

Secondary minerals

The values of the turbidity and alteration indices are 82-99 vol. % and 20-43 vol. %, respectively, and were computed from modal data (Table 3. 1). The observed variations between TX and AX are consistent with the development of these two processes independently.

1-Turbid alkali feldspar: Turbid alkali feldspar is brownish, predominantly with a cloudy appearance, and contains strings of unmixed sodic feldspar

which are the product of late-stage exsolution from an originally homogeneous feldspar (Ferry, 1985).

2-Turbid plagioclase: Turbid plagioclase is similar to turbid alkali feldspar, and occurs as rims to plagioclase crystals. The boundaries between clear and turbid regions are microstructurally distinct (Ferry, 1985; Guthrie and Veblen, 1991). The clear regions are relatively inclusion-free whereas the turbid regions contain fluid inclusions.

3-Epidote: Epidote is colourless to pale green, restricted to samples with significant amounts of plagioclase (see modal data, Table 3.1), and supports the deduction that the epidote is an alteration product of plagioclase .

4-Chlorite: Chlorite is pale greenish yellow and occurs either as a direct replacement of biotite in the mafic inclusions (**Fig. 3. 4 (iv)**) or along grain boundaries of amphibole, biotite and Fe-Ti oxide within the granite.

5-White mica: Muscovite is present as a sericitic alteration of both alkali feldspar and plagioclase commonly along the cleavage direction of the crystals and rarely as individual flakes.

3.2.4 The Marsco Granite

An inequigranular granite, with both alkali feldspar and plagioclase as large crystals up to 20mm across. The groundmass crystals range from 0.2-18mm across. Graphic texture involving quartz and alkali feldspar is commonly developed (**Fig. 3. 5 (i)**). The average modal composition is 28-36 vol.% quartz, 52-60 vol.% alkali feldspar, 0-7.55 vol.% plagioclase, 0-1.85 vol.% olivine, 0-3.85 vol.% pyroxene, 0-3-3.65 vol.% amphibole and 0-2.2.9 vol.% biotite. Zircon with trace apatite are the most prominent accessory minerals, along with some flakes of secondary chlorite and rare calcite.

Fig. 3. 4 (v) Alkali feldspar patches as inclusions within plagioclase crystals, suggesting some form of exsolution (antiperthite). Where: **A**, alkali feldspar; **B**, plagioclase; and, **C**, amphibole. **Glamaig Granite**. Crossed-polars. Field of view: 3mm x 2mm.

Fig. 3. 5 (i) Granophyric texture, resulting from the simultaneous crystallisation of quartz and alkali feldspar. **Marsco Granite**. Crossed-polars. Field of view: 1.25mm x 0.84mm.

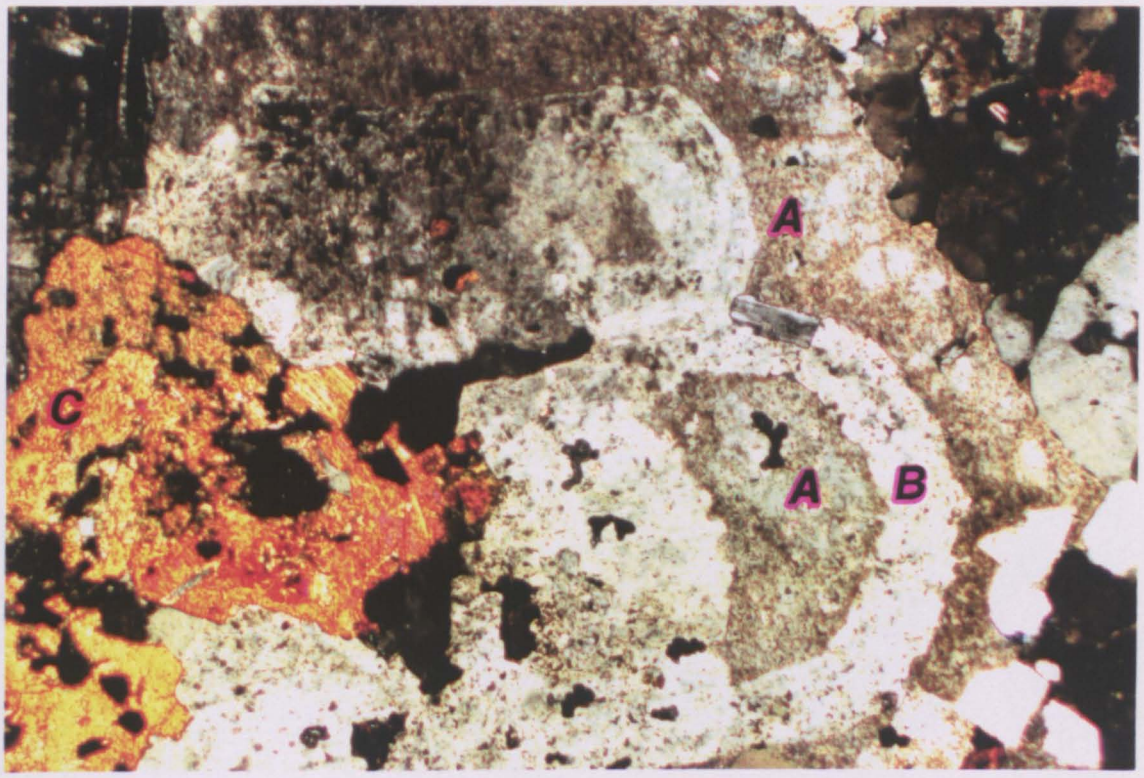
A
C
A
B

Fig. 3. 5 (ii) Quartz in a consertal relation with plagioclase. The plagioclase shows typical albite twinning, and is affected by turbidity in some parts. A pyroxene crystal is partially altered to secondary amphibole, and apatite needles are included within the plagioclase crystal. Where: **A**, quartz; **B**, plagioclase; **C**, pyroxene; **D**, secondary amphibole; and, **E**, apatite. **Marsco Granite**. Crossed-polars. Field of view: 1.25mm x 0.84mm.

Fig. 3. 5 (iii) Calcite crystal surrounded by alkali feldspar and biotite. The calcite appears to be a replacement of either alkali feldspar or biotite. Interaction with water is evident from the fluid inclusions in the quartz. Where: **A**, calcite; **B**, biotite; **C**, alkali feldspar; **D**, quartz; and, **E**, plagioclase. **Marsco Granite**. Crossed-polars. Field of view: 1.25mm x 0.84mm.

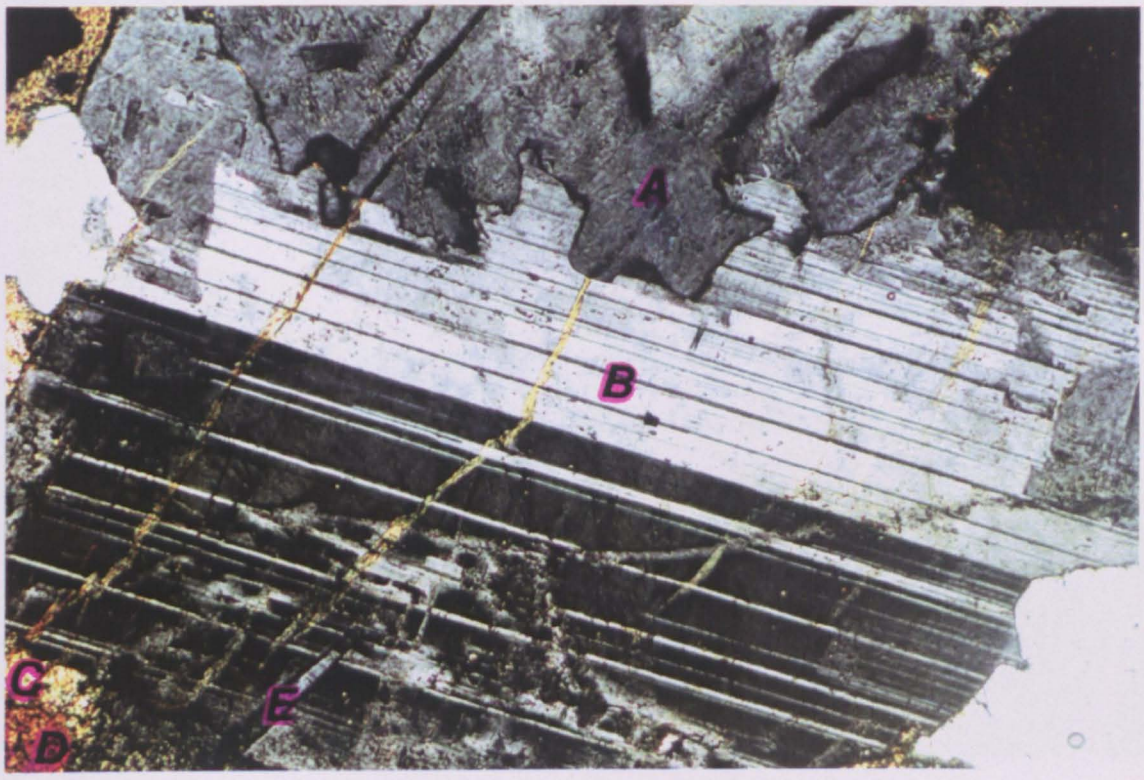
A
B
C
D
E

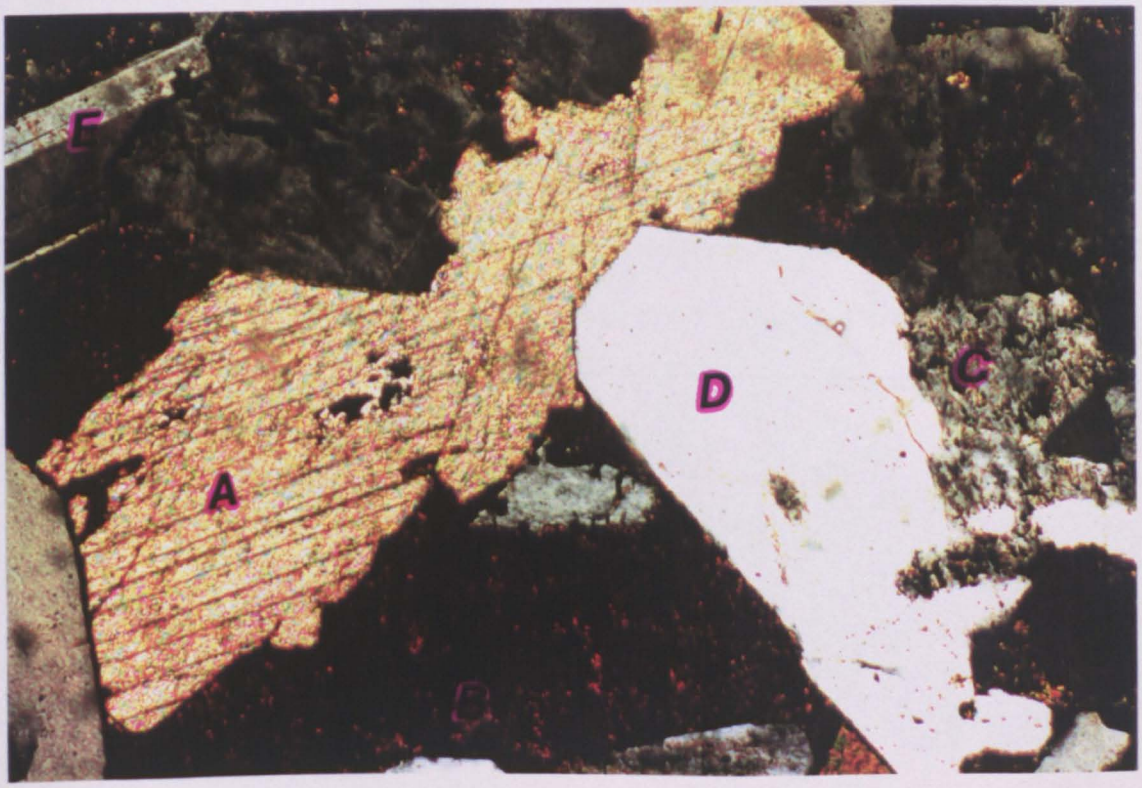
A
C
D
E

Fig. 3. 5 (iv) The distribution of clear and turbid regions within an alkali feldspar crystal; the boundary between the two regions is not sharp. Where: **A**, a turbid region; **B**, a clear region; **C**, amphibole; and, **D**, Fe-Ti oxide. **Marsco Granite**. Crossed-polars. Field of view: 1.25mm x 0.84mm.

Fig. 3. 5 (v) Plagioclase crystal rimmed with alkali feldspar, along with pyroxene crystals (some of it partially altered to uralitic amphibole), quartz and primary amphibole.Where: **A**, plagioclase; **B**, alkali feldspar; **C**, quartz; **D**, pyroxene; **E**, amphibole; and, **F**, partially-altered pyroxene. **Marsco Granite**. Crossed-polars. Field of view: 3mm x 2mm.


A
B
C
D

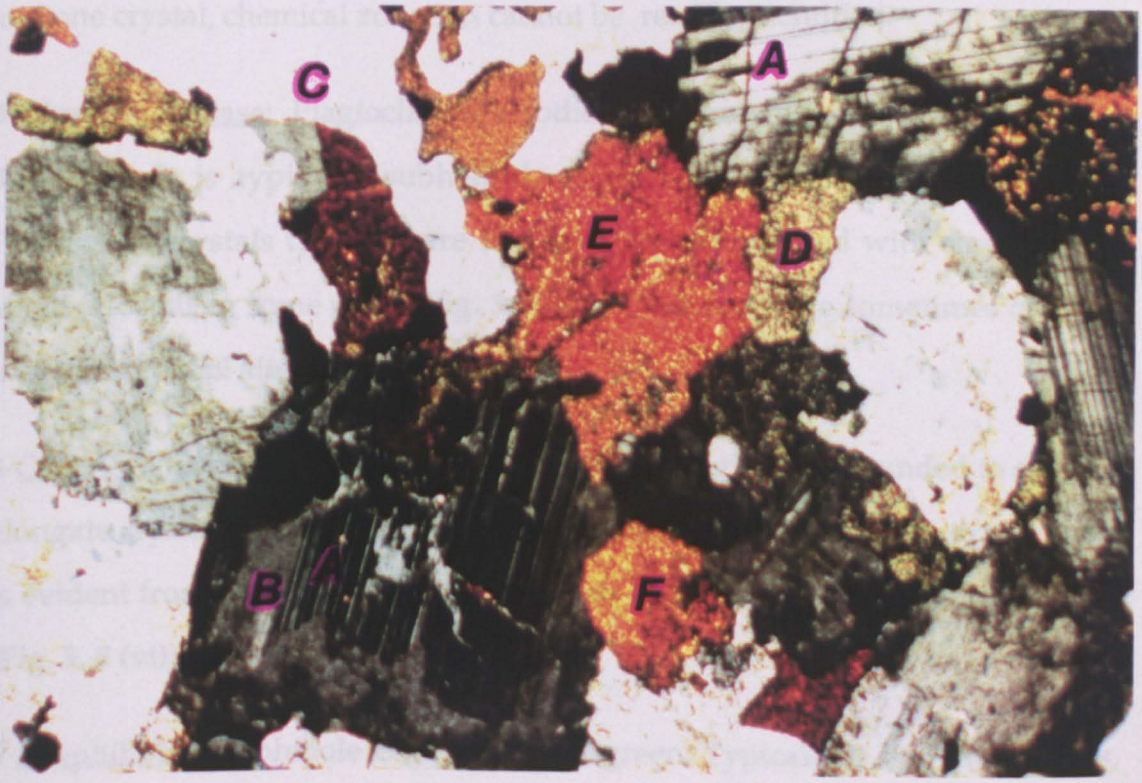
A
B
C
D
E
F

Crystal shapes range between anhedral to subhedral, except for a few euhedral amphibole, zircon and apatite crystals. Modal data are presented in Table 3.1.

Primary minerals

1-Quartz: Quartz is present as colourless, anhedral equant crystals up to 5mm in size, occasionally in linear aggregates suggestive of some sort of recrystallisation, whereas other crystals show evidence of some form of deformation by the development of lamellae. Quartz shows consertal texture with other minerals (for example, plagioclase) (**Fig. 3. 5 (ii)**), whereas interaction with water is evident from the fluid inclusion distribution in some quartz crystals (**Fig. 3. 5 (i) and (iii)**).

2-Clear alkali feldspar: Alkali feldspar is present as anhedral-subhedral prisms, on average 4-16mm (up to 20mm) across. It is commonly strongly perthitic. Clear alkali feldspar is brownish white, and persists in the interior of a number of crystals (**Fig. 3. 5 (iv)**). Because of the distribution of turbid material within any one crystal, chemical zonation cannot be readily identified.

3-Clear plagioclase: Plagioclase is a sodic type, showing albite twinning (**Fig. 3. 5 (ii)**). It is typically subhedral, along with a few euhedral crystals. Plagioclase crystals typically are 12-14mm across, mantled with clear/turbid alkali feldspar in some cases (**Fig. 3. 5 (v)**). Clear cores are sometimes cracked and show partial alteration to sericite.

4-Olivine: Olivine is yellowish orange, with very high relief, rounded to slightly elongate crystals and is often enclosed by pyroxene. The alteration to pyroxene is evident from pyroxene flakes along edges and in fractures in olivine crystals (**Fig. 3. 5 (vi)**).

5-Amphibole: Amphibole is green to pale green. Typically it is 4-7mm across,

Fig. 3. 5 (vi) Olivine showing some form of alteration to pyroxene along fractures, in association with pyroxene, plagioclase, alkali feldspar, quartz and Fe-Ti oxide. Where: **A**, olivine; **B**, pyroxene; **C**, alkali feldspar; **D**, quartz; **E**, plagioclase; and, **F**, Fe-Ti oxide. **Marsco Granite**. Crossed-polars. Field of view: 1.25mm x 0.84mm.

Fig. 3. 5 (vii) Pyroxene crystals partially replaced by amphibole, in close association with primary amphibole, plagioclase, alkali feldspar, quartz and an apatite needle. Where: **A**, pyroxene; **B**, amphibole; **C**, plagioclase; **D**, alkali feldspar; **E**, quartz; and, **F**, apatite. **Marsco Granite**. Crossed-polars. Field of view: 1.25mm x 0.84mm.

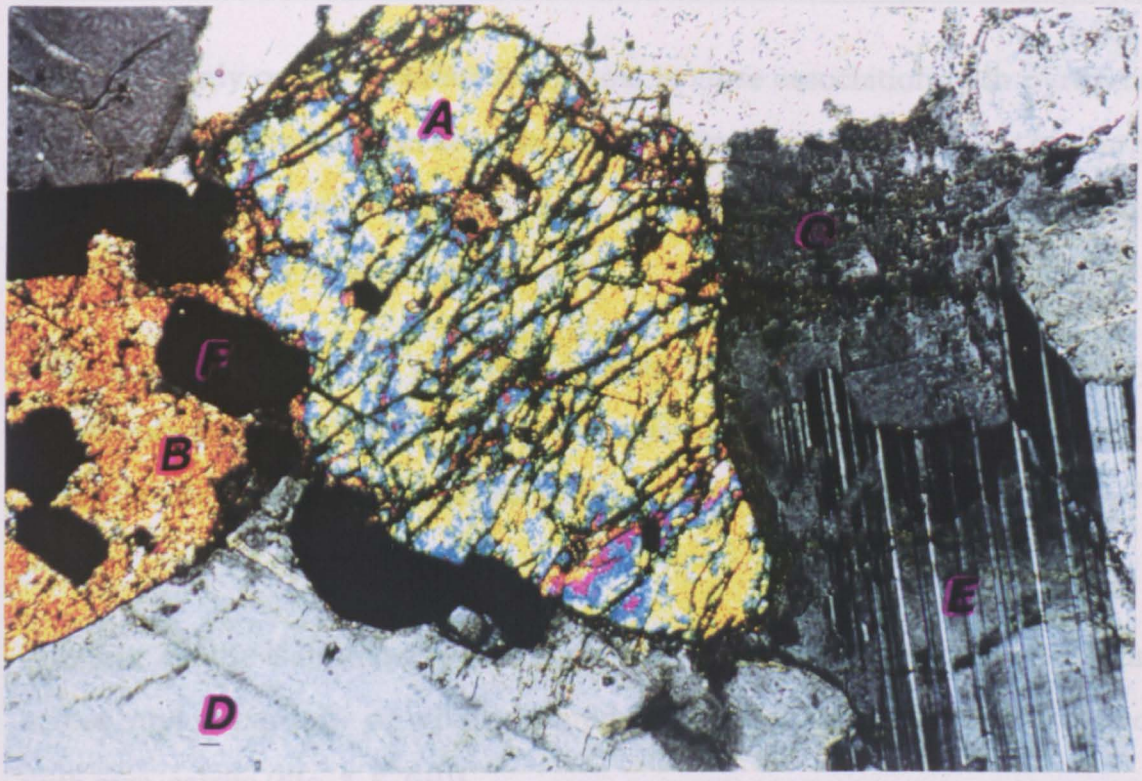
A
C
F
B
E
D

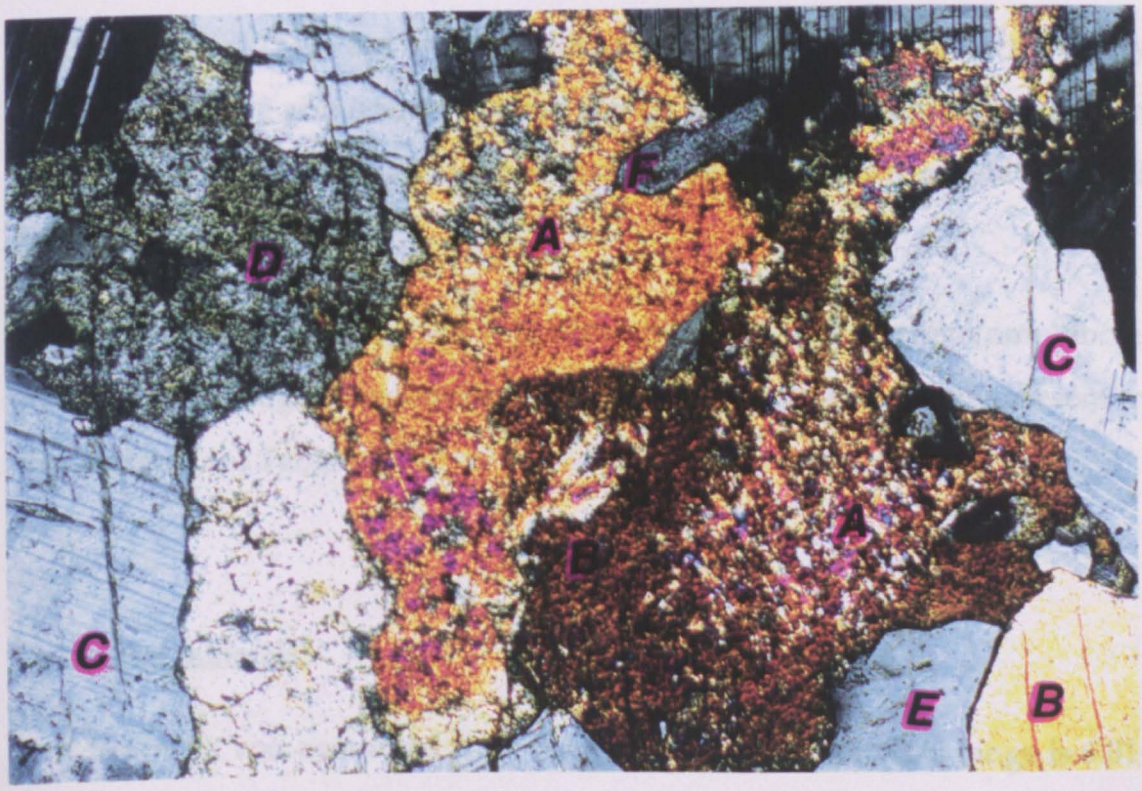
F
D
A
C
A
B
C
E
B

and commonly occurs as subhedral grains in close association with pyroxene and Fe-Ti oxides in the form of mineral aggregates. Individual crystals of nearly euhedral form are also present. There are numerous inclusions within the amphibole, usually of zircon and apatite.

6-Pyroxene: Pyroxene is yellowish-brown, partially altered to secondary amphibole (uralite) (**Fig. 3. 5 (vii)**), whereas some crystals are unaltered and typically occur within mafic clots along with primary amphibole and Fe-Ti oxide.

7-Biotite: Biotite is brown to pale brown, with strong pleochroism, up to 2mm across, and is partially or wholly altered to chlorite. The biotite is associated with rare calcite (**Fig. 3. 5 (iii)**).

8-Zircon: Zircon is colourless and occurs as early-precipitated crystals enclosed within amphibole and plagioclase. It commonly has a euhedral form. Identified magmatic zircons are up to 0.3mm across. Inherited (anhedral) zircons are less common and 0.15-0.2mm in size.

9-Fe-Ti oxides: These are one of the most common and ubiquitous accessory phases in all Skye granites, up to 2mm across, and occur predominantly within early-precipitated minerals and in mafic clots along with amphibole and pyroxene (**Fig. 3. 5 (vi)**).

10-Apatite: Apatite needles, up to 0.15mm in length, occur within amphibole, pyroxene and plagioclase crystals (**Fig. 3. 5 (vii)**). Apatite is rarely present in this granite (see Table 3.1).

Secondary minerals

A value of TX was computed from the data in Table 3. 1 and its range is 0.81-

0.83. This implies that 81-83 vol.% of the feldspar is turbid within the Marsco Granite, and indicates how considerably less the amount of turbid feldspar this intrusion contains relative to other Skye granites. In contrast, a value of 0.13-0.28 was computed for the Alteration Index, and implies that only 13-28 vol. % of mafic minerals are altered to secondary mafic minerals.

1-Turbid alkali feldspar: Wholly or partially replacing clear alkali feldspar, turbid alkali feldspar is easily distinguished from coexisting plagioclase which is considerably clearer. It is typically a microperthite with strings of unmixed sodic plagioclase (**Fig. 3. 5 (iv)**).

2-Turbid plagioclase: Forms only a small vol.% of this granite, and occurs along the rims of clear crystals. The boundaries between clear and turbid plagioclase are microstructurally distinct (Guthrie and Veblen, 1991). Almost all of the plagioclase is inclusion-free, except for rare turbid patches (**Fig. 3. 5 (ii)**).

3-Chlorite: Chlorite is brownish yellow, and occurs as fine-grained aggregates along with Fe-Ti oxides, replacing pyroxene, amphibole, or biotite.

4-Calcite: Calcite is greenish to colourless. Only a single example of a crystal was observed in this intrusion, and shows well developed cleavage. It is surrounded by and appears to be partially replacing, alkali feldspar and biotite crystals (**Fig. 3. 5 (iii)**).

5-Muscovite: It is colourless to light shades of green, and is present as a sericitic alteration of alkali feldspar and occasionally of plagioclase, often along their elongation direction. More rarely, it is found as individual flakes up to 0.5mm across.

3.2.5 Other granites

3.2.5.1 The Glas Beinn Mhor Granite

An inequigranular granite, with alkali feldspar crystals up to 25mm; all other crystals range from 0.2-15mm in grain-size. Quartz and alkali feldspar commonly show micrographic and granophyric textures. Crystals of plagioclase are commonly rimmed by alkali feldspar, but occasionally show a reverse relationship i.e. alkali feldspar patches within plagioclase crystals, which can be attributed to exsolution processes (cf. Smith and Brown, 1988)

The most important ferromagnesian mineral is biotite, although amphibole, pyroxene and olivine are also present. These occur as individual crystals or in aggregates within mafic clots, along with chlorite, Fe-Ti oxides, epidote and zircon, the last of which occurs as inclusions in the mafic minerals. Modal data are presented in Table 3.1.

3.2.5.2 The Beinn Dearg Mhor Granite

A medium- to coarse-grained hypersolvus granite with porphyritic texture involving alkali feldspar phenocrysts. Micrographic and granophyric intergrowths commonly mantle the phenocrysts. Most of the alkali feldspar crystals have been affected by the turbidity-forming process(es), whereas quartz crystals are covered by numerous fluid inclusions.

The most important ferromagnesian mineral is pyroxene, forming rounded to subhedral prismatic grains, along with Fe-Ti oxides. Secondary minerals include: clay minerals, chlorite, muscovite, and rare epidote. The absence of amphibole and biotite is suggestive of a 'dry' melt; thus, the turbid feldspar and the fluid inclusions within the quartz most likely result from subsolidus processes. Modal data are presented in Table 3.1.

3.2.5.3 The Beinn na Caillich Granite

A medium-grained non-porphyritic granite. Spherulitic texture dominates the marginal facies, giving way to granophyric and graphic textures within the interior of the intrusion. Feldspar is turbid within their rims, whereas their cores exhibit smooth featureless surfaces.

Pyroxene is the main ferromagnesian mineral, present either as inclusions in later-precipitated minerals, or at the boundaries of quartz and feldspar crystals. Associated with the pyroxenes are their alteration product (chlorite), and other mafic and accessory minerals (Fe-Ti oxides, rare zircon and a few apatite needles). Modal data are presented in Table 3.1.

3.2.5.4 The Allt Fearna Granite

An inequigranular granite, with quartz, alkali feldspar and plagioclase as phenocrysts up to 20mm across. Quartz and alkali feldspar intergrowths commonly shows granophyric and spherulitic textures.

The only primary ferromagnesian minerals now present are Fe-Ti oxides. Secondary white mica (sericite) occurs as the result of alteration of alkali feldspar and plagioclase within grains and as individual flakes up to 0.4mm. Also present as inclusions in plagioclase is rare zircon. Modal data are presented in Table 3.1.

3.2.5.5 The Creag Strollamus Granite

A medium- to coarse-grained granite, with alkali feldspar as the largest

crystals, up to 20mm across. The groundmass minerals range from 0.3 to 9mm across. Graphic and granophyric textures are common and overgrow the early-formed crystals of both quartz and feldspar.

The main ferromagnesian minerals are clinopyroxene and amphibole, with pyroxene dominant over amphibole. These are partially altered to secondary chlorite, and occur as aggregates of crystals, along with traces of biotite, Fe-Ti oxides, and rare zircon, together with secondary chlorite, calcite and clay minerals in mafic clots. Modal data are presented in Table 3.1.

3.2.5.6 The Southern Porphyritic Granite

This intrusion has been studied by Wager et. al. (1965), Bell (1966), and Thompson (1969). It is a fine- to medium-grained, leucocratic granite, containing quartz and alkali feldspar as phenocrysts (up to 15mm across) within a fine-grained groundmass.

Around each phenocryst, are granophyric intergrowths, which become markedly coarser away from the phenocrysts.

The main ferromagnesian minerals are biotite and their alteration product (i.e. chlorite), along with small grains of amphibole partially altered to chlorite, Fe-Ti oxide, and rare zircon. Fe-Ti oxide is the only easily distinguished mineral within the groundmass, which is dominated by very fine-grained, granular-textured quartz and alkali feldspar formed by rapid cooling during a rapid decrease in the pressure of the magma (Bell, 1966). Modal data are presented in Table 3.1.

3.2.5.7 The Maol na Gainmhich Granite

A one-feldspar granite, with alkali feldspar and quartz phenocrysts in a porphyritic texture, previously called the Coarse Granite (Wager et.al., 1965). There are no quartz-alkali feldspar intergrowths in the groundmass.

The dominant ferromagnesian mineral is a strongly pleochroic, dark greenish blue to yellow amphibole. Chlorite is also present in mafic clots along with amphibole and small patches of biotite. Apart from Fe-Ti oxides, other accessory minerals are rare, very fine-grained, zircon and apatite. Modal data are presented in Table 3.1.

3.2.5.8 The Meall Buidhe Granite

This intrusion was first recognised by Wager et al. (1965) as a distinct mass. It is a medium-grained rock, and contains some plagioclase crystals mantled with turbid alkali feldspar. The groundmass contains independent crystals of alkali feldspar and quartz in a predominantly microgranitic texture.

The main ferromagnesian minerals are a few grains of pyroxene, green amphibole, and greenish biotite. Some of the amphiboles are an alteration product of pyroxene, whereas the rest are magmatic in origin. Secondary minerals are represented by epidote, muscovite and chlorite, in mafic clots, along with Fe-Ti oxide and rare zircon. Apatite and zircon are usually present as inclusions in other early minerals such as amphibole, although sometimes in feldspar and quartz. Mantled plagioclase with alkali feldspar and green pyroxene are suggestive of an affinity towards the Marsco Granite (Wager et al., 1965). Modal data are presented in Table 3.1.

3.2.5.9 The Eas Mor Granite

An inequigranular, hypersolvus granite with a single microperthitic feldspar. These feldspar crystals occur predominantly as phenocrysts (10-15mm), surrounded by graphic and granophyric textured quartz and alkali feldspar, and which become coarser away from the phenocrysts. Quartz is commonly covered by fluid inclusion pits, whereas feldspar has a turbid surface.

Ferromagnesian minerals are predominantly green amphibole, although a few pyroxene grains are present as well, some of which are replaced by amphibole. Fe-Ti oxides are present in aggregates with the ferromagnesian minerals, along with secondary chlorite and muscovite. Also present are rare accessory zircon and apatite. Modal data are presented in Table 3.1.

3.2.5.10 The Northern Porphyritic Felsite

This rock consists of quartz and alkali feldspar predominantly as phenocrysts, along with a few phenocrysts of Fe-Ti oxide and secondary chlorite in a fine-grained groundmass.

Wager et al. (1965) recorded some pyroxene phenocrysts from this intrusion, but which are commonly replaced by low-temperature chlorite, as in the samples examined during the present study. Rare amphibole phenocrysts contain early-precipitated zircon. The groundmass is mainly composed of quartz and alkali feldspar, but their small grain size precludes the identification of any other minerals. Modal data are presented in Table 3.1.

3.2.5.11 The Glen Sligachan Granite

An inequigranular, porphyritic microgranite, with alkali feldspar and quartz as

the dominant phenocrysts (15-20mm across). Quartz grains form clots or aggregates suggestive of some sort of recrystallisation.

Pyroxene is the main ferromagnesian mineral, partially altered to chlorite, and concentrated in mafic clots along with Fe-Ti oxides, secondary epidote, and zircon. Secondary muscovite flakes are mainly concentrated within alkali feldspar phenocrysts, up to 0.3mm across. Modal data are presented in Table 3.1.

3.2.5.12 The Raasay Granite

This intrusion has been studied by Davidson and Walker (1934). It is a porphyritic granite crowded with tabular phenocrysts of alkali feldspar (15mm) and smaller (~8mm) phenocrysts of quartz. Granophyric texture around the quartz and alkali feldspar phenocrysts is common and is coarser away from the phenocrysts.

Biotite is the predominant ferromagnesian mineral, associated occasionally with magnesium-rich clinopyroxene (diopside) in mafic clots, along with zircon, Fe-Ti oxide, rare apatite, and secondary chlorite and epidote. Modal data are presented in Table 3.1.

3.3 Summary and conclusions

From the microscopic study of Skye granites the following features are recognised:

(i) Skye granites have been severely altered by hydrothermal fluids, as shown by the turbidity of feldspar, fluid inclusions in quartz, and the alteration of ferromagnesian minerals to secondary mafic minerals.

(ii) The turbidity of feldspars and the alteration of mafic minerals appear to have developed independently. Since feldspars dissolve incongruently in aqueous solutions to give mica at low temperature and feldspathoids at higher temperatures, (Anderson and Burnham, 1983), it is concluded that the alteration process(es) occurred below 500°C.

(iii) The textures shown by the major phases suggest that they crystallised sequentially. Differences in modal mineral contents even within one intrusion suggest that they formed by more than one magmatic pulse (cf. Gibson, 1984).

(iv) The recognition of inherited zircon throughout the suite suggests a crustal component.

(v) The presence of mafic inclusions within a number of the granites, in particular the Glamaig Granite, suggests the role of magma-mixing during the evolution of the suite.

(vi) The coarsening of granophyric texture outwards from the alkali feldspar phenocrysts suggests it is a primary feature (Dunham, 1965; Carstens, 1983; Gibson, 1984). Dunham (1965) has suggested that as the crystallisation proceeds the acid magma evolves towards a cotectic line in the Or-Ab-SiO_2-H_2O system, and becomes supercooled as the result of a decrease in the water vapour pressure. At this temperature we get maximum nucleation of both alkali feldspar and quartz and granophyric intergrowth develops. As the crystallisation proceeds, the quartz-alkali feldspar intergrowth builds up outwards from the phenocrysts. Any decrease in supercooling will produce larger crystals, resulting in the general coarsening of intergrowth outwards.

Other suggested mechanisms which may produce this sort of intergrowth are: devitrification, and modification of older granitic rocks by partial fusion (Smith and Brown, 1988). Devitrification is ruled out here because it is unlikely that these textures in Skye granites were once glassy. There is no evidence of

modification of older granitic rocks by partial melting processes preserved within or adjacent to the Skye granites. Also, the sub-solidus replacement of myrmekitic plagioclase by alkali feldspar as proposed by Shelley (1966), is rejected due to the absence of any remnants of myrmekite texture.

Table 3.1 Modal and mineral assemblage data for Skye granites

Sample	Beinn an Dubhaich					
	Sk-298	Sk-299	Sk-300	Sk-301	Sk-302	Sk-338
Primary minerals						
Quartz	29.8	28.4	33.15	33.25	35.9	28.95
Clear alkali feldspar	9.6	10.35	11.85	8.75	7.15	8.55
Clear plagioclase	8.4	7.65	6.15	4.65	5.65	7.45
Olivine	0.0	0.0	0.0	0.0	0.0	0.0
Pyroxene	0.0	0.0	0.0	0.0	0.0	0.0
Amphibole	4.6	3.65	9.45	1.1	3.1	6.85
Biotite	1.25	2.95	0.15	0.85	1.15	1.9
Fe-Ti oxide	0.65	0.85	1.25	1.15	1.45	1.65
Zircon	0.25	0.2	0.3	0.0	0.05	0.15
Apatite	0.1	0.05	0.2	0.05	0.0	0.05
Secondary minerals						
Turbid alkali feldspar	40.1	40.45	34.45	41.10	34.35	39.15
Turbid plagioclase	2.25	3.75	1.85	6.05	4.15	3.35
Chlorite	2.75	2.55	1.15	2.45	4.75	1.85
Clay minerals	0.0	0.0	0.0	0.0	0.0	0.0
Epidote	0.0	0.0	0.0	0.55	1.75	0.0
Calcite	0.0	0.0	0.0	0.0	0.0	0.0
Muscovite	0.25	0.15	0.05	0.05	0.55	0.10
TX	0.71	0.70	0.67	0.78	0.75	0.73
AX	0.31	0.22	0.11	0.50	0.52	0.17
Q	33.1	31.3	38.0	35.5	41.2	33.2
A	55.1	56.1	52.9	53.1	47.6	54.5
P	11.8	12.6	9.1	11.4	11.2	12.3

Where: TX, Turbidity Index; AX, Alteration Index.

Table 3.1 continued

Sample	Loch Ainort				Creag Strollamus	
	Sk-313	Sk-316	Sk-317	Sk-318	Sk-305	Sk-306
Primary minerals						
Quartz	31.55	27.25	30.20	27.1	37.4	29.95
Clear alkali feldspar	5.65	5.75	5.10	4.6	2.15	4.25
Clear plagioclase	0.15	0.0	0.1	0.05	0.25	1.75
Olivine	0.0	0.0	0.0	0.1	0.0	0.0
Pyroxene	0.25	3.75	0.0	3.7	0.75	0.0
Amphibole	6.55	3.7	0.0	0.95	0.0	1.15
Biotite	0.0	0.05	2.95	0.0	0.0	0.15
Fe-Ti oxide	1.65	1.05	0.95	1.65	1.15	1.3
Zircon	0.3	0.1	0.05	0.1	0.1	0.05
Apatite	0.1	0.1	0.0	0.05	tr.	0.05
Secondary minerals						
Turbid alkali feldspar	49.20	56.35	59.75	59.3	55.15	52.85
Turbid plagioclase	0.1	0.0	0.05	0.1	0.4	3.85
Chlorite	3.95	1.45	0.65	1.95	2.65	3.45
Clay minerals	0.05	0.0	0.0	0.0	0.0	0.15
Epidote	0.15	0.0	0.15	0.25	0.0	0.0
Calcite	0.0	0.0	0.0	0.0	0.0	0.65
Muscovite	0.35	0.45	0.05	0.1	0.0	0.4
TX	0.90	0.91	0.92	0.93	0.96	0.90
AX	0.37	0.20	0.18	0.29	0.78	0.73
Q	36.5	30.5	31.7	29.7	39.2	32.4
A	63.3	69.5	68.1	70.1	60.1	61.6
P	0.2	0.0	0.2	0.2	0.7	6.0

Where: TX, Turbidity Index; AX, Alteration Index.

Table 3.1 continued

Sample	Marsco			Beinn na Caillich		
	Sk-333	Sk-334	Sk-343	Sk-335	Sk-336	Sk-337
Primary minerals						
Quartz	34.7	36.2	28.3	28.85	30.70	29.10
Clear alkali feldspar	10.35	9.05	6.75	2.05	10.25	8.75
Clear plagioclase	0.0	0.0	4.95	0.0	0.55	0.5
Olivine	0.0	0.0	1.85	0.0	0.0	0.0
Pyroxene	0.0	3.85	2.3	1.85	3.50	2.95
Amphibole	0.0	0.0	3.65	0.0	0.0	0.0
Biotite	2.9	0.0	0.85	0.0	0.0	0.0
Fe-Ti oxide	0.55	0.8	1.2	2.65	1.95	2.15
Zircon	0.25	0.15	0.35	0.0	0.1	0.15
Apatite	0.05	0.05	0.1	0.05	0.05	0.05
Secondary minerals						
Turbid alkali feldspar	50.05	49.3	45.6	61.85	50.3	53.85
Turbid plagioclase	0.0	0.0	2.6	0.0	0.75	1.05
Chlorite	1.15	0.6	1.25	2.65	1.8	1.35
Clay minerals	0.0	0.0	0.0	0.05	0.0	0.0
Epidote	0.0	0.0	0.0	0.0	0.05	0.05
Calcite	0.0	0.0	0.25	0.0	0.0	0.0
Muscovite	0.0	0.25	0.1	0.0	0.0	0.05
TX	0.83	0.84	0.81	0.97	0.83	0.86
AX	0.28	0.19	0.13	0.59	0.34	0.32
Q	36.5	38.3	32.1	31.1	33.2	31.2
A	63.5	61.7	59.3	68.9	65.4	67.1
P	0.0	0.0	8.6	0.0	1.4	1.7

Where: TX, Turbidity Index; AX, Alteration Index.

Table 3.1 continued

Sample	Beinn Dearg Mhor				Allt Fearna	
	Sk-314	Sk-315	Sk-339	Sk-340	Sk-303	Sk-304
Primary minerals						
Quartz	34.8	31.25	29.85	34.6	36.6	38.3
Clear alkali feldspar	1.3	1.15	1.4	1.55	3.45	3.1
Clear plagioclase	0.0	0.0	0.0	0.0	0.5	0.35
Olivine	0.0	0.0	0.0	0.0	0.0	0.0
Pyroxene	0.0	2.45	1.25	3.6	0.0	0.0
Amphibole	0.0	0.0	0.0	0.0	0.0	0.0
Biotite	0.0	0.0	0.0	0.0	0.0	0.0
Fe-Ti oxide	1.35	1.2	0.75	0.8	2.7	2.25
Zircon	0.15	0.2	0.1	0.15	0.1	0.15
Apatite	tr.	0.05	0.0	0.05	tr.	0.05
Secondary minerals						
Turbid alkali feldspar	55.65	59.9	62.75	54.1	49.2	47.9
Turbid plagioclase	0.0	0.0	0.0	0.0	1.35	1.85
Chlorite	1.55	0.85	0.6	1.4	2.75	3.1
Clay minerals	4.8	2.85	3.15	3.4	0.0	0.0
Epidote	0.05	tr.	0.05	0.0	0.0	0.0
Calcite	0.0	0.0	0.0	0.0	0.0	0.0
Muscovite	0.25	0.1	0.1	0.35	3.35	2.95
TX	0.98	0.98	0.98	0.97	0.93	0.94
AX	1.0	0.26	0.34	0.28	1.0	1.0
Q	37.9	33.9	31.8	38.3	40.2	41.9
A	62.1	66.1	68.2	61.7	57.8	55.7
P	0.0	0.0	0.0	0.0	2.0	2.4

Where: TX, Turbidity Index; AX, Alteration Index.

Table 3.1continued

Sample	Glamaig					Eas Mor
	Sk-323	Sk-324	Sk-325	Sk-326	Sk-327	Sk-321
Primary minerals						
Quartz	27.2	32.8	33.4	30.95	27.5	26.95
Clear alkali feldspar	0.5	1.35	4.25	6.65	3.8	2.55
Clear plagioclase	0.0	0.15	3.15	4.1	2.3	0.0
Olivine	0.0	0.0	0.0	0.0	0.0	0.0
Pyroxene	0.3	0.65	tr.	0.0	0.0	0.35
Amphibole	0.0	0.0	3.45	5.85	5.35	4.95
Biotite	5.3	4.35	1.65	0.75	1.15	0.0
Fe-Ti oxide	3.65	2.1	1.2	1.05	0.85	1.65
Zircon	0.05	0.1	0.15	0.25	0.2	0.1
Apatite	0.05	tr.	tr.	0.1	0.05	0.05
Secondary minerals						
Turbid alkali feldspar	58.65	53.7	45.4	45.1	47.05	61.7
Turbid plagioclase	0.0	2.1	4.65	3.55	7.2	0.0
Chlorite	3.45	2.25	1.95	1.35	3.75	1.45
Clay minerals	0.0	0.0	0.0	0.0	0.0	0.0
Epidote	0.0	0.0	0.55	0.2	0.45	0.0
Calcite	0.0	0.0	0.0	0.0	0.0	0.0
Muscovite	0.85	0.45	0.20	0.10	0.35	0.25
TX	0.99	0.97	0.87	0.82	0.90	0.96
AX	0.43	0.35	0.35	0.20	0.41	0.21
Q	31.5	36.4	36.8	34.2	32.6	29.6
A	68.5	61.1	54.6	57.3	60.2	70.4
P	0.0	2.5	8.6	8.5	7.2	0.0

Where: TX, Turbidity Index; AX, Alteration Index.

Table 3.1 continued

Sample	Glas Bheinn Mhor					Meall Buidhe
	Sk-307	Sk-309	Sk-310	Sk-311	Sk-312	Sk-322
Primary minerals						
Quartz	35.1	37.45	30.9	33.7	37.95	33.4
Clear alkali feldspar	0.8	1.1	2.15	0.7	1.35	1.9
Clear plagioclase	0.15	0.25	0.15	0.1	0.95	1.65
Olivine	0.0	0.0	0.95	0.0	0.0	0.0
Pyroxene	0.35	0.0	2.65	0.2	0.35	0.2
Amphibole	0.0	0.0	1.05	0.55	0.85	3.85
Biotite	2.15	0.85	0.35	4.85	0.0	1.15
Fe-Ti oxide	1.2	0.95	0.95	0.6	1.15	0.95
Zircon	tr.	0.15	0.05	0.25	tr.	0.05
Apatite	0.0	0.1	tr.	0.05	0.25	0.0
Secondary minerals						
Turbid alkali feldspar	52.65	54.55	58.4	56.60	52.85	51.75
Turbid plagioclase	4.95	3.85	1.9	0.65	2.75	3.85
Chlorite	1.25	0.3	0.35	0.05	0.0	0.9
Clay minerals	0.0	0.0	0.0	0.0	tr.	0.0
Epidote	tr.	0.45	0.0	0.0	1.05	0.15
Calcite	0.0	0.0	0.0	0.0	0.15	0.0
Muscovite	1.4	tr.	0.15	tr.	0.35	0.15
TX	0.98	0.98	0.96	0.99	0.96	0.94
AX	0.33	0.47	0.07	0.01	0.47	0.17
Q	37.5	38.5	33.0	36.7	39.6	36.1
A	57.1	57.3	64.8	62.5	56.5	58.0
P	5.4	4.2	2.2	0.8	3.9	5.90

Where: TX, Turbidity Index; AX, Alteration Index.

Table 3.1 continued

Sample	Southern Porphyritic					Raasay
	Sk-329	Sk-330	Sk-331	Sk-332	Sk-341	Ra-100
Primary minerals						
Quartz	21.05	24.1	38.9	26.3	36.75	34.5
Clear alkali feldspar	1.9	3.75	5.85	1.9	2.35	1.65
Clear plagioclase	0.0	0.0	0.0	0.0	0.0	0.0
Olivine	0.0	0.0	0.0	0.0	0.0	0.0
Pyroxene	0.0	0.0	0.0	0.0	0.0	0.7
Amphibole	0.0	0.0	0.65	0.0	0.0	0.0
Biotite	3.45	2.65	1.4	0.55	0.0	1.35
Fe-Ti oxide	1.75	1.5	3.85	2.35	0.8	0.8
Zircon	tr.	0.05	0.1	0.0	0.0	0.15
Apatite	tr.	0.0	0.0	0.0	0.0	0.05
Secondary minerals						
Turbid alkali feldspar	32.75	28.7	45.35	38.85	56.8	58.35
Turbid plagioclase	0.0	0.0	0.0	0.0	0.0	0.0
Chlorite	1.45	0.85	0.0	0.0	0.25	1.95
Clay minerals	0.0	0.0	0.0	0.0	0.0	0.0
Epidote	0.0	0.0	0.0	0.0	0.9	0.45
Calcite	0.0	0.0	0.0	0.0	0.0	0.0
Muscovite	0.0	0.0	0.0	0.0	0.0	0.05
Microlite groundmass	37.65	38.4	3.90	30.05	2.15	—
TX	0.95	0.88	0.89	0.95	0.96	0.97
AX	0.30	0.24	0.0	0.0	1.0	0.54
Q	37.8	42.6	43.2	39.2	38.3	36.5
A	62.2	57.4	56.8	60.8	61.7	63.5
P	0.0	0.0	0.0	0.0	0.0	0.00

Where: TX, Turbidity Index; AX, Alteration Index.

Table 3.1 continued

Sample	Northern Porphyritic Sk-320	Glen Sligachan Sk-328	Maol na Gainmhich Sk-319
Primary minerals			
Quartz	12.75	30.6	38.05
Clear alkali feldspar	2.55	0.85	2.75
Clear plagioclase	0.0	0.0	0.0
Olivine	0.0	0.0	0.0
Pyroxene	0.15	1.3	0.0
Amphibole	0.8	0.0	0.35
Biotite	0.0	0.0	0.2
Fe-Ti oxide	0.85	1.95	2.1
Zircon	0.05	0.15	0.1
Apatite	0.0	tr.	tr.
Secondary minerals			
Turbid alkali feldspar	28.7	63.8	55.8
Turbid plagioclase	0.0	0.0	0.0
Chlorite	1.35	0.4	0.0
Clay minerals	0.4	0.0	0.0
Epidote	0.0	0.35	0.0
Calcite	0.0	0.0	0.0
Muscovite	0.15	0.6	0.65
Groundmass	52.95	0.0	0.0
TX	0.92	0.99	0.97
AX	0.59	0.24	0.54
Q	29.0	32.1	39.4
A	71.0	67.9	60.6
0.0	0.0	0.0	0.00

Where: TX, Turbidity Index; AX, Alteration Index.

CHAPTER IV

MINERAL CHEMISTRY

4.1 Introduction

As discussed in Chapter III, the main rock-forming minerals of the Skye granites are: quartz, alkali feldspar, plagioclase, amphibole, pyroxene and biotite. In order to fully characterise their chemical compositions, an electron probe study has been carried out. In addition, the concentration of the rare-earth-elements (REE) have been determined from high purity mineral separates. Data are presented for four granites : Beinn an Dubhaich, Marsco, Loch Ainort and Glamaig.

4.2 Electron probe analyses

4.2.1 *Plagioclase*

Two types of plagioclase are recognised (Tables 4.1 and 4.2; Fig. 4.1):

(i) large, well-developed crystals, of relatively calcic plagioclase, present only in the Glamaig Granite (analyses 10-13, Table 4.2).

(ii) medium to large, well-developed crystals, mainly of oligoclase composition, in the Beinn an Dubhaich, Marsco and Glamaig granites. The compositions of these plagioclases within each of the three granites overlap, with An contents varying from around 2 to about 40 mol.% (i.e. albite-andesine), and the majority between 10 and 30 mol.% (i.e. oligoclase). Electron

probe data are presented in Tables 4.1 and 4.2.

Both types of plagioclase show slight normal zoning, with core compositions of around An_{35} and An_{20}, respectively. The Ab/An ratio of plagioclase from the Beinn an Dubhaich and Marsco granites are within the range of oligoclase, with only one analysed crystal having a core of andesine composition ($An_{35.95}$, analysis 3, Table 4.1). In contrast, plagioclase from the Glamaig Granite has a wide range in composition from albite through oligoclase to andesine (Table 4.2). The most calcic plagioclase in this granite is $An_{35.50}$ lying within the range of plagioclase compositions for the mafic inclusions within the Glamaig Granite (An_{22-45}, Thompson 1980). This compositional overlap may reflect the role played by the inclusions during the crystallisation of plagioclase in the Glamaig Granite and could be evidence in favour of the mixing of acid and intermediate magmas during the crystallisation of the Glamaig Granite (Thompson, 1980).

Other evidence which may support either mixing or assimilation processes, comes from the composition of a plagioclase grain from the Glamaig Granite which has a very low calcium content ($An_{1.97}$) compared with the rest of the analysed crystals, and may represent material incorporated into the magma from another magma or from the wall-rock (analysis of crystal 1(rim), Table 4.2).

The average Or content of the plagioclases in the Skye granites is <5mol %, i.e. within the range where Ab, An and Or components form a solid-solution (Deer et al., 1963a, 1989; Smith and Brown, 1988). However, a few plagioclase crystals contain > 5 mol.% Or, in the oligoclase-andesine range (Fig. 4.1) suggesting a limited submicroscopic antiperthite component (Deer et al., 1993).

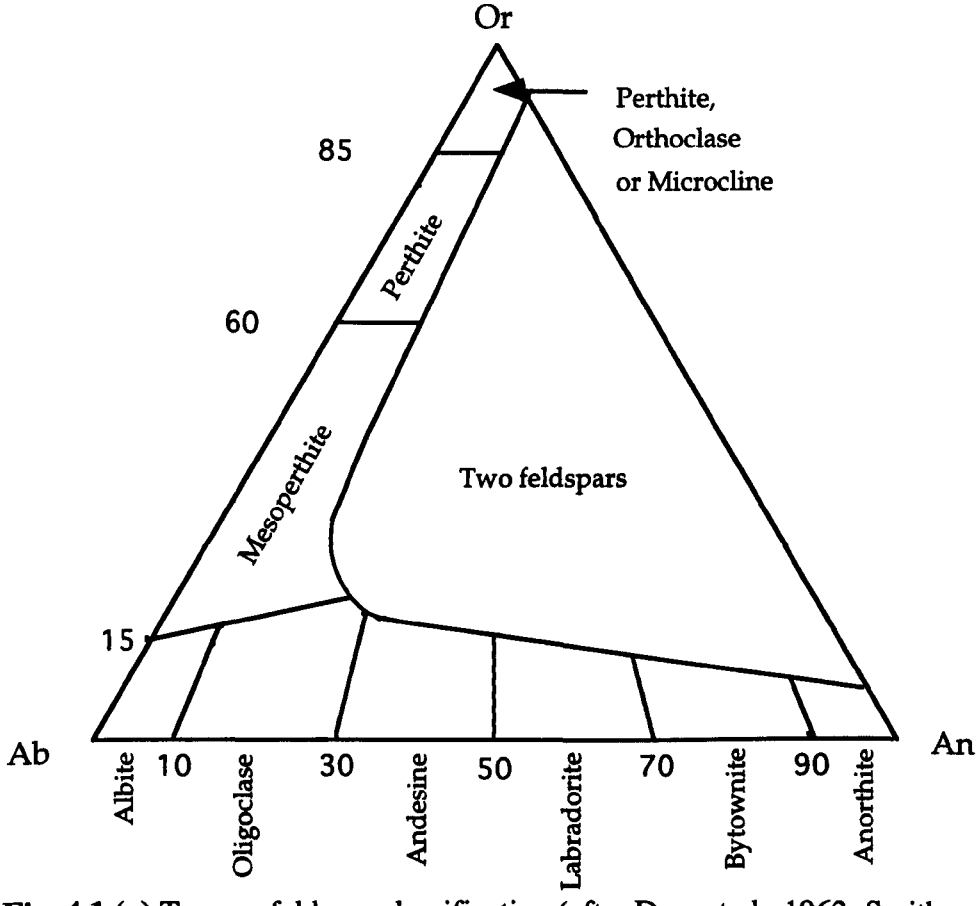

Fig. 4.1 (a) Ternary feldspar classification (after Deer et al., 1962; Smith and Brown, 1988).

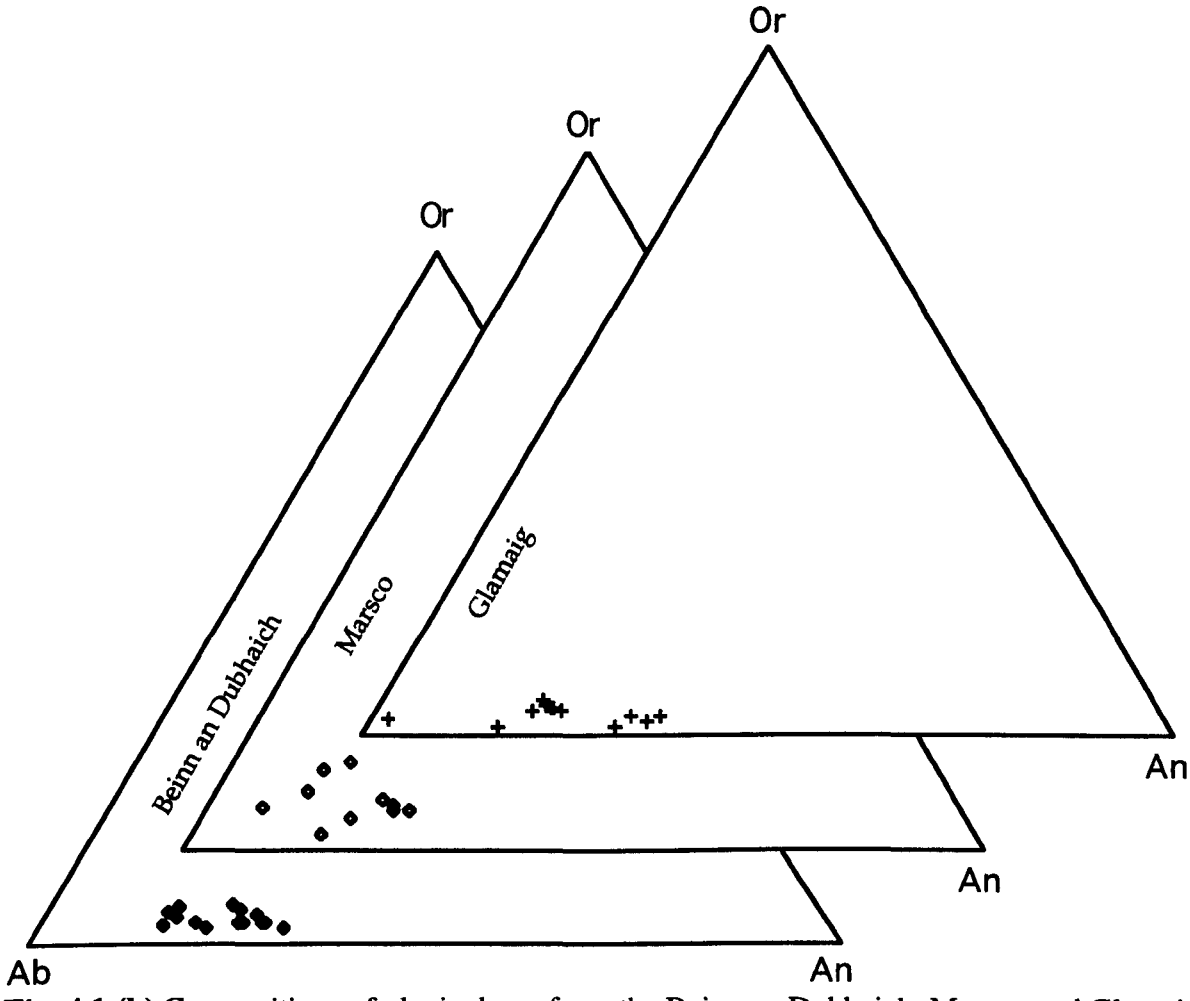

Fig. 4.1 (b) Compositions of plagioclases from the Beinn an Dubhaich, Marsco and Glamaig granites.

4.2.2 *Alkali feldspar*

In terms of crystal size and chemical composition, two different types of alkali feldspar are identified:

(i) fine to medium grain-size, with a lower proportion of perthite, and with a composition in the range Or_{20} to Or_{70}. Most of the analyses are predominantly of Or_{50} composition (Fig. 4.2) i.e. in the range of mesoperthite composition (Evangelakakis et al., 1993).

(ii) large megacrysts, usually perthite and chemically unzoned, with compositions around Or_{90}, lying in the perthitic orthoclase field (analysis of crystal 2(rim), Table 4.3; analyses of crystals 1, 2, 3, 4, 5 Table 4. 4; analysis of crystal 5(rim), Table 4.5; analyses 2(rim), 3(rim), crystal (5), 6(core), and 7(rim) Table 4. 6) (Fig. 4.2) according to the feldspar classification of Smith and Brown (1988).

Whereas type (ii) crystals are dominant in the Loch Ainort Granite, type (i) crystals occur in all Skye granites, i.e. Beinn an Dubhaich, Glamaig , Marsco and Loch Ainort. Electron probe data are presented in Tables 4.3-4.6

The An contents of both varieties of alkali feldspar are very small, i.e. less than 5 mol.%, within the range where Or, Ab and An form a solid-solution (Deer et al., 1963a, 1993). Type (i) show normal chemical zoning in only a few crystals from the Glamaig Granite and varies from a Na-rich ($Na_2O > K_2O$) core to a Na-poor ($Na_2O < K_2O$) rim.

The megacrysts of type (i) and some crystals of type (ii) are altered to a mixture of alkali feldspar and sericite.

Apart from K-Na exchange, there is no real difference in the analysed alkali feldspar of both types in terms of other elements such as Al, which, therefore, rules out any sort of elemental substitution. However, alkali feldspars of type

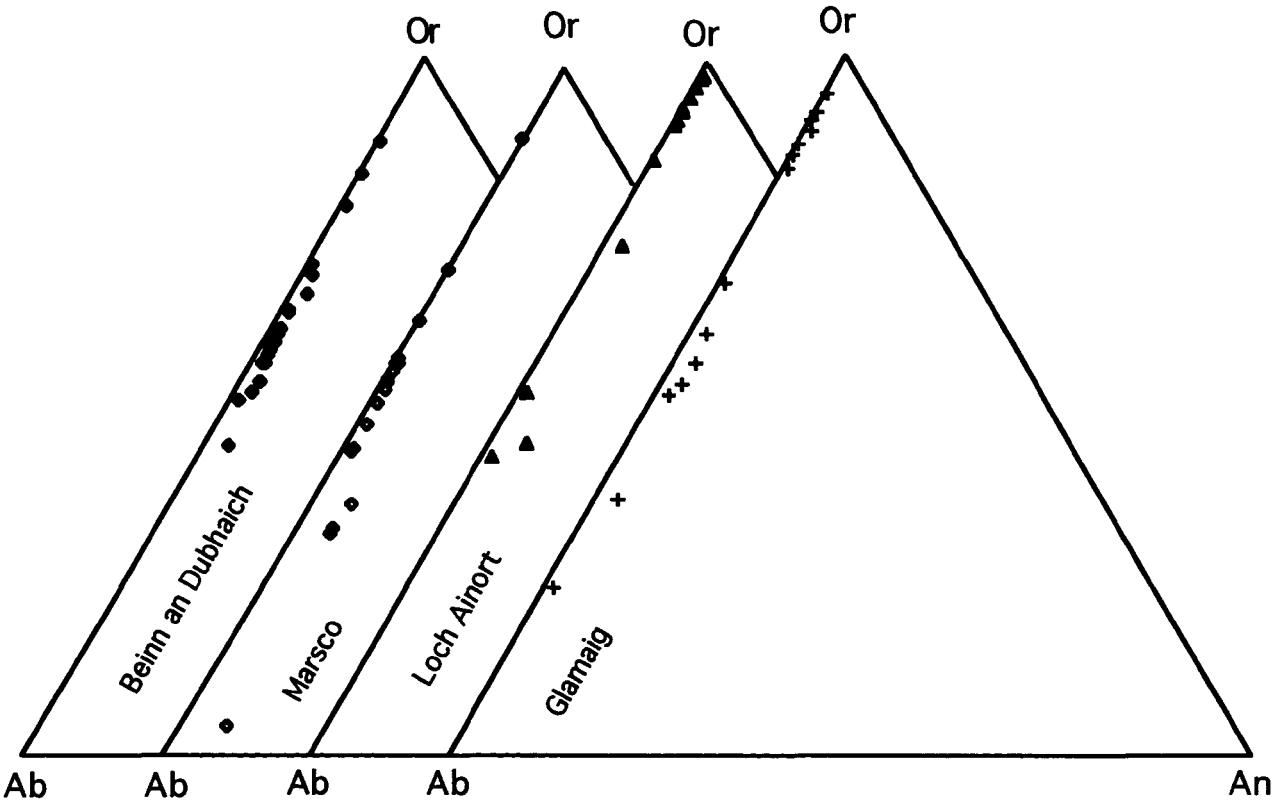

Fig. 4.2 Alkali feldspar compositions from the Beinn an Dubhaich, Marsco, Loch Ainort and Glamaig granites.

(i) have a somewhat lower concentration of K_2O and higher concentration of BaO compared to alkali feldspars of type (ii), despite the limited BaO content in general (<2 mol.%). This is explained by a more pronounced substitution of Ba^{2+} for K^+, since they are nearly identical in their ionic radii (Henderson, 1982).

Feldspar thermometry :

On the basis of the crystallisation of Skye granites at a pressure of about 500 bars (for example, Brown, 1963), the compositions of coexisting clear alkali feldspar and plagioclase were used to calculate feldspar temperatures from the Beinn an Dubhaich, Marsco and Glamaig granites. The compositions of cores and rims were used according to the calibration of Haselton et al. (1983) (see appendix I), which yields temperatures of 790-750°C for Beinn an Dubhaich, 964-825°C for Marsco and 881-771°C for Glamaig .

The temperatures recorded by cores from the three granites (i.e. 790, 964 and 881°C) may be very close or equal to crystallisation temperatures, whereas rim temperatures (i.e. 750, 825 and 771°C) more likely reflect the limited re-equilibration of coexisting alkali feldspar and plagioclase under subsolidus conditions (Ferry, 1985).

Coexisting feldspars from the Marsco Granite record a higher crystallisation temperature, indicating the more primitive nature of the magma, or possibly the incorporation of more primitive magma during the differentiation process(es).

4.2.3 *Amphibole*

Amphibole is commonly associated with other ferromagnesian minerals such as pyroxene and biotite, and with the accessory minerals apatite, zircon and Fe-

Ti oxides, often in mafic clots (see Chapter III). There is no detectable difference between cores and rims of amphibole crystals, or between different crystals within a single intrusion. Electron probe data are presented in Tables 4.7-4.9.

The crystallochemical formulae of amphiboles from the Beinn an Dubhaich, Loch Ainort and Glamaig granites are given in Tables 4.7-4.9. This formula was calculated on the basis of 24 oxygen atoms. By using the computer program of Spear and Kimball (1984), the proportions of Fe^{2+} and Fe^{3+} were also estimated.

All the amphibole formulas were calculated according to a standard formula recommended by Leake (1978), as follows:

$$A_{0-1}\, B_2\, C^{vi}{}_5\, T^{iv}{}_8\, O_{22}\, (OH, F, Cl)_2$$

where:

(i) T is summed to 8, using Si, Al, Cr^3, Fe^{3+}, and then Ti.

(ii) C is summed to 5 using the excess from (i), then Mg, and Fe^{2+}, and then Mn.

(iii) B is summed to 2 using the excess from (ii), then Ca, and then Na.

(iv) A is in the range between 0-1, using the excess from (iii), and then all K.

According to this formula all analysed amphiboles have $(Ca+Na)_B > 1.24$ and $Na_B < 0.67$, which indicates they belong to the calcic amphibole group (Leake, 1978). By taking $(Na+K)_A$, Ti, Fe^{3+} and Al^{vi} into consideration, the majority are ferro-edenite or ferro-edenitic hornblende (Fig. 4.3). In contrast, the amphibole in the Beinn an Dubhaich Granite is partially a hastingsitic hornblende. The variation in silica content of the amphiboles either within one intrusion or between different intrusions may reflect the change in silica activity of the

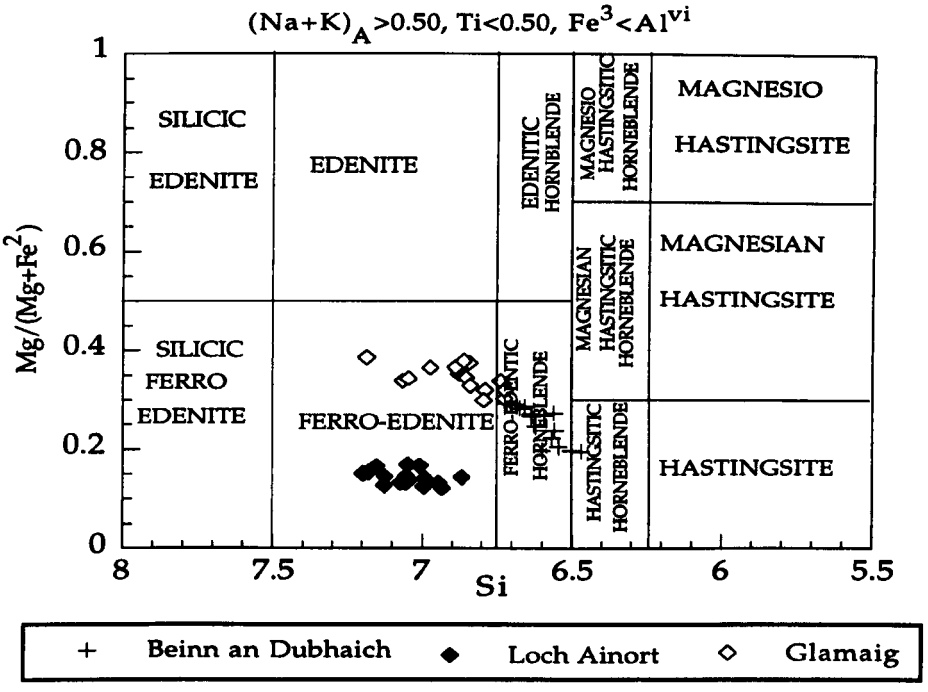

Fig. 4.3 Calcic amphiboles classification for the Beinn an Dubhaich, Loch Ainort and Glamaig granites, according to the scheme proposed by Leake (1978).

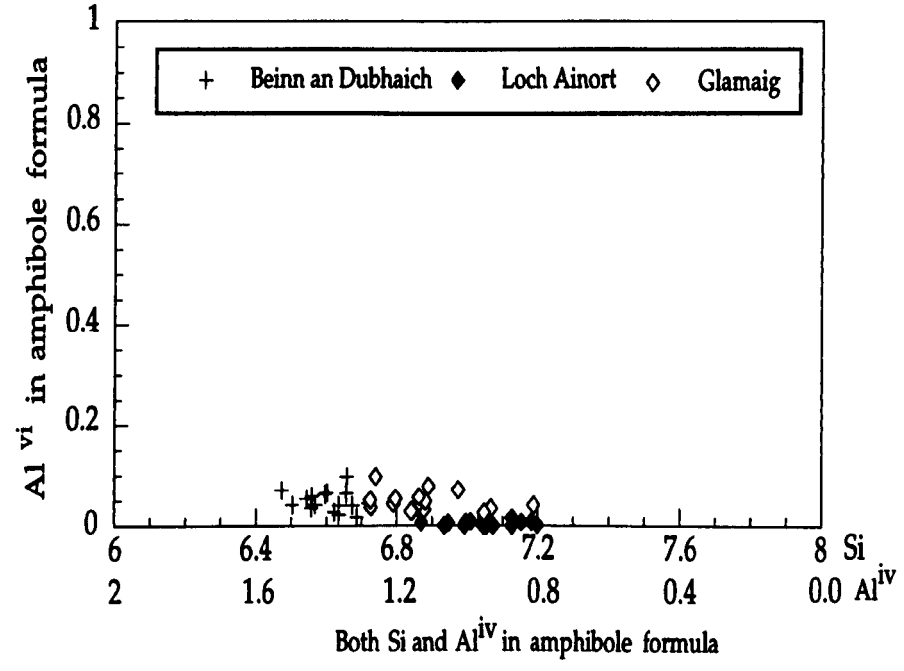

Fig. 4.4 Plot of Al^{vi} against Al^{iv} or Si for Skye granite amphiboles

magma(s) as they crystallised (Wones and Gilbert, 1982).

Leake (1971) demonstrated the relation between Al^{iv} and Si v Al^{vi}, and concluded that Al^{vi} usually increases with increasing Al^{iv} in calciferous amphiboles. However, he ruled out any opposite relation. Leake (1971) also deduced that the concentration of Al^{vi} is a function of rock composition and pressure of formation, with high pressure favouring high Al^{vi}. This relation is examined for amphiboles from the Skye granites (Fig. 4.4). The distribution of Al^{vi} in Loch Ainort amphiboles is relatively low and relatively uniform, whereas Al^{vi} in amphiboles from the Beinn an Dubhaich and Glamaig granites show higher values, up to 0.11. This cannot simply be attributed to differences in whole-rock composition, as amphiboles from the Beinn an Dubhaich Granite show higher Al^{vi} than amphiboles from the Loch Ainort Granite despite the lower whole-rock Al content of the Beinn an Dubhaich Granite (Sk-298 in Table 6.1) relative to the whole-rock Al content of the Loch Ainort Granite (Sk-313 , Table 6.1). Thus, on crystallographic grounds, Ghose (1965) and Cawthorn (1976) concluded that the M_2-sites in the amphibole structure with high Al^{vi} contents should tend to be relatively magnesium rich, because this site is filled with Al^{vi} instead of Fe^{2+}. This conclusion may explain the slight Al^{vi} and $Mg/(Mg+Fe^{2+})$ variations between the Loch Ainort and Beinn an Dubhaich amphiboles, (see Tables 4.7 and 4.8).

The overall uniform Al^{vi} contents in amphiboles either within single or different intrusions, in the range 0-0.11, strongly suggests their crystallisation at almost the same pressure and temperature conditions.

The Ti content of Skye granite amphiboles is in the range 0.07 to 0.2, and increases from Loch Ainort through Glamaig to Beinn an Dubhaich (Fig. 4.5). This variation in Ti content could be related to fluctuations in crystallisation temperature, oxygen fugacity and/or the composition of the granitic magma (Robinson et al., 1982; Gilbert et al., 1982; Wones and Gilbert, 1982). Thus, these

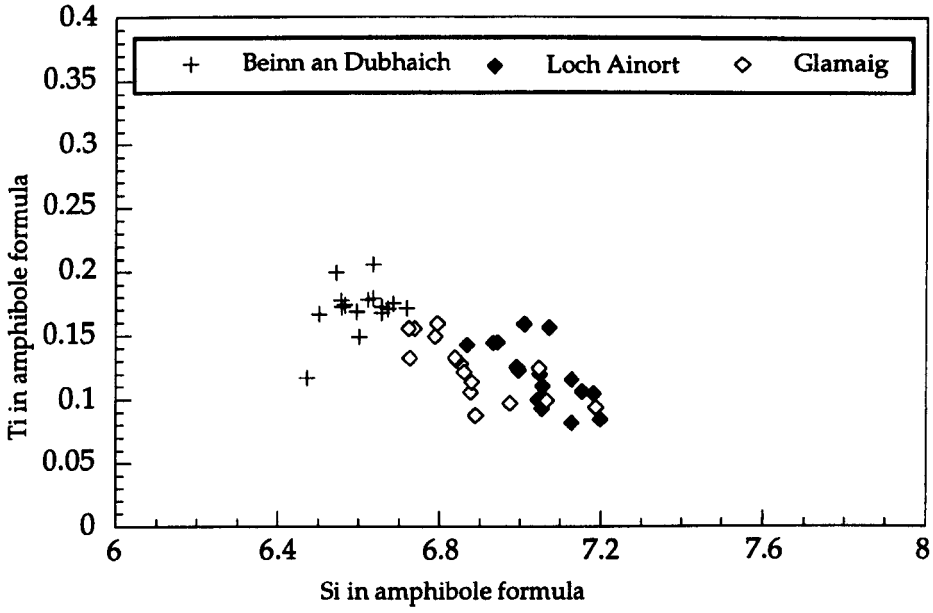

Fig. 4.5 Plot of Si against Ti for Skye granite amphiboles.

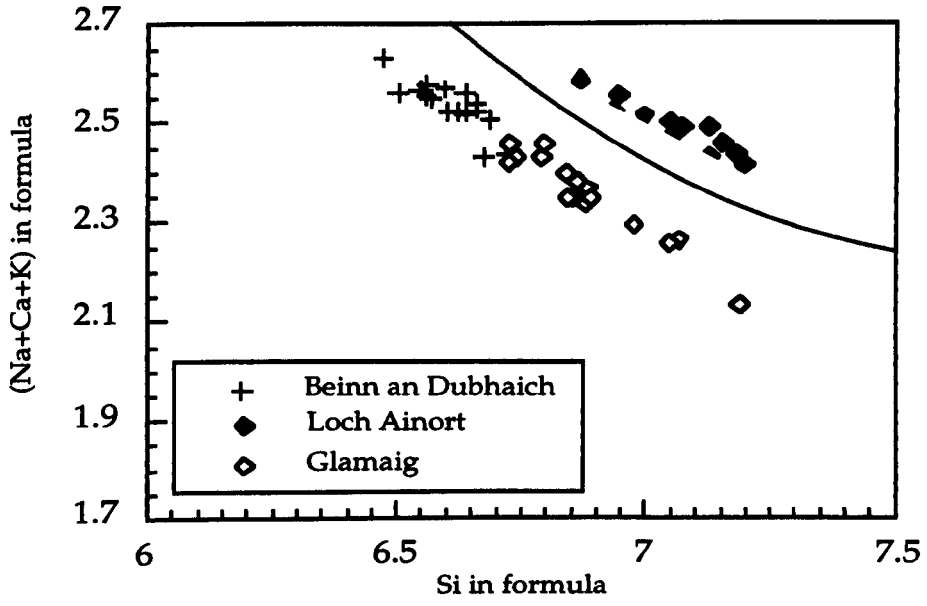

Fig. 4.6 Plot of Si against (Na+Ca+K) in amphibole formula for calcic amphiboles from the Loch Ainort, Glamaig and Beinn an Dubhaich granites. Curved line is the upper limit of igneous amphiboles as proposed by Leake (1971).

slight variations in Si, Ti and Al^{vi} contents of amphiboles from Skye granites are suggestive of different crystallisation temperatures; increasing in the order: Beinn an Dubhaich, Glamaig, Loch Ainort (Leake, 1971 and reference therein). This is in consistent with the crystallisation temperatures recorded by feldspar thermometry earlier (section 4.2.2), and can be explained by the incorporation of different primitive magma(s) during differentiation.

The (Na+Ca+K) content of Skye granite amphiboles is quite close to the curved line determined by Leake (1971) as the upper compositional limit of igneous amphiboles (Fig 4.6). The position of Loch Ainort amphibole above the limiting line is consistent with the assumption made by Leake (1971) (that the crystallisation of such amphibole occurs by the replacement of magmatic pyroxene at some temperature below the liquidus of the magma, as recorded by amphiboles from the Loch Ainort Granite, (see Chapter III).

The observed difference in (Na+Ca+K) values can be attributed to the variation in Na content, as the Ca content of calcic amphiboles is not sensitive to the CaO content of the parent magma, and the K content is unlikely to be affected by either temperature or pressure (Deer et al., 1963b; Cawthorn, 1976). On the other hand, Ca and K show uniform concentrations throughout (Tables 4.7-4.9) and appear to have been unaffected by hydrothermal processes (see Chapter VI), although Thompson (1976) reported different K contents between the core and rim of an alkali amphibole crystal, whereas the Na content may be affected by hydrothermal alteration (Ferry, 1985).

4.2.4 *Pyroxene*

Pyroxene is the dominant ferromagnesian mineral in the Marsco Granite, whereas only a few crystals were found as an inclusion in alkali feldspar in the Loch Ainort Granite. In order to evaluate aspects of the pyroxene chemistry,

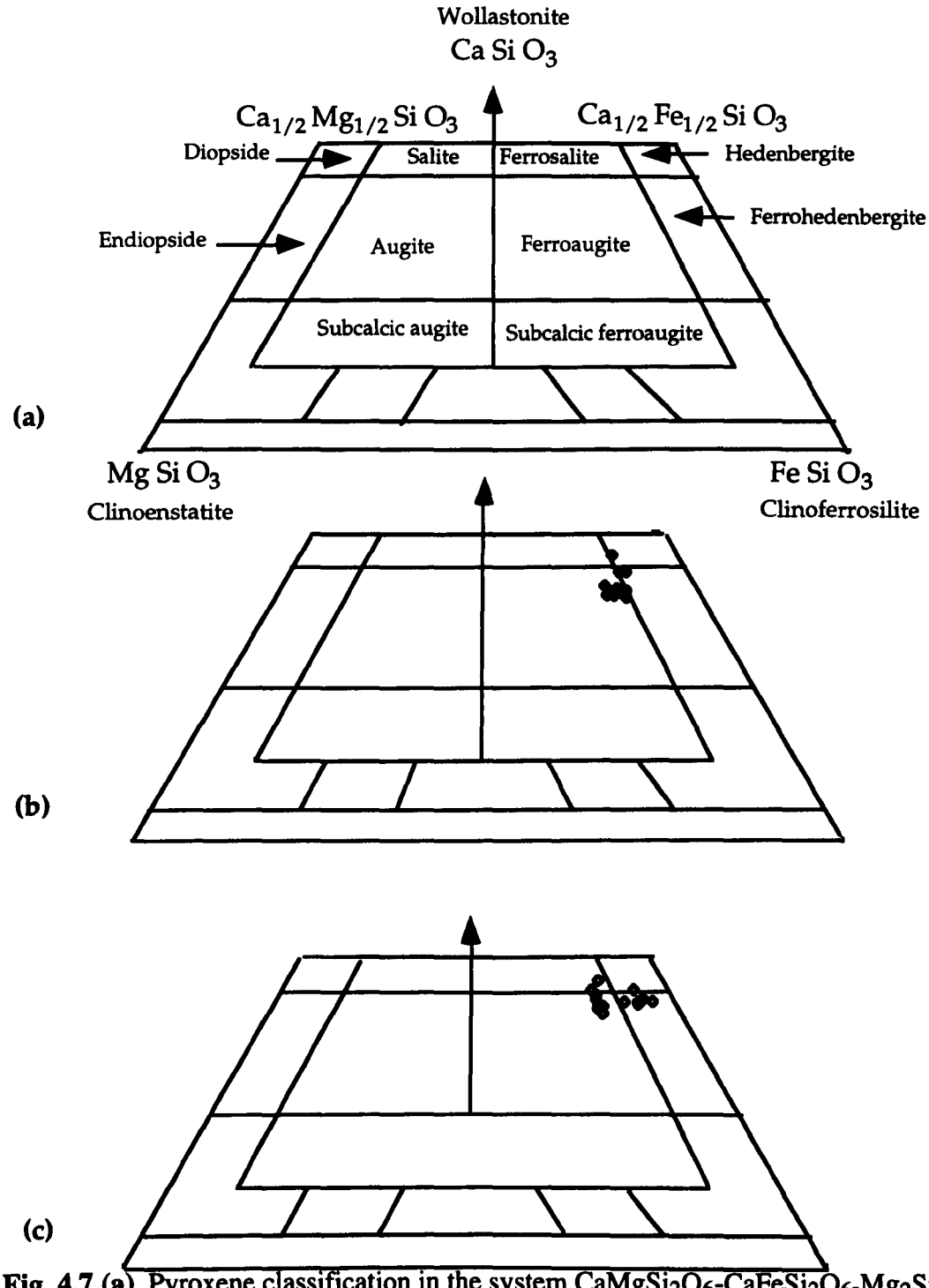

Fig. 4.7 (a) Pyroxene classification in the system $CaMgSi_2O_6$-$CaFeSi_2O_6$-$Mg_2Si_2O_6$-$Fe_2Si_2O_6$ (after Deer et al., 1989). **(b)** and **(c)** are pyroxene compositions from the Loch Ainort and Marsco granites, respectively.

recalculation of the electron probe data were made, and are presented in Tables 4.10 and 4.11.

The general formula for pyroxene can be represented as $XZYO_6$, where X represents Na, Ca, Mn, Fe^{2+}, Mg, and Li in the M_2 site, Z represents Mn, Fe^{2+}, Mg, Fe^{3+}, Al, Cr, and Ti in M_1 site, and Y represents Si and Al (Deer et al., 1963b, 1978). Accordingly, Skye granite pyroxenes can be classified as being calcic since Ca occupies more than two-thirds of the M_2 site (Deer et al., 1978; Cameron and Papike, 1982).

No significant differences were detected within individual crystals or even within a single intrusion, in terms of the major cations i.e. Mg, Fe^{2+} Fe^{3+} and Ca. Since the Skye granite pyroxenes do not contain any significant amounts of cations other than Mg, Fe^{2+}, Fe^{3+} and Ca, (Tables 4.10 and 4.11), they can be considered as members of the four component system: $CaMgSi_2O_6$-$CaFeSi_2O_6$-$Mg_2Si_2O_6$-$Fe_2Si_2O_6$ (Fig.4.7, Deer et al., 1978). All analysed crystals plot in the hedenbergite, ferrohedenbergite and ferro-augite fields.

Fig. 4.8 shows the relationship between Ca (atomic) and Fe*, where Fe* = atomic Fe^{2+}/ (Fe^{2+} +Mg). This plot illustrates the considerable variation in Ca in the Loch Ainort pyroxenes within a very small range of Fe*(0.78-0.83), in contrast to the greater variation in Marsco pyroxene Fe* within a narrow range of atomic Ca. The relatively small ranges of both Ca and Fe* in Skye granite pyroxenes can be explained in terms of fluctuations in temperature during their crystallisation; the highest Fe* values in the Marsco pyroxenes possibly reflect the high Fe content of the Marsco granite magma (Papike, 1982).

The overall uniform Ca, Mg, Fe^{2+} contents in Skye granite pyroxenes (0.76-0.88, 0.06-0.24 and 0.79-0.97, respectively) suggest similar temperatures and pressures during their period of crystallisation. The Fe^{3+} contents are also uniform and very low, most likely reflecting the lower oxygen fugacities that

obtained during the intrusion of the parent granite magma (Papike, 1982).

4.2.5 *Biotite*

Biotite is present only in the Beinn an Dubhaich Granite. It is absent in the Loch Ainort and Marsco granites and has been completely replaced by chlorite in the Glamaig Granite. It occurs as irregular, highly pleochroic flakes, usually associated with amphibole in mafic clots. Electron probe data are presented in Table 4.12.

The crystallochemical formulas were calculated on the basis of 24 oxygen (OH, F, Cl) atoms, dependent on the availability of volatile components. The Al contents were taken as total since the assumption that $Si + Al^{IV} = 8$ was used, with no Al left for Al^{VI} because $Si + Al^{IV} < 8$ (see Table 4.12). This may be due to a shortage of silica in the biotites which is consistent with the enrichment of host-rock with silica (73 wt.%), since the silica content of biotite decreases with increasing silica of host rock (De Albuquerque, 1973; Czamanske, 1981).

Skye granite biotites are members of the phlogopite-annite solid-solution series, as illustrated in Fig.4.9 on the phlogopite-annite-sider0phyllite-eastonite quadrilateral.

The Beinn an Dubhaich biotites have uniform $Fe^{2+}/(Fe^{2+} + Mg)$ (Fig. 4.9). This can be explained either by the crystallisation of all biotite at constant oxygen fugacity and temperature, or that all biotite compositions have re-equilibrated under the same conditions during a uniform post-crystallisation event (Speer, 1982). The observed slight variations in Fe^{2+} : Mg ratio may be attributed to the time of biotite formation (Deer et al., 1962).

Brigatti and Gregnanin (1987) and Deer et al. (1989) reported that the $Mg/(Mg + Fe^{2+})$ ratio in biotites decreases as the silica content of the parent magma

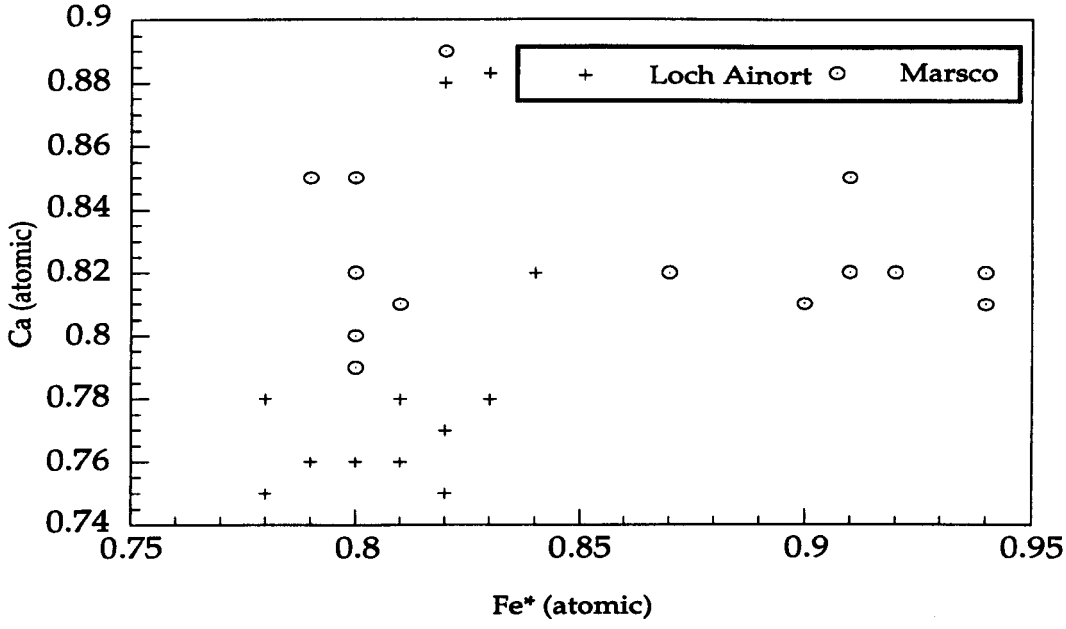

Fig. 4.8 Plot of Ca (atomic) against Fe* for pyroxenes in Skye granites, where Fe*= atomic $Fe^{2+}/(Fe^{2+} + Mg)$.

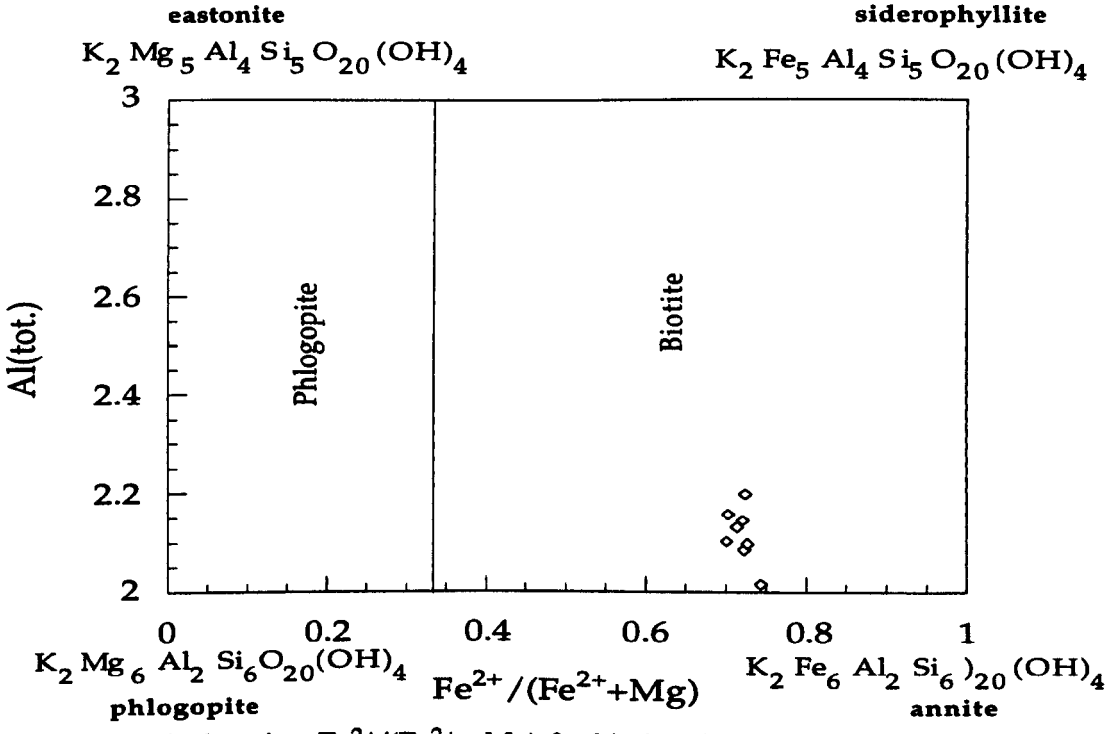

Fig. 4.9 Plot of Al against $Fe^{2+}/(Fe^{2+}+ Mg)$ for biotites from the Beinn an Dubhaich Granite, projected onto the phlogopite-annite-eastonite-siderophyllite quadrilateral .

increases, although this ratio is highly variable in granites. Albuquerque (1973) noted an inverse correlation between Si content of biotites and the Si content of the host-rock, together with a positive correlation between the amount of Al and Fe in biotites and the Si content of the parent magma. Thus, the observed variation within biotite crystals from the Beinn an Dubhaich Granite, in terms of their Al contents, can be explained by crystallisation of these crystals from the same magma under the same conditions, but at relatively different times (i.e early and later biotites) (Brigatti and Gregnanin, 1987; Deer et al., 1989).

4.2.6 *Olivine*

Fresh olivine is a rare phase in the Marsco Granite. Satisfactory analyses were not obtained, although Thompson (1969) reports compositions which are almost of pure fayalite.

4.2.7 *Fe-Ti oxides*

Due to the complexities of exsolution upon cooling, this study has not examined in detail the composition of the Fe-Ti oxides. Detail of the composition of Fe-Ti oxides are reported by Ferry (1985) in which he confirmed that Skye granites contains both ilmenite and magnetite.

4.3 Rare-earth-element (REE) concentrations of minerals

The REE are commonly regarded as immobile elements during alteration processes (Rollinson, 1993), thus their distribution among the rock-forming minerals may produce valuable information on rock petrogenesis. The REE geochemistry of accessory apatite and zircon, and the other main minerals:

amphibole, pyroxene, plagioclase and alkali feldspar, together with whole rock data for the Beinn an Dubhaich, Marsco, Loch Ainort and Glamaig granites has been investigated using inductively coupled plasma mass spectrometric technique (ICP-MS).

To investigate REE concentrations and their relative fractionations, data are typically normalised to a common reference standard. Because chondritic meteorites are thought to be relatively unfractionated samples of the Solar System, they have been recommended for this purpose by several authors (for example, Nakamura, 1974; Thompson, 1982; Rollinson, 1993). Chondrite abundances used in this study were taken from Nakamura (1974) and Potts et al. (1981), which comprise data from ten ordinary chondrites.

The REE abundances of appropriate whole rock are presented in Table 6.2, whereas their component minerals are presented in Tables 4.13-4.14. However, all REE concentrations are plotted as normalised values against atomic number in Figs. 4.10, 4.11, 4.12 and 4.13.

The values of normalised REE data are in the range 1-10^4, reflecting crystal-chemical control on the distribution of these elements in Skye granites. The REE concentrations of amphibole, pyroxene, apatite, Eu in plagioclase and alkali feldspar, and Yb, Lu and Tm in zircon are much higher than the whole -rock concentrations. Both alkali feldspar and plagioclase have very similar patterns with slight enrichment of the light rare-earth-elements (LREE) relative to the heavy rare-earth-elements (HREE), with large positive Eu anomalies ($Eu/Eu^* > 1$) observed in both feldspars in the Beinn an Dubhaich and Glamaig granites. In contrast, smaller positive Eu anomalies are recorded in the (single) alkali feldspar granites (Marsco and Loch Ainort).

Zircon patterns are very similar in all granites (Fig. 4.16), in their slight enrichment in the MREE-HREE (Gd-Yb), and inconsistent concentration of the

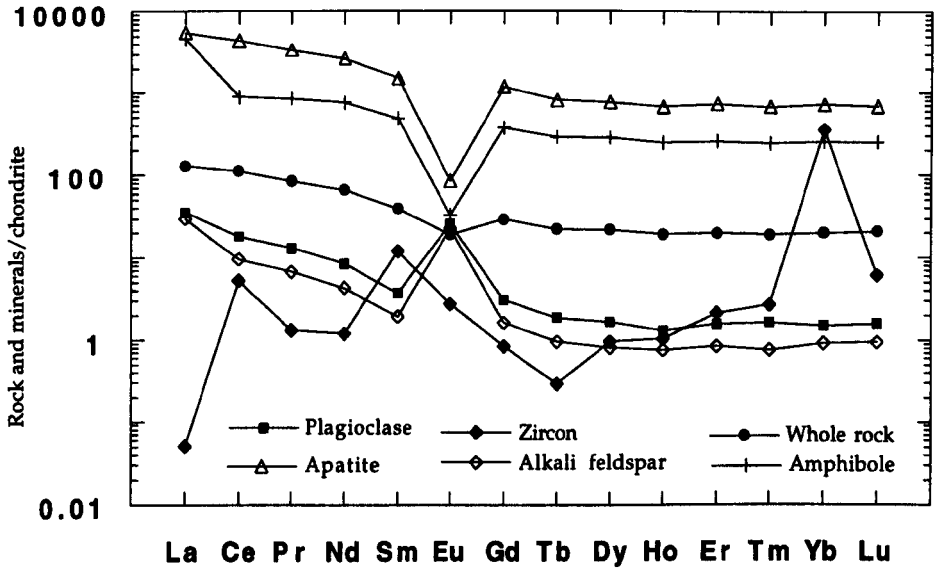

Figure 4.10 Chondrite-normalized REE patterns of whole-rock and minerals in the Beinn an Dubhaich Granite (Sample SK-300).

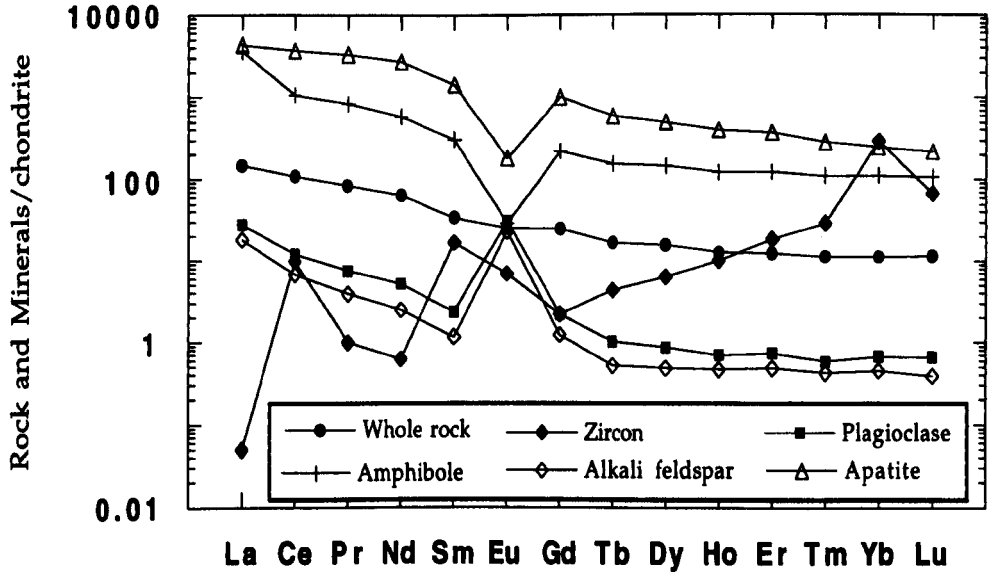

Figure 4.11.Chondrite-normalized REE patterns of whole-rock and minerals in the Glamaig Granite (Sample SK-326).

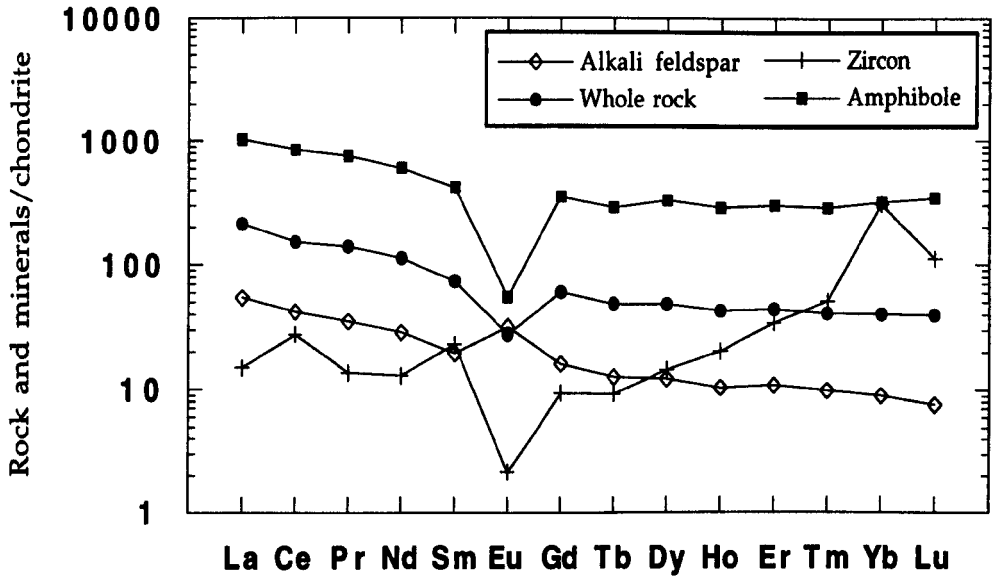

Fig. 4.12. Plot of chondrite normalized REE patterns of whole rock and minerals in the Loch Ainort Granite (Sample SK-313).

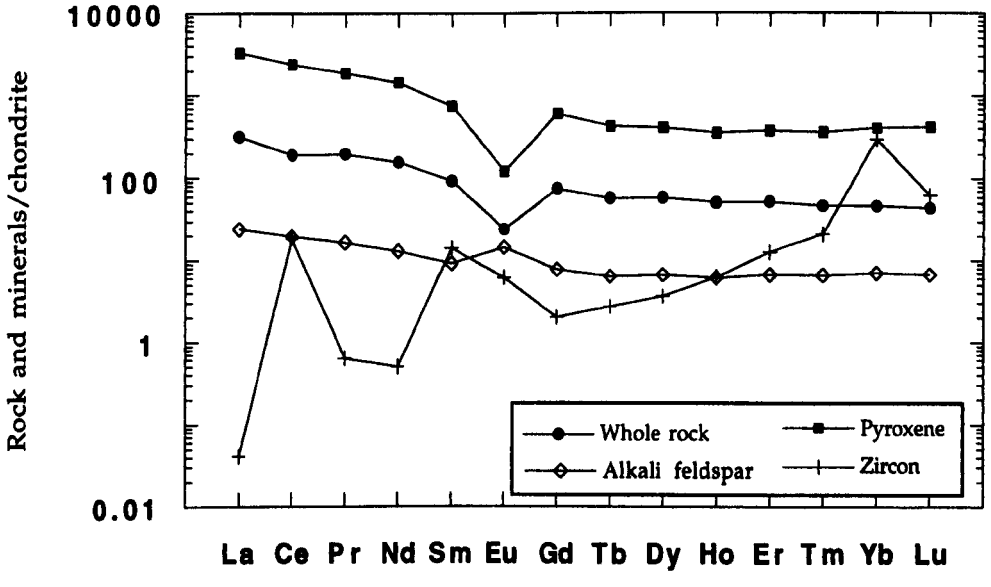

Figure 4.13 Chondrite-normalized REE patterns of whole-rock and minerals in the Marsco Granite (Sample SK-334).

LREE and Lu, which may be due to alteration, or the presence of apatite inclusions (Hinton and Upton, 1991). Loch Ainort zircons show a negative Eu anomaly ($Eu/Eu^* = 0.15$).

The major phases amphibole and pyroxene, along with the accessory phase apatite, show uniformly enriched patterns relative to whole-rock values, with the greatest REE concentrations recorded from the apatite. Apatite has a significant negative Eu anomaly (Fig. 4. 15), with Eu/Eu^* in the range 0.064-0.15. These three phases are recognised as the major hosts for the REE in Skye granites. Their REE enrichment may have had significant controls on the REE concentration and distribution in residual melts during crystallisation .

From a consideration of mineral REE pattern shapes and absolute abundances, the following discussion concentrates on each mineral, to evaluate any information related to the REE contents and their variation over the crystallisation period.

(i) Alkali feldspar and plagioclase. Since these two phases share similar chemical characters, and possess very similar REE patterns, it is useful to deal with them together. Both REE patterns are similar to those for the whole-rock, but with lower concentrations. The alkali feldspar contains an overall lower concentration of the REE relative to plagioclase. Both feldspars have higher Eu concentrations than the whole-rock. The whole-rocks record negative Eu anomalies, whereas both the alkali feldspar and the plagioclase show large positive Eu anomalies ($=Eu/Eu^* = Eu_N/\sqrt{(Sm_N * Gd_N)}$, Taylor and Mclennan, 1985). The smaller positive Eu anomalies recorded for the alkali feldspar from granites with a single feldspar (Loch Ainort (1.8) and Marsco (1.7)), contrast with the alkali feldspars which coexist with plagioclase in the Beinn an Dubhaich and Glamaig granites: the former has positive Eu anomalies of 12.82 and 7.63, respectively, whereas the latter has positive Eu anomalies of 19.41 and 13.84, respectively. In the two feldspar granites the whole-rock shows

a smaller negative Eu anomaly relative to the single feldspar granites. These differences between the two types of granite suggest that the Eu anomalies in the whole-rocks are chiefly controlled by the removal of plagioclase feldspar from the original melt by crystal fractionation, or accumulation as a residue by some form of partial melting process (for example, Skjerlie, 1992; Rollinson, 1993). The observed low concentration of the REE in the feldspars may in part be due to the crystallisation of an early REE-rich phase such as amphibole or pyroxene, and implies that the crystallisation of the feldspar was from a melt with REE contents the same or lower than that of the their whole rocks (Gromet and Silver, 1983).

(ii) Amphibole and Pyroxene. Consideration of the compositional and structural similarity of pyroxene and amphibole (for example, Rollinson, 1993), suggests that these two phases may be examined together (Fig. 4.14). The only granite which contains pyroxene is Marsco, whereas the other granites contain only amphibole. All the amphibole and the pyroxene have similar patterns, but with more enrichment of the LREE in the pyroxene and greater depletion of the HREE in the Glamaig amphibole. In general, this similarity in mineral patterns shape, together with similar whole-rock patterns (Figs. 4.10- 4.13) are suggestive of similar origins for these granites (Gromet and Silver, 1983). The D_{Ce}/D_{Yb} ratios for the amphiboles (where, $D_{Ce}/D_{Yb} = (Ce/Yb)_{N\ amphibole})/(Ce/Yb)_{N\ rock}$), from the Beinn an Dubhaich, Loch Ainort and Glamaig granites are 0.62, 0.70 and 1.00, respectively; this indicates a decrease in $(Ce/Yb)_N$ in the amphiboles relative to their host rocks from the more primitive (Glamaig) granite towards the more evolved (Beinn an Dubhaich) granite (see Chapter VI), suggesting that the fractionation of amphibole caused the $(Ce/Yb)_N$ to increase in the remaining melt, i.e. Ce increased relative to Yb, possibly due to the association of Yb-rich phases with early-crystallising amphiboles such as zircon (see Fig. 4.16).

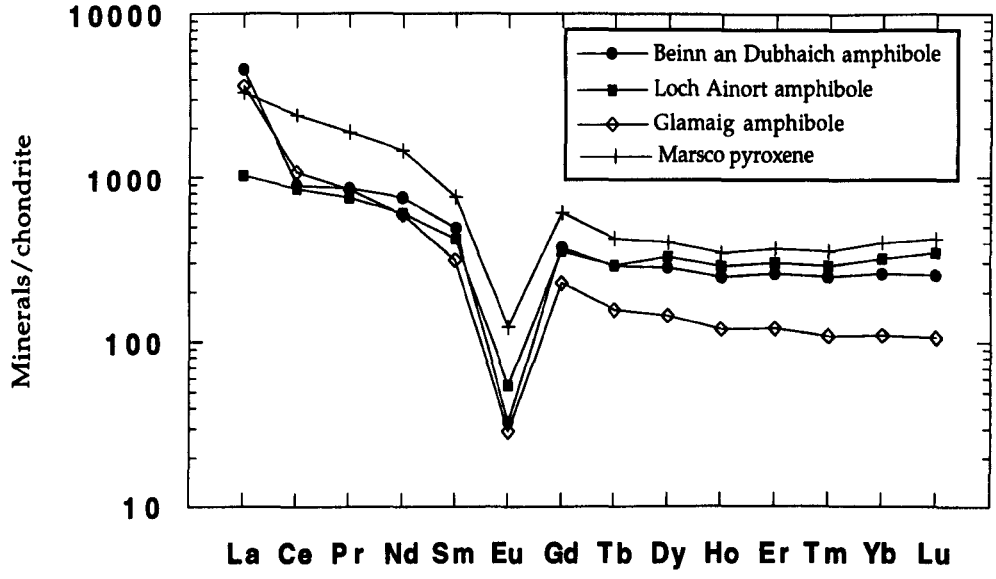

Figure 4.14 Plot of chondrite-normalized REE patterns of amphiboles and pyroxenes in Skye granites.

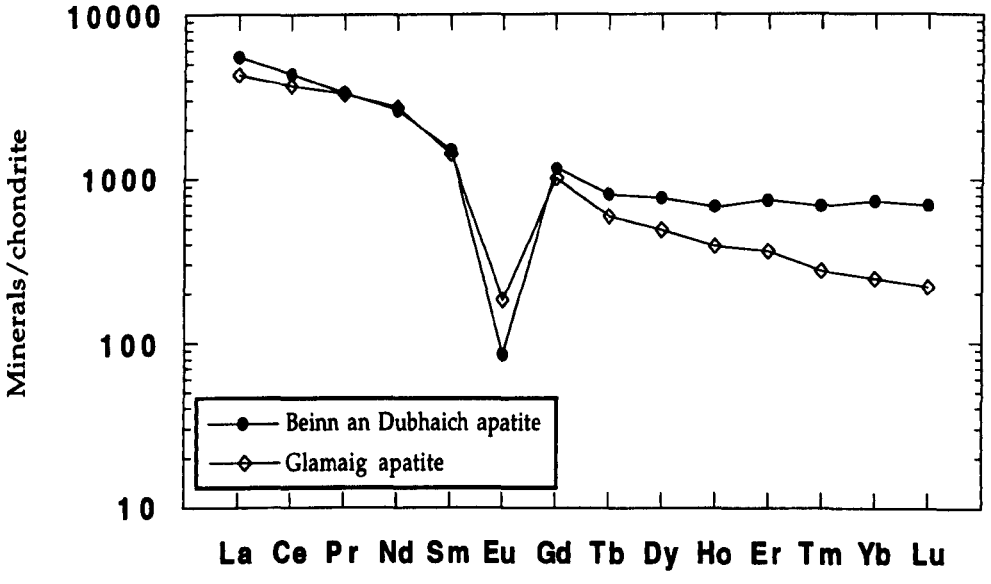

Figure 4.15 Plot of chondrite-normalized REE patterns of apatites in Skye granites.

The observed enrichment of the LREE relative to the HREE in amphibole and pyroxene normalised values compared to the whole-rock data also suggests the early removal or crystallisation of HREE-rich phases such as zircon as differentiation process proceeded.

(iii) Apatite. REE-normalised values for apatites from the Beinn an Dubhaich and Glamaig granites are presented in Fig. 4.15. Both apatites show similar REE patterns, with a greater enrichment in Beinn an Dubhaich in almost all of the REE, and the HREE in particular. The relative depletion of the HREE in the Glamaig apatite may be an indication of the crystallisation and fractionation of early zircon. The apatite patterns show large negative Eu anomalies suggesting that the crystallisation of these apatites occurred after the crystallisation of plagioclase (Nagasawa, 1970). Nagasawa's work yields a D_{Ce}/D_{Yb} ratio for apatite of 1.45; in this study the Beinn an Dubhaich and Glamaig apatites yield values of 1.07 and 1.54, respectively (where $D_{Ce}/D_{Yb} = (Ce/Yb)_{N\ apatite})/(Ce/Yb)_{N\ rock}$), These higher $(Ce/Yb)_N$ values in apatites relative to their host rocks indicate that crystal fractionation of apatite from Skye granite magmas would have lowered the $(Ce/Yb)_N$ of the remaining melt (Exley, 1980).

(iv) Zircon. Data from the four granites are shown in Fig. 4.16. The observed REE patterns reflecting some element anomalies such as Ce, Sm and Lu (Gromet and Silver, 1983). The source of such anomalies is unclear, and possibly due to either analytical problem or these zircon are not completely magmatic(i.e. contain restite zircon) Gromet and Silver (1983), such inherited zircons are evident in Skye granites as accessory minerals investigation reveal (Chapter VIII). The uniform whole-rock-normalised REE for these granites, together with the low REE concentrations of their zircons, and the modal abundance data (Table 3.1) of these zircons, are consistent with the conclusions of Thorpe et al. (1977) and Exley (1980) that the fractionation of zircon does not

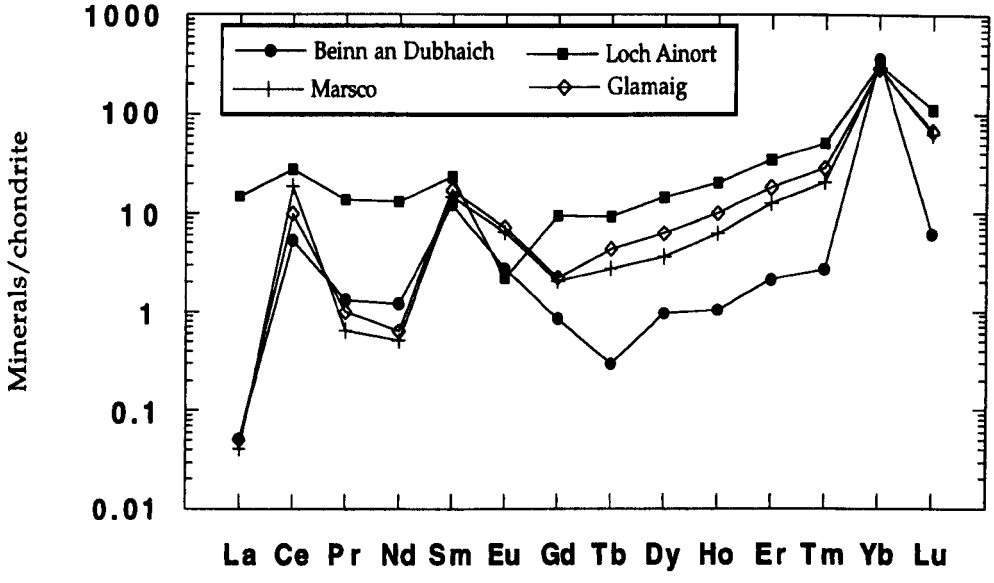

Figure 4.16 Plot of chondrite-normalized REE patterns of zircons in Skye granites.

greatly affect the observed whole-rock REE patterns of the Skye granites. All four zircon patterns are very similar, suggesting that zircons of similar compositional characteristics were crystallised from or incorporated into the Skye granite magmas. Only in the Loch Ainort Granite does the zircon have a negative Eu anomaly, although smaller than that for the coexisting apatite, suggesting that it crystallised prior to the crystallisation of apatite and alkali feldspar (Nagasawa, 1970). Despite their low REE concentrations, Skye granite zircons show HREE-enrichment relative to the LREE, with $(Ce/Yb)_N$ in range 0.015-.09, which is consistent with the electron probe data presented by Exley (1980).

4. 4 Summary and conclusions

From the electron probe analyses and rare-earth-element concentrations of the main and accessory minerals, the following conclusions are made:

(i) Plagioclase compositions in the Glamaig Granite are clearly related to the plagioclase in the associated mafic inclusions (Thompson, 1980).

(ii) The difference in crystallisation temperatures indicated by feldspar thermometry and variations in Si, Ti, and Al^{vi} contents of amphiboles, suggests the independent crystallisation of each granite, or alternatively the incorporation of different amounts of primitive magma (probably with different Ca contents) into each granite during differentiation process(es).

(iii) The low concentration of Fe^{3+} in pyroxene along with the slight variations in Fe^{2+}: Mg ratio of biotite, suggest re-equilibration during a slow cooling history (Papike, 1982; Brigatti and Gregnanin, 1987).

(iv) The smaller negative Eu anomalies for whole rock samples of the two feldspar granites (Beinn an Dubhaich and Glamaig) relative to the signatures

from the single feldspar granites (Loch Ainort and Marsco) demonstrate clearly the important role played by plagioclase fractionation during the evolution of Skye granites.

(v) Rare-earth-element data show that amphibole, pyroxene and apatite are the most important reservoirs for the REE in Skye granites.

(vi) The effect of crystallisation and fractionation of Skye granite minerals on the REE pattern of the residual magmas increases in the order: zircon, alkali feldspar, plagioclase, apatite, and amphibole or pyroxene.

(vii) The REE patterns of zircons are completely inconsistent when compared with the whole rock data and suggest the presence of a restite zircon component in the granites.

(viii) The high crystallisation temperatures recorded for Skye granites by feldspar thermometry (800-950°C, see Section 4. 2. 2), and the incorporation of possible restite zircons indicate the dual importance of mantle-derived materials and crustal components in the origin of the granites.

Table 4-1 Electron probe analyses of plagioclase from the Beinn an Dubhaich Granite

	Beinn an Dubhaich Plagioclase							
Crystal	1(core)	1(rim)	2(rim)	2(core)	3(core)	3(rim)	4(rim)	4(core)
SiO_2	60.24	60.87	60.97	60.96	62.49	64.07	64.75	63.54
TiO_2	0.00	0.00	0.50	0.041	0.00	0.00	0.00	0.02
Al_2O_3	24.90	24.82	24.46	24.39	23.67	22.51	22.11	22.85
MgO	0.00	0.00	0.00	0.00	0.00	0.00	0.00	0.00
CaO	6.19	5.56	5.38	5.64	4.16	3.20	2.98	3.35
MnO	0.00	0.00	0.00	0.00	0.00	0.00	0.00	0.00
FeO	0.28	0.25	0.29	0.25	0.17	0.16	0.06	0.15
SrO	0.00	0.00	0.00	0.00	0.00	0.00	0.00	0.00
BaO	0.02	0.03	0.10	0.10	0.03	0.00	0.00	0.02
Na_2O	7.61	7.91	8.02	7.85	8.60	8.85	9.80	9.16
K_2O	0.33	0.46	0.67	0.46	0.30	0.86	0.69	0.59
Total	99.57	99.91	99.92	99.69	99.42	99.64	99.68	99.68
Si	2.693	2.709	2.718	2.720	2.778	2.838	2.861	2.816
Ti	0.00	0.00	0.002	0.001	0.00	0.00	0.00	0.001
Al	1.312	1.302	1.285	1.283	1.240	1.175	1.151	1.194
Mg	0.00	0.00	0.00	0.00	0.00	0.00	0.00	0.00
Ca	0.297	0.265	0.257	0.270	0.198	0.152	0.141	0.159
Mn	0.00	0.00	0.00	0.00	0.00	0.00	0.00	0.00
Fe	0.010	0.009	0.011	0.009	0.006	0.006	0.002	0.006
Sr	0.00	0.00	0.00	0.00	0.00	0.00	0.00	0.00
Ba	0.00	0.001	0.002	0.002	0.00	0.00	0.00	0.00
Na	0.660	0.683	0.693	0.679	0.741	0.760	0.778	0.787
K	0.019	0.026	0.038	0.026	0.017	0.048	0.039	0.033
Total	4.991	4.994	5.004	4.990	4.981	4.979	4.972	4.997
Ab	67.62	70.05	70.03	69.52	77.45	79.17	81.22	80.32
Or	1.94	2.66	3.85	2.68	1.79	5.04	4.04	3.39
An	30.40	27.23	35.95	27.62	20.72	15.79	14.73	16.25
Cs	0.04	0.06	0.17	0.18	0.04	0.00	0.01	0.04

Table 4.1 continued

	Beinn an Dubhaich Plagioclase						
Crystal	5(core)	5(rim)	6(core)	6(rim)	7(core)	7(rim)	7(rim)
SiO_2	61.641	61.43	61.90	62.65	61.43	62.08	64.20
TiO_2	0.03	0.00	0.06	0.02	0.00	0.00	0.00
Al_2O_3	24.32	24.78	23.75	23.54	24.79	23.97	23.07
MgO	0.00	0.00	0.00	0.001	0.00	0.00	0.001
CaO	4.91	5.10	4.77	3.90	5.02	4.49	3.02
MnO	0.00	0.00	0.00	0.00	0.00	0.00	0.00
FeO	0.18	0.22	0.24	0.12	0.21	0.20	0.18
SrO	0.00	0.00	0.00	0.00	0.00	0.00	0.00
BaO	0.06	0.03	0.12	0.03	0.03	0.10	0.03
Na_2O	8.07	8.17	7.99	8.84	8.38	7.96	9.12
K_2O	0.047	0.442	0.771	0.423	0.450	0.906	0.346
Total	99.69	100.17	99.58	99.51	100.31	99.69	100.01
Si	2.741	2.722	2.759	2.784	2.720	2.762	2.827
Ti	0.001	0.00	0.002	0.001	0.00	0.00	0.001
Al	1.275	1.294	1.248	1.233	1.294	1.257	1.197
Mg	0.00	0.00	0.00	0.00	0.00	0.00	0.00
Ca	0.234	0.242	0.228	0.186	0.238	0.214	0.143
Mn	0.00	0.00	0.00	0.00	0.00	0.00	0.00
Fe	0.007	0.008	0.009	0.004	0.008	0.007	0.007
Sr	0.00	0.00	0.00	0.00	0.00	0.00	0.00
Ba	0.001	0.001	0.002	0.001	0.001	0.002	0.001
Na	0.696	0.702	0.690	0.762	0.719	0.686	0.779
K	0.027	0.025	0.044	0.024	0.025	0.051	0.019
Total	4.982	4.994	4.982	4.993	5.005	4.979	4.973
Ab	72.69	72.37	71.62	78.39	73.14	71.99	82.73
Or	2.79	2.58	4.55	2.46	2.58	5.39	2.07
An	24.41	25.00	23.64	19.10	24.22	22.44	15.15
Cs	0.11	0.05	0.19	0.05	0.06	0.18	0.05

Table 4-2 Electron probe analyses of plagioclase from the Marsco and Glamaig granites

	Marsco Plagioclase							
Crystal	1(core)	1(rim)	2(core)	2(rim)	3(rim)	3(rim)	4(core)	4(rim)
SiO_2	63.24	62.04	63.77	65.21	61.67	61.36	60.62	60.72
TiO_2	0.01	0.05	0.03	0.02	0.01	0.00	0.03	0.06
Al_2O_3	23.62	23.65	22.59	21.82	24.12	24.32	24.88	24.57
MgO	0.00	0.00	0.00	0.00	0.00	0.00	0.00	0.00
CaO	3.37	3.84	2.47	1.53	4.46	4.81	5.29	4.98
MnO	0.00	0.01	0.00	0.01	0.00	0.01	0.00	0.00
FeO	0.15	0.61	0.24	0.16	0.34	0.33	0.30	0.38
SrO	0.05	0.02	0.02	0.00	0.04	0.05	0.05	0.03
BaO	0.29	0.32	0.82	0.81	0.29	0.35	0.28	0.26
Na_2O	9.19	8.59	8.58	9.97	8.05	7.99	7.77	8.10
K_2O	0.33	0.72	1.71	0.85	1.16	1.02	0.92	0.96
Total	100.25	99.84	100.22	100.38	100.12	100.26	100.14	100.04
Si	2.791	2.771	2.831	2.881	2.743	2.727	2.702	2.711
Ti	0.00	0.00	0.00	0.00	0.00	0.00	0.00	0.00
Al	1.230	1.241	1.181	1.131	1.261	1.281	1.312	1.291
Mg	0.00	0.00	0.00	0.00	0.00	0.00	0.00	0.00
Ca	0.161	0.182	0.120	0.065	0.211	0.230	0.251	0.242
Mn	0.00	0.00	0.00	0.00	0.00	0.00	0.00	0.00
Fe	0.010	0.020	0.011	0.009	0.008	0.007	0.007	0.010
Sr	0.00	0.00	0.00	0.00	0.00	0.00	0.00	0.00
Ba	0.001	0.005	0.010	0.011	0.004	0.008	0.004	0.00
Na	0.792	0.740	0.742	0.852	0.693	0.692	0.671	0.701
K	0.021	0.042	0.101	0.051	0.066	0.061	0.051	0.051
Total	5.004	5.009	5.001	5.008	5.004	5.001	5.002	5.022
Ab	76.35	81.11	76.33	86.43	71.01	70.13	68.42	70.23
Or	4.20	1.94	10.03	4.85	6.72	5.91	5.34	5.46
An	18.88	16.43	12.17	7.31	21.75	23.34	25.76	23.85
Cs	0.57	0.52	1.47	1.41	0.52	0.62	0.48	0.46

Table 4-2 continued

	Marsco Plagioclase		Glamaig Plagioclase				
Crystal	5(rim)	5(core)	1(core)	1(rim)	2(core)	2(core)	2(rim)
SiO_2	62.90	63.79	61.86	67.73	61.98	62.11	63.45
TiO_2	0.04	0.04	0.05	0.00	0.01	0.01	0.00
Al_2O_3	23.08	22.65	23.94	20.50	24.28	24.05	23.56
MgO	0.00	0.00	0.00	0.00	0.00	0.00	0.00
CaO	3.12	2.42	4.05	0.40	4.47	4.42	3.28
MnO	0.00	0.02	0.00	0.03	0.01	0.00	0.00
FeO	0.11	0.16	0.15	0.07	0.10	0.20	0.00
SrO	0.04	0.03	0.00	0.00	0.02	0.03	0.07
BaO	0.83	0.87	0.87	0.10	0.20	0.13	0.04
Na_2O	8.22	9.14	8.91	10.94	8.49	8.48	9.35
K_2O	1.97	1.17	0.34	0.35	0.64	0.65	0.19
Total	100.30	100.28	100.18	100.13	100.19	100.09	99.94
Si	2.801	2.831	2.749	2.961	2.751	2.764	2.801
Ti	0.00	0.00	0.00	0.00	0.00	0.00	0.00
Al	1.211	1.180	1.261	1.062	1.272	1.261	1.232
Mg	0.00	0.00	0.00	0.00	0.00	0.00	0.00
Ca	0.148	0.121	0.192	0.022	0.211	0.209	0.161
Mn	0.00	0.00	0.00	0.00	0.00	0.00	0.00
Fe	0.004	0.011	0.009	0.004	0.008	0.010	0.00
Sr	0.00	0.00	0.00	0.00	0.00	0.00	0.00
Ba	0.010	0.009	0.012	0.00	0.00	0.00	0.00
Na	0.711	0.789	0.773	0.931	0.731	0.728	0.801
K	0.110	0.071	0.773	0.931	0.731	0.728	0.801
Total	5.003	5.001	5.010	4.990	5.00	5.00	4.990
Ab	72.07	80.02	77.17	95.79	74.36	74.51	82.82
Or	11.34	6.75	1.91	2.06	3.66	3.78	1.08
An	15.13	11.70	19.39	1.97	21.63	21.48	16.02
Cs	1.46	1.53	1.53	0.18	0.35	0.23	0.08

Table 4-2 continued

	Glamaig Plagioclase							
Crystal	3(core)	3(rim)	4(rim)	4(core)	5(rim)	5(core)	6(core)	6(rim)
SiO_2	61.38	61.85	62.30	62.13	59.81	58.80	58.35	59.16
TiO_2	0.01	0.00	0.05	0.00	0.02	0.04	0.00	0.04
Al_2O_3	24.36	24.22	23.48	24.13	25.84	26.60	26.57	25.95
MgO	0.00	0.00	0.00	0.00	0.00	0.00	0.001	0.00
CaO	4.72	4.29	4.03	4.18	6.28	7.03	7.28	6.60
MnO	0.00	0.00	0.01	0.04	0.20	0.02	0.00	0.04
FeO	0.25	0.12	0.22	0.16	0.10	0.25	0.21	0.26
SrO	0.03	0.04	0.08	0.08	0.06	0.08	0.07	0.10
BaO	0.13	0.19	0.26	0.22	0.04	0.08	0.18	0.12
Na_2O	8.35	8.59	8.46	8.50	7.72	7.25	6.98	7.48
K_2O	0.60	0.65	0.81	0.64	0.19	0.31	0.43	0.41
Total	99.87	99.94	99.70	100.06	100.08	100.47	100.08	100.17
Si	2.729	2.754	2.779	2.761	2.667	2.622	2.613	2.643
Ti	0.00	0.00	0.00	0.00	0.00	0.00	0.00	0.00
Al	1.281	1.269	1.234	1.261	1.359	1.394	1.401	1.369
Mg	0.00	0.00	0.00	0.00	0.00	0.00	0.00	0.00
Ca	0.222	0.199	0.191	0.201	0.304	0.343	0.352	0.321
Mn	0.00	0.00	0.00	0.00	0.00	0.00	0.00	0.00
Fe	0.011	0.002	0.010	0.011	0.007	0.010	0.011	0.011
Sr	0.00	0.00	0.00	0.00	0.00	0.00	0.00	0.00
Ba	0.00	0.00	0.00	0.00	0.00	0.00	0.00	0.00
Na	0.721	0.739	0.728	0.731	0.669	0.632	0.611	0.652
K	0.029	0.039	0.052	0.040	0.011	0.020	0.029	0.020
Total	5.00	5.010	4.990	5.00	5.00	5.00	5.010	5.010
Ab	73.36	75.17	75.05	75.45	68.19	63.84	61.65	65.48
Or	3.47	3.76	4.72	3.71	1.12	1.79	2.52	2.39
An	22.94	20.94	19.77	20.45	30.62	34.23	35.51	31.51
Cs	0.23	0.34	0.46	0.39	0.07	0.14	0.32	0.21

Table 4-3 Electron-probe analyses of alkali feldspar from the Beinn an Dubhaich Granite

	Beinn an Dubhaich Alkali feldspar							
Crystal	1(core)	1(core)	1(rim)	1(rim)	2(rim)	2(core)	3(rim)	3(core)
SiO_2	64.72	64.72	65.20	64.64	65.06	65.16	64.82	64.90
TiO_2	0.00	0.03	0.07	0.00	0.00	0.00	0.04	0.00
Al_2O_3	20.16	19.95	19.92	19.79	19.33	19.78	19.97	19.64
MgO	0.01	0.00	0.00	0.00	0.00	0.00	0.00	0.00
CaO	0.38	0.39	0.18	0.19	0.00	0.14	0.15	0.26
MnO	0.00	0.00	0.00	0.00	0.00	0.00	0.00	0.00
FeO	0.11	0.06	0.09	0.07	0.16	0.03	0.15	0.11
SrO	0.00	0.00	0.00	0.00	0.00	0.00	0.00	0.00
BaO	1.02	0.78	0.55	1.08	0.12	0.69	0.63	0.82
Na_2O	4.81	5.08	4.56	4.11	1.68	4.07	4.26	4.32
K_2O	8.53	8.66	9.13	9.91	13.46	9.86	9.82	9.86
Total	99.52	99.66	99.70	99.79	99.82	99.74	99.83	99.91
Si	2.938	2.942	2.956	2.951	2.979	2.962	2.948	2.955
Ti	0.00	0.001	0.002	0.00	0.00	0.00	0.001	0.00
Al	1.082	1.069	1.065	1.065	1.043	1.060	1.070	1.054
Mg	0.00	0.00	0.00	0.00	0.00	0.00	0.00	0.00
Ca	0.019	0.019	0.009	0.009	0.00	0.007	0.007	0.013
Mn	0.00	0.00	0.00	0.00	0.00	0.00	0.00	0.00
Fe	0.004	0.002	0.004	0.003	0.006	0.001	0.006	0.004
Sr	0.00	0.00	0.00	0.00	0.00	0.00	0.00	0.00
Ba	0.018	0.014	0.010	0.019	0.002	0.012	0.011	0.015
Na	0.424	0.448	0.401	0.364	0.149	0.359	0.375	0.382
K	0.496	0.502	0.528	0.577	0.786	0.572	0.570	0.573
Total	4.981	4.997	4.974	4.988	4.968	4.973	4.988	4.995
Ab	44.35	45.56	42.33	37.54	15.93	37.75	38.95	38.86
Or	51.82	51.10	55.73	59.52	83.84	60.23	59.14	58.33
An	1.93	1.94	0.90	0.94	0.00	0.73	0.74	1.31
Cs	1.90	1.40	1.04	2.00	0.23	1.29	1.17	1.50

Table 4-3 continued

	Beinn an Dubhaich Alkali feldspar							
Crystal	4(core)	4(core)	4(core)	4(rim)	5(rim)	5(core)	5(core)	5(core)
SiO_2	65.23	65.21	65.61	64.72	65.37	63.95	64.34	65.94
TiO_2	0.00	0.00	0.01	0.02	0.00	0.00	0.00	0.01
Al_2O_3	19.82	19.80	19.76	19.34	19.71	19.78	19.89	20.34
MgO	0.00	0.00	0.00	0.00	0.00	0.00	0.00	0.00
CaO	0.16	0.24	0.17	0.04	0.15	0.17	0.17	0.53
MnO	0.00	0.00	0.00	0.00	0.00	0.00	0.00	0.00
FeO	0.08	0.10	0.10	0.10	0.08	0.03	0.21	0.20
SrO	0.00	0.00	0.00	0.00	0.00	0.00	0.00	0.00
BaO	0.55	0.39	0.64	0.31	0.66	0.84	0.73	0.38
Na_2O	4.33	4.52	5.24	2.21	4.26	4.03	4.29	5.37
K_2O	9.42	9.50	8.25	12.84	9.71	10.82	10.30	7.06
Total	99.57	99.76	99.77	99.58	99.93	99.60	99.93	99.82
Si	2.963	2.958	2.965	2.971	2.965	2.937	2.938	2.956
Ti	0.00	0.00	0.00	0.00	0.00	0.00	0.00	0.00
Al	1.061	1.059	1.052	1.047	1.053	1.071	1.070	1.075
Mg	0.00	0.00	0.00	0.00	0.00	0.00	0.00	0.00
Ca	0.008	0.012	0.008	0.002	0.007	0.008	0.008	0.025
Mn	0.00	0.00	0.00	0.00	0.00	0.00	0.00	0.00
Fe	0.003	0.004	0.004	0.004	0.003	0.001	0.008	0.007
Sr	0.00	0.00	0.00	0.00	0.00	0.00	0.00	0.00
Ba	0.010	0.007	0.011	0.006	0.012	0.015	0.013	0.007
Na	0.381	0.398	0.459	0.197	0.375	0.359	0.380	0.467
K	0.546	0.550	0.475	0.752	0.562	0.634	0.600	0.404
Total	4.971	4.986	4.976	4.979	4.976	5.025	5.017	4.941
Ab	40.36	41.18	48.11	20.56	39.21	35.30	37.95	52.73
Or	57.81	56.91	49.82	78.66	58.79	62.40	59.93	44.71
An	0.80	1.19	0.88	0.20	0.77	0.81	0.83	2.81
Cs	1.03	0.72	1.19	0.58	1.23	1.49	1.29	0.75

Table 4-3 continued

	Beinn an Dubhaich Alkali feldspar							
Crystal	6(core)	6(rim)	6(rim)	7(rim)	7(core)	8(rim)	8(core)	8(rim)
SiO_2	64.47	64.59	63.95	64.67	64.93	64.36	64.74	63.91
TiO_2	0.00	0.00	0.02	0.04	0.03	0.00	0.00	0.09
Al_2O_3	19.96	19.52	19.22	19.49	19.67	19.42	19.74	19.76
MgO	0.00	0.00	0.00	0.00	0.00	0.00	0.00	0.00
CaO	0.31	0.11	0.01	0.21	0.25	0.08	0.38	0.09
MnO	0.00	0.00	0.00	0.00	0.00	0.00	0.00	0.00
FeO	0.12	0.11	0.04	0.06	0.07	0.11	0.00	0.08
SrO	0.00	0.00	0.00	0.00	0.00	0.00	0.00	0.00
BaO	0.37	0.11	0.21	0.07	0.07	0.34	0.49	0.52
Na_2O	4.80	3.38	1.32	3.32	4.64	3.24	3.55	4.00
K_2O	9.74	12.04	15.22	11.81	10.23	12.09	11.20	11.08
Total	99.77	99.86	99.99	99.68	99.88	99.62	100.10	99.53
Si	2.936	2.954	2.957	2.958	2.951	2.956	2.950	2.935
Ti	0.00	0.00	0.001	0.001	0.001	0.00	0.00	0.003
Al	1.071	1.053	1.047	1.051	1.053	1.051	1.060	1.070
Mg	0.00	0.00	0.00	0.00	0.00	0.00	0.00	0.00
Ca	0.015	0.006	0.00	0.010	0.012	0.004	0.019	0.004
Mn	0.00	0.00	0.00	0.00	0.00	0.00	0.00	0.00
Fe	0.005	0.004	0.002	0.002	0.003	0.004	0.00	0.003
Sr	0.00	0.00	0.00	0.00	0.00	0.00	0.00	0.00
Ba	0.007	0.002	0.004	0.001	0.001	0.006	0.009	0.009
Na	0.424	0.299	0.119	0.295	0.408	0.288	0.414	0.356
K	0.566	0.703	0.897	0.689	0.593	0.708	0.651	0.949
Total	5.024	5.021	5.027	5.007	5.022	5.017	5.002	5.030
Ab	41.93	29.65	11.62	29.60	40.25	28.59	31.62	34.95
Or	55.94	69.61	87.97	69.25	58.43	70.40	65.63	63.71
An	1.47	0.55	0.03	1.02	1.21	0.40	1.86	0.41
Cs	0.66	0.19	0.38	0.13	0.11	0.61	0.89	0.93

Table 4-4 Electron-probe analyses of alkali feldspar from the Loch Ainort Granite

	Loch Ainort Alkali feldspar							
Crystal	1(core)	1(rim)	2(core)	2(rim)	3(rim)	3(core)	4(core)	4(rim)
SiO_2	64.02	63.59	63.75	63.25	63.37	63.14	63.06	63.26
TiO_2	0.24	0.07	0.02	0.09	0.01	0.00	0.07	0.03
Al_2O_3	18.88	19.12	19.01	18.86	19.10	19.31	19.20	19.41
MgO	0.00	0.00	0.00	0.00	0.00	0.00	0.00	0.00
CaO	0.03	0.00	0.02	0.00	0.00	0.00	0.00	0.03
MnO	0.00	0.00	0.00	0.00	0.00	0.00	0.00	0.00
FeO	0.04	0.04	0.03	0.12	0.02	0.00	0.00	0.00
SrO	0.00	0.00	0.00	0.00	0.00	0.00	0.00	0.00
BaO	0.21	0.71	0.36	0.40	0.70	0.93	0.45	0.37
Na_2O	0.88	0.71	0.20	0.25	0.71	0.57	0.41	0.76
K_2O	15.82	15.90	16.53	16.56	15.75	15.84	16.44	15.69
Total	99.90	100.15	99.92	99.52	99.65	99.79	99.62	99.56
Si	2.968	2.954	2.964	2.959	2.956	2.946	2.946	2.946
Ti	0.001	0.003	0.001	0.003	0.00	0.00	0.003	0.001
Al	1.032	1.047	1.042	1.040	1.050	1.062	1.058	1.065
Mg	0.00	0.00	0.00	0.00	0.00	0.00	0.00	0.00
Ca	0.002	0.00	0.001	0.00	0.00	0.00	0.00	0.002
Mn	0.00	0.00	0.00	0.00	0.00	0.00	0.00	0.00
Fe	0.002	0.002	0.001	0.004	0.001	0.00	0.00	0.00
Sr	0.00	0.00	0.00	0.00	0.00	0.00	0.00	0.00
Ba	0.004	0.013	0.007	0.007	0.013	0.017	0.008	0.007
Na	0.079	0.064	0.018	0.023	0.064	0.015	0.037	0.069
K	0.936	0.942	0.981	0.988	0.937	0.943	0.980	0.932
Total	5.022	5.024	5.014	5.024	5.020	5.020	5.031	5.021
Ab	7.71	6.28	1.79	2.21	6.31	5.06	3.58	6.83
Or	91.78	92.45	97.45	97.06	92.43	93.25	95.62	92.34
An	0.14	0.00	0.10	0.01	0.00	0.00	0.00	0.16
Cs	0.37	1.27	0.66	0.72	1.26	1.69	0.80	0.67

Table 4-4 continued

	Loch Ainort Alkali feldspar					
Crystal	5(core)	5(rim)	6(rim)	6(core)	7(rim)	7(core)
SiO_2	63.80	63.60	65.16	65.42	64.17	64.28
TiO_2	0.00	0.00	0.02	0.02	0.01	0.00
Al_2O_3	18.93	18.91	19.82	20.04	19.78	20.48
MgO	0.00	0.00	0.00	0.00	0.00	0.00
CaO	0.02	0.01	0.11	0.22	0.43	0.87
MnO	0.00	0.00	0.00	0.00	0.00	0.00
FeO	0.06	0.98	0.15	0.16	0.18	0.36
SrO	0.00	0.00	0.00	0.00	0.00	0.00
BaO	0.19	0.43	0.27	0.25	0.76	0.36
Na_2O	0.79	0.96	5.24	6.25	2.63	5.73
K_2O	15.93	14.87	8.91	7.40	12.00	7.78
Total	99.72	99.77	99.68	99.76	99.98	99.86
Si	2.965	2.957	2.954	2.948	2.943	2.911
Ti	0.00	0.00	0.001	0.001	0.00	0.00
Al	1.037	1.036	1.059	1.064	1.069	1.093
Mg	0.00	0.00	0.00	0.00	0.00	0.00
Ca	0.001	0.001	0.005	0.011	0.021	0.042
Mn	0.00	0.00	0.00	0.00	0.00	0.00
Fe	0.002	0.038	0.006	0.006	0.007	0.014
Sr	0.00	0.00	0.00	0.00	0.00	0.00
Ba	0.004	0.008	0.005	0.004	0.012	0.006
Na	0.071	0.087	0.461	0.546	0.234	0.503
K	0.944	0.882	0.515	0.426	0.702	0.449
Total	5.024	5.009	5.005	5.005	4.991	5.019
Ab	6.95	8.87	46.71	55.34	24.10	50.25
Or	92.62	90.26	52.27	43.15	72.34	44.87
An	0.09	0.06	0.54	1.07	2.15	4.24
Cs	0.34	0.81	0.48	0.44	1.41	0.64

Table 4-5 Electron-probe analyses of alkali feldspar from the Marsco Granite

	Marsco Alkali feldspar					
Crystal	1(core)	1(rim)	2(rim)	2(core)	3(core)	3(rim)
SiO_2	64.31	65.63	64.67	64.57	65.93	65.52
TiO_2	0.03	0.00	0.06	0.02	0.00	0.00
Al_2O_3	20.90	20.78	20.99	21.22	20.04	19.79
MgO	0.00	0.00	0.01	0.00	0.01	0.01
CaO	0.96	0.88	0.88	0.92	0.22	0.16
MnO	0.00	0.00	0.00	0.00	0.00	0.00
FeO	0.22	0.32	0.12	0.08	0.10	0.04
SrO	0.00	0.00	0.00	0.00	0.00	0.00
BaO	1.17	0.78	1.02	1.03	0.04	0.09
Na_2O	6.64	8.46	7.08	7.22	5.78	5.47
K_2O	5.81	3.50	5.49	5.14	8.23	8.69
Total	100.05	100.34	100.33	100.23	100.34	99.80
Si	2.901	2.921	2.901	2.893	2.951	2.957
Ti	0.00	0.00	0.00	0.00	0.00	0.00
Al	1.110	1.092	1.111	1.121	1.062	1.049
Mg	0.00	0.00	0.00	0.00	0.00	0.00
Ca	0.048	0.041	0.039	0.040	0.010	0.008
Mn	0.00	0.00	0.00	0.00	0.00	0.00
Fe	0.009	0.009	0.004	0.001	0.004	0.001
Sr	0.00	0.00	0.00	0.00	0.00	0.00
Ba	0.019	0.011	0.016	0.018	0.001	0.003
Na	0.581	0.731	0.622	0.628	0.491	0.476
K	0.330	0.201	0.310	0.291	0.470	0.501
Total	5.002	5.001	5.009	5.008	5.001	5.001
Ab	59.13	74.18	62.19	63.82	51.06	48.41
Or	34.02	20.17	31.74	29.88	47.81	50.64
An	4.75	4.26	4.25	4.47	1.06	0.78
Cs	2.10	1.39	1.82	1.83	0.07	0.17

Table 4-5 contimued

	Marsco Alkali feldspar					
Crystal	4(rim)	4(rim)	4(core)	5(rim)	5(core)	5(core)
SiO_2	65.11	65.08	65.59	63.56	65.20	66.13
TiO_2	0.00	0.03	0.01	0.03	0.01	0.00
Al_2O_3	19.98	20.01	19.89	19.49	19.98	20.00
MgO	0.00	0.00	0.00	0.00	0.00	0.00
CaO	0.08	0.08	0.17	0.01	0.18	0.21
MnO	0.00	0.00	0.00	0.00	0.01	0.02
FeO	0.20	0.14	0.17	0.11	0.22	0.15
SrO	0.00	0.00	0.00	0.00	0.00	0.00
BaO	0.37	0.43	0.16	0.38	0.16	0.09
Na_2O	4.81	4.71	5.19	1.26	5.24	6.28
K_2O	9.52	9.63	9.28	15.12	8.96	7.61
Total	100.07	100.11	100.47	99.98	99.97	100.49
Si	2.947	2.950	2.948	2.941	2.949	2.959
Ti	0.00	0.00	0.00	0.00	0.00	0.00
Al	1.069	1.071	1.049	1.059	1.061	1.049
Mg	0.00	0.00	0.00	0.00	0.00	0.00
Ca	0.001	0.001	0.009	0.00	0.009	0.010
Mn	0.00	0.00	0.002	0.00	0.001	0.00
Fe	0.009	0.004	0.008	0.004	0.008	0.009
Sr	0.00	0.00	0.00	0.00	0.00	0.00
Ba	0.008	0.008	0.001	0.009	0.001	0.003
Na	0.419	0.409	0.449	0.111	0.459	0.540
K	0.548	0.558	0.531	0.889	0.518	0.429
Total	5.009	5.007	5.002	5.030	5.008	5.011
Ab	42.98	42.15	45.43	11.15	46.50	54.95
Or	55.98	56.68	53.47	88.10	52.31	43.86
An	0.37	0.40	0.81	0.07	0.90	1.02
Cs	0.67	0.77	0.29	0.68	0.29	0.17

Table 4-5 continued

	Marsco Alkali feldspar					
Crystal	6(rim)	6(rim)	6(rim)	6(core)	7(core)	7(rim)
SiO_2	65.26	64.85	65.18	65.96	64.80	64.21
TiO_2	0.02	0.02	0.00	0.00	0.00	0.02
Al_2O_3	20.12	19.96	19.69	19.99	19.95	19.69
MgO	0.00	0.01	0.00	0.00	0.00	0.00
CaO	0.15	0.16	0.10	0.27	0.08	0.06
MnO	0.00	0.00	0.00	0.00	0.00	0.00
FeO	0.02	0.19	0.21	0.17	0.15	0.10
SrO	0.00	0.00	0.00	0.00	0.00	0.00
BaO	0.31	0.84	0.45	0.50	0.64	0.52
Na_2O	4.67	4.89	5.09	6.10	4.15	3.32
K_2O	9.44	9.19	9.11	7.34	10.55	11.85
Total	99.99	100.11	99.85	100.31	100.31	99.78
Si	2.949	2.941	2.959	2.961	2.938	2.939
Ti	0.00	0.00	0.00	0.00	0.00	0.00
Al	1.071	1.049	1.048	1.061	1.069	1.061
Mg	0.00	0.00	0.00	0.00	0.00	0.00
Ca	0.010	0.004	0.003	0.009	0.002	0.001
Mn	0.00	0.00	0.00	0.00	0.00	0.00
Fe	0.00	0.010	0.011	0.008	0.008	0.004
Sr	0.00	0.00	0.00	0.00	0.00	0.00
Ba	0.009	0.009	0.010	0.010	0.010	0.010
Na	0.409	0.431	0.449	0.528	0.369	0.300
K	0.541	0.529	0.531	0.422	0.611	0.691
Total	4.991	5.001	5.00	4.991	5.009	5.008
Ab	42.36	43.68	45.34	54.57	36.85	29.52
Or	56.33	54.02	53.34	43.20	61.60	69.24
An	0.74	0.78	0.51	1.33	0.40	0.30
Cs	0.57	1.52	0.81	0.90	1.15	0.94

Table 4-6 Electron-probe analyses of alkali feldspar from the Glamaig Granite

	Glamaig Alkali feldspar							
Crystal	1(rim)	1(core)	2(core)	2(rim)	3(core)	3(rim)	4(core)	4(rim)
SiO_2	62.76	62.56	62.49	63.93	65.31	63.68	65.81	64.39
TiO_2	0.02	0.03	0.05	0.00	0.01	0.02	0.02	0.00
Al_2O_3	20.44	20.79	20.83	19.45	20.56	19.59	20.09	19.62
MgO	0.00	0.00	0.00	0.00	0.00	0.001	0.001	0.00
CaO	0.43	0.57	0.61	0.00	0.60	0.00	0.41	0.19
MnO	0.00	0.00	0.009	0.030	0.00	0.00	0.029	0.00
FeO	0.11	0.21	0.17	0.04	0.07	0.05	0.07	0.09
SrO	0.00	0.00	0.00	0.00	0.00	0.00	0.00	0.00
BaO	2.14	2.33	2.42	0.28	0.16	0.32	0.15	0.14
Na_2O	4.20	4.85	4.52	0.85	7.06	0.88	5.16	3.54
K_2O	9.60	8.22	8.77	15.51	6.41	15.84	8.71	11.60
Total	99.71	99.22	99.87	100.09	100.20	100.37	100.43	99.56
Si	2.902	2.882	2.878	2.948	2.919	2.941	2.952	2.951
Ti	0.00	0.001	0.001	0..00	0.00	0.00	0.00	0.00
Al	1.111	1.131	1.129	1.061	1.092	1.072	1.061	1.059
Mg	0.00	0.00	0.00	0.00	0.00	0.00	0.00	0.00
Ca	0.021	0.034	0.032	0.00	0.031	0.00	0.021	0.009
Mn	0.00	0.00	0.001	0.001	0.00	0.00	0.00	0.00
Fe	0.004	0.012	0.009	0.00	0.00	0.00	0.002	0.003
Sr	0.00	0.00	0.00	0.00	0.00	0.00	0.00	0.00
Ba	0.041	0.044	0.005	0.00	0.001	0.009	0.001	0.001
Na	0.379	0.432	0.394	0.082	0.612	0.081	0.451	0.311
K	0.568	0.481	0.521	0.909	0.371	0.931	0.501	0.678
Total	5.020	5.010	5.020	5.010	5.020	5.030	4.991	5.011
Ab	37.55	43.89	40.65	7.61	60.54	7.74	46.29	31.30
Or	56.46	49.00	51.91	91.88	36.21	91.69	51.41	67.56
An	2.13	2.85	3.04	0.00	2.98	0.00	2.04	0.90
Cs	3.86	4.26	4.40	0.51	0.27	0.57	0.26	0.24

Table 4-6 continued

	Glamaig Alkali feldspar						
Crystal	5(core)	5(rim)	5(rim)	6(core)	6(rim)	7(rim)	7(core)
SiO_2	62.28	63.31	64.25	63.83	66.37	63.50	63.71
TiO_2	0.00	0.01	0.00	0.05	0.01	0.00	0.01
Al_2O_3	19.47	19.54	19.57	19.49	20.48	19.50	19.54
MgO	0.00	0.00	0.00	0.00	0.00	0.001	0.01
CaO	0.20	0.00	0.05	0.05	0.32	0.00	0.12
MnO	0.00	0.00	0.00	0.00	0.03	0.00	0.01
FeO	0.06	0.25	0.09	0.03	0.03	0.01	0.25
SrO	0.00	0.00	0.00	0.00	0.00	0.00	0.00
BaO	0.67	0.36	0.00	0.27	0.22	0.36	0.23
Na_2O	1.02	0.55	1.49	1.33	8.44	0.99	1.67
K_2O	15.18	16.25	14.61	14.99	4.05	15.35	14.24
Total	99.72	100.26	100.06	100.05	99.95	99.72	99.80
Si	2.931	2.941	2.949	2.948	2.951	2.951	2.941
Ti	0.00	0.00	0.00	0.00	0.00	0.00	0.00
Al	1.081	1.073	1.061	1.061	1.071	1.071	1.057
Mg	0.00	0.00	0.00	0.00	0.00	0.00	0.00
Ca	0.010	0.00	0.00	0.00	0.010	0.00	0.009
Mn	0.00	0.00	0.00	0.00	0.00	0.00	0.00
Fe	0.002	0.011	0.003	0.001	0.001	0.00	0.010
Sr	0.00	0.00	0.00	0.00	0.00	0.00	0.00
Ba	0.010	0.009	0.00	0.00	0.00	0.012	0.00
Na	0.094	0.051	0.129	0.121	0.731	0.093	0.154
K	0.901	0.957	0.862	0.882	0.233	0.911	0.843
Total	5.031	5.030	5.011	5.020	4.991	5.020	5.021
Ab	9.15	4.87	13.38	11.81	74.54	8.89	15.01
Or	88.65	94.49	86.37	87.44	23.52	90.46	83.97
An	0.98	0.00	0.25	0.26	1.55	0.00	0.61
Cs	1.22	0.64	0.00	0.49	0.39	0.65	0.41

Table 4-7 Electron-probe analyses of amphibole from the Beinn an Dubhaich Granite

	Beinn an Dubhaich Amphibole							
Crystal	1(rim)	1(core)	1(rim)	2(rim)	2(core)	2(rim)	3(rim)	3(core)
SiO_2	41.51	42.13	41.59	41.71	41.76	42.21	41.83	42.25
TiO_2	1.45	1.43	1.49	1.50	1.42	1.43	1.73	1.45
Al_2O_3	8.05	7.84	7.49	7.40	7.89	7.34	7.51	7.58
FeO(tot.)	27.69	27.05	28.55	27.91	27.78	27.55	27.51	27.13
MnO	0.52	0.79	0.80	0.64	0.64	0.61	0.70	0.66
MgO	5.25	5.30	4.86	5.38	5.11	5.63	5.38	5.42
CaO	10.00	10.03	9.84	9.86	10.00	9.81	9.60	9.93
Na_2O	2.08	2.07	1.96	2.10	2.09	1.97	2.15	2.08
K_2O	1.24	1.14	1.17	1.15	1.19	1.06	1.12	1.12
H_2O	1.09	1.14	0.99	1.15	1.04	0.90	1.12	0.99
F	1.67	1.59	1.86	1.54	1.78	2.07	1.61	1.89
Total	100.55	100.49	100.60	100.27	100.70	100.58	100.25	100.53
O=F	-0.704	-0.669	-.0782	-0.648	-0.751	-0.872	-0.679	-0.797
Total	99.84	99.83	99.81	99.62	99.95	99.71	99.57	99.73
T								
Si	6.5593	6.6583	6.6222	6.6358	6.5952	6.6732	6.6363	6.6570
Al(IV)	1.4407	1.3417	1.3778	1.3642	1.4048	1.3268	1.3637	1.3430
Total	8.000	8.000	8.000	8.000	8.000	8.000	8.000	8.000
C								
Al(VI)	0.0596	0.0983	0.0278	0.0231	0.0633	0.0409	0.0409	0.0645
Ti	0.1723	0.1677	0.1785	0.1795	0.1685	0.1705	0.2058	0.1723
Fe(3+)	0.3733	0.4519	0.2537	0.1878	0.3638	0.2800	0.2353	0.3706
Mg	1.2353	1.2316	1.1540	1.2745	1.2024	1.3261	1.2711	1.2732
Fe(2+)	3.1595	3.0505	3.3860	3.3351	3.2020	3.1825	3.2469	3.1194
Total	5.000	5.000	5.000	5.000	5.000	5.000	5.000	5.000
B								
Fe(2+)	0.1262	0.0229	0.1617	0.1910	0.1036	0.1804	0.1681	0.0851
Mn	0.0692	0.1048	0.1078	0.0857	0.0855	0.0814	0.0935	0.0886
Ca	1.6929	1.6742	1.6785	1.6801	1.6921	1.6614	1.6319	1.6758
Na	0.1117	0.1981	0.0520	0.0432	0.1188	0.768	0.1065	0.1505
Total	2.000	2.000	2.000	2.000	2.000	2.000	2.000	2.000
A								
Na	0.5252	0.4266	0.5543	0.6053	0.5202	0.5283	0.5558	0.4849
K	0.2498	0.2275	0.2371	0.2324	0.2391	0.2132	0.2265	0.2290
Total	0.7750	0.6541	0.7914	0.8377	0.7593	0.7415	0.7823	0.7139

Table 4-7 continued

	Beinn an Dubhaich Amphibole							
Crystal	4(rim)	4(core)	4(rim)	5(rim)	5(core)	6(core)	6(rim)	(rim)
SiO_2	41.12	40.50	40.99	41.05	41.42	40.59	42.13	42.77
TiO_2	1.48	0.97	1.66	1.45	1.24	1.39	1.47	1.45
Al_2O_3	7.87	8.49	8.01	7.82	7.80	8.15	7.12	7.16
FeO(tot.)	28.73	29.82	29.31	29.12	30.12	30.07	27.19	27.36
MnO	0.77	0.74	0.77	0.83	0.57	0.67	0.66	0.72
MgO	4.63	3.47	3.88	4.27	3.68	3.72	5.94	5.93
CaO	9.85	10.41	9.96	9.78	9.92	9.92	9.83	9.55
Na_2O	2.04	1.92	2.02	2.04	1.93	1.95	2.07	2.09
K_2O	1.18	1.26	1.17	1.19	1.15	1.23	0.99	0.97
H_2O	1.64	1.25	1.31	1.22	1.25	1.29	0.98	1.07
F	1.48	1.28	1.18	1.35	1.30	1.19	1.91	1.75
Total	100.32	100.11	100.26	100.12	100.38	100.18	100.27	100.82
O=F	-0.624	-0.539	-0.496	-0.566	-0.549	-0.502	-0.802	-0.737
Total	99.69	99.57	99.76	99.55	99.83	99.68	99.47	100.08
T								
Si	6.5571	6.4724	6.5452	6.5676	6.6011	6.5027	6.6862	6.7185
Al(IV)	1.4429	1.5276	1.4548	1.4324	1.3989	1.4973	1.3138	1.2815
Total	8.000	8.000	8.000	8.000	8.000	8.000	8.000	8.000
C								
Al(VI)	0.0360	0.0719	0.0537	0.0426	0.0666	0.0423	0.0175	0.0446
Ti	0.1775	0.1171	0.1995	0.1740	0.1490	0.1669	0.1752	0.1716
Fe(3+)	0.3139	0.6035	0.3402	0.3268	0.4550	0.4214	0.1733	0.2561
Mg	1.1004	0.8264	0.9231	1.0180	0.8748	0.8877	1.4055	1.3893
Fe(2+)	3.3722	3.3811	3.4835	3.4386	3.4546	3.4817	3.2285	3.1384
Total	5.000	5.000	5.000	5.000	5.000	5.000	5.000	5.000
B								
Fe(2+)	0.1462	0.0008	0.0909	0.1306	0.1055	0.1263	0.2068	0.2003
Mn	0.1036	0.1002	0.1046	0.1126	0.0767	0.0912	0.0893	0.0963
Ca	1.6828	1.7827	1.7040	1.6768	1.6931	1.7033	1.6710	1.6067
Na	0.0674	0.1163	0.1005	0.0800	0.1247	0.0792	0.0329	0.0967
Total	2.000	2.000	2.000	2.000	2.000	2.000	2.000	2.000
A								
Na	0.5646	0.4774	0.5240	0.5518	0.4714	0.5278	0.6044	0.5411
K	0.2409	0.2573	0.2388	0.2431	0.2330	0.2514	0.2009	0.1934
Total	0.8055	0.7347	.7628	0.7949	0.7044	0.7792	0.8053	0.7345

Table 4-8 Electron-probe analyses of amphibole from the Loch Ainort Granite

	Loch Ainort Amphibole							
Crystal	1(core)	1(rim)	1(rim)	2(rim)	2(core)	2(rim)	3(rim)	3(core)
SiO_2	42.43	43.80	43.49	43.43	44.46	43.22	43.50	44.55
TiO_2	1.17	0.99	1.31	0.76	0.87	0.81	0.90	0.70
Al_2O_3	5.96	5.09	5.25	4.78	4.50	4.79	4.95	4.21
FeO(tot.)	31.89	31.13	31.23	32.53	31.30	32.73	32.66	32.06
MnO	0.56	0.49	0.46	0.88	0.76	0.89	0.87	0.88
MgO	2.99	3.47	3.48	3.13	3.44	2.96	2.79	3.20
CaO	9.72	9.59	9.34	9.21	9.38	9.11	9.09	9.19
Na_2O	2.177	2.090	2.071	2.170	2.139	2.184	2.176	2.058
K_2O	1.46	0.94	0.94	0.90	0.85	0.86	0.88	0.97
H_2O	1.07	1.02	0.98	1.26	0.89	0.91	1.19	1.11
F	1.64	1.78	1.85	1.23	2.06	1.96	1.39	1.57
Total	100.65	100.38	100.40	100.28	100.65	100.43	100.40	100.41
O=F	-0.690	-0.750	-0.781	-0.518	-0.868	-0.826	-0.586	-0.662
Total	99.96	99.63	99.62	99.76	99.78	99.61	99.81	99.74
T								
Si	6.8694	7.0495	7.0109	7.0542	7.1541	7.0452	7.0563	7.1985
Al(IV)	1.1306	0.9505	0.9891	0.9145	0.8459	0.9205	0.9437	0.8015
Ti	0.00	0.00	0.00	0.0313	0.00	0.0343	0.00	0.00
Total	8.000	8.000	8.000	8.000	8.000	8.000	8.000	8.000
C								
Al(VI)	0.0065	0.0160	0.0077	0.00	0.0075	0.00	0.0033	0.0010
Ti	0.1423	0.1195	0.1588	0.0614	0.010580.0651		0.1100	0.0845
Fe(3+)	0.0374	0.0921	0.0443	0.00	0.0431	0.00	0.0193	0.0056
Mg	0.7203	0.8315	0.8363	0.7574	0.8256	0.7191	0.6735	0.7715
Fe(2+)	4.0935	3.9409	3.9529	4.1812	4.0180	4.2158	4.1939	4.1374
Total	5.000	5.000	5.000	5.000	5.000	5.000	5.000	5.000
B								
Fe2+	0.1880	0.1577	0.2130	0.2370	0.1504	0.2461	0.2178	0.1896
Mn	0.0772	0.0667	0.0632	0.1212	0.1029	0.1225	0.1197	0.1206
Ca	1.6860	1.6542	1.6133	1.6023	1.6176	1.5918	1.5797	1.5905
Na	0.0488	0.1214	0.1105	0.0395	0.1291	0.0396	0.0828	0.0993
Total	2.000	2.000	2.000	2.000	2.000	2.000	2.000	2.000
A								
Na	0.6347	0.5309	0.5368	0.6439	0.5382	0.6507	0.6016	0.5454
K	0.2161	0.1939	0.1929	0.1869	0.1747	0.1795	0.1819	0.1800
Total	0.8508	0.7248	0.7297	0.8308	0.1729	0.8302	0.7835	0.7254

Table 4-8 continued

	Loch Ainort Amphibole							
Crystal	4(core)	4(core)	4(rim)	5(core)	5(rim)	5(core)	6(core)	6(rim)
SiO_2	44.50	43.17	44.06	42.50	43.80	42.99	42.71	43.53
TiO_2	0.86	1.01	0.67	1.17	0.94	1.02	1.18	1.28
Al_2O_3	4.34	5.28	4.66	5.55	4.37	5.01	5.53	4.63
FeO(tot.)	31.70	32.62	32.40	32.61	32.75	32.57	31.97	32.41
MnO	0.70	0.71	0.79	0.65	0.77	0.67	0.65	0.78
MgO	3.19	2.60	3.03	2.54	2.70	3.01	2.72	2.78
CaO	9.33	9.48	8.87	9.43	9.08	9.52	9.64	9.00
Na_2O	2.10	2.14	2.26	2.13	2.30	1.97	2.15	2.33
K_2O	0.80	0.95	0.91	0.97	0.87	0.99	0.96	0.92
H_2O	0.97	1.13	1.15	1.16	1.11	1.14	1.15	0.99
F	1.87	1.53	1.47	1.43	1.54	1.49	1.46	1.82
Total	100.37	100.62	100.27	100.13	100.24	100.37	100.12	100.44
O=F	-0.787	-0.643	-0.620	-0.601	-0.649	-0.625	-0.615	-0.764
Total	99.58	99.97	99.65	99.53	99.59	99.74	99.50	99.67
T								
Si	7.1817	6.9968	7.1268	6.9338	7.1271	6.9924	6.9456	7.0728
Al(IV)	0.8183	1.0032	0.8732	1.0662	0.8414	0.9597	1.0544	0.8864
Ti	0.00	0.00	0.00	0.00	0.0315	0.0479	0.00	0.0408
Total	8.000	8.000	8.000	8.000	8.000	8.000	8.000	8.000
C								
Al(IV)	0.0081	0.0063	0.0154	0.0004	0.000	0.000	0.0055	0.000
Ti	0.1044	0.1226	0.0813	0.1438	0.0837	0.0772	0.1443	0.1153
Fe(3+)	0.0465	0.0361	0.0884	0.0028	0.000	0.000	0.0312	0.000
Mg	0.7669	0.6278	0.7302	0.6179	0.6555	0.7294	0.6590	0.6725
Fe(2+)	4.0741	4.2072	4.0847	4.2351	4.2608	4.1934	4.1600	4.2122
Total	5.000	5.000	5.000	5.000	5.000	5.000	5.000	5.000
B								
Fe(2+)	0.1575	0.1789	0.2102	0.2114	0.1957	0.2368	0.1572	0.1919
Mn	0.0954	0.978	0.1084	0.0891	0.1057	0.0926	0.0889	0.1075
Ca	1.6131	1.6469	1.5373	1.6485	1.5823	1.6597	1.6791	1.5662
Na	0.1340	0.0764	0.1441	0.0510	0.1163	0.0109	0.0748	0.1344
Total	2.000	2.000	2.000	2.000	2.000	2.000	2.000	2.000
A								
Na	0.5240	0.5958	0.5644	0.6238	0.6100	0.6116	0.6044	0.5985
K	0.1651	0.1962	0.1870	0.2023	0.1804	0.2046	0.1996	0.1916
Total	0.6891	0.7920	0.7514	0.8261	0.7904	0.8162	0.8040	0.7901

Table 4-9 Electron-probe analyses of amphibole from the Glamaig Granite

	Glamaig Amphibole							
Crystal	1(rim)	1(core)	1(core)	1(rim)	2(core)	2(core)	2(rim)	2(core)
SiO_2	44.15	43.48	45.12	44.17	44.32	44.49	43.39	44.28
TiO_2	0.90	1.27	0.93	1.09	0.97	0.75	1.33	1.13
Al_2O_3	6.29	6.81	6.02	6.47	6.38	6.51	7.42	6.52
FeO(tot.)	26.04	26.54	25.43	26.25	25.48	25.56	25.82	25.23
MnO	0.58	0.59	0.69	0.61	0.55	0.57	0.54	0.62
MgO	7.25	6.41	7.18	7.11	7.31	7.11	6.31	7.72
CaO	9.88	10.09	9.97	9.84	10.06	10.01	9.96	10.03
Na_2O	1.80	1.95	1.68	1.81	1.79	1.73	1.95	1.73
K_2O	0.74	0.78	0.72	0.85	0.79	0.86	0.92	0.87
H_2O	1.26	1.51	1.35	1.28	1.30	1.15	1.31	1.37
F	1.39	0.85	1.21	1.35	1.30	1.62	1.26	1.18
Total	100.26	100.27	100.20	100.83	100.25	100.36	100.210	100.66
O=F	-0.583	-0.356	-0.508	-0.568	-0.546	-0.684	-0.531	-0.496
Total	99.68	99.91	99.69	100.26	99.70	99.67	99.68	100.17
T								
Si	6.8781	6.7900	6.9746	6.8541	6.8812	6.8897	6.7392	6.8427
Al(IV)	1.1219	1.2100	1.0254	1.1459	1.1188	1.1103	1.2608	1.1573
Total	8.000	8.000	8.000	8.000	8.000	8.000	8.000	8.000
C								
Al(VI)	0.0324	0.0442	0.0712	0.0367	0.0488	0.0785	0.0978	0.0311
Ti	0.1052	0.1490	0.0968	0.1274	0.1135	0.0871	0.1557	0.1309
Fe(3+)	0.3100	0.2887	0.4094	0.2796	0.3304	0.4620	0.4880	0.2926
Mg	1.6828	1.4909	1.6548	1.6446	1.6910	1.6415	1.4600	1.7773
Fe(2+)	2.8696	3.0272	2.7678	2.9117	2.8163	2.7309	2.7985	2.7681
Total	5.000	5.000	5.000	5.000	5.000	5.000	5.000	5.000
B								
Fe(2+)	0.2132	0.1503	0.1108	0.2151	0.1625	0.1179	0.0673	0.1999
Mn	0.0764	0.0780	0.0902	0.0796	0.0723	0.0744	0.0705	0.0805
Ca	1.6494	1.6887	1.6514	1.6365	1.6736	1.6606	1.6581	1.6610
Na	0.0610	0.0830	0.1476	0.0688	0.0916	0.1471	0.2041	0.0586
Total	2.000	2.000	2.000	2.000	2.000	2.000	2.000	2.000
A								
Na	0.4836	0.5059	0.3566	0.4754	0.4482	0.3724	0.3844	0.4589
K	0.1461	0.1558	0.1420	0.1681	0.1557	0.1703	0.1831	0.1711
Total	0.6297	0.6617	0.4986	0.6437	0.6039	0.5427	0.5675	0.6300

Table 4-9 continued

	Glamaig Amphibole							
Crystal	3(core)	3(rim)	4(core)	4(rim)	5(rim)	5(core)	5(core)	5(core)
SiO_2	44.57	42.94	43.46	43.11	46.58	43.66	45.50	45.22
TiO_2	1.05	1.12	1.35	1.32	0.81	1.12	0.85	1.06
Al_2O_3	6.59	7.10	6.83	7.22	4.69	6.44	5.29	5.33
FeO(tot.)	25.10	27.25	26.84	26.57	24.83	26.18	26.19	25.94
MnO	0.43	0.71	0.72	0.65	0.73	0.69	0.85	0.61
MgO	7.69	5.95	5.84	6.21	8.11	6.59	7.02	7.21
CaO	10.05	10.17	10.15	10.19	9.76	10.26	9.99	9.97
Na_2O	1.82	1.86	1.94	1.78	1.38	1.66	1.59	1.53
K_2O	0.92	0.93	0.86	0.91	0.55	0.86	0.63	0.66
H_2O	1.36	1.46	1.32	1.38	1.45	1.51	1.30	1.46
F	1.21	0.94	1.24	1.12	1.01	0.82	1.31	0.95
Total	100.78	100.43	100.54	100.44	99.90	99.81	100.51	99.95
O=F	-0.508	-0.394	-0.522	-0.469	-0.426	-0.347	-0.553	-0.402
Total	100.28	100.03	100.02	99.96	99.48	99.46	99.96	99.55
T								
Si	6.8620	6.7262	6.7956	6.7240	7.1873	6.8398	7.0664	7.0474
Al(IV)	1.1380	1.2738	1.2760	1.2760	0.8127	1.1602	0.9336	0.9526
Total	8.000	8.000	8.000	8.000	8.000	8.000	8.000	8.000
C								
Al(VI)	0.0577	0.0377	0.0547	0.0512	0.0412	0.0297	0.0345	0.0265
Ti	0.1210	0.1323	0.1590	0.1552	0.0940	0.1320	0.0989	0.1241
Fe(3+)	0.3319	0.3617	0.3145	0.3883	0.2367	0.3014	0.2270	0.1818
Mg	1.7656	1.3885	1.3615	1.4436	1.8646	1.5381	1.6250	1.6739
Fe(2+)	2.7238	3.0798	3.1103	2.9617	2.7635	2.9988	3.0146	2.9939
Total	5.000	5.000	5.000	5.000	5.000	5.000	5.000	5.000
B								
Fe(2+)	0.1763	0.1287	0.0842	0.1159	0.2042	0.1302	0.1602	0.2056
Mn	0.0565	0.0937	0.0951	0.0855	0.0949	0.0917	0.1124	0.0800
Ca	1.6583	1.7069	1.7006	1.7026	1.6140	1.7227	1.6628	1.6650
Na	0.1089	0.0707	0.1201	0.0960	0.0869	0.0554	0.0646	0.0494
Total	2.000	2.000	2.000	2.000	2.000	2.000	2.000	2.000
A								
Na	0.4339	0.4948	0.4668	0.4417	0.3257	0.4485	0.4151	0.4135
K	0.1815	0.1857	0.1709	0.1803	0.1081	0.1727	0.1238	0.1320
Total	0.6154	0.6805	0.6377	0.6220	0.4338	0.6212	0.5389	0.5455

Table 4-10 Electron-probe analyses of pyroxene from the Loch Ainort Granite

	Loch Ainort Pyroxene							
Crystal	1(rim)	1(rim)	1(core)	2(core)	2(rim)	2(core)	3(rim)	3(core)
SiO_2	47.65	47.73	47.98	47.30	47.43	48.43	47.43	48.64
TiO_2	0.23	0.28	0.07	0.32	0.37	0.00	0.25	0.07
Al_2O_3	0.55	0.56	0.25	0.51	0.59	0.17	0.50	0.22
Fe_2O_3	3.34	3.72	3.80	3.91	4.21	3.32	3.50	2.74
Cr_2O_3	0.00	0.00	0.03	0.00	0.05	0.00	0.00	0.00
FeO	25.47	25.71	23.50	25.68	24.98	24.80	26.02	24.39
MnO	1.12	1.07	1.28	1.15	1.04	1.10	1.10	1.09
MgO	3.74	3.55	2.81	3.30	4.06	3.90	3.07	4.00
CaO	17.39	17.59	20.37	17.40	17.19	17.87	17.67	18.05
Na_2O	0.35	0.38	0.32	0.39	0.38	0.46	0.35	0.53
K_2O	0.01	0.01	0.02	0.00	0.01	0.01	0.02	0.02
Total	99.85	100.57	100.41	99.95	100.30	100.05	99.90	99.72
Si	1.9423	1.9354	1.9467	1.9335	1.9246	1.9636	1.9410	1.9720
Al	0.0264	0.0268	0.0117	0.0246	0.0282	0.0079	0.0240	0.0107
Ti	0.0071	0.0086	0.0021	0.0097	0.0112	0.000	0.0075	0.0020
Fe 3	0.1026	0.1136	0.1162	0.1202	0.1285	0.1014	0.1079	0.0836
Cr	0.0001	0.000	0.0009	0.000	0.0016	0.000	0.000	0.0001
Mg	0.2276	0.2147	0.1699	0.2010	0.2453	0.2359	0.1874	0.2403
Fe 2	0.8682	0.8717	0.7972	0.8780	0.8477	0.8408	0.8905	0.8271
Mn	0.0385	0.0367	0.0439	0.0398	0.0356	0.0376	0.0381	0.0374
Ca	0.7592	0.7642	0.8854	0.7620	0.7474	0.7763	0.7747	0.7841
Na	0.0273	0.0281	0.0252	0.0312	0.0296	0.0361	0.0278	0.0415
K	0.0005	0.0003	0.0010	0.000	0.0003	0.0004	0.0011	0.0011
Total	3.9991	3.9987	4.0010	4.0001	3.9999	3.9988	4.0011	4.0001
Wo	40.09	40.49	46.69	40.52	39.84	41.06	40.97	41.51
En	12.02	11.38	8.96	10.69	13.08	12.48	9.91	12.72
Fs	47.89	48.13	44.35	48.80	47.08	46.46	49.12	45.77

Table 4-10 continued

	Loch Ainort Pyroxene				
Crystal	4(rim)	4(core)	5(rim)	5(core)	5(core)
SiO_2	47.77	47.84	47.43	47.38	48.36
TiO_2	0.33	0.36	0.15	0.17	0.03
Al_2O_3	0.54	0.52	0.41	0.37	0.08
Fe_2O_3	2.53	3.16	4.16	4.01	3.64
Cr_2O_3	0.05	0.00	0.02	0.00	0.00
FeO	26.63	26.34	25.34	24.86	24.86
MnO	1.06	1.08	1.07	0.82	1.52
MgO	3.31	3.19	3.44	2.82	2.60
CaO	17.11	17.65	17.79	18.89	18.87
Na_2O	0.41	0.39	0.33	0.41	0.53
K_2O	0.00	0.00	0.01	0.00	0.06
Total	99.73	100.52	100.09	99.72	100.54
Si	1.9535	1.9435	1.9348	1.9404	1.9640
Al	0.0258	0.0251	0.0197	0.0177	0.0039
Ti	0.0100	0.0109	0.0046	0.0052	0.0009
Fe 3	0.0779	0.0966	0.1276	0.1236	0.1111
Cr	0.0016	0.000	0.0006	0.000	0.000
Mg	0.2017	0.1932	0.2093	0.1720	0.1572
Fe 2	0.9107	0.8951	0.8645	0.8514	0.8446
Mn	0.0367	0.0370	0.0348	0.0283	0.0523
Ca	0.7498	0.7682	0.7775	0.8288	0.8210
Na	0.0323	0.0304	0.0263	0.0324	0.0417
K	0.0000	0.0000	0.0004	0.0002	0.0032
Total	4.0001	4.0000	3.9991	4.0002	4.0000
Wo	39.48	40.57	41.22	44.07	43.79
En	10.62	10.21	11.10	9.15	8.38
Fs	49.89	49.23	47.68	46.78	47.83

Table 4-11 Electron-probe analyses of pyroxene from the Marsco Granite

	Marsco Pyroxene							
Crystal	1(rim)	1(rim)	1(core)	2(rim)	2(rim)	2(core)	3(rim)	3(core)
SiO_2	46.82	47.09	48.09	46.69	46.70	47.33	46.34	46.86
TiO_2	0.38	0.61	0.16	0.72	0.82	0.15	0.80	0.29
Al_2O_3	0.64	1.01	0.27	0.99	1.23	0.47	1.08	0.68
Fe_2O_3	4.34	3.67	3.59	4.03	3.29	3.95	4.71	5.44
Cr_2O_3	0.00	0.00	0.02	0.00	0.00	0.02	0.00	0.00
FeO	26.23	24.93	23.42	24.58	25.09	23.97	24.16	23.00
MnO	0.84	0.97	0.96	0.89	1.00	1.03	0.97	0.97
MgO	2.28	3.36	2.88	3.53	3.43	3.35	3.47	3.38
CaO	18.62	18.56	20.49	18.33	17.96	19.39	18.31	19.59
Na_2O	0.29	0.24	0.41	0.25	0.27	0.18	0.28	0.26
K_2O	0.00	0.03	0.00	0.02	0.03	0.02	0.01	0.00
Total	100.45	100.46	100.28	100.03	99.81	99.86	100.13	100.46
Si	1.9173	1.9113	1.9496	1.9028	1.9065	1.9309	1.8887	1.9020
Al	0.0310	0.0484	0.0127	0.0477	0.0590	0.0226	0.0518	0.0326
Ti	0.0118	0.0187	0.0050	0.0219	0.0251	0.0045	0.0246	0.0087
Fe 3	0.1339	0.1120	0.1096	0.1235	0.1009	0.1213	0.1445	0.1662
Cr	0.000	0.000	0.0007	0.000	0.000	0.0006	0.000	0.000
Mg	0.1390	0.2031	0.1738	0.2144	0.2089	0.2039	0.2111	0.2046
Fe 2	0.8983	0.8461	0.7939	0.8376	0.8564	0.8179	0.8235	0.7807
Mn	0.0292	0.0333	0.0330	0.0308	0.0347	0.0356	0.0336	0.0333
Ca	0.8167	0.8069	0.8898	0.8005	0.7854	0.8473	0.7996	0.8517
Na	0.0228	0.0186	0.0320	0.0199	0.0217	0.0144	0.0222	0.0202
K	0.0001	0.0017	0.000	0.0008	0.0014	0.0009	0.0005	0.000
Total	4.0000	4.0001	3.9998	3.9996	3.9997	4.0001	4.0000	3.9999
Wo	43.37	42.71	47.07	42.50	41.66	44.48	42.81	45.54
En	7.38	10.75	9.19	11.38	11.08	10.71	11.30	10.94
Fs	49.25	46.54	43.74	46.11	47.26	44.81	45.89	43.52

Table 4-11 continued

	Marsco Pyroxene						
Crystal	4(core)	4(rim)	5(rim)	5(core)	6(rim)	6(rim)	6(core)
SiO_2	46.44	45.69	45.98	46.07	46.02	46.47	46.91
TiO_2	0.57	0.58	0.63	0.65	0.60	0.33	0.09
Al_2O_3	0.86	0.75	0.94	0.83	0.83	0.54	0.22
Fe_2O_3	5.42	5.03	4.41	3.79	3.85	4.54	4.60
Cr_2O_3	0.00	0.00	0.00	0.02	0.00	0.03	0.00
FeO	23.70	27.61	27.00	26.95	27.96	27.05	26.04
MnO	0.93	1.01	1.01	0.98	1.02	1.05	0.97
MgO	3.37	0.99	1.66	1.59	1.00	1.38	1.49
CaO	18.74	18.24	18.39	18.48	18.40	18.55	19.27
Na_2O	0.30	0.30	0.22	0.25	0.26	0.32	0.39
K_2O	0.00	0.01	0.01	0.02	0.00	0.01	0.00
Total	100.32	100.19	100.22	99.62	99.93	100.26	99.98
Si	1.8908	1.8971	1.8979	1.9106	1.9114	1.9189	1.9361
Al	0.0411	0.0367	0.0459	0.0405	0.0406	0.0261	0.0104
Ti	0.0173	0.0181	0.0196	0.0204	0.0186	0.0101	0.0027
Fe 3	0.1662	0.1572	0.1370	0.1184	0.1203	0.1409	0.1429
Cr	0.000	0.000	0.000	0.0005	0.000	0.0011	0.0001
Mg	0.2047	0.0613	0.1021	0.0981	0.0620	0.0851	0.0914
Fe 2	0.8069	0.9582	0.9312	0.9348	0.9712	0.9342	0.8987
Mn	0.0319	0.0356	0.0352	0.0344	0.0358	0.0368	0.0340
Ca	0.8176	0.8115	0.8132	0.8210	0.8190	0.8205	0.8523
Na	0.0235	0.0237	0.0173	0.0203	0.0210	0.0256	0.0310
K	0.000	0.0005	0.0005	0.0010	0.000	0.0006	0.0002
Total	4.0002	4.0000	3.9998	3.9999	3.9995	4.0003	4.0001
Wo	43.93	43.47	43.22	48	43.38	43.72	45.42
En	11.00	3.29	5.42	5.19	3.28	4.53	4.87
Fs	45.07	53.24	51.36	51.33	53.34	51.74	49.71

Table 4-12 Electron-probe analyses of biotite from the Beinn an Dubhaich Granite

	Beinn an Dubhaich Biotite							
Crystal	1(rim)	1(rim)	1(core)	2(rim)	2(core)	3(core)	3(core)	3(rim)
SiO_2	34.98	35.21	34.88	35.31	35.32	34.91	35.45	35.27
TiO_2	4.03	3.92	3.94	3.66	3.18	2.97	3.03	3.05
Al_2O_3	11.83	12.18	12.08	12.12	11.54	12.56	12.06	12.29
FeO(Tot)	29.62	29.41	29.35	29.91	31.51	30.59	29.76	29.35
MnO	0.35	0.25	0.35	0.28	0.33	0.30	0.39	0.35
MgO	5.41	5.62	5.43	5.35	5.17	5.56	6.04	5.93
CaO	0.01	0.01	0.01	0.00	0.01	0.01	0.01	0.01
Na_2O	0.26	0.35	0.39	0.22	0.25	0.14	0.28	0.21
K_2O	9.20	9.12	9.06	9.07	8.98	8.65	8.83	9.49
H_2O	2.72	2.72	2.42	3.31	3.11	2.99	2.98	2.74
F	2.09	2.25	2.72	0.88	1.28	1.53	1.59	2.09
Total	100.48	100.92	100.64	100.09	100.66	100.29	100.42	100.77
O=F	-0.882	-0.904	-1.145	-0.370	-0.537	-0.643	-0.670	-0.881
Total	99.60	100.02	99.49	99.72	100.13	99.65	99.75	99.89
Si	5.230	5.231	5.254	5.190	5.234	5.181	5.244	5.251
Al(tot.)	2.086	2.132	2.145	2.098	2.016	2.198	2.103	2.157
Ti	0.453	0.438	0.447	0.405	0.354	0.331	0.338	0.341
Fe(3+)	0.556	0.548	0.555	0.551	0.586	0.570	0.552	0.548
Fe(2+)	3.148	3.105	3.143	3.125	3.319	3.227	3.130	3.106
Mg	1.206	1.244	1.219	1.171	1.142	1.230	1.332	1.315
Mn	0.044	0.031	0.044	0.035	0.042	0.038	0.049	0.045
Ca	0.000	0.001	0.001	0.000	0.001	0.009	0.002	0.001
Na	0.076	0.099	0.113	0.062	0.071	0.041	0.080	0.061
K	1.755	1.728	1.741	1.702	1.697	1.638	1.666	1.803
Total	14.755	14.557	14.662	14.339	14.462	14.462	14.496	14.628

Table 4-13. Rare-earth-element concentrations of minerals from the Beinn an Dubhaich and Loch Ainort granites (in ppm.)

	Beinn an Dubhaich					Loch Ainort		
	Alkali feldspar	Plago-clase	Amphi-bole	Zircon	Apatite	Alkali feldspar	Amphi-bole	Zircon
La	9.877	11.77	1511	------	1811	17.88	337.5	4.887
Ce	8.424	15.85	773.2	4.605	3764	36.21	733.4	23.77
Pr	0.849	1.621	105.3	0.163	412.0	4.352	92.51	1.676
Nd	2.755	5.424	475.0	0.757	1665	18.23	380.3	8.185
Sm	0.395	0.757	99.21	2.448	309.5	3.977	85.16	4.674
Eu	1.750	1.989	2.541	0.211	17.44	2.460	4.264	0.166
Gd	0.446	0.846	102.3	0.235	324.8	4.437	97.40	2.600
Tb	0.050	0.098	14.97	0.015	42.25	0.659	15.01	0.481
Dy	0.278	0.569	96.72	0.330	263.6	4.163	112.8	4.948
Ho	0.059	0.101	19.19	0.081	52.81	0.806	22.42	1.566
Er	0.189	0.352	58.05	0.479	166.0	2.423	67.54	7.669
Tm	0.026	0.056	8.362	0.092	23.27	0.331	9.783	1.723
Yb	0.201	0.328	56.95	78.65	160.3	1.960	69.79	67.60
Lu	0.032	0.053	8.604	0.207	23.54	0.257	11.71	3.769
(Ce/Yb)N	10.66	12.29	3.45	0.015	5.97	4.70	2.67	0.089
Eu/Eu*	12.82	7.63	0.078	0.860	0.064	1.80	0.14	0.15

Table 4-14. Rare-earth-element concentration of minerals from the Glamaig and Marsco granites (in ppm).

	Glamaig					Marsco		
	Alkali feldspar	Plago-clase	Amphi-bole	Zircon	Apatite	Alkali feldspar	Pyrox-cene	Zircon
La	5.975	9.148	1192	------	1417	7.938	1087	------
Ce	5.828	10.45	925.5	8.599	3190	16.99	2053	16.06
Pr	0.485	0.932	103.2	0.122	406.2	2.068	232.4	0.079
Nd	1.581	3.320	370.9	0.396	1725	8.467	919.2	0.318
Sm	0.238	0.481	63.59	3.461	294.9	1.924	154.4	2.952
Eu	1.794	2.432	2.248	0.544	14.28	1.141	9.505	0.487
Gd	0.339	0.607	62.43	0.611	282.8	2.168	167.8	0.564
Tb	0.027	0.053	8.082	0.225	30.91	0.334	22.02	0.143
Dy	0.166	0.295	49.21	2.138	167.9	2.283	137.6	1.243
Ho	0.036	0.054	9.282	0.778	30.36	0.473	27.06	0.484
Er	0.108	0.165	26.98	4.077	80.80	1.482	82.76	2.807
Tm	0.014	0.020	3.665	0.962	9.346	0.224	11.94	0.703
Yb	0.098	0.146	24.11	62.69	53.96	1.526	87.86	64.48
Lu	0.013	0.022	3.594	2.274	7.408	0.230	14.25	2.124
(Ce/Yb)N	15.07	18.17	9.76	0.035	15.03	2.83	6.03	0.06
Eu/Eu*	19.41	13.84	0.11	1.15	0.15	1.72	0.18	1.16

CHAPTER V

Thermometric and stable isotope geochemistry of fluid inclusions

5.1. Introduction

Micro-thermometric analysis has been used to measure the homogenisation, and first and last melting temperatures of fluid inclusions in quartz crystals from Skye granites. The homogenisation temperatures were used with an assumed hydrostatic pressure of fluid i.e. 250 bars, to calculate trapping temperatures according to charts proposed by Potter (1977). It is assumed that the Skye granites crystallised at a pressure around 500 bars (Hoersch, 1981), and were emplaced at their present exposure level (Thompson, 1969).

The $\delta^{18}O$ values for fluid inclusions, have been calculated from the $\delta^{18}O$ values of host quartz and homogenisation temperatures (Matsuhisa et al., 1979), whereas the δD values were measured directly from the inclusions.

The thermometric data suggest that the trapped fluid is a mixture of low-temperature meteoric water and a more saline, higher-temperature water which may have at least been partly magmatic. This is consistent with hydrogen and oxygen isotope data for inclusions in quartz which suggest that the fluid which 'associated' with the Skye granites was formed by limited mixing between magmatic and meteoric waters.

5.2 Fluid inclusion Studies

Micro-thermometric measurements were carried out on individual inclusions in quartz from three different Skye granites, prepared as free-standing doubly-polished wafers following the method of Shepherd et al. (1985). The micro-thermometric analyses were carried out using a calibrated LINKAM THM 600 heating/freezing stage (Shepherd, 1981).

The morphologies of inclusions were either ellipsoidal or irregular, and their size range from 15 to 35μm. Phase relationships at room temperature display only one type of inclusion, liquid-vapour aqueous inclusions (L+V) in all three samples.

5.2.1 Beinn an Dubhaich

These consist of a few random inclusions concentrated through out the crystals, indicating them to be of primary origin, up to 35 μm across (Barr, 1990; Gallagher et al., 1992), together with planar groupings of pseudosecondary and secondary inclusions of smaller size (20-30 μm). The pseudosecondary planars terminate before the crystal edges, and the secondary planars are continuous to the edge of crystals (cf. Boullier et al., 1991).

All inclusions, without exception, show a domination of the liquid phase over the vapour phase, and have a high degree of fill, i.e. F=0.85-0.9; where: F=volume of liquid phase / (volume of liquid phase + volume of vapour phase). All inclusions showed homogenisation to the liquid state.

5.2.2 Loch Ainort

Quartz crystals in the Loch Ainort Granite contain two generations of fluid inclusions of small to medium size (15-25 μm). The first one consists of ellipsoidal-shaped, pseudosecondary inclusions with slightly variable

liquid-vapour ratios, i.e. F=0.8-0.9. The second generation comprises secondary inclusions which are typically irregularly-shaped (cf. Batchelor et al., 1992). The degree of fill for the secondary inclusions is in the range F=0.9-0.95.

In general, the Loch Ainort inclusions are similar to inclusions from Beinn an Dubhaich, but there is no sign of any primary inclusions. The pseudosecondary and secondary inclusions in planar arrays along fractures are dominant.

5.2.3 Beinn Dearg Mhor

Only 18 inclusions in quartz from the Beinn Dearg Mhor Granite were studied because of their small size (10-15μm). These are similar to the inclusions in the Loch Ainort Granite in terms of their distribution and morphologies (irregular) (Feely and Hogelsberger, 1991), and their mode of homogenisation to the liquid state, with F=0.95. The termination of pseudosecondary inclusions before the edges of crystals and the continuation of secondary inclusions to the crystal edges are the main distinguishing features between these two types, beside the inclusion's shape.

5.3 Thermometric analyses

The results of thermometric analyses are given in Tables 5.1, 5.2 and 5.3 and Figs. 5.1, 5.2 and 5.3. All the aqueous inclusions measured from all three granites have temperatures of first ice melting in the range -24°C to -32°C, with a mean of about -27°C. Consideration of eutectic temperatures for aqueous systems suggests a Na-Mg-Cl dominated system (Shepherd et al., 1985). Inclusions from Beinn an Dubhaich quartz have low initial and last

melting temperatures relative to inclusions from the other two intrusions, suggestive of the presence of either Ca Cl_2 or Mg Cl_2 within the fluid phase (Potter and Clynne, 1978; Lamb et al., 1991; Feely and Hogelsberger, 1991).

Furthermore, certain inclusions in quartz from the Beinn an Dubhaich Granite have higher homogenisation temperatures (Th) than most other intrusions, whilst they have similar final melting temperatures (Tm). These differences can be attributed to their trapping under a different pressure (cf. Sterner et al., 1988; Ratajeski et al., 1994). Indeed, if the higher temperature inclusions from Beinn an Dubhaich quartz are primary, and the rest are pseudosecondary or secondary inclusions, then these inclusions must have trapped at different pressures and therefore represent different trapping events (i.e. different homogenisation temperatures).

Assuming 1:1 NaCl: $MgCl_2$, and using the relationships between salt wt.% and depression of freezing point (Shepherd et al., 1985), the Beinn an Dubhaich Granite inclusions have temperatures of last melting (Tm) ranging from -8.9 to -12.8°C. These values yield estimated salinity values between 11.9 and 15 equiv.wt.% NaCl (Table 5.1). Similarly, the Loch Ainort inclusions have temperatures of last melting ranging from -8.3 to -11.2°C, which yield salinity estimates of between 10.8 to 13 equiv. wt.% NaCl (Table 5.2). The Beinn Dearg Mhor inclusions have temperatures of last melting ranging from -10.2 to -13.2°C, which corresponds to salinities of 12 to 15.1 equiv. wt.% NaCl (Table 5.3).

All inclusions in this study showed final homogenisation into the liquid State (L+V --> L). Homogenisation temperatures (Th) for the Beinn an Dubhaich inclusions range from 273°C to 420°C, with a mean of about 333°C. The Loch Ainort inclusions range from 285°C to 388°C, with a mean of about 332°C, whereas the Beinn Dearg Mhor inclusions show homogenisation temperatures from 284°C to 356°C, with a mean of 323°C.

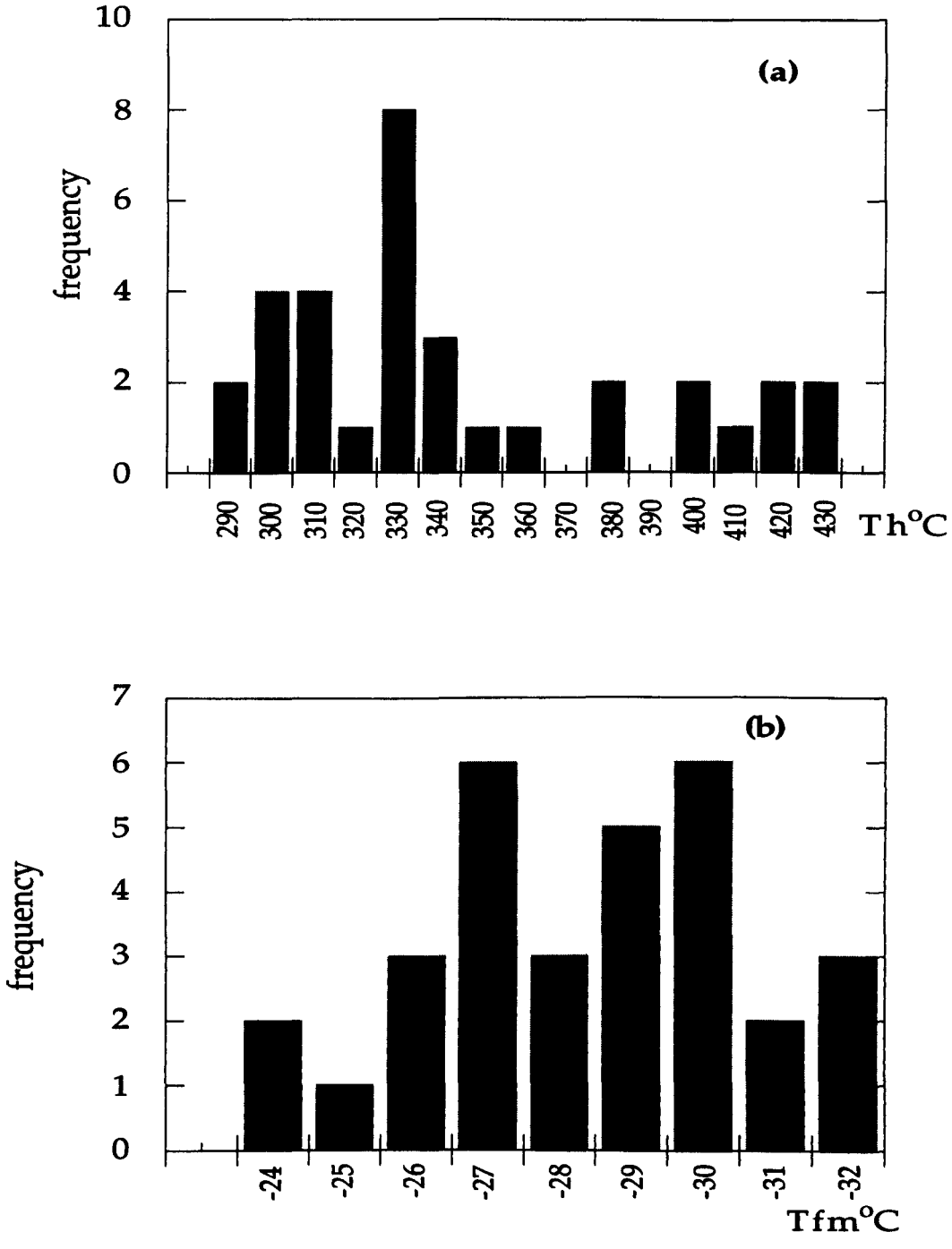

Fig. 5. 1 (a) and **(b)**. Homogenization (Th) and first melting (Tfm) temperatures of the inclusions in quartz from the Beinn an Dubhaich Granite.

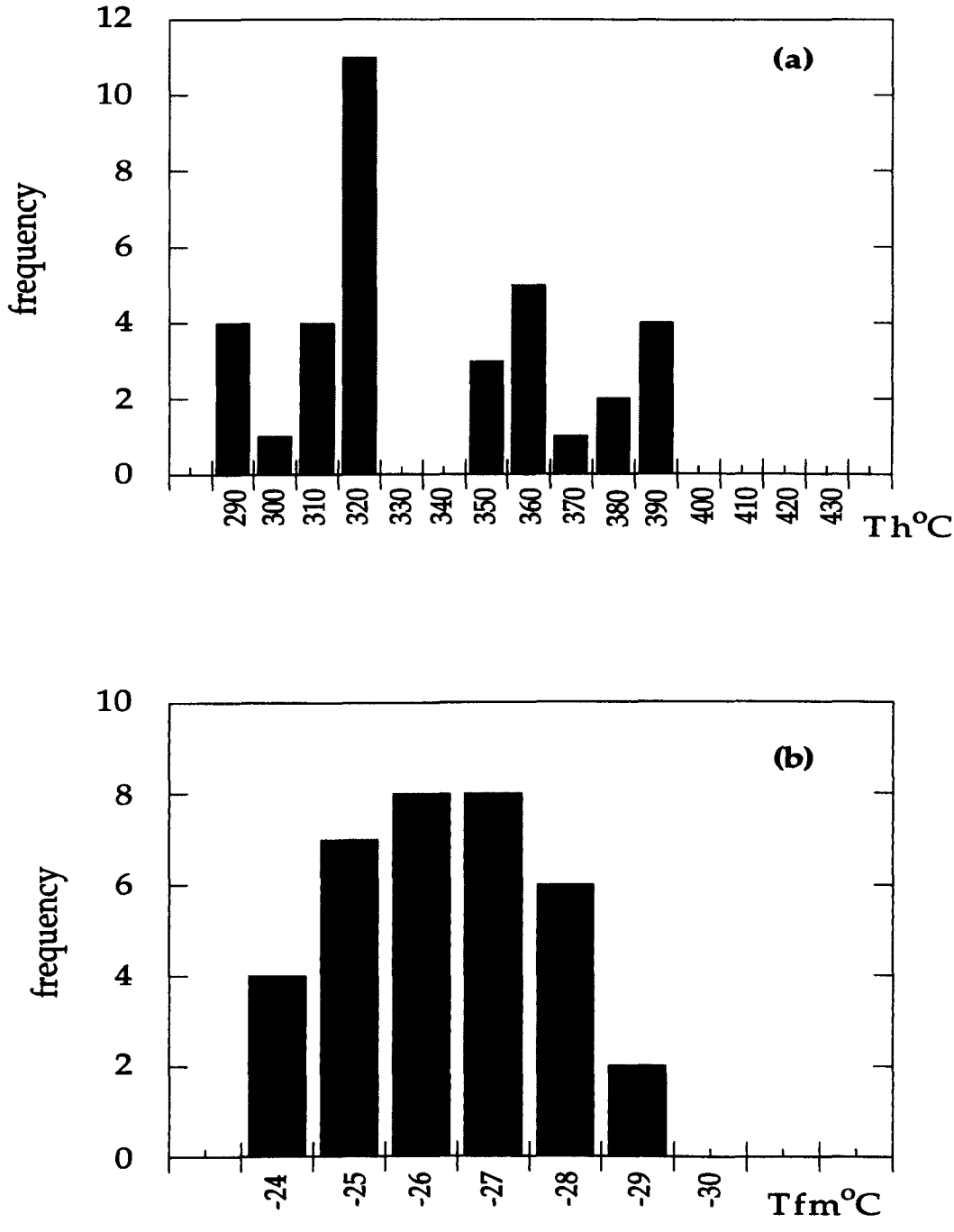

Fig. 5. 2 (a) and (b). Homogenization (Th) and first melting (Tfm) temperatures of the inclusions in quartz from the Loch Ainort Granite.

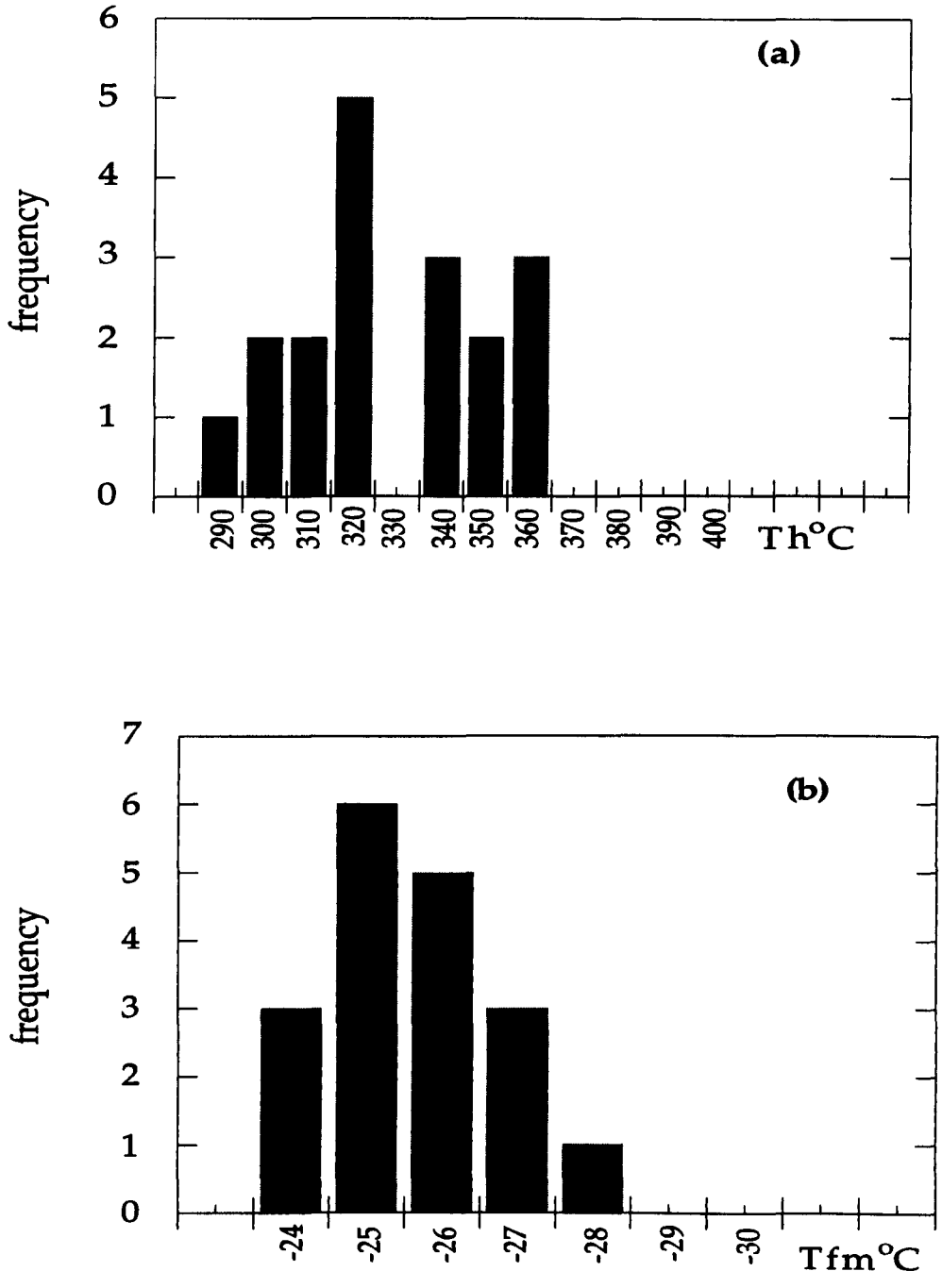

Fig. 5. 3 (a) and **(b).** Homogenization and first melting temperatures of the inclusions in quartz from the Beinn Dearg Mhor Granite.

These homogenisation temperatures theoretically can only be used as a minimum trapping temperature when assuming homogeneous trapping (Schwartz, 1989).

The Th-salinity pairs for Skye granite inclusions form a grouping which exhibits a wide range of homogenisation temperature values (280-410°C), and a rather limited salinity range (12-15 equiv. wt.% NaCl, Fig. 5.4). This wide spread of homogenisation temperatures with a reasonably constant salinity value probably indicates necking down of inclusions (Pecher, 1981; Yardley, 1983; Shepherd et al., 1985). The apparent compositional gaps between salinities of 12 and 13 equiv. wt.% NaCl, 13 and 14 equiv. wt.% NaCl are considered to be due to the difficulty of identification of halite daughter minerals, because of their small size, and since the halite crystals are difficult to identify in inclusions containing less than 24 equiv. wt.% NaCl (Shepherd et al., 1985).

Feely and Hogelsberger (1991) record approximately similar homogenisation and salinity values for inclusions in quartz crystals from the Galway Granite and related mineralised veins, i.e. ~350°C and ~10 equiv. wt.% NaCl, respectively. Subsequently, Gallagher et al. (1992), based upon their study of fluid inclusions from the Galway Granite, together with the stable isotope (O and H) mineralogical data presented by Jenkin et al. (1992), concluded that both late-stage magmatic fluids and post-magmatic meteoric waters were involved in the crystallisation and mineralization events.

Skye granites crystallised at a lithostatic pressure close to 500 bars (Brown, 1963; Hoersch, 1981). Assuming a hydrostatic pressure control on the fluid inclusion trapping temperatures, by using the relation between lithostatic and hydrostatic pressures, we can assume the fluid inclusion pressure in Skye granite quartz crystals is in the range 200 to 250 bars.

From approximate salinities in Tables 5.1, 5.2 and 5.3, and homogenisation temperatures, the trapping temperatures estimated from curves produced by Potter (1977) are listed in Tables 5.1, 5.2 and 5.3.

These trapping temperatures are just 8-13°C above the homogenisation temperatures in the range 300 to 430°C, which indicates that trapping occurred at sub-solidus temperatures (cf. Hansteen and Lustenhouwer, 1990), and most likely during episodes of hydrothermal fluid circulation, which is consistent with the hydrothermal alteration temperatures determined by Ferry (1985). Thus, the fluid responsible for these inclusions may be the product of the mixing of a low-temperature meteoric water with a more saline, higher-temperature fluid which may have been at least partly magmatic (cf. Rankin and Alderton, 1985), or long-lived aqueous fluid (cf. Jenkin et al., 1992).

Wilkinson (1990), in his study of fluid inclusions within quartz crystals in mineralised veins associated with the Cornubian granite batholith of south Cornwall, concluded that the fluid involved in the mineralising and alteration events resulted from mixing between ideal magmatic and metamorphic end-members.

5.4 Stable isotope data

Hydrogen isotope ratios of fluid inclusions in quartz from the Beinn an Dubhaich, Loch Ainort and Beinn Dearg Mhor granites were measured directly on water released by decrepitation of fluid inclusions, whereas oxygen isotope ratios for the fluids were obtained from the analyses of the quartz and utilizing homogenisation temperatures of the fluid inclusions based on the assumption that both quartz and fluids were at equilibrium, using established isotopic fractionation relationships (Matsuhisa et al.,

1979).

The results of the stable isotope study are presented in Table 5.4, and Fig. 5. 5. The homogenisation temperatures which were used in the calculations were selected to represent the minimum trapping temperatures in each intrusion. Higher homogenisation temperatures determined for primary and/or pseudosecondary inclusions in quartz from the granite, are more likely to be close to the mineral formation temperature (Vityk et al., 1993).

Forester and Taylor (1977) and Taylor (1979) estimated δD values for Skye Eocene meteoric water to be in the range -85 to -100°/oo, and δ^{18}O values in the range -12 to -14°/oo. Magmatic water signatures calculated by Taylor (1974) define a region on δD v δ^{18}O diagrams between δD values of -40 and -80°/oo and δ^{18}O values of 5.5 and 9.0°/oo. The range for metamorphic waters is: δD values between 0 and -65°/oo and δ^{18}O values between 2 and 20°/oo (Sheppard, 1986; Rollinson, 1993).

The δD value for the fluid inclusions in the Beinn an Dubhaich quartz is close to -86°/oo, whereas the δD value from the Loch Ainort Granite is -90°/oo and from Beinn Dearg Mhor Granite is -93.5°/oo. These δD values suggest that the fluids were dominantly of meteoric origin, and the observed difference in δD values of the fluids between these granites are unlikely to be due to water-rock interaction, since hydrogen is usually a trace-element in rocks (Sheppard, 1986). Such differences can be attributed to the different H-isotope compositions of the fluids 'associated' with each intrusion (Curtis et al., 1993).

The δD value for each intrusion represents fluids trapped over a wide range in temperature. This difference could be explained by the limited mixing of magmatic and meteoric waters in the Beinn an Dubhaich Granite, which contains primary inclusions as well as pseudosecondary and

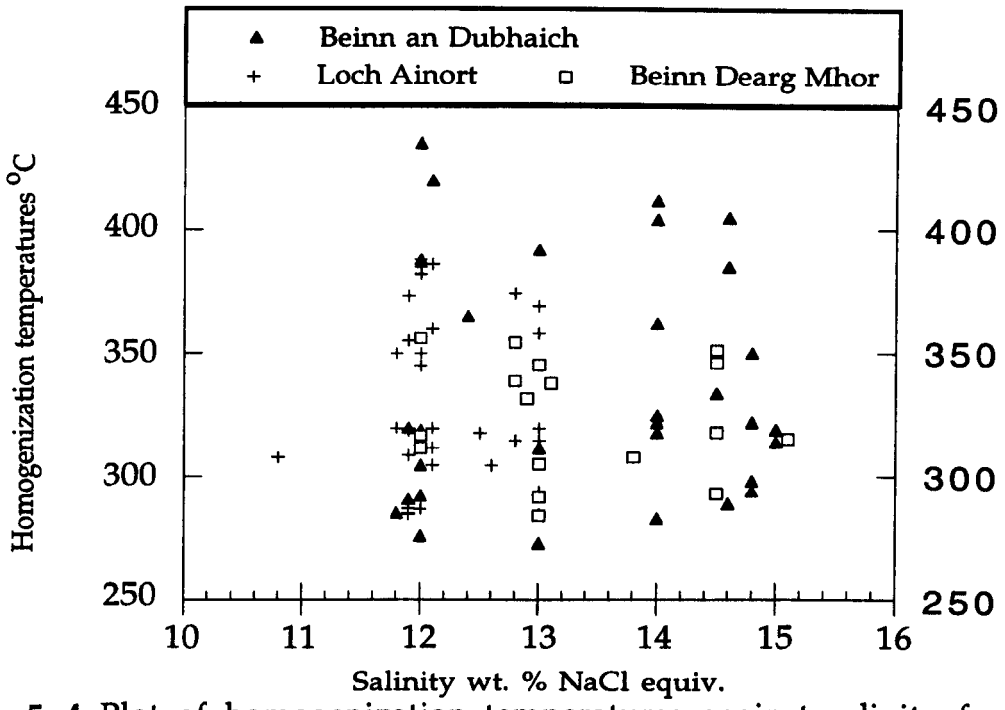

Fig. 5. 4 Plot of homogenization temperatures against salinity for fluid inclusions in quartz crystals.

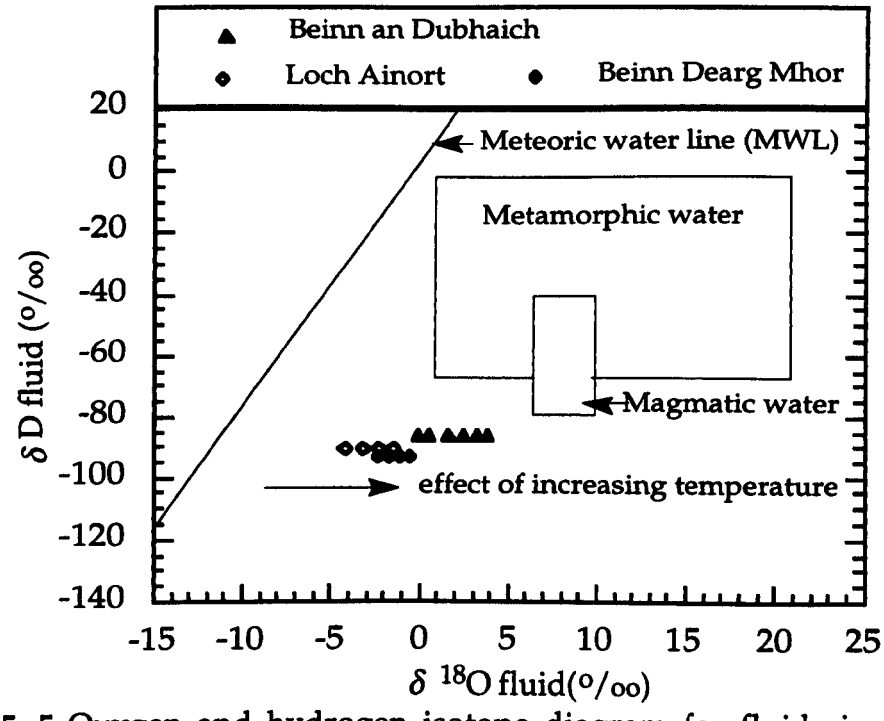

Fig. 5. 5 Oxygen and hydrogen isotope diagram for fluids in quartz from Skye granites over a range in temperatures (see main text for details).

secondary inclusions. The more depleted δD values in the Loch Ainort and Beinn Dearg Mhor granites suggest a greater importance for meteoric water during the hydrothermal circulation process.

Maximum homogenisation temperature values were identified in the Beinn an Dubhaich inclusions where the only primary inclusions recognised in this study are present. The minimum homogenisation temperature values correspond to all the secondary inclusions in all three intrusions.

The $\delta^{18}O$ values of quartz from the Beinn an Dubhaich, Loch Ainort and Beinn Dearg Mhor granites are 7.5‰, 3.0‰ and 4.5‰, respectively. However, The $\delta^{18}O$ values for fluids in each intrusion, reflect, different degrees of positive oxygen isotope shift from the isotopic composition of meteoric water as a result of the difference in water-rock ratio at comparable temperatures of exchange (see Chapter VII; and, Sheppard, 1986). Consequently, these shifts usually increase with an increase in temperature of the fluid, as seen in Fig. 5.5, because the mineral-water fractionation factors decrease with increasing temperature and also the rate of oxygen isotope exchange increases with increasing temperature (Jenkin, 1988).

5. 5 Summary and conclusions

(i) Fluid inclusion microthermometric analysis and stable isotope data indicate that limited mixing of magmatic and meteoric waters was responsible for the fluids 'associated with' the Skye granites. However, the relative significance of the circulating long-lived meteoric waters is difficult to quantify (cf. Jenkin et al., 1992).

(ii)The thermometric and isotopic data demonstrate that the fluids

'associated' with the Beinn an Dubhaich Granite had the largest magmatic component relative to the other two granites studied.

(iii) The pseudosecondary and secondary inclusions are most likely the result of reactions caused by 'associated' hydrothermal fluids (i.e. predominantly meteoric water) (cf. Turpault et al., 1992).

Table 5.1 Thermometric data for inclusions in quartz from the Beinn an Dubhaich Granite.

Th (°C)	Tfm (°C)	Tm (°C)	salinity %NaCl (equiv)	ΔTc (°C)	Trapping T (°C)
285	-30.4	-11.2	13	11.5	296.5
314	-25.4	-12.7	15	11	325
322	-25.2	-11.8	14	10.8	330.8
314	-26.4	-12.6	15	11	325
334	-26.2	-12.2	14.5	10.5	344.5
285.4	-22.4	-9.4	11.8	12	297.4
320	-23.1	-8.9	11.9	11.5	331.5
298.2	-22.1	-12.4	14.8	12	310.2
322	-27.4	-12.3	14.8	10.8	332.8
291	-28.3	-9.8	11.9	11.8	302.8
420	-31.4	-10.4	12.1	9	429
273	-31.6	-11.2	13	12.5	285.5
435	-27.4	-10.2	12	8.5	443.5
388	-27.4	-10.2	12	10.5	398.5
350	-25.2	-12.4	14.8	10	360
392	-31.1	-11.2	13	9	401
404	-30.6	-11.7	14	8.5	412.5
276	-28.4	-10.3	12	12	288
319	-26.3	-12.8	15	10.8	329.8
294	-24.8	-12.4	14.8	11	306
325	-27.2	-11.8	14	10.5	335.5
318	-25.1	-11.6	14	10.6	328.6
314	-25.3	-10.2	12	11	325
319.2	-24.5	-10.1	12	11	330.2
283	-28.2	-11.7	14	12	295
312	-25.2	-10.9	13	11	323
305	-24.5	-9.9	12	11.5	316.5
292.4	-30.1	-9.7	12	12	304.4
412	-28.1	-11.6	14	8.8	420.8
385	-28.2	-12	14.6	9.8	394.8
405	-30	-12.1	14.6	9.9	414.9
362	-28	-11.6	14	10.5	372.5
289	-28.4	-12.1	14.6	12.6	301.6
365	-29.2	-10.6	12.4	10.5	375.5

Where: Th, Homogenisation temperature; **Tfm,** First melting temperature; **Tm,** last melting temperature.

Table 5.2 Thermometric data for inclusions in quartz from the Loch Ainort Granite.

Th (°C)	Tfm (°C)	Tm (°C)	salinity %NaCl (equiv)	ΔTc (°C)	Trapping T (°C)
345	-27.3	-10.3	12	11	356
350	-28.2	-10.2	12	11	361
350	-28.4	-9.5	11.8	11	361
294.3	-25.2	-11.2	13	11.5	305.8
285.2	-26.2	-9.9	11.9	12.5	297.5
287	-26	-10.3	12	12.5	299.5
320	-24	-9.5	11.8	11	331
285	-25.3	-9.8	11.9	12.5	297.5
320	-26.2	-10.4	12.1	11.5	331.5
373	-24.8	-10	11.9	10.5	383.5
312	-27	-10.4	12.1	11	323
382	-24.5	-10.3	12	10	392
309	-26.2	-9.9	11.9	11.5	320.5
305	-27.2	-10.4	12.1	11.5	316.5
318	-25.3	-10.2	12	11	329
369	-24.7	-10.9	13	11	380
386	-27.3	-10.4	12.1	10.5	396.5
305	-25.5	-10.6	12.6	11.5	316.5
315	-26.3	-11.2	13	10.5	325.5
320	-23.8	-11.1	13	10.5	330.5
360	-27.4	-10.4	12.1	11	371
287.4	-24.3	-10.1	11.9	12.5	299.9
355	-24	-10	11.9	11	366
315	-26	-10.8	12.8	10.5	325.5
308	-23.8	-8.3	10.8	11.5	319.5
385	-24.6	-10.3	12	10	395
319	-25.1	-9.9	11.9	11	330
316	-26.4	-10.1	12	11	327
318	-27.4	-10.8	12.5	11	329
356	-25.8	-10.1	12	11	367
358	-24.1	-11	13	10.5	368.5
374	-24.8	-10.8	12.8	9.5	383.5
320	-26.4	-9.8	11.9	11.5	331.5
388	-27.2	-10.3	12	10	398
355	-26.9	-10	11.9	11	366

Where: Th, Homogenisation temperature; **Tfm,** First melting temperature; **Tm,** last melting temperature.

Table 5.3 Thermometric data for inclusions in quartz from the Beinn Dearg Mhor Granite.

Th (°C)	Tfm (°C)	Tm (°C)	salinity %NaCl (equiv)	ΔTc (°C)	Trapping T (°C)
356.2	-29.4	-10.4	12	10	366.2
339	-28.7	-10.9	12.8	10	349
315.2	-28.8	-13.2	15.1	11	326.2
312	-28.5	-10.2	12	9	321
284.4	-30.2	-11.3	13	11	295.4
346.2	-28.2	-12.1	14.5	10	356.2
292	-29.8	-10.9	13	11	303
351.2	-29.4	-12.3	14.5	10	361.2
308.1	-30.4	-11.5	13.8	11	319.1
318	-27.4	-12.1	14.5	10.5	328.5
345.4	-30.2	-11.3	13	10	355.4
293	-28.4	-12.4	14.5	11	304
317	-29.3	-10.4	12	12	329
338	-29.1	-11.4	13.1	11	349
354.2	-27.3	-10.8	12.8	10	364.2
332	-28.4	-11.2	12.9	11	343
305.6	-31.1	-11.3	13	11	316.6
315	-27.2	-10.8	12.8	10.5	325.5

Where: Th, Homogenisation temperature; **Tfm,** First melting temperature; **Tm,** last melting temperature.

Table 5. 4 Stable isotope (δD and δ^{18}O) data for fluid inclusions in quartz crystals from Skye granites.

Sample description	T °C	T K	δD, °/oo (SMOW)	δ^{18}O quartz, °/oo	δ^{18}O fluid, °/oo
Beinn an Dubhaich	280	553.15	-86	7.5	-0.1
	300	573.15	-86	7.5	0.64
	330	603.15	-86	7.5	1.63
	360	633.15	-86	7.5	2.48
	390	663.15	-86	7.5	3.22
	420	693.15 -	-86	7.5	3.86
Loch Ainort	290	563.15	-90	3.0	-4.22
	320	593.15	-90	3.0	-3.18
	350	623.15	-90	3.0	-2..29
	380	653.15	-90	3.0	-1.52
Beinn Dearg Mhor	300	573.15	-93.5	4.5	-2.36
	320	593.15	-93.5	4.5	-1.68
	340	613.15	-93.5	4.5	-1.07
	360	633.15	-93.5	4.5	-0.52

CHAPTER VI

Whole Rock Chemistry

6.1 Introduction

Representative major-trace- including rare-earth-element whole rock analyses of granites from the Western and Eastern Red hills Centres, together with CIPW norms and other derived parameters, are presented in Tables 6.1 and 6.2.

In order to characterise the possible effects of hydrothermal processes on element mobility, bivarient plots involving alteration and turbidity indices (AX and TX) from Table 3.1 in Chapter III (where AX= total volume of secondary mafic minerals divided by the total volume of primary and secondary mafic minerals; and, TX= total volume of turbid feldspar divided by total volume of clear and turbid feldspars) and selected major- and trace-elements are presented in Figs. 6.1a-6.1j and 6.2a-6.2f. These plots show extreme scatter and a complete lack of correlation. This lack of correlation in Figs. 6.1a-6.1j and 6.2a-6.2f suggests that enrichment or depletion of major-and trace-elements did not systematically occur during hydrothermal alteration and secondary mineral formation. By comparison, Ferry 's (1985) study of Skye granites identified an increase in H_2O^+ and a decrease in calcium and iron during progressive hydrothermal alteration .

In Figs. 6.2a-6.2f the proportion of turbid feldspar is plotted against selected major- and trace-elements. The observed scatter indicates that the formation of turbid feldspar during hydrothermal alteration appears to have been

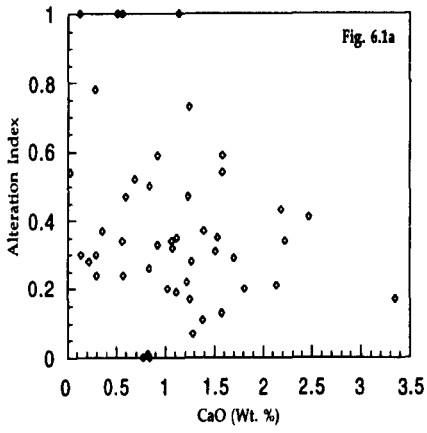
Fig. 6.1a
Alteration Index
CaO (Wt. %)

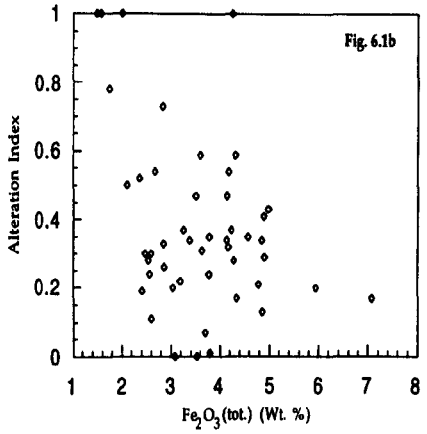
Fig. 6.1b
Alteration Index
Fe2O3(tot.) (Wt. %)

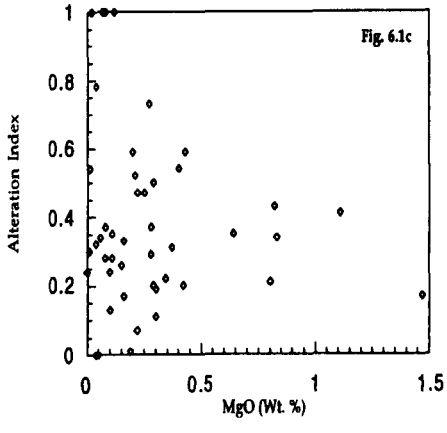
Fig. 6.1c
Alteration Index
MgO (Wt. %)

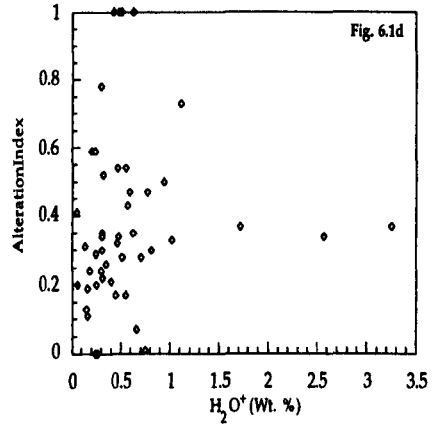
Fig. 6.1d
AlterationIndex
H2O+ (Wt. %)

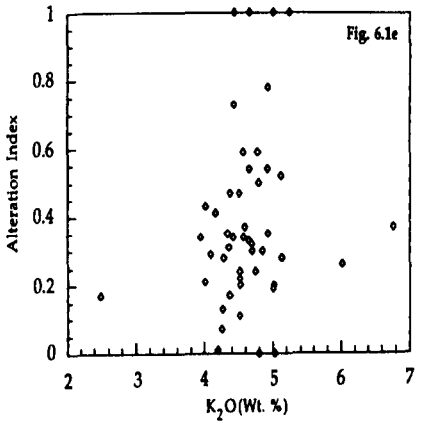
Fig. 6.1e
Alteration Index
K2O(Wt. %)

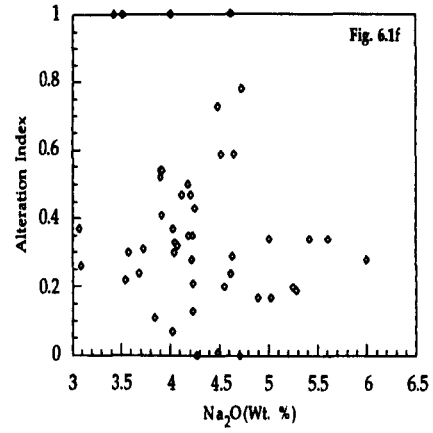
Fig. 6.1f
Alteration Index
Na2O(Wt. %)

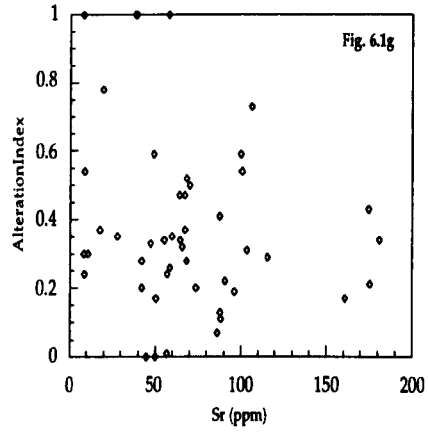

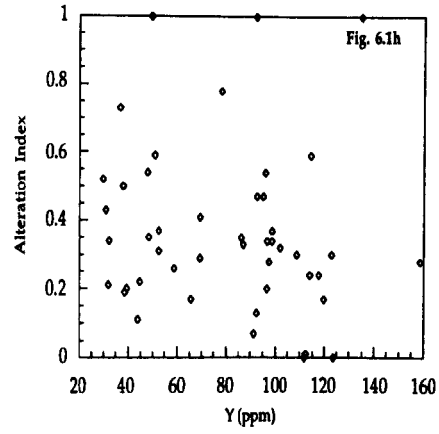

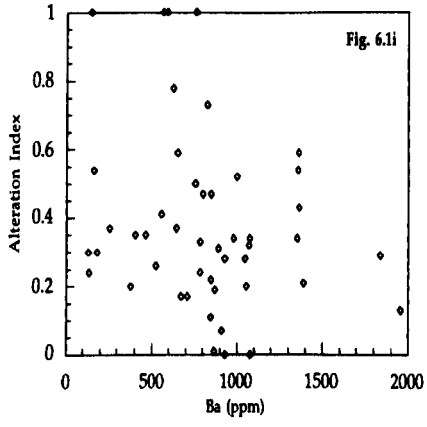

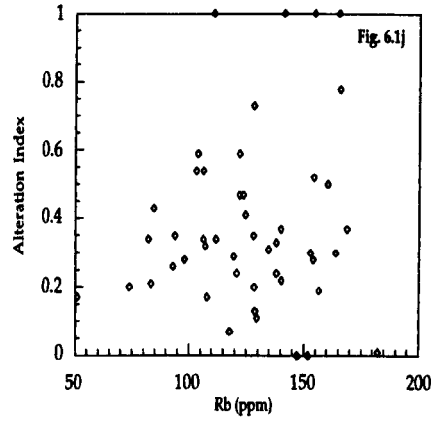

Figs 6.1a-6.1j Plots of Alteration Index (AX) against selected major- and trace-elements.

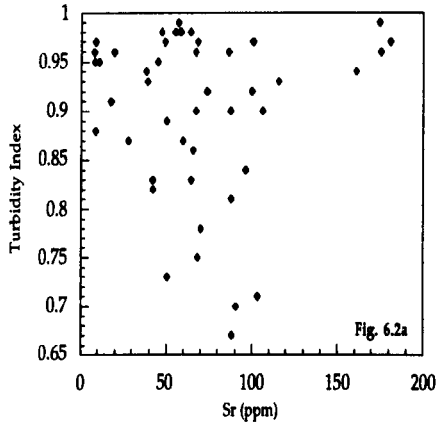

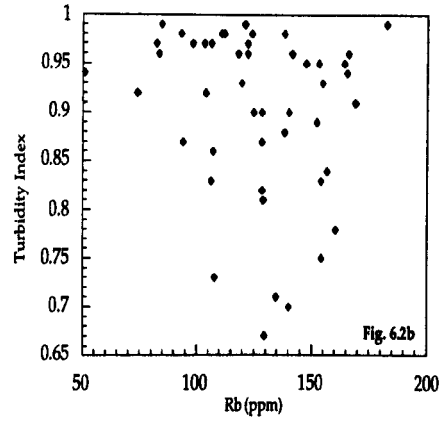

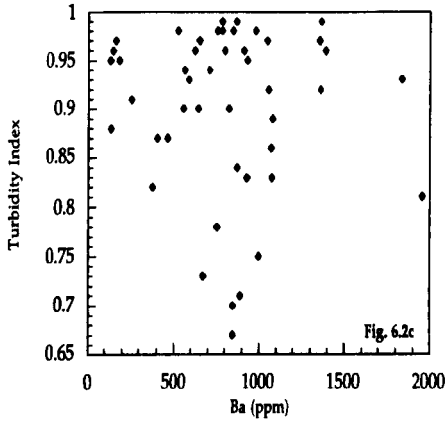

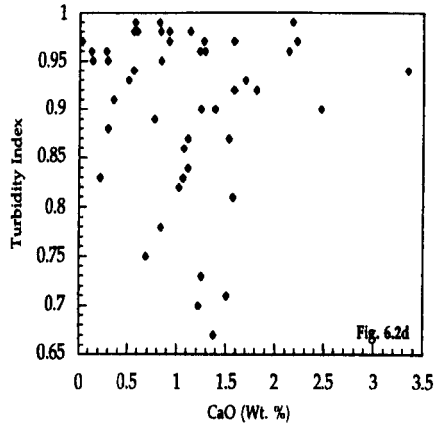

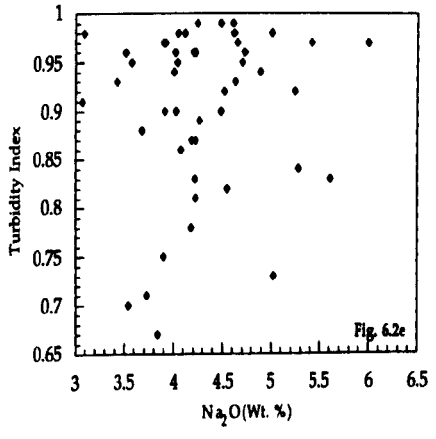

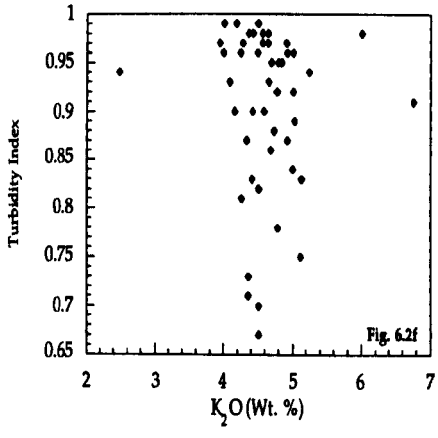

Figs 6.2a-6.2f Plots of Turbidity Index (TX) against selected major- and trace-elements.

isochemical. Thus, both the formation of turbid feldspar and other secondary minerals during hydrothermal alteration of Skye granites was isochemical, or nearly so, and both the major- and trace-element concentrations most likely record primary (i.e. magmatic) values.

Four intrusions, which cover the compositional variations within the two centres, have been examined in detail, in terms of their petrography, mineral chemistry, and isotope geochemistry. More attention is therefore given to these granites. They are, in order of emplacement (Bell, 1976): Glamaig (GL), Loch Ainort(LA), Marsco (MA) and Beinn an Dubhaich (BD).

6-2 Major -elements

Major-element variation diagrams are presented in Figs 6.3-6.12, utilizing the Thornton and Tuttle Differentiation Index [for Skye granites,TTDI = normative (Q+Or+Ab)] (Thornton and Tuttle, 1960) and SiO_2 wt.% as fractionation indices.

These bivarant plots show the following features:-

(A) SiO_2 v TTDI. Over the range of TTDI, silica increases from 67wt.% to 77.5wt.% (Fig. 6.3). The positive correlation between SiO_2 and TTDI from low silica (Glamaig) towards high silica (Marsco) is consistent with some form of differentiation process. However, the high SiO_2 concentration in the Marsco Granite may not represent a liquid composition, because from petrographic data certain samples (Table 3.1, samples SK-333 and SK-334) of the Marsco Granite contain more than 34.5 vol.% quartz, in contrast with the other sample from the Marsco Granite (SK-343) which contains 28 vol.% of quartz. It is suspected, therefore, that accumulation of quartz crystals within the magma has occurred (cf. McCormick, 1989). Sample SK-343 from the Marsco Granite

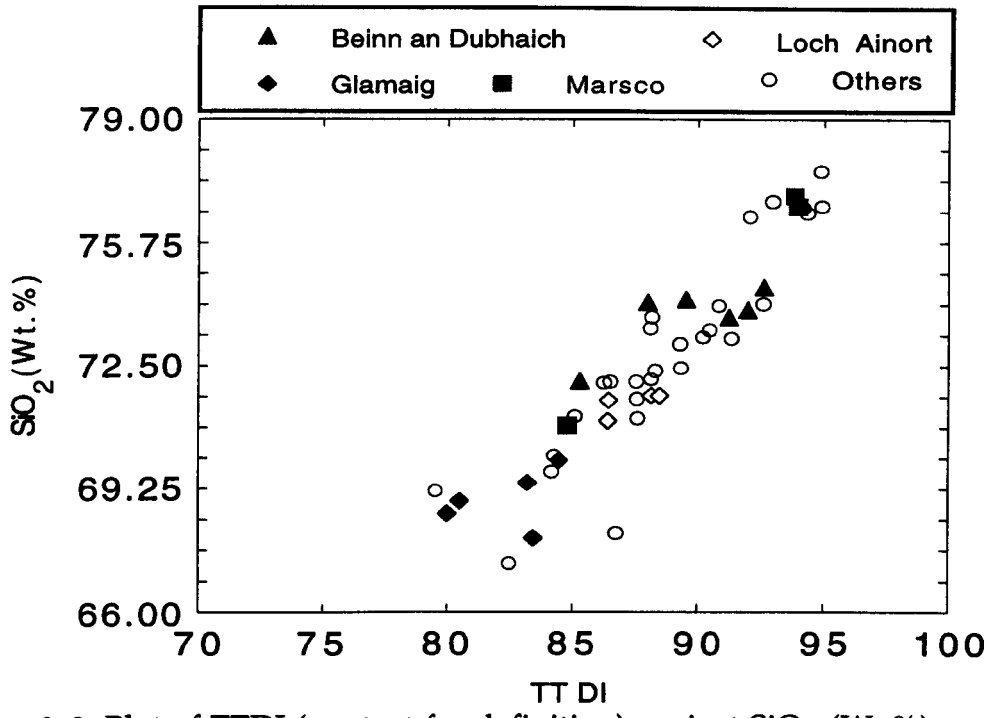

Fig. 6. 3. Plot of TTDI (see text for definition) against SiO_2 (Wt.%).

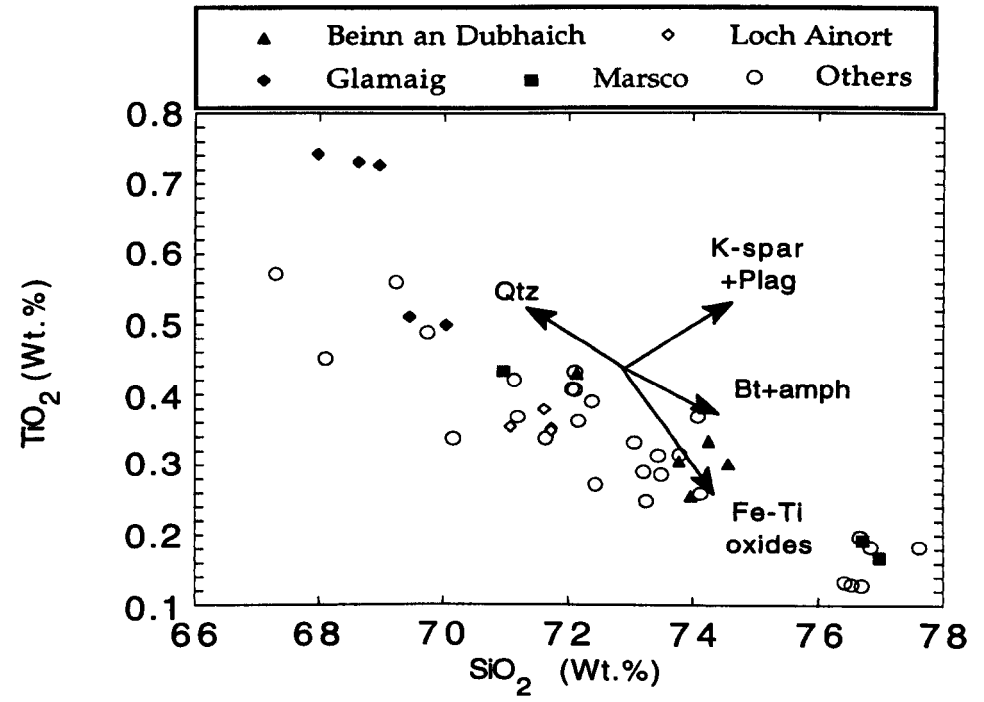

Fig. 6.4. SiO_2 (Wt.%) against TiO_2 (Wt.%).

has other significantly different compositional features, which will be discussed below.

(B) TiO_2 shows a compatible behaviour (Fig. 6.4), decreasing in the sequence: Glamaig, Loch Ainort, Beinn an Dubhaich and Marsco. The affinities of TiO_2, into which it mainly concentrated, are ilmenite and magnetite, and to a lesser extent amphibole and biotite. Thus, the observed relation between TiO_2 and SiO_2 is consistent with the fractionation of these minerals as the vectors show. Alternatively mixing, of a high TiO_2 and low SiO_2 liquid with a low TiO_2 and high SiO_2 liquid cannot be ruled out.

(C) Over the range of silica concentration, Al_2O_3 shows a rather broad scatter, with a decrease from 13.7wt.% in the Glamaig Granite to 11.2wt,% in the Marsco, Allt Fearna and Creag Strollamus granites (Fig. 6.5). These relationships between silica and alumina are consistent with plagioclase and alkali feldspar fractionation (cf. McCormick, 1989). This conclusion is supported by the lack of plagioclase in the highly evolved granites (i.e. Marsco, Allt Fearna and Creag Strollamus, see modal data, Chapter III).

(D) In a plot of Fe_2O_3 * (i.e. total iron) against SiO_2 (Fig. 6.6), the observed trend is a decrease in iron with increasing silica concentration, from Glamaig through Loch Ainort and Beinn an Dubhaich to Marsco. The variation in iron content with silica is consistent with the fractionation of ferromagnesian silicates (i.e. pyroxene, amphibole and biotite) and Fe-Ti oxides, as indicated by the mineral subtraction vectors (cf. Gamble et al., 1992), or, alternatively, by magma-mixing (see (B), above).

(E) The concentration of MnO through the suite apparently shows two different trends (Fig. 6.7). Trend (1) represents incompatible behaviour from Glamaig towards Glen Sligachan (SK-328), whereas, trend (2) shows a compatible relation with SiO_2, extending from Glen Sligachan (SK-328), through most of

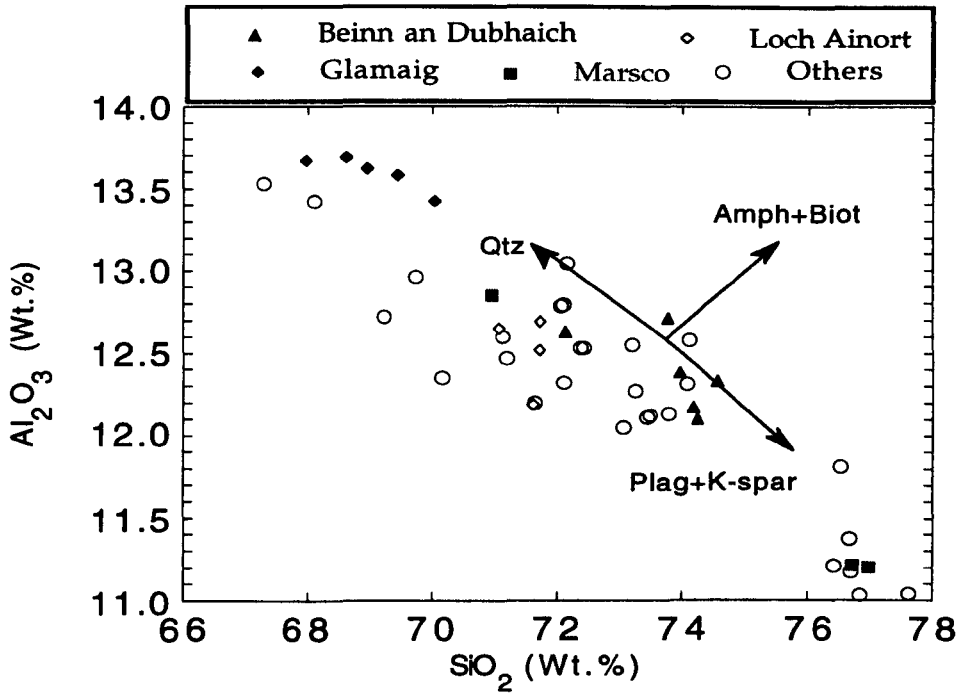

Fig. 6.5. SiO_2 (Wt.%) against Al_2O_3 (Wt.%).

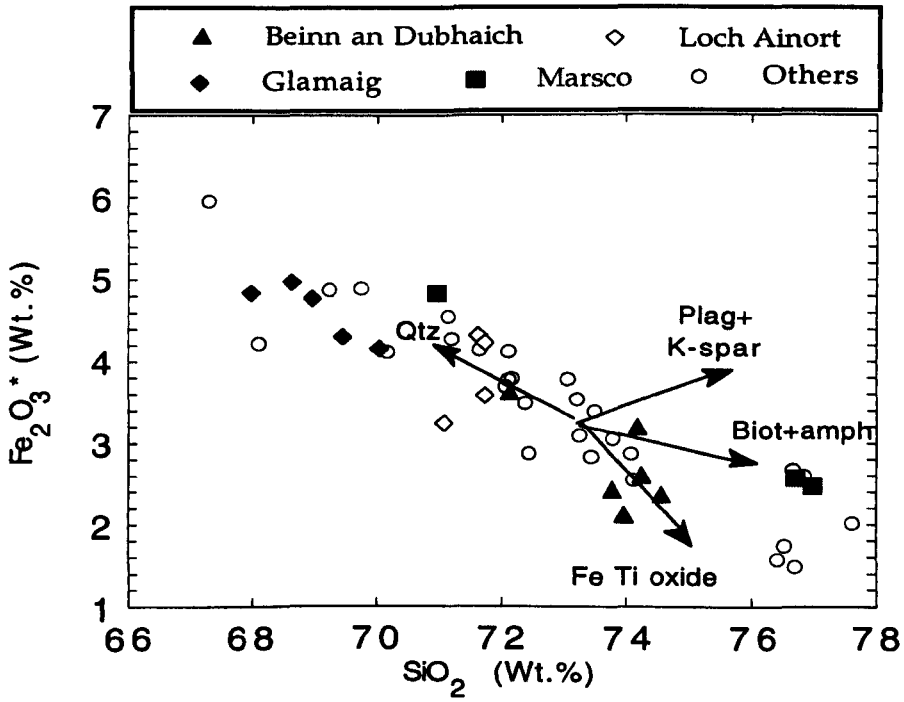

Fig. 6.6. SiO_2 (Wt.%) against $Fe_2O_3^*$ (total iron)(Wt.%).

the suite to highly evolved intrusions (i.e. Marsco, Allt Fearna and Creag Strollamus). Trend (1) may be explained either by incorporation of pyroxene from new basic pulses during differentiation process or fractionation of MnO-depleted phases, for example plagioclase, from the most primitive composition represented by Glamaig Granite, up to the more evolved magma(s) composition as represented by Glen Sligachan Granite (SK-328), (see Wilson, 1989). Thereafter, fractionation of MnO-rich phases will produce the negative correlation between MnO and SiO_2. The unusually high concentration of manganese in the relatively silica-poor Eas Mor Granite (SK-321) may be explained in terms of significant amounts of quartz fractionation.

(F) The majority of Skye granites have MgO concentrations of less than 0.5wt.%. Certain of the Glamaig samples fall above 0.5wt.% (Fig. 6.8). In general, there is a decrease in MgO content within the more evolved granites, despite an observable poor correlation between MgO and SiO_2. However, the enrichment of MgO in Glamaig and Beinn an Dubhaich, relative to Loch Ainort and Marsco, and the majority of the suite in general, can explain their magnesum-rich amphiboles, for example, Glamaig (7.3 wt.%) and Beinn an Dubhaich (5.5 wt.%) compared with Loch Ainort (0.8 wt.%), despite the similar modal amounts of amphibole in the three intrusions. In addition, the MgO content of the pyroxenes from Loch Ainort are higher than in the Marsco pyroxenes (averages of 3.5 and 2.5 wt.%, respectively).

This contrast in amphibole and pyroxene compositions in the Loch Ainort Granite suggests that mixing between evolved Loch Ainort magma with its low-MgO amphiboles with more refractory (MgO-rich) pyroxene has occurred. The origin of the pyroxene is unclear, although it is evident that they were not precipitated directly from the Loch Ainort magma. It may be explained by the refluxing of the magma chamber with new batches of more primitive magma, i.e. the influx of a new magma pulse and its mixing with residual evolved

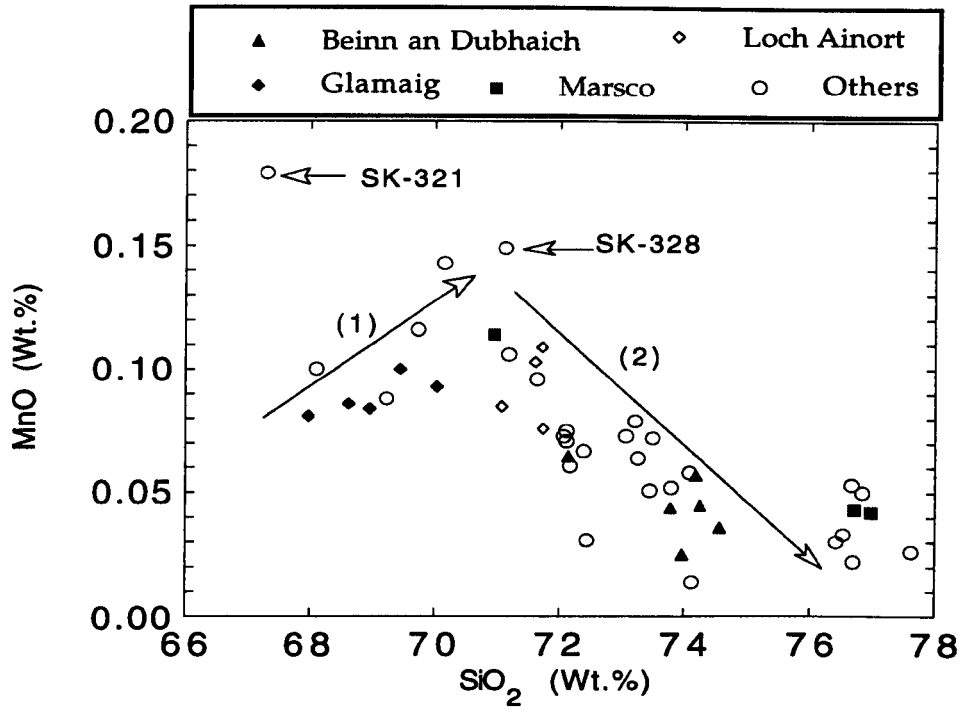

Fig. 6.7. SiO_2 (Wt.%) against MnO (Wt.%).

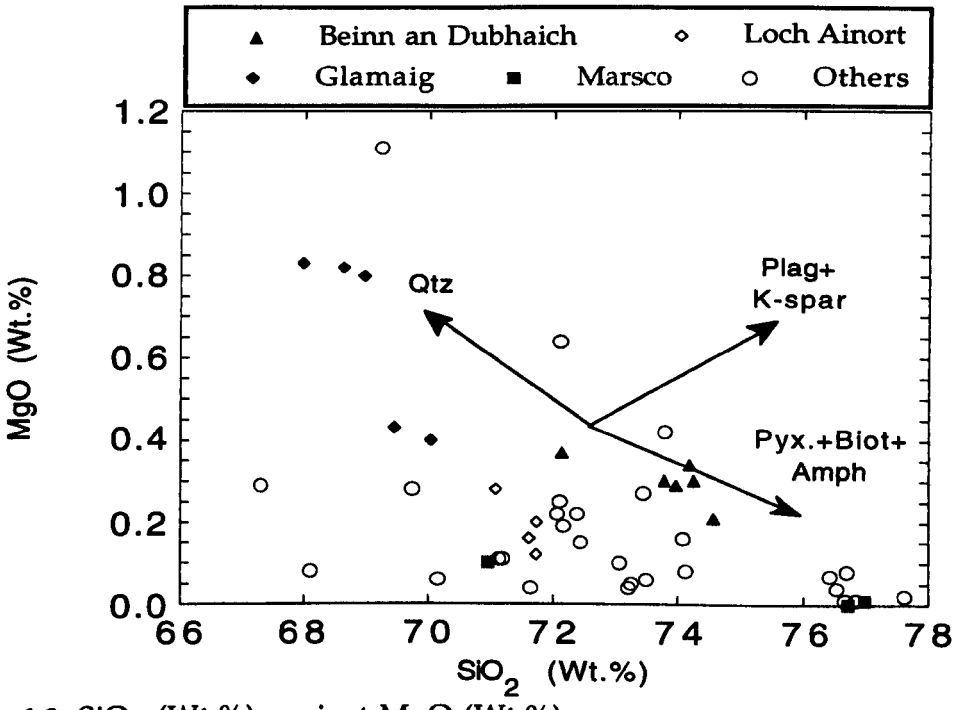

Fig. 6.8. SiO_2 (Wt.%) against MgO (Wt.%).

magma.

The MgO enrichment of the Beinn an Dubhaich Granite could be evidence in favour of a crystal mush origin of this granite (cf. Hood, 1981), i.e. the intrusion represents a mixture of refractory material and evolved liquid. This type of mixing process may commonly be involved in the generation of granitic magmas, as the heat provided by basaltic magmas can melt a significant proportion of a rock of granitic composition, and the residual (refractory) component is carried upward within the anatectic liquid, as a crystal mush (Fourcade and Allègre, 1981; but see also, Hildreth, 1979)).

(G) Skye granites have CaO contents of up to 2.5wt.%, with the majority of analyses clustering between 0.5wt.% and 1.6wt.% (Fig. 6.9). The observed CaO trend is consistent with plagioclase and/or amphibole and, to a lesser extent, apatite fractionations, as shown by the fractionation vectors. The observed low CaO concentration in the Northern Porphyritic Felsite (SK-320) is consistent with the lack of plagioclase, amphibole and apatite in this intrusion.

(H) In general, Skye granites show wide variations in Na_2O content, in the range 3.1wt.% to 6wt.% (Fig. 6.10) compared with a small range for the Mourne granites (3.4 -3.6 wt.%, McCormick, 1989). The poorly-defined negative correlation between Na_2O and SiO_2 is broadly consistent with plagioclase fractionation. However, the enrichment in Na_2O (and Al_2O_3) in G1 and G3 intrusions relative to the other intrusions from the Mourne suite led Hood (1981) to attributed to higher water vapour pressure during crystallisation. Thus, the slight enrichment of Loch Ainort in Na_2O may be due to the same process. Such variations in water pressure could cause the shifting of the minimum towards the Ab apex in the Or-Ab-SiO_2 -H_2O system (for example, Winkler 1974, Table 18.2, p 283). The vectors on Fig. 6. 10 represent the effect of plagioclase, alkali feldspar and quartz fractionation, reflecting the importance of plagioclase fractionation during the evolution of the Skye granites. This

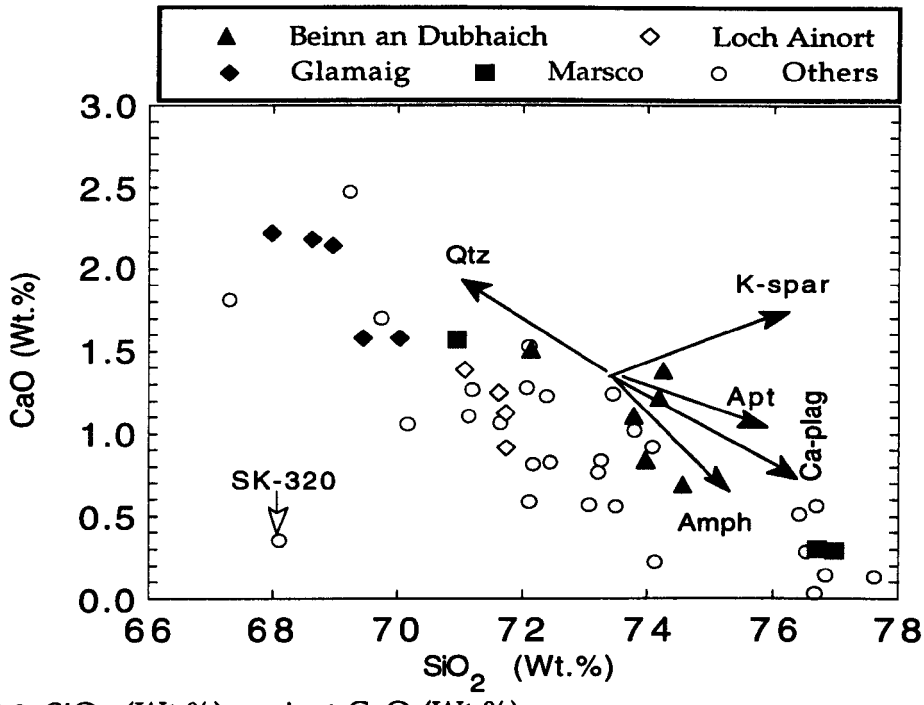

Fig. 6.9. SiO_2 (Wt.%) against CaO (Wt.%).

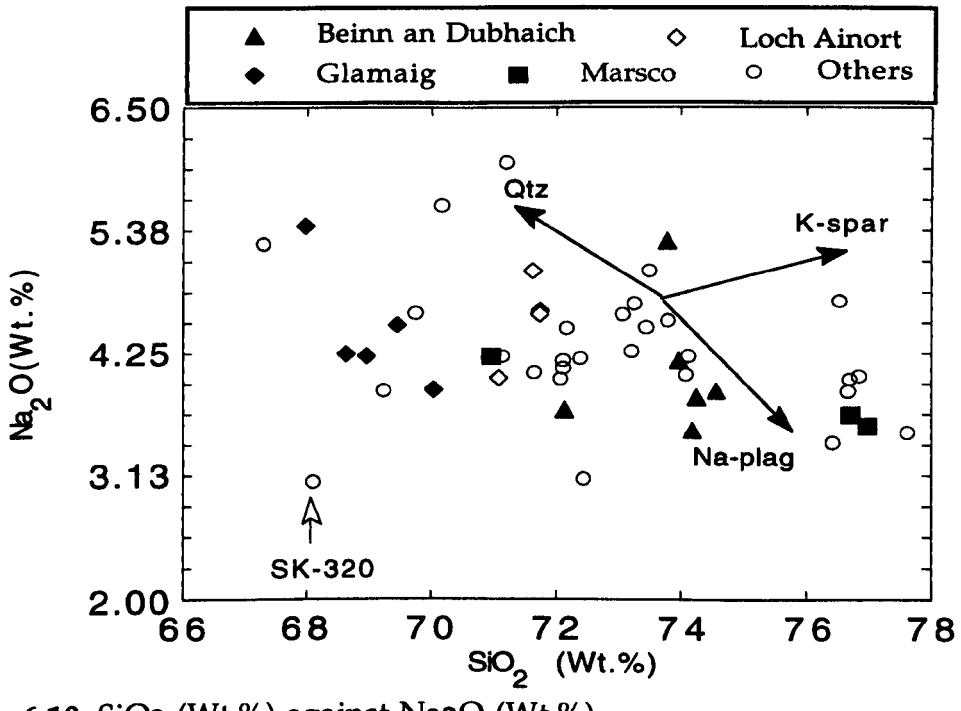

Fig. 6.10. SiO_2 (Wt.%) against Na_2O (Wt.%).

conclusion is supported by a lack of plagioclase in the more evolved intrusions such as Marsco, whereas the Na_2O content of the Northern Porphyritic Felsite (SK-320), along with its lower SiO_2 content, argues strongly for an origin other than by crystal fractionation.

(I) Although the observed positive correlation between SiO_2 content and K_2O content (Fig. 6.11) is consistent with the fractionation of K-depleted phases such as plagioclase, the data show a divergence in K_2O concentration as the evolution of the suite proceeds, as shown by trends 1 and 2. Outlying members of the trends include: the Northern Porphyritic Felsite (SK-320); the Eas Mor Granite (SK-321); and, the Maol na Gainmhich Granite (SK-319). All are rich in alkali feldspar and biotite compared with the other granites (see modal data in Table 3.1, Chapter III).

Thus, the K_2O contents of certain of the granites may not represent liquid compositions, and consequently selective accumulation of biotite and/or alkali feldspar during the evolution process seems the most reasonable explanation for the K_2O trend(s) seen in granites. This accumulation process may develop to a small extent and produce the divergent trend, or occur to a large extent and produce the outlying members (SK-320, SK-321, and SK-319).

(J) The correlation between P_2O_5 and SiO_2 (Fig. 6. 12), is not particularly well constrained but, in general, the compatible behaviour of P_2O_5 is consistent with apatite fractionation during progressive differentiation (Askren et al., 1991), or selective accumulation of apatite by the less evolved melts. Significantly, there is an almost complete lack of apatite in the Loch Ainort Granite.

In order to compositionally classify Skye granites, the scheme set out by Streckeisen and Le Maitre (1979) is used to avoid any uncertainty within the

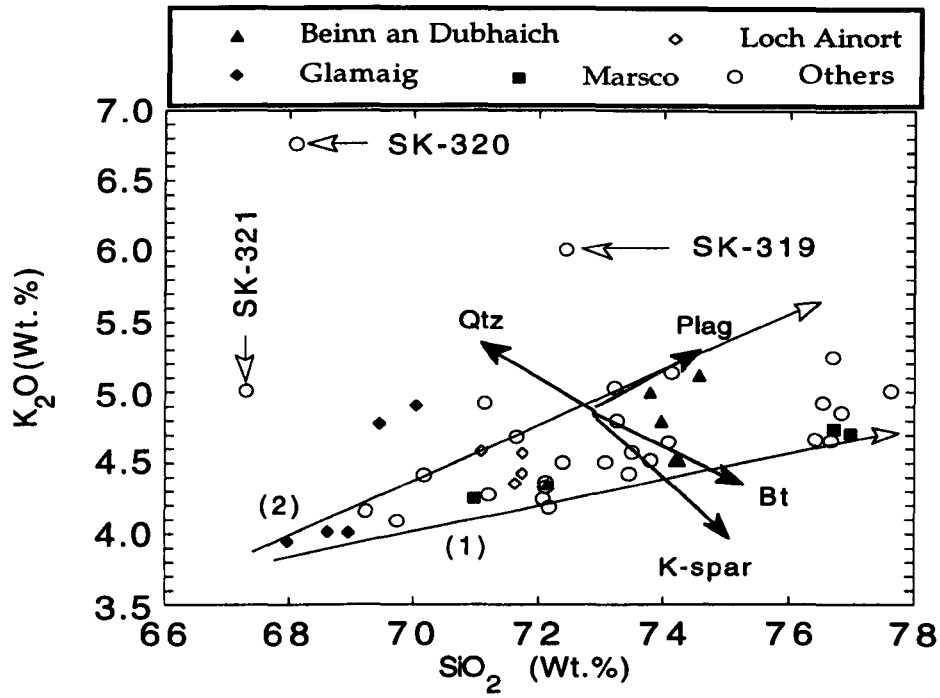

Fig. 6.11. SiO_2 (Wt.%) against K_2O (Wt.%).

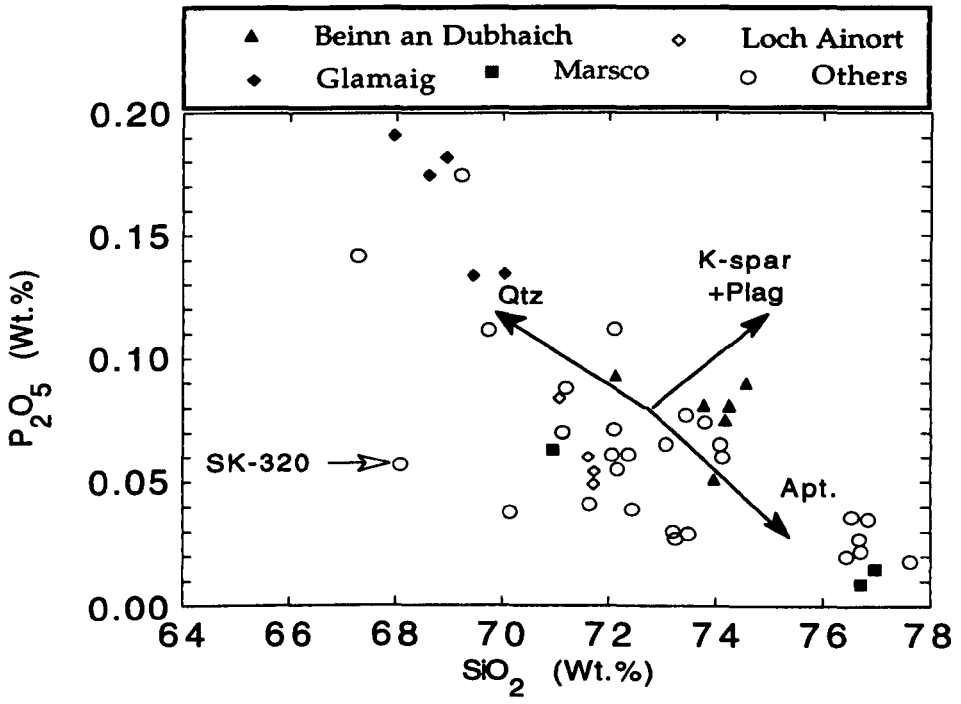

Fig. 6.12. SiO_2 (Wt.%) against P_2O_5 (Wt.%).

point counting data, since this approach is dependent on CIPW normative data. Normative proportions in the form of the ratio ANOR [$=10^2$ * An/(Or+An)], and Q' [$=10^2$ * Q/(Q+Ab+An+Or)], are presented in Fig. 6.13.

Using the granitic field positions of Streckeisen (1976), the mineral norms for the Skye granites concentrate across fields 2 and 3a, corresponding to alkali feldspar granite and syenogranite. However, there are a few samples which fall in field 6 Fig. (6.13), corresponding to quartz-alkali feldspar syenite. The small range of normative composition within each intrusion e.g. Glamaig, Beinn an Dubhaich and Marsco, may possibly be attributed to the slight difference in temperatures of crystallisation, or due to different proportions of accumulated or fractionated alkali feldspar, plagioclase, biotite and amphibole, which will affect the concentrations of K_2O, Na_2O and CaO.

From a consideration of aluminium saturation and undersaturation, terms such as peraluminous and metaluminous can be used to discriminate between granitic rocks, even within one intrusion (Shand, 1947). The I-type and S-type granites of Chappell and White (1974) are distinguished as metaluminous and peraluminous, respectively, whereas Avila-Salinas (1990) defined this boundary at an ASI = 1.1, where the Aluminium Saturation Index (ASI), defined by Zen (1986), is the ratio of the molecular proportions $Al_2O_3/(CaO+Na_2O+K_2O)$, often abbreviated to A/CNK, and is illustrated in Fig. 6.14.

Here we classify Skye granites according to the original definition of 'peraluminous' by Shand (1947) as a rock characterised by an ASI value of more than 1. ASI values for the studied samples range from about 0.8 to around 1.07, with the majority concentrated in the range from 0.9 to 1.05. Thus, all Skye granites fall in the I-type field and suggest a mantle contribution (Chappell and Stephens, 1988). As none of the analysed granites are in the S-type field, this implies a diminished crustal protolith contribution (White and Chappell, 1988),

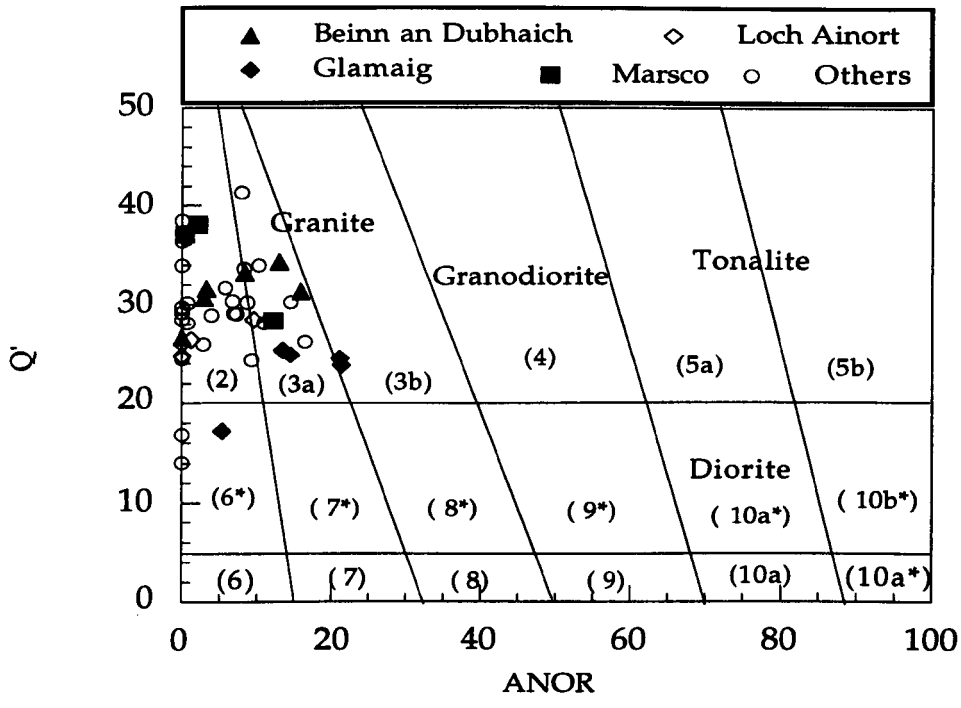

Fig. 6. 13. Classification diagram based on ANOR[=10^2 x An/(An + Or)] against Q'[= 10^2 x Q/(Q + Ab + An + Or)]. After Streckeisen and Le Maitre (1979). Where: **2**, alkali feldspar granite; **3a**, syenogranite; **3b**, monzogranite; **4**, granodiorite; **5**, tonalite; **6***, quartz alkali feldspar syenite; **7***, quartz syenite; **8***, quartz monzonite; **9***, quartz monzodiorite, quartz monzogabbro; **10***, quartz diorite, quartz gabbro, quartz anorthosite; **6**, alkali feldspar syenite; **7**, syenite; **8**, monzonite; **9**, monzodiorite, monzogabbro; **10**, diorite, gabbro, anorthosite.

although, many I-type granites are peraluminous in the original sense (cf. Chappell and White, 1992).

Chappell and White (1992) in their study of I-and S-type granites from the Lachlan Fold Belt pointed out that compositionally similar granitic rocks can be produced from different sources by different processes, such as low degrees of partial melting predominantly by consuming quartz and feldspar, and differentiation of more mafic materials.

Fig. 6.14 shows a very narrow range of ASI for the Glamaig, Beinn an Dubhaich and Marsco granites around the peraluminous-metaluminous boundary, despite their wide variations in silica content. This could be attributed to the role played by fractionation and/or accumulation of Ca, Na and K-rich minerals such as plagioclase, amphibole, biotite and K-feldspar during crystallisation of these intrusions. This is consistent with the Chappell and White (1992) proposal that the S-type granites have higher molecular proportions (ASI) than the I-type due to their lower Ca and Na content and not to a higher Al content.

The Loch Ainort Granite shows the widest range in ASI, from 0.85 to 0.99 at almost constant silica content. This, accompanied by Na_2O/K_2O ratios in the range 0.79 to 1.16, is consistent with there being heterogeneities in the composition of the parent magma, or possibly some form of selective accumulation of Ca, Na and K-rich minerals.

6. 3 Trace-elements

6. 3. 1 Trace-element chemistry

Consideration of the geochemical behaviour of rubidium during crystal-liquid fractionation and partial melting suggests that it is an excellent monitor of

these processes within a suite of cogenetic intrusions (for example, Gamble et al., 1992). Despite the fact that Rb shows a lack of correlation with both the turbidity and alteration indices, Rb was excluded as differentiation index in the following discussion to avoid any uncertainty about the behaviour of the trace-elements during hydrothermal alteration (Ferry, 1985). In Figs. 6.15-6-27 SiO_2 is used to examine a number of trace-element relationships in the Skye granites.

(A) Potassium-rubidium ratio: The average K/Rb ratio for continental crust ranges from 250 to 280 (Taylor and Mclennan, 1985). High K/Rb ratios are recorded for "primitive" Skye granites e.g. Glamaig and Loch Ainort (285-399 and 272 - 338, respectively), whereas low K/Rb values are observed in more "evolved" intrusions such as Beinn an Dubhaich and Marsco (248-289 and 238-285), respectively (Fig. 6.15).

K/Rb ratios vary from about 190 to around 560, with an average of 310. This wide range is caused by wide ranges in concentrations of both potassium and rubidium (Table 6.1) and is considerably higher than the average crustal ratio of 250-280. Bowden and Kinnaird (1984) record low K/Rb ratios (down to 35) for Nigerian granites due to their higher Rb concentration (1500 ppm), and attribute Rb enrichment to post magmatic recrystallisation of albite, which they recognised by a negative correlation of K against Rb.

Since, the Rb shows a colse geochemical affinity towards K (cf. Bowden and Kinnaird 1984), and enter into K-minerals with enrichment relative to K in the more evolved rocks (Lang et al., 1966; Green, 1980). The observed general decrease in K/Rb ratio towards more evolved intrusions is consistent with fractionation of K-rich minerals (biotite and alkali feldspar).

Away from the main trend, samples from the Glas Bheinn Mhor Granite (SK-310 and SK-312) and the Beinn na Caillich Granite (SK-336), show higher K/Rb ratios despite their consistent K_2O contents with the rest of the suite ($\approx$4.35),

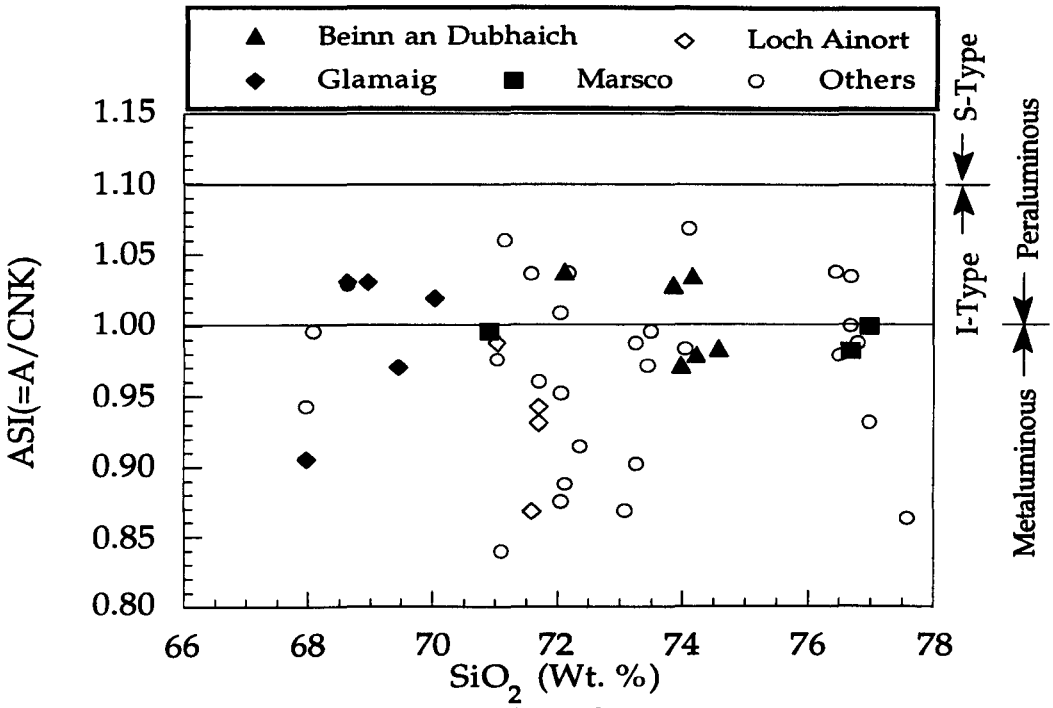

Fig. 6.14. SiO_2 (Wt.%) against ASI[=A/CNK].

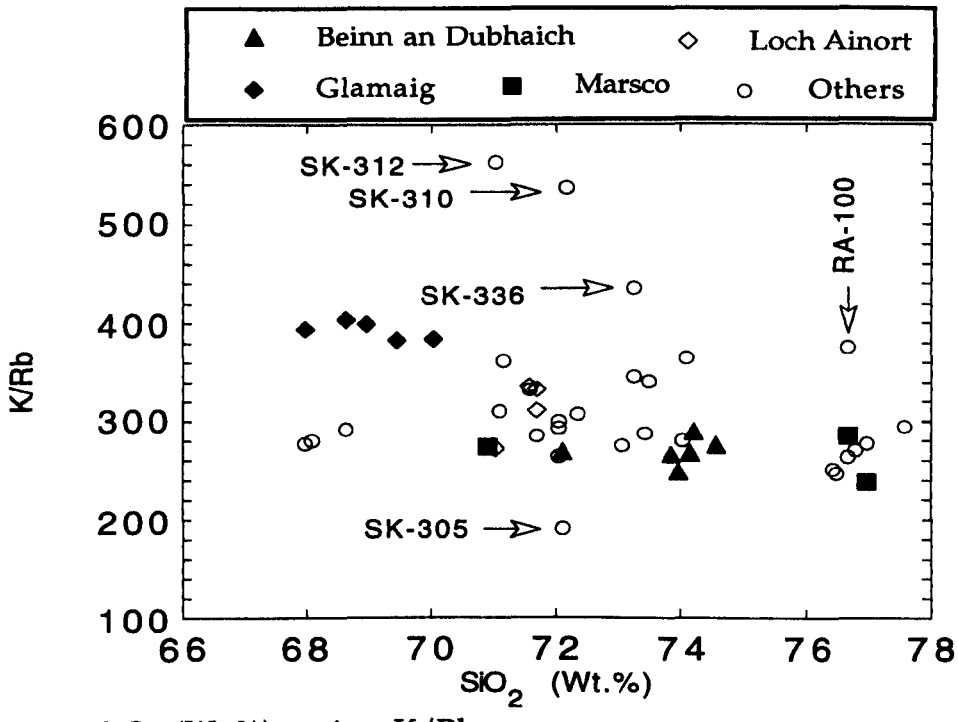

Fig. 6.15. SiO_2 (Wt.%) against K/Rb.

indicating their relative depletion in Rb, which are consistent of early alkali feldspar, with less extent amphibole and biotite fractionations (see Table 3.1). In contrast, sample SK-305 (the Creag Strollamus Granite) has a high Rb concentration (166 ppm), suggesting a failure of alkali feldspar fractionation .

(B) The Skye granites are an intermediate Rb suite relative to other granites from the Province (for example, Lundy, 450-700ppm, Thorpe et al., 1990; Mourne, 210-830 ppm, Hood, 1981). Rb concentrations are within the range 70-175 ppm, with the higher concentrations in the more evolved granites (Fig. 6.16). The observable increase of Rb from Glamaig through Loch Ainort to Marsco and Beinn an Dubhaich, is consistent with the fractionation of alkali feldspar, plagioclase, and amphibole (Taylor, 1965; Hanson, 1978; McCormick, 1989; Askren et al, 1991). In contrast, the high Rb concentration of the Northern Porphyritic Felsite (SK-320) and the Glas Bheinn Mhor Granite (SK-311) suggest the accumulation of Rb-rich and silica-poor phases such as biotite.

(C) The Skye granites are conspicuously enriched in Sr compared to other granites from the BTVP e.g. Arran (Meighan, 1979); Lundy (Thorpe et al., 1990). In Fig. 6.17, Sr shows a negative correlation with silica. The depletion in Sr, from Glamaig through Loch Ainort to Marsco, is consistent with the removal of a Sr-rich mineral(s) from the evolving liquid, for example, plagioclase, alkali feldspar, and apatite. The variation in Sr is very significant within the Glamaig Granite suggestive of extensive amounts of plagioclase fractionation.

The Eas Mor Granite (SK-321), the Northern Porphyritic Felsite (SK-320) and the Glen Sligachan Granite (SK-328), have Sr concentrations away from the main trend, suggesting early and extensive plagioclase fractionation.

(D) The ionic radius and charge of Ba are such that it can only substitute for potassium, and consequently is fractionated by crystallisation of K-bearing

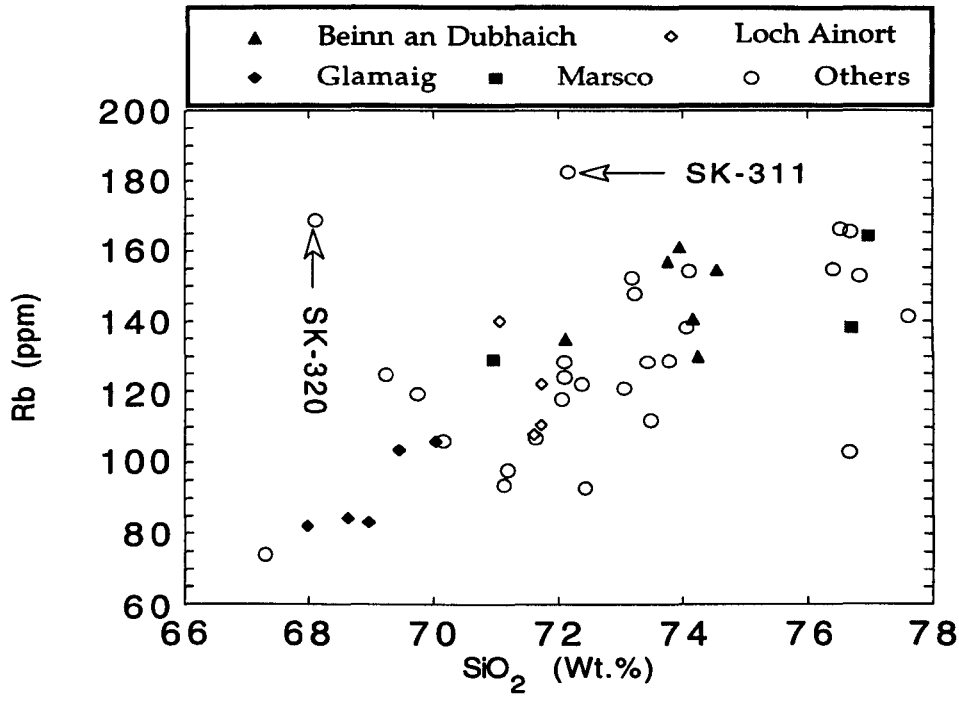

Fig. 6.16. SiO_2 (Wt.%) against Rb (ppm).

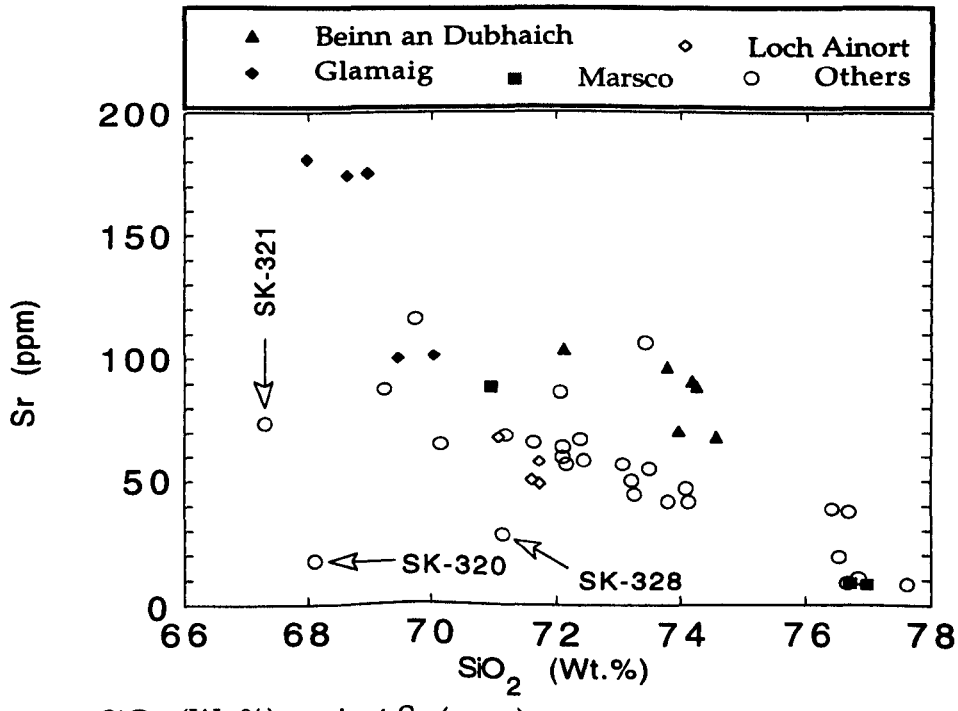

Fig. 6.17. SiO_2 (Wt.%) against Sr (ppm).

minerals such as alkali feldspar and biotite. In Fig. 6.18, Ba shows a steady decrease from Glamaig through Loch Ainort to Marsco, consistent with crystal-liquid fractionation (Fourcade and Allègre, 1981).

The highest Ba values are in one of the Marsco samples and in the Meall Buidhe Granite (SK-343 and SK-322, respectively, Table 6.1) and indicates their more primitive nature. This conclusion is supported by the low K-content in the alkali feldspar from SK-343 (see alkali feldspar analyses, Chapter IV). The Beinn an Dubhaich Granite contains a higher Ba content compared to the Loch Ainort Granite, which again may be due to accumulation of alkali feldspar crystals. The Northern Porphyritic Felsite (SK-320) records a low Ba concentration suggesting some sort of early feldspar crystallisation.

Both Ba and Sr (Fig. 6.19) show associated depletion towards the more fractionated intrusions, i.e. they behave compatibly with respect to silica. At the primitive end of the composition spectrum (higher Ba and Sr) there is an apparent divergence in the Ba and Sr concentrations. The Sr/Ba ratios throughout the suite are in the close range (0.04-0.13), despite the fact that this ratio should increase during fractionation (Green, 1980; Askren et al., 1991); Glamaig samples comprise the most primitive rocks represented by higher Sr and Ba concentrations and high Sr /Ba values (0.13) relative to the more evolved Marsco Granite (Sr/Ba=0.06). These data, along with the variation of Sr/Ba within the Glamaig Granite, suggest that Ba behaved in an almost incompatible way. Thus, the observed convergence reflects extensive plagioclase and alkali feldspar fractionation, possibly from a range of primitive compositions.

Fig. 6.20 shows the relation between Sr/Rb and Ba/Rb; trend (1) shows extensive depletion of Sr, probably due to Ca-plagioclase fractionation, and consequently the melt will become enriched in Ba relative to Sr. However, when alkali feldspar started to crystallise along with the plagioclase, the melt

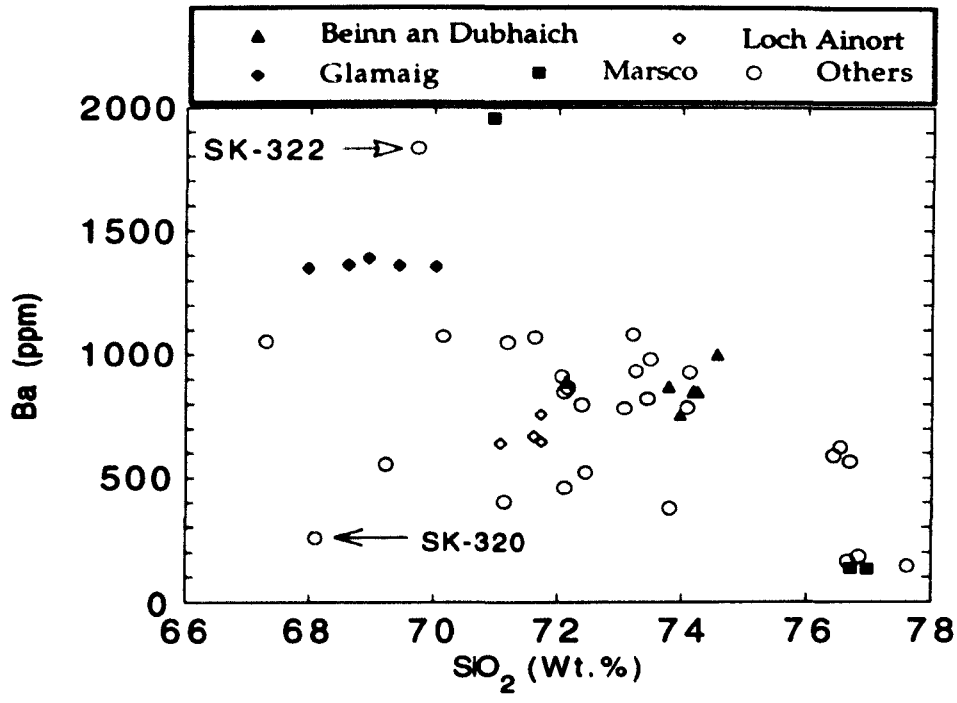

Fig. 6.18. SiO_2 (Wt.%) against Ba (ppm).

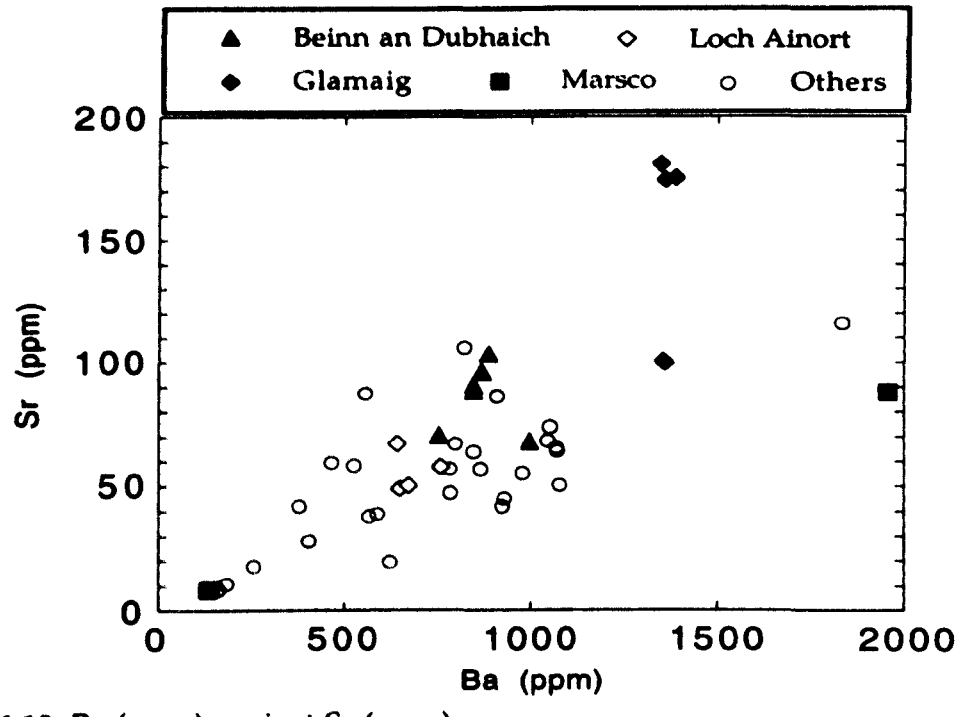

Fig. 6.19. Ba (ppm) against Sr (ppm).

became depleted in both Ba and Sr (trend 2). Thus, any early alkali feldspar crystallisation and fractionation at the beginning of trend (1) must have been Ba-rich.

(E) Zr behaves as an incompatible element during the crystallisation of most common rock-forming minerals (Green, 1980). Consequently, it occurs only within accessory phases such as zircon (Fourcade and Allègre, 1981), and some pyroxene and amphibole (Gamble, 1975; Tindle and Pearce, 1981). Chao and Fleischer (1960) and Tindle and Pearce (1981) point out that Zr enters into ferromagnesian minerals in the order: pyroxene, amphibole and biotite; therefore, in the most evolved rocks Zr should be depleted.

Zr in Skye granites ranges in concentration from around 780ppm to about 150ppm. These concentrations (apart from Beinn an Dubhaich) show a positive relation with trend (1) (Fig. 6.21), starting from Glamaig through Loch Ainort to Marsco, reflecting the incompatible behaviour of Zr during the differentiation process. The high concentration of Zr in the Marsco Granite, which contains insignificant amounts of zircon may not represent the magmatic Zr, and suggesting the accumulative nature of the pyroxene in this evolved sample, as this pyroxene may host most of the Zr (see Table 3.1, Chapter III). Alternatively, it could be attributed to the fractionation of Zr-poor phases.

The Beinn an Dubhaich Granite, the Creag Strollamus Granite (SK-305 and SK-306) and the Allt Fearna Granite (SK-303 and SK-304), all have lower Zr values and do not plot on trend (1), suggesting removal of Zr by fractionation of zircon, pyroxene and amphibole during differentiation. Inspite of the low Zr concentration recorded from the Beinn an Dubhaich Granite, it still has a reasonable amount of zircon compared with the rest of the suite. According to the zircon-solubility model of Watson and Harrison (1983), magmas similar to the Beinn an Dubhaich composition (i.e. per-metaluminous) become saturated

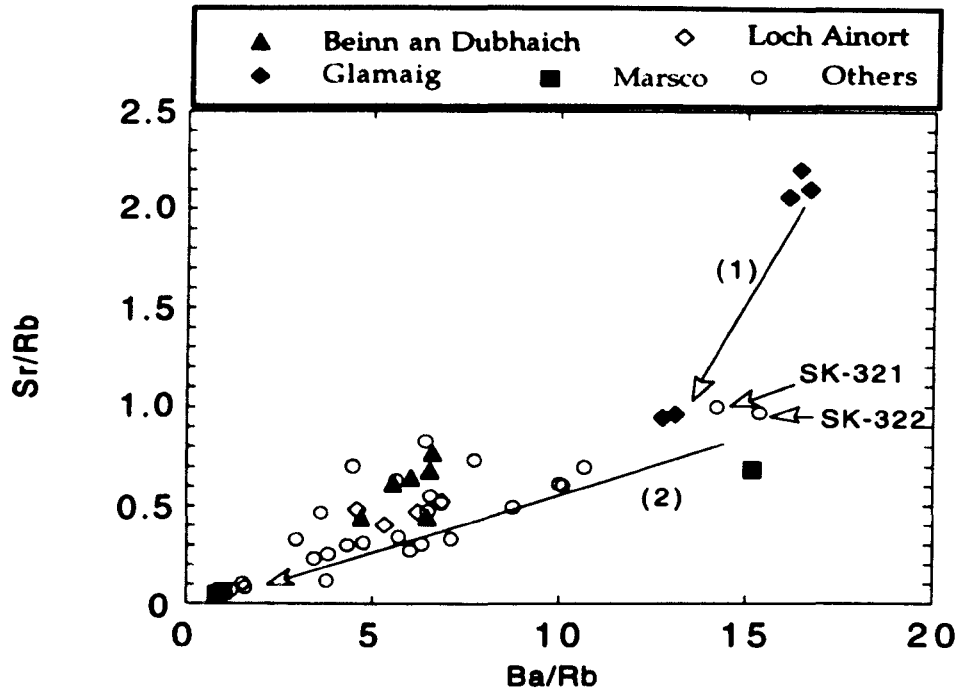

Fig. 6.20. Ba/Rb against Sr/Rb (ppm).

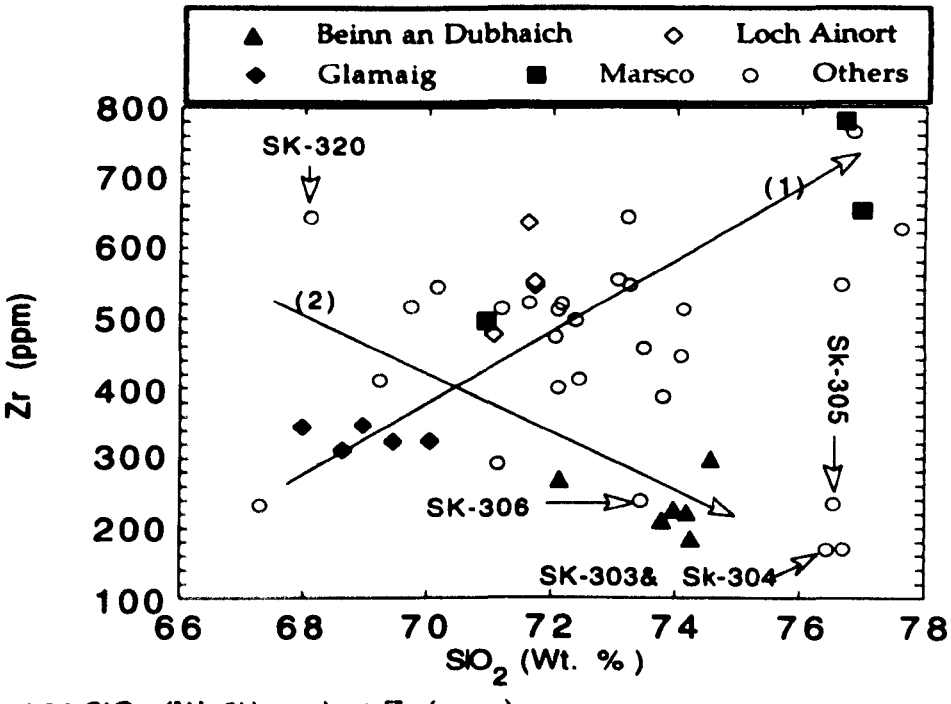

Fig. 6.21 SiO_2 (Wt.%) against Zr (ppm).

with zircon with as little as 100ppm Zr in the melt, which will lead to crystallisation of zircon as appears to be the case here. However in peralkaline liquids much high concentrations were required to cause zircon crystallisation.

(F) Skye granites are depleted in Th compared to other British Tertiary granites (for example, Ailsa Craig, 18ppm, Meighan, 1979; Mourne, 20-65ppm, McCormick, 1989). Th shows a positive correlation with silica (Fig. 6.22) indicating its incompatible behaviour, and the failure of phases such as zircon to be effectively fractionated.

(G) The yttrium concentration of Skye granites varies from around 30ppm to about 160ppm . Low Y values ($\leq$ 75ppm) are typified by Glamaig and Beinn an Dubhaich, and high Y values ($\geq$ 75ppm) are typified by Loch Ainort and Marsco. Generally Y behaves as an incompatible element, i.e. it should correlate positively with SiO_2 as indicated by trend (1) (Fig. 6.23) which shows an increase in Y from Glamaig towards Marsco. This behaviour is consistent with the fractionation of Y-depleted phases (Green, 1980).

The low concentration of Y in the Beinn an Dubhaich Granite together with the Allt Fearna Granite (SK-303 and SK-304) and the Creag Strollamus Granite (SK-306), corresponds with the low Zr group (at high SiO_2 content) shown in Fig 6.21. This suggests that the Y content of the granites is essentially related to the behaviour of zirconium as discussed above, which confirms that Y concentrates in zircon, as proposed by McCormick (1989).

(H) The bulk of Nb in granites occurs within (in decreasing order of importance): biotite, ilmenite and zircon (Henderson, 1982), although the substitution of Ti^{4+} by Nb^{5+} in pyroxene is possible.

In Skye granites Nb shows similar behaviour to that of Y (Fig. 6.24), but with lower concentrations i.e. 9-29ppm. The incompatible behaviour of Nb is observed from Glamaig through Loch Ainort to Marsco, suggesting a lack of

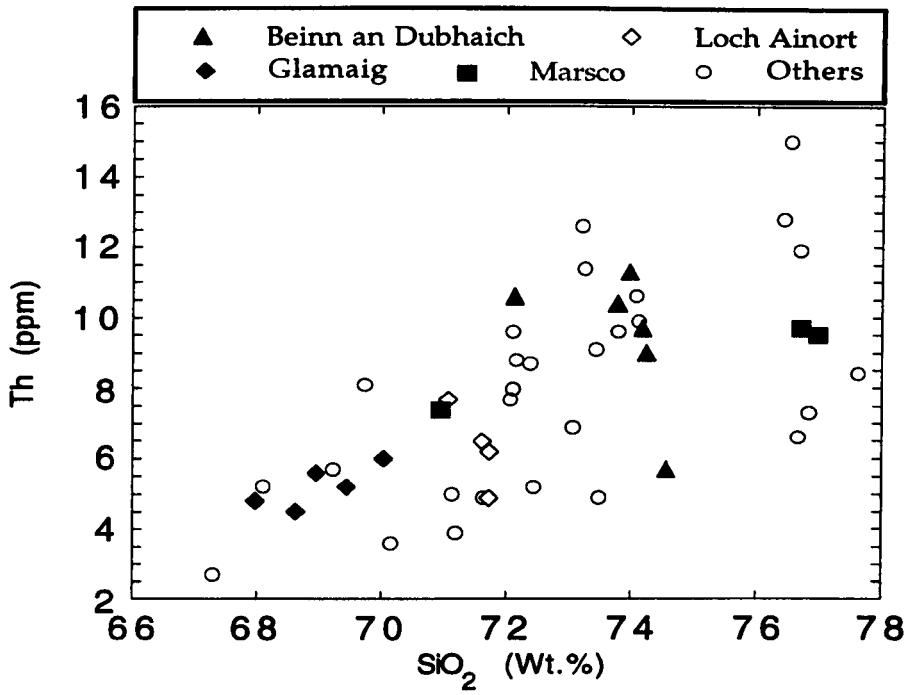

Fig. 6.22. SiO_2 (Wt.%) against Th (ppm).

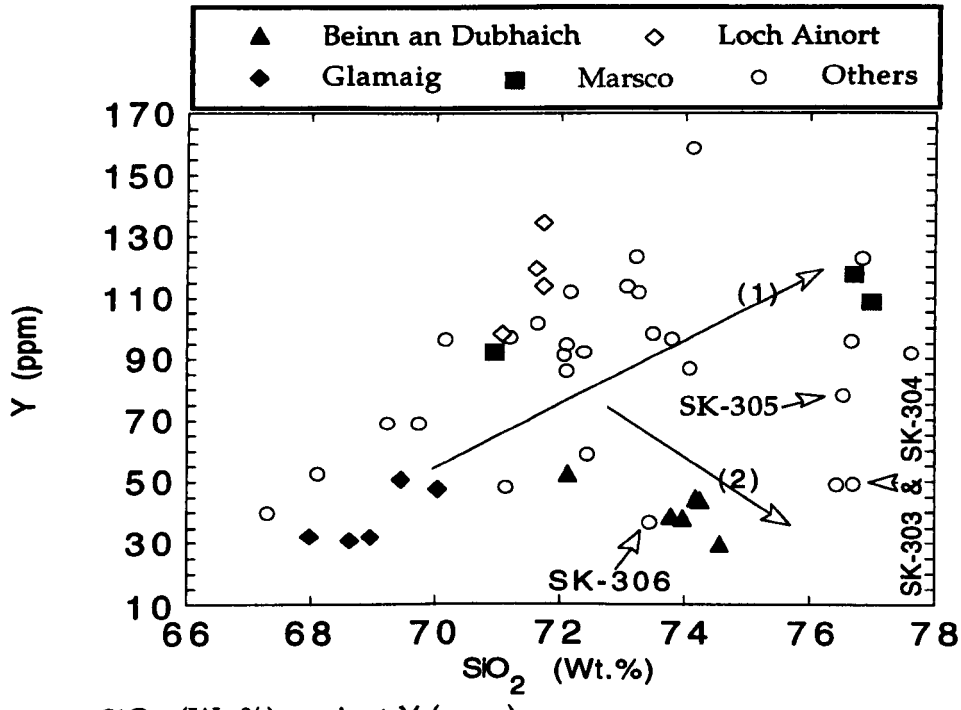

Fig. 6.23. SiO_2 (Wt.%) against Y (ppm).

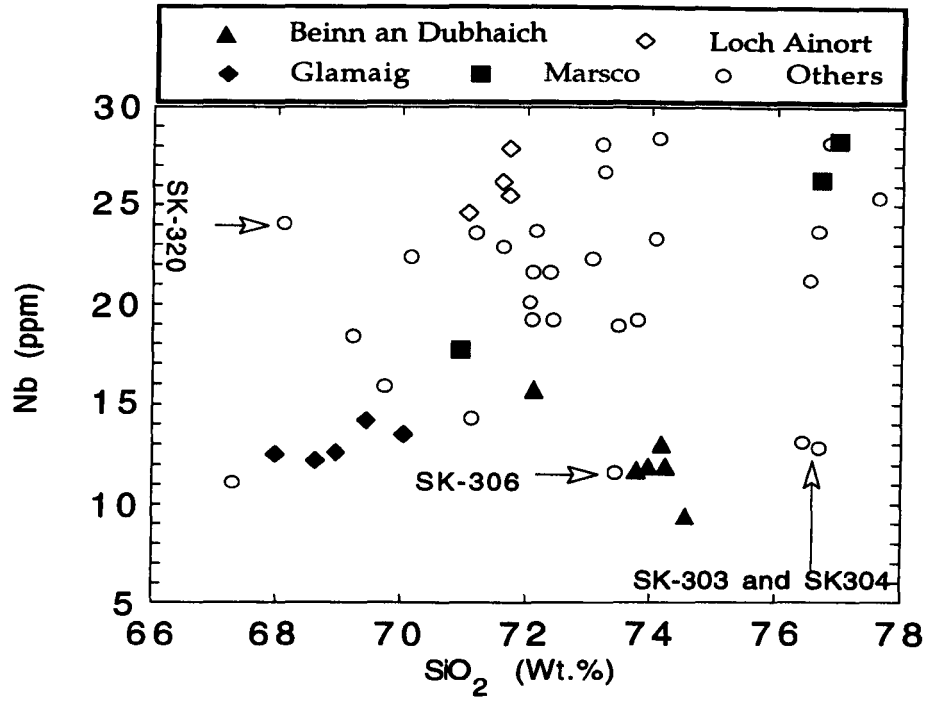

Fig. 6.24. SiO_2 (Wt.%) against Nb (ppm).

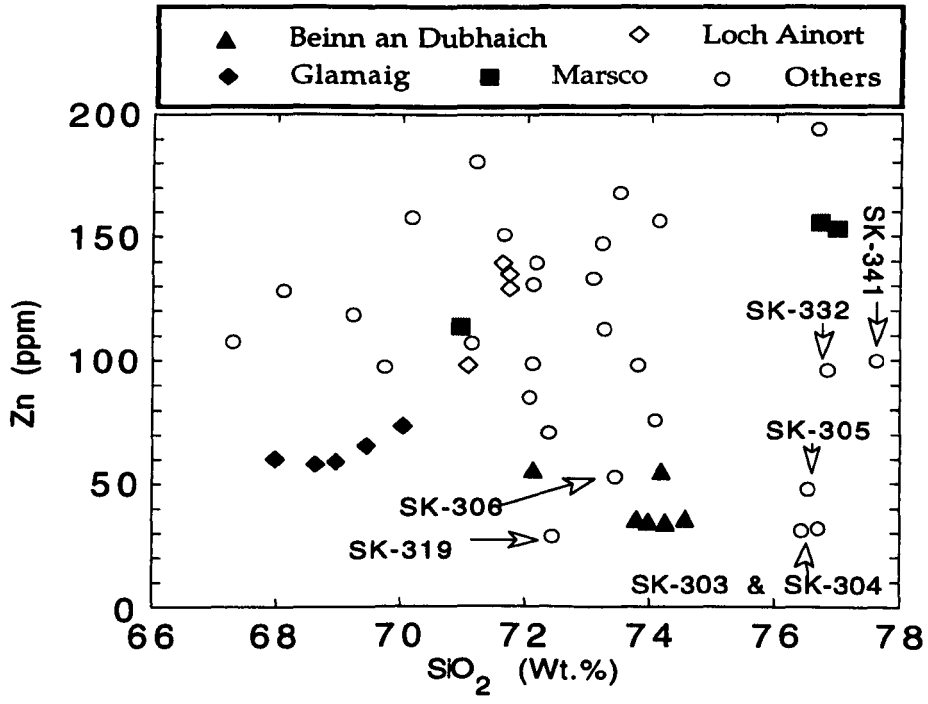

Fig. 6.25. SiO_2 (Wt.%) against Zn (ppm).

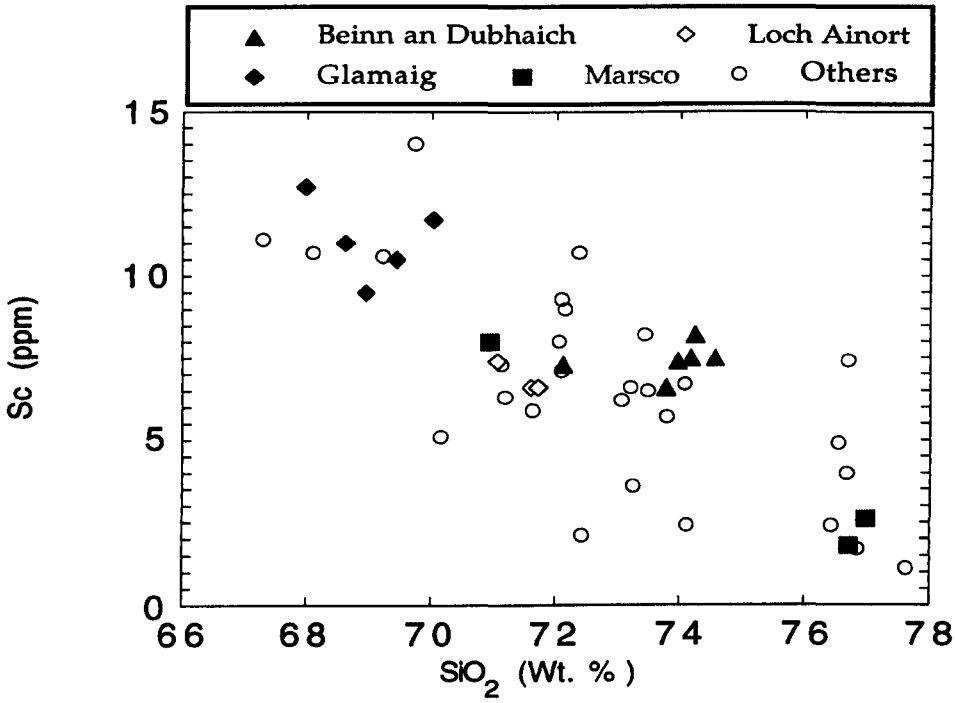

Fig. 6.26. SiO_2 (Wt.%) against Sc (ppm).

fractionation of appropriate minerals. The Beinn an Dubhaich, Allt Fearna (SK-303 & SK-304) and Creag Strollamus (SK-306) granites all show lower Nb concentrations but are silica-rich. This behaviour is consistent with pyroxene fractionation.

(I) No simple correlation can be identified between Zn and SiO_2 (Fig. 6. 25). Zinc is consistently higher in Marsco and Loch Ainort (100-170ppm) compared to Glamaig and Beinn an Dubhaich granites (40-90ppm). Zn was depleted with progressive fractionation, this depletion suggests pyroxene, and probably amphibole, biotite and magnetite fractionation (McCormick, 1989). The latter conclusion could explain the lower Zn concentration in the Beinn an Dubhaich Granite.

(j) Scandium values for Skye granites range from 1ppm to 14ppm, with the highest concentrations being recorded in the Glamaig intrusion (Fig. 6.26). This behaviour suggests the fractionation of early amphibole and pyroxene, with the Sc occupying Fe^{2+} sites in those minerals (cf. Buma et al., 1971).

6.3.2 Trace-element modelling

Crystal-liquid fractionation models can be tested by using whole-rock trace-element abundance data and the relevant equilibrium and Rayleigh equations (for example, Cox et al., 1979; McBirney, 1984; Philpotts, 1990; Rollinson, 1993). During fractionation, incompatible trace-elements will increase in concentration, whereas compatible trace-elements will decrease in concentration. Depending upon the minerals which fractionate, a number of geochemical trends will develop. In general terms, during Rayleigh fractionation, incompatible trace-elements (i.e. $K_D < 1$) will become more depleted in the residual and compatible trace-elements ($K_D > 1$) will become more enriched in the fractionated minerals, than during equilibrium

crystallisation.

In the Skye granites, based upon the major-element compositional relationships, it is clear that feldspar (both alkali feldspar and plagioclase) have played important roles in the evolution of the suite (cf. Figs. 6.5, 6.9, 6.10 and 6.11). Consequently, it is useful to examine the behaviour of the associated trace-elements: Ba, Rb and Sr.

For the Skye granites, based upon the major-element relationships and the relatively large ranges in trace-element concentrations within the suite, the Rayleigh model is likely to be the most realistic.

An initial starting composition of: Rb = 75ppm; Sr = 190ppm and Ba = 1500ppm, was chosen. This is slightly more primitive than the Glamaig Granite (SK-323, SK-324, SK-325, SK-326, SK-327), which contains: Rb = 82-106 ppm; Sr = 100-181 ppm and Ba = 1348-1388 ppm, see Table 6.1). A bulk distribution coefficient (D) was calculated using a reasonable fractionation assemblage (cf. Table 6.1) of: 30 vol.% alkali feldspar; 30 vol.% quartz; and, 40 vol.% plagioclase (cf. Gamble et al., 1992). D_{Rb} was held constant to simplify the modelled trends, due to its incompatible behaviour relative to Ba and Sr, and, more importantly, variation in D_{Rb} does not affect the calculated Rb values to any large extent (for example, if D_{Rb}= 0.276, 60% crystallisation results in C_L= 108.56ppm, whereas if D_{Rb}=0.246, C_L=110.23ppm (with C_O=75ppm)) (Gibson, 1984; Gamble et al., 1992). Due to the wide variations of partition coefficients for trace elements in high-silica rocks (see for example, Mahood and Hildreth, 1983; Nash and Crecraft, 1985; Michal, 1988), the values of Kd were taken within the range of values presented by Henderson (1982).

The calculated value of D_{Rb} is 0.276, and along with the range of values of D_{Ba} and D_{Sr},was used in order to bracket the whole-rock compositional data presented in Figs. 6.27 and 6.28. Consequently, it was calculated that D_{Ba} must

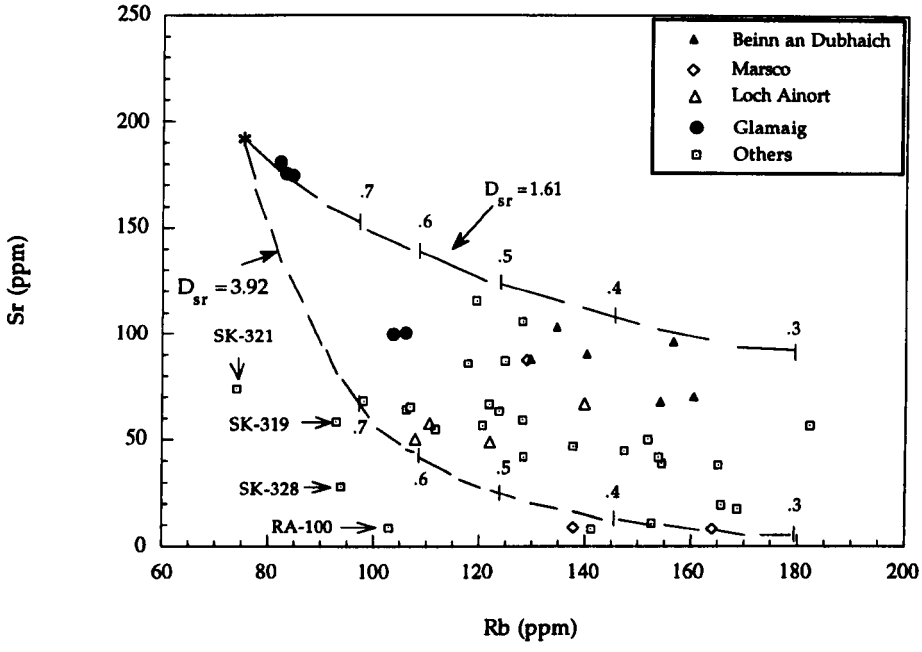

Fig. 6.27a. Plot of Rb in ppm against Sr in ppm. Curves are calculated trajectories for Rayleigh fractionation of a 'Ternary minimum' assemblage of quartz, alkali feldspar and plagioclase, (see text for further explanation).

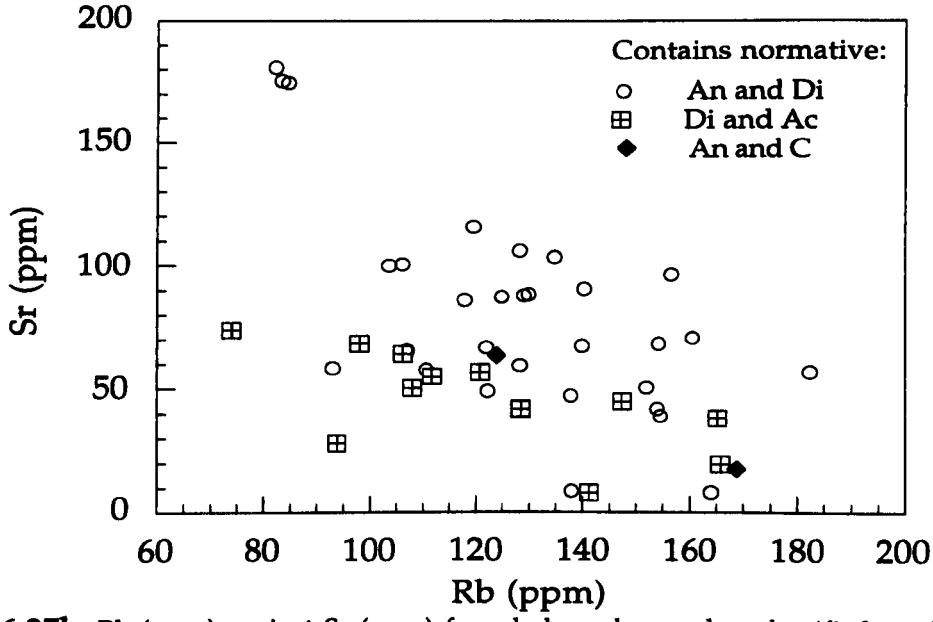

Fig. 6.27b. Rb (ppm) against Sr (ppm) for whole rock samples, classified on the basis of aluminum saturation. Where, An, anorthite; and, Di, diopside.

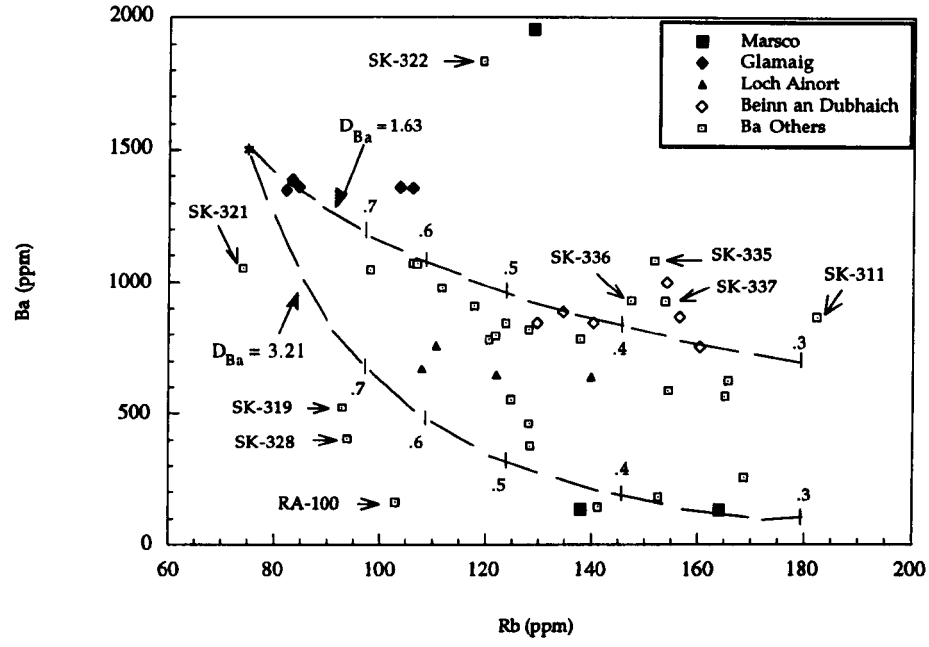

Fig. 6.28a. Plot of Rb in ppm against Ba in ppm. Curves are calculated trajectories for Rayleigh fractionation of a 'Ternary minimum' assemblage of quartz, alkali feldspar and plagioclase, (see text for further explanation).

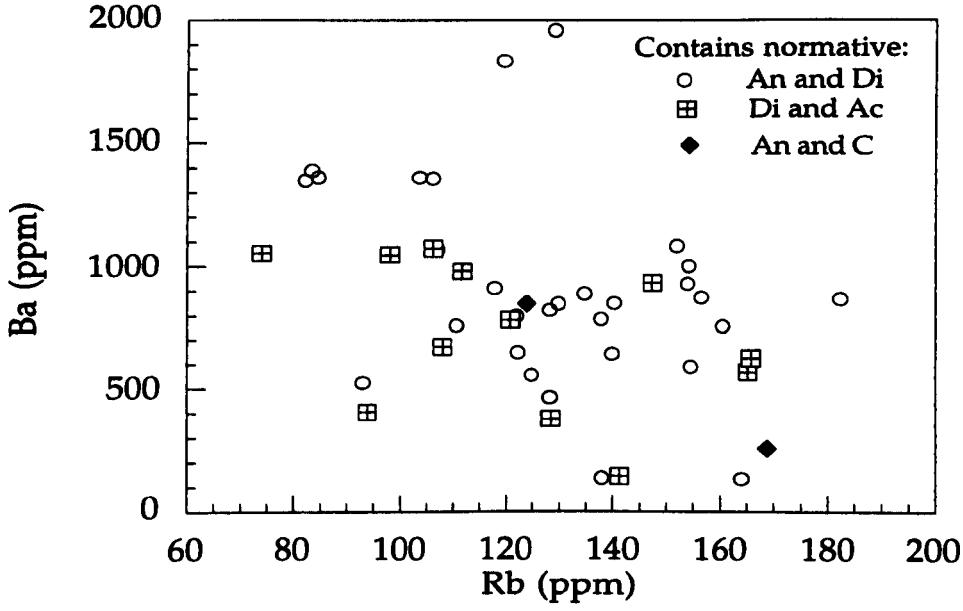

Fig. 6.28b. Rb (ppm) against Ba (ppm) for whole rock samples, classified on the basis of aluminum saturation. Where, An, anorthite; and, Di, diopside.

lie within the range 1.63 to 3.21, and D_{Sr} must lie within the range 1.61 to 3.92, in order to cover the compositional range within the suite. Samples that fall outside these ranges in D are: the Raasay Granite (RA-100), the Maol na Gainmhich Granite (SK-319), the Eas Mor Granite (SK-321), the Glen Sligachan Granite (SK-328), a sample from the Glas Bheinn Mhor Granite (SK-311), and the Beinn na Caillich Granite (SK-335, SK-336 and SK-337).

The following points are noted:

(i) The large scatter in the plot of Sr against Rb (Fig. 6.27a) and Ba against Rb (Fig. 6.28a) suggests that simple (with constant proportions of quartz, alkali feldspar and plagioclase) fractionation cannot, alone, explain these data;

(ii) The value of D_{Ba} is most likely towards the lower end of the selected range of values based upon the distribution of data points in Fig. 6.28a.

(iii) Some peralkaline granites lie outside the range of calculated trends, but in a trend approximately parallel to the high $D_{Sr,Ba}$ trends. These granites are: Eas Mor (SK-321), Maol na Gainmhich (SK-319)(cf. Wager et al., 1965, Table 1), Glen Sligachan (SK-328) and Raasay (RA-100).

(iv) In Fig. 6. 27b certain normative assemblages are distinguished: (a) both normative An and Di; (b) normative An only, and with normative C; and, (c) normative Di only, and with normative Ac. Those samples which contain both normative An and Di form a distinct trend paralleling the low D_{Sr} calculated trend, in contrast to the samples which contain normative Di only (and contain normative Ac, and therefore, by definition, are peralkaline) which form a distinct trend paralleling the high D_{Sr} calculated trend. The coherence of these trends suggests that Sr and Rb have behaved in a robust manner and have not been significantly disturbed during the hydrothermal events subsequent to

crystallisation of the silicate minerals. In contrast to the behaviour of Sr, the Ba data do not define simple fractionation trends when plotted against Rb (Fig. 6.28b). The most likely explanation for this is the redistribution of Ba during hydrothermal alteration (Nabelek, 1986) and turbidity development of alkali feldspar in particular.

(v) It is suggested that slight changes in the modal assemblage (e.g. increase in plagioclase and/or biotite contents at the expense of alkali feldspar) in conjunction with lower Kd_{Ba} values could account for the low ultimate D_{Ba} necessary to model the samples which lie above the low D_{Ba} trend. An increase in alkali feldspar content at the expense of either plagioclase or biotite, in conjunction with higher $Kd_{Sr, Ba}$ values could account for the high ultimate $D_{Sr, Ba}$ necessary to model certain peralkaline samples (i.e. SK-321, SK-319, SK-328 and RA-100).

(vi) The variations observed in these compatible elements (i.e. Sr = 10-180 ppm; Ba = 100-1900 ppm) are unlikely to have been produced by partial melting processes alone, since they should remain fairly constant throughout a series produced by such a process (cf. Hanson, 1978).

(vii) Both D_{Sr} calculated trends bracket most of the suite, and this is consistent with a higher proportion of plagioclase fractionation during the early stages, which consequently decreased as fractionation proceeded.

From the measured and calculated trends it appears that:

(a) The fractionation process was controlled mainly by alkali feldspar and plagioclase. As fractionation proceeded alkali feldspar become dominant.

(b) Fractional crystallisation (at depth) of a primitive magma with the Ba, Sr and Rb concentrations chosen here would produce magmas with the compositions of Glamaig Granite samples before 30% crystallisation. Most of

the remainder of the suite would have formed after 40% crystallisation and before 70% crystallisation (see Figs 6.27a and 6.28a).

Thus, the Skye granites could be generated by either:

(i) Differentiation of individual batches of basaltic magma to produce the different granites and/or different samples from one granite; or,

(b) Formation of a magma with the composition of the Glamaig Granite by partial melting of a mantle source to produce a basaltic magma, *followed* by fractional crystallisation to generate the rest of the suite.

6.4 Rare-earth-element chemistry

Forty-one samples of Skye granites have been analysed for fourteen REE by Inductively coupled plasma mass spectrometer. The analytical procedures are presented in Appendices III and IV. Nineteen of these samples are representative of the four granites studied in detail (Beinn an Dubhaich, Marsco, Loch Ainort and Glamaig). The other samples represent most of the other Skye granites. Data are presented in Table 6.2.

The data have been normalised to the chondrite abundances of Nakamura (1974) and Potts et al. (1981), and plotted in Figs. 6.29-6.38. Figs. 6.29 to 6.32 present data for the Beinn an Dubhaich, Glamaig, Loch Ainort and Marsco granites, respectively, whereas Figs. 6.33 to 6.37 represent combinations of the rest of the Skye granites and Fig. 6.38 shows comparisons between the Beinn an Dubhaich, Marsco, Loch Ainort and Glamaig granites. The chondrite-normalised REE patterns show the following features:

(A) Samples from the Beinn an Dubhaich Granite (Fig. 6.29) show very similar REE concentrations, with enrichment in LREE relative to HREE, $[(Ce/Yb)_N =$

5.56-9.04] and with moderate Eu anomalies (0.44-0.7).

(B) Fig. 6.30 presents data for samples from the Glamaig Granite and a mafic inclusion (SK-325A). The samples from the granite show very similar LREE concentrations with small Eu anomalies (0.83-0.87), but significantly different HREE concentrations [$(Ce/Yb)_N$ = 5.99-10.24]. The mafic inclusion has a large negative Eu anomaly relative to the granite itself (0.42) and has a higher total REE concentration. The inclusion also has a small negative Ce anomaly.

(C) Loch Ainort samples are presented in Fig. 6.31 and have similar patterns, with LREE enrichment [$(Ce/Yb)_N$ = 3.76-4.94], but with relatively variable HREE concentrations and negative Eu anomalies (0.41-0.49).

(D) For the Marsco Granite (Fig. 6.32), the overall patterns are similar, with LREE enrichment [$(Ce/Yb)_N$ = 4.17-5.31]. The most evolved sample (SK-334) has a higher total REE content and a large Eu anomaly (0.29), in contrast to the more primitive samples which have lower overall abundances and smaller Eu anomalies.

(E) Fig. 6.33 presents normalised REE concentrations of samples of the Allt Fearna and Creag Strollamus granites [(SK-303 and SK-304) and (SK-305 and SK-306)], respectively. Both intrusions are very similar in terms of LREE; however, the Creag Strollamus samples show significant variations in their HREE contents. Allt Fearna has $(Ce/Yb)_N$ values of 6.59 and 7.07, whereas Creag Strollamus has $(Ce/Yb)_N$ values of 3.39 and 10.05. Both granites have large to moderate Eu anomalies (0.28-0.30 and 0.41-0.5).

(F) REE data for the Glas Bheinn Mhor (SK-307, SK-309, SK-310 and SK-312) and the Beinn na Caillich (SK-335 and SK-337) granites are presented in Figs. 6.34 and 6.35. Overall, both granites show similar patterns but variable REE concentrations [$(Ce/Yb)_N$ = 4.04-5.45 and 3.42-4.48 for Glas Bheinn Mhor and Beinn na Caillich, respectively]. The Beinn na Caillich Granite has a higher total

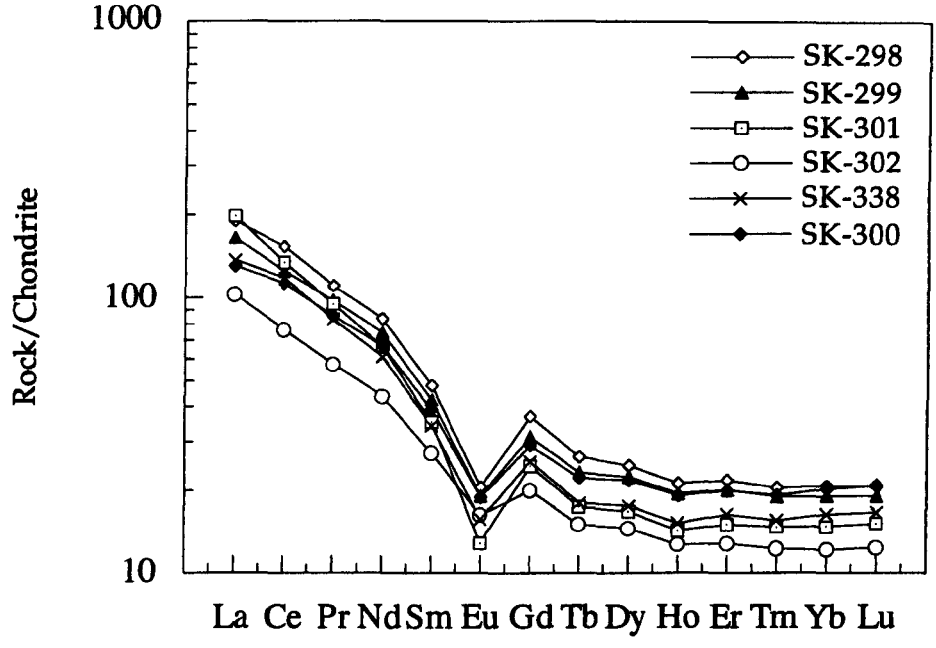

Fig. 6.29. Chondrite-normalised REE patterns for samples from the Beinn an Dubhaich Granite.

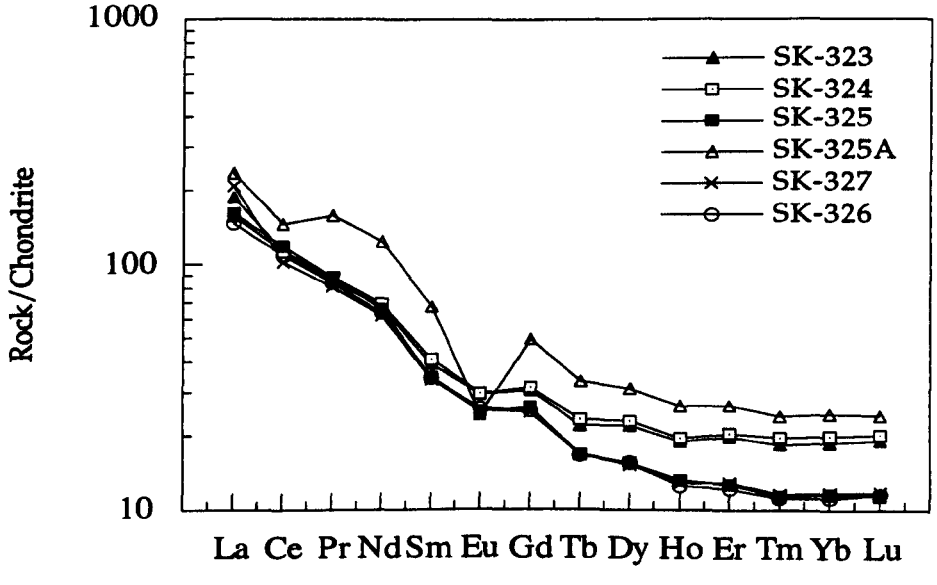

Fig. 6.30. Chondrite-normalised REE patterns for samples from the Glamaig Granite.

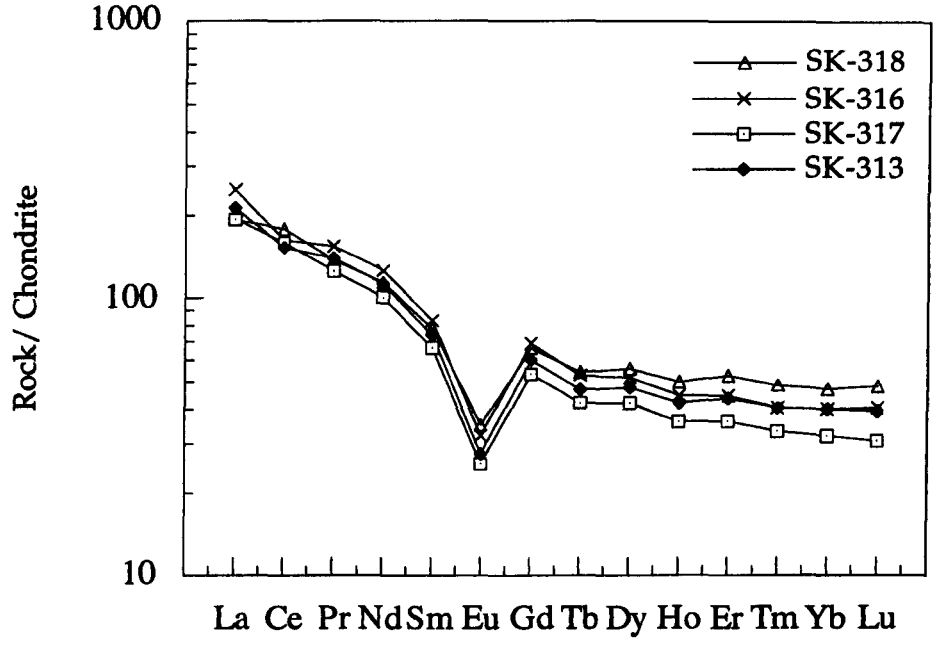

Fig. 6.31. Chondrite-normalised REE patterns for samples from the Loch Ainort Granite.

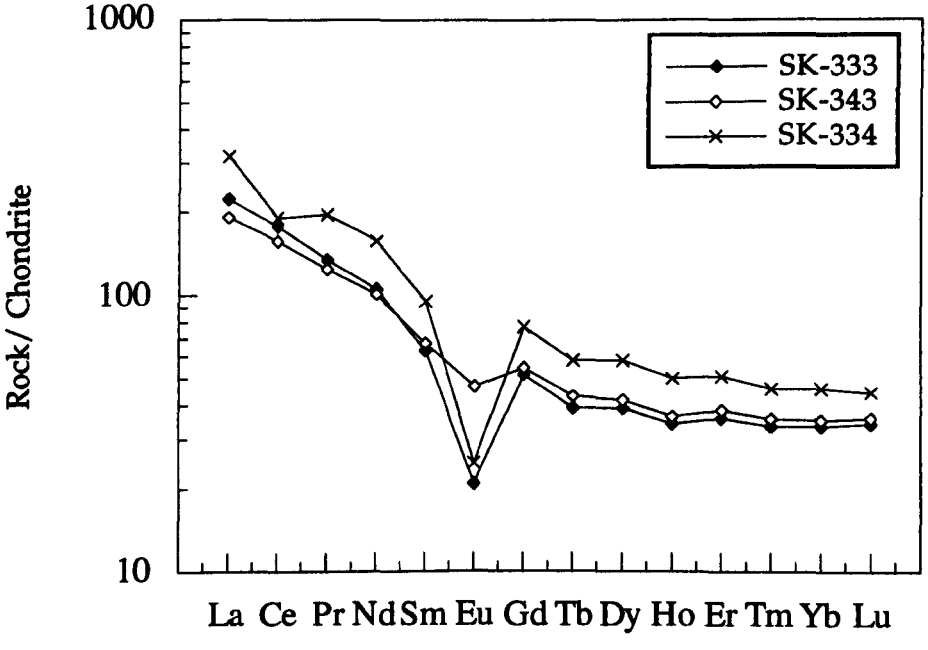

Fig. 6.32 Chondrite-normalised REE patterns for samples from the Marsco Granite.

REE concentration than the Glas Bheinn Mhor Granite. All patterns have negative Eu anomlies of 0.35-0.52 for Glas Bheinn Mhor and 0.47-0.49 for Beinn na Caillich.

(G) The normalised REE patterns for the Beinn Dearg Mhor Granite (SK-315, SK-339 and SK-340) and the Southern Porphyritic Granite (SK-329, SK-332 and SK-341) are presented in Fig. 6.36. These two intrusions are very similar in terms of their LREE enrichment [$(Ce/Yb)_N$ = 4.26-6.84 for Beinn Dearg Mhor and 4.06-6.27 for Southern Porphyritic]. The latter has larger negative Eu anomalies (0.27-0.3) relative to the former (0.51-0.58).

(H) Normalised REE data for the Maol na Gainmhich Granite (SK-319), the Northern Porphyritic Felsite (SK-320), the Eas Mor Granite (SK-321), the Meall Buidhe Granite (SK-322) and the Glen Sligachan Granite (SK-328) are presented in Fig. 6.37. All of these intrusions show similar LREE enrichment, with [$(Ce/Yb)_N$ = 9.17 in SK-319; 8.33 in SK-320; 6.49 in SK-321; 5.34 in SK-322; and, 6.3 in SK-328]. SK-319, SK-320, SK-322 and SK-328 have negative Eu anomaly values of 0.49, 0.27, 0.92 and 0.56, respectively, whereas SK-321 yields a positive Eu anomaly of 1.13.

From these data the following conclusions are made:

(i) In general, the similarity of the REE patterns of Skye granites indicates that these patterns have not been significantly disturbed by alteration processes and confirm that they are chemically related (cf. Thorpe et al., 1990).

(ii) All Skye granites are light REE-enriched, with chondrite-normalised Ce values of 76-218 and chondrite-normalised Yb values of 11-49 and $(Ce/Yb)_N$ in the range 3.4-10.2. Therefore, Skye granites have very similar pattern shapes with their absolute REE contents varying by a factor of 3-4.

(iii) With the exception of the Eas Mor Granite, which has a positive Eu

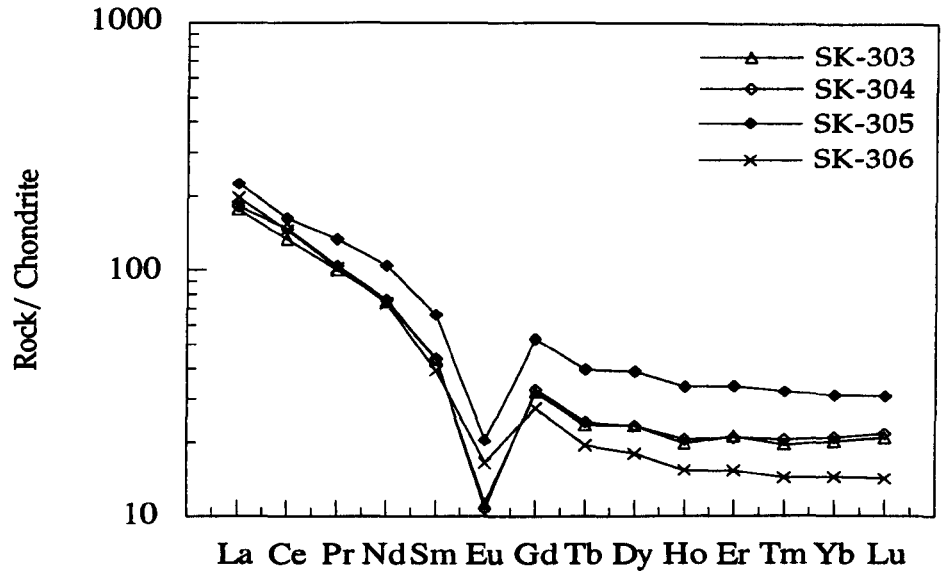

Fig. 6.33 Chondrite-normalised REE patterns for samples from the Allt Fearna Granite (SK-303 and SK-304) and the Creag Strollamus Granite (SK-305 and Sk-306).

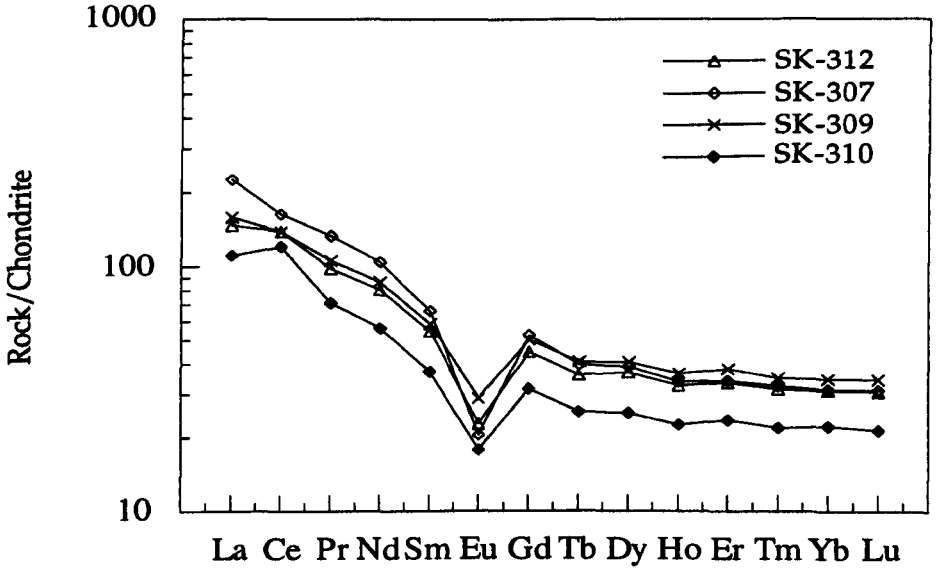

Fig. 6.34 Chondrite-normalised REE patterns for samples from the Glas Bheinn Mhor Granite.

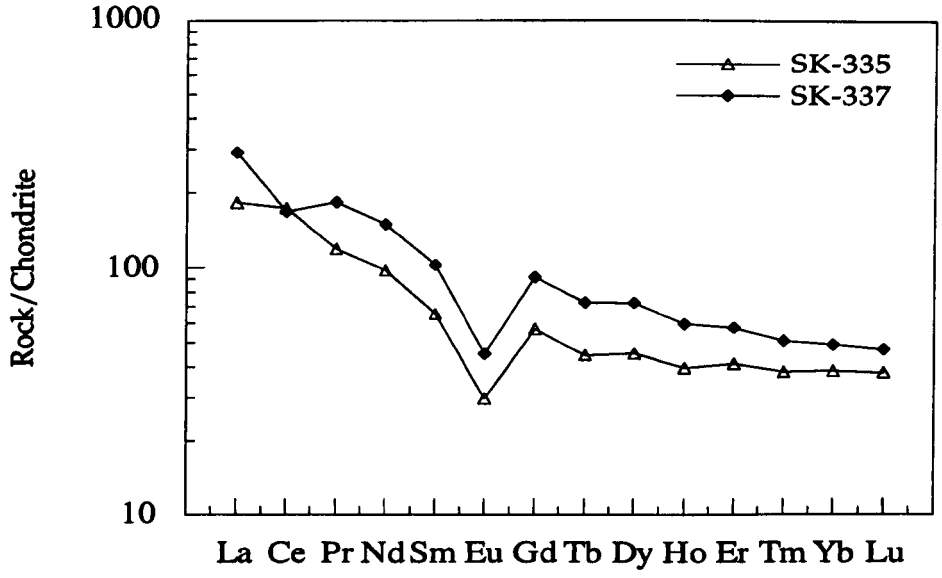

Fig. 6.35 Chondrite-normalised REE patterns for samples from the Beinn na Caillich Granite.

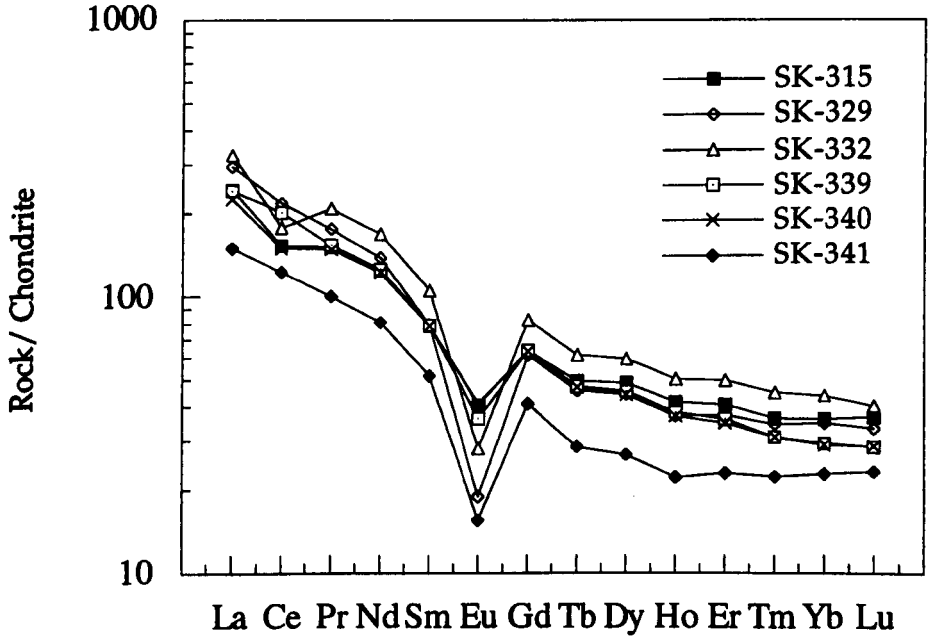

Fig. 6.36 Chondrite-normalised REE patterns for samples from the Beinn Dearg Mhor Granite (SK-315, SK-339, and SK-340) and the Southern Porphyritic Granite (SK-329, SK-332, and SK-341).

anomaly, and the Glamaig Granite which has a small negative Eu anomaly, all other Skye granites have clear negative Eu anomalies, (i.e.< 0.92) where, ($Eu/Eu^* = Eu_N / \sqrt{(Sm_N * Gd_N)}$) (Taylor and Mclennan, 1985). Thorpe et al. (1977) explain the small Eu anomaly in the Glamaig Granite as an indication of its derivation from a basaltic parental magma with no Eu anomaly by fractional crystallisation.

Thorpe et al. (1977) pointed out that the processes of fractional crystallisation and partial melting to produce granitic magmas with minerals which have $D^{REE} < 1$ and plagioclase which has $D^{Eu} \geq 1$, would produce melts with similar REE patterns to their parent, but with different degrees of REE enrichment, and Eu depletion inversely proportional to the amount of melt produced. From Fig. 6.38, the more primitive (Glamaig) Granite shows the lowest REE contents and has no significant Eu anomaly. In contrast, the younger granites, Loch Ainort and Marsco, have higher REE contents together with larger negative Eu anomalies. The Beinn an Dubhaich Granite has a REE content and Eu anomaly intermediate between the Glamaig and Loch Ainort granites.

Values of $(Ce/Yb)_N$ for the samples are:

Glamaig: 9.73 Beinn an Dubhaich: 5.56

Loch Ainort: 3.81 Marsco: 4.17

As the absolute abundance of the REE increases, the value of $(Ce/Yb)_N$ tends to decrease: the more evolved granites show smaller amounts of REE fractionation. Whatever process or processes have been involved in the formation of the granites, it is necessary to explain this change in REE distribution. The increase in the size of the Eu anomaly (Eu/Eu*) is most easily explained in terms of feldspar fractionation during the evolution of the granite magmas (Gamble et al., 1992).

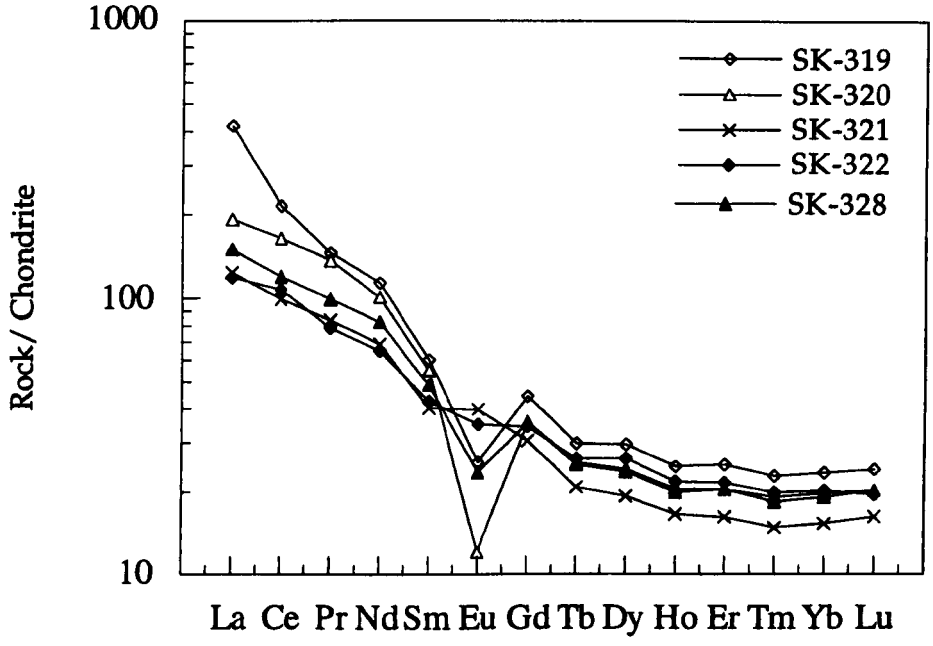

Fig. 6.37 Chondrite-normalised REE patterns for samples from the Maol na Gainmhich Granite (SK-319), the Northern Porphyritic Felsite (SK-320), the Eas Mor Granite (SK-321), the Meal Buidhe Granite (SK-322) and the Glen Sligachan Granite (SK-328).

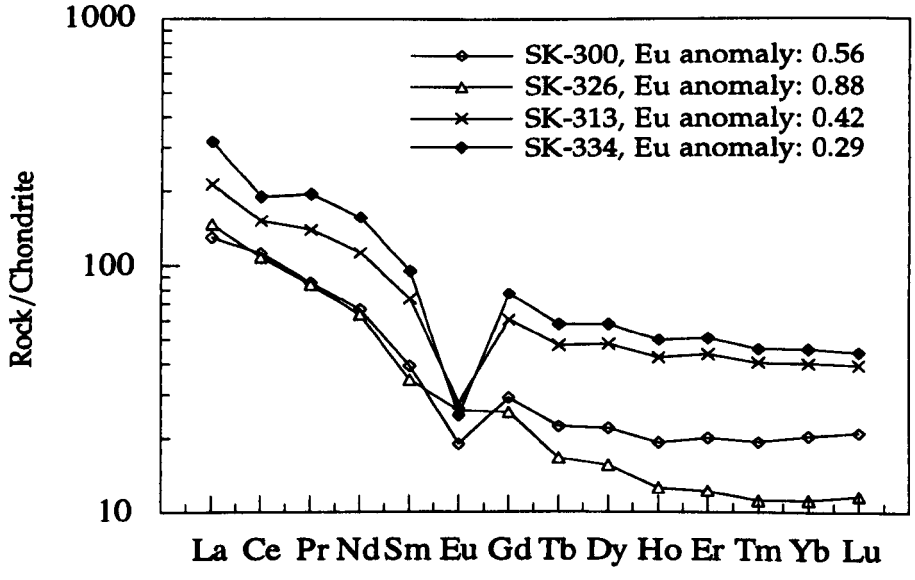

Fig. 6.38. Selected chondrite-normalized REE patterns for samples from the Beinn an Dubhaich Granite (SK-300), the Glamaig Granite (SK-326), the Loch Ainort Granite (SK-313) and the Marsco Granite (SK-334).

Two proposed crustal sources for the Skye granites are Lewisian gneiss and Torridonian sandstone (Thorpe et al., 1977). Both have lower overall REE contents and greater values of [(Ce/Yb)N = (8-18)] than the Skye granites, suggestive that these two lithologies are unlikely sources for the granites (Thorpe et al., 1977). Thus, Thorpe et al. (1977) suggest that the Glamaig Granite may have originated by fractional crystallisation of a more basic magma with a similar REE pattern, whereas the Loch Ainort and Marsco granites may result from further fractional crystallisation of Glamaig magma or from a magma with a composition similar to Glamaig magma. In contrast, the Beinn an Dubhaich Granite may also have been derived by fractional crystallisation, but from a different parental basic magma.

6. 5 Combined major-, trace- and rare-earth-element chemistry

The compositional significance of a mineral during fractional crystallisation is completely dependent on its relative abundance and its Kd value for a given trace-element (Hanson, 1978; but see also, Wager, 1956; Walsh, et al., 1979). In order to assess the role of constituent minerals in controlling the geochemical evolution of Skye granitic magma(s), it is necessary to consider the effects of fractionation of individual minerals. To do so, it is important to examine how the rock-forming minerals can affect the compositions of various elements, including: the LIL elements, Zr, P, Ti, and the REE.

Crystallisation of alkali feldspar will deplete the residual liquid in Ba and fractionation of plagioclase will deplete the residual liquid in Sr. Fractionation of alkali feldspar, which has a high Rb distribution coefficient, will increase the K/Rb ratio in the residual melt relative to the parental liquid. Negative Eu anomalies will increase in size with progressive plagioclase fractionation.

The affect of ferromagnesium minerals during fractionation processes are

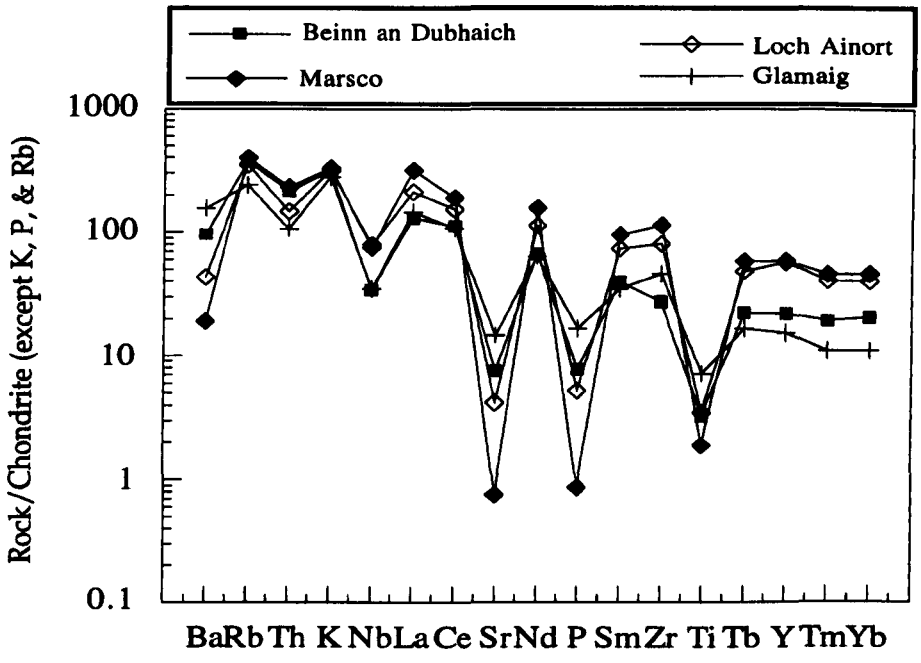

Fig. 6. 39. Normalized compatible and incompatible-element patterns for, Beinn an Dubhaich granite (SK-300), Loch Ainort Granite (SK-313), Glamaig Granite (SK-326) and Marsco Granite (SK-334).

limited because of the low abundances of Ca, Mg and Fe affiliated trace-elements in the magmas. Fractionation of biotite will contribute to the depletion of Ba and also aid the depletion of Ti in conjunction with the oxide phases. Amphibole fractionation will affect the Zn and REE concentrations. Apatite fractionation will reduce the amount of P in the residual liquid together with the LREE. Zircon fractionation will deplete the melt in Zr and the HREE.

Fig. 6.39 shows chondrite-normalised patterns for the Beinn an Dubhaich, Loch Ainort, Marsco and Glamaig granites. The factors used in normalise these data are those recommended by Thompson (1982). Without exception, all four rocks display very similar patterns. The observable negative Nb, Sr, P and Ti anomalies and declining Ba and Th levels are consistent with fractional crystallisation of pyroxene, plagioclase, apatite, Fe-Ti oxide (with biotite), alkali feldspar and zircon.

6. 6 Summary and conclusions

The whole-rock compositional data for the Skye granites indicate (in terms of petrogenetic processes):

(i) There is a strong geochemical coherence within the suite;

(ii) The lower abundances of CaO and MgO, together with higher Fe/Mg, Nb and Zr relative to S and I-type granites described elsewhere (for example Collins, et at., 1982), classify these granites as A-type granite (i.e. anorogenic), see also Clarke, (1992).

(iii) The generation of the Glamaig Granite magma may have been by crystal -liquid fractionation from a more primitive (basic) magma, or by partial melting of material with a similar REE distribution;

(iv) The rest of the granites have, in general, higher concentrations of the incompatible trace-elements (Rb, Zr, Th, Y, Nb), including the REE, but with less fractionated REE signatures (i.e. smaller values of $(Ce/Yb)_N$);

(v) The geochemical trends are consistent with either crystal-liquid fractionation, involving variable proportions of quartz, alkali feldspar, plagioclase, amphibole, biotite, apatite, Fe-Ti oxide, and zircon, or the mixing of end-member compositions such as the Glamaig Granite (i.e. the most primitive composition) and the Marsco Granite (the most evolved composition). Combined crystal-liquid fractionation and mixing represents a third possibility;

(vi) Simple mixing does not, however, explain: (a) the inflection present in the plot of MnO against SiO_2 (Fig. 6.7); (b) the non-linear and divergent relationships between K_2O, Rb, Sr and ?Nb against SiO_2 (Figs. 6.11, 6.16, 6.17 and 6.24, respectively); (c) the presence of an anomalous group of granites which are characterised by *low* Zr, Y and Nb, but with *high* SiO_2 contents (Figs. 6.21, 6.23 and 6.24, respectively).

Table 6. 1 Whole-rock major- and trace-element analyses, normative CIPW data, and other derived parameters for Skye granites.

	RA-100	SK-305	SK-306	SK-335	SK-336	K-S337
Major-elements (wt. %)						
SiO_2	76.67	76.53	73.44	73.21	73.25	74.12
TiO_2	0.198	0.130	0.313	0.29	0.248	0.259
Al_2O_3	11.37	11.81	12.11	12.55	12.27	12.58
Fe_2O_3	1.16	0.36	0.79	1.31	1.07	0.83
FeO	1.36	1.24	1.83	2.00	1.81	1.54
MnO	0.053	0.033	0.051	0.079	0.064	0.014
MgO	0.01	0.04	0.27	0.04	0.05	0.08
CaO	0.03	0.28	1.24	0.77	0.84	0.22
Na_2O	3.90	4.73	4.49	4.27	4.71	4.22
K_20	4.655	4.923	4.424	5.031	4.801	5.134
L.O.I.	0.55	0.30	1.11	0.26	0.24	0.71
P_2O_5	0.027	0.036	0.077	0.03	0.027	0.060
Total	99.99	100.41	100.13	99.84	99.38	99.77
Norm CIPW						
Ap	0.05	0.09	0.19	0.07	0.07	0.14
Il	0.38	0.25	0.59	0.55	0.48	0.50
Mt	1.49	0.00	1.02	1.91	0.02	1.22
Or	27.70	29.04	26.38	29.85	28.61	30.60
Ab	32.72	33.31	38.05	36.28	36.70	36.05
An	0.00	0.00	0.00	0.22	0.00	0.23
Di	0.00	1.00	4.89	3.03	3.55	0.41
Hy	1.45	1.69	0.55	0.77	1.29	1.73
Ac	0.41	1.04	0.28	0.00	3.08	0.00
C	0.00	0.00	0.00	0.00	0.00	0.00
Q	35.80	32.30	28.05	27.32	26.20	29.11
Ns	0.00	1.28	0.00	0.00	0.00	0.00
Total	100.00	100.00	100.00	100.00	100.00	99.99
Trace-elements (ppm)						
Nb	23.7	21.2	11.6	28.1	26.7	28.4
Zr	546.7	234.8	239.4	645.2	548.2	513.0
Y	95.6	77.0	36.7	123.7	111.9	158.7
Sr	8.7	19.5	106.0	50.3	44.9	41.8
Rb	102.9	165.7	128.0	151.8	147.3	153.8
Th	6.6	15.0	9.1	12.6	11.4	9.9
Pb	16.7	14.2	14.3	21.7	14.4	26.5
Zn	193.8	47.8	52.8	147.7	113.1	156.9
Cu	b.d.l.	0.1	5.9	1.7	0.5	2.7
Ni	7.7	8.9	8.1	7.5	7.9	9.3
Ce	201.1	110.2	104.5	146.2	134.9	183.7
Cr	b.d.l.	b.d.l.	2.5	b.d.l.	b.d.l.	b.d.l.
Nd	112.5	52.4	43.9	80.8	72.7	116.1
La	103.8	54.3	92.2	77.7	68.3	106.5
V	3.4	5.1	13.7	3.3	7.1	3.0
Ba	162.7	623.6	821.2	1078.4	929.5	925.4
Sc	4.0	4.9	8.2	6.6	3.6	2.4
Element ratios						
K/Rb	375.48	246.6	286.87	275.08	270.52	277.06
K/Ba	237.47	65.52	44.71	38.72	42.87	46.05
Rb/Sr	11.83	8.5	1.21	3.02	3.28	3.68
Sr/Ba	0.05	0.03	0.13	0.05	0.05	0.05
TTDI	94.20	94.37	90.47	91.34	90.19	92.63

L.O.I.= Loss on ignition.; **b.d.l.** = below detection limit; TTDI, Thornton and Tuttle Differentiation Index
Where: **RA-100**, Raasay; **SK-305, SK-306**, Creag Strollamus; **SK-335, SK-336, SK-337**, Beinn na Caillich.

TABLE 6. 1(Continued)

	SK-298	SK-299	SK-300	SK-301	SK-302	SK-338
Major-elements (wt.%)						
SiO_2	72.13	74.18	74.25	73.97	74.57	73.87
TiO_2	0.43	0.381	0.333	0.255	0.301	0.303
Al_2O_3	12.63	12.17	12.10	12.38	12.33	12.71
Fe_2O_3	1.03	0.77	0.73	0.55	0.72	0.60
FeO	2.34	2.18	1.68	1.4	1.48	1.64
MnO	0.065	0.057	0.045	0.025	0.036	0.045
MgO	0.37	0.34	0.30	0.29	0.21	0.27
CaO	1.51	1.22	1.38	0.84	0.69	1.10
Na_2O	3.73	3.54	3.84	4.18	3.90	3.74
K_2O	4.354	4.515	4.517	4.793	5.117	4.861
L.O.I.	0.14	0.31	0.16	0.94	0.32	0.19
P_2O_5	0.093	0.075	0.081	0.051	0.090	0.054
Total	98.82	99.74	99.40	99.68	99.77	99.38
Norm CIPW						
Ap	0.22	0.19	0.19	0.12	0.21	0.19
Il	0.83	0.73	0.63	0.50	0.57	0.57
Mt	1.51	1.12	1.07	0.81	1.05	0.88
Or	26.05	26.86	26.91	28.67	30.42	28.95
Ab	31.98	30.12	32.73	35.82	33.18	31.90
An	4.94	3.99	2.45	0.88	1.02	3.57
Di	1.77	1.35	3.35	2.56	1.57	1.21
Hy	2.93	3.02	1.08	1.19	1.43	2.17
Ac	0.00	0.00	0.00	0.00	0.00	0.00
C	0.00	0.00	0.00	0.00	0.00	0.00
Q	29.78	32.61	31.58	29.45	30.54	30.57
Ns	0.00	0.00	0.00	0.00	0.00	0.00
Total	100.01	99.99	99.99	100.00	99.99	100.01
Trace-elements (ppm)						
Nb	15.7	13.0	11.9	11.9	9.4	11.7
Zr	268.9	222.4	184.7	226.5	298.2	211.0
Y	52.6	44.7	44.0	38.0	29.7	38.7
Sr	103.3	90.4	88.2	70.3	68.0	96.1
Rb	134.5	140.2	129.6	160.4	154.1	156.5
Th	10.6	9.7	9.0	11.3	5.7	10.4
Pb	13.0	13.5	12.3	12.8	14.2	13.8
Zn	55.6	55.2	34.3	34.6	36.1	35.7
Cu	0.4	-0.7	0.6	1.4	1.5	0.8
Ni	10.1	7.0	8.3	8.0	7.9	9.0
Ce	113.8	101.2	90.3	98.9	61.9	88.0
Cr	b.d.l.	0.00	b.d.l.	0.2	b.d.l.	b.d.l.
Nd	55.7	49.4	44.4	38.7	31.0	40.4
La	58.4	54,2	44.1	74.8	32.2	44.9
V	14.3	13.0	11.8	9.4	10.4	15.1
Ba	887.7	847.2	846.7	753.9	998.2	868.9
Sc	7.3	7.5	8.2	7.4	7.5	6.6
Element ratios						
K/Rb	268.68	267.29	289.29	248.02	275.61	257.8
K/Ba	40.71	44.23	44.28	52.77	42.55	46.43
Rb/Sr	1.30	1.55	1.47	2.28	2.27	1.63
Sr/Ba	0.12	0.11	0.10	0.09	0.07	0.11
TTDI	85.28	88.01	89.54	92.00	92.65	91.26

L.O.I.= Loss on ignition.; **b.d.l.** = below detection limit; TTDI, Thornton and Tuttle Differentiation Index
Where: **SK-298, SK-299, SK-300, SK-301, SK-302, SK-338,** Beinn an Dubhaich.

Table 6. 1 continued

	SK-307	SK-309	SK-310	SK-311	SK-312	SK-303	SK-304
Major-elements (wt. %)							
SiO_2	74.08	72.10	72.07	72.16	72.38	76.43	76.70
TiO_2	0.368	0.432	0.407	0.362	0.390	0.133	0.128
Al_2O_3	12.31	12.79	12.78	13.04	12.53	11.21	11.17
Fe_2O_3	1.05	1.59	1.43	1.46	1.30	0.35	0.26
FeO	1.63	2.29	2.04	2.11	1.96	1.1	1.1
MnO	0.058	0.075	0.073	0.061	0.067	0.03	0.022
MgO	0.16	0.25	0.22	0.19	0.22	0.07	0.08
CaO	0.92	0.59	1.28	0.82	1.23	0.51	0.56
Na_2O	4.05	4.12	4.02	4.49	4.21	3.43	4.01
K_2O	4.646	4.367	4.251	4.191	4.506	4.663	5.246
L.O.I.	1.02	0.77	0.66	0.75	0.59	1.905	0.48
P_2O_5	0.065	0.071	0.061	0.055	0.061	0.02	0.022
Total	100.36	99.46	99.30	99.69	99.56	99.85	99.77
Norm CIPW							
Ap	0.16	0.17	0.14	0.13	0.14	0.05	0.05
Il	0.71	0.83	0.79	0.69	0.75	0.23	0.25
Mt	1.53	2.34	2.10	2.14	1.91	0.52	0.00
Or	27.66	26.16	25.46	24.03	26.96	28.12	31.24
Ab	34.49	35.33	34.49	38.40	36.03	29.64	28.42
An	1.69	2.50	4.33	3.08	1.99	1.46	0.00
Di	2.11	0.00	1.47	0.55	3.26	0.87	2.38
Hy	0.95	2.99	1.84	2.40	0.91	1.34	0.82
Ac	0.00	0.00	0.00	0.00	0.00	0.00	0.76
C	0.00	0.38	0.00	0.00	0.00	0.00	0.00
Q	30.70	29.29	29.37	27.57	28.05	37.77	34.94
Ns	0.00	0.00	0.00	0.00	0.00	0.00	1.14
Total	100.00	99.99	99.99	98.99	100.00	100.00	100.00
Trace-elements (ppm)							
Nb	23.3	21.6	20.1	23.7	21.6	13.1	12.8
Zr	446.5	512.6	4.74.5	521.6	498.2	170.0	171.4
Y	86.8	94.9	91.4	112.2	92.3	49.1	49.3
Sr	47.1	63.7	86.1	56.7	66.9	39.0	38.1
Rb	137.7	123.7	117.7	182.3	121.8	154.4	165.1
Th	10.6	9.6	7.7	8.8	8.7	12.8	11.9
Pb	16.9	13.9	16.4	19.6	13.6	11.3	12.9
Zn	76.0	98.0	85.2	140.2	70.9	31.0	31.8
Cu	2.6	7.5	4.2	6.5	4.0	b.d.l.	b.d.l.
Ni	8.0	9.7	10.0	9.5	8.5	7.5	7.8
Ce	145.6	119.7	94.3	128.8	113.6	125.4	125.3
Cr	0.3	0.3	0.4	0.00	b.d.l.	b.d.l.	b.d.l.
Nd	74.3	59.3	52.7	75.5	60.6	58.1	56.0
La	76.5	58.4	43.3	75.7	52.8	66.9	67.6
V	8.8	10.5	6.4	7.9	9.8	3.6	4.8
Ba	784.6	846.9	910.1	865.4	797.9	587.8	565.6
Sc	6.7	7.1	8.0	9.0	10.7	2.4	7.4
Element ratios							
K/Rb	280.04	293.02	299.77	190.81	307.06	250.67	263.73
K/Ba	49.15	42.80	38.77	40.20	46.87	65.84	76.98
Rb/Sr	2.92	1.94	1.37	3.22	1.82	3.96	4.33
Sr/Ba	0.06	0.08	0.09	0.07	0.08	0.07	0.07
TTDI	90.85	87.55	86.24	88.13	88.29	92.07	94.93

L.O.I.= Loss on ignition.; b.d.l. = below detection limit; TTDI, Thornton and Tuttle Differentiation Index
Where: SK-307, SK-309, SK-310, SK-311, SK-312, Glas Bheinn Mhor; SK-303, SK-304, Allt Fearna.

Table 6.1 continued

	SK-314	SK-315	SK-339	SK-340	SK-333	SK-334	SK-343
Major-elements (wt. %)							
SiO_2	70.15	72.22	73.49	71.19	76.98	76.71	70.95
TiO_2	0.337	0.352	0.286	0.368	0.168	0.193	0.433
Al_2O_3	12.35	12.34	12.12	12.47	11.20	11.21	12.85
Fe_2O_3	1.32	1.31	1.00	1.30	0.58	0.67	1.33
FeO	2.53	2.60	2.14	2.68	1.70	1.71	3.16
MnO	0.143	0.102	0.072	0.106	0.042	0.043	0.114
MgO	0.06	0.06	0.06	0.11	0.01	0.0	0.10
CaO	1.06	1.07	0.56	1.27	0.29	0.30	1.57
Na_2O	5.61	4.19	5.01	6.00	3.58	3.68	4.23
K_2O	4.420	4.748	4.577	4.280	4.703	4.735	4.26
L.O.I.	2.57	0.24	0.31	0.52	0.31	0.30	0.15
P_2O_2	0.038	0.038	0.029	0.088	0.015	0.009	0.63
Total	100.59	99.27	99.65	100.38	99.57	99.57	99.22
Norm CIPW							
Ap	0.14	0.10	0.05	0.12	0.05	0.02	0.14
Il	0.66	0.67	0.55	0.70	0.33	0.36	0.82
Mt	0.00	1.92	0.00	0.00	0.85	0.98	1.95
Or	25.37	28.35	27.25	25.33	28.00	28.22	25.42
Ab	41.03	35.80	37.08	40.38	30.52	31.37	36.13
An	0.00	0.84	0.00	0.00	0.61	0.07	3.52
Di	4.41	3.77	2.36	5.29	0.63	1.22	3.48
Hy	2.26	1.49	2.51	2.01	2.15	1.72	2.65
Ac	3.90	0.00	2.91	3.77	0.00	0.00	0.00
C	0.00	0.00	0.00	0.00	0.00	0.00	0.00
Q	21.50	27.07	26.76	20.96	36.90	36.04	25.87
Ns	0.71	0.00	0.53	1.44	0.00	0.00	0.00
Total	99.98	100.01	100.00	100.00	100.03	100.00	99.98
Trace-elements (ppm)							
Nb	22.4	22.9	18.9	23.6	28.3	26.3	17.7
Zr	544.8	522.5	457.4	514.6	652.3	780.1	496.1
Y	96.5	101.7	98.3	97.2	108.5	117.6	92.3
Sr	64.2	65.5	55.1	68.2	8.2	8.8	87.7
Rb	106.1	106.9	111.6	98.0	164.0	137.9	128.8
Th	3.6	4.9	4.9	3.9	9.5	9.7	7.4
Pb	20.5	15.5	41.9	28.4	25.7	12.8	12.9
Zn	158.0	151,1	168.3	180.7	153.2	155.7	113.9
Cu	3.6	1.7	b.d.l.	0.7	9.3	7.3	9.6
Ni	9.2	9.4	7.2	8.7	9.3	7.3	9.6
Ce	163.1	147.1	134.6	134.0	161.8	179.8	114.1
Cr	0.00	0.3	0.00	b.d.l.	b.d.l.	b.d.l.	b.d.l.
Nd	86.6	79.1	73.5	70.8	82.4	93.8	61.8
La	85.8	96.1	65.5	65.8	77.8	80.7	51.3
V	4.1	3.1	3.0	3.6	0.8	2.5	2.6
Ba	1072.1	1069.7	979.0	1046.7	132.3	136.0	1956.2
Sc	5.1	5.9	6.5	6.3	2.6	1.8	8.0
Element ratios							
K/Rb	345.77	368.65	340.4	362.49	238.02	284.99	274.52
K/Ba	34.22	36.84	38.8	33.94	295.05	288.97	18.07
Rb/Sr	1.65	1.63	2.03	1.44	20	15.67	1.47
Sr/Ba	0.06	0.06	0.06	0.07	0.06	0.06	0.04
TTDI	84.26	87.57	88.11	85.08	93.85	93.96	84.78

L.O.I.= Loss on ignition.; b.d.l. = below detection limit; TTDI, Thornton and Tuttle Differentiation Index
Where: SK-314, SK-315, SK-339, SK-340, Beinn Dearg Mhor; SK-333, SK-334, SK-343, Marsco.

Table 6. 1 continued

	SK-323	SK-324	SK-325	SK-325A	SK-326	SK-327	SK-322
Major-elements (wt. %)							
SiO_2	70.03	69.44	68.95	64.99	68.62	67.97	70.28
TiO_2	0.50	0.511	0.727	0.950	0.731	0.742	0.502
Al_2O_3	13.42	13.58	13.62	13.57	13.69	13.67	13.10
Fe_2O_3	0.69	0.82	0.99	3.2	0.97	1.05	0.87
FeO	3.13	3.14	3.41	3.48	3.6	3.41	3.67
MnO	0.093	0.10	0.084	0.138	0.086	0.081	0.117
MgO	0.4	0.43	0.8	1.47	0.82	0.83	0.26
CaO	1.58	1.58	2.14	3.35	2.18	2.22	1.74
Na_2O	3.92	4.52	4.23	4.89	4.25	5.42	4.03
K_2O	4.912	4.783	4.009	2.485	4.015	3.947	4.107
L.O.I.	0.47	0.24	0.4	0.45	0.57	0.48	0.25
P_2O_5	0.135	0.134	0.182	0.265	0.175	0.191	0.086
Total	99.28	99.27	99.53	99.23	99.72	100.01	99.02
Norm CIPW							
Ap	0.34	0.31	0.43	0.65	0.43	0.45	0.22
Il	0.96	0.98	1.40	1.83	1.40	1.41	0.96
Mt	1.01	1.20	1.45	4.70	1.42	1.53	1.28
Or	29.36	28.52	23.90	14.89	23.96	23.45	24.59
Ab	33.57	38.62	36.10	41.87	36.27	46.07	34.52
An	4.57	2.67	6.38	7.82	6.46	1.31	5.58
Di	2.11	3.79	2.66	5.89	2.78	7.21	2.24
Hy	4.49	3.60	5.08	3.29	5.48	2.76	4.97
Ac	0.00	0.00	0.00	0.00	0.00	0.00	0.00
C	0.00	0.00	0.00	0.00	0.00	0.00	0.00
Q	23.59	20.31	22.59	19.06	21.84	15.80	25.63
Ns	0.00	0.00	0.00	0.00	0.00	0.00	0.00
Total	100.00	100.00	99.99	100.00	100.04	99.99	99.99
Trace-elements (ppm)							
Nb	13.5	14.2	12.6	19.9	12.2	12.5	15.9
Zr	324.6	323.7	347.2	160.3	311.5	344.3	516.6
Y	47.7	50.7	32.0	65.6	30.9	32.2	69.0
Sr	100.4	99.8	175.4	160.9	174.6	180.9	115.6
Rb	106.0	103.6	83.3	51.0	84.5	82.1	119.3
Th	6.0	5.2	5.6	4.8	4.5	4.8	8.1
Pb	16.3	13.2	11.6	8.6	10.7	12.2	12.1
Zn	73.6	65.4	59.0	85.0	58.1	60.1	97.5
Cu	10.1	8.4	8.4	10.2	7.5	6.7	4.0
Ni	8.8	8.9	9.0	13.5	10.4	11.0	8.6
Ce	88.0	95.5	95.3	153.5	86.9	80.0	76.1
Cr	b.d.l.	0.1	4.5	13.0	4.0	2.4	b.d.l.
Nd	41.5	45.2	41.1	79.7	42.7	38.4	44.8
La	43.9	49.2	51.6	66.8	44.7	51.9	40.9
V	11.3	12.1	48.0	103.9	47.2	49.0	6.8
Ba	1355.1	1359.3	1388.2	709.2	1361.2	1348.2	1833.5
Sc	11.7	10.5	9.5	20.5	11.0	12.7	14.0
Element ratios							
K/Rb	384.62	383.19	399.46	404.42	394.37	399.03	285.73
K/Ba	30.09	29.21	23.97	29.08	24.48	24.30	18.59
Rb/Sr	1.06	1.04	0.47	0.32	0.48	0.45	1.03
Sr/Ba	0.07	0.07	0.13	0.23	0.13	0.13	0.06
TTDI	84.45	83.20	80.48	70.94	79.98	83.44	84.15

L.O.I.= Loss on ignition.; **b.d.l.** = below detection limit; TTDI, Thornton and Tuttle Differentiation Index
Where: **SK-323, SK-324, SK-325, SK-326, SK-327,** Glamaig, and mafic inclusion **(SK-325A); SK-322,** Meall Buidhe.

Table 6.1 continued

	SK-313	SK-316	SK-317	SK-318	SK-321	SK-320	SK-319
Major-elements (wt.%)							
SiO_2	71.90	71.61	71.07	71.72	67.29	68.10	73.26
TiO_2	0.354	0.379	0.354	0.348	0.572	0.451	0.283
Al_2O_3	12.73	12.19	12.65	12.52	13.53	13.42	12.64
Fe_2O_3	0.84	0.77	0.76	0.87	1.16	0.88	0.71
FeO	2.48	3.2	2.24	3.03	4.31	3.01	2.01
MnO	o.73	0.103	0.085	0.109	0.79	0.10	0.035
MgO	0.12	0.29	0.08	0.12	0.29	0.08	0.12
CaO	o.93	1.25	1.39	1.13	1.81	0.35	0.84
Na_2O	5.95	5.02	4.03	4.62	5.25	3.07	3.28
K_2O	4.725	4.362	4.588	4.432	5.012	6.759	6.099
L.O.I.	0.09	0.55	1.72	0.51	0.25	3.25	0.44
P_2O_5	0.070	0.06	0.084	0.049	0.142	0.057	0.04
Total	100.35	99.66	99.25	99.46	99.82	99.57	99.77
Norm CIPW							
Ap	0.12	0.14	0.19	0.12	0.33	0.15	0.10
Il	0.67	0.73	0.68	0.67	1.09	0.89	0.54
Mt	1.23	0.00	1.13	1.27	0.48	1.33	1.04
Or	27.27	26.00	27.81	26.46	29.74	41.49	36.30
Ab	39.64	38.77	34.97	39.51	41.89	26.98	27.94
An	0.23	0.00	2.94	0.34	0.00	1.40	1.76
Di	3.55	5.17	3.11	4.41	7.11	0.00	1.91
Hy	3.37	3.16	2.24	2.50	4.06	4.61	2.04
Ac	0.00	2.23	0.00	0.00	2.41	0.00	0.00
C	0.00	0.00	0.00	0.00	0.00	0.58	0.00
Q	23.93	23.42	26.92	24.72	12.88	22.58	28.39
Ns	0.00	0.36	0.00	0.00	0.00	0.00	0.00
Total	100.01	100.00	99.99	100.00	99.99	100.01	100.02
Trace-elements (ppm)							
Nb	27.9	26.2	24.6	25.5	11.1	24.1	19.2
Zr	546.9	637.6	477.7	553.5	232.8	643.5	413.0
Y	114.0	119.7	98.4	134.6	39.7	52.5	58.8
Sr	49.1	50.4	67.2	57.8	73.8	17.6	58.4
Rb	122.0	107.9	139.8	110.5	74.0	168.7	92.9
Th	6.2	6.5	7.7	4.9	2.7	5.2	5.2
Pb	23.9	10.2	17.8	14.7	11.9	19.2	7.4
Zn	129.6	139.9	98.3	135.3	107.6	128.1	28.5
Cu	1.5	5.6	4.8	1.6	6.6	1.0	151.9
Ni	8.3	9.1	9.7	8.6	9.4	9.0	9.3
Ce	136.9	157.2	130.8	126.6	70.4	155.9	151.8
Cr	b.d.l.	b.d.l.	3.2	b.d.l.	0.8	b.d.l.	b.d.l.
Nd	73.6	83.2	66.1	67.0	40.9	74.8	66.8
La	64.9	74.1	59.9	61.9	38.3	70.0	71.6
V	7.3	5.0	19.3	3.0	12.9	5.3	16.3
Ba	648.5	671.8	641.1	758.4	1052.7	256.6	524.6
Sc	6.6	6.6	7.4	6.6	11.1	10.7	2.1
Element ratios							
K/Rb	311.25	338.36	272.39	332.9	562.16	332.54	544.91
K/Ba	585.54	53.89	59.4	48.50	39.52	218.63	96.50
Rb/Sr	2.48	2.14	2.08	1.91	1.00	9.58	1.59
Sr/Ba	0.76	0.08	0.10	0.08	0.07	0.07	0.11
TTDI	88.14	86.43	86.41	88.47	82.48	86.76	89.33

L.O.I.= Loss on ignition.; **b.d.l.** = below detection limit; TTDI, Thornton and Tuttle Differentiation Index
Where: **SK-313, SK-316, SK-317, SK-318,** Loch Ainort; **SK-321,** Eas Mor; **SK-320,** Northern Porphyritic Felsite; **SK-319,** Maol na Gainmhich.

Table 6.1 continued

	SK-329L	SK-329D	SK-330	SK-331	SK-332	SK-341	SK-328
Major-elements (wt. %)							
SiO_2	73.79	72.10	69.22	73.07	76.84	77.62	71.1
TiO_2	0.314	0.406	0.561	0.331	0.183	0.183	0.412
Al_2O_3	12.13	12.32	12.72	12.05	11.03	11.04	12.58
Fe_2O_3	0.48	0.65	1.60	0.67	0.41	0.32	0.65
FeO	2.30	2.82	2.95	2.80	1.97	1.52	3.50
MnO	0.052	0.071	0.088	0.073	0.05	0.026	0.147
MgO	0.42	0.64	1.11	0.1	0.01	0.02	0.12
CaO	1.02	1.53	2.47	0.57	0.14	0.13	1.10
Na_2O	4.55	4.19	3.91	4.61	4.04	3.52	4.68
K_2O	4.519	4.334	4.165	4.508	4.851	5.008	4.94
L.O.I.	0.06	0.63	0.05	0.19	0.81	0.43	0.30
P_2O_5	0.074	0.112	0.175	0.065	0.035	0.018	0.061
Total	99.72	99.80	99.01	99.03	100.37	99.83	99.59
Norm CIPW							
Ap	0.17	0.26	0.43	0.18	0.10	0.05	0.17
Il	0.59	0.79	1.07	0.63	0.34	0.34	0.78
Mt	0.13	0.95	2.34	0.03	0.00	0.07	0.00
Or	26.81	25.80	24.89	26.96	28.79	29.78	29.37
Ab	37.36	35.74	33.42	37.30	29.86	29.06	37.54
An	0.00	2.04	4.89	0.00	0.00	0.00	0.00
Di	3.98	4.18	5.25	2.12	0.39	0.46	4.45
Hy	2.74	3.60	3.55	3.90	3.25	2.33	4.13
Ac	1.13	0.00	0.00	1.91	1.19	0.79	1.89
C	0.00	0.00	0.00	0.00	0.00	0.00	0.00
Q	27.09	26.63	24.15	26.99	35.36	37.11	21.63
Ns	0.00	0.00	0.00	0.00	0.73	0.00	0.04
Total	100.00	99.99	99.99	100.02	100.01	99.99	100.00
Trace-elements (ppm)							
Nb	19.2	19.2	18.4	22.3	28.2	25.4	14.3
Zr	387.3	400.4	411.2	555.7	764.4	626.1	292.6
Y	96.6	86.1	69.1	113.9	122.8	91.8	48.3
Sr	42.0	59.5	87.2	56.9	10.8	8.1	28.1
Rb	128.3	128.1	124.7	120.6	152.6	141.2	93.8
Th	9.6	8.0	5.7	6.9	7.3	8.4	5.0
Pb	13.9	13.6	19.3	11.2	8.2	9.7	14.9
Zn	98.4	131.2	118.5	133.6	96.0	99.8	107.3
Cu	b.d.l.	0.9	11.2	b.d.l.	b.d.l.	b.d.l.	2.4
Ni	10.5	13.0	16.6	9.7	8.4	7.9	8.6
Ce	185.9	183.5	125.6	172.7	192.1	183.8	93.5
Cr	3.0	9.7	16.1	b.d.l.	0.3	b.d.l.	1.4
Nd	105.3	103.4	66.4	107.2	118.3	93.7	50.8
La	113.4	124.3	64.8	94.3	116.2	90.6	44.4
V	17.5	26.0	42.9	7.3	0.8	4.2	3.8
Ba	377.4	463.5	555.7	782.7	182.5	144.5	404.8
Sc	5.7	9.3	10.6	6.2	1.7	1.1	7.3
Element ratios							
K/Rb	292.34	280.81	277.22	310.25	263.85	294.38	437.12
K/Ba	99.38	77.61	62.21	47.80	220.62	287.66	101.29
Rb/Sr	3.05	2.15	1.43	2.12	14.13	17.43	3.34
Sr/Ba	0.11	0.13	0.16	0.07	0.06	0.07	0.07
TTDI	88.16	86.49	79.52	89.30	92.97	94.89	87.60

L.O.I.= Loss on ignition.; **b.d.l.** = below detection limit; TTDI, Thornton and Tuttle Differentiation Index
Where: **SK-329L, SK-329D, SK-330, SK-331, SK-332, SK-341**, Southern Porphyritic Granite; **SK-328**, Glen Sligachan.

Table 6. 2 Rare-earth-element concentrations of whole rocks (in ppm).

	SK-298	SK-299	SK-300	SK-301	SK-302	SK-338	SK-303	SK-304
La	62.4	54.20	42.77	64.99	33.78	44.90	57.99	59.73
Ce	132.07	107.63	97.44	115.48	66.01	101.43	115.14	127.17
Pr	13.56	11.99	10.52	11.64	7.04	10.24	12.28	12.77
Nd	52.83	46.98	41.98	41.81	27.62	38.34	47.20	47.82
Sm	9.73	8.63	7.98	7.16	5.54	6.95	8.85	8.93
Eu	1.58	1.47	1.46	0.99	1.25	1.21	0.87	0.83
Gd	10.23	8.66	8.05	6.79	5.54	7.03	8.84	9.08
Tb	1.38	1.21	1.15	0.91	0.78	0.94	1.23	1.26
Dy	8.46	7.71	7.48	5.77	5.02	6.04	8.01	8.02
Ho	1.66	1.52	1.50	1.12	1.00	1.18	1.55	1.61
Er	4.90	4.52	4.51	3.38	2.89	3.67	4.76	4.71
Tm	0.70	0.65	0.65	0.50	0.42	0.54	0.67	0.70
Yb	4.56	4.20	4.46	3.24	2.68	3.60	4.44	4.61
Lu	0.70	0.65	0.71	0.51	0.42	0.56	0.71	0.74
(Ce/Yb)N	7.37	6.52	5.56	9.04	6.26	7.17	6.59	7.07
Eu/Eu*	0.49	0.52	0.56	0.44	0.70	0.53	0.30	0.28

Where: **SK-298, SK-299, SK-300, SK-301, SK-302, SK-338,** Beinn an Dubhaich; **SK-303, SK-304,** Allt Fearna.

Table 6. 2 continued

	SK-323	SK-324	SK-325	SK-325A	SK-326	SK-327	SK-328
La	61.58	51.48	52.76	76.82	48.27	68.16	49.32
Ce	97.06	97.46	102.43	125.73	93.60	88.02	103.91
Pr	10.50	10.92	10.89	19.40	10.36	9.99	12.25
Nd	42.17	43.67	41.43	77.84	40.14	38.93	51.94
Sm	7.95	8.31	6.99	13.67	6.98	6.86	9.90
Eu	2.26	2.28	1.93	1.88	1.99	1.97	1.81
Gd	8.46	8.65	7.18	13.66	6.99	6.89	9.88
Tb	1.14	1.21	0.87	1.73	0.86	0.87	1.31
Dy	7.53	7.86	5.31	10.66	5.33	5.20	8.11
Ho	1.48	1.52	1.03	2.05	0.98	1.01	1.55
Er	4.44	4.60	2.86	5.95	2.74	2.92	4.59
Tm	0.63	0.67	0.39	0.82	0.38	0.39	0.62
Yb	4.12	4.38	2.54	5.37	2.45	2.58	4.20
Lu	0.65	0.68	0.39	0.82	0.39	0.40	0.69
(Ce/Yb)N	5.99	5.65	10.24	5.95	9.73	8.69	6.30
Eu/Eu*	0.85	0.83	0.84	0.42	0.88	0.88	0.56

Where: **SK-323, SK-324, SK-325, SK-326, SK-327,** Glamaig; and **SK-325A** a mafic inclusion; **SK-328,** Glen Sligachan.

Table 6. 2 continued

	SK-305	SK-306	SK-307	SK-309	SK-310	SK-312	SK-335	SK-337
La	53.35	65.05	73.89	51.72	36.44	48.20	59.97	95.74
Ce	97.88	126.3	140.53	119.3	104.16	119.57	149.74	145.23
Pr	10.74	12.55	16.35	13.05	8.72	12.04	14.68	22.52
Nd	44.14	46.37	65.91	54.79	35.42	50.51	61.32	94.10
Sm	9.95	7.99	13.40	11.90	7.54	11.11	13.24	20.80
Eu	1.39	1.28	1.57	2.22	1.37	1.75	2.30	3.49
Gd	11.06	7.64	14.54	13.91	8.70	12.37	15.72	25.34
Tb	1.76	1.02	2.07	2.12	1.32	1.86	2.34	3.78
Dy	12.07	6.20	13.41	13.98	8.64	12.64	15.67	24.88
Ho	2.46	1.20	2.64	2.85	1.76	2.54	3.11	4.66
Er	7.62	3.47	7.66	8.54	5.32	7.52	9.29	12.96
Tm	1.12	0.49	1.10	1.19	0.74	1.07	1.30	1.74
Yb	7.35	3.20	6.85	7.59	4.86	6.79	8.50	10.80
Lu	1.13	0.48	1.05	1.16	0.72	1.04	1.29	1.60
(Ce/Yb)N	3.39	10.05	5.22	4.04	5.45	4.48	4.48	3.42
Eu/Eu*	0.41	0.50	0.35	0.53	0.52	0.46	0.47	0.51

Where: **SK-305, SK-306,** Creag Strollamus; **SK-307, SK-309, SK-310, SK-312,** Glas Bheinn Mhor; **SK-335, SK-337,** Beinn na Caillich.

Table 6. 2 continued

	SK-313	SK-316	SK-317	SK-318	SK-319	SK-320	SK-321	SK-322
La	70.10	81.27	63.53	63.20	137.64	63.45	40.68	39.21
Ce	131.69	139.82	136.83	153.79	185.93	142.21	85.95	93.13
Pr	17.16	18.92	15.42	16.87	17.93	16.84	10.32	9.64
Nd	71.22	79.21	63.45	71.94	71.67	63.66	43.24	40.76
Sm	14.97	16.92	13.50	15.87	12.22	11.23	8.18	8.63
Eu	2.13	2.48	1.96	2.71	1.97	0.93	3.07	2.71
Gd	16.62	19.03	14.81	18.37	12.31	9.95	8.48	9.57
Tb	2.51	2.77	2.21	2.84	1.57	1.33	1.08	1.38
Dy	16.47	17.90	14.52	19.27	10.18	8.31	6.60	9.08
Ho	3.30	3.51	2.83	3.92	1.93	1.60	1.29	1.70
Er	9.82	10.05	8.14	11.90	5.64	4.59	3.64	4.85
Tm	1.37	1.38	1.13	1.66	0.77	0.65	0.50	0.67
Yb	8.78	8.81	7.05	10.41	5.15	4.34	3.37	4.44
Lu	1.33	1.37	1.04	1.64	0.82	0.69	0.55	0.66
(Ce/Yb)N	3.81	4.04	4.94	3.76	9.17	8.33	6.49	5.34
Eu/Eu*	0.42	0.42	0.43	0.49	0.49	0.27	1.13	0.92

Where: **SK-313, SK-316, SK-316, SK-317,** Loch Ainort; **SK-319,** Maol na Gainmhich; **SK-320,** Northern Porphyritic Felsite; **SK-321,** Eas Mor; **SK-322,** Meall Buidhe.

Table 6. 2 contiued

	SK-333	SK-334	SK-343	SK-315	SK-339	SK-340	SK-329	SK-332
La	73.11	104.35	62.82	80.09	79.36	73.93	97.28	107.17
Ce	153.24	164.60	135.12	132.60	173.70	129.24	188.53	153.87
Pr	16.56	24.03	15.34	18.61	18.90	18.28	21.71	25.67
Nd	66.61	99.02	63.69	78.30	79.40	77.41	87.28	106.75
Sm	12.80	19.35	13.67	15.89	16.03	15.90	16.05	21.37
Eu	1.60	1.90	3.60	3.12	2.78	3.16	1.45	2.17
Gd	14.22	21.18	15.01	17.61	17.61	17.55	16.92	22.77
Tb	2.03	3.01	2.23	2.57	2.46	2.44	2.37	3.19
Dy	13.31	19.79	14.26	16.64	15.56	15.16	15.20	20.34
Ho	2.68	3.89	2.83	3.24	2.97	2.88	2.88	3.91
Er	8.04	11.40	8.60	9.14	8.10	7.83	8.38	11.17
Tm	1.14	1.56	1.21	1.23	1.05	1.05	1.17	1.53
Yb	7.34	10.05	7.75	7.91	6.46	6.38	7.65	9.63
Lu	1.16	1.50	1.21	1.24	0.96	0.97	1.13	1.37
(Ce/Yb)N	5.31	4.17	4.43	4.26	6.84	5.15	6.27	5.39
Eu/Eu*	0.36	0.29	0.77	0.57	0.51	0.58	0.27	0.34

Where: **SK-333, SK-334, SK-343,** Marsco; **SK-315, SK-339, SK-340,** Beinn Dearg Mhor; **SK-329, SK-332,** Southern Porphyritic.

CHAPTER VII

Stable Isotope Geochemistry

7.1 Introduction

Previous isotope studies of Skye granites have mainly been concerned with **either** deciphering their hydrothermal history, by examination of oxygen and hydrogen isotope data (for example, Taylor and Forester, 1971; Forester and Taylor, 1977; Dickin et al., 1980; Ferry, 1985; Elsenheimer and Valley, 1993) to assess the amount of fluid-rock interaction and the mechanisms(s) involved in these subsolidus processes, **or,** have considered aspects of magma genesis by examination of radiogenic isotope data (for example, Dickin, 1981; Dickin et al., 1984).

The apparently contradictory evidence that these studies have provided raises a number of important questions concerning the application of stable and radiogenic isotope data in the investigation of high-level (subvolcanic) intrusions such as the Skye granites (see Chapter II).

In this chapter new oxygen and hydrogen isotope data for whole-rock and mineral separates from the Beinn an Dubhaich, Loch Ainort, Marsco and Glamaig granites are presented (Tables 7.1 and 7.2). In Chapter VIII new radiogenic isotope data (Sr and Nd) are reported **for the same samples.** The aim of producing such a complete isotopic data set is to assess the relative influence of hydrothermal processes (quantified by the stable isotope data)

on the magmatic signatures of the granites (quantified, predominantly, by the radiogenic isotope data).

7. 2 Oxygen isotopes

7. 2. 1 Results

The $\delta^{18}O$ values of whole rock samples and individual minerals and mineral-mineral fractionations for the four granites under investigation are presented in Table 7. 1. The oxygen isotope ratios are expressed in parts per thousand (°/oo) relative to Standard Mean Ocean Water (SMOW) (Craig, 1961), and are reported as a δ value, where $\delta^{18}O$ is calculated as follows:

$$\delta^{18}O\ (°/oo)=\left[\left(^{18}O/^{16}O_{(sample)}-{}^{18}O/^{16}O_{(SMOW)}\right)/{}^{18}O/^{16}O_{(SMOW)}\right] \times 10^3$$

All of the granites analysed here have whole-rock $\delta^{18}O$ values less than that of typical unaltered granites (+6 to +8; +8 to+10 °/oo, values correspond to I- and S-type granites, respectively) (Taylor, 1978). The range of values lies between the relatively undepleted value of +5.5 °/oo for the Beinn an Dubhaich Granite and the considerably depleted value of -1.8 °/oo for the Loch Ainort Granite (Table 7.1). The range of whole-rock values reported by Forester and Taylor (1977) is comparable (cf. Figs. 3 and 4 in their paper).

The $\delta^{18}O$ signatures of the Skye granites are similar to the signatures recorded from granites associated with the Mull and Ardnamurchan Central Complexes (Beckinsale, 1974; Forester and Taylor, 1976) and the Slieve Gullion Central Complex (Gamble et al., 1992), and which were explained in terms of depletion of 'normal' granites by reaction with heated meteoric waters. In contrast, granites belonging to the Mourne Central Complex, Northern Ireland (McCormick et al., 1993) and the North Arran Granite (Dickin et al., 1981; Meighan et al., 1992) preserve near-normal $\delta^{18}O$

signatures, with whole rock values of +6 to +9.5 °/oo and +5.1 to +9.7 °/oo, respectively.

Mineral separates from each of the four granites have been analysed and quartz, alkali feldspar and Fe-Ti oxide have been isolated from all four intrusions. Plagioclase separates were obtained from Beinn an Dubhaich and Glamaig (there is no plagioclase present in Loch Ainort and Marsco, see Chapter III); amphibole separates have been obtained from Beinn an Dubhaich, Loch Ainort and Glamaig, and a pyroxene separate has been obtained from Marsco (see Chapter III).

$\delta^{18}O$ values for quartz are in the range +3.06 °/oo (Loch Ainort) to +7.51 °/oo (Beinn an Dubhaich). Only the Beinn an Dubhaich and Glamaig granites contain quartz with $\delta^{18}O$ typical of 'normal' granites; both Loch Ainort and Marsco have signatures which are significantly lower than 'normal' granites (cf. Taylor, 1978).

$\delta^{18}O$ values for alkali feldspar lie between -1.88 °/oo for Loch Ainort and +4.32 °/oo for Beinn an Dubhaich. The plagioclase from the Beinn an Dubhaich and Glamaig granites have $\delta^{18}O$ of +4.79 °/oo and +0.63 °/oo, respectively. These values are very similar to those of co-existing alkali feldspar (+4.32 °/oo and +0.57 °/oo, respectively).

Amphiboles from Beinn an Dubhaich, Loch Ainort and Glamaig have $\delta^{18}O$ of +4.66 °/oo, -1.1 °/oo and +2.71 °/oo, respectively. The pyroxene separate analysed in this study from the Marsco Granite has $\delta^{18}O$ of +0.70 °/oo. Fe-Ti oxides were analysed from all four granites and their $\delta^{18}O$ values are in the range -2.55 to +1.85 °/oo.

7. 2. 2 Discussion

The susceptibility of coexisting minerals to oxygen isotope exchange with heated meteoric waters is highly variable (O'Neil and Taylor, 1967; Taylor, 1968; Forester and Taylor, 1980; Criss and Taylor, 1986; Jenkin et al., 1994). Open system behaviour of rocks should result in a wide range of $\delta^{18}O$ in coexisting minerals, in contrast to closed system-behaviour where a limited range of oxygen isotope signatures for coexisting minerals in δ-δ space occurs (Gregory and Criss, 1986, but see Jenkin et al., 1991).

As quartz is considered to be a common rock-forming mineral relatively resistant to oxygen isotope exchange (Faure, 1986), its O-isotope composition should be a useful indicator of the $\delta^{18}O$ of the source magma, although late fluid(s) may have modified the oxygen isotopic signature (see Chapter V), the majority of the quartz grains are likely to retain magmatic values. The $\delta^{18}O$ of quartz from the Beinn an Dubhaich and Glamaig granites lies within normal igneous signatures. In contrast, quartz in the Marsco and Loch Ainort granites records $\delta^{18}O$ values lower by about 3 $^{o}/_{oo}$ than the values reported for normal igneous granites.

Since quartz and alkali feldspar data are available for all four granites, it is instructive to examine these data first. Fig. 7.1 illustrates the distribution of these data and, in general, their positive relationship. No simple relationship between position on the plot and degree of compositional evolution is identified.

Similar data are reported by Forester and Taylor (1977). Values of $\Delta_{Q\text{-}Af}$ lie within the range +1.56 to +6.32 $^{o}/_{oo}$. Typical equilibrium values are approximately +1 to +2 $^{o}/_{oo}$ (Forester and Taylor, 1980) and therefore indicate that, apart from Marsco, the granites examined here record considerable disequilibrium, by >+1 $^{o}/_{oo}$, possibly due to open system water-

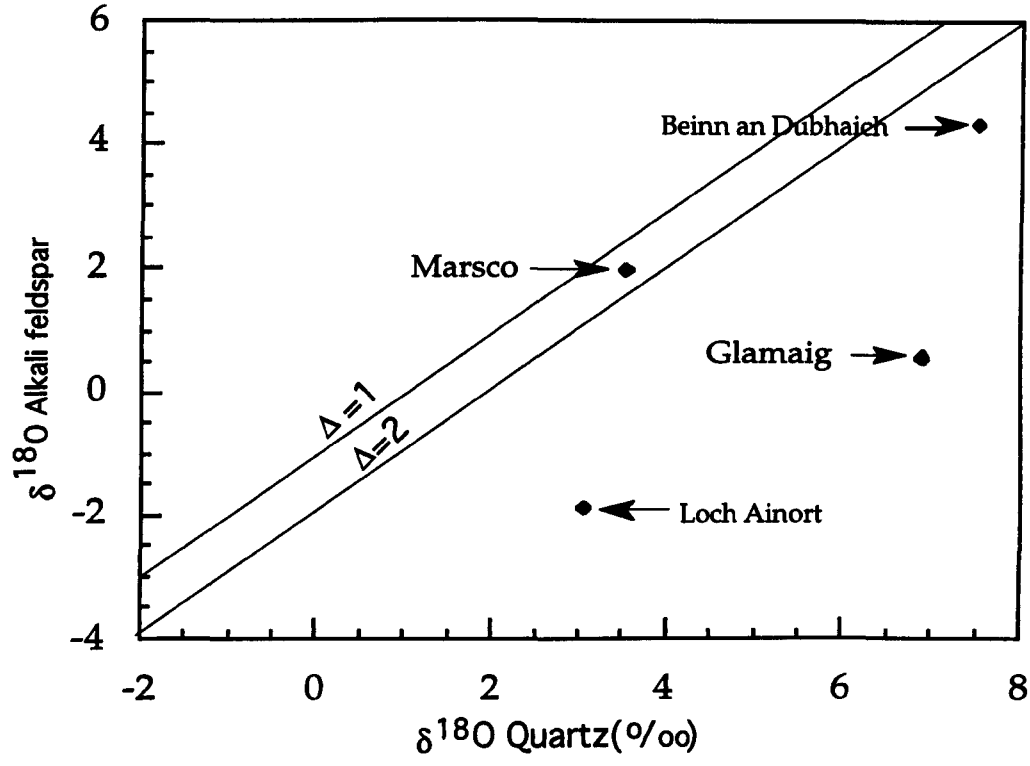

Fig. 7. 1 Plot of $\delta^{18}O_{quartz}$ against $\delta^{18}O_{alkali\ feldspar}$ for Skye granites. Diagonal lines show the location of alkali feldspar and quartz pairs in equilibrium conditions at about 400 and 500°C (Clayton et al., 1989).

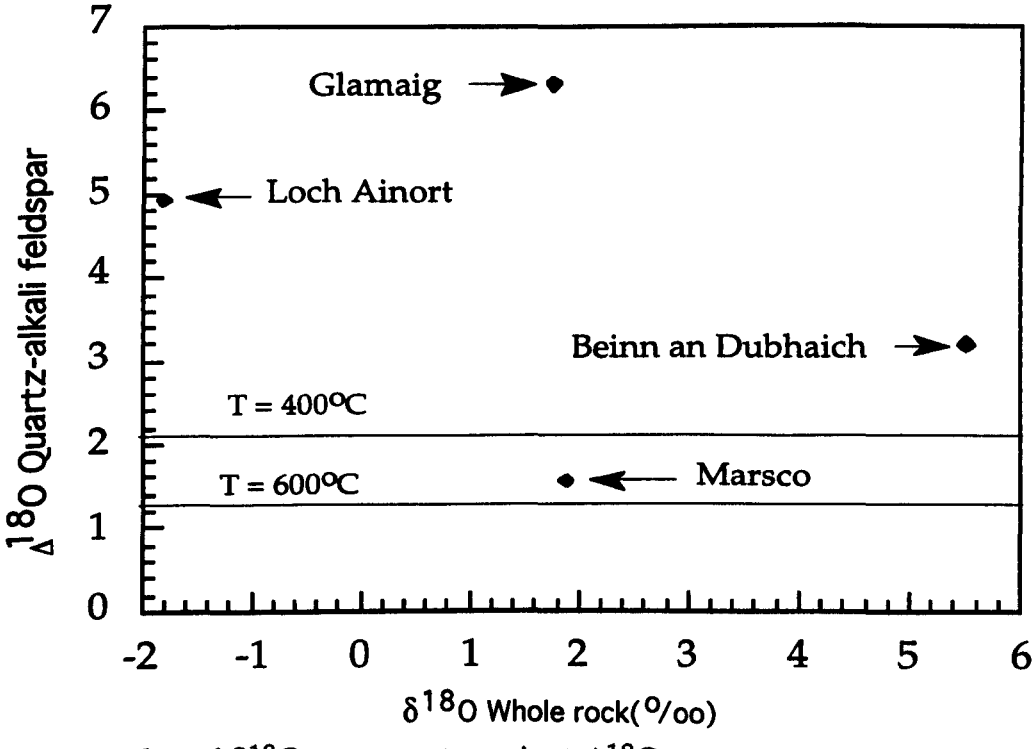

Fig.7. 2 Plot of $\delta^{18}O_{\text{whole rock}}$ against $\Delta^{18}O_{\text{quartz-alkali feldspar}}$. Horizontal lines exhibit equilibrium oxygen isotope fractionation at 400 and 600°C (Clayton et al., 1989).

rock reaction. These disequilibrium quartz-alkali feldspar O-isotope fractionations are independent of the $\delta^{18}O$ value of whole rocks (Fig. 7. 2), suggesting that these granites either have been affected by different batches of water with different O-isotope signatures (cf. McCormick et al., 1993), or, crystallised from different protoliths with different O-isotope signatures.

However, considering the three Western Redhills granites (Glamaig, Loch Ainort and Marsco), there is a correlation between the order of emplacement and the value of $\Delta_{Q\text{-}Af}$, with: Glamaig (emplaced first, with 6.32), then Loch Ainort (with 4.94), then Marsco (with 1.56). This might be interpreted in terms of the reacting meteoric water becoming less depleted in ^{18}O, with time. Alternatively, different, discrete batches of meteoric water may have interacted with each of these intrusions. The Beinn an Dubhaich Granite from the younger Eastern Redhills Centre has a value of 3.19 and was, uniquely, emplaced into Cambro-Ordovician dolostones.

$\Delta_{Q\text{-}Plag}$ values are +2.72 and +6.26 for the Beinn an Dubhaich and Glamaig granites, respectively, and are very similar to their counterpart $\Delta_{Q\text{-}Af}$ values (i.e. +3.19 and +6.32 for Beinn an Dubhaich and Glamaig, respectively), and they record a near-equilibrium value for the Beinn an Dubhaich Granite and a far from equilibrium value for the Glamaig Granite. The similar $\delta^{18}O$ values for alkali feldspar and plagioclase in each granite are possibly due to a closed-system process (i.e., no fluid infiltrated into these granites after their crystallisation) (Jenkin et al., 1991), based on the assumption that both oxygen isotope fractionation and rate of oxygen diffusion in alkali feldspar and plagioclase are effectively identical (see Giletti et al., 1978; Richter and Hoernes, 1988; Jenkin et al., 1991). However, the turbidity of both feldspars (Chapter III), the fluid inclusion studies (Chapter V), and the difference in Sr isotopic signatures of both residue and leachate feldspars (Chapter VIII), suggest that the observed $\delta^{18}O$ values for alkali feldspar and plagioclase

have also been influenced by hydrothermal processes. Similarly, the non-magmatic quartz-feldspar fractionations for Glamaig argue against the closed-system model.

The $\delta^{18}O$ of igneous amphiboles is considered to lie in the range + 6 to + 8 °/oo (Jenkin, 1988, p.181); thus, $\Delta_{Q\text{-}Amph}$ fractionations should be in the range 0 to 2 °/oo. Three of the granites in this study contain amphibole, with $\delta^{18}O$ values in the range -1.1 to +4.66 °/oo. Consequently, the range of $\Delta_{Q\text{-}Amph}$ values is +2.85 to +4.18 °/oo. Only the Beinn an Dubhaich Granite records a $\Delta_{Q\text{-}Amph}$ value (of 2.85 °/oo) close to the equilibrium range (Table 7.1). The Marsco Granite contains pyroxene with a $\Delta_{Q\text{-}Px}$ value of +4.23 °/oo, well outside the range for isotopic equilibrium and close to the $\Delta_{Q\text{-}Amph}$ values for the Glamaig and Loch Ainort granites. Based on the amphibole and pyroxene data it is clear that the Beinn an Dubhaich Granite has suffered considerably less ^{18}O exchange than the other three granites and has maintained a mineralogy which is in isotopic equilibrium (see Holness and Fallick, 1994).

The values of $\Delta_{Q\text{-}Ox}$ are relatively uniform, in the range +5.04 to +6.57 °/oo. Equilibrium $\Delta_{Q\text{-}Ox}$ values should lie within the range 0 to +3 °/oo (Forester and Taylor, 1980). The granite which records the largest apparent degree of disequilibrium is Beinn an Dubhaich, with a $\Delta_{Q\text{-}Ox}$ value of +6.57 °/oo. These unexpected data are possibly due to the dominance of ilmenite over magnetite in the Beinn an Dubhaich Granite (see Ferry, 1985, Table 1), which strongly influences equilibrium $\delta^{18}O$ Fe-Ti oxide values (Taylor and Forester, 1979, p 397, but see also Chiba et al., 1989).

McCormick et al. (1993) note that in samples from the Mourne Central Complex, which have whole-rock signatures at the lower end of the spectrum (i.e. +6 °/oo), the individual minerals are not in isotopic

equilibrium, whereas the samples with the 'normal' signatures preserve minerals which are in isotopic equilibrium.

It is clear, therefore, that all of the whole rock and minerals separates analysed here show some degree of depletion in ^{18}O relative to 'normal' igneous rocks as defined by Taylor (1968, 1978). Based on a detailed study of the Skye granites, Forester and Taylor (1977) attribute such low ^{18}O values to the crystallisation of the granites from low $\delta^{18}O$ magmas and further ^{18}O-depletion by subsolidus exchange with meteoric water.

Guthrie and Veblen (1991) present evidence from a study of fluid inclusion distributions in alkali feldspars in the Skye granites that late-stage magmatic fluids may also have been involved in the Beinn an Dubhaich Granite which, uniquely, records a near-normal $\delta^{18}O$ whole-rock signature.

Many factors may contribute to the extent of ^{18}O depletion in a given suite of igneous rocks, but the two most important are: the ^{18}O signature of the magma protolith; and, the degree to which any water-rock interaction takes place and the type of water involved (meteoric or sea water) and the temperature at which they interact.

Water/rock (w/r) ratios are calculated from the equations of Taylor (1974, 1977) as follows:

$$W/R=[\delta^{18}O_{final(rock)}-\delta^{18}O_{initial(rock)}] / [\delta^{18}O_{initial(water)}-\delta^{18}O_{final(water)}]$$

and are presented in Table 7.3.

Fluid inclusion data (Chapter V) confirm the interaction between heated meteoric waters and Skye granites at temperatures of about 350-450 ^{o}C, which is consistent with previous studies (for example, Taylor and Forester, 1971; Forester and Taylor, 1977).

The primary $\delta^{18}O$ value of most granitic rocks has been estimated by Taylor (1978) to lie in the range +6 to +10 °/oo. These values correspond approximately to values for normal granites derived from mantle and crustal sources, respectively (Pankhurst et al., 1978; White and Chappell, 1988; Clarke, 1993). The value of +8 °/oo (average) was adopted in the following water/rock (w/r) ratio calculations and assumes a mixed source. The composition of meteoric water present during the Palaeocene and therefore involved in the Skye Igneous Centre is assumed to be $\delta^{18}O_{water}$ = -12 ‰ (Forester and Taylor, 1977).

Since alkali feldspar is a dominant mineral in granites and is the most susceptible mineral to O-isotope exchange (Taylor and Forester, 1979; Ferry, 1985), the water rock fractionation(Δ) assumed by O'Neil and Taylor (1967) for plagioclase (An_{30}), (see Appendix II) was used to calculate the $\delta^{18}O$ composition of the final (reacted) water. The resultant calculations for both closed and open systems are presented in Table 7. 3. The calculated w/r ratios for the granites investigated here range from 0.19-1.46 and 0.27-1.15 at 350°C and 450°C, respectively, during closed system exchange. Thus, the highest w/r ratios were observed in the Loch Ainort and Glamaig granites, whereas the lowest w/r ratios are recorded from the Beinn an Dubhaich and Marsco granites. Taylor (1978) reports a similar w/r ratio for the Beinn an Dubhaich Granite, and attributed its low value to the emplacement of this granite into relatively impermeable limestones.

Despite the small range of w/r ratios between the Loch Ainort, Glamaig and Marsco granites, both Loch Ainort and Marsco show lower $\delta^{18}O_{quartz}$ by about 2.5 °/oo than Glamaig, which contains a $\delta^{18}O_{quartz}$ value close to normal values of granite quartz (Forester and Taylor, 1977). These data suggest that subsolidus exchange with meteoric water at about 400 °C (Elsenheimer and Valley, 1993; and this study), may not be the only factor

responsible for the observed $\delta^{18}O$ depletion in quartz, and that crystallisation of the Skye granites from low-$\delta^{18}O$ magma(s), as suggested by Forester and Taylor (1977), may be involved.

7. 3 Hydrogen isotopes

7. 3. 1 Results

Limited hydrogen isotope analyses have been carried out on amphiboles and fluid inclusions in quartz, from Beinn an Dubhaich, Loch Ainort and Glamaig, and fluid inclusions only from the Marsco Granite. The hydrogen isotope ratios for fluid inclusions in quartz were measured directly on the water released by decrepitation of the inclusions. The oxygen isotope ratios for the fluids were calculated from the O-isotope composition of the quartz, according to oxygen isotopic fractionation in the quartz-water system as proposed by Matsuhisa et al. (1979), and utilizing a subsolidus exchange temperature of 400°C (see oxygen isotope section, and Chapter V).

Similar to the oxygen isotope data, hydrogen isotope ratios are measured in parts per thousand ($^{o}/_{oo}$) relative to SMOW and are calculated in a similar way to oxygen isotope values and reported as δD ‰, as calculated from the following equation:

$$\delta D = \left[\left((D/H)_{sample}-(D/H)_{SMOW}\right)/(D/H)_{SMOW}\right] \times 10^3$$

The measured δD values of water 'associated with' the Skye granites lie between -51 $^{o}/_{oo}$ (Marsco) to -111‰ (Glamaig); Beinn an Dubhaich and Loch Ainort have δD values of -86 ‰ and -90.5 ‰, respectively. The three amphibole samples from the Beinn an Dubhaich, Loch Ainort and Glamaig granites yield δD values of -130 ‰, -145 ‰ and -138 ‰, respectively.

The measured hydrogen and calculated oxygen isotope compositions of water from Skye granites are presented in Table 7. 2.

7. 3. 2 Discussion

Fig. 7.3 illustrates the isotopic composition of water 'associated with' the Skye granites, and the compositions of natural waters as proposed by several authors (for example, Forester and Taylor, 1977; Taylor, 1974, 1979; Sheppard, 1986; Rollinson, 1993).

The fluid compositions determined in this study all show normal or slightly depleted δD values, relative to the estimated composition of the meteoric/hydrothermal waters (-85 $^{o}/_{oo}$) circulating within the Skye Igneous Centre during the Palaeocene (Forester and Taylor, 1977; Taylor, 1978), except for the Marsco Granite, which records a fluid considerably enriched in D (δDwater = -51 $^{o}/_{oo}$). Significantly, the Marsco Granite does not contain any hydroxyl-bearing minerals (see Chapter III). Based upon its position in Fig 7.3, the origin of the fluid involved in the Marsco Granite may have been: (i) a D-enriched fluid, such as reported for metamorphic fluids; or, (ii) a meteoric water which has attained a high δD signature by extensive reaction with lithologies which have high δD values (for example, metamorphic rocks, cf. Valley, 1986).

The δD signatures for the fluids from the Loch Ainort and Beinn an Dubhaich granites can be interpreted as the product of mixing between meteoric water and a magmatic fluid or a meteoric water which has exchanged with igneous rocks (cf. Taylor and Sheppard, 1986). The fluid from the Glamaig Granite has the most depleted signature, with δD = -111 $^{o}/_{oo}$, approximately 20-30 $^{o}/_{oo}$ less than the composition of meteoric water (-85 $^{o}/_{oo}$) circulating within the Skye Igneous Centre during the Palaeocene

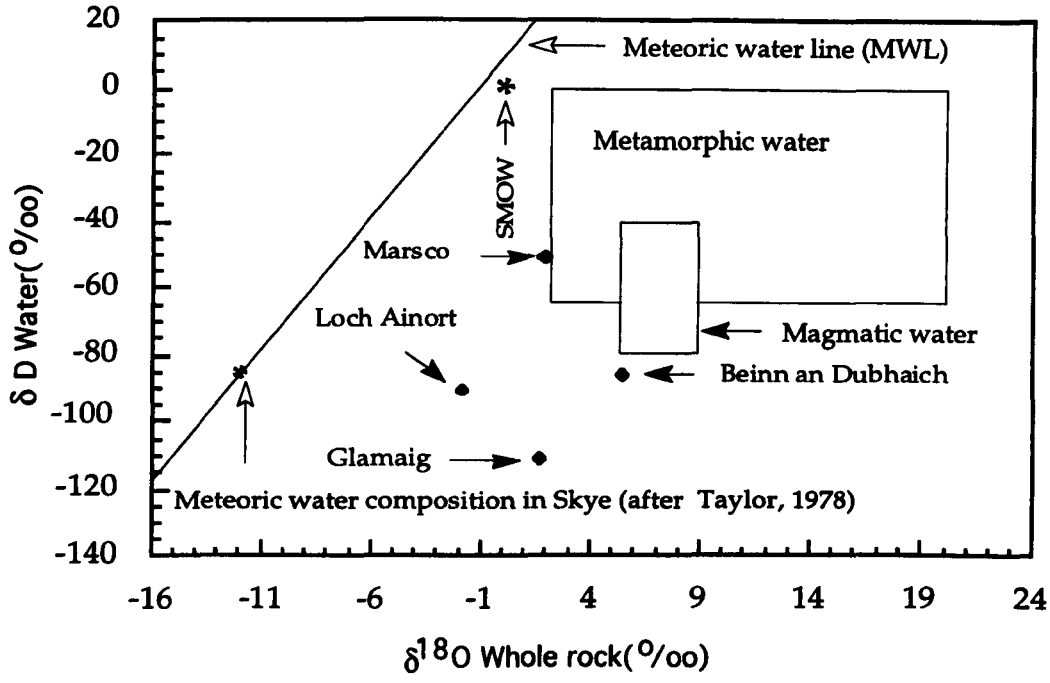

Fig.7. 3 Plot of $\delta^{18}O$ whole rock against δD_{water} for Skye granites. The fields of natural waters are also shown (Forester and Taylor, 1977; Taylor, 1974, 1979; Sheppard, 1986; Rollinson, 1993).

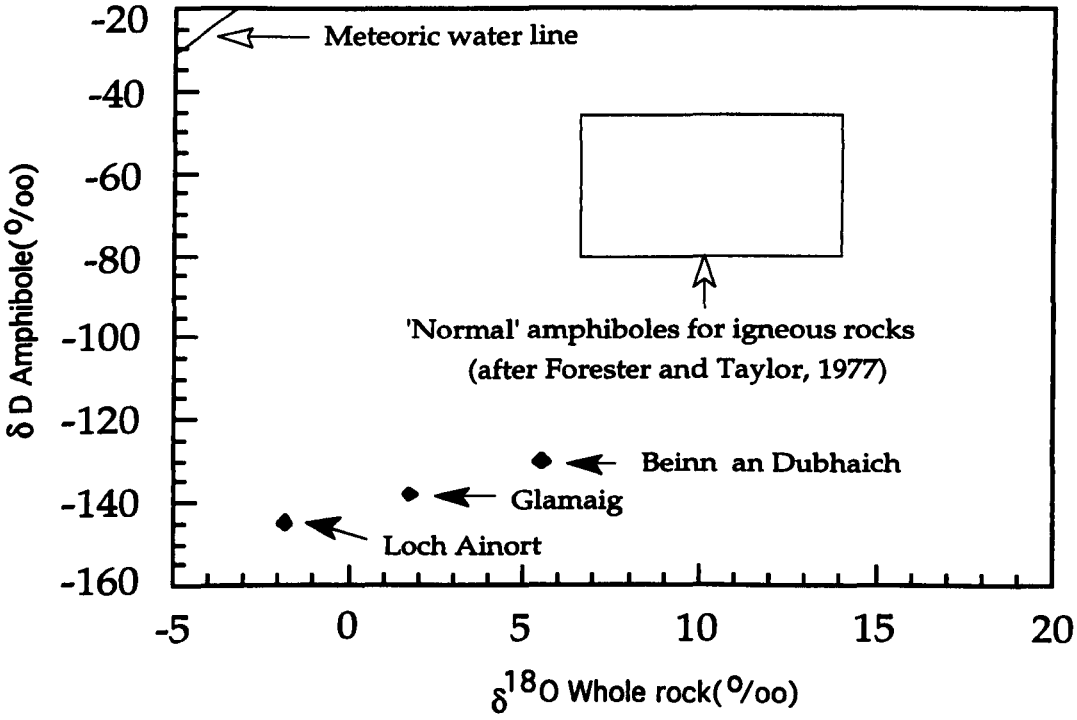

Fig.7.4 Plot of $\delta^{18}O$ whole rock against δD_{amph} for Skye granites. The field of igneous amphibole (see Jenkin, 1988, p. 181) is also shown, as is the meteoric water line (Craig, 1961).

(Forester and Taylor, 1977; Taylor, 1978). One possible explanation for this is that the low D signature is the result of a meteoric water interacting with previously-altered lithologies which had already achieved relatively D-depleted signatures. (Taylor, 1977, 1978; Taylor and Sheppard, 1986).

The calculated $\delta^{18}O$ compositions of the fluids (water) associated with the granites are presented in Table 7.2 and range between -1 $^{o}/_{oo}$ (Loch Ainort) to +3.44 $^{o}/_{oo}$ (Beinn an Dubhaich). All of these values lie between the composition of meteoric water in the Palaeocene at Skye (see Fig. 7.3) and values typical of igneous rocks. Therefore, these data can be explained, as before, either in terms of the mixing of a meteoric water with a magmatic fluid, or, by a positive "^{18}O shift" (Craig, 1961; Taylor, 1978) due to a meteoric water having partially equilibrated with ^{18}O-rich lithologies typical of the Skye Igneous Centre and its surrounding country-rocks (mainly Palaeocene lavas).

The δD signatures of the amphiboles in the Beinn an Dubhaich, Loch Ainort and Glamaig granites (-130 to -145 $^{o}/_{oo}$) are all depleted relative to the δD values of igneous amphiboles (Fig. 7.4) (-102 to -109 $^{o}/_{oo}$; Forester and Taylor, 1977; Taylor, 1977; Taylor and Sheppard, 1986). The δD values of the Skye amphiboles decrease with increasing w/r ratio, as set out in Table 7.3, with the lowest δD signature in the Loch Ainort amphibole corresponding to a w/r ratio of 1.46, and the highest δD value (Beinn an Dubhaich amphibole) corresponding to a w/r ratio of 0.19.

Fig. 7.4 is a plot of $\delta^{18}O_{whole\ rock}$ against δD_{amph} and illustrates that a positive correlation exists between these two parameters, i.e. the most ^{18}O-depleted rock contains amphiboles with the most depleted δD signature. As noted above, the most ^{18}O-depleted rock has the highest w/r ratio, thus, the δD signature of these amphiboles must be controlled to some extent by w/r

ratios. As the amount of hydrogen in a rock is very small compared to its oxygen content (for example, Forester and Taylor, 1977; Criss and Taylor, 1986), then the 'hydrogen sensitivity' can be used to show that even at low w/r ratios the δD value of a rock can be drastically lowered (Taylor, 1978).

The slope of the positive correlation in Fig. 7.4, however, has a very shallow gradient and does not intersect the field of 'normal' amphiboles for igneous rocks and suggests that the original amphiboles in the Skye granites were relatively depleted in D.

The δD value for rocks of granitic composition is estimated to lie within the range -50 to -85 °/oo (Nabalek et al., 1983; Taylor and Sheppard, 1986) and any values lower than this range are considered to be the result of interaction with meteoric water (Criss and Taylor, 1986). As noted already, the Beinn an Dubhaich Granite has interacted with a relatively high δD fluid (-86 °/oo) when compared to the water(s) which have 'associated with' the Loch Ainort Granite (-90.5 °/oo) and the Glamaig Granite (-111 °/oo).

Fig. 7.5 illustrates the relation between the hydrogen isotope compositions and water contents of Skye granite amphiboles. The exsolution or degassing of a vapour phase from a crystallising magma will progressively deplete the magma in both water and deuterium (Taylor et al., 1983; Nabelek et al. 1983). The observed scatter in Fig. 7.5 suggests that degassing (i.e. exsolution of a vapour phase) processes are not responsible for the δD variations within the Skye granites (O'Neil et al., 1977; O'Neil and Chappell, 1977; Nabelek et al., 1983; McCormick et al. 1993).

As noted in Section 7. 2. 2, based on the depleted signatures of the quartz, both the Loch Ainort and Marsco granites most likely crystallised from magmas depleted in ^{18}O. In addition, the Loch Ainort Granite interacted with a low-deuterium (meteoric) water, thus, the involvement of this water

is an important factor in controlling the δD value in this granite (cf. Taylor, 1978, 1979). In contrast, the Glamaig Granite magma has a 'normal' O-isotope signature (based upon $\delta^{18}O_{quartz}$ = +6.89°/oo), but a low δD_{amph} (-138°/oo) signature, accompanied by a high water content in its amphibole. Thus, the low δD_{amph} value in Glamaig can be attributed partially to interaction with a D-depleted fluid, and also its partial chloritisation (see Chapter III) (cf. Sheppard and Taylor, 1974; Clauer et al., 1982), since chloritisation increases the water content of the sample (Nabelek et al., 1983).

Utilizing the measured δD values of amphibole in each intrusion with a subsolidus exchange temperature of 400°C (based upon fluid homogenisation temperatures, see Chapter 5), together with the D/H (amph-water) fractionation factor-temperature equation of Suzuoki and Epstein (1976), the hydrogen isotope composition of the water 'associated with' each granite has been calculated. These data show the following δD values: -85 °/oo for Beinn an Dubhaich; -100 °/oo for Loch Ainort; -94 °/oo for Glamaig.

Whereas the water involved in the Beinn an Dubhaich Granite exhibits limited mixing between magmatic and meteoric waters, the data for the other two intrusions suggest the involvement of meteoric water only. In the case of the Loch Ainort Granite, the high w/r ratio and the possible involvement of a low-D protolith may be factors responsible for the very low δD value of the Loch Ainort amphibole. Finally, for the Glamaig Granite, interaction with meteoric water and chloritisation are the most reasonable explanations for the δD_{amph} value.

With the exception of Marsco, the mean quartz fluid inclusion and amphibole δD values are relatively consistent at -96 ± 13 °/oo and -138 ± 8 °/oo, respectively. The average amphibole-water hydrogen isotope

fractionation ($\Delta^{D}_{amph-water}$) is thus -42 ± 14 °/oo, which is just consistent with the value suggested by Suzuoki and Epstein (1976) for hornblende at 400°C. $\Delta^{D}_{amph-water}$. It is inferred, therefore, that the aqueous fluid associated with all three granites had δD around -95 ± 15 °/oo. This is a somewhat surprising inference given the conventional picture of limited influence of meteoric (and so low δD) water for Beinn an Dubhaich.

Additionally, the single Marsco fluid inclusion δD value of -51°/oo tentatively suggests that the magmatic fluid associated with this system was **not** D-depleted; clearly, further work is required to substantiate this observation, for the combination of a low $\delta^{18}O$ but normal (in the sence of Taylor and Sheppard, 1986) δD composition would be highly intriguing.

Suzuoki and Epstein (1976) have shown that the chemical (i.e. non isotopic) composition of hydrous minerals also affects the δD values of amphiboles, i.e. the equilibrium distribution of D between amphibole and water increases with decreasing Fe/Mg ratio in the amphibole. Fig. 7. 6 shows that there is no simple relationship between hydrogen isotope composition and Fe/Mg ratio for Skye granite amphiboles, and that the δD_{amph} signatures have been reset by interaction with heated meteoric waters (cf. Graham et al., 1984). Kuroda et al. (1986) attribute such scattered relations to the difference in geological conditions of crystallisation (i.e. magma water content and H-isotope composition of circulating waters).

7. 4 Significance of $\delta^{18}O$ and δD variations

The data presented here for the Skye granites (see also: Forester and Taylor, 1977: Taylor, 1977, 1978; Taylor and Sheppard, 1986) make it abundantly clear that meteoric hydrothermal fluids, together with crystallisation from ^{18}O

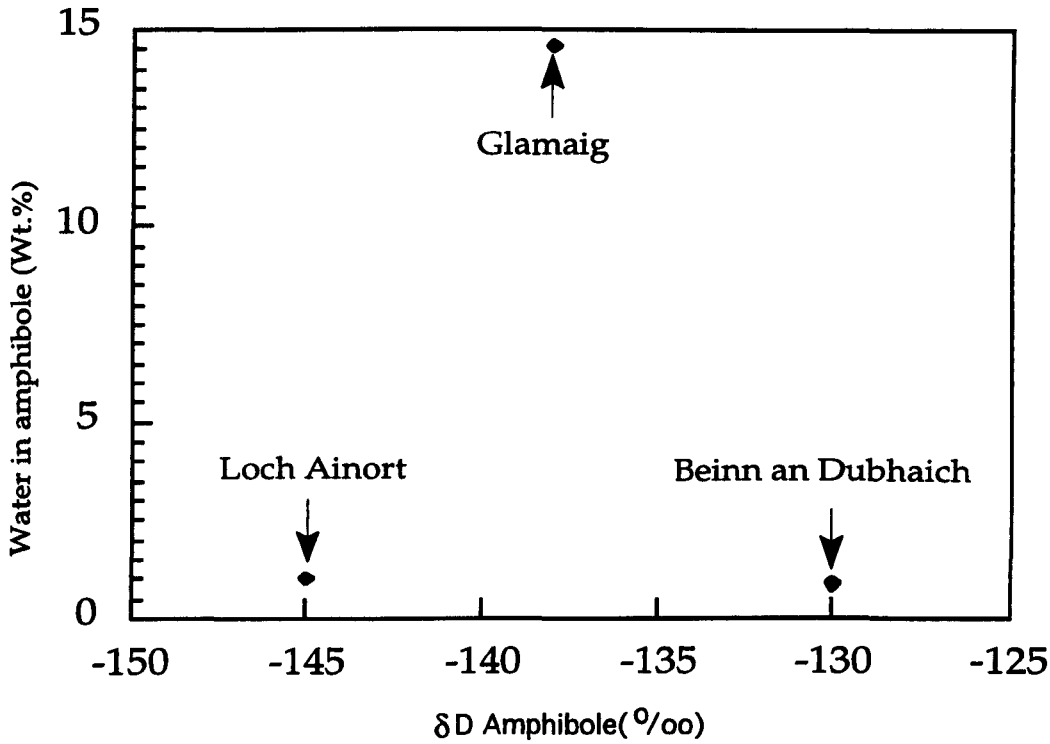

Fig. 7.5 Plot of δDamph against H_2O^+ for amphiboles. The lack of correlation means that processes other than outgassing are responsible for the observed low D-isotope signature of amphiboles from the Skye granites.

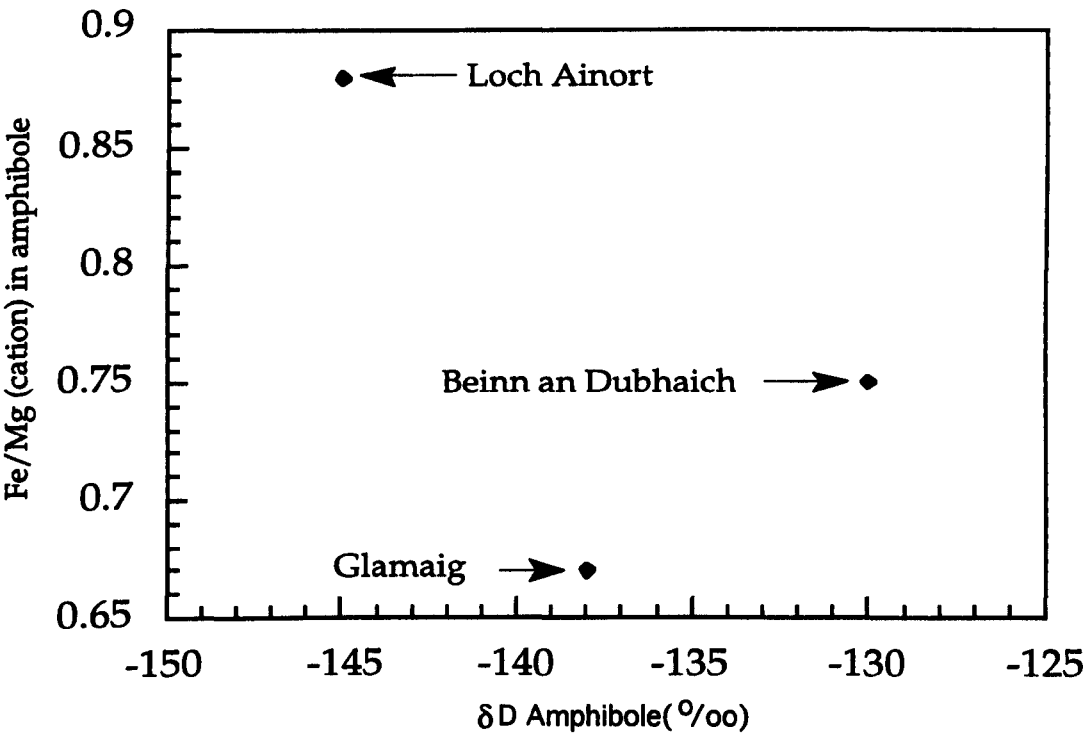

Fig. 7.6 Plot of Fe/Mg (cation) ratio against δD for Skye granite amphiboles. The absence of any correlation means that the D-isotope signature of these amphiboles is not controlled by their chemical compositions.

(and possibly D) -depleted magmas, are the dominant geological processes responsible for the stable isotope signatures.

Forester and Taylor (1977) argue that, based on the accepted order of emplacement, and considering $\delta^{18}O$ quartz values, that the granites on Skye preserve a complex history of magmas with variable amounts of ^{18}O depletion which they link to a variety of igneous and tectonic processes. The cause of the ^{18}O depletion is attributed to the influx of meteoric water into the granite magma bodies via hydrothermal fracture systems. Subsequently, Taylor and Forester (1979) discuss the hydrodynamic problems associated with a meteroric water gaining access to a body of magma and indicate that a ^{18}O depleted signature need not necessarily involve a direct meteoric water input.

The difficulty of direct influx of low-^{18}O meteoric waters into magma chambers, together with the large quantities of water required to reduce the $\delta^{18}O$ of such magma bodies, argues against this model being the dominant process involved in the ^{18}O mineral signatures now preserved. However, the ^{18}O-depleted signature of the quartz from the Marsco Granite, together with its equilibrium value of ΔQ-Af, suggests that, either, ^{18}O-depleted magmas were formed on a small scale, or, that meteoric water reacted with the quartz and alkali feldspar at temperatures just below the granite solidus and resulted in the equilibrium fractionation now preserved.

Another possible process involved in the formation of the Skye granites, which can have an important effect on the oxygen isotopic signature, is the incorporation of partial melts from low-^{18}O hydrothermally-altered country-rocks, i.e. the involvement of crustal materials in the magmatic processes that formed the Skye granites (cf. Moorbath and Bell, 1965; Moorbath and Welke, 1969; Dickin, 1981; Dickin et al., 1984).

Partial melting of such country-rocks will have required that a significant amount of heat was available. Geophysical evidence (Brown and Mussett, 1976) suggests that a large and possibly contemporaneous basaltic magma chamber developed below the Redhills granites and would have supplied sufficient heat for the partial melting process (see also Bell, 1966). Heat will also be liberated during the crystallisation of the granite bodies themselves, however, this requires assimilation (and so heat releases) before crystallisation. In addition, dehydration of the hydrothermally-altered country-rocks by the granitic magmas, may also be considered as a mechanism involved to produce the ^{18}O-depleted signature of these granites (cf. Taylor and Sheppard, 1986).

Thus, the most primitive granite (Glamaig) crystallised with an almost normal O-isotope composition and, with time, the magmas isotopically exchanged with hydrothermally-altered country-rocks and this resulted in low-^{18}O magmas (Loch Ainort and Marsco). Beinn an Dubhaich is the only granite on Skye emplaced entirely into carbonate country-rocks (Harker, 1904) and so it has been argued (Forester and Taylor, 1977) was less affected by hydrothermally-altered country-rocks (see also Holness and Fallick, 1994). As far as degree of fractionation is concerned, the Beinn an Dubhaich Granite is one of the more evolved intrusions (with modal biotite, see Chapter III), and thus its $\delta^{18}O$ enrichment is consistent with the more evolved nature of this intrusion (O'Neil and Taylor, 1967; O'Neil et al., 1977).

Consideration of the temperature of equilibration under subsolidus conditions (400°C, see Chapter V) the measured δD values for amphiboles and meteoric waters from the Skye granites suggest that the D-depleted signature of the magmas are due to either: addition of meteoric water by partial melts or by incorporation of hydrothermally-altered country-rocks

resulting in lowering δD values of the magma by 30 to 50 ‰ than that of the meteoric water (see Taylor, 1978). These depleted signatures are due to the fact that in the temperature range 200-500°C water strongly concentrates D relative to OH-bearing minerals (Taylor, 1977, 1978; Taylor and Sheppard, 1986).

Thus, the δD values of the Skye amphiboles may not represent magmatic values, and consequently the magmas may have had higher δD signatures than the δD values recorded from their amphiboles. This result is quite logical for the Glamaig and Beinn an Dubhaich granites which have almost normal O-isotope quartz compositions. However, the Loch Ainort Granite, crystallised from an ^{18}O-depleted magma possibly due to the access of meteoric fluid into the magma with high w/r ratio at higher temperature (high than temperature of hydrothermal event) since this granite had crystallised at high temperature (see Chapter VIII), or due to their isotopic exchange with hydrothermally-altered country-rocks (see above), either process may will depleted D-isotope signature of its amphibole.

7. 5 Summary and conclusions

(i) The hydrogen and oxygen isotope compositions of the water(s) circulating in the Skye granites indicate they were predominantly of meteoric origin, although limited mixing with a magmatic water is also possible.

(ii) The composition of the fluids which interacted with the Skye granites was: a δD value in the range -85 to -111 $^{o}/_{oo}$ and a $\delta^{18}O$ value in the range -1.00 to +3.44$^{o}/_{oo}$. When compared with the recorded composition of Palaeocene meteoric water (-85$^{o}/_{oo}$ and -12$^{o}/_{oo}$, Forester and Taylor 1977;

Taylor 1978, 1979), this argues strongly for a mixed origin for the measured waters.

(iii) The interaction between this mixed water and each intrusion, individually affected by the w/r ratio and the composition of the country-rock lithologies which the water had reacted with, has led to the highest w/r ratio for the Loch Ainort Granite and the lowest w/r ratio for the Beinn an Dubhaich Granite.

(iv) The proposed country-rocks should be similar in their $\delta^{18}O$ and δD compositions for all of the intrusions, except for the Marsco Granite which may have involved country-rock with a higher δD value. However, we cannot rule out the possibility of limited mixing between meteoric water and metamorphic water in the case of the Marsco Granite fluid.

(v) The ^{18}O-depleted signature of the quartz from the Marsco Granite, together with its equilibrium value of $\Delta Q\text{-}Af$, suggests that either, ^{18}O-depleted magmas were formed on a small scale, or, that meteoric water reacted with the quartz and alkali feldspar at temperatures just below the granite solidus and resulted in the equilibrium fractionation now preserved.

(vi) The ^{18}O-depleted signature of the quartz from the Loch Ainort and Marsco granites, suggests that these granites may have formed from ^{18}O-depleted protolith(s).

(vii) Although the hydrogen isotope signature for Skye amphiboles may have been attributed to the low-D protolith(s), interaction with meteoric water significantly influenced their δD values.

(viii) Interaction with meteoric hydrothermal fluids, together with crystallisation from ^{18}O (and possibly D) -depleted magmas, are the

dominant geological processes responsible for the stable isotope signatures of Skye granites.

However, the observed similarity of the calculated fluid δD for Beinn an Dubhaich, Loch Ainort and Glamaig from measured amphibole values and measured fluid inclusion δD values, but the single different value for Marsco, make further hydrogen isotope studies a high priority for further work.

Table 7. 1 Oxygen isotope data for whole rock and mineral separates, along with mineral-mineral fractionations.

	Beinn an Dubhaich	Loch Ainort	Glamaig	Marsco
$\delta^{18}O$ Whole rock	5.66 5.35 (5.51*)	-1.50 -2.11 (-1.81*)	1.53 1.95 (1.74*)	1.93 1.81 (1.88*)
$\delta^{18}O$ (Q) Quartz	7.52 7.50 (7.51*)	3.06	7.01 6.76 (6.89*)	3.44 3.61 (3.53*)
$\delta^{18}O$ (Af) Alkali feldspar	4.14 4.49 (4.32*)	-1.88	0.57	1.98 1.96 (1.97*)
$\delta^{18}O$ (Plag) Plagioclase	4.58 5.00 (4.79*)	——	0.69 0.57 (0.63*)	——
$\delta^{18}O$ (Amph) Amphibole	4.62 4.70 (4.66*)	-1.1	2.81 2.61 (2.71*)	——
$\delta^{18}O$ (Px) Pyroxene	——	——	——	-0.80 -0.60 (-0.70*)
$\delta^{18}O$ (Ox) Fe-Ti oxide	.94	-2.57 -2.53 (-2.55*)	1.85	-1.87
$\Delta^{18}O$ (Q-Af.)	3.19	4.94	6.26	1.56
$\Delta^{18}O$ (Q-Plag.)	2.72	----------	6.32	----------
$\Delta^{18}O$ (Q-Amph.)	2.85	4.16	4.18	——
$\Delta^{18}O$ (Q-Px.)	——	——	——	4.23
$\Delta^{18}O$ (Q-Ox)	6.57	5.61	5.04	5.40

(*) Mean of duplicate analyses.

Table 7. 2 Hydrogen isotope data for water and amphiboles

sample name	Beinn an Dubhaich	Loch Ainort	Glamaig	Marsco
$\delta D(w)$ °/oo	-86	-90.5	-111	-51
$\delta^{18}O(q)$ °/oo	7.52	3.06	7.01	3.44
	7.50 (7.51*)		6.76 (6.89*)	3.60 (3.5*)
$\delta^{18}O(w)$ °/oo	3.44	-1.00	2.83	-.56
δD(amph.) °/oo	-130	-145	-138	------
(Fe/Mg)amph.	.75	.88	.67	------
H_2O+(wt.% amph)	.86	1.01	14.58	-------

(*) Mean of duplicate analyses.

Table 7. 3 Water /rock (interaction) data in closed and open systems of studying samples where BD, Beinn an Dubhaich; LA, Loch Ainort; GL, Glamaig and MA, Marsco granites.

Sample	$\delta^{18}O$	$\delta^{18}O(w)$final		W/R(closed)		W/R(open)	
name	Af	350ºC	450ºC	350ºC	450ºC	350ºC	450ºC
SK-300 (BD)	4.32	.93	2.71	.19	.27	.17	.24
SK-313 (LA)	-1.88	-5.27	-3.49	1.46	1.15	.90	.77
SK-326 (GL)	.57	-2.82	-1.04	.68	.57	.52	.45
SK-334 (MA)	1.97	-1.42	0.36	.58	.50	.46	.41

CHAPTER VIII

Radiogenic Isotope Geochemistry

8.1 Introduction

In this chapter the genesis and evolution of the Skye granite magmas will be examined in terms of their radiogenic isotope geochemistry.

New Sr and Nd isotopic data for whole rocks and individual minerals from the Beinn an Dubhaich, Loch Ainort, Marsco and Glamaig granites are presented in Tables 8. 1 and 8. 2. Previously published Sr and Nd data for Skye granites and possible protoliths are also discussed (for example, Carter et al., 1978; Moorbath and Thompson, 1980; Dickin, 1981; Dickin and Jones, 1983; Dickin, et al., 1987). Refractory accessory phases are also examined, in order to identify any crustal components involved in the evolution of the Skye granites.

The following discussion is mainly concerned with assessing the petrogenesis of the granites: are they derived by differentiation of basaltic magma, the products of crustal of crustal melting, or a combination of these two processes. However, the Skye granites are severely disturbed by

hydrothermal meteoric water (see Chapters, III, V and VII); in order to minimise the effects of such alteration processes on Sr isotopic data, feldspars were strongly leached to remove any hydrothermal Sr. The effects of these hydrothermal alteration processes, together with crustal contamination and source heterogeneity, are examined in the following discussion. Analytical techniques are presented in Appendix III.

8. 2 Rb-Sr isotopes

8. 2 . 1 Results

To investigate possible hypotheses for the origin of Skye granites, it is necessary to assess their initial strontium isotopic compositions. Rb-Sr isotope analyses have been carried out on whole rock and mineral separates (including separate analyses for residue and leached feldspars) from the Beinn an Dubhaich, Marsco, Loch Ainort and Glamaig granites and these data are presented in Table 8. 1.

The measured Rb-Sr isotope data for the four granites comprise:

(a) The whole rock and mineral separates for the Beinn an Dubhaich Granite have $^{87}Sr/^{86}Sr$ values in the range 0.713215 ± 17 to 0.718481 ± 16 for plagioclase residue and whole rock, respectively. Leachate samples of alkali feldspar and plagioclase yield $^{87}Sr/^{86}Sr$ values of 0.719153 ± 29 and 0.713357 ± 36, respectively. The $^{87}Rb/^{86}Sr$ values range from 0.5082 in quartz to 11.0434 in alkali feldspar leachate.

(b)The $^{87}Sr/^{86}Sr$ values of the Marsco Granite range from 0.725976 ± 16 to 0.758195 ± 17 for a pyroxene separate and the whole rock, respectively, with alkali feldspar leachate recording a value of 0.743804 ± 23. The $^{87}Rb/^{86}Sr$

Table 8.1 Rb-Sr isotope data for whole rock and mineral separates from Skye granites

Sample name	Rb (ppm)	Sr (ppm)	Rb/Sr	$^{87}Rb/^{86}Sr$	$(^{87}Sr/^{86}Sr) \pm 2se$	$(^{87}Sr/^{86}Sr)_i$
Beinn an Dubhaich (SK-300) (Age: 59.1 Ma)						
Whole rock	122.4	80.7	1.5167	4.3940	0.716158 ± 17	0.71247
Quartz	0.73	4.04	0.1755	0.5082	0.713313 ± 29	0.71289
Amphibole	14.9	16.1	0.9248	2.6775	0.714882 ± 17	0.71263
Alkali feldspar R.	292.3	126.1	2.3186	6.7154	0.718481 ± 16	0.71284
Plagioclase R.	27.9	208.9	0.1336	0.3867	0.713215 ± 17	0.71289
Alkali feldspar L.	156.4	41.0	3.8128	11.0434	0.719153 ± 29	0.70988
Plagioclase L.	26.4	56.9	0.4634	1.3415	0.713357 ± 36	0.71223
Marsco Granite (SK-334) (Age: 59.9 Ma)						
Whole rock	137.5	6.34	21.825	59.9241	0.758195 ± 17	0.70720
Pyroxene	37.9	5.72	6.7080	19.4442	0.725976 ±16	0.70943
Alkali feldspar R.	175.5	9.53	18.454	50.8210	0.752689 ± 42	0.70944
Alkali feldspar L.	3048.6	213.1	14.307	41.5402	0.743804 ± 23	0.70845
Loch Ainort Granite (SK-313) (Age: 58 Ma)						
Whole rock	109.9	32.2	3.4172	9.8899	0.712186 ±18	0.70404
Quartz	1.43	0.45	3.6316	10.3448	0.714724 ± 26	0.70620
Amphibole	13.8	5.24	2.6513	7.6667	0.712572 ± 30	0.70625
Alkali feldspar R.	168.9	67.0	2.5195	7.2926	0.711605 ±17	0.70560
Alkali feldspar L.	149.7	68.6	2.1842	6.3221	0.711907 ± 18	0.70670
Glamaig Granite (SK-326) (Age: 56.6 Ma)						
Whole rock	65.4	137.2	0.4766	1.3792	0.709906 ± 16	0.70880
Quartz	1.78	6.72	0.2640	0.7615	0.709405 ± 17	0.70879
Amphibole	5.74	17.7	0.3214	0.9305	0.709732 ± 21	0.70898
Alkali feldspar R.	189.7	154.0	1.2323	3.5667	0.711817 ± 27	0.70895
Plagioclase R.	65.1	222.2	0.2932	0.8483	0.709629 ± 18	0.70895
Alkali feldspar L.	190.6	140.2	1.3591	3.9340	0.711685 ± 38	0.70852
Plagioclase L.	88.9	93.9	0.9462	2.7383	0.709852 ±16	0.70765

Where: **R**, residue samples; **L**, leachate samples.

values are relatively high, ranging from 19.4442 to 59.9241 for the pyroxene and the whole rock, respectively.

(c) The Loch Ainort Granite has $^{87}Sr/^{86}Sr$ values ranging from 0.711605 ± 17 to 0.714724 ± 26 for alkali feldspar residue and whole rock respectively. The leachate sample of alkali feldspar has a $^{87}Sr/^{86}Sr$ value of 0.711907 ± 18. Values of $^{87}Rb/^{86}Sr$ ratios range from 6.3221 for the alkali feldspar leachate to 10.3448 for quartz.

(d) $^{87}Sr/^{86}Sr$ ratios for whole rock and mineral separates from the Glamaig Granite record values in the range 0.709405 ± 17 to 0.711817 ± 27 for quartz and the alkali feldspar residue, respectively. In contrast, the alkali feldspar and plagioclase leachates have $^{87}Sr/^{86}Sr$ values of 0.711685 ± 38 and 0.709852 ± 16 respectively. $^{87}Rb/^{86}Sr$ ratios range from 0.7615 to 3.9340 for quartz and alkali feldspar leachate.

8. 2. 2 Geochronological investigations

From the Sr-isotope compositions and Rb and Sr contents of whole rocks and mineral separates for the granites given in Table 8.1 preliminary isochrons have been determined and are presented in Figs. 8.1 to 8.4. Ages were determined using the algorithm of York (1969).

To reduce the influence of alteration processes (due to the relative mobility of Rb and Sr), only the residues from the leached alkali feldspar and plagioclase separates, together with amphibole or pyroxene, were used to construct mineral isochrons. Quartz from the studied granites contains a large number of fluid inclusions (see chapter V); as these inclusions may contain all the Sr and Rb of the quartz, the measured $^{87}Sr/^{86}Sr$ ratios possibly represent fluid compositions and not the quartz itself. For this

reason the quartz was also excluded initially from the mineral isochron determinations. Thus, the ages produced here most likely represent the magmatic ages of these granites, and the close fit of the points to a linear array suggests isotopic homogenisation within each granite at the time of crystallisation (Moorbath and Bell, 1965; Dickin, et al., 1986; Wendt, 1993).

Three intrusions yield Rb-Sr ages of: 59.1±6.2 Ma with an initial $^{87}Sr/^{86}Sr$ ratio of 0.7128 ± 4 (MSWD = 7.4) for Beinn an Dubhaich (Fig. 8.1); 59.9±0.9 Ma with an initial $^{87}Sr/^{86}Sr$ ratio of 0.7094 ± 4 (from two points only) for Marsco (Fig. 8.2); and, 56.6±4.6 Ma with an initial $^{87}Sr/^{86}Sr$ ratio of 0.7089 ± 1 (MSWD = 0.11) for Glamaig (Fig. 8.4) (MSWD is the Mean Square Weighted Deviates). However, when the quartz compositions are included in the isochron calculations for the Beinn an Dubhaich and Glamaig granites, the resulting initial ratios (0.7128 ± 2; and, 0.7089 ± 1, respectively) are identical to those calculated without the quartz. These results indicate that the Sr isotopic compositions of the fluids in the quartz from the Beinn an Dubhaich and Glamaig granites are magmatic (see Chapters V and VI).

In contrast, minerals from the Loch Ainort Granite do not yield a satisfactory isochron (Fig. 8.3), demonstrating that its isotopic composition was not completely homogeneous at the time of crystallisation, or it may not have remained a closed system (Moorbath and Thompson, 1980; Faure, 1986; Dickin, et al., 1986; Wendt, 1993).

Only the Glamaig Granite has a MSWD value lower than 2.5, which has been proposed by several researchers as the upper limit of analytical error (for example, Brooks et. al., 1972; Rollinson, 1993). The Beinn an Dubhaich Granite defines an errorchron with an MSWD value of 7.4, reflecting some scatter in the data which most likely represents the influence of hydrothermal activity, for example, some hydrothermal alteration is still

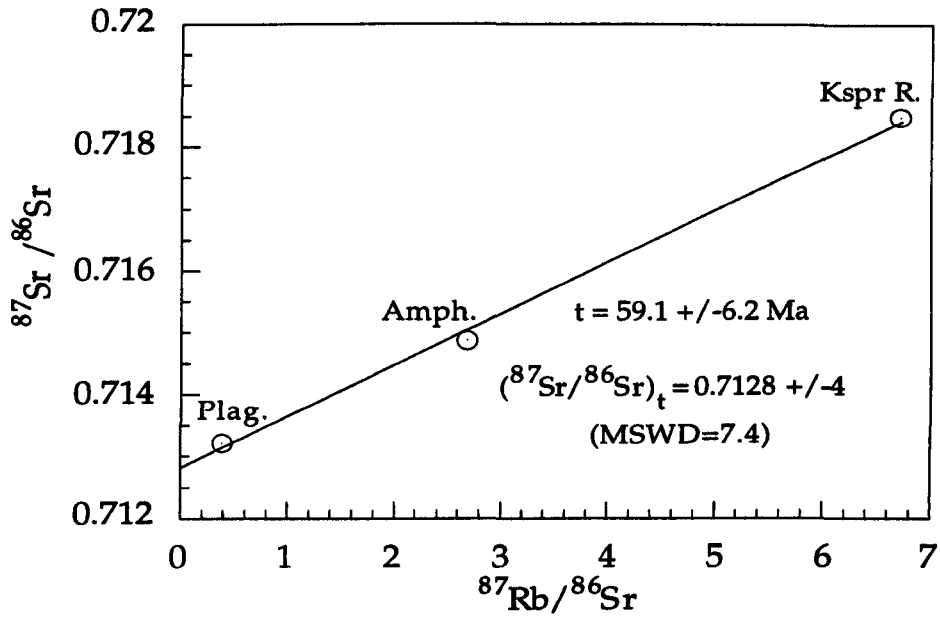

Fig. 8.1 Rb-Sr mineral isochron diagram for the Beinn an Dubhaich Granite. Where: Af. R., alkali feldspar (residue); Plag. R., plagioclase (residue); Amph., amphibole.

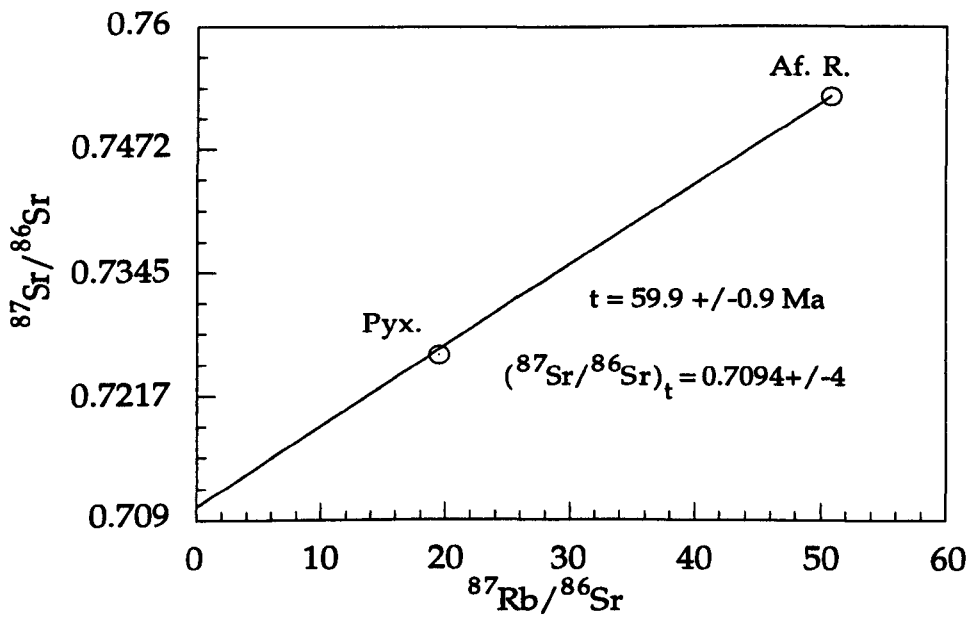

Fig. 8.2 Rb-Sr mineral isochron diagram for the Marsco Granite. Where: Af. R., alkali feldspar (residue); Pyx., pyroxene.

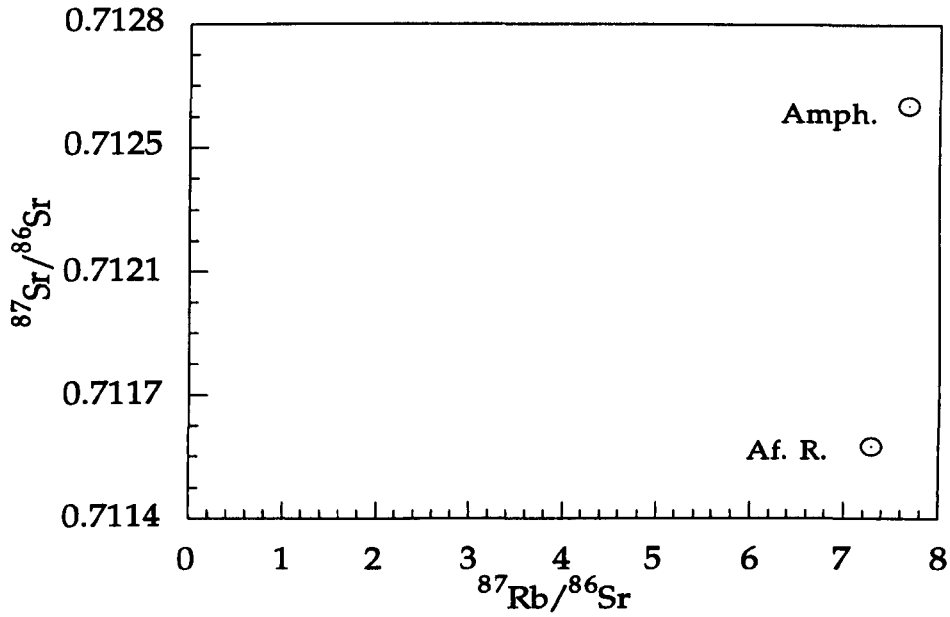

Fig. 8. 3 Rb-Sr mineral isochron diagram for the Loch Ainort Granite. Where: Af. R., alkali feldspar (residue); Amph., amphibole.

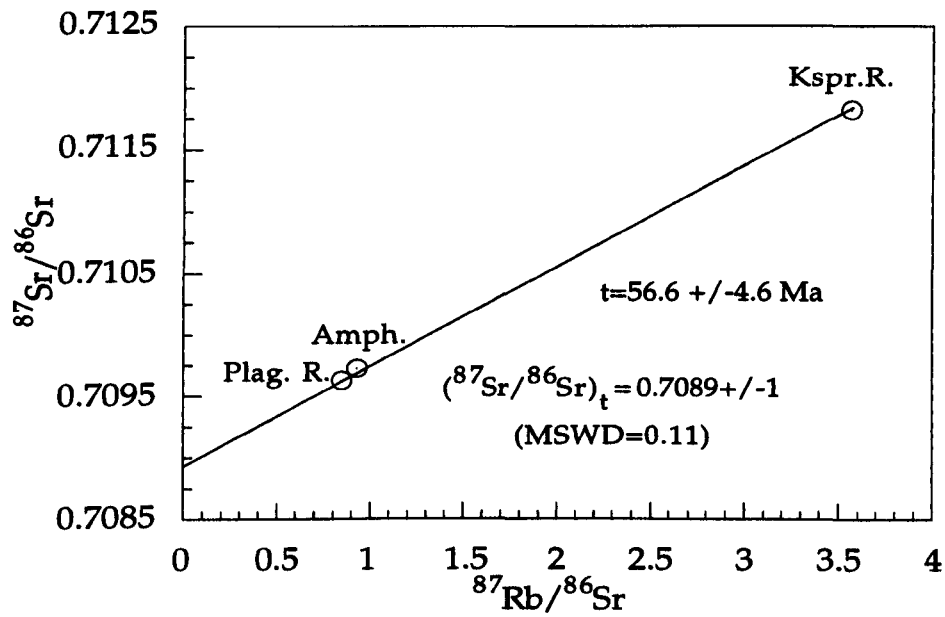

Fig. 8.4 Rb-Sr mineral isochron diagram for the Glamaig Granite. Where: Af. R., alkali feldspar (residue); Plag. R., plagioclase (residue); Amph., amphibole.

present, either in feldspars or amphibole (but see also, Moorbath and Thompson, 1980; Dickin et al., 1986).

Dickin (1981) reported whole rock isochrons for the Glamaig, Loch Ainort and Marsco granites, yielding ages of 59 Ma, 58.7 ± 1.7 Ma and 57 Ma respectively, whereas, Moorbath and Bell (1965) determined an age of 55 ± 4 Ma for the Beinn an Dubhaich Granite based on coexisting biotite and plagioclase. The new age calculations are consistent within error, with other previous studies (for example, Moorbath and Bell, 1965; Wager et al., 1965, Bell, 1966) and field relations (for example, Bell and Harris, 1986; and Chapter II), suggesting that the Loch Ainort Granite crystallised after the Glamaig Granite and prior to the Marsco and Beinn an Dubhaich granites.

From the data presented in this study, as the Glamaig Granite yields an age of 56.6 ± 4.6 Ma, Beinn an Dubhaich Granite yields an age of 59.1 ± 6.2 Ma and the Marsco Granite records an age of 59.9 ± 0.9 Ma, these ages were used in calculating initial $^{87}Sr/^{86}Sr$ ratios for whole rock and mineral separates for those granites. Accordingly, all analysed granites, including the Loch Ainort, must have crystallised between 55 and 60 Ma. The associated errors in these age calculations indicate that the crystallisation ages of the Skye granites are indistinguishable. Hence, an age of 58 Ma has been assumed in all subsequent calculations for the Loch Ainort Granite, this will make an age determination a high priority in any further study and may be acquired by K-Ar isotopic systems (see for example, Miller and Mohr, 1965; Evans and Miller, 1973) . The resulting data are presented in Table 8.1 (all errors quoted to 2se i.e. 2 standard errors of the mean).

In conclusion, from previous studies and the age data presented here, it is concluded that the emplacement and crystallisation of the Skye granites occurred within a very short time (5 Ma) at approximately 55-60Ma.

8. 2. 3 Discussion

8. 2. 3. 1 Variations in Sr isotope signatures within the Skye granites

From the discussion in section 8. 2. 2 on geochronology, apart from the Loch Ainort Granite, all of the isochron calculations indicate that the minerals in the analysed specimen of each granite had a uniform or nearly uniform initial strontium isotopic composition at the time of its crystallisation. However, the Loch Ainort Granite may also have had a uniform Sr isotopic composition at the time of crystallisation, but it appears that hydrothermal fluids may have subsequently disturbed the Rb-Sr systematics. As Sr isotopic data are available for mineral separates for each of the four granites, the initial $^{87}Sr/^{86}Sr$ variations within each granite will be discussed individually. Values are tabulated in Table 8.1:

(i) The Beinn an Dubhaich Granite. This granite has the highest initial Sr ratio of the samples studied (0.7128 ± 4). The initial $^{87}Sr/^{86}Sr$ ratios of minerals calculated at 59.1 Ma are 0.71289, 0.71263, 0.71284 and 0.71289 for quartz, amphibole, magmatic alkali feldspar and plagioclase, respectively. Variation between these minerals is very small. Dickin et al. (1980) have shown that the hydrothermal fluids which passed through the Coire Uaigneich Granophyre (see Chapter II) were less radiogenic than the magma from which the granophyre crystallised. This conclusion is consistent with the Sr isotopic compositions of leached samples of residues and leachates from alkali feldspar and plagioclase in this study. The initial Sr isotopic compositions of the residues (0.71284 and 0.71289, respectively) are considered to represent those of magmatic alkali feldspar and plagioclase which have reacted with hydrothermal fluids which have passed through

the Beinn an Dubhaich Granite. In contrast, the leachates, whose Sr isotopic composition may reflect that of the hydrothermal fluid or at least mixtures of hydrothermal and magmatic Sr, have initial $^{87}Sr/^{86}Sr$ ratios of 0.70988 and 0.71223 for the alkali feldspar and plagioclase, respectively. This model requires that the hydrothermal alteration of the granite took place ≥11Ma ago, after which time the feldspar leachate has a higher $^{87}Sr/^{86}Sr$ than the residue.

(ii) The Marsco Granite. The initial Sr isotopic compositions of the whole rock, pyroxene, and alkali feldspar (residue and leachate) separates are 0.70720, 0.70943, 0.70944 and 0.70845, respectively. The higher ($^{87}Sr/^{86}Sr$) initial value of the alkali feldspar residue compared to the leachate indicates that the water passing through the Marsco Granite was less radiogenic (Table 8.1) than the magma.

(iii) The Loch Ainort Granite. The initial Sr isotopic compositions are 0.70404, 0.70620, 0.70625, 0.70560, and 0.70670 for the whole rock, quartz, amphibole, magmatic alkali feldspar and leachate alkali feldspar. It is unlikely that the composition of the alkali feldspar has been modified to a less radiogenic composition by hydrothermal processes because the initial $^{87}Sr/^{86}Sr$ ratio of the magmatic alkali feldspar (i.e. the residue) is low relative to the leached alkali feldspar, which suggests that the Sr isotopic composition of fluids passing through the Loch Ainort Granite was more radiogenic than the magma (Table 8.1). This controversy makes an age determination a high priority in further work for this granite.

A $^{87}Sr/^{86}Sr$ ratio for 'magmatic' alkali feldspar from the Loch Ainort Granite (0.7056) at an age of 58 Ma was used as the best indicator of the intrusion's Sr isotopic composition at the time of crystallisation, on the assumption that all the altered Sr was removed by the leaching process. This

initial $^{87}Sr/^{86}Sr$ ratio is slightly lower than the initial ratio (0.70614) obtained from a whole rock isochron by Dickin (1981).

(iv) The Glamaig Granite. The most primitive granite examined in this study has initial $^{87}Sr/^{86}Sr$ ratios of minerals in the range 0.70879 (quartz) to 0.70898 (amphibole). The whole rock also has an initial $^{87}Sr/^{86}Sr$ ratio of 0.70880, which, coupled with the small MSWD value for the isochron (0.11), suggests the minerals in this sample of granite had a homogeneous Sr isotopic composition at the time of crystallisation (cf. Dickin et al., 1980; McCormick, 1989), and that the influence of any hydrothermal alteration on the rock composition has been very limited. The lower initial $^{87}Sr/^{86}Sr$ of the leachates would be attributed to the isotopic composition of the hydrothermal fluids associated with these granites, and also stressing the timing constraints on such alteration.

From the above discussion, it may be concluded that the Glamaig Granite is certainly the least isotopically disturbed granite in the studied intrusions. We may also conclude, that the four granites had distinct and different initial strontium isotopic compositions.

Quartz in Skye granites contains large numbers of fluid inclusions (Chapter V). On the assumption that the Sr and Rb in the quartz are in the fluid inclusions, then the $^{87}Sr/^{86}Sr$ ratio for the quartz is that of the trapped fluid.

From thermometric studies of fluid inclusions (Chapter V) in the Beinn an Dubhaich and Loch Ainort granites, primary (magmatic) inclusions are present only in the quartz from the Beinn an Dubhaich Granite, together with some secondary inclusions. The primary inclusions are larger and therefore contain a relatively large quantity of fluid, compared to the secondary and pseudosecondary inclusions (Shepherd et al., 1985). Thus, the Sr isotopic compositions of quartz containing both types of inclusions is

likely to be dominated by the composition of the primary inclusions, due to the large amount of fluid in primary inclusions and assuming that the secondary inclusions do not have significantly higher Sr contents than the primary inclusions.

For the Beinn an Dubhaich and Glamaig granites, the initial $^{87}Sr/^{86}Sr$ ratios of the quartz are approximately in isotopic equilibrium with the other minerals, further suggesting that the Sr in the inclusions is magmatic in origin. Also, the initial $^{87}Sr/^{86}Sr$ ratio of quartz in the Loch Ainort Granite (which contains no primary inclusions) is in isotopic equilibrium with the amphibole; on the other hand the magmatic alkali feldspar is not in isotopic equilibrium with coexisting amphibole, indicating that the amphibole may contain a component of hydrothermal Sr. Therefore, the $^{87}Sr/^{86}Sr$ ratios of fluids in the Beinn an Dubhaich and Glamaig granites possibly represent mixing of magmatic and meteoric waters (see Chapter V and VII), whereas the fluid in the Loch Ainort Granite is mainly meteoric. Indeed, Guthrie and Veblen (1991) recognise evidence for reaction between the alkali feldspar of the Loch Ainort Granite with two different types of fluid.

8. 2. 3. 2 Possible causes of Sr isotope variations

The $(^{87}Sr/^{86}Sr)_i$ ratios increase from the more primitive Glamaig Granite (0.7089) towards the more evolved Marsco and Beinn an Dubhaich granites (0.7094 and 0.7128, respectively), but with the Loch Ainort Granite having the lowest $(^{87}Sr/^{86}Sr)_i$ ratio (0.7056). Variations in initial $^{87}Sr/^{86}Sr$ ratio in granites can be explained by the following processes: (i) interaction with and contamination by hydrothermal fluids; (ii) source mantle heterogeneity; (iii) derivation by partial melting of isotopically heterogeneous crustal

lithologies, or contamination of mantle-derived magma by crustal lithologies.

(i) Hydrothermal Sr alteration: Skye granites record a marked ^{18}O depletion due to their pervasive interaction with meteoric water, as has been shown in Chapters V and VII. Taylor and Forester (1971) and Forester and Taylor (1977) suggested that this hydrothermal process may have disturbed the Sr isotope compositions of the various lithologies of the Intrusive Complex and the surrounding (older) lava field, although Paul (1979), in his study of Indian kimberlites, has shown that the initial $^{87}Sr/^{86}Sr$ ratios are not related to the degree of alteration.

As shown earlier, the initial $^{87}Sr/^{86}Sr$ ratios of the whole rocks and magmatic minerals, such as amphibole or pyroxene, are completely different in both the Loch Ainort and Marsco granites (Table 8.1), suggesting that their Sr isotopic compositions may have been disturbed by hydrothermal fluids. In contrast, the Glamaig and Beinn an Dubhaich granites record whole rock initial $^{87}Sr/^{86}Sr$ compositions which are nearly identical with those of separated amphiboles and leached feldspars, indicating that their whole rock Sr isotopic compositions have not been significantly affected by hydrothermal fluids (Hawkesworth and Morrison, 1978).

Fig.8.5a shows the relation between $\delta^{18}O$ and $(^{87}Sr/^{86}Sr)_i$ of whole rock samples from Skye granites. The data define a positive correlation line, suggesting some sort of relation between the hydrothermal process (as represented by the $\delta^{18}O$ whole rock data) and the Sr isotopic compositions. However, in Section 7.2.2, the oxygen isotope data indicated that the Marsco and Loch Ainort granites crystallised from low-^{18}O magmas. Consequently, such a positive correlation between $\delta^{18}O$ and initial $^{87}Sr/^{86}Sr$ ratios in Fig. 8.5a cannot be the result of hydrothermal alteration of magmas with a

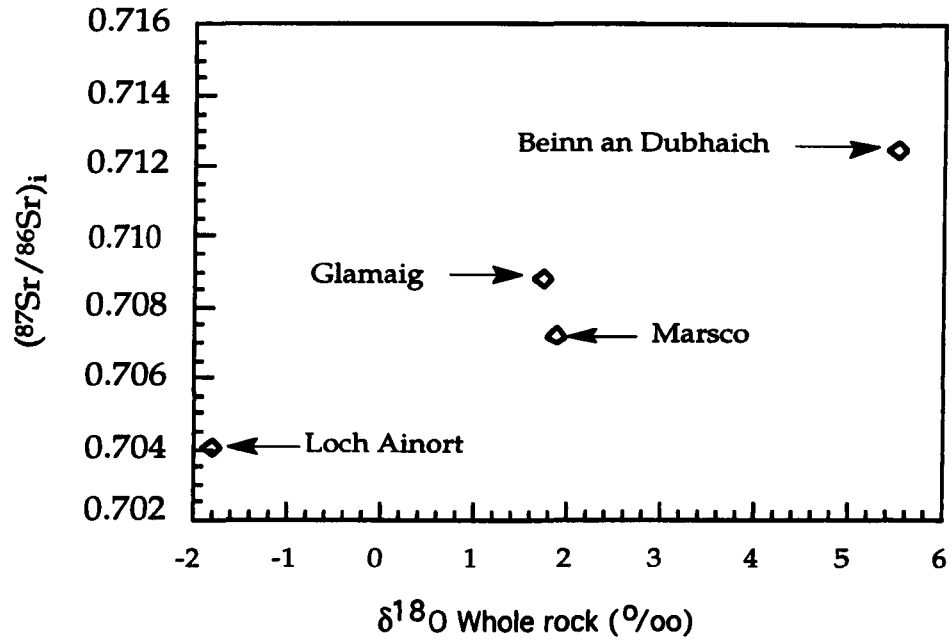

Fig.8.5a Co-variation between oxygen and initial strontium isotopic composition for whole rock samples of Skye granites.

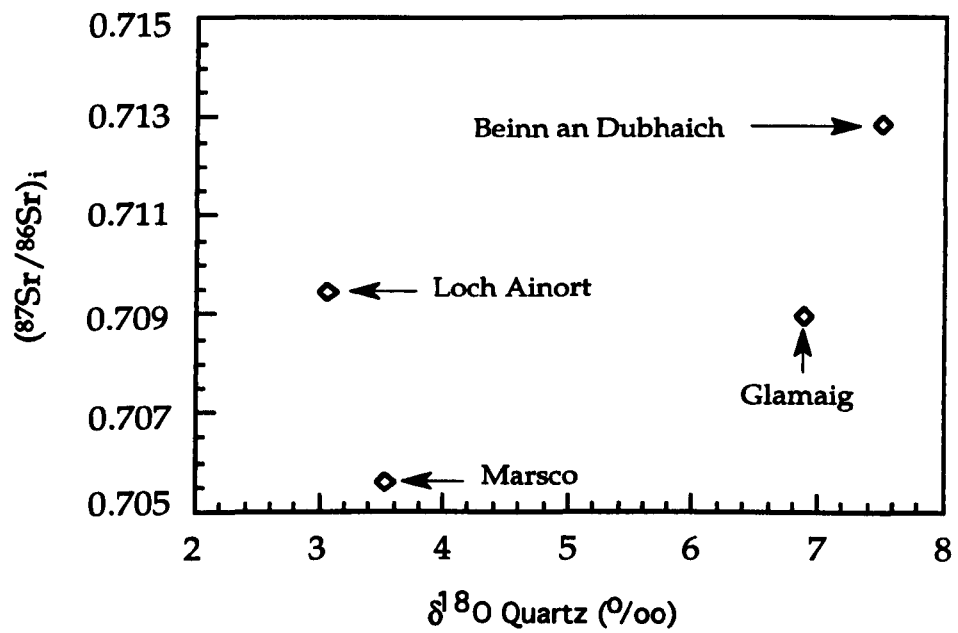

Fig.8.5b Co-variation between oxygen isotopic composition for quartz and initial strontium isotopic composition for 'magmatic' alkali feldspar.

uniform initial Sr and "normal" O isotopic composition. Moreover, the Loch Ainort magma appears to have interacted with a fluid with a higher initial Sr isotopic composition than its own, whereas the Beinn an Dubhaich, Marsco and Glamaig magmas have interacted with a less radiogenic fluid (Section 8.2.3.1), thus suggesting that there was not a unique hydrothermal fluid involved in the alteration of the Skye granites.

Dickin et al. (1980) showed that Sr exchange between rocks and hydrothermal fluid does not occur to such a large extent as oxygen exchange. In Fig. 8.5b the relationship between magmatic oxygen isotope signatures (considered to be represented by the $\delta^{18}O$ for quartz) and magmatic initial Sr isotopic compositions ($^{87}Sr/^{86}Sr$ for alkali feldspar residue) is presented, which shows a poor correlation. This further suggests that hydrothermal alteration of any crustal source rocks for the Skye granites is unlikely to be the sole cause of the initial $^{87}Sr/^{86}Sr$ variation between the granites.

Therefore, as hydrothermal alteration may be excluded as being responsible for the variations in initial $^{87}Sr/^{86}Sr$ ratios between the Skye granites, variations must be due to magmatic processes.

(ii) Mantle heterogeneity: The Sr isotopic signatures of a number of suites of continental volcanic rocks have been attributed to inheritance from an isotopically heterogeneous continental lithospheric source (Brooks et al., 1976; Pankhurst, 1977; Cohen et al., 1980; Dupré and Allègre, 1980). Thus, the effect of mantle heterogeneity on isotopic composition must be considered before magma-crust interaction is taken into account (Dickin et al., 1984).

Fig. 8. 6 shows the relation between initial $^{87}Sr/^{86}Sr$ ratios and Sr contents of whole rocks. The data show no correlation (i.e. neither positive nor negative). Moorbath and Thompson (1980) attributed such a lack of correlation in Skye lavas to contamination of the magma with variable

amounts of Sr derived from crustal rocks. However, as these granites are highly affected by hydrothermal alteration, their whole rock initial $^{87}Sr/^{86}Sr$ are not representative of the magma (at least for Loch Ainort and Marsco) and contain a component of hydrothermal alteration. Such an observation, together with an overall close association in time and space for the Skye granites, implies that mantle heterogeneity is unlikely to be an important contributor to the observed Sr isotopic variations (Dickin, 1981; Dickin and Jones, 1983). Consequently, it is necessary to consider the role of crustal materials to generate the recorded Sr isotopic variations.

(iii) Partial melting of crustal rocks or contamination of mantle-derived material by crustal rocks: Several authors (for example, Brown, 1963; Wager et al., 1965, Thompson 1969) have interpreted the Skye granites as partial melts of ancient crustal rocks such as the Torridonian (Upper Proterozoic) sandstones, or amphibolite facies and granulite facies gneisses from the (Archaean) Lewisian Complex. Torridonian rocks have an $^{87}Sr/^{86}Sr$ ratio at 60Ma of 0.7406; granulite facies gneiss has an $^{87}Sr/^{86}Sr$ at 60Ma of 0.7030, and amphibolite facies gneiss has an $^{87}Sr/^{86}Sr$ at 60Ma of 0.7174 (Dickin and Jones, 1983). The intermediate initial $^{87}Sr/^{86}Sr$ ratios of the Skye granites, in the range 0.7062-0.7128, suggest a contribution of both crustal rocks along with mantle-derived material with an initial $^{87}Sr/^{86}Sr$ composition of 0.7028 (Dickin and Jones, 1983).

Dickin (1981), in presenting Pb isotopic data for Skye granites, was able to show from a mixing diagram (involving: mantle-amphibolite facies gneiss-granulite facies gneiss), the lack of any clustering of granite Pb analyses near the composition of crustal gneiss (either amphibolite or granulite facies), which he suggested indicated the involvement of a mantle component and argues against a purely crustal origin.

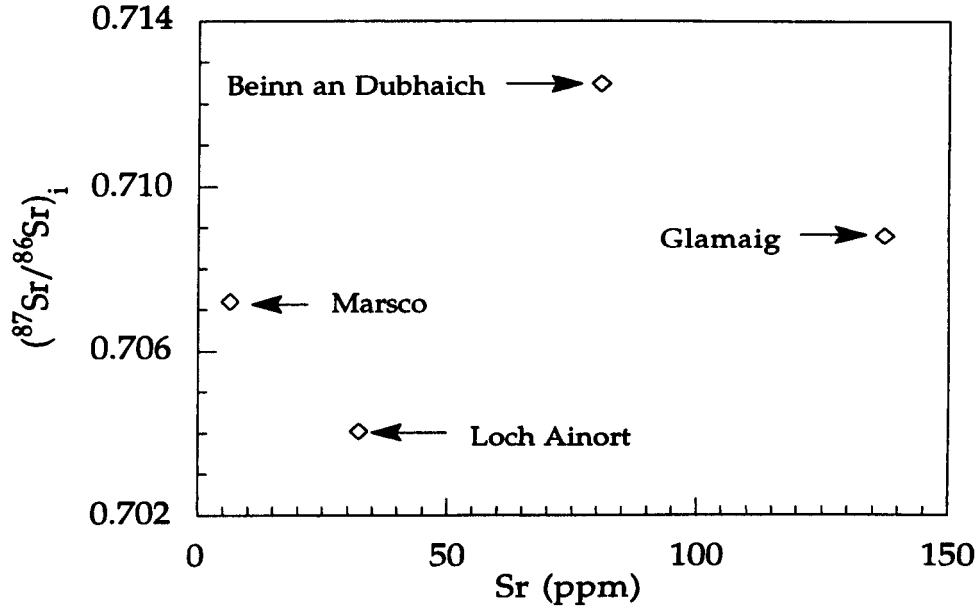

Fig.8.6 Plot of $(^{87}Sr/^{86}Sr)_i$ against Sr content for whole rock samples.

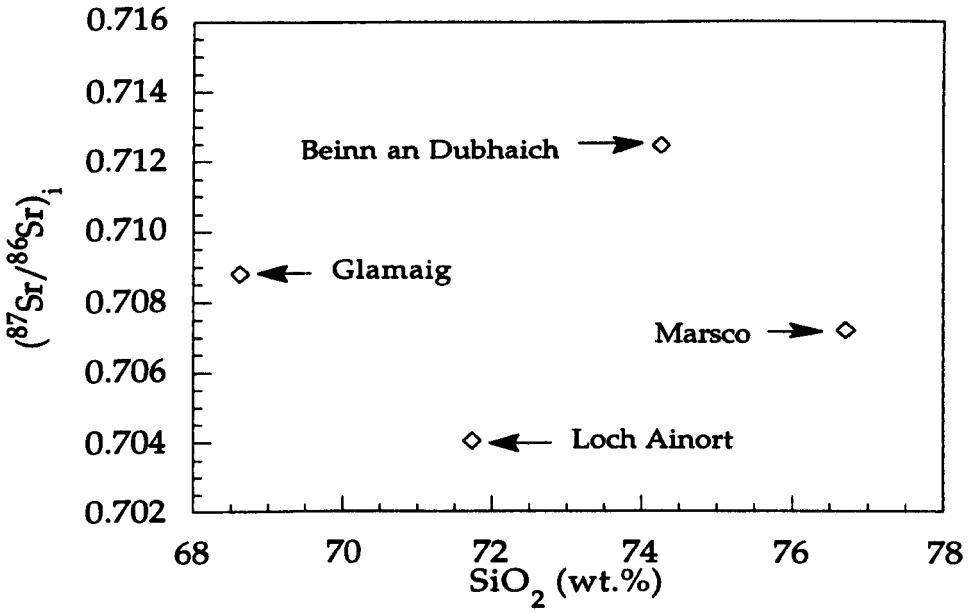

Fig.8.7 Plot of $(^{87}Sr/^{86}Sr)_i$ against SiO_2 content for whole rock samples.

Of the various processes which may have caused the considerable Sr isotopic variations between Skye granites, it is possible to reject mantle heterogeneity, and partial melting of heterogeneous crustal rocks as the sole cause of this isotopic variation. Hydrothermal alteration may have been responsible to a small extent, for some of the recorded isotopic variation. The alternative explanation is that the $^{87}Sr/^{86}Sr$ variations are the result of assimilation of crustal rocks by mantle-derived magma.

Dickin (1981), on discussing normative quartz contents of Lewisian gneiss (18 wt. %) within the normative Q-Or-Ab-An tetrahedron, was able to show that a small degree of partial melting of crustal rocks by basic magma, will produce substantial amounts of quartz, and consequently this will increase the silica content of the fractionated magmas. It is apparent from Fig. 8. 7 that there is no obvious correlation between SiO_2 content and initial $^{87}Sr/^{86}Sr$ ratio for the Skye granites, which may be due to the presence of variable alteration products in these granites, as suggested by the w/r (water/rock) ratios (see Chapter VI). However, the observed relation (Fig. 8.7) also excludes the possibility of bulk contamination on a regional scale (i.e. all the granites are not related to each other through variable degrees of bulk crustal contamination of a unique more basic magma which then did not fractionate any further), although, for each intrusion, variable degrees of crustal contamination of a more basic magma followed by fractionation could explain the scatter in Fig 8.7 (but see, Dickin, 1981; Thirlwall and Jones, 1983; Dickin et al., 1984; Bell et al., 1994).

8. 3 Sm-Nd isotopes

Since Sm-Nd isotope systematics have been shown to be robust even in areas of extensive hydrothermal activity (see Dickin, 1981; Darbyshire and

Shepherd, 1994), they are used here in order to examine the genesis and evolution of Skye granites which have significantly interacted with hydrothermal water as deduced from petrography (Chapter III), fluid inclusions studies (Chapter V) and stable isotope geochemical data (Chapter VII).

8. 3. 1 Results

Sm-Nd isotope analyses have been carried out on whole rocks and amphiboles or pyroxenes from the Beinn an Dubhaich, Marsco, Loch Ainort and Glamaig granites, and the data are listed in Table 8. 2.

The measured $^{143}Nd/^{144}Nd$ ratios and initial $^{143}Nd/^{144}Nd$ ratios at an age of 58 Ma for whole rocks and amphiboles are:

(i) The measured $^{143}Nd/^{144}Nd$ values for whole rocks and amphiboles from the Beinn an Dubhaich, Loch Ainort and Glamaig granites are: 0.511559 $\pm$ 5 and 0.511570 $\pm$ 7; 0.511897 $\pm$ 8 and 0.511899 $\pm$ 6 ; and 0.511282 $\pm$ 7 and 0.511272 $\pm$ 7, respectively. The values for the whole rock and pyroxene from the Marsco Granite are 0.511466 $\pm$ 6 and 0.511456 $\pm$ 9, respectively.

(ii) The initial $^{143}Nd/^{144}Nd$ values for whole rocks and amphiboles from Beinn an Dubhaich, Loch Ainort and Glamaig are: 0.511515 and 0.511517; 0.511847 and 0.511845; 0.511242 and 0.511235, respectively. The values for whole rock and pyroxene from the Marsco Granite are 0.511421 and 0.511412, respectively.

Initial $^{143}Nd/^{144}Nd$ ratios are reported in the epsilon (ε) notation as deviations in parts per 10^4 from the reference reservoir, CHUR (Chondritic Uniform Reservoir) (DePaolo and Wasserburg, 1976), as follows:

Table 8.2 Sm-Nd isotope data for whole rock and mineral separates from Skye granites

Sample name	Sm (ppm)	Nd (ppm)	Sm/Nd	$^{147}Sm/^{144}Nd$	$(^{143}Nd/^{144}Nd)$ (±2se)	$^{143}Nd/^{144}Nd$ (58Ma)	ε_{Nd} (58Ma)
Beinn an Dubhaich Granite (SK-300)							
Whole rock	8.15	41.84	0.19	0.1178	0.511559 ± 5	0.511515	-20.5
Amphibole	109.36	468.29	0.23	0.1412	0.511570 ± 7	0.511517	-20.4
Apatite	1429.83	8240	0.17	0.1049	0.511542 ± 8	0.511502	-20.7
Zircon A	134.45	510.54	0.26	0.1592	0.511592 ± 16	0.511533	-20.1
Zircon P	18.07	61.20	0.30	0.1785	0.511591 ± 8	0.511524	-20.3
Marsco Granite (SK-334)							
Whole rock	21.17	115.24	0.20	0.1185	0.511466 ± 6	.511421	-22.3
Pyroxene	194.48	1015.14	0.19	0.1158	0.511456 ± 9	.511412	-22.5
Zircon A	21.02	263.08	0.08	0.0483	0.511567 ± 29	.511548	-19.8
Zircon P	23.54	716.03	0.03	0.0199	0.511605 ± 18	.511597	-18.9
Loch Ainort Granite (Sk-313)							
Whole rock	10.65	49.32	0.21	0.1306	0.511897 ± 8	0.511847	-14.0
Amphibole	130.05	558.84	0.23	0.1407	0.511899 ± 6	0.511845	-14.0
Zircon A	9.22	19.55	0.47	0.2852	0.511987 ± 17	0.511880	-13.3
Zircon P	47.50	196.11	0.24	0.1464	0.511847 ± 18	0.511792	-15.0
Glamaig Granite (SK-326)							
Whole rock	9.63	55.10	0.17	0.1056	0.511282 ± 7	0.511242	-25.8
Amphibole	60.78	383.13	0.16	0.0959	0.511272 ± 7	0.511235	-25.9
Apatite	292.51	1862.16	0.16	0.0949	0.511284 ± 6	0.511248	-25.7
Zircon A	31.83	8034.58	0.004	0.0024	0.511609 ± 21	0.511609	-18.6
Zircon P	2.92	488.0	0.006	0.0036	0.511542 ± 23	0.511541	-19.9

Where: **A**, anhedral; **P**, prismatic.

$$\varepsilon^{t}_{Nd} = \left[\left((^{143}Nd/^{144}Nd)_{t,\,sample} / (^{143}Nd/^{144}Nd)_{t,CHUR} \right) - 1 \right] * 10^{4}$$

The resultant data show equilibrium conditions between the whole rock and analysed minerals in each intrusion at the time of crystallisation. The ε^{58}_{Nd} values for the whole rock and amphibole from the Beinn an Dubhaich Granite are -20.5 and -20.4, respectively; the ε^{58}_{Nd} values for the whole rock and pyroxene from the Marsco Granite are -22.3 and-22.5, respectively; the ε^{58}_{Nd} values for the whole rock and amphibole from the Loch Ainort Granite are -14.0 and -14.0, respectively; and the ε^{58}_{Nd} values for the whole rock and amphibole from the Glamaig Granite are -25.8 and -25.9, respectively.

8. 3. 2 Discussion

The results reported here for the Loch Ainort Granite are slightly higher than a single analysis of the same intrusion presented by Dickin et al. (1984), which had an initial $^{143}Nd/^{144}Nd$ of 0.511777. The initial $^{143}Nd/^{144}Nd$ ratios for the Marsco Granite are much lower than that reported by Dickin et al. (1984) (0.511797) for the Marsco Granite, and by Carter et al. (1978) (0.511680) for the Marsco Granite. Thus, comparing the Skye granites with other acid rocks from British Tertiary Volcanic Province in terms of their Nd isotopic signature (for example, Carter et al., 1978; Dickin and Jones, 1983; McCormick, 1989; Dickin, 1994), only the Mourne, Arran and Lundy granites show (much) higher initial $^{143}Nd/^{144}Nd$ (0.512368-0.512430, McCormick, 1989; 0.51204-0.5210, Dickin, 1994; 0.512334-0.512403, Thorpe et al., 1990, respectively). The comparison of the Skye granites with Skye basalts, Mourne and Arran granites is presented in Fig. 8.8, in terms of initial Nd and Sr isotopic compositions.

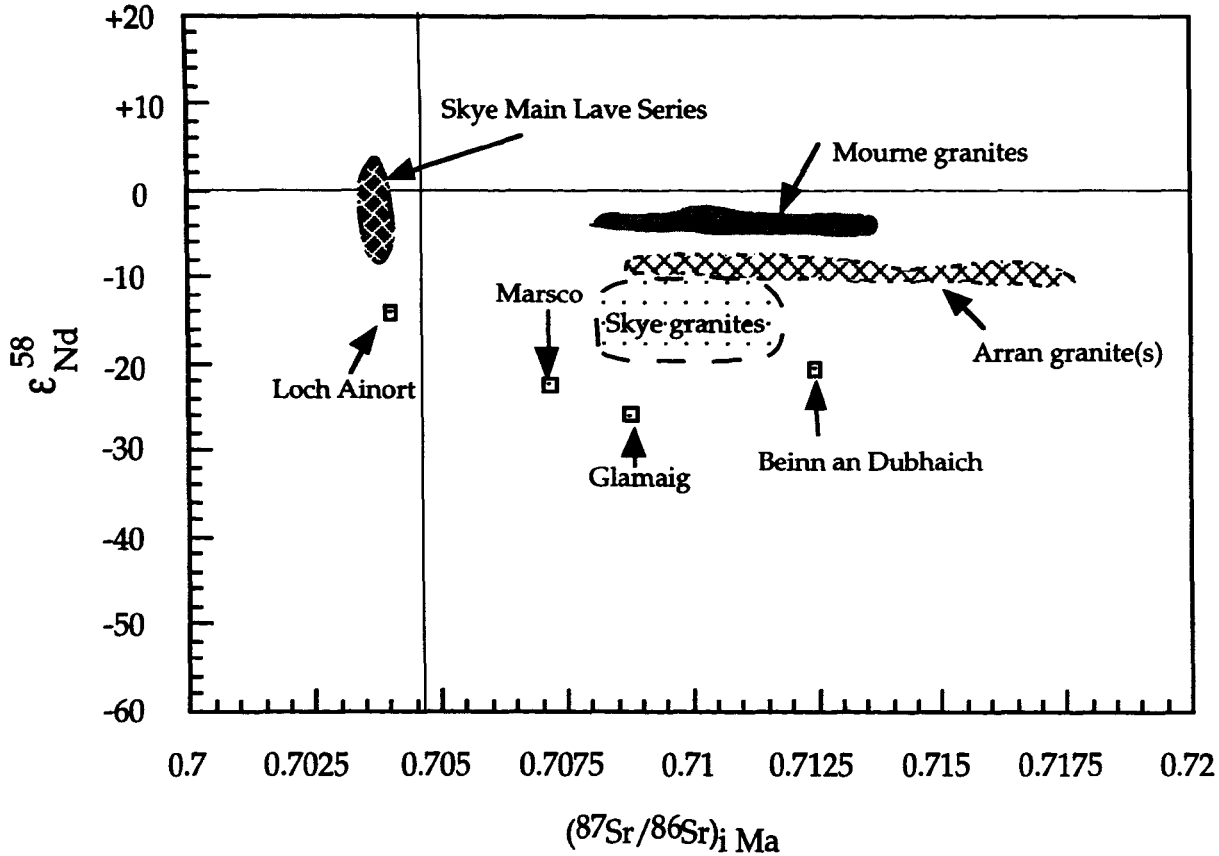

Fig. 8.8 Plot of initial Nd and Sr isotopic compositions for Skye granites, compared with other British Tertiary Volcanic Province rocks: Skye Main Lava Series (data from, Carter et al., 1978; Dickin et al., 1987); Mourne granites (data from, McCormick, 1989); Arran granite(s) (data from, O'Connor, 1976; Dickin et al., 1980; Dickin, 1994); Skye granites (data from Carter et al., 1978; Dickin et al., 1984).

The average $^{143}Nd/^{144}Nd$ isotopic compositions at 60 Ma of possible source rocks for Skye granites are: 0.5129-0.5130 for the Hebridean lithospheric mantle (Carter et al., 1978; Dickin and Jones, 1983; Dickin et al., 1987; Bell et al., 1994); and an average of 0.5108 for both granulite and amphibolite facies gneiss from the Lewisan Complex, calculated from the data of Hamilton et al. (1979) (Dickin and Jones, 1983). The analyses of the Skye granites cluster at intermediate Nd isotopic compositions between mantle and crustal compositions, suggesting some sort of combination between crustal and mantle-derived materials to produce the Skye granites (see also Fig. 8.12).

As with the Sr isotopic signatures, the observed Nd isotopic variations in the Skye granites could have originated by several processes:

(i) Hydrothermal Nd alteration: Alteration of granites after their crystallisation by hydrothermal fluids generally affects mobile elements such as Cs, Sr, K, Rb and Ba; however, it is accepted that Nd is largely immobile during such processes (for example, Dickin, 1981; Darbyshire and Shepherd, 1994, and references therein). However, because the Skye intrusive centres and the surrounding country-rocks have been heavily affected by meteoric/hydrothermal water, as indicated by their significant $\delta^{18}O$ depletions (Taylor and Forester, 1971; Forester and Taylor, 1977; Dickin et al., 1980; Chapters V and VII of this study) the effect of such processes on their Nd isotopic composition has been examined. Fig. 8.9 shows the lack of correlation between $\delta^{18}O$ and initial $^{143}Nd/^{144}Nd$ for whole rock samples, which suggests that the overall variation in initial $^{143}Nd/^{144}Nd$ ratios is independent of hydrothermal alteration.

(ii) Mantle heterogeneity: The role of possible mantle heterogeneity was examined by Carter et al. (1978), Thirlwall and Jones (1983), and Dickin et al. (1984) during investigations of the Nd isotopic variations in Skye lavas; Dickin et al. (1981) on the Tertiary igneous rocks of the Isle of Arran; and, by

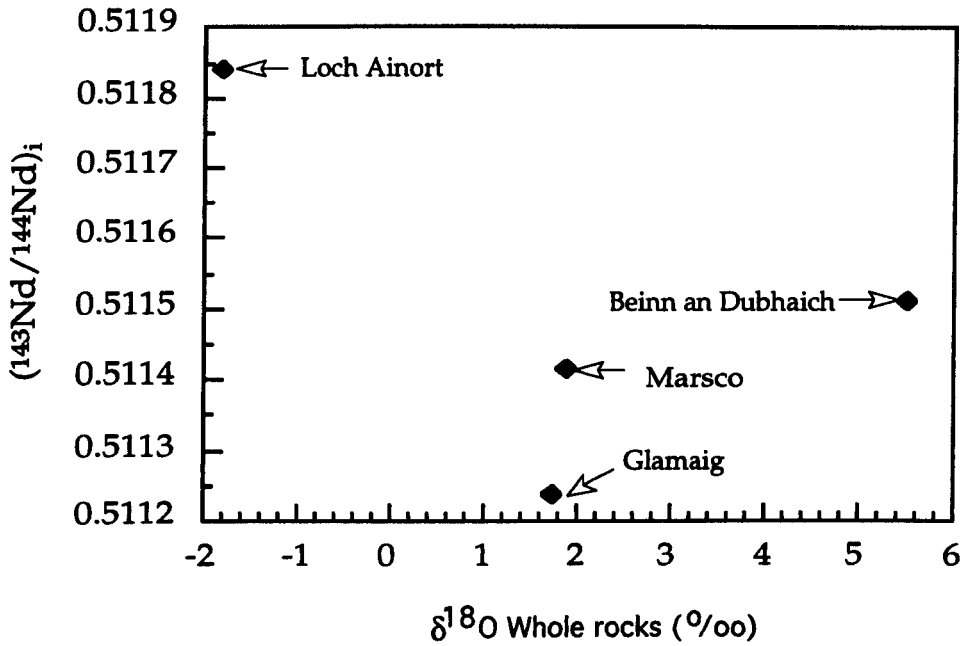

Fig. 8.9 Co-variation between oxygen and initial Nd isotopic composition for whole rock samples.

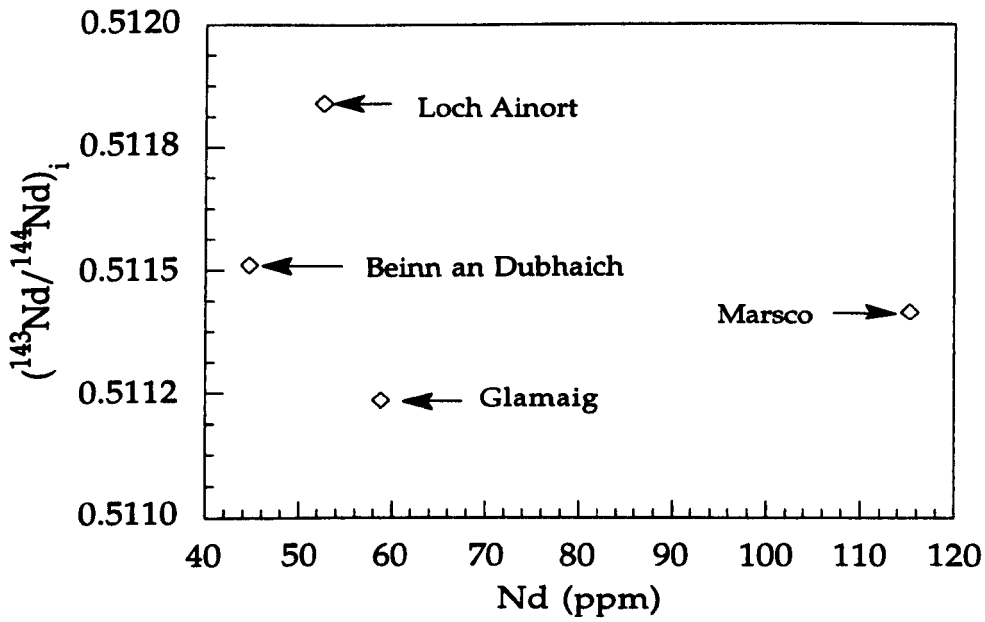

Fig. 8.10 Plot of $(^{143}Nd/^{144}Nd)_i$ against Nd content for whole rock samples.

Dickin and Jones (1983) on the pitchstones and felsites from Eigg. Carter et al. (1978) attributed the apparent contradictory ages for Hebridean rocks from Rb-Sr and Sm-Nd pseudo-isochrons to crustal contamination, and not to mantle differentiation events.

Thirlwall and Jones (1983) showed that ε^{i}_{Nd} correlates with the ratio FeO/{FeO + MgO}, and since the Fe/Mg ratio for Skye lavas has been controlled by fractional crystallisation, they concluded that the ε^{i}_{Nd} compositions must have been related to fractional crystallisation rather than mantle heterogeneity. Dickin and Jones (1983) used the close association in time and space of the pitchstones and felsites from the Isle of Eigg to exclude any influence of mantle heterogeneity in the isotopic variations they identified. Fig. 8.10 illustrates the relationship between initial $^{143}Nd/^{144}Nd$ and Nd contents for whole rock samples: the plot shows a lack of correlation which suggests that the granites are not related to each other through simple binary mixing processes between mantle and crustal end members. However, this scatter could be due to extreme fractionation after mixing (i.e. the different granites representing different proportions of mixing), as was concluded from the Sr isotope data.

It may therefore be concluded that the initial $^{143}Nd/^{144}Nd$ variations in the Skye granites should be attributed to higher level processes in the crust, and that mantle heterogeneity may have played a secondary role in the observed Nd isotopic variations.

(iii) Partial melting of crustal rocks or contamination of mantle-derived material by crustal rocks: From previous studies (for example, Dickin and Exley, 1981; Dickin, 1981; Dickin et al., 1984) and the above discussion, it is considered most likely that the Nd isotopic variations in the Skye granites are due to involvement of crustal materials, together with mantle-derived materials. Their intermediate Nd isotopic compositions between Hebridean

mantle and average Lewisian crustal rocks (granulite and amphibolite facies gneisses) is consistent with contamination of basaltic differentiates, by crustal melts.

The relationship between 100/Nd content and the initial $^{143}Nd/^{144}Nd$ ratio for whole rock samples of the Skye granites is shown in Fig.8.11, in order to explore possible mixing models. The average Nd content of Lewisian Gneiss is assumed to be 26 ppm (Dickin and Jones, 1983) and its initial $^{143}Nd/^{144}Nd$ composition at 60 Ma was 0.5108 (calculated from the data of Hamilton et al., 1979), the value of the Hebridean mantle at 60 Ma is assumed to be 0.5130 (Carter et al., 1978; Thirlwall and Jones, 1983; Dickin et al., 1987; Bell et al., 1994). The data presented here cluster far away from any possible mixing line involving the average Lewisian Gneiss composition and a pure mantle-derived magma. To produce the Nd composition of Skye granites by bulk assimilation, one would need a Nd-rich mantle derived magma contaminated with Lewisian gneiss containing at least 100ppm Nd. Alternatively, the Skye magmas have been fractionated after the mixing between mantle and crustal end members occured, which will increase the Nd contents of the granites. Thus, this may reinforce the role of assimilation and fractional crystallisation (AFC) processes in enhancing the Nd content of the Skye granites.

8. 4 Implications of the Sr and Nd isotope data for granite petrogenesis

In the above discussion (Sections 8.2 and 8.3), the Nd and Sr isotopic variations have been attributed, principally, to crustal contamination of mantle-derived magmas. Hydrothermal processes may have slightly affected the Sr isotope composition; the role of the mantle heterogeneity in

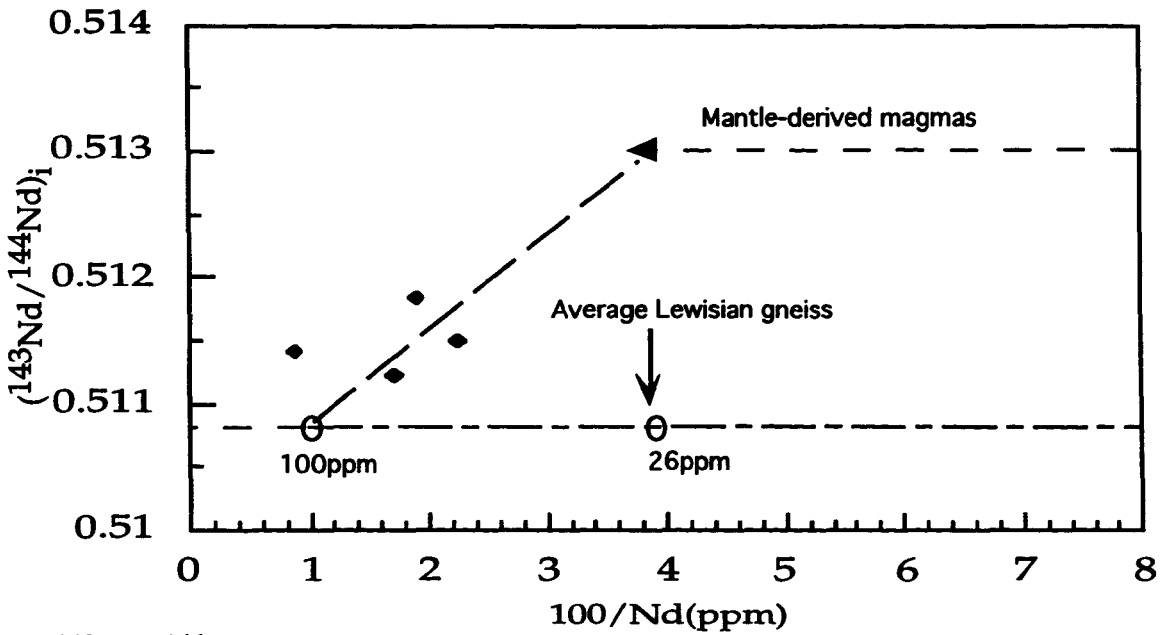

Fig. 8.11 Plot of $(^{143}Nd/^{144}Nd)_i$ against 100/Nd for Skye granites and their possible protoliths (see text for explanation).

controlling the variations of both isotopic systems is considered to be minimal.

The Nd and Sr isotopic compositions of the Beinn an Dubhaich, Loch Ainort, Marsco and Glamaig granites are plotted on Fig. 8.12, together with the fields of possible sources (data from: Hamilton et al., 1979; Dickin, 1981; McCulloch and Chappell, 1982; Dickin and Jones, 1983; Dickin et al. 1987; Dempsey et al., 1990; Wallace et al., 1994). The wide range in initial $^{87}Sr/^{86}Sr$ ratios and ε^{i}_{Nd} values in the Skye granites (0.7062-0.7128 and -14.0- -25.8, respectively) preclude a simple, unique origin for these granites (for example, derived wholly from the Hebridean mantle or from Lewisian amphibolite facies gneiss).

The very unradiogenic Nd isotopic compositions of the granites clearly suggest the presence of an old crustal component such as Lewisian gneiss (Halliday, 1984; Halliday et al., 1985; Hansmann and Oberli, 1991). Indeed, Halliday (1984) has proposed, in his study of Scottish Caledonian granitoids, that values of ε_{Nd} less than -6 are a good indication of the incorporation of crustal melts in granitoid sources. The variation in initial Sr isotopic composition could reflect the involvement of upper crust (Lewisian amphibolite facies gneiss) along with a mantle-derived component, with or without a lower crust component (Lewisian granulite facies gneiss), especially in Loch Ainort Granite.

The distribution of data points on Fig. 8.12 suggests the involvement of Lewisian amphibolite facies gniess in the Beinn an Dubhaich, Glamaig and Marsco granites, whereas the contribution of lower crustal Lewisian granulites is suggested from the position of the Loch Ainort sample. Thus, this scatter of the data could reflect the heterogeneous nature of the contaminants; indeed Thirlwall and Jones (1983) have indicated a large range in ε^{60}_{Nd} for Lewisian amphibolites and granulites.

Dempsey et al. (1990) attributed the narrow range in Sr isotopic composition of the Donegal granitoids to the low Sr content of crustally-derived partial melts, because of plagioclase acting as a stable residual phase. In contrast, at mantle depths, plagioclase is generally unstable during melting processes, and thus the mantle-derived component will have a high Sr concentration. In this respect, the initial $^{87}Sr/^{86}Sr$ ratio of the magma will be generally little changed by low degrees of crustal contamination, whereas the Nd isotopic signature will be affected more easily by any interaction with highly variable (in terms of Nd isotopic signatures) crustal material (Dempsey et al., 1990). This is because the Nd concentration in mantle-derived melts is low, whereas in crustal melts it is higher. However, the Skye granites have a large range in $(^{87}Sr/^{86}Sr)_i$ and more limited range in $(^{143}Nd/^{144}Nd)_i$: this could be an indication of larger amounts of contamination, because if the contamination occurs with a more evolved magma or during later stages of fractional crystallisation, where the Nd concentration of the magma has risen and the Sr concentration has fallen, then it will have a greater effect on $^{87}Sr/^{86}Sr$ and a lesser effect on $^{143}Nd/^{144}Nd$.

The Skye granites display a wide range of Sr contents (6-137 ppm) presumably due to variable degrees of plagioclase fractionation (see Chapters, III, IV, VI). The unknown amount of crustal Sr which contributed to each granite, and the effect of residual plagioclase in controlling the Sr content of crustal melts, precludes the use of the Sr isotope evidence to draw quantitative conclusions about the proportion of crustal (upper or lower) materials in each granite (cf. Dickin, 1981).

Due to the similarity of the Nd isotopic compositions of the Lewisian granulite and Lewisian amphibolite facies gneisses, Nd evidence also cannot be used to discriminate between upper and lower crustal materials.

On the basis of the Pb contents of the Skye granites, Dickin (1981) estimated that the proportion of melt derived from amphibolite facies gneiss in each granite is as follows: Glamaig (5%), Loch Ainort (8%), both Marsco and Beinn an Dubhaich (17%). This gives the impression that greater degrees of upper crustal contamination occurred in the more evolved granites. However, the effect of alkali feldspar fractionation on the Pb content of crustal melts and each granite may raise questions with the estimates of Dickin (1981).

However, the systematic variation of initial Nd and Sr isotopic compositions could, as was pointed out above, be the result of the mixing of two components in different proportions to produce the source materials of the Skye granites. These components could have been Palaeocene Hebridean mantle-derived melts and Lewisian amphibolite facies gneiss or melts derived therefrom. Possible crustal and mantle component compositions are indicated on Fig. 8.12, and their estimated average Sr and Nd contents are 130ppm, and 26ppm, and 180ppm and 16ppm, for amphibolite and mantle, (data from: Dickin, 1981; Dickin and Jones, 1983; Dickin et al., 1984; Dickin et al., 1987; Dempsey et al., 1990; Wallace et al., 1994). The average values of ε^{58}_{Nd}Ma are +8.5 and -34 for mantle and crust, respectively, (data from: Dickin and Jones, 1983, Frost and O'Nions, 1985; Dempsey et al., 1990; Cohen et al., 1991) and the average initial Sr ratios at 58 Ma are 0.7174 for amphibolite facies gneiss and 0.7028 for mantle (data from: Carter et al., 1978; Dickin, 1981; Dickin and Jones, 1983; Frost and O'Nions, 1985).

The mixing line between these two components was calculated according to the equation set out by Faure (1977; 1986, page 148, see Appendix II). The model gives a qualitative fit through the analysed data. However, given the heterogeneous nature of the Lewisian amphibolites and the fact that

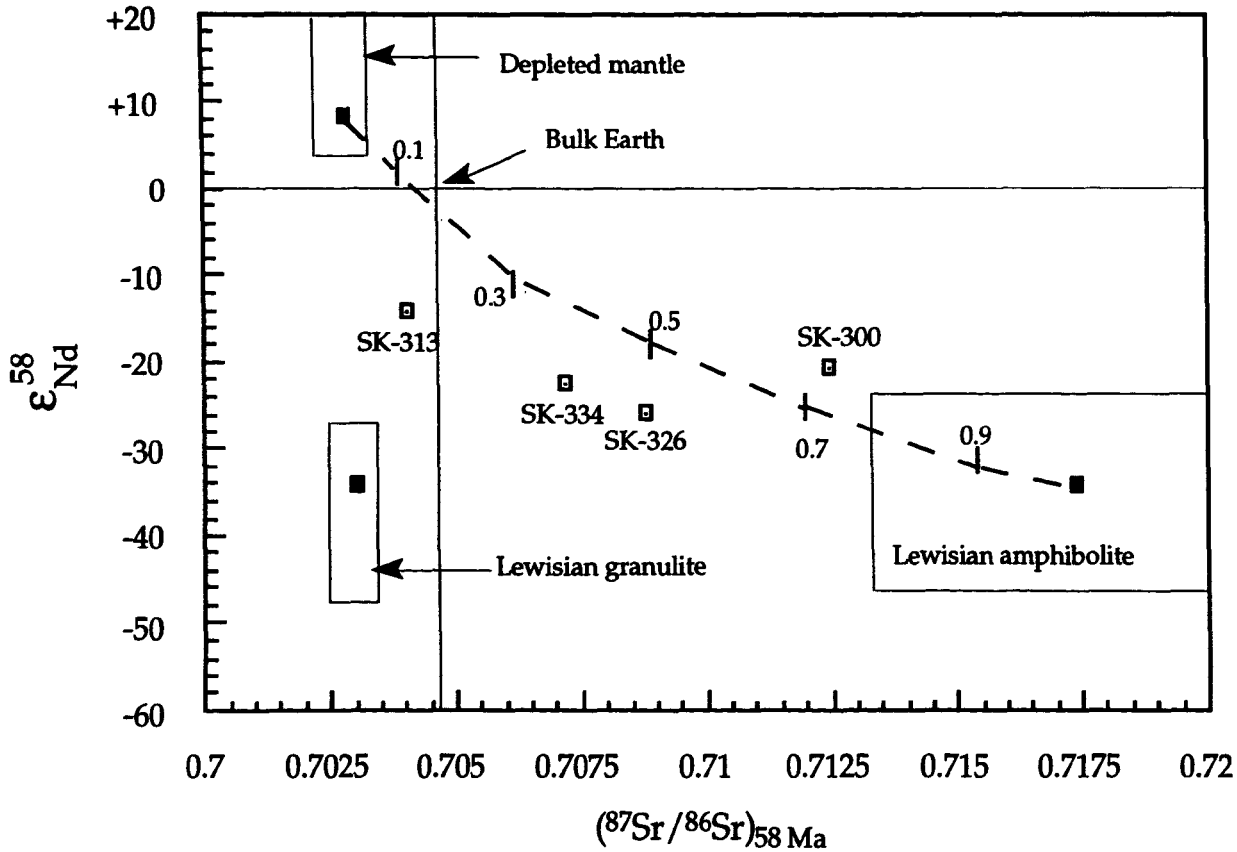

Fig. 8.12 Initial Nd and Sr isotopic compositions of Skye granites and their possible country (source) rocks. Data for source rocks are from: (Dickin, 1981; Dickin and Jones, 1983; Dempsey et al., 1990). Where: SK-300, Beinn an Dubhaich; SK-313, Loch Ainort; SK-326, Glamaig; SK-334, Marsco. See main text for discussion.

average compositions were used for both end members in this calculation, mixing between mantle and Lewisian amphibolite with a ε^{58}_{Nd} value higher than -34 will more closely approximate to the Beinn an Dubhaich Granite, whereas values lower than -34 could produce the remaining granites. The lower values could also be produced by either having a higher Sr/Nd in the mantle-derived end member, or a lower Sr/Nd in the crustal-derived end member, such that the mixing curve would become more pronounced. The contribution of Lewisian amphibolites to each granite are (10%) for Loch Ainort, (40%) for Marsco, (50%) for Glamaig and (72%) for Beinn an Dubhaich. These results do not agree with Dickin's estimations, possibly because Dickin (1981) based his estimation on Pb contents of these granites, and Pb contents are highly dependent on alkali feldspar fractionation.

These proportions of Lewisian amphibolite in the Skye granites indicates that the Beinn an Dubhaich Granite has the largest crustal component, whereas the Loch Ainort has the smallest crustal component. DePaolo and Wasserburg (1979) have noted that ε^{i}_{Nd} values of continental basalts which cluster near ε^{i}_{Nd}= 0 do not represent a mixture between a mantle-derived magma with positive ε^{i}_{Nd} and crustal material with negative ε^{i}_{Nd}. Indeed, DePaolo (1981) has shown that this sort of clustering near any one of the mixing end members could result due to extensive crustal assimilation only. In the case of the Skye granites, the major- and trace-element data (Chapter VI) argue against the compositional variations being due to magma mixing, and thus the isotopic trends are more likely to be due to extensive degrees of crustal contamination of basic magmas.

Therefore, it is most likely that the four granites are the products of the differentiation of different pulses of basaltic magma which rose independently into the upper crust and were contaminated with different

crustal lithologies, as suggested by the refractory zircons in the Glamaig and Marsco granites (Section 8.6)(but see also, Patchett, 1980; Palacz, 1985).

8. 5 Model ages

Despite the fact that the Skye granites may be composites of material derived from the mantle at different times (e.g. during the Archaean and the early Tertiary), and their Sm/Nd ratios may have been influenced by crustal processes (Wilson et al., 1985), model ages are tested here, to evaluate an estimate of the average time that the material in each sample has been resident in the continental crust, i.e. older components are involved in the measured $^{143}Nd/^{144}Nd$ for granites.

The T_{CHUR}^{Nd} model age is the time since a sample would last have had a Nd isotopic composition the same as CHUR. Similarlly, the T_{DM}^{Nd} model age is the time since a sample would last have had a Nd isotopic composition the same as depleted mantle (DM). Both model ages are calculated for whole rock samples, by using the following formula:

$$T_{CHUR}^{Nd} = (1/\lambda)\ln[((^{143}Nd/^{144}Nd)_{sample} - (^{143}Nd/^{144}Nd)_{CHUR}) / ((^{147}Sm/^{144}Nd)_{sample} - (^{147}Sm/^{144}Nd)_{CHUR}) + 1)]$$

The same equation is used for calculating T_{DM} by substituting the appropriate $(^{143}Nd/^{144}Nd)$ and $(^{147}Sm/^{144}Nd)$ values for DM instead of CHUR, where:

$(^{143}Nd/^{144}Nd)_{CHUR,\ today} = 0.512638$; $(^{143}Nd/^{144}Nd)_{DM,\ today} = 0.513148$; and,

$(^{147}Sm/^{144}Nd)_{CHUR} = 0.1967$; $(^{147}Sm/^{144}Nd)_{DM} = 0.2136$; (values are from Jacobsen, 1988; Rollinson, 1993).

The calculated ages are as follows:

Granite	T_{CHUR}^{Nd} (Ma)	T_{DM}^{Nd} (Ma)
Beinn an Dubhaich	2077	2515
Marsco	2275	2681
Loch Ainort	1705	2288
Glamaig	2259	2619

The results show that the average ages of separation of Nd in the Skye granites from Chondrite Uniform and Depleted Mantle reservoirs are about 1700 to 2270 Ma and 2290 to 2680 Ma, respectively. The Beinn an Dubhaich Granite has a younger T_{DM} model age than the Glamaig Granite and this is consistent with its ε_{Nd}^{58} value being significantly higher (Table 8.2). This may reflect their components being derived from the mantle at different times, with Glamaig's components being older. Alternatively, the granites may represent mixtures of components separated from the mantle at similar times, in this case the Glamaig Granite contains a higher proportion of older components than the Beinn an Dubhaich.

The Marsco Granite has a slightly lower ε_{Nd}^{58} value (-22.3) and an older T_{DM} model age compared with the Beinn an Dubhaich Granite, suggesting the involvement of older crustal components (Wilson et al., 1985). The Loch Ainort Granite has the highest ε_{Nd}^{58} value (-14.0) and the lowest model age, indicating the involvement of either younger crustal components, or a greater proportion of Tertiary mantle-derived material.

The measured T_{CHUR}^{Nd} model ages are less than the T_{DM}^{Nd} model ages, and thus provide estimates of the minimum ages of the oldest components involved in the Skye granite source(s) (cf. McCulloch and Chappell, 1982). The Nd data for the Skye granites indicate that some of their source crustal materials were derived from the mantle at about 2300 Ma or older. This is consistent with the involvement of Lewisian crustal materials which are thought to have separated from an undifferentiated mantle at 2920 Ma

(Carter et al., 1978, Hamilton et al., 1979). A crustal contribution to the Skye granites is further supported by the presence of inherited zircon in certain intrusions (See section 8.6 below), and the intermediate $^{143}Nd/^{144}Nd$ signatures of the granites between mantle and crustal sources (see Sections 8.3.2 and 8.4).

It may be concluded that if the Nd in the granites had a simple two-stage growth history: firstly of Nd growth in CHUR between the formation of the Earth and the generation of the granite protoliths, and then subsequently with the granite's present day Sm/Nd ratio, the time of separation from a chondritic reservoir would have been between 1705 and 2275 Ma, whereas the time of separation from a depleted mantle would have been between 2288 and 2681 Ma. The wide range of Nd model ages for the Skye granites may best be interpreted, therefore, as representing variable mixtures of older crustal and Tertiary mantle-derived materials (cf. Arndt and Goldstein, 1987).

8. 6 Accessory minerals

The Sm-Nd isotopic composition of granitic rocks is often dominantly controlled by REE-rich accessory phases which may be refractory (Mittlefehldt and Miller, 1983; Paterson and Stephens, 1992; Paterson et al., 1992a, b; Evans and Hanson, 1993). The refractory mineral phases routinely identified within granitic rocks (for example, Paterson et al. 1992a, b; Williams, 1992) are unlikely to have been derived from the mantle (Kresten et al., 1975; Davis, 1978; Hansmann and Oberli, 1991). Therefore, identified inherited components in granitoid rocks can provide information about the crustal components of granitic magmas. Given the large crustal input to the Skye granites shown by the Sr and Nd data (Sections 8.2 and 8.3), apatite and

zircon from the Skye granites have been investigated, in the light of their textural and isotopic characteristics.

Accessory minerals (zircon and apatite) are extremely difficult to investigate with transmitted light, due to their small size and high refractive indices (cf. Paterson et al., 1989). Thus, other techniques are widely used to investigate these small grains (zircon in particular): backscattered electron imaging, which displays mean atomic number (Z)-contrast images (ZCI), and cathodoluminescence (CL) images (for example, Paterson et al., 1989, 1992a, b; Hancher and Miller, 1993; Vavra, 1993, 1994).

Zircon and apatite crystals were separated from crushed samples, using normal separation techniques as described in Appendix III. Due to the low modal abundances of these minerals, backscattered electron (BSE) and cathodoluminescence (CL) images were carried out using grains mounts. Whereas apatite crystals are inclusion free, zircon grains contain apatite needles.

8. 6. 1 Textural behaviour and refractory nature

(i) Zircon:

Zircon crystals from Beinn an Dubhaich (SK-300), Loch Ainort (SK-313), Marsco (SK-334) and Glamaig (SK-326) have been investigated texturally.

Sector zoning is a common feature in accessory minerals, and is often superimposed on continuous and discontinuous zoning (cf. Hoffman and Long, 1984; Paterson et al., 1989). This type of zoning has been observed by ZCI textural studies within the Beinn an Dubhaich and Loch Ainort zircons (Figs. 8.13 and 8.14), possibly indicating a post-crystallisation event which has caused changes to these zircons (Paterson et al., 1989).

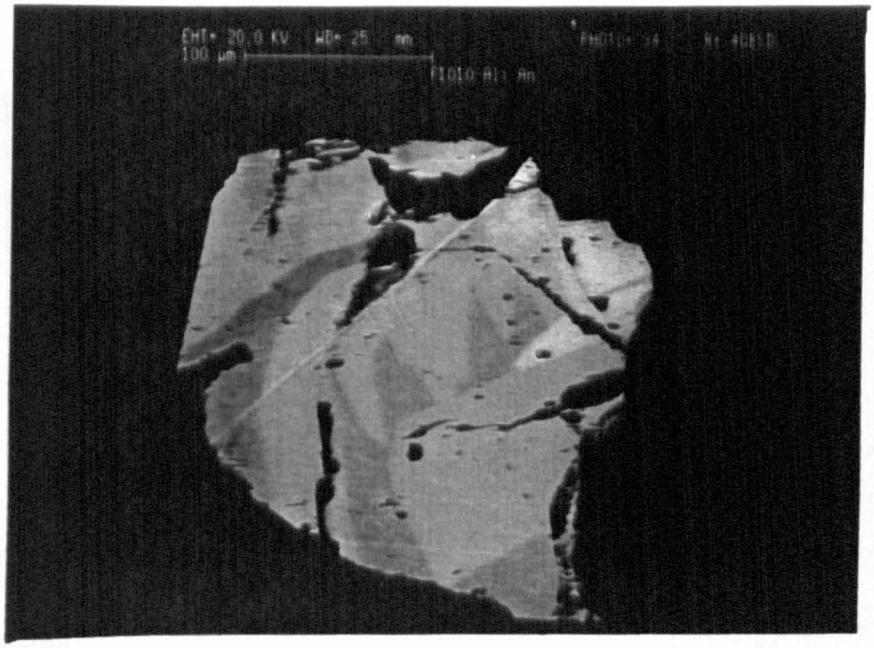

Fig.8.13 A Z-contrast image of a zircon from the Beinn an Dubhaich Granite, illustrating sector zoning. Scale bar at top of image.

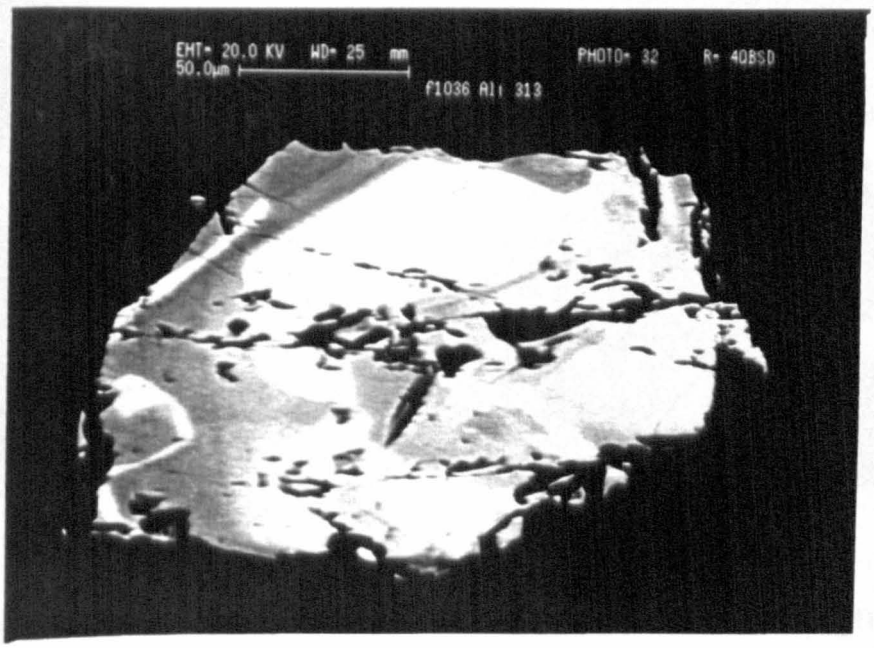

Fig.8.14 A Z-contrast image of a zircon from the Loch Ainort Granite, illustrating sector zoning. Scale bar at top of image.

Fig.8.15 Two cathodoluminescence images of zircon grains from the Glamaig Granite, showing euhedral refractory cores (R) included within magmatic grains (M). Field of view: 0.31mm x 0.22mm.

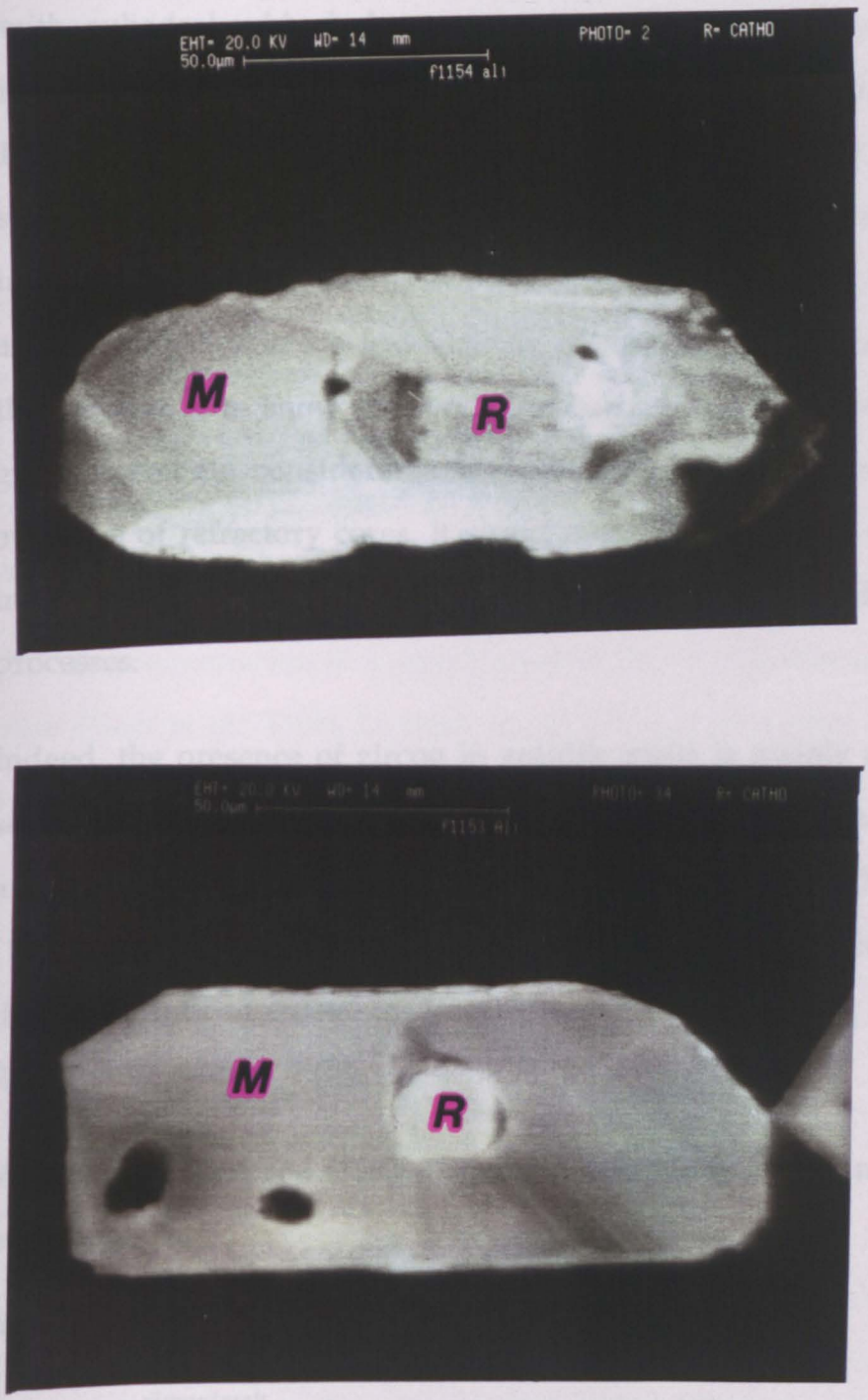

Fig.8.16 Two Z-contrast images of zircon grains from the Marsco Granite, showing euhedral refractory cores (R) included in magmatic grains (M). Scale bar at top of images.

ZCI and CL investigations reveal some refractory cores among Marsco and Glamaig zircons. These cores have a euhedral shape (Figs. 8.15 and 8.16), with euhedral-subhedral overgrowths. The euhedral cores suggest that inherited zircon does not always occur as anhedral cores (cf. Paterson et al., 1992b), and, most importantly, indicates that the refractory zircons were not significantly disturbed by mechanical abrasion before their incorporation into the granite magma(s).The amounts of inherited zircon are about 10% and 50% for the Marsco and Glamaig granite zircons, respectively. Although the isotopic data show that both the Loch Ainort and Beinn an Dubhaich granites contain considerable amounts of crustal components, there is no evidence of refractory cores. It seems most likely that the inherited zircons in these two granites have been completely dissolved during magmatic processes.

Indeed, the presence of zircon in granitic melts is mainly dependent on Zr solubility and the dissolution kinetics of the inherited phases (Hansmann and Oberli, 1991). Based on experimental studies, Dietrich (1968), Watson (1979) and Watson and Harrison (1983) have shown that Zr solubility during periods of crustal melting increases with increasing temperature and the cationic ratio M = (Na + K + 2 Ca)/(Si x Al) of the melt.

Watson and Harrison (1983) provide a saturation model in the form of the equation:

$$\ln D_{Zr}^{zircon/melt} = -3.80 - [0.85 \times (M-1)] + (12900/T)$$

Where: $D_{Zr}^{zircon/melt}$ is the concentration ratio of Zr in a stoichiometric zircon to that in the melt; T is the absolute temperature (i.e. in K); and M is the cation ratio (Na + K + 2 Ca)/(Si x Al). In this model the melt should contain at least ~ 2wt.% H_2O.

This equation can be used to calculate a zircon saturation temperature (i.e. possibly the peak temperature of anatexis (Harrison et al., 1987), based on the source Zr concentration, and the likelihood that the granites contain inherited zircon cores. The uncertainty of the saturation temperature is recommended by Harrison et al. (1987) as ± 30°C of the calculated temperature.

Paterson et al. (1992a) pointed out that a granite without inherited zircon should have a whole-rock Zr concentration close to the concentration of Zr that was dissolved in the melt. In this respect, measured whole-rock Zr concentrations of the Beinn an Dubhaich and Loch Ainort granites should represent the Zr dissolved in their magmas.

The Zr concentration in a stoichiometric zircon was assumed to be 517000 ppm (Deer et al., 1989), in order to calculate Zr saturation temperatures for samples SK-300, SK-313, SK-326 and SK-334 (Table 8.3).

Table 8. 3 Zircon and apatite solubility data

Sample	M	SiO_2 (Wt.%)	Zr (ppm)	P_2O_5 (Wt.%)	Zr saturation T(°C)	P_2O_5saturation T(°C)
SK-300	0.909	74.25	184.7	0.081	833 ± 30	929 ± 25
SK-313	0.943	71.73	546.9	0.054	943 ± 30	867 ± 25
SK-326	0.974	68.62	311.5	0.175	812 ± 30 a	955 ± 25
SK-334	0.816	76.71	780.1	0.009	986 ± 30 b	770 ± 25

a Corrected for 50% inherited zircon: uncorrected temperature is 879°C; b corrected for 10% refractory zircon: uncorrected temperature is 999°C. Where, SK-300, Beinn an Dubhaich; SK-313, Loch Ainort; SK-326, Glamaig; SK-334, Marsco.

From these calculations, the Glamaig Granite (SK-326) has a Zr saturation temperature of 879 ± 30°C, and correcting for 50% refractory zircon lowers the calculated temperature to 812 ± 30°C. The Marsco Granite (SK-334) has a Zr saturation temperature of 999°C, and correction for 10% inherited zircon lowers the calculated temperature by 13°C to 986°C.

These Zr saturation temperatures may correspond to the temperatures at the peak of anatexis (Harrison et al., 1987). However, some physical

processes can change the Zr concentration of the melt, which consequently will affect the apparent saturation temperatures (Watson et al., 1989). These processes are: incorporation or fractionation of zircon crystals into or from the melt; and, less importantly, the physical isolation of accessory phases from the melt as inclusions in other minerals.

Used in conjunction with temperatures derived from feldspar thermometry (Chapter IV) for the Beinn an Dubhaich Granite, sample SK-300 (790°C), and the Glamaig Granite, sample SK-326 (881°C), the Zr saturation temperature and the equilibrium temperature of coexisting clear plagioclase and alkali feldspar are consistent within their expected errors (i.e. ± 30°C for Zr saturation temperature (Harrison et al., 1987) and ± 50°C for feldspar thermometry (Ferry, 1985)).

Consideration of the calculated temperatures indicates that only the Beinn an Dubhaich and Glamaig granites have crystallised at temperatures reasonable for a granitoid magma (Clarke, 1992). In contrast, both the Loch Ainort and Marsco granites appear to have crystallised at considerably higher temperatures, suggesting higher temperatures of their parental magmas (Watson and Harrison, 1983), possibly due to the influx of more basic magma pulses into these magmas before their final emplacement.

(ii) Apatite:

Due to the very low modal abundance of apatite in the Loch Ainort Granite (SK-313) and the Marsco Granite (SK-334), apatite needles were separated only from the Beinn an Dubhaich and Glamaig granites, SK-300 and SK-326, respectively.

From ZCI textural studies, the apatite needles from the Beinn an Dubhaich Granite show normal zoning (Fig. 8.17), whereas these from Glamaig show oscillatory zoning (Fig. 8.18). Pidgeon (1992) reports oscillatory zoning in

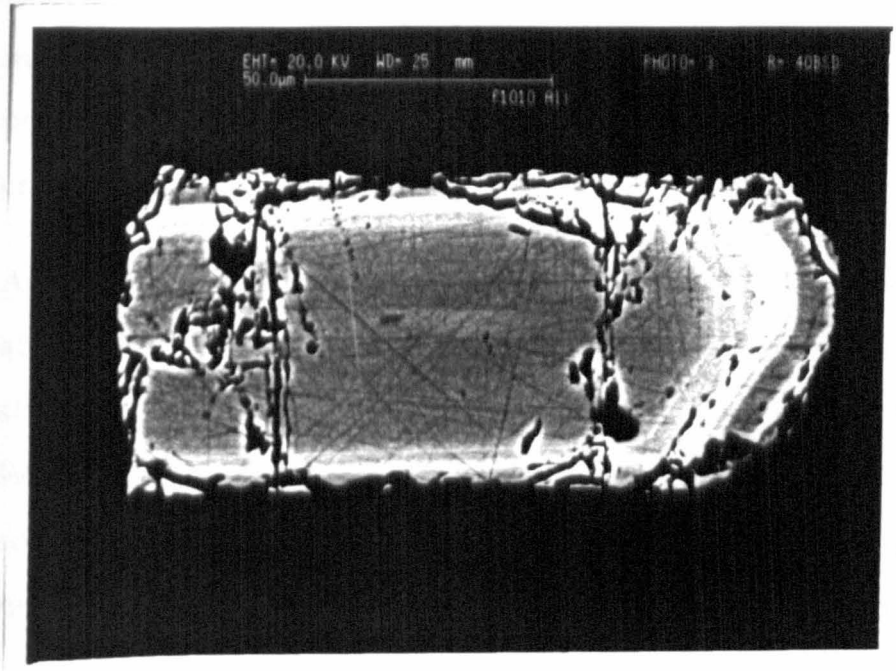

Fig.8.17 A Z-contrast image of apatite from the Beinn an Dubhaich Granite, showing normal zoning. Scale bar at top of the image.

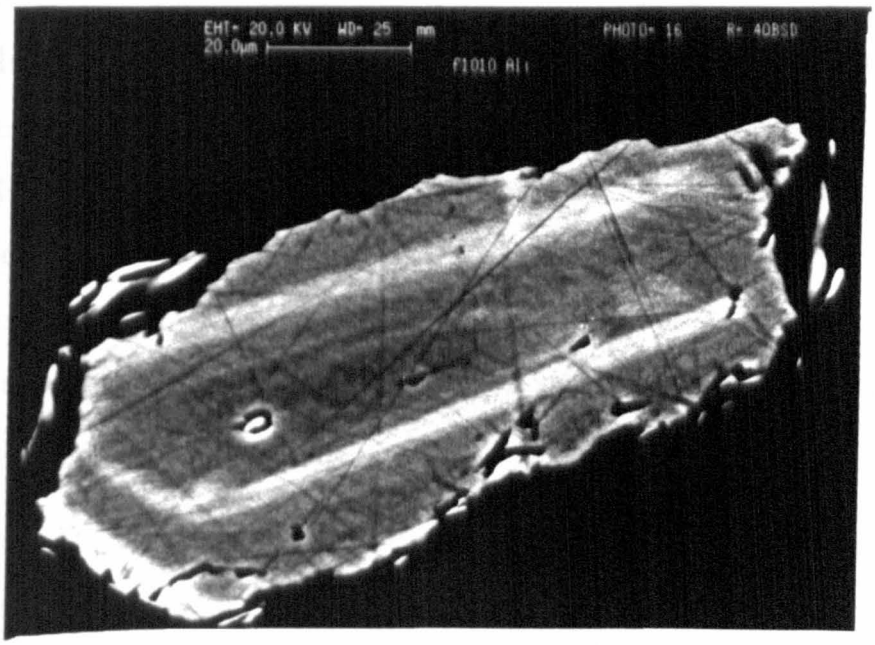

Fig.8.18 A Z-contrast image of apatite from the Glamaig Granite, showing oscillatory zoning. Scale bar at top of the image.

zircon grains and concludes that the occurrence of such zoning is due to magmatic processes. This oscillatory zoning in the Glamaig apatite is possibly due to the changes in undercooling of the Glamaig magma during crystallisation (Loomis, 1982).

An accessory mineral's saturation may be limited by a single, low-abundance component in the melt. Such components are called essential structural constituents (ESC's) (Sun and Hanson, 1975; Harrison and Watson, 1984). In the case of apatite, the ESC is phosphorus (P); because the solubility of P in a felsic melt is limited, apatite saturation in the melt is reached at low concentrations of P_2O_5 (Harrison and Watson, 1984).

Harrison and Watson (1984) describe apatite solubility as a function of absolute temperature and melt composition by the following expression:

$$\ln D_P^{apatite/melt} = [(8400 + ((SiO_2 - 0.5) \times 2.64 \times 10^4))/T] - [3.1 + (12.4(SiO_2 - 0.5))]$$

Where: $D_P^{apatite/melt}$ is the concentration ratio of P in a stoichiometric fluorapatite to that in the melt; SiO_2 is the weight fraction of silica in the melt; and T is temperature in K. The P concentration in a stoichiometric fluorapatite was assumed to be 40 wt.%. This model appears to be valid between: 45 and 75 wt.% SiO_2, 0 and 10 wt.% H_2O, and for the range of pressures expected in the crust (Harrison and Watson, 1984). The uncertainties associated with these saturation temperatures are ~ $\pm$ 25°C (Evans and Hanson, 1993).

Theoretical phosphorus saturation temperatures have been calculated for four samples; by using XRF data (Table 6.1) for SiO_2 and P_2O_5, results are presented in Table 8.3. Samples which have a very low modal abundance of apatite needles (SK-313 and SK-334, Loch Ainort and Marsco, respectively) give phosphorus saturation temperatures of 867°C and 770°C, respectively. These temperatures are lower than their counterpart Zr saturation

temperatures, possibly due to the low P_2O_5 concentrations as a result of small amounts of modal apatite. The Beinn an Dubhaich and Glamaig granites (SK-300 and SK-326, respectively) have phosphorus saturation temperatures of 929°C and 955°C, respectively, well in excess of the calculated Zr saturation temperatures.

Zr saturation temperatures for samples SK-300 (Beinn an Dubhaich) and SK-326 (Glamaig) granites were considered earlier as reasonable for granitic magmas. Thus, their P saturation temperatures appear relatively high. These higher P saturation temperatures could be attributed to one of the following possibilities:

(a) Both the Beinn an Dubhaich and Glamaig granites contain refractory apatite. However, apatite cores are not observed in either granite. This could be due to diffusion erasing chemical heterogeneities (Paterson et al., 1992a), although the textural evidence suggests otherwise (i.e. the presence of zoned apatite);

(b) The P_2O_5 concentration does not represent that of the liquid composition of the magma due to the cumulus nature of the apatite;

(c) There are other parameters which may affect apatite solubility in felsic melts, other than those identified by Harrison and Watson (1984). These parameters include: CaO activity and the alkalinity of the melt (Watson and Capoblanco, 1981). Indeed, these two samples are metaluminous, with (Na + K)/Al = 0.93 for SK-300 and 0.83 for SK-326. Significantly, Watson and Capoblanco (1981), recorded a lower apatite temperature (~ 850°C) for highly-silicic peralkaline melts, with (Na + K)/Al = 1.2-2.0.

It may be concluded that:

(1) From textural observations there is no evidence of a refractory apatite component within the samples studied;

(2) The textural investigations show no evidence for refractory zircons in the Beinn an Dubhaich and Loch Ainort granites, despite the crustal contribution into these granites, suggesting that any refractory zircons may have been completely dissolved during magmatic evolution;

(3) Inherited zircon occurs only in the Glamaig and Marsco granites, with about 50% of the total zircon in the Glamaig Granite being inherited, and only 10% of the total zircon present in the Marsco Granite being inherited;

(4) The high Zr saturation temperatures of the Loch Ainort and Marsco granites are possibly due to higher temperatures of their magmas, whereas the higher P saturation temperatures of the Beinn an Dubhaich and Glamaig granites are possibly due to the metaluminous nature of these granites.

8. 6. 2.Isotope studies

As each mineral within a rock has a different Sm/Nd ratio, then consequently, through time, it will evolve to have a different ε_{Nd} value. Therefore, phases which are incorporated into a granitic magma and do not equilibrate with it (i.e. are refractory) will have Nd isotopic signatures different from the same mineral which was precipitated from that magma. Analogous behaviour forms the basis for the identification of inherited Pb in zircons (e.g. Pidgeon and Aftalion, 1978; Rogers et al., 1989; Rogers et al., 1990).

Several studies have shown that zircon should have higher Sm/Nd ratios relative to average continental crust and many REE-rich accessory phases precipitated from granitic melts (for example, Gromet and Silver, 1983; Sawka, 1988; Hinton and Upton, 1991). Consequently, zircons which have crystallised from a melt should evolve to more positive ε_{Nd} values in a given period of time than their host rock. Thus, inherited zircon is expected to have higher ε_{Nd} values than its granitic host at the time of magmatism (Paterson et al., 1992a)

The Sm-Nd isotope data for whole-rock and mineral separates, including accessory phases, are given in Table 8.2 for the four studied granites. All grains used for isotope analysis were hand-picked; indeed, zircon grains were separated according to their morphology (i.e. anhedral and prism crystals, zircon A and P, respectively, Table 8.2), as in the light of U-Pb studies on granites prismatic grains are more likely to represent melt-precipitated grains (i.e. new magmatic) whereas anhedral grains could potentially be inherited (for example, Rogers et al., 1989). Earlier in this chapter all Sm-Nd isotopic compositions of ferromagnesian minerals (either pyroxene or amphibole) were shown to be in equilibrium with their respective whole rock compositions.

From the data in Table 8.2, the most important features concerning the accessory phases are:

(i) The ε^{58}_{Nd} values of -20.7 for apatite, and -20.1 and -20.3 for anhedral and prismatic zircons, from the Beinn an Dubhaich Granite are in equilibrium with each other and with their host rock.

(ii) The ε^{58}_{Nd} values of -19.8 and -18.9 for anhedral and prismatic zircons from the Marsco Granite, are in equilibrium with each other. However, they

are approximately 2.5 ε_{Nd} units more positive than their host rock, although their Sm/Nd ratios are very small.

(iii) In the Loch Ainort Granite, the ε^{58}_{Nd} values of anhedral and prismatic zircons are: -13.3 and -15.0, and these are in equilibrium with their host rock.

(iv) The ε^{58}_{Nd} value of -25.7 for apatite from the Glamaig Granite is in equilibrium with the whole rock value (-25.8). However, the values of their counterpart zircons (-18.6 and -19.9 for the anhedral and prismatic morphologies, respectively) are about 6 ε_{Nd} units more positive. They also have very low Sm/Nd ratios.

The above observations indicate that:

1) the analysed apatite appears to be in equilibrium with coexisting amphibole and their respective whole rocks, indeed these two minerals hold the bulk of the whole rock's REE (see Chapter VI);

2) zircons from the Beinn an Dubhaich and Loch Ainort granites are also in Nd isotopic equilibrium with their respective whole rocks and with the other minerals in their respective whole rock;

3) Nd isotopic disequilibrium between zircons and the other phases does exist in the Marsco Granite and, to a larger extent, in the Glamaig Granite, suggesting the presence of refractory components; and,

4) the refractory zircons have unusually low Sm/Nd ratios.

(A) Equilibrium accessory phases:

The recorded equilibrium in initial Nd isotopic composition that exists between: zircons and apatite in the Beinn an Dubhaich Granite; zircons in the Loch Ainort Granite; and apatite in Glamaig Granite, to their respective host rocks, suggests that none of these phases has refractory components, or,

if they did, that they equilibrated during the Palaeocene magmatic episode. This is consistent with the textural observations as demonstrated by the absence of refractory cores (Figs. 8. 13, 8.14, 8.17 and 8.18)

(B) Disequilibrium accessory phases:

As noted above, only zircons from the Glamaig and Marsco granites exhibit disequilibrium with respect to their co-existing minerals and host rocks. These zircons have unusual, very low, Sm/Nd ratios relative to their co-existing minerals and to typical continental crust. Any explanation of this disequilibrium must take into consideration both the nature of the disequilibrium, and, why these zircons have such low Sm/Nd ratios.

Paterson et al. (1992a) assumed three possible causes of such disequilibrium:

(i) Post-crystallisation disturbance: This model implies that the zircons were in equilibrium with the other phases at the time of crystallisation, but were subsequently open to Sm-Nd isotopic exchange. As the Marsco Granite was emplaced after the Loch Ainort Granite, then any post-crystallisation processes affecting the Marsco Granite should have at least partially affected the Loch Ainort Granite, which is not the case. Further, the observations of Futa (1981) and the diffusion experiment of Watson et al. (1985) suggest that apatite should be disturbed by long duration, high temperature events. However, the apatite and amphibole from the Glamaig Granite were in isotopic equilibrium at the time of crystallisation, which suggests they have not been isotopically disturbed. Therefore, any disturbance of the zircons would have to have been at low T (less than 300°C).

As noted above, zircons should have higher Sm/Nd ratios relative to many REE-rich accessory phases (see Hinton and Upton, 1991) and to continental crust (Taylor and McLennan, 1985). Consequently, equilibration between zircon and such materials will lower the ε_{Nd} value of the equilibrated

zircon. Thus, if equilibrium is achieved between magmatic zircon and any other material to produce the current ε Nd values (i.e. the initial ε Nd values for Glamaig and Marsco zircons), the other coexisting minerals should also be affected, which is not the case. Therefore, the observed Nd-isotopic disequilibrium is unlikely to be due solely to post-crystallisation disturbance.

(ii) Mixing of isotopically distinct magmas: The ε_{Nd} values of zircons from the Glamaig and Marsco granites could be the result of mixing of partially crystallised magmas. This implies that two isotopically distinct magma sources were involved and that each had crystallised at least some zircon before mixing. This process will produce two different zircon populations. However, if the zircons crystallise at a relatively late (magmatic) stage, as suggested by Wark and Miller (1993), then the mixed magma should produce zircons with near or identical equilibrium Sm-Nd isotopic compositions. However, as the possibility of magma mixing being a dominant process was eliminated during the discussion of the major- and trace-elements (Chapter VI), then such a mixing model cannot be used as the sole explanation of apparent Nd isotopic disequilibrium.

(iii) Inheritance of Sm-Nd isotope signature: The textural evidence suggests that zircons from two granites (Glamaig and Marsco) contain refractory cores (Figs. 8.15 and 8.16). If the cores were actually produced during the Tertiary magmatic event, then it is most likely that the core should have the same initial Nd isotopic signature as the other minerals precipitated from the melt. The fact that the zircons which show textural cores are in initial Nd isotopic disequilibrium strongly suggests that the cores are inherited. Consequently, the measured ε^{58}_{Nd} values for the analysed zircons will be an average of the refractory and magmatic components.

In this respect, these zircons should have rims which are in initial Nd isotopic equilibrium with other phases precipitated from the granitic melts (i.e. have approximately ε^{58}_{Nd} values of -25.7 for the Glamaig Granite and -22.3 for the Marsco Granite). In contrast, the ε^{58}_{Nd} values of the cores will be more positive than those of the measured whole-grain values (i.e. more positive than about -18 for both granites). Their actual ε^{58}_{Nd} values will depend on the relative proportions of the core and rim components, their respective Nd isotopic compositions, and their Sm and Nd concentrations (Paterson et al., 1992a, b).

All of the equilibrium accessory phases in this study record 'normal' Sm/Nd ratios (Gromet and Sliver, 1983; Wark and Miller, 1993), whereas the zircons which show initial Nd isotopic disequilibrium have very low Sm/Nd ratios relative to their host rocks. If this isotopic disequilibrium is due to the presence of refractory cores, then the low Sm/Nd ratios of the zircons in the Glamaig and Marsco granites may be due to the unusually low Sm/Nd ratios in the inherited cores, as the zircons in the Loch Ainort and Beinn an Dubhaich granites, which do not show evidence for inherited cores, have high Sm/Nd ratios. There are two possible explanations for such low Sm/Nd ratios, which are not mutually exclusive:

(a) The refractory cores contain phases with very high Nd concentrations: phases such as apatite, for example, which will reduce the Sm/Nd ratio of the 'bulk' zircon grain. However, all of the analysed zircons (i.e. from all four granites) contain apatite needles as inclusions, randomly distributed in the zircon grains. These apatite needles have no apparent effect on the zircons from the Beinn an Dubhaich and Loch Ainort granites. Thus, the apatite inclusions in the zircon cores from the Glamaig and Marsco granites must have unusually high Nd concentrations and low Sm/Nd ratios to satisfy the low Sm/Nd ratio of the refractory cores.

(b)The equilibration of zircons with normal Sm/Nd ratios (but higher $^{143}Nd/^{144}Nd$ values than average bulk rock Skye granites) with a mineral with a low Sm/Nd ratio will reduce the Sm/Nd ratio of the equilibrated zircon. This type of equilibration behaviour is presented as a schematic model in Fig. 8.19, in which it is assumed that the zircons were open to isotopic exchange (Futa, 1981; Paterson et al., 1992a). These equilibrated zircons will maintain a nearly constant $^{143}Nd/^{144}Nd$ value after coming into contact with the low Sm/Nd mineral. Subsequently, the equilibrated zircons are incorporated into the Skye granite magmas (Marsco and Glamaig) (Fig. 8.20).

Therefore, the Nd isotopic compositions of the zircons from the Glamaig and Marsco granites represent the Nd isotopic compositions of refractory zircons (which have a low Sm/Nd ratio) and magmatic zircons from each granite magma. Assuming that the chemical and isotopic composition of the refractory zircons were the same in both cases and that these controlled the REE and isotopic composition of the mixed zircon after granite magmatism, then, the greater shift in $^{143}Nd/^{144}Nd$ of the zircon whole-grain value from magmatic value in the Glamaig Granite compared to that in the Marsco Granite (Fig. 8.20) is qualitatively consistent with the greater proportion of refractory core material in the former (50% compared to 10%).

8.7 Summary and conclusions

The Sr and Nd isotope data indicate:

(i) Crystallisation of the analysed samples from Skye granites appears to have occurred within a very short period of time (5Ma) at approximately 55-60Ma.

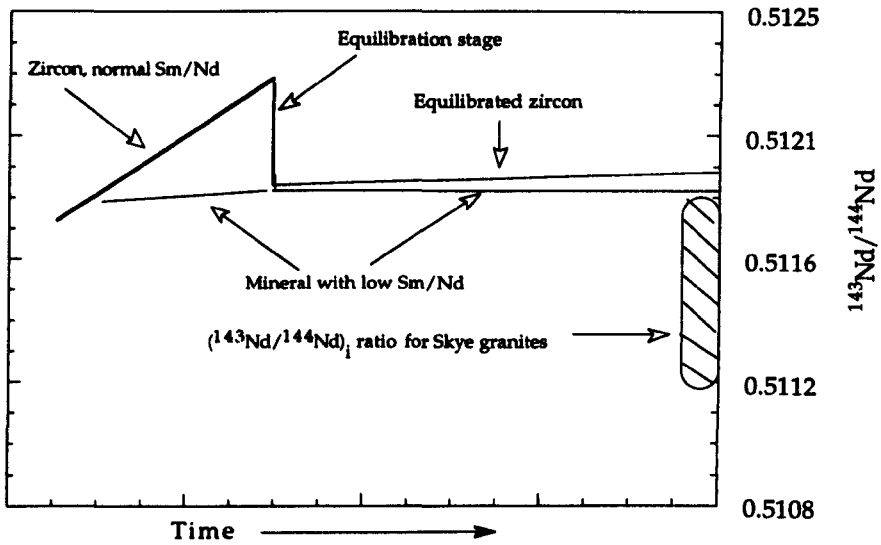

Fig. 8. 19 A model illustrating how equilibration between zircon with normal Sm/Nd and a mineral with low Sm/Nd, would produce, through time, zircon with low Sm/Nd. See main text for discussion.

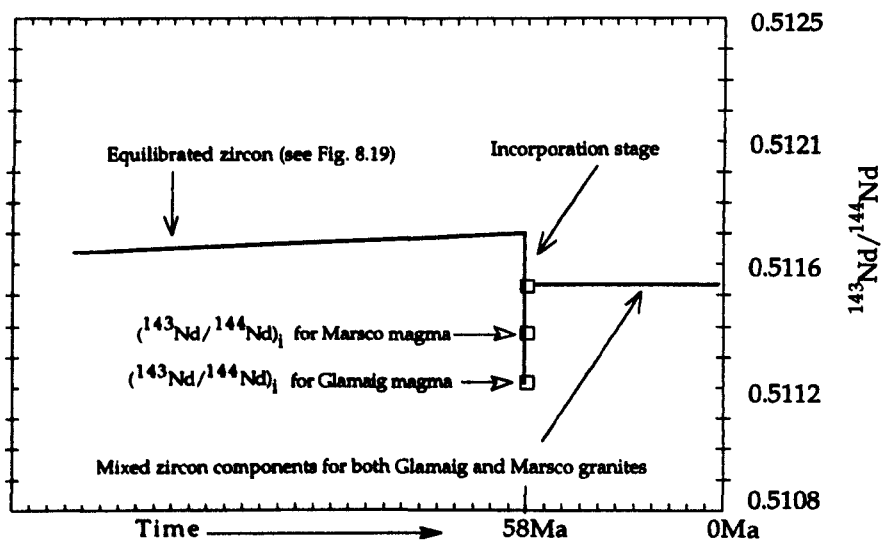

Fig. 8.20 A model illustrating the incorporation of a low Sm/Nd zircon into Skye granite magmas. See main text for discussion.

(ii) The observed heterogeneity in initial $^{87}Sr/^{86}Sr$ ratios between minerals from the Marsco and Loch Ainort granites is mainly due to hydrothermal alteration. This indicates that these two magmas have been severely affected by hydrothermal fluids, as suggested by the high water/rock ratios (see Chapter VII).

(iii) The four granites have distinct and different initial $^{87}Sr/^{86}Sr$ and ε^{58}_{Nd} isotopic compositions.

(iv) The observed variations in Sr and Nd isotopic compositions between the granites are unlikely to be due to either post-magmatic processes or due to source mantle heterogeneity, and most likely are the result of magma-crust interaction.

(v) Model age calculations indicate that the crustal components in the Skye granites were separated from a Chondritic Uniform Reservoir at, or before, about 1705 - 2275 Ma, or separated from a depleted mantle at, or before, about 2288 -2681Ma.

(vi) Sm/Nd values for whole rock samples are very similar and, consequently, imply that neither partial melting nor crystal fractionation has had a significant affect on this ratio during the evolution of the Skye granites.

(vii) The contribution of crustal lithologies to basaltic differentiates in the petrogenesis of the Skye granitic magmas is evident from the refractory zircons in the Glamaig and Marsco granites, and also from their intermediate isotopic composition between Hebridean mantle and crustal compositions. However, in the Beinn an Dubhaich and Loch Ainort granites, the absence of inherited zircons could just imply that the inherited zircons dissolved in the melts.

(viii) From Zr saturation calculations the Beinn an Dubhaich and Glamaig granites crystallised at temperatures reasonable for a granitoid magma. In contrast, both the Loch Ainort and Marsco granites appear to have crystallised at relatively high temperatures.

(ix) The inherited zircons in the Glamaig and Marsco granites have unusually low Sm/Nd ratios, possibly due to equilibration between the zircon and other mineral(s) with low Sm/Nd ratios.

(x) The Sr and Nd isotopic data indicate that regional bulk assimilation of Lewisian amphibolite facies gneisses into mantle-derived-magmas has affected the Skye granites during their evolution.

Therefore, from the above points, it may be concluded that due to:

(1) the presence of refractory zircons in the Glamaig and Marsco granites; (2) the heterogeneous isotopic compositions of Lewisian amphibolites and granulites; (3) the different proportions of crustal components in each granite; (4) the difference in the calculated crystallisation temperatures of the granites;

the Skye granites are most likely the products of the differentiation of different pulses of basaltic magma, and that each magma was contaminated with crustal lithologies which had distinct and different Sr and Nd isotope signatures.

CHAPTER IX

Petrogenesis

The primary mineralogy of the Skye granites is dominated by the following main rock-forming minerals: alkali feldspar, quartz, plagioclase, amphibole, biotite, pyroxene, Fe-Ti oxide and accessory zircon and apatite. Accessory sphene and allanite were not identified, although both sphene and trace allanite have been reported in Skye granite by Exley (1980) and Ferry (1985). This set of primary minerals are accompanied by a set of secondary minerals such as chlorite, epidote, clay minerals, calcite and muscovite. Both feldspars are severely disturbed by turbidity phenomenon, and quartz contains numerous fluid inclusions. These features together with the presence of secondary mafic phases are suggestive of interaction between these granites and hydrothermal fluids. The primary phases appear to be crystallised sequentially, the late introduction of mafic magma is evident from the presence of biotite as inclusions in amphibole. The granites contain mafic inclusion (e.g. Glamaig Granite) which suggest mantle involvement in their origin. Zircon does exist as inherited crystals suggesting a crustal component in these granite.

Most of the primary phases have been totally or partially affected by hydrothermal alteration either by turbidity process as in both feldspars, fluid inclusions in quartz or alteration of mafic phases to secondary minerals, Isotopic compositions of these granites have also been severely disturbed (see Table 3.1; $\delta^{18}O$ values of whole rock and mineral separates together

with mineral-mineral fractionation Tables 7.1 and 7.2 and initial $^{87}Sr/^{86}Sr$ ratios, Table 8.1). The turbidity of feldspar considered by Folk (1955) as a common phenomenon in igneous rocks that crystallised from a hydrous magma. However, Loch Ainort and Marsco granites appear to have crystallised from anhydrous parents (due to the presence of a single feldspar, and absence of hydrous minerals), yet still contain significant amount of turbid feldspar. The distribution of turbid regions along the boundary of feldspar crystals, the presence of secondary inclusions through quartz grains indicate that the fluid was introduced to granites after they has been cooled to the temperature of hydrothermal event (350-450°C, see Chapter V), consequently the turbidity of feldspars is considered as subsolidus phenomenon. As the granites cooled, quartz decreased in volume much more than feldspar (Skinner, 1966; Ferry, 1985) which resulted in set of channel ways along grain boundaries (see for example, Fig. 3.3 (vi)).

The composition of the fluids responsible for the alteration processes in these granites are variable. Beinn an Dubhaich and Glamaig granites are associated with both magmatic and meteoric fluids as shown by the distribution of primary and secondary fluid inclusions, oxygen isotopic signatures of the quartz and small variations in $^{87}Sr/^{86}Sr$ ratios between magmatic minerals and their leachates. Whereas, in Loch Ainort and to lesser extent Marsco granites two different probably higher temperature meteoric fluids were involved, which have disturbed the oxygen and strontium isotopic compositions for their minerals. However, the variations in initial $^{87}Sr/^{86}Sr$ ratios between the granites are more likely to be dominated by the difference in country rocks which have contaminated each granitic magma during their differentiation (cf. Meighan, 1979). The effect of hydrothermal alteration on mafic minerals is represented by 1) replacement of primary pyroxene by secondary amphibole, possibly due the action of hydrothermal fluids (high w/r ratio table 7.2) along fractures

during the late stage of crystallisation (for example, Loch Ainort amphibole (Fig. 4.6)) ; 2) secondary biotite replacing amphibole (Fig. 3.2(v)); 3) formation of other secondary minerals such as chlorite, clay minerals, and little epidote and calcite, as replacement of amphibole, pyroxene, biotite, and olivine. Both types of alteration (turbidity and alteration to secondary minerals) appear to have been developed independently possibly due to the presence of different type of hydrothermal fluids as by the $\delta^{18}O$ and δD values for fluids associated with Skye granites (see Chapters V and VII; and, see also, Guthrie and Veblen, 1991). Plots of turbidity and alteration indices against selected major and trace elements (Figs. 6.1 and 6.2) have shown that these two process have no significant effect on the whole rock chemistry, which suggests that the variation in major and trace elements between different intrusions are due to difference in degree of differentiation and/or the difference in parent magmas composition. Thus, the derivation of each granite from a different basic magma and/or incorporation of a different amount of basic pulses during differentiation processes are likely process involved in the formation of these granites.

The peraluminous mineralogy for the four granites (Beinn an Dubhaich, SK-300; Loch Ainort, SK-313; Marsco, SK-334; and Glamaig, SK-326, see Tables 3.1; 6.1), high initial $^{87}Sr/^{86}Sr$ along with low ε_{Nd} values, and presence of inherited zircon indicate that the Skye granites contain crustal components. However, a comparison of the difference in REE patterns and concentrations between granites (Ce_N/Yb_N=3-10, with higher concentrations) and the possible crustal parents (Lewisian and Torridonian rocks, Ce_N/Yb_N=8-18, with lower concentration, Thorpe et al., 1977), the iron enrichment, and the presence of fayalite and ferrohedenbergite (see Chapter III) indicate that the granite cannot be derived solely from the crustal rocks. The contribution of both mantle and crust to the magma source for the Skye granites is evident from the calculated modal ages which

indicate that both old crustal and Tertiary-derived materials were involved, and the significant variations in major and trace element chemistry for whole rock presented. Examples of such chemical variations are presented in Chapter VI and include higher concentrations of compatible elements such as Ti, Fe, Al, Mg, Ca, Sr, and Ba in more primitive granites (for example, Glamaig) relative to their abundances in more evolved granites (Beinn an Dubhaich and Marsco). These are consistent with the derivation of some of these elements from mantle and crustal sources (cf. Pearce et al., 1984). However, such chemical variations are expected to correlate with the oxygen, strontium and neodymium isotopic ratios (Rollinson, 1993). No such correlations have been observed in this study, possibly due to an effect of hydrothermal alteration on both element concentrations (mobile) and isotopic ratios (oxygen and strontium in particular).

The low $\delta^{18}O$ values associated with higher crystallisation temperatures (980°C, see Table 8.3) for the Loch Ainort and Marsco granites , indicate that both granites have invaded by a later basic pulses before their final differentiation and emplacement, accompanied by isotopic exchange of both magmas with hydrothermal country rock(s). Alternatively, after they had cooled several hundred degrees, the hydrothermal fluids gained access to them. Thereafter, isotopic exchange between both rocks and fluids would occur which result in lowering the ^{18}O-signatures for their minerals which result in equilibrium isotopic fractionation between quartz and feldspar in Marsco (ΔQ-Af=1.56). Such temperature would be sufficiently high to protect primary igneous minerals from any sort of alteration to secondary minerals. Another generation of fluid gained access to both granites (see, Guthrie and Veblen, 1991) during hydrothermal temperatures (350-450°C) with larger quantity into Loch Ainort Granite (see w/r ratios, Table 7.3) this affected the both isotopic compositions and mineralogy, whereas, in Marsco both

isotopic signatures and mineralogy have experienced little change (for example, survival of olivine crystals, Fig. 3.5 (vi)).

The above discussion has clearly demonstrated that Skye granites contain both crustal and mantle components, possibly with the incorporation of different amounts of later basic pulses. Simple mixing is regarded as an unlikely mechanism due to the inflection present in the plot of MnO against SiO_2 (Fig. 6.7); the non-linear and divergent relationships between K_2O, Rb and Sr against SiO_2, together with the presence of an anomalous group of granites such as the Beinn an Dubhaich Granite which are characterised by low Zr, Y and Nb, but with high SiO_2 (Figs. 6.21; 6.23 and 6.24). Moreover, the Sr and Nd isotopic compositions of analysed samples in a mixing model away from any possible mixing line between average Lewisian Genesis composition and a pure mantle-derived materials (Fig. 8.11) mitigates against simple mixing as the sole process responsible for the compositional variations within the granites. The observed chemical and isotopic variations between different intrusions could be attributed to the different degree of crustal contamination (possibly with involvement of different crustal lithologies) at different crustal levels of basaltic magmas. Therefore, the contribution of mantle and crust to these granitic magma(s) requires some form of contamination process involving the mantle-derived melt passing through the continental lithosphere (assimilation and fractional crystallisation, AFC).

The derivation of granite from mantle-crustal sources would involve substantial fractional crystallisation of a range of major and accessory minerals. Fractionation of the following minerals from the parental magma would account for the indicated chemical characteristic: alkali feldspar (low Ba), plagioclase (low Sr, and high Rb/Sr and Eu/Eu*), Fe-Mg minerals (low Mg, high Fe/Mg), Fe-Ti oxide (low Ti), zircon (low Zr) and apatite (low P).

From a consideration of some compatible (Sr and Ba) and incompatible (Rb) trace element variations in the suite, together with the difference in negative Eu anomalies for samples with single feldspar (large Eu anomaly) compared to samples with two feldspar (small Eu anomaly), the feldspars have played an important role in the evolution of the suite. Most Skye granites may have formed by 30-70% fractional crystallisation (Figs. 6.27a and 6.28a). However, the fractionation or incorporation of accessory phases from or to the granites magma(s) will affect the elements concentrated within these phases, for example apatite and zircon contamination will modify REE concentrations. Only the Glamaig and Marsco granites contain refractory inherited zircons. The REE patterns of the analysed zircons (Fig. 4.16) show that with exception of Loch Ainort zircon the patterns are very different from their respective whole rock patterns, although they are more or less consistent with each other. In fact REE patterns of zircons from Marsco and Glamaig are very similar despite the estimated difference in the amount of inherited zircon in the zircon population of each granite (10% for Marsco and 50% for Glamaig). The high REE concentrations in some of inherited the zircons (Table 8.2) indicate that the present REE patterns of the bulk zircons may have been dominated by the REE concentration of the inherited zircons in both of these granites and hence presumably these zircons are derived from the same source (see Fig. 8.20).

The generation of these granites from different pulses of basic magma is also supported by, 1) the difference of crystallisation temperatures as indicated by feldspar thermometry and variations of Si and Ti contents of amphibole together with difference between phosphorus and zirconium saturation temperatures, 2) the ^{18}O-depleted signature of the quartz from Marsco and Loch Ainort granites together with equilibrium value of ΔQ-Af for Marsco Granite. A Tertiary magmatic contribution to these granites would clearly by represented a basic magma which pre-dated the granite emplacement in

BTVP such as Skye Main Lava Series. These basic magmas are varied in chemical composition and show a wide variation in Sr and Nd isotope ratios as result of contamination of these basaltic magma with various Archaean rocks (Moorbath and Thompson, 1890; Dickin, 1981; Thirlwall and Jones, 1983; Thorpe et al., 1991) (but see also, Wallace et al., 1994). Mattey et al., (1977) reported REE concentrations of basaltic magma-types on Skye which represent two broad chemical groups (alkali basalt and olivine tholeiite), and these are: (i) Preshal Mhor with $(Ce/Yb)_N < 1.0$; (ii) Fairy Bridge with $Ce/Yb)_N=1.7\text{-}2.4$ and (iii) Skye Main Lava Series with $(Ce/Yb)_N > 2.4$. The Skye granites having $(Ce/Yb)_N=3\text{-}8$, such composition may be derived by fractional crystallization of pyroxene and amphibole from basaltic types (ii) and (iii), respectively (see Thorpe et al., 1978). However, accepting that the granites are unlikely to be derived from a single source, the parental basaltic magmas could be alkali basalts or olivine tholeiitees. The lowest $(^{87}Sr/^{86}Sr)_i$ for these basalts 0.70307 to 0.70308 (see for example Dickin, 1980; Moorbath and Thompson, 1980) are consistent with their formation by successive phases of partial melting from upper mantle (Moorbath and Thompson, 1980).

The relative mantle and crustal contributions to these granites is difficult to evaluate due to wide range of Sr contents (6-137ppm) in these granites which possibly reflects the different degrees of plagioclase fractionation, uncertainty of the Sr and Nd compositions of Tertiary component, and the amounts of subsequent Sr and Nd fractionation. It will also reflect the mechanism of crust and mantle interaction (cf. Thirlwall and Jones, 1983; Thorpe et al., 1991), and the relative contributions to each element present in the granite will depend on their concentrations in the crustal and mantle components. Possible sources of Sr and Nd in the Skye granites have been modelled by mixing of mantle-derived magmas and Lewisian amphibolite compositions (see section 8.4; Fig. 8.12). The mixing curve is convex

downward and passes through the analysed data (i.e. below the Beinn an Dubhaich and above Marsco, Loch Ainort and Glamaig). Curves which will fit the lower samples (Loch Ainort, Glamaig and Marsco) may be produced by either having high Sr/Nd in the mantle-derived component, or a lower Sr/Nd in the crustal material, whereas the other way around will fit in the Beinn an Dubhaich Granite. The contribution of crustal lithologies to the Skye granites are variable and increase in order Loch Ainort (10%), Marsco (40%), Glamaig (50%) and Beinn an Dubhaich (70%). These crustal ratios are consistent with crystallisation temperatures as presented by the solubility of the zircon (table 8.3). Although they contradict the amount of inherited zircon contents, suggesting that different crustal rocks were involved.

In summary it is suggested that the granitic rocks included in this study originated predominantly by differentiation of 'contaminated' basaltic magmas (Skye Main Lava Series) of variable compositions. The compositions of these basaltic magmas must be more primitive than the composition of Glamaig magma from which some of these intrusions may have differentiated. Such differentiation may have occurred (magma chambers) at different crustal level, at which some of the crustal zircon crystals remain refractory, and some of the earlier acid derivatives are invaded by later basic pulses (eventually they rise their crystallisation temperature). Thereafter, each acid magma have been invaded by different generation of hydrothermal meteoric fluids through permeable basaltic rocks (Skye Main lava Series) after they had cooled 200 to 300°C from their crystallisation temperatures. Those intrusions which crystallised at higher temperature, their oxygen isotopic signatures are severely disturbed (Loch Ainort and Marsco granites), although the second generation of these hydrothermal fluids at (350-450°C) also affect their mineralogy and isotopic compositions each intrusion according to their w/r ratio. Whereas, other intrusions that crystallised at lower temperatures for granitic compositions

(750-800°C) like Glamaig and Beinn an Dubhaich granites, these hydrothermal fluids are corresponding to hydrothermal alteration events (350-450°C), and have disturbed both their mineralogy and isotopic compositions based on the w/r ratios in each intrusion.

CHAPTER X

Summary and conclusions

New data concerning the petrography, mineral chemistry, fluid inclusions and whole rock geochemistry of the Palaeocene granites of the Skye Intrusive Centre, NW Scotland, are presented. In addition, stable and radiogenic isotope geochemistry data (whole rock and mineral separates) on selected intrusions (Beinn an Dubhaich, Loch Ainort, Marsco and Glamaig) are also documented. These new data are used to decipher the petrogenesis of the magmas and the nature of subsequent subsolidus modifications which have affected the granites.

The main conclusions of this study may be summarised as follows:

I- Emplacement and crystallisation of the Skye granites occurred within a very short period of time (5 Ma) at approximately 55-60Ma **(Chapter VIII)**. The order of crystallisation is indistinguishable, but based upon the calculated isochrons is: Glamaig (56.6 Ma); Beinn an Dubhaich (59.1 Ma); Marsco (59.9 Ma). A useful isochron for the Loch Ainort Granite could not be obtained.

II- Skye granites have been severely affected by hydrothermal meteoric water, as shown by the turbidity of feldspar, alteration of ferromagnesian

minerals to secondary mafic minerals (**Chapter III**), secondary fluid inclusions in quartz (**Chapter V**), $\delta^{18}O$ whole rock values (**Chapter VII**), and mineral-mineral oxygen isotope fractionations (**Chapter VII**).

III- Micro-thermometric analysis and stable isotope data from fluid inclusions in quartz (**Chapter V**) indicate that the limited mixing of magmatic and meteoric waters was responsible for the fluids 'associated with' the Skye granites.

IV- In terms of mineral chemistry, the low concentrations of Fe^{3+} in pyroxenes from the Loch Ainort and Marsco granites, together with the variations in the Fe^{2+}: Mg ratio of biotite from the Beinn an Dubhaich Granite (**Chapter IV**), point to the slow cooling history of the suite.

V- The crystallisation of each granite (and even different samples from a single intrusion) involved different amounts of different basic compositions, indicated by differences in modal mineral contents (**Chapter III**), the difference in crystallisation temperatures as illustrated by feldspar thermometry, variations in Si, Ti, and Al^{vi} contents of amphiboles (**Chapter IV**), and differences in zirconium and phosphorus saturation temperatures (**Chapter VIII**).

VI- Major-, trace- and rare-earth-element compositional variation of whole rock samples (**Chapter VI**) is consistent with crystal-liquid fractionation (involving variable proportions of quartz, alkali feldspar, plagioclase, amphibole, biotite, apatite, Fe-Ti oxide, and zircon), but is not consistent with the mixing of end-member compositions such as the Glamaig Granite (i.e. the most primitive composition) and the Marsco Granite (the most evolved composition). Combined crystal-liquid fractionation and mixing remains a viable third possibility.

VII- The similarity of the REE patterns of Skye granites **(Chapter VI)** indicate that these patterns have not been significantly disturbed by alteration processes, and imply that the Skye granites are chemically related.

VIII- The observed strong geochemical coherence within the suite **(Chapter VI)**, together with the smaller negative Eu anomalies for whole rock samples of two-feldspar granites relative to single feldspar granites **(Chapters IV and VI)**, indicate that the fractional crystallisation processes were dominated by plagioclase removal, together with lesser amounts of biotite and alkali feldspar. As the differentiation processes proceeded, alkali feldspar removal became dominant over plagioclase removal.

IX- The Glamaig Granite contains mafic inclusions **(Chapter IV)**, and refractory zircon **(Chapter VIII)**, pointing to a mixed mantle-crustal parentage.

X- Sm/Nd values for whole rock samples **(Chapter VIII)** are very similar and, consequently, imply that neither partial melting nor crystal fractionation had a significant effect on these two elements during the evolution of the Skye granites. The most important reservoirs for the REE in the Skye granites are amphibole, pyroxene and apatite **(Chapter IV)**.

XI- The ^{18}O-depleted signature of quartz in the Marsco Granite, together with its equilibrium value of $\Delta Q\text{-}Af$ **(Chapter VII)**, suggest that either, ^{18}O-depleted magmas were formed on a small scale, or, that meteoric water reacted with the quartz and alkali feldspar at temperatures just below the granite solidus and resulted in the equilibrium fractionation now preserved.

XII- The ^{18}O-depleted signature of quartz from the Loch Ainort and Marsco granites **(Chapter VII)** suggests that these granites may have originated from ^{18}O-depleted protolith(s).

XIII- The resultant $\delta^{18}O$ (whole rock and mineral separates) signatures **(Chapter VII)** have been controlled by the water/rock ratio (w/r) (involving **Palaeocene** meteoric water and each granite), and by the $\delta^{18}O$ signatures of **country-rock** lithologies with which the water reacted.

XIV- The hydrogen isotope compositions of Skye amphiboles are related to **each** other, and their δD signatures increase with decreasing w/r ratio. The **amphiboles**, in a plot of $\delta D_{amphibole}$ against $\delta^{18}O_{whole\ rock}$, define a positive **shallow** gradient, but which does not intersect the field of 'normal' **amphiboles** for igneous rocks **(Chapter VII)**, suggesting that the original **amphiboles** in the Skye granites were relatively depleted in D.

XV-The Beinn an Dubhaich and Glamaig granites crystallised at calculated **temperatures** reasonable for a granitoid magma, whereas both the Loch **Ainort** and Marsco granites appear to have crystallised at relatively high **temperatures (Chapter VIII)**. These high crystallisation temperatures, in **association** with the presence of pyroxene **(Chapter III)**, point to the **incorporation** of batches of basaltic magma into the Loch Ainort and Marsco **granite** magmas (i.e. they are of high temperature parentage).

XVI- The observed heterogeneity in initial $^{87}Sr/^{86}Sr$ ratio between minerals **in** each granite is most likely due to hydrothermal alteration rather than **magmatic** processes. The observed variation in Sr and Nd isotopic **composition** between the granites is unlikely to be due to either post-**magmatic** processes or source mantle heterogeneity, and most likely is the **result** of magma-crust interaction **(Chapter VIII).**

XVII- Model age calculations **(Chapter VIII)**, indicate that the crustal **components** within the granites were separated from a Chondrite Uniform **Reservoir** (derived from the mantle) over a relatively short period of time; **however**, each granite records a different mean crustal residence time.

XVIII- The intermediate Sr and Nd isotopic compositions of Skye granites, between Hebridean mantle and crustal compositions (basement (amphibolite and granulite) Lewisian gneisses) (Chapter VIII), together with the presence of refractory zircons in the Glamaig and Marsco granites (Chapter VIII), indicate contributions from both the crust and the mantle in Skye granite petrogenesis.

XVIX- The inherited zircons in the Glamaig and Marsco granites came from the same source and did not suffer much mechanical abrasion during transportation (Chapter VIII). These refractory zircons have unusually low Sm/Nd ratios, possibly due to equilibration between the zircon and other mineral(s) with low Sm/Nd ratios prior to their incorporation into the granite magmas.

Finally, from these data it may be concluded that the Skye granites are most likely the products of the differentiation of different pulses of basaltic magma, and that each magma was contaminated with different crustal lithologies which had distinct and different geochemical compositions.

Epilogue

This thesis represents a small episode in the study of the Skye granites, and clearly much more work is required to investigate their petrogenesis. Potentially, more detailed investigations on petrography, mineral chemistry, together with more whole rock geochemical analyses of other intrusions, is needed. Indeed, as this study has highlighted, Skye granites have been highly disturbed by heated meteoric-hydrothermal waters, and, subsequently, more data on fluid inclusions, and the oxygen and hydrogen isotope characteristics of constituent minerals are needed to elucidate further this important process. The open system behaviour indicated by Rb-

Sr isotope data for the Marsco and Loch Ainort granites suggests that more accurate geochronological information is required and may be acquired by the U-Pb and Ar-Ar isotopic systems. The presence of refractory zircons with very low Sm/Nd ratios in some granites, makes further Sm-Nd isotope studies for both the granites and their country-rocks a high priority for future work.

This thesis may represent a basis for these studies.

APPENDIX I

List of samples

In this section the list of analysed samples includes sample number, rock type and location.

SK-298: granite, Beinn an Dubhaich Intrusion, coastal exposures, between Camas Malag and Allt na Leth-pheighinne [NG581193];

SK-299: granite, with mafic clots, Beinn an Dubhaich Intrusion, coastal exposures, between Camas Malag and Allt na Leth-pheighinne [NG581194];

SK-300: heterogeneous granite, with areas devoid of ferromagnesian minerals, Beinn an Dubhaich Intrusion, coastal exposures, between Camas Malag and Allt na Leth-pheighinne [NG581195];

SK-301: quartz-feldspar pegmatite from vugh, Beinn an Dubhaich Intrusion, coastal exposures, between Camas Malag and Allt na Leth-pheighinne [NG581195];

SK-302: small (c.20cm wide) microgranite dyke, Beinn an Dubhaich Mass, coastal exposures, between Camas Malag and Allt na Leth-pheighinne [NG581195];

SK-303: porphyritic (quartz-feldspar) felsite, roadside cutting (south of road), west of Camas na Sgianadin, at Fasair-choille [NG6222258];

SK-304: porphyritic (quartz-feldspar) felsite, roadside cutting (south of road), west of Camas na Sgianadin, at Fasair-choille [NG6222258];

SK-305: coarse granite, altered, roadside cutting (south of road), NE of Creag Strollamus [NG611265];

SK-306: coarse granite, ?plagioclase-rich, altered, quarry, NW of Creag Strollamus [NG604267];

SK-307: coarse granite, Glas Bheinn Mhor Intrusion, 15m from contact, ?altered, roadside exposures (south of road) between Strollamus and Dunan roadsigns [NG590273];

SK-308: metamorphosed ?sandstone, roadside exposures (south of road) between Strollamus and Dunan roadsigns [NG590273];

SK-309: granite, Glas Bheinn Mhor Intrusion, with inclusion, roadside exposures (south of road) between Strollamus and Dunan roadsigns [NG585280];

SK-310: granite, Glas Bheinn Mhor Intrusion, with inclusion of ferromagnesian minerals, roadside (disused quarry) (SE side of road), NE of Luib [NG569285];

SK-311: microgranite dyke, cutting Glas Bheinn Mhor Intrusion, at least 80cm wide (only one side exposed), roadside (disused quarry) (SE side of road), NE of luib [NG569285];

SK-312: coarse granite, Glas Bheinn Mhor Intrusion, roadside between Luib and Aricharnach [NG553275];

SK-313: porphyritic (feldspar) granite, Loch Ainort Intrusion, Eas a' Bhradain, SE face of waterfall, head of Loch Ainort [NG533265];

SK-314: coarse granite, Beinn Dearg Mhor Intrusion, ?altered, roadside (east side of road), immediately north of the Allt Mhic Mhoirein [NG530278];

SK-315: granite, Beinn Dearg Mhor Intrusion, ?altered, roadside (east side of road), SW of Druim nan Cleochd, east of tributaries of Abhainn Torra-mhichaig [NG534287];

SK-316: granite, Loch Ainort Intrusion, roadside, (south side of road), south of Allt Mhic Mhoireinn [NG532278];

SK-317: porphyritic (feldspar) felsite, roadside (south of road), Sron Ard a' Mhullaich [NG542272];

SK-318: granite, Loch Ainort Intrusion, disused quarry, Maol Ban, Loch Ainort [NG565297];

SK-319: granite, Maol na Gainmhich Intrusion, weathered, roadside (west side of road), south of Maol na Gainmhich [NG561310];

SK-320: porphyritic (quartz-feldspar) felsite, Northern Porphyritic Felsite, highly fractured and veined, north side of forestry track, Coire Mor [NG557302];

SK-321: granite, Eas Mor Intrusion, ?mafic, above Eas Mor, north face of Glamaig [NG516308];

SK-322: microgranite, Meall Buidhe Intrusion, Allt a' Bhealaich Bhric, NE of Meallan a' Bhealaich Bhric, above E-W-flowing tributary [NG542311];

SK-323: granite, Glamaig Intrusion, Abhainn Torr-mhichaig, due west of Meallan a' Bhealaich Bhric [NG538309];

SK-324: granite, Glamaig Mass, ?altered, Abhainn Torr-mhichaig, due west of Meallan a' Bhealaich Bhric [NG538309];

SK-325: granite, Glamaig Intrusion, with clots of ferromagnesian minerals **(SK-325A)**, Allt na Mearanroch, first exposures east of path [NG497272];

SK-326: granite, Glamaig Intrusion, with clots of ferromagnesian minerals, Allt na Mearanroch, first exposures east of path [NG497272];

SK-327: granite, Glamaig Intrusion, with clots of ferromagnesian minerals, Allt na Mearanroch, first exposures east of path [NG497272];

SK-328: granite, Glen Sligachan Intrusion, east of track, at base of Harker's Gully, Marsco [NG496261];

SK-329: porphyritic (quartz-feldspar) felsite, Southern Porphyritic Felsite, at contact with marscoite, Harker's Gully, immediately below Shelter Stone Level [NG499259];

SK-330: porphyritic (quartz-feldspar) felsite, Southern Porphyritic Felsite, c.1m from contact with marscoite, Harker's Gully, immediately below Shelter Stone Level [NG499259];

SK-331: porphyritic (quartz-feldspar) felsite, Southern Porphyritic Granite, c.1m from contact with felsite, Harker's Gully, immediately below Shelter Stone Level [NG499259];

SK-332: porphyritic (quartz-feldspar) felsite, Southern Porphyritic Granite, c.15m from contact with felsite, Harker's Gully, immediately below Shelter Stone Level [NG499259];

SK-333: granite, Marsco Intrusion, c.100m above Shelter Stone level, stream south of Harker's Gully (loose block) [NG498258];

SK-334: granite, Marsco Intrusion, immediately below Shelter stone level, stream south of Harker's Gully (loose block) [NG498258];

SK-335: felsite, margin of Beinn na Caillich Intrusion, Allt Slapin Gorge [NG584218];

SK-336: microgranite, c.3m from contact of Beinn na Caillich Intrusion, Allt Slapin Gorge [NG584218];

SK-337: granite, c.100m from margin of Beinn na Caillich Intrusion, Allt Slapin Gorge [NG584218];

SK-338: granite, margin of Beinn an Dubhaich Mass, Kilchrist Manse, (location S4, Figure 20, p. 190, Bell and Harris, 1986) [NG616201];

SK-339: granite, Beinn Dearg Mhor Intrusion, Allt Coire nam Bruadaran [NG526258];

SK-340: granite, Beinn Dearg Mhor Intrusion, Allt Mam a' Phobuill [NG519256];

SK-341: porphyritic (quartz-feldspar) granite, Southern Porphyritic Granite, tributary of the Allt Mam a' Phobuill, NE face of Marsco [NG518252];

SK-342: Lewisian Gneiss xenolith in ferrodiorite, Marscoite Ring-dyke, Allt Coire nam Bruadaran [NG520249];

SK-343: granite, Marsco Intrusion, col between Coire nam Bruadaran and Am Fraoch-choire [NG519243];

RA-100: porphyritic (quartz-feldspar) felsite, southern side Isle of Raasay [NG5523354];

APPENDIX II

Equations

II-1 Equation used for calculating mixing line between two magmas with two distinct isotopic compositions (after Faure, 1986 p. 148):

$$[(^{87}Sr/^{86}Sr)_M = (^{87}Sr/^{86}Sr)_A \times Sr_A(ppm)\ FA + (^{87}Sr/^{86}Sr)_B \times Sr_B(ppm) \times (1-F_A)] / [Sr_A(ppm) \times F_A + Sr_B(ppm) \times (1-F_A)].$$

Where: M, calculated component; A and B, representing the acid and basic end members, respectively; F, is the weight fraction of A. The $^{143}Nd/^{144}Nd$ ratio can be calculated using the same formula.

II-2 Feldspar thermometry (after Haselton et al., 1983):

$$T_K=[(X^{Af}_{Or})^2 (18810 + 17030\, X^{Af}_{Ab} + 0.364\ P) - (X^{Pl}_{An})^2 (28230-39520\, X^{Pl}_{Ab})] / 10.3\, (X^{Af}_{Or})^2 + 8.3143 \ln\{(X^{Pl}_{Ab})^2 (2-X^{Pl}_{Ab})/X^{Af}_{Ab}\}.$$

Where: Af and Pl, refers to the mole fraction of the alkali feldspar and plagioclase respectively; T, in Kelvin; P, pressure in bars.

II-3 Oxygen isotopic fractionation between quartz and water (after Matsuhisa et al., 1979):

$$\Delta\ Q\text{-}W = 3.34\ (10^6\ T^{-2}) - 3.31,$$ for the temperature range: 250 to 500 °C.

Where: T, in Kelvin.

II-4 Oxygen isotopic fractionation between amphibole and water (after Suzuoki and Epstein, 1976):

Δ Amph-W = -23.9 (10^6 T^{-2}) +7.9, for the temperature range: 450 to 800 °C.

Where: T, in Kelvin.

II-5 Equation used for calculating oxygen isotopic composition of fluid (after Taylor, 1974, 1977):

δ^{18}spr- δ^{18}Ow= -3.52+2.682 ($10^6/T^2$), Where: T, in Kelvin.

APPENDIX III

Methods

III. 1 Sample collection and preparation

44 samples were collected from the main outcrops of the Skye granites (see Appendix II). Fresh material was collected were possible, with at least 4-8 kg sample sizes for whole rock chemical and isotope analysis. All samples were slabbed to obtain totally unweathered material; thin-sections were obtained from all samples, together with probe sections for selected samples, and accessory minerals were also mounted on probe sections.

Initial preparation of samples for chemical analysis consisted of passing the samples through a jaw crusher, followed by a Roller crusher, then powdering them in a Tema mill until a rock powder of the appropriate grain-size was obtained.

III. 2 Electron probe, BSE and CL studies

All of the electron probe analyses (Chapter 4), were taken by a sun workstation- controlled Cameca SX-50 electron probe microanalyser (at Glasgow University) fitted with four wavelength spectrometers:

SP1 PC1, TAP, LIF, PET

SP2 LIF, PET

SP3 PCO, TAP, Pc2, PC3

SP4 LIF, PET

The generating conditions of the probe were 15 kV and nA, with 10s counting time on the peak and 5s on each the positive and negative backgrounds. The vacuum was typically 4 x 10^{-5} Pa in the chamber and 4 x 10^{-6} Pa at the electron gun. Standards comprised a series of pure elements and compound standards supplied by Cameca and Micro analysis Consultants Ltd.

For accessory minerals such as zircon and apatite, both backscattered electron and cathodoluminescence studies were used. Backscattered electron studies were carried out using a Cambridge Stereoscan 360 electron microscope, with 4 quadrant BSE detector (SI-N type), whereas cathodoluminescence studies were carried out using a SEM based cathodoluminescence detection system and optical techniques. The latter used a Technosyn model 8200 MK2 with autohold, at typical operating conditions of 20 kV, 200 μA, and a vacuum of approximately 0.05 torr.

III. 3 Mineral Separation

As noted above (section III. 1), large samples were crushed to approximately sand-size grains to separate most of the rock-forming minerals, including those with small grain-sizes (zircon and apatite).

Two main separation techniques were used: magnetic separation, and heavy liquids separation, using tetrabromo-ethane (2.96) and methylene-iodide (3.3). This was followed by hand-picking where necessary to purify the separates.

III. 4 X-Ray Fluorescence

Whole rock major- and trace-element analyses were carried out using a Philips PW 1480 automatic x-ray fluorescence spectrometer in the Department of Geology and Geophysics in the University of Edinburgh. The

spectrometer was equipped with a La heavy absorber and an on-line PC for data processing. The accuracy and precision of the analyses are comparable to those quoted by Fitton and Dunlop (1985) and Thirlwall et al. (1994). The preparation method is described by Fitton and Dunlop (1985) and summarised below:

III. 4. 1 Major elements analyses

Samples were made into fused glass discs, according to the method of Harvey et al. (1973), in duplicate, from 0.9-1.0g of dried sample and 4.5-5.0g of Spectroflux 105 (containing lithium carbonate, lithium tetraborate and lanthanum oxide).

III. 4. 2 Trace elements analyses

Samples were prepared as pressed pellets, containing 6g of the rock powder and 4 drops of Mowiol, covered by 1 tablespoon of Boric acid powder.

III. 5 Ferrous iron determination

To determine ferrous iron contents, 0.5 g of rock powder from each sample was ground in acetone to prevent iron oxidation. The rock powder was mixed in a Pt crucible with 50% H_2SO_4, 40% HNO_3, 40% HF and concentrated H_3PO_4, and heated on a hot plate at 160°C for about 10 minutes. This was titrated with potassium dichromate solution with a 0.2% solution of sodium diphenylamine sulphonate as an indicator. The FeO concentration be determined as follows:

$$\% FeO = 0.2 \times \text{vol. dichromate} / \text{weight of sample}$$

Consequently, the percentage of Fe_2O_3 can be calculated from the following relationship:

$$Fe_2O_3 = Fe\ (total) - (FeO \times 1.1113)$$

III. 6 Loss on ignition

The samples were dried overnight in a oven at 110°C, weighted out into crucibles and mixed with about 5 times its weight of flux. The mixture was ignited at 1100°C for 20 minutes, and then place on a cool block for about 5 minutes. After this, the samples were re-weighed and the loss on ignition (LOI) was calculated:

$LOI = [wt\ (sample + crucible + flux)_0 - wt\ (sample + crucible + flux)_t] / wt\ (sample)$, where: 0 and t, refer to wt. before and after ignition, respectively.

III. 7 ICP-MS (Rare earth elements determination)

About 0.1g of whole rock and major rock-forming mineral samples, and 0.04-0.05g of accessory mineral samples were weighted out into PTFE beakers. All samples were mixed with 5 ml hydrofluoric acid (40%) and 5 ml nitric acid (conc.) and placed on a hot plate at 80°C for 24 hours.

The contents were allowed to evaporate to dryness at 200°C on the hot plate, and then 25 ml of 2% nitric acid was added to those samples which had completely dissolved. However, this processes could not cope with insoluble minerals such as zircon, and eventually 2 ml hydrofluoric acid (40%) and 2 ml nitric acid (conc.) were added to the undissolved samples

and they were placed in a stainless steel bomb and put in an oven at 200°C for a minimum of 2 days.These samples were then collected to cool and were dried under lamps and again 25 ml of 2% nitric acid was added.

The samples were then slightly heated on a hot plate and transfered by a filtration process to a volumetric flask. Blank and some duplicate samples were also prepared.

For the REE analyses, a VG plasma Quad PQ2 Turbo plus (Fisons Instruments Elemental Analysis) ICP-MS at SURRC, East kilbride was used. The ICP-MP operating conditions were as follows:

	Plasma Quad PQ2	
(i) Sample introduction:		
Method	Liquid nebulisation	
Uptake	0.8 ml^{-1}	
(ii) Plasma:		
RF power	Forward	1350 W
	Reflected	< 5W
Gas controls:	Auxiliary	0.75 1 min^{-1}
	Coolant	14.0 1 min^{-1}
	Nebuliser	0.90 1 min^{-1}
Nebuliser	De Galan V-groove	
Spray chamber	Scott type double bypass, water cooled	
(iii) Ion sampling:		
Sampling cone	Nickel, 1.0 mm orifice	
Skimmer cone	Nickel, 0.75 mm orifice	
Sampling distance	10 mm from load coil	
(iv) Vacuum:		
Expansion stage	2.5 mbar	
Intermediate stage	2×10^{-4} mbar	
Analyser	2×10^{-6} mbar	
(v) Data acquisition:		
Acquisition time	30 s	
Acquires per sample	3	

Measured masses were: ^{138}Ba, ^{139}La, ^{140}Ce, ^{141}Pr, ^{143}Nd, ^{146}Nd, ^{147}Sm, ^{150}Nd, ^{151}Eu, ^{157}Gd, ^{159}Tb, ^{162}Dy, ^{165}Ho, ^{166}Er, ^{169}Tm, ^{174}Yb, ^{175}Lu.

III. 8 Fluid inclusion wafers

Fluid inclusions were studied on doubly-polished rock wafers 45 μm thick which optimise light transmission and the preservation potential of large

inclusions. These wafers were prepared by embedding a sawn rock fragment in resin; cleaning, grinding and polishing of one face; then sawing to 1.5mm thick and grinding the opposite face until the wafer is of the required thickness, then polishing this face.

Measurement of heating and cooling temperatures of the fluids in the wafers was carried out on a heating/freezing stage, and a thermal cell with upper and lower heat insulating glass windows. Heating was by means of an element mounted in the centre of the stage below the specimen, and cooling is effected by a stream of nitrogen gas which has previously been cooled by passage in a coil through a bath of liquid nitrogen. Temperature, temperature gradient and limit were controlled from, and displayed on, a box connected to the element and temperature sensors within the stage.

Observation was by transmitted light (PPL), through the stage windows which protect the optics from the temperature ranges and gradients within. A powerful microscope, with magnifications in the range 320 x up to 1250 x, and capable of a resolution of 1 μm, was used.

III. 9 Hydrogen and Oxygen isotopes

III. 9. 1 Hydrogen isotope analysis of minerals

H-isotope analysis of amphibole separates was carried out followed the method of Godfrey (1962). The structural water was extracted by induction heating to melting, and the reduction of H_2O to H_2 was obtained by passage over uranium at 850°C. D/H ratios were determined with a mass spectrometer (VG-Micromass 602 B with a modified inlet system).

III. 9. 2 Hydrogen isotope and volatile analysis of fluid inclusions

Analysis of the bulk hydrogen isotopic composition of quartz was carried out using nearly the same procedure as for amphibole separates (III. 9.1).

This was measured directly on water released by the decrepitation of fluid inclusions in quartz. However, to obtain enough hydrogen for analysis, large amounts of quartz separate was used (1-3g).

III. 9. 3 Oxygen analysis of oxide and silicate minerals

Oxygen was extracted from oxide and silicate minerals by using ClF_3 as a reagent (Brothwick and Harmon, 1982), using the vacuum extraction methods of Clayton and Mayeda (1963). The oxygen was then reduced to CO_2 and collected for analysis on a VG-SIRA 10 mass spectrometer.

For fluid inclusions, oxygen isotopic ratios were calculated using the quartz-H_2O fractionation equation of Matsuhisa et al. (1979) (see Appendix II), and temperatures were provided by thermometric data (i.e. homogenization temperatures of fluid inclusions).

III. 10 Strontium and Neodymium

III. 10. 1 Chemistry:

(i) *Leaching experiments* :

All alkali feldspar and plagioclase samples were leached to separate "altered" from "magmatic" materials. 2M mls of 5% HF were added to the weighed samples in PFA Teflon screw-top beakers (Savillex) and left for 10 minutes. The solution and sample were then transferred to a centrifuge tube and centrifuged for about 2 minutes in ultrasonic centrifuge. The liquid was then dried down under lamps. The residue was dried to a constant weight (i.e. weight of "magmatic" materials), then was subtracted from the original weight of the sample to get the weight of "leached" materials.

(ii) *Sample Dissolution* :

Samples were dissolved in PFA Teflon screw-top beakers (Savillex) using 10mls 40% HF and 1ml 14M HNO_3 on a hot plate overnight. The beakers were removed, cooled, and then the solution was dried down under lamps. The residue was then dissolved in 3 mls 14M HNO_3 overnight on a hot plate, and dried down as before. The residue was now dissolved in 8 mls 6M HCl overnight on a hot plate. After cooling, a weighed aliquot of about 1/3 the volume of the solution was taken, to which was added weighed quantities of ^{145}Nd and ^{149}Sm spikes for isotope dilution determination of Sm and Nd concentrations. The remaining 2/3 aliquot was used for the determination of the isotopic composition of both Sr and Nd. ^{87}Rb and ^{84}Sr spikes were also added to this solution for the determination of Rb and Sr concentrations by isotope dilution analysis. Both solutions were dried down and the final residues each taken up in 2 mls 2.5M HCl.

(iii) *Column chemistry* :

Sr and the REE were separated using standard cation exchange chromatography techniques. The sample was transferred to a centrifuge tube and any residue was centrifuged off. The solution was then loaded onto a preconditioned cation exchange column containing 10 mls Bio-Rad AG50W x 8, 200-400 mesh resin. The sample was washed in with 2 * 1 ml 2.5M HCl. For samples where Rb and Sr were to be collected 29 mls 2.5M HCl were eluted, followed by collection of Rb in 7 mls 2.5M HCl; this was then evaporated to dryness. 10 mls 2.5M HCl was then eluted. The Sr fraction was collected with a further 10 mls 2.5M HCl, and evaporated to dryness. Sr blanks were less than 1 ng. For Sm and Nd spiked samples the Sr fraction did not need to be collected, and so 56 mls 2.5M HCl were eluted.

The REE were separated by further eluting 20 mls 2.5M HCl and 10 mls 3M HNO_3. The next 26 mls 3M HNO_3 were collected, and evaporated to dryness.

Sm and Nd were isolated from Ba and the other REE using 3 columns.

Column 1 (initial Ba clean-up):

The residue from the REE fraction from the Sr columns was dissolved in 1 ml of a solution of 75% CH_3COOH - 25% 5M HNO_3 (hereafter called 75/25). This was loaded onto a column containing 8ml of Bio-Rad AG1 x8, 200-400 mesh anion exchange resin which had been preconditioned with 5 mls of a solution of 90% CH_3COOH - 10% 5M HNO_3 (90/10). The sample was washed in with 2 * 1 ml 90/10 solution, and then eluted with 50 mls 90/10 solution. The REE's were collected with 15 mls 0.05M HNO_3, and evaporated to dryness.

Column 2 (Sm and Nd separation):

The residue from column 1 was dissolved in 1 ml of "orange cocktail". This cocktail consisted of 75% CH_3OH - 25% orange cocktail mix: the mix is made of 1336 mls H_2O - 406 mls CH_3COOH - 256 mls 5M HNO_3. The sample was loaded onto a column containing 8 ml of Bio-Rad AG1 x8, 200-400 mesh anion exchange resin which had been preconditioned with 5 mls "orange cocktail". This column was encased in a water jacket through which water kept at 25°C by a thermostatically-controlled water bath was circulated. The sample was washed in with 2 * 1 ml "orange cocktail", and eluted with 10 mls "orange cocktail". For spiked samples the next 17 mls "orange cocktail" were collected which contained the Sm fraction; this was evaporated to dryness. A further 12 mls "orange cocktail" were then eluted. For unspiked samples 29 mls "orange cocktail" were eluted. The next 29 mls "orange cocktail" containing the Nd fraction were then collected, and the solution evaporated to dryness.

Column 3 (final Ba clean-up):

The residue from the Nd fraction from column 2 (both spiked and unspiked) was dissolved in 1 ml 75/25 solution, and loaded onto a column containing 5 ml of Bio-Rad AG1 x8, 200-400 mesh anion exchange resin which had been preconditioned with 3 mls 90/10 solution. The sample was washed in with 2 * 1 ml of 90/10 solution and eluted with 15 mls 90/10 solution. The Nd was collected with 10 mls 0.05M HNO_3, and evaporated to dryness. Sm and Nd blanks were less than 0.2 ng.

III. 10. 2 Mass Spectrometry

(i) *Rb* :

Rb samples were run on single collecter VG MM30 thermal ionisation mass spectrometer. Rb samples were dissolved in a few ml of RO H_2O in a glass spitzer, loaded onto a Ta side filament of an outgassed triple Ta filament assembly, and carefully dried down so as to avoid the sample bubbling up on the filament. Beams were managed to give a peak intensity of about 5 pA ^{87}Rb. Peak intensities were corrected for zero and dynamic memory.

(ii) *Sr* :

Sr samples were run on a single collector VG 54E thermal ionisation mass spectrometer. Sr samples were dissolved in 1ml 1M H_3PO_4 and were loaded onto a single outgassed Ta filament. A small current is passed through the filament to dry the sample which is then increased slowly until the H_3PO_4 fumes off and the filament glows dull red. Sr beams were managed to give an intensity of 1.5 pA ^{86}Sr. Peak intensities were corrected for zero, dynamic memory and Rb interference (if necessary). The $^{87}Sr/^{86}Sr$ ratio was corrected for mass fractionation using $^{86}Sr/^{88}Sr = 0.1194$. Repeat analysis of NBS 987 Sr standard gave $^{87}Sr/^{86}Sr = 0.710236 \pm 19$ (2s.d.).

(iii) *Nd* :

Nd analyses were performed on a VG Sector 54-30 thermal ionisation mass spectrometer with 8 Faraday collectors. Nd samples were dissolved in water and loaded on the Ta side filaments of an outgassed triple filament assembly with a Re centre filament. The sample was dried very carefully at 0.5A. For Nd isotopic composition runs beams were managed to give a ^{144}Nd intensity of 10pA with a centre filament current of 4 A. Data were acquired in multi-dynamic mode (to avoid inter-collector gain calibration uncertainties) using a 5 collector peak jumping routine. The data were collected in 12 blocks of 10 cycles/block, giving 120 ratios in total. Each cycle comprised 4 sequences; after each sequence the magnet was switched to place a different isotope into any given collector. The integration time for each sequence within a cycle was 5 seconds with a 2 second wait time between each sequence to allow the magnet to settle. $^{143}Nd/^{144}Nd$ ratios were corrected for mass fractionation using $^{146}Nd/^{144}Nd = 0.7219$. Peak intensities were corrected for background and the ^{144}Nd peak was corrected for Sm interference. During the course of this study the JM Nd standard gave $^{143}Nd/^{144}Nd = 0.511500 \pm 10$ (2s.d.).

For Nd isotope dilution runs the ^{143}Nd beam intensity was 0.5 pA. The analyses were performed in static mode, with 3 blocks of 10 cycles being collected. The integration time for each cycle was 5 seconds. Peak intensities are corrected for zero and Sm interference (where necessary).

(iv) *Sm* :

Sm analyses were also performed on the Sector 54-30 instrument. Loading techniques were the same as those for Nd. Sm beams were managed to give a ^{149}Sm beam intensity of 0.5 pA. The analyses were performed in static mode, with 3 blocks of 10 cycles being collected. The integration time for each cycle was 5 seconds. Peak intensities are corrected for background. Measured Sm/Nd ratios are considered to be better than 0.15% (2 s.d.)

APPENDIX IV

Techniques

IV. 1 Electron probe, BSE and CL studies

(i) Electron probe microanalyser:

A Cameca SX50 Electron probe microanalyser with four spectrometers each carrying a range of crystals (LIF, TAP, PET and other synthetic crystals for light element analysis) was used to determine major element analyses of minerals. An electron beam is released from the electron gun with an accelerating voltage of 15kV, current of 20nA and focussed on the surface of the sample. To prevent the electron beam from scattering or dropping in voltage, the electron column and specimen chamber must be maintained under conditions of high vacuum (10^{-7} to 10^{-8} Torr) by using rotary and diffusion pumps. The focused electron beam on the surface of the sample leads to the generation of x-rays characteristic (wavelength dispersive) of the atoms present. These x-rays are diffracted by the analysing crystals in the specrometers, the intensity of the x-rays are measured by a gas flow proportional counter using wavelength dispersive spectrometers. The measured intensities require certain corrections the chief source of which is the continuous x-ray spectrum. The composition at analysed point is calculated from the corrected intensities by applying matrix corrections which take account of various factors governing the relationship between intensity and composition. Calibrations were done on accredited mineral standards of similar composition to the samples where possible and on pure standards otherwise. These process yield detection limits in the range 0.03 to 0.24 % oxide, which are 50 to 100 times poorer than those expected for bulk analysis by x-ray fluorescence. The associated Sun work station computer running a Unix operating system is used to facilitate the control and coordinate the movement and operation of the stages, and spectrometer, to

record x-ray data and to calculate matrix corrections. (for further details, see Potts, 1987).

(ii) Scanning electron microscope:

Backscattered electron studies were carried out using a Cambridge Stereoscan 360 electron microscope, this scanning electron microscope (SEM) techniques is very similar to those described above for electron probe microanalysis, however, scanning electron microscope procedures designed to show high resolution scanning electron microscope images (Lloyd, 1987; Paterson et al, 1989). The incident backscattered electrons (BSE) on the target sample are reflected by elastic scattering events, and imaged with the scanning electron microscope (SEM), image resolutions were obtained by using an accelerating voltage of 20 kV. The mean atomic number of the sample is the main controller of the proportion of electrons that have been backscattered (see, Potts, 1987). The intensity of backscattered is displayed as a scan on cathode ray tube, by allowing the electron beam to be scanned in synchronism with the passage of that beam over the sample under investigation, consequently high resolution scanning electron images may be viewed and recorded.

(iii) Cathodoluminescence:

The Cathodoluminescence technique used was a SEM-based cathodoluminescence detection system and optical techniques to identify some of crystal-texture characteristics (see Finch and Walker, 1991; Hayward and Jones, 1991;Varva, 1993, 1994). This technique is based on the semiconductor properties of a mineral under investigation. Such properties will mean that two bands of energy were occupied by electrons within the crystal lattice, the higher band and the ground state band. Any interactions between primary electron beam and the sample can cause electrons to be excited from ground to higher energy bands, or viceversa, such a process will involves some energy release. The energy differences between these bands is emitted as electromagnetic radiation in the visible region (cathodoluminescence).

IV. 2 X-Ray Fluorescence

Whole rock major (fused glass discs) and trace (compressed powder pellets) element analyses were carried out using a Philips PW 1480 automatic x-ray fluorescence spectrometer. In such an analysis a specimen is bombarded with x-rays generated by an x-ray tube operated at a potential of between 10 and 100 kV, that causes secondary fluorescent radiation from each of the elements present. The choice of x-ray target is dependent on the wavelength of elements of interest, absorbtion by other elements, and interference from other elements or tube lines (see Harvey et al., 1973). For each element the operating potential (kV), and current (mA) of the tube is selected so that the energy of the x-rays exceeds the critical excitation energy of the element and to optimise the peak to the ground ratio. The primary radiation causes electrons to be knocked out of electron shells of atoms (ionization), and characteristic x-ray fluorescence occurs when vacancies in inner shells are filled by electrons from outer shells.

Prior to diffraction on the crystal lattice the radiation is collimated in the primary collimator to provide a parallel beam of x-rays. The collimators consist of a series of parallel plates, the coarse collimators for use with lighter elements, where loss of intensity is more critical and a fine collimator for the heavier elements. Incident x-rays pass through a thin window, causing ionization of the argon and the production of electrons. A potential between the casing (cathode) and the wire (anode) attracts these electrons towards the anode wire, thereby producing an electric current proportional to the intensity and energy of the x-ray photons. An x-ray radiation is then diffracted on a crystal of known lattice spacing, and the diffracted rays collected in a counter. Different peaks of x-ray radiations will occur and determine the emitting elements, because each element has an associated x-ray wavelength. Calibration of these peaks according to standards of known concentration lead to determination of concentration of different elements.

IV. 3 Inductively coupled plasma-mass spectrometry (ICP-MS)

An inductively coupled argon plasma technique was used as a source of ions to determine the concentration of rare earth elements (REE) by using a VG plasma Quad PQ2 Turbo plus (Fisons Instruments Elemental Analyser) mass spectrometer. This mass spectrometry consists of three components: 1, the argon plasma; 2, a quadrupole mass spectrometer and associated data

collection electronics; 3, an interface unit which permits sampling of the plasma gases and transfer of the ion beam into the mass spectrometer proper (Potts, 1987). After the samples have been taken into a solution (Appendix, III), then they are aspirated into the argon plasma, the interface unit will controlled the plasma gases to enter the spectrometer for analysis. For a satisfactory analyses, this mass spectrometers require a very high vacuum (usually better than 10^{-7} Torr). The ion beam have been collimated and then passes through a number of plates biased at appropriate potential. These plates have created an electrostatic field which focusses the ion beam in a form suitable for transmission through the mass filter. However, the presence of spectrum peaks as small peaks and tails are result in wide variations of energies of ions, the effect of such tails on spread of ions reaching the detector is controlled by adjusting the mass filter. Moreover, the losses of ions due collisions are reduced by pumping away any species accompanying the plasma from the expansion chamber. Spectra, however, are built up by scanning a selected mass range with using a sweep time (0.1-1s), from each sweep the intensity data have been accumulated in a multi-channel analyser. Thereafter, the output count pulses from the ion detector are added to the appropriate channel, selected in synchronization with the quadrupole mass sweep. Analyses were quantified by integrating selected mass peaks over an appropriate channel range, and comparing the resultant data for duplicate samples.

IV. 4 Stable isotopes

Samples have been heated to extract the structural water as described in Appendix III.

IV. 4. 1 Hydrogen isotope mass spectrometry

Gas sample were transferred into an evacuated sample tube and then to the mass spectrometer. The hydrogen was isotopically analysed using a VG-Micomass 602B with a modified inlet system. Such an inlet system allows the use of mercury pistons to enable very small samples to be introduced in to the mass spectrometer. In this mass spectrometer a stream of electrons are generated by bombardment source, and then fired into a chamber containing the gas of interest. Some fraction of the gas molecules are struck

and ionized out of the chamber electrostatically, and accelerated through a potential difference to collimate the beam of ions. These ions pass into a magnetic field where the beam is split up according to the mass to charge ratio of the ions (by adjusting the magnetic field). Ions of a chosen mass to charge ratio are focused on the collector slit by selecting the appropriate value of the magnetic field. Isotope ratios are measured by monitoring molecular masses $2H_2^+$ and $3HD^+$; this 3/2 mass ratio of the gas sample was measured relative to the standard gas of $\partial D \approx -50$ °/oo, then a correction to mass 3 (according to Craig, 1957) has been applied to allow for the presence of H_3^+. The precision of data produced by this method is about 2°/oo or better.

IV. 4. 2 Oxygen isotope mass spectrometry

As the oxygen gas is reactive and suffers too great a risk of contamination from the atmosphere if measured directly by mass spectrometry, therefore the extracted gas is normally first converted to carbon dioxide by passing over a carbon rod heated to 550-600°C. A VG Sira 10 dynamic gas source mass spectrometer fitted with a triple collector was used. The mechanism of mass spectrometer is similar to those used of hydrogen isotope analyses (above).The ions monitored were 44 ($^{12}C^{16}O^{16}O^+$), 45 ($^{13}C^{16}O^{16}O^+$with minor $^{12}C^{16}O^{17}O^+$) and 46 ($^{12}C^{16}O^{18}O^+$with minor $^{13}C^{17}O^{16}O^+$and $^{13}C^{17}O^{17}O^+$). After correction for the interfering low abundance minor ions (see Craig, 1957), $^{18}O/^{16}O$ (and so $\partial^{18}O$) was calculated from the 46/44 and 45/44 ratios. The precision of data produced by this method is about 0.2°/oo or better.

The effect of blanks on measured isotopic composition of samples was calculated by the following equation (after Jenkin, 1988):

$$\partial Dm = \{(\partial Dsamp \times Msamp) + (\partial Dblank \times Mblank)\} / Mm$$

where: $\partial Dm = \partial D$ of measured gas at mass spectrometer; $\partial Dsamp = \partial D$ of uncontaminated gas from the sample; $\partial Dblank = \partial D$ of blank gas; Msamp = moles of gas from sample; Mblank = moles of gas from blank and Mm = Msamp + Mblank i.e. moles of measured gas.

IV. 5 Radiogenic isotopes

IV. 5. 1 Ionic exchange technique

An ion exchange technique was used to separate and purify elements before determining their isotopic ratios. Such procedure involving using column chemistry (see appendix III), on the basis of reversible exchange of ions between a solid phase {the resin, which normally packed into a suitable glass tube, however, two types of resins were used, (a)Bio-Rad AG50W and (b) Bio-Rad AG1 x8, see Appendix III} and a mobile phase {a solution of ions}. Ions of different elements are separated from one another due the differences in their affinity towards the ion exchange resin, the more strongly an ion is attracted to the ion exchange resin, the larger the volume of eluent required to wash that ion out of the ion exchange column. Different types of eluent was used according to the element of interest, for example in order to collect Sr and Rb, HCl was used, whereas, HNO_3 was used in REE collection.

IV. 5. 2 Isotope Dilution Analysis

Thermal ionisation mass spectrometry have been used to determine the concentration of an element which exists as two or more naturally occurring isotopes by isotope dilution analysis. This method is based on the measurement of the isotopic composition of an element in a mixture of a known weight of sample and a spike which consists of a precisely known amount of the element enriched in one isotope of that element. The spike and sample solutions are allowed to equilibrate prior to a chemical separation (ion exchange) to isolate the element of interest. This isolated element fraction is then analysed by the thermal ionisation mass spectrometry to determine the ratio between the spiked and unspiked masses, and hence the concentration of the element of interest is the sample.

IV. 5. 3 Thermal ionisation mass spectrometry

Thermal ionisation mass spectrometry has been used for all analysed radiogenic isotope elements in this study (Rb, Sr, Sm, and Nd). In a thermal

ionisation mass spectrometer ions are generated by passing an electric current through the filament on which the sample has been loaded, thus heating it up. The highest possible degree of ionisation is obtained by running the ionisation filament at the maximum possible temperature. The ions are accelerated out of the source using a potential difference across a source collimation block of typically 8000 volts. The ion beam is also focused within this source collimator.

After emerging from the ion source, the ions pass into magnetic field where the beam is split up according to the mass to charge ratio of the ions (by changing the magnetic field). Ions of a chosen mass to charge ratio are focused on the collector slit by selecting the appropriate value of the magnetic field. After passing through the collector slit the intensity of the selected ion beam is measured either by means of a Faraday Cup Collector or by means of a multiplier system. Typically the Faraday Cup will be used for beam sizes up to 10^{-11} amps, whereas multiplier system will be used in cases where the ion beam is less than 5×10^{-13} amps.

In a single collector ionisation mass thermal ionisation mass spectrometer (VG MM30 and VG 54E instruments) the different isotopes of a given element are sequentially cycled into the collector by systematically changing the intensity of the magnetic field. In the multiple collector instruments (VG sector 54-30) two types of data were employed. Firstly, static collection, in which each isotope is always collected in the same cup throughout the analysis; this enables rapid collection to occur, though uncertainties in data reproducibility are introduced due to small variations in the gains between the different collectors. Static multicollector was used for Sm and Nd isotope dilution analysis. Secondly, multi-dynamic collection, in which some peak jumping occurs. Although this take longer than static analysis, the uncertainties due to inter-collector gain variation do not occur, and the data produced are potentially more accurate. This technique was used for the measurement of the Nd and Sr isotopic compositions.

REFERENCES

Anderson, G.M. and Burnham, C. W., (1983) Feldspar solubility and the transport of aluminium under metamorphic conditions. *Am. J. Sci.*, **283A**: 283-297.

Arndt, N.T. and Goldstein, S. L., (1987) Use and abuse of crust-formation ages. *Geology*, **15**: 893-895.

Askren, D. R. R., Whitney, J. A. and Roden, M, F., (1991) Petrology and geochemistry of the Huerto Andesite, San Juan volcanic field, Colorado. *Contrib. Mineral. Petrol.*, **107**: 373-386.

Avila-Salinas, W.A., (1990) Tin-bearing from the Cordillera Real, Bolivia; a petrological and geochemical review. *Geol. Soc. Am. Spec. Pap.*, **241**: 145-159.

Bailey, E.B., (1947) Chilled and "baked" edges as criteria of relative age. *Geol. Mag.*, **84**: 126-128.

Barbarin, B., (1990) Granitoids: main petrogenetic classifications in relation origin and tectonic setting. *Geol. J.*, **25**: 227-238.

Barr, H., (1990) Preliminary fluid inclusion studies in a high-grade bluechist terrain, Syros, Greece. *Mineral. Mag.*, **54**: 159-168.

Batchelor, R. A., Armstrong, D. C. and McDonald, M., (1992) Composition of fluids in quartz: discrimination of magma pulses in Caledonian granitoid. *Mineral. Mag.*, **56**: 335-342.

Bates, L.R. and Jackson, J. A., (1980) Glossary of Geology. American Geological Institute.

Beckinsale, R. D., (1974) Rb-Sr and K-Ar age determinations, and oxygen isotope data for the Glen Cannel granophyre, Isle of Mull, Argyllshire, Scotland. *Earth Planet Sci. Lett.*, **22**: 267-274.

Bell, J.D., (1966) Granites and associated rocks of the eastern part of the Western Red Hills Complex, Isle of Skye. *Trans. Roy. Soc. Edin*b., **66**: 307-343.

Bell, J.D., (1976) The Tertiary intrusive complex on the Isle of Skye. *Proc. Geol. Assoc.*, **87**: 247-271.

Bell, B. R., (1982) The evolution of the Eastern Red Hills Tertiary igneous centre, Skye, Scotland. PhD. Thesis. London University.

Bell, B.R. and Harris, J. W., (1986) An excursion guide to the Geology of the Isle of Skye. *Geol. Soc. Glasgow.*, 1-317.

Bell, B. R., Claydon, R. V. and Rogers, G., (1994) The petrology and geochemistry of cone-sheets from the Cuillin Igneous Complex, Isle of Skye: Evidence for combined assimilation and fractional crystallisation during lithospheric extension. *J. Petrol.*, **34**: 1055- 1094.

Borthwick, J. and Harmon, R. S., (1982) A note regarding ClF_3 as an alternative to BrF_5 for oxygen isotope analysis. *Geochim. Cosmochim. Acta.*, **46**: 1665-1668.

Boullier, A.M., Lanord, C. F., Dubessy, J., Adamy, J. and Champenois, M., (1991) Linked fluid and tectonic evolution in the high Himalaya mountains (Nepal). *Contrib. Mineral. Petrol.*, **107**: 358-372.

Bowden, P. and Kinnaird, J. A., (1984) The petrology and geochemistry of alkaline granites from Nigeria. *Phys. Earth Planet. Inter.*, **35**: 199-211.

Brigatti, M. F. and Gregnanin, A., (1987) Crystal chemistry of igneous rock biotites. *Mineral. Petrol.*, **37**: 323-341.

Brooks, C., Hart, S. R. and Wendt, T., (1972) Realistic use of two-error regression treatments as applied to rubidium-strontium data. *Rev. Geophys. Space Phys.*, **10**: 551-577.

Brooks, C., James, D. E. and Hart, S. R., (1976) Ancient lithosphere: its role in young continental volcanism. *Science.*, **193**: 1086-1094.

Brown, G. M., (1963) Melting relations of Tertiary granitic rocks in Skye and Rhum. *Mineral. Mag.*, **33**: 533-562.

Brown, G. C. and Mussett, A. E., (1976) Evidence for two discrete centre in Skye. *Nature.*, **261**: 218-220.

Brown, G. C., Thorpe, R. S. and Webb, P. C., (1984) The geochemical characteristics of granitoids in contrasting arcs and comments on magma sources. J. *Geol. Soc. Lond.*, **141**: 413-426.

Bryon, D. N., Atherton, M. P., and Hunter, R. H., (1994) The description of the primary textures of "Cordilleran" granitic rocks. *Contrib. Mineral. Petrol.*, **117**: 66-75.

Buma, G., Frey, F. A., and Wones, D. R., (1971) New England Granites: Trace element evidence regarding their origin and differentiation. *Contrib. Mineral. Petrol.*, **31**: 300-320.

Cameron, M. and Papike, J.J., (1982) Crystal chemistry of Silicate pyroxenes. *Rev. Mineralogy, Mineral. Soc. Am.*, **7**: 5-92.

Capdevila, R. and Floor, P., (1970)*Boletín de Geologiá y Mineralogiá, España,* **81**: 215-225.

Capdevila, R., Gorretegé, G. and Floor, P., (1973) *Bulletin de la Société géologique de France,* **15**: 209-228.

Carstens, C., (1983) Simultaneous crystallisation of quartz and alkali feldspar intergrowth from granitic magmas. *Geology,* **11**: 339-341.

Carter, S.R., Evensen, N. M., Hamilton, P. J. and O'Nions, R. K., (1978) Neodymium and strontium isotope evidence for crustal contamination of continental volcanics. *Science,* **202**: 743-747.

Cawthorn, R. G., (1976) Some chemical controls on igneous amphibole compositions. *Geochim. Cosmochim. Acta.*, **40**: 1319-1328.

Chao, E. C.T. and Fleischer, M., (1960) Abundance of zirconium in igneous rocks. *Rep. Int. Geol. Congr. XXI Session (Norden),* **I**: 106-131.

Chappell, B.W. and White, A. J. R., (1974) Two contrasting granite types. *Pacific Geol.*, **8**:173-174.

Chappell, B.W. and White, A. J. R., (1984) I-and S-type granites in the Lachlan Fold Belt, south-eastern Australia. In: Xu Kegin and Tu Guangchi (eds), Geology of Granites and their Metallogenetic Relations. Proceedings of the international Symposium, Nanjing University. *Science Press, Beijing*. 87-101.

Chappell, B.W. and Stephens, W. E., (1988) Origin of infracrustal (I-Type) granite magmas. *Trans. Roy. Soc. Edinb. Earth sciences.*, **79**: 71-86.

Chappell, B.W. and White, A. J. R., (1992) I- and S-type granites in the Lachlan Fold Belt. *Trans. Roy. Soc. Edinb. Earth scienes.*, **83**: 1-26.

Chayes, F., (1985) IGBADAT: a word data base for igneous petrology. *Episodes*, **8**: 245-251.

Chiba, H., Chacko, T., Clayton, R. N. and Goldsmith, J. R., (1989) Oxygen isotope fractionations involving diopside, forsterite, magnetite and calcite: application to geochemistry. *Geochim. et Cosmochim. Acta*, **53**: 2985-2995.

Clarke, D.B., (1992) Granitoid Rocks. London,: Chapman & Hall. 1-283.

Claur, N., O'Neil, J. R., and Bonnot-Courtois, C., (1982) The effect of natural weathering on the chemical and isotopic compositions of biotites. *Geochim. Cosmochim. Acta.*, **46**: 1755-1762.

Clayton, R.N. and Mayeda, T. K., (1963) The use of bromine pentafluoride in the extraction of oxygen from oxides and silicates for isotopic analysis. *Geochim. Cosmochim. Acta*, **27**: 43-52.

Clayton, R. N., Goldsmith, J. R., and Mayeda, T. K., (1989) Oxygen isotope fractionation in quartz, albite, anorthite and calcite. *Geochim. Cosmochim. Acta*, **53**: 725-733.

Clemens, J. D., Holloway, J. R. and White, A. J. R., (1986) Origin of an A-type granite: experimental constraints. *Am. Mineral.*, **71**: 317-324.

Cohen, R. S., Evensen, N. M., Hamilton, P. J. and O'Nions, R. K., (1980) U-Pb, Sm-Nd and Rb-Sr systematics of mid-ocean ridge basalt glasses. *Nature*, **283**: 149-153.

Cohen, A. S., O'Nions, R. K. and O'Hara, M. J., (1991) Chronology and mechanism of depletion in Lewisian granulites. *Contrib. Mineral. Petrol.*, **106**: 142-153.

Collins, W.J., Beams, S. D., White, A. J. R. and Chappell, B. W., (1982) Nature and origin of A-type granites with particular reference to south-eastern Australia. *Contrib. Mineral. Petrol.*, **80**: 189-200.

Cox, K. G., Bell, J. D. and Pankhurst, R. J., (1979) The interpretation of igneous rocks. Allen and Unwin, London.

Craig, H., (1957) Isotopic standards for carbon and oxygen and correction factors for mass spectrographic analysis of carbon dioxide. *Geochim. Cosmochim. Acta*, **12**: 133-149.

Craig, H., (1961) Isotope variations in meteoric water. *Science*, **133**: 1702-1703.

Creaser, R. A., Price, R. C. and Wormald, R. J., (1991) A-type granites revisited: assessment of a residual-source model. *Geol.*, **19**: 163- 166.

Criss, H., and Taylor, H. P., Jr., (1986) Meteoric hydrothermal Systems. In: Valley, J. W., Taylor, H. P., Jr., & O'Neil, J. R. (eds.) Stable isotopes in high temperature geological processes. *Rev. Mineralogy, Mineral. Soc. Am.*, **16**: 373-424.

Curtis, S. F., Pattrick, R. A. D., Jenkin, G. R. T., Fallick, A. E., Boyce, A. J. and Treagus, J. E., (1993) Fluid inclusion and stable isotope study of fault-related mineralisation in Tyndrum area, Scotland. *Trans. Instn. Min. Metall. (Sect. B: Appl. earth sci.)*, **102**: B39-B47.

Czamanske, G. K., Ishihara, S. and Atkin, S. A., (1981) Chemistry Of rock-forming minerals of the Cretaceous-Palaeocene batholith in south-western Japan and implications for magma genesis. *J. Geophy. Resch.*, **86**: 10431-10469.

Darbyshire, D. P. F. and Shepherd, T. J., (1994) Nd and Sr isotope constraints on the origin of the Cornubian batholith, SW England. *J. Geol. Soc. Lond.*, **151**: 795-802.

Davidson, C.F. and Walker, F., (1934) The Tertiary Geology of Raasay, Inner Hebrides. *Trans. Roy. Soc. Edinb.*, **58**: 374-407.

Davis, G.L., (1978) Zircons from mantle. In: Zartmann RE (ed) Fourth Int Conf Geochron Cosmochron Isotope Geol. *US Geol. Surv. Open-File Rep.*, **78-701**: 86-88.

De Albuquerque, C. A. R., (1973) Geochemistry of biotites from granitic rocks, Northern Portugal. *Geochim. Cosmochim. Acta.*, **37**: 1779-1802.

De la Roche, L., J., Grande C. P. & Marchal, M., (1980) A classification of volcanic and plutonic rocks using R1-R2 diagrams and major element analyses-its relationships and current nomenclature. *Chem. Geol.*, **29**: 183-210.

De la Roche, H., (1986)*Bulletin de la Societe geologique de France.*, **8 (11)**: 337-353.

Debon, F. and Le Fort, P., (1988)*Bulletin de Mineralogie.*, **111**: 493-510.

Deer, W. A., Howie, R. A. and Zussman, J., (1962) Rock forming-minerals, sheet silicates. 1st ed. **Vol.3**, William clowes and sons, London.

Deer, W. A., Howie, R. A. and Zussman, J., (1963a) Rock forming-minerals, Framework silicates. 1st. ed. **Vol. 4**, William Clowes and sons, London.

Deer, W. A., Howie, R. A. and Zussman, J., (1963b) Rock forming-minerals, Chain silicates. 1st. ed. **Vol. 2**, William clowes and sons, London.

Deer, W. A., Howie, R. A. and Zussman, J., (1978) Rock forming-minerals, Single-chain silicates. 2nd ed. **Vol. 2A**, Longman, London.

Deer, W. A., Howie, R. A. and Zussman, J., (1989) An introduction to the rock-forming minerals. 2nd ed. Longman, London and New York.

Deer, W. A., Howie, R. A. & Zussman, J., (1993) An introduction to the rock-forming minerals. 2nd ed. Longman, London.

Dempsey, C. S., Halliday, A. N. and Meighan, I. G., (1990) Combined Sm-Nd and Rb-Sr isotope systematics in the Donegal granitoids and their petrogenetic implications. *Geol. Mag.*, **127**: 75-80.

DePaolo, D.J. and Wasserburg, G. J., (1976) Nd isotope variations and Petrogenetic models. *Geophy. Res. Lett.*, **3**: 249-252.

DePaolo, D.J., (1981) Trace element and isotopic effects of combined wall rock assimilation and fractional crystallisation. *Earth Planet. Sci. Lett.*, **53**: 189-202.

Dickin, A.P., Exley, R. A. and Smith, B. M., (1980) Isotope measurement of Sr and O exchange between meteoric-hydrothermal fluid and the Coire Uaigneich Granophyre, Isle of Skye, N. W. Scotland. *Earth Planet. Sci. Lett.*, **51**: 58-70.

Dickin, A.P. and Exley, R. A., (1981) Isotope and geochemical evidence from magma mixing in the petrogenesis of the Coire Uaigneich Granophyre, Isle of Skye, N. W. Scotland. *Contrib. Mineral. Petrol.*, **76**: 98-108.

Dickin, A.P., Moorbath, S. and Welke, H. J., (1981) Isotope, trace element and major element geochemistry of Tertiary igneous rocks, Isle of Arran, Scotland. *Transc. Roy. Soc. Edinb.: Earth Sci.*, **72**: 159-170.

Dickin, A.P., (1981) Isotope geochemistry of Tertiary igneous rocks from the Isle of Skye, N. W. Scotland. *J. Petrol.*, **22**: 155-189.

Dickin, A. P. and Jones, N. W., (1983) Isotope evidence for the age and origin of pitchstones and felsites, Isle of Eigg, N. W. Scotland. J. *Geol. Soc. Lond.*, **140**: 691-700.

Dickin, A.P., Brown, J.L., Thompson, R.N., Halliday, A. N. and Morrison, M. A., (1984) Crustal contamination and the granite problem in the British Tertiary Volcanic Province. *Phil. Trans. Roy. Soc.Lond.*, **A 310**: 755-780.

Dickin, A.P., Fallick, A. E., Halliday, A. N., Macintyre, R. M. and Stephens, W. E., (1986) An isotopic and geochronological investigation of the younger igneous rocks of the Seychelles microcontinent. *Earth planet. Sci. Lett.*, **81**: 46-56.

Dickin, A. P., Jones, N. W., Thirlwall, M. F. and Thompson, R. N., (1987) A Ce/Nd isotope study of crustal contamination processes affecting Palaeocene magmas in Skye, Northwest Scotland. *Contrib. Mineral. Petrol.*, **96**: 455-464.

Dickin, A. P., (1994) Nd isotope chemistry of Tertiary igneous rocks from Arran, Scotland: implications for magma evolution and crustal structure. *Geol. Mag*, **131**: 329-333.

Didier, J. and Lameyre, J., (1969) Les granites du Massif Central francais: Etude comparee des leucogranites et granodiorites. *Contrib. Mineral. Petrol.*, **24**: 219-238.

Didier, J., Duthou, J. L. and Lameyre, J., (1982) Mantle and crustal granites: genetic classification of orogenic granites and the nature of their enclaves. *J. Vol. Geotherm. Res.*, **14**: 125-132.

Didier, J. and Barbarin, B. (eds), (1991) Enclaves and Granite Petrology. 2nd ed. Elsevier. Amsterdam.

Dietrich, R.V., (1968) Behaviour of zirconium in certain artificial magmas under diverse P-T conditions. *Lithos*, **1**: 20-29.

Dunham, A. C., (1965) The nature and origin of the groundmass textures in felsites and granophyres from Rhum, Inverness-shire. *Geol. Mag.*, **102**: 8-23.

Dunham, A. C. and Thompson, R. N., (1967) The origin of granitic magmas: Skye and Rhum. *J. Geol. Soc. Aust.*, **14**: 339-343.

Dupre, B. and Allègre, C. J., (1980) Pb-Sr-Nd isotopic correlation and the chemistry of the North Atlantic mantle. *Nature*, **286**: 17-22.

Elsenheimer, D. and Valley, J.W., (1993) Submillimeter scale zonation of ^{18}O in quartz and feldspar, Isle of Skye, Scotland. *Geochim. Cosmochim. Acta*, **57**: 3669-3676.

Emeleus, C.H., (1982) The central complex. In: Igneous of British Isles , **Chapter 29**. John Wiley and Sons Ltd.

Emeleus, C.H., (1989) Tertiary igneous activity. In: Geology of Scotland, **Chapter 14**. John Wiley and Sons Ltd.

Evangelakakis, C., Kroll, H., Voll, G., Wenk, H.R., Meisheng, Hu. and Köpcke, J., (1993) Low-temperature coherent exsolution in alkali feldspars from high-grade metamorphic rocks of Sri Lanka. *Contrib. Mineral. Petrol.*, **114**: 519-532.

Evans, A.l., Fitch, G.J., and Miller,J. A., (1973) Potassium-Argon age determinations of some British Tertiary Igneous rocks. *J. Geol. Soc.*, **129**: 419-443.

Evans, O.C., and Hanson, G. N., (1993) Accessory-mineral fractionation of rare-earth element (REE) abundances in granitoid rocks. *Chem. Geol.*, **110**: 69-93.

Exley, R.A., (1980) Microprobe studies of REE-rich accessory minerals: Implications for Skye Granite petrogenesis and REE mobility in hydrothermal systems. *Earth. Planet. Sci. Lett.*, **48**: 97-110.

Faure, G., (1977) Principles of isotope geology. **1st ed.** Wiley, New York.

Faure, G., (1986) Principles of isotope geology. **2nd ed.** J. Wiley & sons, New York.

Feely, M., and Högelsberger, H., (1991) Preliminary fluid inclusion studies of the Mace Head Mo-Cu deposit in the Galway Granite. *Irish J. Earth Sci.*, **11**: 1-10.

Ferry, J. M., (1979) Reaction mechanisms, physical conditions, and mass transfer during hydrothermal alteration of mica and feldspar in granitic rocks from south-central Maine, USA. *Contrib. Mineral. Petrol.*, **68**: 125-139.

Ferry, J. M., (1985) Hydrothermal alteration of Tertiary igneous rocks from the Isle of Skye, Northwest Scotland. II Granites. *Contrib. Mineral. Petrol.*, **91**: 283-30-4.

Finch, A. A. and Walker, F. D. L., (1991) Cathodoluminescence and microporosity in alkali feldspars from the Blå Måne SØ perthosite, South Greenland. *Mineral. Mag.*, **55**: 583-589.

Fitton, J. G. and Dunlop, H. M., (1985) The Cameroon line, West Africa, and its bearing on the origin of oceanic continental alkali basalt. *Earth Planet. Sci. Lett.*, **72**: 23-38.

Floyd, P. A. and Winchester, J. A., (1975) Magma type and tectonic setting discrimination using immobile elements. *Earth Planet. Sci. Lett.*, **27**: 211-218.

Folk, R.L., (1955) Note on the significance of "turbid" feldspars. *Am. Mineral.*, **40**: 356-357.

Forbes, J.D., (1845) Notes on the petrography and geology of the Cuchullin Hills in Skye, and on the traces of ancient glaciers which they present. *Edinb. New Phil. JI.*, **40**: 76-99.

Forester, R.W. and Taylor, H. P., Jr, (1976) ^{18}O-depleted igneous rocks from the Tertiary complex of the Isle of Mull, Scotland. *Earth Planet Sci. Lett.*, **32**: 11-17.

Forester, R.W. and Taylor, H. P., (1977) $^{18}O/^{16}O$, D/H, and $^{13}C/^{12}C$ studies of the Tertiary Igneous Complex of Skye, Scotland. *Am. J. Science*, **277**: 136-177.

Forester, R.W., and Taylor, H. P., (1980) Oxygen, hydrogen, and carbon isotope studies of the Stony Mountain Complex, Western San Juan Mountains, Colorado. *Econ. Geol*, **75**: 362-383.

Fourcade, S. and Allègre, C. J., (1981) Trace elements behaviour in Granite Genesis: A Case study the calc-alkaline plutonic association from the Querigut complex (Pyrenees, France). *Contrib. Mineral. Petrol.*, **76**: 177-195.

Frost, C. D. and O'Nions, R. K., (1985) Caledonian magma genesis and crustal recycling. *J. Petrol.*, **26**: 515-544.

Futa, K., (1981) Sm-Nd systematic of a tonalitic augen gneiss and its constituent minerals from northern Michigan. *Geochim. Cosmochim. Acta*, **45**: 1245-1249.

Gallagher, V., Feely, M., Högelsberger, H., Jenkin, G. R. T. and Fallick, A. E., (1992) Geological, fluid inclusion and stable isotope studies of Mo mineralisation, Galway Granite, Ireland. *Mineral Deposita*, **27**: 314-325.

Gamble, J.A., (1975) The structure, petrology and geochemistry of the central complex of Slieve Gullion. PhD thesis. The Queen's University of Belfast.

Gamble, J.A., Meighan, I. G. and McCormick, A. G., (1992) The petrogenesis of Tertiary microgranites and granophyres from the Slieve Gullion Central Complex, NE Ireland. *Jour. Geol. Soc. Lond.*, **149**: 93-106.

Geikie, A., (1897) The ancient volcanoes of Great Britain. **2 Volumes**. Macmillan, London.

Ghose, S., (1965) A scheme of cation distribution in the amphiboles. *Mineral. Mag.*, **35**: 46-54.

Gibson, D., (1984) The petrology and geochemistry of the Western Mourne Granites, Co Down, N. Ireland. PhD Thesis, The Queen's University, of Belfast.

Gilbert, M. C., Helz, R. T., Popp, R. K. and Spear, F. S., (1982) Experimental studies of amphibole stability. *Rev. Minerlogy, mineral. Soc. Am.*, **9B**: 229-353.

Giletti, B. J., Semet, M. P. and Yund, R. A., (1978) Studies in diffusion-III. Oxygen in feldspars, an ion microprobe determination. *Geochim. Cosmochim. Acta.*, **42**: 45-57.

Godfrey, J.D., (1962) The deuterium of hydrous minerals from the East-Central Sierra Nevada and Yosemite National Park. *Geochim. Cosmochim. Acta.*, **26**: 1215-1245.

Graham, C.M., Harmon, R. S., and Sheppard, S. M.F., (1984) Experimental hydrogen isotope studies: hydrogen isotope exchange between amphibole and water. *Am. Mineral.*, **69**: 128-138.

Green, T.H., (1980) Island arc and continent-building magmatism: a review of petrogenetic models based on experimental petrology and geochemistry. *Tectonophysics.*, **63**: 367-385.

Gregory, R.T., and Criss, R. E., (1986) Isotopic exchange in open and closed systems. In: Valley, J.W., Taylor, H. P., Jr., & O'Neil, J. R. (eds) Stable isotopes in high temperature Geological processes. *Rev. Mineralogy, Mineral. soc. Am.*, **16**: 91-127.

Gromet, L.P., and Silver, L. T, (1983) Rare earth element distributions among minerals in granodiorite and their petrogenetic implications. *Geochim. Cosmochim. Acta*, **47**: 925-939.

Guthrie, G.D., Jr., and Veblen, D. R., (1991) Turbid alkali feldspar from the Isle of Skye, N.W.Scotland. *Contrib. Mineral. Petrol.*, **108**: 298-304.

Halliday, A.N., Stephens, W. E. and Harmon, R. S., (1981) Isotope and chemical constraints on the development of peraluminous Caledonian and Acadian granites. *Can. Mineral.*, **19**: 205-216.

Halliday, A.N., (1984) Coupled Sm-Nd and U-Pb systematics in late Caledonian granites and the basement under northern Britain. *Nature.*, **284**: 542-543.

Halliday, A. N., Stephens, W. E., Hunter, R. H. Menzies, M. A., Dickin, A. P. and Hamilton, P. J., (1985) Isotopic and chemical constraints on the building of the deep Scottish lithosphere. *Scottish J. Geol.*, **21**: 465-491.

Hamilton, P.J., Evensen, N. M., O'Nions, R. K. and Tarney, J., (1979) Sm-Nd systematics of Lewisian gneisses: implications for the origin of granulites. *Nature*, **277**: 25-28.

Hanchar, J. M., and Miller, C. F., (1993) Zircon zonation patterns as revealed by cathodoluminescence and backscattered electron images: Implications for interpretation of complex crustal histories. *Chem. Geol.*, **110**: 1-13.

Hansmann, W., and Oberli, F., (1991) Zircon inheritance in an igneous rock suite from the southern Adamello batholith (Italian Alps). *Contrib. Mineral. Petrol.*, **107**: 501-518.

Hanson, G.N., (1978) The application of trace elements to the petrogenesis of igneous rocks of granitic composition. *Earth and Planet. Sci. Lett.*, **38**: 26-43.

Hansteen, T. H. and Lustenhouwer, W. J., (1990) Silicate melt inclusions from a mildy peralkaline granite in the Oslo paleorift, Norway. *Mineral. Mag.*, **54**: 195-205.

Harker, A., (1904) The Tertiary Igneous rocks of Skye. *Mem. Geol. Surv. Great Britain..*

Harker, A., (1909) The natural history of igneous rocks; Methuen, London.

Harrison, R. K., Stone, P., Cameron, I. B., Elliot, R.W. and Harding, R. R., (1987) Geology, petrology and geochemistry of Ailsa Craig, Ayrshire. *Brit. Geol. Surv. Rep.*, **16, No 9**: 29. H.M.S.O.

Harrison, T.M., and Watson, E. B., (1984) The behaviour of apatite during crustal anatexis: equilibrium and kinetic considerations. *Geochim. Cosmochim. Acta*, **48**: 1467-1477.

Harrison, T. M., Aleinikoff, J. N., and Compston, W., (1987) Observations and controls on the occurrence of inherited zircon in Concord-type granitoids, New Hampshire. *Geochim. Cosmochim. Acta*, **51**: 2549-2558.

Harvey, P.K., Taylor, D. M., Hendry, R. D. and Bancroft, F., (1973) An accurate fusion method for the analysis of rocks and chemically related materials by X-ray fluorescence spectrometry. *X-ray spectrometry.*, **2**: 33-44.

Haselton, H. T. J., Hovis, G. L., Hemingway, B. S. and Robie, R. A., (1983) Calorimetric investigation of the excess entropy of mixing in an albite-sanidine solid solutions: Lack of evidence for Na, K short range order and implications for two-feldspar thermometry. *Am. Mineral.*, **68**: 398-413.

Hatch, F. H., Wells, A. K. and Wells, M. K., (1972) Petrology of igneous rocks, London: George Allen & Unwin Ltd.

Haung, W. T., (1962) Petrology. McGraw-Hill Book Company, Inc. London.

Hawkesworth, C.J. and Morrison, M. A., (1978) A reduction in $^{87}Sr/^{86}Sr$ during basalt alteration. *Nature.*, **276**: 381-383.

Hayward, C. L. and Jones, A. P., (1991) Cathodoluminescence petrography of Middle Proterozoic extrusive carbonate from Qasiarsuk, South Greenland. *Mineral. Mag.*, **55**: 591-603.

Henderson, P., (1982) Inorganic Geochemistry. Pergamon Press, Oxford.

Hildreth, W., (1979) The Bishop Tuff: Evidence for origin of compositional zonation in silicic magma chambers. *Geol. Soc. Am. Spec. Paper*, **180**: 43-76.

Hinton, R.W. and Upton, B. G. J., (1991) The chemistry of zircon: Variations within and between large crystals from Syenite and alkali basalt xenoliths. *Geochim. Cosmochim. Acta.*, **55**: 3287-3302.

Hoffman, J., E. and Long, J. V. P., (1984) Unusual sector zoning in Lewisian zircons. *Mineral. Mag.*, **48**: 513-517.

Hoersch, A.L., (1981) Progressive metamorphism of chert-bearing Durness limestone in the Beinn a Dubhaich aureole, Isle of Skye, Scotland: A reexamination. *Am. Mineral.*, **66**: 491-506.

Holness, M. B. and Fallick, A. E., (1994) Palaeohydrology of the Beinn an Dubhaich aureole, Skye, and inferred mechanisms of fluid infiltration in carbonates. *Mineral. Mag.*, **58A**: 428-429.

Hood, D.N., (1981) Geological, petrological and structural studies on the Tertiary granites and associated rocks of the Eastern Mourne Mountains, Co. Down, N. Ireland. Ph.D thesis, The Queen's University of Belfast.

Huang, W.T., (1962) Petrology. Mc Graw-Hill, New York.

Ishihara, S., (1977) *Mining Geology Japan.*, **27**: 293-300.

Jacobsen, S.B., (1988) Isotopic constraints on crustal growth and recycling. *Earth Planet. Sci. Lett.*, **90**: 315-329.

Jenkin, G.R.T., (1988) Stable isotope studies in the Caledonides of SW Connemara, Ireland. PhD Thesis, University of Glasgow.

Jenkin, G.R.T., Linklater, C. and Fallick, A. E., (1991) Modelling of mineral $\delta^{18}O$ values in an igneous aureole: Closed-system model predicts apparent open-system $\delta^{18}O$ values. *Geol.*, **19**: 1185-1188.

Jenkin, G.R.T., Fallick, A. E. and Leake, B. E., (1992) A stable isotope study of retrograde alteration in S. W. Connemara, Ireland. *Contrib. Mineral. Petrol.*, **110**: 269-288.

Jenkin, G.R.T., Farrow, C.M., Fallick, A.E. and Higgins, D., (1994) Oxygen isotope exchange and closure temperatures in cooling rocks. *J. Metamorphic Geol.*, **12**: 221-235.

Johannsen, A., (1931) A descriptive petrology of the igneous rocks. Baker and Taylor, New York.

Judd, J.W., (1874) The secondary rocks of Scotland. Second Paper. On the ancient volcanoes of the highlands and the relations of their products to the Mesozoic strata. *Q. JI. geol. Soc. Lond.*, **30**: 220-301.

Keith, M. L. and Tuttle, O. F., (1952) Significance of variation in the high-low inversion of quartz. *Am. J. Sci.*, **Bowen Vol.**: 203-280.

King, B. C., (1960) The form of the Beinn an Dubhaich Granite, Skye. *Geol. Mag.*, **97**: 326-333.

Kleeman, A.W., (1965) The origin of granitic magmas. *J. Geol. Soc. Aust.*, **12**: 35-52.

Kleeman, A.W., (1967) The origin of granitic rocks: Skye and Rhum. *J. Geol. Soc. Aust.*, **14**: 345-347.

Kresten, P., Fels, P., and Berggren, G., (1975) Kimberlitic zircons-A possible aid in prospecting from kimberlites. *Mineral deposita*, **10**: 47-56.

Kuroda, Y., Yamada, T., Kobayashu, H., Othoma, Y., Yagi, M., and Matsuo, S., (1986) Hydrogen isotope study of the granitic rocks of the Ryoke belt, central Japan. *Chem. Geol. (Isot. Geosci. Sec.)*, **58**: 283-302.

Lacroix, A., (1898) *Bulletin du Service de la carte géologique de France.*, **64**, (10): 241-306.

Lamb, W.M., Brown, P. E. and Valley, J. W., (1991) Fluid inclusions in Adirondack granulites: implication for retrograde P-T path. *Contrib. Mineral. Petrol*, **107**: 472-483.

Lameyre, J., (1980) Les magmas granitiques: leurs compartements, leurs associations et leurs sources. In: *Livre Jubilaire Soc. Geol. France, Mem. hors-serie.*, **10**: 51-62.

Lameyre, J. and Bowden, P., (1982) Plutonic rock type series: discrimination of various granitoid series and related rocks. *J. Vol. Geotherm. Res.*, **14**: 169-186.

Lang, I. M., Reynolds, R.C. and Lyons, J. B., (1966) K/Rb ratios in coexisting K-feldspars and biotites from some new England granites and Metasediments. *Chem. Geol.*, **1**: 317-322.

Le Bas, M.J. and Streckeisen, A. L., (1991) The IUGS systematics of igneous rocks. *J. Geol. Soc. Lond.*, **148**: 825-833.

Le Maitre, R.W., Bateman, P. Dudek, A. and Keller, J., (1989) A classification of igneous rocks and glossary terms: recommendation of IUGS Subcommission on the systematics of igneous rocks. Blackwell Scientific Publications. Oxford: 1-193.

Leake, B.E., (1971) On aluminous and edenitic hornblendes. *Min. Mag.*, **38**: 389-407.

Leake, B.E., (1978) Nomenclature of amphiboles. *Min Mag.*, **42**: 533-563.

Liggett, D.L., (1990) Geochemistry of the garnet-bearing Tharps Peak granodiorite and its relation to other members of the Lake Kaweah intrusive suite, south-western Sierra Nevada, California. In, Anderson, J. L.(ed), The nature and origin of Cordilleran Magmatism. *Geol. Soc. Am. Mem.*, **174**: 224-236.

Lloyd, G. E., (1987) Atomic number and crystallographic contrast images with the SEM: a review of backscattered electron techniques. *Mineral. Mag.*, **51**: 3-19.

Loiselle, M. C. and Wones, D. R., (1979) Characteristic and origin of anorogenic granites. *Geol. Soc. Am. Abs. with Prog.*, **11**: 468.

Loomis, T.P., (1982) Numerical simulations of crystallisation processes of plagioclase in complex melts: the origin of major and oscillatory zoning in plagioclase. *Contrib. Mineral. Petrol.*, **81**: 219-229.

Macculloch, J., (1819) A description of the Western Island of Scotland, including the Isle of Man: Comprising an account of their geological structure; with remarks on their agriculture, scenery, and

antiquities. **3 volumes. (Skye, vol. 1, 262-419).** Hurst Robinson, London.

Mahood, G. and Hildreth, W., (1983) Large partition coefficients for trace elements in high-silica rhyolites. *Geochim. Cosmochim. Acta*, **47**: 11-30.

Manier, P.D. and Piccoli., P. M., (1989) *Geol. soc. Am.*, **101**: 635-643.

Mattey, D. P., Gibson, I. L., Marriner, G. F., and Thompson, R. N., (1977) The diagnostic geochemistry, relative abundance and spatial distribution of high -calcium, low-alkali olivine tholeiite dykes in the Lower Tertiary regional swarm of the Isle of Skye, N. W. Scotland. *Mineral. Mag.*, **41**: 273-285.

Matsuhisa, Y., Goldsmith, J. R., and Clayton, R. N., (1979) Oxygen isotopic fractionation in the system quartz-albite-anorthite-water. *Geochim. Cosmochim. Acta*, **43**: 1131-1140.

McCormick, A.G., (1989) Isotopic studies on the Eastern Mourne Centre and other Tertiary acid igneous rocks of North East Ireland, PhD thesis. The Queen's University of Belfast.

McCormick, A. G., Fallick, A. E., Harmon, R.S., Meighan, I. G., and Gibson, D., (1993) Oxygen and Hydrogen isotope geochemistry of the Mourne Mountains Tertiary granites, Northern Ireland. *Jour. Petrol.*, **34, part 6,**: p. 1177-1202.

McIntyre, D.B. and Reynolds, D. L., (1947) Chilled and "baked" edges as criteria of relative age. *Geol. Mag.*, **84,**: p. 61-64.

McBirney, A. R., (1984) Igneous Petrology. Freeman Cooper and company, San Francisco.

McCulloch, M.T. and Chappell, B. W., (1982) Nd isotopic characteristic of S- and I-type granites. *Earth Planet. Sci. Lett.*, **58**: 51-64.

Mehnert, K.R., (1968) Migmatites and Origin of Granitic Rocks. 1st.ed. Elsevier. Amsterdam.

Meighan, I.G., (1979) The acid igneous rocks of the British Tertiary province. *Bull. Geol. Surv. U.K.*, **70**: 10-22.

Meighan, I.G.,Fallick, A. C. and McCormick, A. C. (1992) Anorogenic granite magma genesis: new isotopic data for the southern sector of the British Tertiary Igneous Province. *Trans. Roy. Soc. Edinb. Earth Sci.*, **83**: 227-233.

Michael, P.J., (1988) Partition coefficients for rare earth elements in mafic minerals of high silica rhyolites: the importance of accessory mineral inclusions. *Geochim. Cosmochim. Acta*, **52**: 275-282.

Miller, J.A. and Mohr, P.A., (1965) Potassium-aragon age determination from St. Kilda and Rockall. *Scott. J. Geol.*, **1**: 93-99.

Miller, C.F., Wooden, J. L. and Bennett, V. C., (1990) Petrogenesis of the composite peraluminous-metaluminous Old Woman-Piute Range batholith, south-eastern California; isotropic constraints. In, Anderson, J. L. (ed) The nature and origin of Cordilleran Magmatism. *Geol. Soc. Am. Mem.*, **174**: 99-109.

Mittlefehldt, D.W., and Miller, C. F., (1983) Geochemistry of the Sweet water Wash pluton, California: implications for 'anomalous' trace element behaviour during differentiation of felsic magmas. *Geochim. Cosmochim. Acta.*, **47**: 109-124.

Moorbath, S. and Bell, J. D., (1965) Strontium isotope abundance studies and rubidium-strontium age determinations on Tertiary igneous rocks from the Isle of Skye, North-west Scotland. *J. Petrol.*, **6**: 37-66.

Moorbath, S. and Welke, H., (1969) Lead isotope studies on igneous rocks from the Isle of Skye, Northwest Scotland. *Earth Planet. Sci. Lett.*, **5**: 217-230.

Moorbath, S. and Thompson, R. N., (1980) Strontium isotope geochemistry and petrogenesis of the early Tertiary lava pile on the Isle of Skye, Scotland, and other basic rocks of British Tertiary Province: an example of magma-crust interaction. *J. Petrol.*, **21**: 295-321.

Morse, S. A., (1970) Alkali feldspars with water at 5 kb pressure. *J. Petrol.*, **11**: 221-253.

Nabelek, P.I., O'Neil, J.R., and Papike, J. J., (1983) Vapour phase exsolution as a controlling factor in hydrogen isotope variation in granitic rocks:

the Notch Peak granitic stock, Utah. *Earth Planet. Sci. Lett.*, **66**: 137-150.

Nabelek, P.I., (1986) Trace-element modelling of the petrogenesis of granophyres and aplites in the Notch Peak granitic stock, Utah. *Am. Minerl.*, **71**: 460-471.

Nachit, H. et al., (1985) *Comptes rendu de l' Acadèmie des scince, Paris.*, **301**: 813-818.

Nagasawa, H., (1970) Rare earth concentrations in zircons and apatites and their host dacites and granites. *Earth Planet. Sci. Lett.*, **9**: 359-364.

Nakamura, N., (1974) Determination of REE, Ba, Fe, Mg, Na and K in carbonaceous and ordinary chondrites. *Geochim. Cosmochim. Acta*, 38: 757-775.

Nash, W.P. and Crecraft, H. R., (1985) Partition coefficients for trace elements in silicic magmas. *Geochim. Cosmochim. Acta*, **49**: 2309-2322.

Nicholson, R., (1970) A note on deformed igneous sheets in the Durness Limestone of Strath district of Skye. *Geol. Mag.*, **107**: 229-233.

Nockolds, S. R., Knok, R.W. O. B., and Chinner, G. A., (1978) Petrology for students, London.

O'Connor, P. J., (1976) Strontium isotope ratios of some acid rocks from Mull and Arran, Scotland. *Geol. Mag.*, **113**: 389-391.

O'Neil, J.R and Chappell, B., W., (1977) Oxygen and hydrogen isotope relations in the Berrridale Batholith, South-eastern Australia. *J. Geol. Soc. London.*, **133**: 559-571.

O'Neil, J.R. and Taylor, H. P., (1967) The oxygen isotope and cation exchange chemistry of feldspar. *Am. Mineral.*, **52**: 1414-1437.

O'Neil, J. R., Shaw, S. E., and Flood, R. H., (1977) Oxygen and Hydrogen Isotope compositions as indicators of granite genesis in the New England Batholith, Australia. *Contrib. Mineral. Petrol.*, **62**: 313-328.

Orsini, J.B., (1979)*Comptes rendu de l'Acadèmie des sciences, Paris*, **289**: 981-984.

Palacz, Z.A., (1985) Sr-Nd-Pb isotope evidence for crustal contamination in the Rhum intrusion. *Earth Planet. Sci. Lett.*, **74**: 35-44.

Pankhurst, R.J., (1977) Strontium isotope evidence for mantle events in the continental lithosphere. *J. Geol. Soc. Lond.*, **134**: 255-268.

Pankhurst, R.J., Walsh, J.N, Beckinsale, R.D. and Skelhorn, R.R., (1978) Isotope and other geochemical evidence for the origin of the Loch Usig Granophyre, Isle of Mull, Scotland. *Earth Planet. Sci. Lett.*, **38**: 355-363.

Papike, J.J., (1982) Pyroxene mineralogy of the Moon and Meteorites. *Rev. Mineralogy, Mineral. Soc. Am.*, **7**: 495-524.

Patchett, P.J., (1980) Thermal effects of basalt on continental crust and crustal contamination of magmas. *Nature.*, **283**: 559-561.

Paterson, B. A., Stephens, W. E., and Herd, D. A., (1989) Zoning in granitoid accessory minerals as revealed by backscattered electron imagery. *Mineral. Mag.*, **53**: 55-61.

Paterson, B.A. and Stephens, W. E., (1992) Kinetically induced compositional zoning in titanite: implications for accessory-phase/melt partitioning of trace elements. *Contrib. Mineral. Petrol.*, **109**: 373-385.

Paterson, B. A., Rogers, G., and Stephens, W. E., (1992a) Evidence for inherited Sm-Nd isotopes in granitoid zircons. *Contrib. Mineral. Petrol.*, **111**: 378-390.

Paterson, B.A., Stephens, W. E., Rogers, G., Williams, I. S., Hinton, R. W., and Herd, D. A., (1992b) The nature of zircon inheritance in two granite plutons. *Trans. R. Soc. Edinb.: Earth Sci.*, **83**: 459-471.

Paul, D., K., (1979) Isotopic composition of strontium in Indian kimberlites. *Geochim. Cosmochim. Acta*, **43**: 389-394.

Pearce, J.A., Harris, N. B. W. and Tindle, A. G., (1984) Trace element discrimination diagrams for tectonic interpretation of granitic rocks. *J. Petrol.*, **25**: 956-983.

Pecher, A., (1981) Experimental decrepitation and reequilibration of fluid inclusions in synthetic quartz. *Tectonphysics.*, **78**: 567-584.

Philpotts, A.R., (1990) Principles of igneous and metamorphic petrology. Prentice Hall. New Jersey.

Pidgeon, R. T. and Aftalion, M., (1978) Cogenetic and inherited zircon U-Pb systems in granites: Palaeozoic granites of Scotland and England. In: Bowes DR, Leake BE (eds) Crustal evolution in north-western Britain and adjacent. *Geol. J. Spec. Issue*, **10**: 183-248.

Pidgeon, R.T., (1992) Recrystallisation of oscillatory zoned zircon: some geochronological and petrological implications. *Contrib. Mineral. Petrol.*, **110**: 463-472.

Pitcher, W.S., (1982) Granite type and tectonic environment. In, Hsu, K. J. (ed), Mountain Building processes, Academic Press, London: 19-40.

Pitcher, W.S., (1983) In: Hsu, K. (ed.), Mountain Building Processes. Academic Press: 19-40, London.

Pitcher, W.S., (1987) *Geologie Rundschau.*, **76**: 51-79.

Pitcher, W.S., (1993) Tha nature and origin of granite. Chapman and Hall, London.

Potter, R.W., (1977) Pressure corrections for fluid-inclusion homogenisation temperatures based on the volumetric properties of the system NaCl-H_2O. J. *Res. U. S. Geol. Sur.*, **5**: 603-607.

Potter, R.W. and Clynne, M. A., (1978) Solubility of highly soluble salts in aqueous media part 1, NaCl, KCl, $CaCl_2$, Na_2SO_4 and K_2SO_4 solubilities to 100oC. *J. Reas. U. S. Geol. Sur.*, **6**: 701-705.

Potts, P.J., (1987) A handbook of silicate rock analysis. Blackie and son Limited, Glasgow.

Potts, P.J., Thorpe, O. W., Watson, J. S., (1981) Determination of the REE abundances in 29 international rock standards by instrumental neutron activation analysis: A critical appraisal of calibration errors. *Chem. Geol.*, **34**: 331-352.

Pupin, J.P., (1980) Zircon and Granite Petrology. *Contrib. Mineral. Petrol.*, **73**: 207-220.

Pupin, J.P., (1985) Magmatic zoning of Hercynian granitoids in France based on zircon typology. Schweiz. *Mineral. Petrogr. Mitt.*, **65**: 29-56.

Rankin, A.H. and Alderton, D. H. M., (1985) In high heat production (HHP) granites, hydrothermal circulation and ore genesis. *Instn. Mining Metall.*, London: 287-299.

Ratajeski, K. and Campbell, A. R., (1994) Distribution of fluid inclusions in igneous quartz of the Capitan pluton, New Mexico, USA. *Geochim. Cosmochim. Acta*, **58, No. 3**: 1161-1174.

Richey, J.E., Stewart, F. H. and Wager, L. R., (1946) Age relations of certain granites and marscoite in Skye. *Geol. Mag.*, **83**: 293.

Richey, J.E., Stewart, F. H. and Wager, L. R., (1947) Age relations of certain granites in Skye. *Geol. Mag.*, **84**: 128.

Richter, R. and Hoernes, S., (1988) The application of the increment method in comparison with experimentally derived and calculated O-isotope fractionations: *Chemische Erde*, **48**: 1-18.

Robinson, P., Spear, F. S., Schumacher, J. C., Laird, Jo., Klein, C., Evans, B. W. and Doolan, B. L., (1982) Phase relations of metamorphic amphiboles: Natural occurrence and theory. *Rev. Mineralogy, Mineral. Soc. Am.*, **9B**: 1-227.

Rogers, G., Krogh, T. E., Bluck, B. J. and Kwok, Y. Y., (1990) Provenance ages of the Torridonian sandstone of NW Scotland using single grain U-Pb zircon analysis. *Geol. Soc. Aust. Abstr. (ICOG)*, **27**: 84.

Rogers, G., Dempster, T. J., Bluck, B. J. and Tanner, P. W. G. (1989) A high precision U-Pb age for the Ben Vuirich granite: implication for the evolution of the Scottish Dalradian Supergroup. *J. G. S. Lond.*, **146**: 789-798.

Rollinson, H. (1993) Using geochemical data: evaluation, presentation, interpretation. John Wiley and Sons, Inc., New York.

Rossi, P. and Cheveremont, P., (1987)*Gèochronique.*, **21**: 14-18.

Sawka, W.N., (1988) REE and trace element variations in accessory minerals and hornblende from the strongly zoned McMurry Meadows Pluton, California. *Trans. R. Soc. Edinb.: Earth Sci.*, **79**: 157-168.

Schwartz, M.O., (1989) Determining phase volumes of mixed CO_2-H_2O inclusions using microthermometric measurements. *Mineral Deposita.*, **24**: 43-47.

Shand, S.J., (1943) Eruptive Rocks. T. Murby and Co. (2 ed.), London.

Shand, S.J., (1947) Eruptive Rocks. Their genesis, composition, classification, and their relation to Ore-Deposits, 3rd ed. J. Wiley and Son, New York.

Shelley, D., (1966) The significance of granophyric and myrmekitic textures in the Lundy Granites. *Min. Mag.*, **35**: 678-692.

Shepherd, T.J., (1981) Temperature-programmable heating-freezing stage for microthermometric analysis of fluid inclusions. *Econ. Geol.*, **76**: 1244-1247.

Shepherd, T.J., Rankin, A. H. and Alderton, D. H. M., (1985) A practical guide to fluid inclusion studies. Blackie, Glasgow.

Sheppard, S.M.F., and Taylor, H. P., Jr., (1974) Hydrogen and oxygen isotope evidence for the origins of water in the Boulder batholith and the Butte ore deposits, Montana. *IEcon. Geol.*, **69**: 926-946.

Sheppard, S. M. F., (1986) Characterisation and isotopic variations in natural waters: In: Valley, J. W., Taylor, H. P. Jr., O'Neil, J.R. (eds) Stable isotopes in high temperature geological processes. *Rev. Mineralogy, Mineral. Soc. Am.*, **16**: 165-183.

Skinner, B. J., (1966) Thermal expansion. In: Clark S (ed) Handbook of Physical Constants. *Geol. Soc. Am. Mem.*, **97**: 75-96.

Skjerlie, K. P. (1992) Petrogenesis and significance of late Caledonian granitoid magmatism in Western Norway. *Contrib. Minarl. Petrol.*, **110**: 473- 487.

Smith, J.V., (1974) Feldspar minerals, **Vols. 1, 2,** Springer-Verlag,. New York.

Smith, J.V. and Brown, W. L., (1988) Feldspar minerals, Volume **1**. Crystal structures, Physical, Chemical, and Microstructural properties. Berlin Heidelberg: Springer-Verlag.

Spear, F. S. and Kimball, K. L., (1984) Recamp: a FORTRAN IV program for estimating Fe^{3}+ contents in amphiboles. *Comp. Geosci.*, **10**: 317-325.

Speer, J.A., (1982) Micas in igneous rocks. *Rev. Mineralogy, Mineral. Soc. Am.*, **13**: 299-356.

Sterner, S.M., Hall, D. L. and Bodnar, R. J., (1988) Synthetic fluid inclusions: V. Solubility relations in the system NaCl-KCl-H_2O under vapour-saturated conditions. *Geochim. Cosmochim. Acta.*, **52**: 989-1005.

Stewart, F.H., (1965) Tertiary igneous activity. In Craig (Ed.): The geology of Scotland 1st. ed. Oliver and Boyd, Edinburgh.

Streckeisen, A.L., (1976) To each plutonic rock its proper name. *Earth. Sci. Rev.*, **12**: 1-33.

Streckeisen, A. L.and Le Maitre, R. W., (1979) A chemical approximation to the modal QAPF classification of the igneous rocks. *Neues Jahrb. Mineral. Abh.*, **136**: 169-206.

Sun, S. S., and Hanson, G. N., (1975) Origin of Ross Island basanitoids and limitations upon the heterogeneity of mantle sources for alkali basalts and nephelinites. *Contrib. Mineral. Petrol.*, **52**: 77-106.

Suzuoki, T., and Epstein, S., (1976) Hydrogen isotope fractionation between OH-bearing minerals and water. *Geochim. Cosmochim. Acta*, **40**: 1229-1240.

Tauson, L.V. and Kozlov, Y. D., (1973)*Transactions of the Instituition of Mining and Metallurgy*, London., **4**: 37-44.

Taylor, B., E., Eichelberger, J., C. and Westrich, H., R. (1983) Hydrogen isotopic evidence of rhyolitic magma degassing during shallow intrusion and eruption. *Nature*, **306**: 541-545.

Taylor, H.P., (1968) The oxygen isotope geochemistry of igneous rocks. *Contrib. Mineral. and Petrol.*, **19**: 1-71.

Taylor, H.P.J., and Forester, R. W., (1971) Low-^{18}O igneous rocks from the intrusive Complexes of Skye, Mull, and Ardnamurchan, Western Scotland.,. *J. Petrol.*, **12**,: 465-97.

Taylor, H.P., (1974) The application of oxygen and hydrogen isotope studies to problems of hydrothermal alteration and ore deposition. *Econ. Geol.*, **69**: 843-883.

Taylor, H.P., (1977) Water/rock interactions and the origin of H_2O in granitic batholiths. *J. Geol. Soc. Lond.*, **133**: 509-558.

Taylor, H.P., (1978) Oxygen and hydrogen isotope studies of plutonic granitic rocks. *Earth Planet. Sci. Lett.*, **38**,: p. 177-210.

Taylor, H.P., Jr., Forester, R. W., (1979) An oxygen and hydrogen isotope study of the Skaergaard Intrusion and its country Rocks: a description of a 55-M. Y. Old Fossil hydrothermal system. *J. Petrol.*, **20**: 355-419.

Taylor, H. P., (1979) Oxygen and hydrogen isotope relationships in hydrothermal mineral deposits. In: Barnes H. L. (ed.), Geochemistry of hydrothermal ore deposits, **2nd ed.** Wiley, New York.

Taylor, H. P. and Sheppard, S. M. F., (1986) Igneous rocks: I. Processes of isotopic fractionation and isotope systematics. In: Valley, J. W., Taylor, H. P., Jr., & O'Neil, J.R. (eds.) Stable Isotope in high temperature geological processes. *Rev. Mineralogy, Mineral. Soc. Am.*, **16**: 227-271.

Taylor, S.R., (1965) The application of trace element data to problems in petrology. *Phs. Chem. earth.*, **6**: 133-213.

Taylor, S. R. and McLennan., S. M., (1985) The continental crust: its composition and evolution. Blackwell Scientific, Oxford.

Thirlwall, M. F. and Jones, N. W., (1983) Isotope geochemistry and contamination mechanisms of Tertiary Lavas from Skye, N. W., Scotland. In Continental basalts and mantle xenoliths (ed. C. J. Hawkesworth & M. J. Norry)., : p. 186-208. Nantwich, Shiva.

Thirlwall, M.F., Upton, B. G. J. and Jenkins, C., (1994) Interaction between Continental Lithosphere and the Iceland Plume-Sr-Nd-Pb Isotope

Geochemistry of Tertiary Basalts, NE Greenland. *J. Petrol.*, **35**: 839-879.

Thompson, R.N., (1969) Tertiary granites and associated rocks of the Marsco area, Isle of Skye. *Q. Jl. geol. Soc. Lond.*, **124**: 349-385.

Thompson, R.N., (1976) Short communications: Alkali amphibole in the Eocene high-level granites of Skye, Scotland. *Min. Mag.*, **40**: 891-893.

Thompson, R.N., (1980) Askja 1875, Skye 56Ma: Basalt-triggered, Plinian, mixed-magma eruptions during the emplacement of the Western Red Hills granites, Isle of Skye. *Geol. Rundsch.*, **69**: 245-262.

Thompson, R.N., (1982) Magmatism of the British Tertiary Volcanic Province. *Scott. J. Geol.*, **18**: 49-107.

Thornton, C. P. and Tuttle, O. F. (1960) Chemistry of igneous rocks. I. Differentiation index,. *Am. J. Sci.*, **258**: 664-684.

Thorpe, R.S., Potts, P. J. and Sarre, M. B., (1977) Rare earth evidence concerning the origin of granites of the Isle of Skye, Northwest Scotland. *Earth. Planet. Sci. Lett.*, **36**: 111-120.

Thorpe, R.S., (1978) The parental basaltic magma of granites from the Isle of Skye, N. W. Scotland. *Min. Mag.*, **42**: 157-158.

Thorpe, R.S., Tindle, A. G . and Gledhill, A., (1990) The Petrology and Origin of the Tertiary Lundy Granite (Bristol Channel, UK.). *J. Petrol.*, **31**: 1379-1406.

Tindle, A. G., and Pearce, J. A., (1981) Petrogenetic Modelling of in situ Fractional Crystallisation in the Zoned Loch Doon Pluton, Scotland. *Contrib. Mineral. Petrol.*, **78**: 196-207.

Tischendorf, G. and Pälchen, W., (1985) *Zeitschrift fur Geologische Wissenschaften, Berlin*, **13**: 615-627.

Turpault, M.P., Meunier, A., Guilhaumou, N. and Touchard, G., (1992) Analysis of hot fluid infiltration in fractured granite by fluid inclusion study. *Appl. Geoch. Suppl.*, **1**: 269-276.

Tuttle, O.F. and Bowen, N. L., (1950) High temperature Albite and Contiguous feldspars. *J. Geol.*, **58**: 572-583.

Tuttle, O.F., (1952) Origin of contrasting mineralogy of extrusive and plutonic salic rocks. *J. Geol.*, **60**: 107-124.

Tuttle, O.F. and Keith, M. L., (1954) The granite problem: evidence from the quartz and feldspar of a Tertiary granite. *Geol. Mag.*, **91**: 61-72.

Tuttle, O.F. and Bowen, N. L., (1958) Origin of granite on the light of experimental studies in system Ab-Or-Q-H2O. *Geol. Soc. Amer. Mem.*, **74**: 153 pp.

Valley, J.W., (1986) Stable isotope geochemistry of Metamorphic rocks. *Rev. Mineralogy Mineral. Soc. Am.*, **16**: 445-489.

Vavra, G., (1993) A guide to quantitative morphology of accessory zircon. *Chem. Geol.*, **110**: 15-28.

Vavra, G., (1994) Systematics of internal zircon morphology in major Variscan granitoid types. *Contrib. Mineral. Petrol.*, **117**: 331-344.

Vityk, M.O., Krouse, H. R. and Demihov, Y. N., (1993) Preservation of ^{18}O values of fluid inclusion in quartz over geological time in an epithermal environment: Beregovo deposit, Transcarpathia, Ukraine. *Earth Planet. Sci. Lett.*, **119**: 561-568.

Von Oeynhausen, C. and Von Dechen, H., (1829) Die Insel Skye. *Karsten's Archiv. fur Min. etc.*, **1**: 56-104.

Wager, L.R., Weedon, D. S. and Vincent, E. A., (1953) A granophyre from Coire Uaigneich, Isle of Skye, containing quartz paramorphs after tridymite. *Min. Mag.*, **30**: 263-275.

Wager, L. R., (1956) A chemical definition of fractionation stages as a basis for comparision of Hawaiian, Hebridean, and other basic lavas. *Geochim. Cosmochim.Acta*, **9**: 217-248.

Wager, L. R. and Vincent, E. A., (1962) Ferrodiorite from the Isle of Skye. *Min. Mag.*, **33**: 26-36.

Wager, L.R., Vincent, E. A., Brown, G. M. and Bell, J. D., (1965) Marscoite and related rocks from the Western Red Hills Complex, Isle of Skye. *Phil. Trans. R. Soc. Lond.*, **A257**: 273-307.

Wallace, J. M., Ellam, R. M., Meighan., I. G., Lyle, P. and Rogers, N. W., (1994) Sr isotope data for the Tertiary lavas of Northern Ireland: evidence for open system petrogenesis. *J. Geol. Soc. Lond.*, **151**: 869-877.

Walsh, J. N., Beckinsale, R. D., Skelhorn, R. R. and Thorpe, R. S., (1979) Geochemistry and petrogenesis of Tertiary granitic Rocks from Isle of Mull, N.W.Scotland. *Contrib. Mineral. Petrol.*, **71**: 99-116.

Wark, D. A., and Miller, C. F., (1993) Accessory mineral behaviour during differentiation of a granite suite: monazite, xenotime and zircon in the Sweet water Wash pluton, south-eastern California, U. S. A. *Chem. Geol.*, **110**: 49-67.

Watson, E.B., (1979) Zircon saturation in felsic liquids: experimental results and applications to trace element geochemistry. *Contrib. Mineral. Petrol.*,**70**: 407-419.

Watson, E.B., and Capobianco, C. J., (1981) Phosphorus and the rare earth elements in felsic magmas: an assessment of the role of apatite. *Geochim. Cosmochim. Acta*, **45**: 2349-2358.

Watson, E. B. and Harrison, T. M., (1983) Zircon saturation revisited: temperature and composition effects in a variety of crustal magma types. *Earth.Planet. Sci. Lett.*, **64**: 295-304.

Watson, E. B., Harrison, T. M., and Ryerson, F. J., (1985) Diffusion of Sm, Sr and Pb in fluoroapatite. *Geochim. Cosmochim. Acta*, **49**: 1813-1823.

Watson, E. B., Vicenzi, E. P. and Rapp, R. P., (1989) Inclusion/host relations involving accessory minerals in high-grade metamorphic and anatectic rocks. *Contrib. Mineral. Petrol.*, **101**: 220-231.

Wendt, I., (1993) Isochron or mixing line? *Chem. Geol. (Isotope Geosience section)*, **104**: 301-305.

Whalen, J.B., Currie, K. L. and Chappell, B. W., (1987) A-type granites: geochemical characteristics, discrimination and petrogenesis. *Contrib. Mineral. Pertol.*, **95**: 407-419.

White, A.J.R., (1979) Sources granite magmas. *Geol. Soc. Am. Abs. with Prog.*, **11**: 539.

White, A.J. and Chappell, B. W., (1988) Some supra-crustal (S-type) granites of Lachlan Fold Belt. *Trans. Roy. Soc. Edinb. Earth science*, **79**: 169-181.

Whitten, E.H.T., (1961) Modal variation and the form of the Beinn an Dubhaich Granite, Skye. *Geol. Mag.*, **98**: 467-472.

Wilkinson, J.J., (1990) The role of metamorphic fluids in the development of the Cornubian orefield: fluid inclusion evidence from south Cornwall. *Min. Mag.*, **54**: 219-230.

Williams, I. S., (1992) Some observations on the use of zircon U-Pb geochronology in the study of granitic rocks. *Trans. Roy. Soc.: Edinb. Earth Sci.*, **83**: 447-458.

Wilson, M.R., Hamilton, P. J., Fallick, A. E., Aftalion, M. and Michard, A., (1985) Granites and early Proterozoic crustal evolution in Sweden: evidence from Sm-Nd, U-Pb and O isotope systematics. *Earth Planet. Sci. Lett.*, **72**: 376-388.

Wilson, M., (1989) Igneous Petrogenesis. **1st. ed.** Chapman and Hall, London.

Winkler, H. G. F., (1974) Petrogenesis of metamorphic rocks. **3rd ed.** Springer Verlag, Berlin.

Wones, D. R. and Gilbert, M. C., (1982) Amphiboles in igneous environment. *Rev. Mineralogy, Mineral. Soc. Am.*, **9B**: 355-390.

Xu Kegin, S.N., Wang Dezi, Hu Shouxi, Liu Yingjun and Ji Shouyuan., (1984): In: Xu Kegin and Tu Guangchi (eds), Geology of Granites and their Metallogenetic Relations. Proceedings of the international Symposium, Nanjing University. *Science Press. Beijing*, pp 1-3.

Yang Chaoqun, (1984) In: Xu Kegin and Tu Guangchi (eds), Geology of Granites and their Metallogenetic Relations. Proceedings of the international Symposium, Nanjing University. *Science Press, Beijing*, 253-276.

Yardley, B.W.D., (1983) Quartz veins and devolatilization during metamorphism. *J. Geol. Soc. Lond.*, **140**: 657-663.

Yoder, H. S., Stewart, D. B. and Smith, J. R., (1957) Ternary feldspar. *Yb. Carnegie Instn. Wash.*, **56**: 206-214.

York, D. (1969) Least squares fitting of a straight line correlated errors. *Earth Planet. Sci. Lett.*, **5**: 320-334.

Zen, E-an, (1986) Aluminium enrichment in silicate melts by fractional crystallisation: some mineralogic and petrologic constraints. *J. Petrol.*, **27**: 1095-1117.